VOLUME 25 / NUMBER 2 / 1983

Radiocarbon

Published by THE AMERICAN JOURNAL OF SCIENCE

11th INTERNATIONAL RADIOCARBON CONFERENCE

1982 Seattle, Washington

Edited by Minze Stuiver and Renee Kra

ology Laboratory
versity
ven, Connecticut 06511

ISSN: 0033-8222

RADIOCARBON

Editor: Minze Stuiver
Managing Editor: Renee S Kra
Published by
THE AMERICAN JOURNAL OF SCIENCE
Editors: John Rodgers, John H Ostrom, Robert A Berner
Managing Editor: Marie C Casey

Published three times a year, in Winter, Spring, and Summer, at Yale University, New Haven, Connecticut 06511.

Subscription rate $75.00 (for institutions), $50.00 (for individuals), available only in whole volumes. The price of the full volume 22, nos. 1-4, is $60.00 for individuals and $80.00 for institutions. The Proceedings of the Tenth International Radiocarbon Conference, vol 22, nos. 2 and 3, are available for $60.00. The Proceedings of the Eleventh International Radiocarbon Conference is $50.00.

All correspondence and manuscripts should be addressed to the Managing Editor, RADIOCARBON, Kline Geology Laboratory, Yale University, 210 Whitney Ave, PO Box 6666, New Haven, Connecticut 06511.

Reprints. The minimum reprint order for each article will be 50 copies without cover. No reprints will be furnished free of charge unless page charges are paid. The cost of additional copies will, of course, be greater if the article is accompanied by plates involving unusual expense. Copies will be furnished with a printed cover giving the title, author, volume, page, and year, when specially ordered.

Page charges. Each institution sponsoring research reported in a technical paper or a date list, will be asked to pay a charge of $80.00 per printed page, due when galley proof is returned. Institutions or authors paying such charges will be entitled to 100 free reprints without covers. No charge will be made if the author indicates that his institution is unable to pay them, and payment of page charges on an article will *not* in any case be a condition for its acceptance.

Back issues and price lists may be obtained from the office of RADIOCARBON.

Missing issues will be replaced without charge only if claim is made within three months (six months for India and Australia) after the publication date. Claim for missing issues will not be honored if absence results from failure by the subscriber to notify the Journal of an address change.

Illustrations should include explanation of symbols used. Copy that cannot be reproduced cannot be accepted; it should be capable of reduction to not more than 10 by 17.5, all lettering being at least 1/6 inch high after reduction. When necessary, one large map or table can be accepted, if it will not exceed 17.5 inches in width after reduction. Line drawings should be in black India ink on white drawing board, tracing cloth, or coordinate paper printed in blue and should be accompanied by clear ozalids or reduced photographs for use by the reviewers. Photographs should be positive prints. Photostatic and typewritten material cannot be accepted as copy for illustrations. *Plates* (photographs) and *figures* (line drawings) should each be numbered consecutively through each article, using arabic numerals. If two photographs form one plate, they are figures A and B of that plate. **All measurements should be given in SI (metric units).**

Citations. **A number of radiocarbon dates appear in publications without laboratory citation or reference to published date lists. We ask that laboratories remind submitters and users of radiocarbon dates to include proper citation (laboratory number and date-list citation) in all publications in which radiocarbon dates appear.**

Radiocarbon Measurements: Comprehensive Index, 1950-1965. This index covers all published ^{14}C measurements through Volume 7 of RADIOCARBON, and incorporates revisions made by all laboratories. It is available to all subscribers to RADIOCARBON at $20.00 US per copy.

List of laboratories. The comprehensive list of laboratories at the end of each volume appears in the third number of each volume. Changes in names or addresses should be reported to the Managing Editor by May 1.

Annual Index. All dates appear in index form at the end of the third number of each volume.

VOLUME 25 / NUMBER 2 / 1983

Radiocarbon

Published by THE AMERICAN JOURNAL OF SCIENCE

Proceedings of the Eleventh International Radiocarbon Conference—Seattle

Editors
MINZE STUIVER and RENEE S KRA

Kline Geology Laboratory
Yale University
New Haven, Connecticut 06511

FOREWORD

The Eleventh International Radiocarbon Conference was held June 21-26, 1982 in Seattle (state of Washington), USA. The organization of the conference was in the hands of Minze Stuiver, P M Grootes, and G W Farwell, all of the University of Washington at Seattle. The meeting was hosted by the Department of Geological Sciences, the Department of Physics, and the Quaternary Research Center. One-hundred and fifty-five scientists from 30 countries participated in a successful meeting at which about 125 papers and contributions were presented.

The major topics of the conference were natural ^{14}C variations, ^{14}C applications, accelerator mass spectrometry, general aspects of the ^{14}C technique, hydrology, oceanography, archaeology, anthropogenic ^{14}C variations, and ^{14}C applications. The international Calibration Committee was reconvened to continue the work on an international cross-calibrated radiocarbon time scale.

Invited lectures were presented by Walter Kutschera, W G Mook, K O Münnich, Hans Oeschger, and H T Waterbolk.

RADIOCARBON volume 25, no. 2, constitutes the proceedings of the Seattle meeting. A few "overflow" articles will be published in volume 25, no. 3. The standard review procedures of RADIOCARBON were followed for the submitted papers. The cooperation of the reviewers of these papers is greatly appreciated.

The next International Radiocarbon Conference is planned for the summer of 1985, in Trondheim, Norway.

Minze Stuiver

CONTENTS

I. NATURAL ^{14}C VARIATIONS

II. HYDROLOGY

III. ^{14}C APPLICATIONS

IV. OCEANOGRAPHY

V. GENERAL ASPECTS OF ^{14}C TECHNIQUE

VI. ANTHROPOGENIC ^{14}C VARIATIONS

VII. ARCHAEOLOGY

VIII. TECHNICAL ASPECTS OF ACCELERATOR MASS SPECTROMETRY

BUSINESS MEETING

PARTICIPANTS

Marisa Alessio
Institute of Physics "G Marconi"
Rome, Italy

L David Arnold
Alberta Environmental Centre
Vegreville, Canada

Gordon C Ball
Atomic Energy of Canada, Ltd
Chalk River, Canada

Cathy W Barnosky
University of Washington, Seattle

Bernd Becker
University of Hohenheim
Stuttgart, West Germany

Jürg Beer
University of Bern, Switzerland

C R Berger
University of California, Los Angeles

Jeanne Berry
University of Waterloo, Canada

Donald J Blakeslee
Wichita State University, Kansas

D Q Bowen
University of Wales, Aberystwyth

Robert Henry Brown
Loma Linda University
Loma Linda, California

Robert M Brown
Atomic Energy of Canada, Ltd
Chalk River, Canada

Thomas Brown
Simon Fraser University
Burnaby, Canada

Richard Burleigh
The British Museum, London

William F Cain
Loyola Marymount University
Los Angeles, California

Gilberto Calderoni
Institute of Geochemistry
Rome, Italy

Jack Liu Chao-li
Illinois State Geological Survey
Champaign, Illinois

Chen Chenghui
Third Institute of Oceanography
Fujian, China

Dennis D Coleman
Illinois State Geological Survey
Champaign, Illinois

Cesarina Cortesi
Institute of Geochemistry
Rome, Italy

Dagmar Cronn
Washington State University, Pullman

Lloyd A Currie
National Bureau of Standards
Washington, D C

Paul E Damon
University of Arizona, Tucson

John Delmonte
Delsen Testing Laboratory
Glendale, California

Douglas J Donahue
University of Arizona, Tucson

Robert J Drimmie
University of Waterloo, Canada

Ellen M Druffel
Woods Hole Oceanographic Institution
Woods Hole, Massachusetts

Lorenz Eichinger
GSF-Institut für Radiohydrometrie
Neuherberg, West Germany

David Elmore
University of Rochester, New York

Youhanna Fares
Texas A&M University, College Station

George W Farwell
University of Washington, Seattle

C W Ferguson
University of Arizona, Tuscon

Jürgen C Freundlich
University of Köln, West Germany

Mebus Geyh
Niedersächsisches Landesamt für
Bodenforschung, Hannover, West Germany

Robert Giegengack
University of Pennsylvania, Philadelphia

Richard Gillespie
Oxford University, England

Pierre Glynn
University of Quebec-Montreal, Canada

Harry E Gove
University of Rochester, New York

J A J Gowlett
Oxford University, England

David L Graham
Rockwell Hanford Operations
Richland, Washington

John Gray
University of Alberta
Edmonton, Canada

Pieter M Grootes
University of Washington, Seattle

Steinar Gulliksen
University of Trondheim, Norway

Debbie M Gurfinkel
University of Toronto, Canada

Herbert Haas
Southern Methodist University
Dallas, Texas

Sören Håkansson
University of Lund, Sweden

Douglas D Harkness
University of Glasgow, Scotland

Vance Haynes
University of Arizona, Tucson

R E M Hedges
Oxford University, England

Jan Heinemeier
University of Aarhus, Denmark

Andrew Herozeg
Lamont-Doherty Geological Observatory
Palisades, New York

John W Hess
Desert Research Institute
Las Vegas, Nevada

Keith Hobson
Simon Fraser University
Burnaby, Canada

Gert Hut
University of Groningen, The Netherlands

Salvatore Improta
Institute of Physics "G Marconi"
Rome, Italy

Margaret Jope
Queen's University, Belfast, Ireland

Edward Martyn Jope
Queen's University, Belfast, Ireland

A J T Jull
University of Arizona, Tucson

Tuovi Kankainen
Geological Survey of Finland, Espoo

John W King
University of Minnesota, Minneapolis

Jeffrey Klein
University of Pennsylvania, Philadelphia

Gundolf H Kohlmaier
University of Frankfurt, West Germany

Serge A Korff
New York University, New York

Renee Kra
Yale University, New Haven, Connecticut

Gerhard Kratz
University of Frankfurt, West Germany

Bernd Kromer
University of Heidelberg, West Germany

Theodore H Kruse
Rutgers University
Piscataway, New Jersey

Sheela Lalbhai Kusumgar
Physical Research Laboratory
Ahmedabad, India

Walter Kutschera
Argonne National Laboratory
Argonne, Illinois

Valmore C Lamarche, Jr
University of Arizona, Tucson

Sara Langer
Lamont-Doherty Geological Observatory
Palisades, New York

Steven W Leavitt
University of Arizona, Tucson

Juan-Carlos Lerman
University of Arizona, Tucson

Leona Marshall-Libby
University of California, Los Angeles

Timothy W Linick
University of California, San Diego

Austin Long
University of Arizona, Tucson

Nancy Lovell
Simon Fraser University
Burnaby, Canada

Wilfrid B Mann
National Bureau of Standards
Washington, D C

Leslie Marcus
Page Museum, Los Angeles, California

Daniel C McCorkle
University of Washington, Seattle

Roger McNeely
Geological Survey of Canada, Ottawa

Stephen Malcolm McPhail
Sydney University, Australia

Howard Melville
Brock University
St Catherines, Canada

Henry N Michael
University of Pennsylvania, Philadelphia

Willem G Mook
University of Groningen, The Netherlands

Heribert Moser
GSF-Institut für Radiohydrometrie
Neuherberg, West Germany

Anthony B Muller
Sandia National Laboratories
Albuquerque, New Mexico

K O Münnich
University of Heidelberg, West Germany

Erle Nelson
Simon Fraser University
Burnaby, Canada

John E Noakes
University of Georgia, Athens

Reidar Nydal
University of Trondheim, Norway

Hans Oeschger
University of Bern, Switzerland

Ingrid U Olsson
University of Uppsala, Sweden

H Gote Östlund
University of Miami, Florida

Robert Leon Otlet
AERE, Harwell, England

Howard D Paap
Lakewood Community College
Whitebear Lake, Minnesota

Richard R Pardi
Queen's College, New York

Frederick J Pearson, Jr
INTERA Environmental Consultants, Inc
Houston, Texas

Gordon W Pearson
Queen's University, Belfast, Ireland

Tsung-Hung Peng
Oak Ridge National Laboratory
Oak Ridge, Tennessee

Johnathan Pilcher
Queen's University, Belfast, Ireland

Henry Polach
Australian National University, Canberra

Pavel Povinec
Comenius University
Bratislava, Czechoslovakia

Christopher John Radnell
University of Arizona, Tucson

Omar Rahmouni
Nuclear Center, Algiers, Algeria

Werner Rauert
GSF-Institut für Radiohydrometrie
Neuherberg, West Germany

Stephen W Robinson
U S Geological Survey
Menlo Park, California

Meyer Rubin
U S Geological Survey
Reston, Virginia

William Raymond Schell
University of Pittsburgh, Pennsylvania

Fred H Schmidt
University of Washington, Seattle

John C Sheppard
Washington State University, Pullman

B L K Somayajulu
University of Washington, Seattle

Charles P Sonett
University of Arizona, Tucson

Eloni Sonninen
University of Helsinki, Finland

John Southon
Simon Fraser University
Burnaby, Canada

Jim D Spaulding
University of Georgia, Athens

W Geoffrey Spaulding
University of Washington, Seattle

Dušan Srdoč
Rudjer Boskovic Institute
Zagreb, Yugoslavia

Michael J Stenhouse
University of Glasgow, Scotland

Robert S Sternberg
University of Arizona, Tucson

Biancamaria Stievano
Laboratori Nazionali DiLegnaro
Legnaro Padova, Italy

Jerry J Stipp
University of Miami, Florida

Boyd R Strain
Duke University
Durham, North Carolina

Robert Stuckenrath
Smithsonian Institution
Rockville, Maryland

Minze Stuiver
University of Washington, Seattle

Shinyal Sugita
University of Washington, Seattle

Charles H Sullivan
Geochron Laboratories
Cambridge, Massachusetts

Roy Switsur
Cambridge University, England

Murry A Tamers
University of Miami, Florida

Henrik Tauber
National Museum
Copenhagen, Denmark

R E Taylor
University of California, Riverside

Jaan Terasmae
Brock University
St Catherines, Canada

Roy Thompson
University of Edinburgh, Scotland

Donald C Thorstenson
U S Geological Survey
Reston, Virginia

John R Toggweiler
Lamont-Doherty Geological Observatory
Palisades, New York

Allen B Tucker
San Jose State University
San Jose, California

Joe Uzdzinski
University of Pennsylvania, Philadelphia

Sam Valastro
University of Texas, Austin

Mark Van Strydonck
Institut Royal du Patrimoine Artistique
Brussels, Belgium

John Vogel
Simon Frazer University
Burnaby, Canada

J C Vogel
National Physical Research Laboratory
Pretoria, South Africa

Martin Wahlen
New York State Department of Health
Albany, New York

Alison Jill Walker
AERE, Harwell, England

Gavin Wallace
Institute of Nuclear Sciences
Lower Hutt, New Zealand

H T Waterbolk
University of Groningen, The Netherlands

Esmée Webb
University of London, England

James White
Lamont-Doherty Geological Observatory
Palisades, New York

Nicholas R White
Oxford University, England

Horst Willkomm
University of Kiel, West Germany

Jürgen Wittenberg
Saskatchewan Research Council
Saskatoon, Canada

Willy Wölfli
Laboratory of Nuclear Physics
Zurich, Switzerland

In Che Yang
U S Geological Survey, Arvada, Colorado

Chen Yee-Chein
Institute of Geology, Beijing, China

Ted Zabel
University of Arizona, Tucson

I. NATURAL ^{14}C VARIATIONS

[Radiocarbon, Vol 25, No. 2, 1983, P 171-178]

DENDROCHRONOLOGY AT BELFAST AS A BACKGROUND TO HIGH-PRECISION CALIBRATION

M G L BAILLIE, J R PILCHER, AND G W PEARSON

Palaeoecology Centre, Queen's University, Belfast

Northern Ireland

INTRODUCTION

The tree-ring program at Belfast originally aimed at the construction of a 6000-year oak chronology. The stimulus for this work came from the large numbers of sub-fossil oaks uncovered in Northern Ireland during land drainage and motorway construction in the late 1960's (Pilcher *et al* 1977). It became clear that any attempt to build such a long chronology would break naturally into two distinct units. One unit related to the construction of a prehistoric (BC era) chronology dependent on the sampling of large numbers of essentially random sub-fossil timbers. For this unit to be successful, timbers would have to survive relatively uniformly through time. The second chronology building unit was related principally to the AD era, with a natural extension into the first millennium BC at least. This unit was envisaged as the link between the present day and the necessarily floating sub-fossil chronologies. This AD chronology was based on modern, historic, and archaeologic timbers.

Work on these two units of chronology has been proceeding in parallel since the early 1970's. The two units will be complete when the chronology is consolidated for the first millennium BC. Currently, the absolute Belfast chronology extends from the present to 13 BC (Baillie 1980; 1982).

In this issue high-precision calibration results are presented for most of the last six millennia (Pearson and Baillie, 1983; Pearson, Pilcher, and Baillie, 1983). Oak timber was used for all the calibrations. We aim to establish the credibility of these chronologies and to indicate the limitations and difficulties of constructing a long oak chronology. Compared with the very long-lived bristlecone pines used to construct a 7104-year chronology (Ferguson, 1969), and also used, to check the most recent five millennia (LaMarche and Harlan, 1973) the problems associated with the construction of a similarly long chronology using a species such as oak are quite different. The short age span of individual trees means that many more overlapping patterns are needed and problems associated with short overlaps become critical. On the other hand oak does not normally show missing or double rings.

METHODOLOGY

Our approach has been to process groups of individual ring patterns into more robust, replicated, site units which represent the chronology building blocks. We do this because by selecting groups of timbers that occur together, there is a greater probability of finding cross-dating between the individuals. Also, mean chronologies tend to improve the common signal by cancelling some of the random noise associated with individual ring patterns.

All cross-dating between ring patterns has been visual and statistical. The Belfast CROS program (Baillie and Pilcher, 1973) was used as standard, and only matches that were visually acceptable and produced 't' values well in excess of 3.0 were accepted. More important from the point of view of overall chronology integrity is insistence on replication. In dendrochronology, replication comes at three levels: 1) Cross-dating of individuals, 2) cross-dating of chronologies, 3) Tertiary replication, which is available in Europe in the parallel oak chronologies produced by independent workers in Ireland and Germany (Becker and Schmidt, 1982; Schmidt and Schwabedissen,1982). Constant replication yields chronologies that stand up well to independent verification.

It is necessary at this stage to examine one particular problem facing a dendrochronologist seeking to build or extend a chronology involving many short lived timbers. Let us assume that there are two chronologies placed approximately end to end on the basis of non-tree-ring evidence and the dendrochronologist can find only a low correlation associated with a short overlap. The true situation could be either a) a real gap exists between the chronologies, b) the chronologies lie exactly end to end, or c) a short overlap exists (a short overlap is likely to be just as difficult to identify as a non-overlap).

The dendrochronologist faces the dilemma of not being able to separate c) where the match is genuine from a) where in fact no significant overlap exists and any possible 'match' is simply the highest random correlation resulting from comparison of the two chronologies. In order to avoid errors in such situations secondary and tertiary levels of replication are required.

VALIDATION OF THE BELFAST CHRONOLOGIES

It is now desirable to justify the chronologies that were used for calibration. The three principal sections of chronology at Belfast are the absolute chronology from the present to 13 BC (Baillie, 1980, 1982), the Garry Bog 2 chronology spanning from the 2nd to the 10th centuries BC, and the recently extended Belfast 'Long' chronology (Pilcher and Baillie, 1978) now spanning the 10th to the 53rd century BC.

THE AD CHRONOLOGY. The Belfast chronology back to 13 BC is made up of multiple site chronologies and cannot be separated from other chronologies of Scotland, Ireland, and England with which it cross-matches and by which it is replicated. Thus an overall British Isles chronology complex exists which is independent and precisely correct. As a final check, various English chronologies, within the British Isles complex have been dated to precisely the same year against the independent German chronologies. Examples of these stepwise correlations are shown in Fig 1, which illustrate the tertiary level of replication.

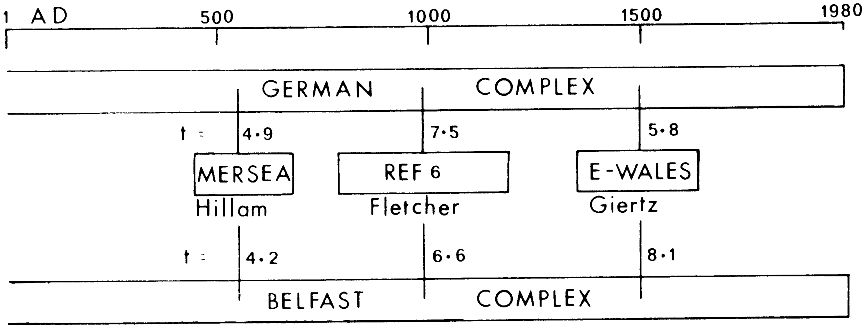

Fig 1. Tertiary replication of the German and Irish chronology complexes via England. For details see Baillie (1982).

THE BC ERA: THE LONG CHRONOLOGY - GB2 LINK. Substantial sections of sub-fossil chronology were completed by the late 1970's including the chronology of 2990 years placed approximately between 1000 and 4000 BC, (now extended to 5300 BC) and the Garry Bog 2 chronology of 719 years, dated to the first millennium BC. No cross-dating could be found between the ends of the chronologies. Recently, two new strands of evidence were obtained, the first of these relates to the high-precision ^{14}C analysis of samples from GB2. Both the long chronology and GB2 were "wiggle" matched against the bristlecone-pine results derived by Suess (1978). The exercise suggests that the long chronology spans 5300 to 940 BC (± 20) while GB2 spans 940 to 220 BC (± 20). The second innovation involves the chance discovery of a new group of sub-fossil oaks from Swan Carr near Durham (northern England). An initial collection of 20 samples from the site yielded a 750-year chronology, falling broadly within the first millennium BC. Comparison of this Swan Carr chronology with GB2 yielded an excellent agreement ($t = 6.0$). The oldest portion of the chronology extended the GB2 chronology back 208 years and suggested that a significant overlap, potentially of the order of two centuries should exist with the long chronology. Unfortunately, any match must be between timbers from northern Ireland and north eastern England. Is matching to be expected? Since Swan Carr and GB2 show good agreement over more than 500 years of overlap it is not unreasonable to expect at least some agreement between Swan Carr and the end of the long chronology. In practice a significant match is found with the final year of the long chronology equivalent to year 207 of the Swan Carr chronology ($t = 4.8$) (Fig 2). (If this is correct the long chronology and GB2 were separated in real time by a single year). To seek some replication for this match, the long chronology was divided into its constituent site units, ie, GB1 and Ballymacombs More. A consistent match is found with the Swan Carr chronology at this position $t = 4.7$ (cf GB1) and $t = 3.6$ (cf BMcC). No other consistent match exists. It is interesting that this match occurs within the likely time period specified by the high-precision "wiggle" matching (Pearson, Pilcher and Baillie, 1983). If this tentative match can be further replicated it will ensure that the Belfast calibration for the BC period is made on a continuous chronology. Recently further confirmation of this link has been obtained by comparison with chronologies for N Germany.

THE BC ERA: INTEGRITY OF THE LONG CHRONOLOGY. At this critical juncture in both the dendrochronologic and the high-precision debate, the existing long chronology (Pilcher, et al 1977) should be re-examined. Since that time, replication has become more formalized; normally, secondary and, preferably, tertiary replication is now sought for all sections of chronology. The site units of which the Belfast Long chronology is composed (Fig 3) show two points where secondary replication is not available. These occur ca 1900 BC where only the Garry Bog site chronology is represented and at ca 2550 BC. If problems of

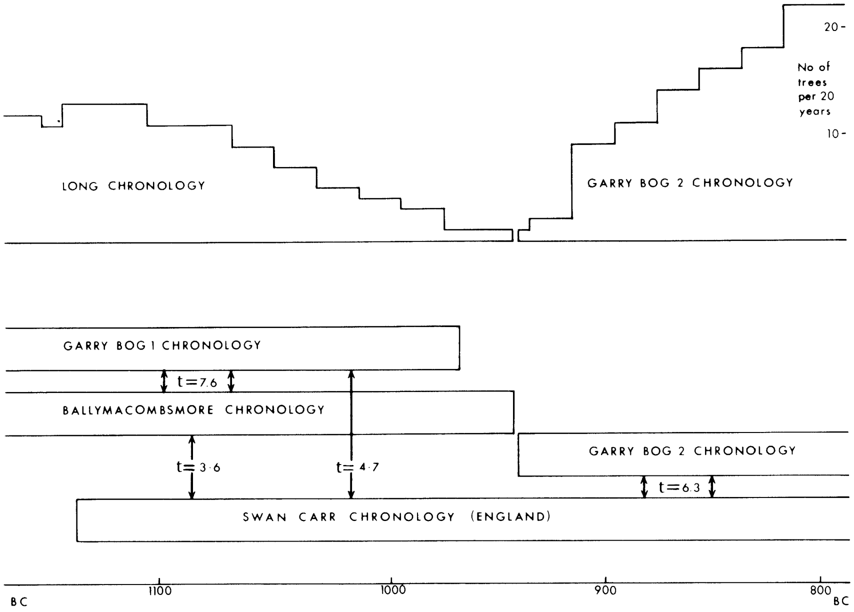

Fig 2. Possible matching position between the Belfast Long chronology and the Swan Carr/Garry Bog 2 chronology. This tentative link requires further replication but is consistent with the ^{14}C information.

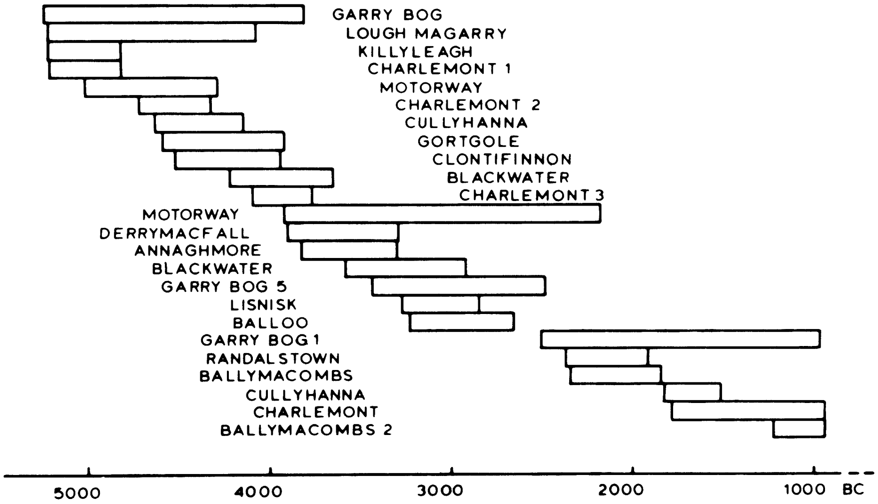

Fig 3. Site units included in the Belfast Long chronology. Only two points lack secondary replication, (ca 1900 and 2500 BC).

the type discussed above were to affect the Long chronology it is at these points that the chronology would be vulnerable. Around 1900 BC, the Garry Bog chronology, although it is only a single site chronology, is so well replicated internally with many trees of over 300 years in length that it need not be considered here. This leaves only one vulnerable point in the Long Chronology. At circa 2550 BC the Motorway chronology relies on a single ring pattern QUB 1546. This has to be the weakest point in the Belfast Chronology.

THE 1546 LINK. Figure 4 visualizes the 1546 situation. Solid replicated blocks of ring patterns are available in an essentially "end to end" mode. Had tree 1546 not been acquired a gap would undoubtedly have occurred in the Long chronology at this point. Thus, is 1546 an adequate link across this gap? The relationship between 1546 and the younger group of the ring patterns is firm, supported by individual 't' values of 6.1 and 7.3 and a value of 't' 7.2 when compared with the mean of the four trees. Thus, the weakest point in the whole Long chronology complex depends on the relationship between 1546 and the four older ring patterns. The evidence in Figure 4 is self-explanatory. Each of the individual ring patterns replicates the match with 1546 and, in this case, the mean of the four ring patterns gives 't' = 6.3. The correlation seems strong.

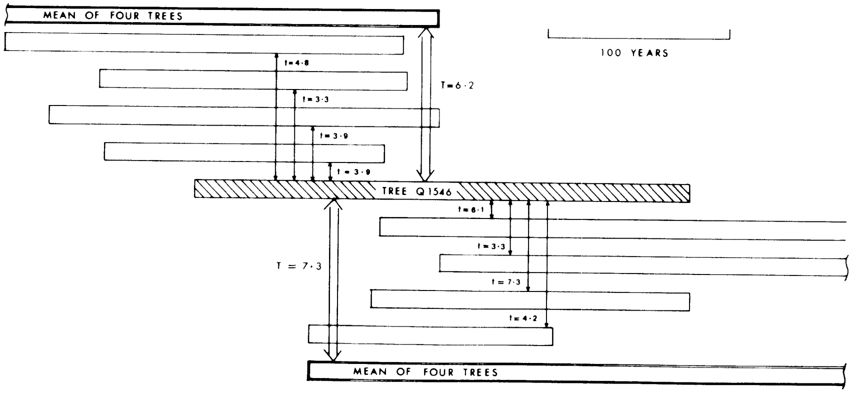

Fig 4. Weakest link in the Belfast Long chronology. Tree QUB1546 is the only link between two well-replicated blocks of chronology. The diagram shows that consistent primary replication is achieved at both sides of this link. Had this tree not been found, the chronology would still be in two parts.

CONCLUSION

Confirming evidence has been presented for the internal integrity of the two main sections of chronology so far constructed at Belfast. If the various correlations supporting the Swan Carr/Long chronology link are borne out by further replication, it would appear that a continuous chronology now exists from ca 200 BC to around 5300 BC. With recent advances in German sub-fossil and prehistoric dendrochronology, as well as Roman advances in England, it is only a matter of time before the entire chronology complex is precisely established. This consolidation will make the tree-ring axis of the high-precision calibration absolute.

ACKNOWLEDGEMENTS

The authors wish to express their gratitude to all those who have contributed to the acquisition and processing of the sub-fossil oaks, in particular, J Hillam, E Halliday, and D Brown. The tree-ring work at Belfast has been generously supported by grants from the Science and Engineering Research Council.

REFERENCES

Baillie, M G L, 1980, Dendrochronology - the Irish view: Current Archaeol, v 7, no 2, p 61 - 63.

Baillie, M G L, 1982, Tree-ring dating and archaeology: London, Croom-Helm, pp 274.

Baillie, M G L and Pilcher, J R, 1973. A simple cross-dating program for tree-ring research: Tree-ring Bulletin, v 33, p 7 - 14.

Becker, B and Schmidt, B, 1982, Verlangerung der Mitteleuropaischen Eichenjahrringchronologie in das Zweite Vorchristliche Jahrtausand: Archaol Korrespondenzblatt, v 12, p 101 - 106.

Ferguson, C W, 1969, A 7104 year annual tree-ring chronology for bristlecone pine for the White Mountains of California: Tree-Ring Bull, v 29, p 3 - 29.

LaMarche, V C Jr and Harlan, T P, 1973 Accuracy of tree-ring dating of bristlecone pine for calibration of the radiocarbon timescale: Jour Geophys Research, v 78, p 8849 - 8859.

Pearson, G W and Baillie, M G L, 1983, High-precision ^{14}C measurement of Irish oaks to show the natural atmospheric ^{14}C variations of the AD time scale, in Stuiver, Minze and Kra, Renee, eds, Internatl radiocarbon conf, 11th, Proc: Radiocarbon, v 25.

Pearson, G W, Pilcher, J R, and Baillie, M G L, 1983, High-precision ^{14}C measurement of Irish oaks to show the natural ^{14}C variations from 200 BC to 4000 BC, in Stuiver, Minze and Kra, Renee, eds, Internatl radiocarbon conf, 11th, Proc: Radiocarbon, v 25.

Pilcher, J R, Hillam, J, Baillie, M G L, and Pearson, G W, 1977, A long sub-fossil tree-ring chronology from the north of Ireland: New Phytologist, v 79, p 713 - 729.

Pilcher, J R and Baillie, M G L, 1978, Implications of a European radiocarbon calibration: Antiquity, v 52, p 217 - 222.

Schmidt, B and Schwabedissen, H, 1982, Ausbau des Mitteleuropaischen Eichenjahrringkalenders bis in Neolithische Zeit: Archaol Korrespondenzblatt v 12, p 107 - 108.

Suess, H E, 1978, La Jolla measurements of radiocarbon in tree-ring dated wood: Radiocarbon, v 20, p 1 - 18.

[Radiocarbon, Vol 25, No. 2, 1983, P 179-186]

HIGH-PRECISION ^{14}C MEASUREMENT OF IRISH OAKS TO SHOW THE NATURAL ^{14}C VARIATIONS FROM 200 BC to 4000 BC

G W PEARSON, J R PILCHER, and M G L BAILLIE

Palaeoecology Centre, The Queen's University of Belfast

Northern Ireland

ABSTRACT. Bi-decade samples of dendrochronologically matched Irish Oak, measured with a precision of ca ± 20 years, covering the period 200 to 4000 BC are presented. The data are compared with the published data of Suess, de Jong, and Mook to provide a general calibration of the ^{14}C time scale for this period. Although the dendrochronologic sequences presented are not absolutely tied to present, the best fit (based on ^{14}C evidence) of the Belfast data to absolute chronologies, the error and evidence associated with such positioning is given. The intervals chosen for analysis were 20 years, reducing slightly the resolution of short-term variations when compared to 10-year intervals, which are sometimes measured. However, this calibration would suffice for most scientific purposes and certainly for the calendrical conversion of ^{14}C dates derived from archaeologic samples.

INTRODUCTION

High-precision measurement of European oak can now provide a ^{14}C time-scale calibration from ca 300 to 4000 BC. De Jong, Mook, and Becker (1979) published some 700 years of calibration which was wiggle-matched to the bristlecone-pine chronology of Suess (1978) to give a zero date for the German Neolithic chronology of 4032 BC.

The Belfast laboratory has now made high-precision measurements ($\sigma = \pm 17$ years standard deviation including all errors on corrections) (Pearson, 1979; 1980) of some bi-decade /decade samples of Irish oak covering a time period of some 5700 years; 3700 years in the BC period overlapping the calibration published by de Jong, Mook, and Becker, (1979). The AD ^{14}C measurements of Belfast and tree-ring standard on which the calibration is based appear in this volume (Pearson and Baillie, 1983). Full advantage was taken of technical improvements in counting systems with the large samples obtainable from British Isles oak chronology. The 300 dates, each measured for 300,000 counts, are calculated to have a realistic precision of ± 17 years and are statistically equivalent to 4800 average ^{14}C measurements to ± 68 years precision.

METHOD

Analysis was made essentially as described in Pearson (1979; 1980) and Pearson and Baillie (1983). Because the system was for high-precision measurement, care was taken to investigate all likely sources of error; many factors were continuously monitored for the last seven years to assist in evaluating the accuracy of measurement. Some samples measured in 1975/76 carry a higher precision of ca ± 20 years to allow for the increased uncertainty of errors associated with weighing due to the use of plastic vial caps, the weight of which is variable with temperature and humidity (Pearson, 1979).

VALIDITY AND ACCEPTABILITY OF CALIBRATION CURVES

A calibration should have two meaningful axes. For the BC period the choice has been limited to either low-precision ^{14}C measurement associated with an assumed absolute bristlecone pine calibration. In the past, neither of these alternatives have offered an ideal calibration curve, but recent developments in European dendrochronology and the high-precision ^{14}C measurement of a long Irish oak series now make the estimated error on the calendrical fixing of the dendro-age axis small, probably < 20 years.

Baillie, Pilcher, and Pearson (1983) show a preliminary dendrochronologic match which fixes the position of the two floating Irish oak series (fig 1) in relation to each other. If this long floating sequence can soon be tied to the present, the high-precision measurement of European oak would be completely valid for ^{14}C time-scale calibration and, once independently duplicated, it would probably be universally acceptable.

CALENDRICAL FIXING OF IRISH OAK DENDRO-AGE BC BY ^{14}C MEASUREMENTS

de Jong, Mook and Becker (1979) showed that a calendrical fix can be obtained for the German chronology by wiggle matching in a comparison between German oak and bristlecone-pine. The technique consists of constructing cubic spline functions through both sets of data using the Reinsch algorithm (Reinsch, 1967). The area under the curves are compared for a fixed number of years and the minimum difference in area is found by moving one curve incremently over the other. Such a plot gave a minimum value and, hence, a fixing for the zero point

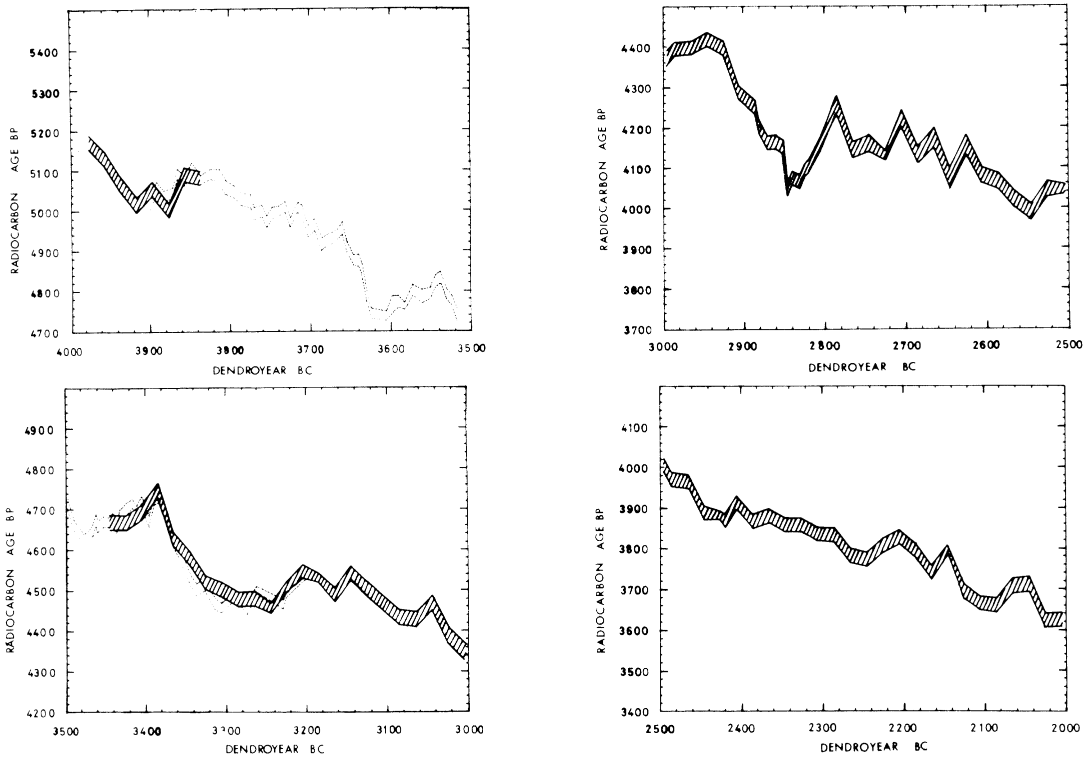

Fig 1A Bi-decade/decade interval measurements of Irish oak. Shaded area is ± 1σ error band. Dotted lines show data of de Jong, Mook, and Becker (1979), de Jong (1981).

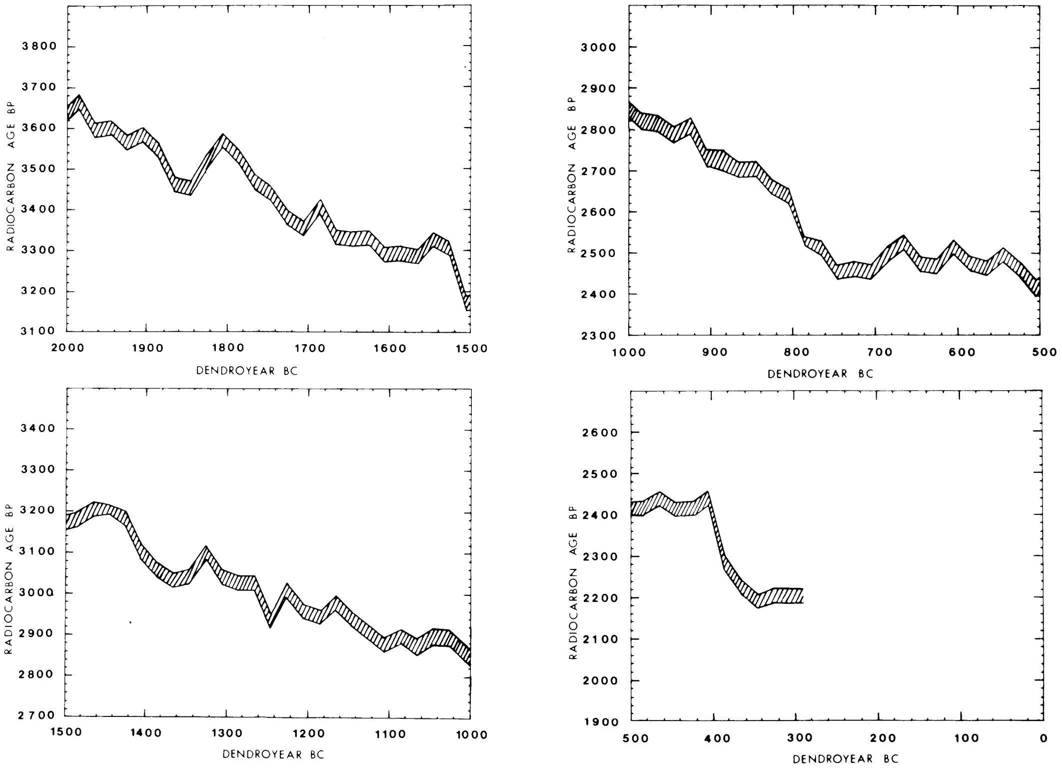

Fig 1B Bi-decade/decade interval measurements of Irish oak. Shaded area is ± 1σ error band.

of the South German Neolithic chronology of 4032 BC (de Jong, ms). A similar technique was used by Kruse et al (1980) to fix the same zero point using the independent ^{14}C measurement of German oak (Suess, 1978) compared to the same laboratory's measurement of bristlecone pine. The zero point for the South German Neolithic chronology from this method was identical to the most recent figure of 4032 BC (de Jong, ms).

Ca 1400 years of the Irish oak ^{14}C measurements were treated in a similar manner and gave a fixing for the 0 tree-ring year, 2075 ± 10 years BC (Pearson, 1980). If the Irish tree-ring year 0 is fixed at 2085 BC then the agreement with de Jong's published data over > 300 years is excellent (fig 1). Assuming the bristlecone-pine chronology is absolute then with agreement among three laboratories for fixing of the German and Irish oak floating chronologies, it is likely that the error in the calendrical fixing of the dendroage given by each chronology does not exceed ± 10 years.

A second floating Irish oak series, in which the zero point was provisionally fixed at 975 BC by wiggle matching, provided material for dating from ca 290 to 975 BC. The curve was visually wiggle matched to the bristlecone-pine measurements for the 1st millennium BC and to the German oak measurements, both of Suess. Unfortunately, the German dates end at ca 500 BC and overlap little, but are significant because of the variations in the ^{14}C concentration for that period. The end of this floating series at 975 BC has now been extended (Baillie, Pilcher, and Pearson 1983) and material that overlaps the long chronology of Irish oak dating from 900-400 BC is being measured at present. The provisional ^{14}C measurements agree sufficiently for the dendrochronologically fixed overlap to be considered correct within a possible variation of ± 10 years. If the above evidence is accepted for fixing the floating sequences, then the main weakness in European high-precision time-scale calibration for the BC period is removed.

INTER-LABORATORY COMPARISON

Almost 2000 years of calibration has been compared between Belfast and Seattle laboratories (Pearson and Baillie 1983). The agreement, showing a bias of 3 ± 5 years is excellent. (Seattle data (Stuiver, 1982) can only be read to the nearest 5 years).

Results of several inter-laboratory studies conducted by the Belfast laboratory are discussed in Pearson and Baillie (1983). Also five identical wood samples of different bi-decades were measured by the Belfast and Groningen laboratories; the results show a mean bias of ca 20 years, Belfast results being slightly older. However, the bias is less between the Belfast and Groningen laboratories for the overlap period in the 4th millennium BC (fig 1) where the general agreement is compatible with the error limits quoted.

CALIBRATION CURVES

There is probably no individual calibration curve that would suffice for all ^{14}C date "conversion" since so many variables exist, eg the error associated with the ^{14}C date, ie, the precision quoted that should include all inaccuracies, the error in the calibration, the choice of sample material and knowledge of the growth period. The minimum precision quoted on a date is a statistical combination of the Poisson statistical counting errors derived from the total counts accumulated from sample standard and background measurement. The precision quoted should be increased to allow for all uncertainty, "an error multiplier" (Stuiver, 1982; Scott, Baxter, and Aitchison, 1981) established by the laboratory from inter-laboratory comparison and internal replication of analysis. "Accurate dates", or those "being without bias" even if accompanied by a low-precision error are needed. If a date is accurate with an appropriately corrected and propogated precision, maximum benefit can be obtained from a high-precision calibration curve with reliable dendro-age bands for interpretation.

The error on the calibration, itself, is dependent upon the precision obtained on the individual data points forming the curve. Before any data is combined it is essential that no significant bias exists among the proposed independent calibration measurements in order to justify a statistical average of the data.

Choice of sample material is not often made by the laboratory except for isolation of specific components of submitted samples. A homogeneous sample that provides a mean date for interpretation, or dates an event, at least as accurately as the ^{14}C measurement allows, is preferred. Knowledge of the growth period of sample carbon is important for correct conversion. If the sample's growth period is less than the calibration interval, eg, single-year samples, such as seeds, nuts, straw, while dating a particular year of growth, it may carry an increased error if converted to a dendro-age using a decade or bi-decade calibration curve (Pearson and Baillie, 1983; Stuiver, 1982; de Jong, 1981 pers comm), because allowances have to be made for the smoothing function of the curve, particularly at points of inflection. Samples with growth period falling between 10 and 30 years are ideal for conversion to a calendar or dendro-age and may also justify high-precision measurement. Dating samples with growth period exceeding 100 years involves errors of averaging because of variation in the growth pattern. As it is extremely unlikely that an equal quantity of sample material is produced, this error is probably greater than the error in the calibration and may not warrant very high-precision measurement.

USE OF CALIBRATION

The conversion of a ^{14}C age to a dendro-age has been fully discussed (de Jong, ms ; Pearson and Baillie, 1983; Stuiver, 1982) and can be summarized as follows:
Evaluate the three errors discussed above

σ_1=The error on the date incorporating any allowance for inaccuracies outside of Poisson statistical counting error

σ_2=The error on the calibration, ie, half the average depth is ^{14}C years of the time period between the upper and lower error limits (normally ± 17 years)

σ_3=Any allowance for samples of short growth period, it is recommended that 15 years is used for sample year's growth falling to zero as the growth period approaches 20 years.
The corrected error the date σ_0 can be calculated from

$$\sigma_0 = \sqrt{\sigma_1^2 + \sigma_2^2 + \sigma_3^2}$$

To convert the ^{14}C age to dendro-age, draw a horizontal line across parallel to the X axis at the calculated date error limits and project the intercept with the calibration to the X axis; all dendro-ages falling between the upper and lower intervals of the calibration curve are valid calendar ages for the converted date. The dendro-age band varies considerably for ^{14}C dates measured to the same precision, giving rise to multiple band widths in some cases and, in other cases, a reduction of the error in dendroyears to that quoted in ^{14}C years.

CONCLUSION

The ^{14}C measurements presented here, together with those of Pearson and Baillie (1983) Stuiver (1982), and de Jong, Mook, and Becker (1979) provide a 6000-year high-precision curve for the conversion of ^{14}C dates. The curve shows significant repetitive detail of ca 150 years' periodicity although the amplitude varies considerably. Good agreement exists among the Belfast, Seattle, and Groningen laboratories for the periods compared and the possibility of an absolute dendrochronologic axis for the last 8000 years looks very promising.

With continued effort, a full 8000-year high-precision calibration should be possible within the next three years.

ACKNOWLEDGMENTS

G W Pearson would like to thank all members past and present of the ^{14}C laboratory who participated in this research. Particular thanks are given to F Qua for her support and complete dedication to this project over many years and to Y McCartney and E Glass who were responsible for the routine analysis of samples. Many additional hours of hard work were given freely by the above members of staff and also by our secretary, J Brown. Thanks are also given to the SERC for a grant to G W Pearson to carry out this research.

REFERENCES

Baillie, M G L, Pilcher, J R, and Pearson, G W, 1983, Dendrochronology at Belfast as a background to high-precision calibration, in Stuiver, Minze and Kra, Renee, eds, Internatl radiocarbon conf, 11th Proc: Radiocarbon, v 25.

de Jong, A F M, (ms) 1981 Natural ^{14}C variations: Unpub Phd dissert, University Groningen.

de Jong, A F M, Mook, W G and Becker, B 1979, Confirmation of the Suess wiggles: 3200-3700 BC: Nature, v 280 p 48-49.

Kruse, H H, Linick, T W, Suess, H E and Becker, B, 1980, Computer-matched radiocarbon dates of floating tree-ring series, in Stuiver, Minze and Kra, Renee, eds, Internatl radiocarbon conf, 10th Proc: Radiocarbon v 22, no 2, p 260-266.

Pearson, G W, 1979, Precise ^{14}C measurement by liquid scintillation counting: Radiocarbon, v 21, p 1-21.

Pearson, G W, 1980, High precision radiocarbon dating by liquid scintillation counting applied to radiocarbon timescale calibration: in Stuiver, Minze, and Kra, Renee, eds, Internatl radiocarbon conf, 10th Proc: Radiocarbon, v 25.

Reinsch, C H, 1967, Smoothing by spline functions: Numerische Mathematik, v 10, p 177-183.

Scott, E M, Baxter, M S, and Aitchison, T C, in press, ^{14}C dating reproducibility: Evidence from a combined experimental and statistical programme, in Internatl symposium on ^{14}C and archaeology, 1st, Proc: Groningen, 1981, in press.

Stuiver, Minze, 1982, A high-precision calibration of the AD radiocarbon timescale: Radiocarbon, v 24, p 1-26

Suess, H E, 1978, La Jolla measurements of radiocarbon in tree-ring dated wood: Radiocarbon, v 20, p 1-18.

[Radiocarbon, Vol 25, No. 2, 1983, P 187-196]

HIGH-PRECISION ^{14}C MEASUREMENT OF IRISH OAKS TO SHOW THE NATURAL ATMOSPHERIC ^{14}C VARIATIONS OF THE AD TIME PERIOD

G W PEARSON and M G L BAILLIE

Palaeoecology Centre, The Queen's University of Belfast

Northern Ireland

ABSTRACT. The high-precision ^{14}C measurement of bi-decade and decade samples of Irish Oak for the time period AD 50 to 1830 is presented. The samples were taken from dendrochronologically dated Irish Oak providing an absolute chronology for this period. While the natural atmospheric ^{14}C concentration shows cyclic deviations from a constant value, the amplitudes of such deviations vary considerably. Repeated measurement and interlaboratory checks justify a claim to accuracy in the data given. Comparison of a large number of data sets between Belfast and Seattle show that the different techniques of scintillation counting of $^{14}C_6H_6$ and gas counting of $^{14}CO_2$ derived from different wood species grown in different continents give no significant bias. Thus, it is justifiable to use this data set as a high-precision calibration curve for the AD period. Over most of this period bi-decade samples were measured giving a slightly reduced resolution of short-term variation when compared to the measurement of decade intervals; however, any difference is not apparent when such curves are compared. It is of much greater importance that a comparison of data sets is without bias if a combined calibration curve is to have sufficient integrity for general use. Averaging the data from Belfast and Seattle would improve the validity of such an AD ^{14}C calibration curve since it would tend to smooth out slight local variations and become internationally more acceptable.

INTRODUCTION

Since the early 1970's G W Pearson has been responsible for the ^{14}C dating laboratory and M G L Baillie for the dendrochronology of the AD era. Over the last few years improvement of technique has led to high-precision ^{14}C measurement. When this improvement is applied to the measurement of tree rings the fine detail of variation in the atmospheric ^{14}C concentration is exposed (Bruns, Munnich, and Becker, 1980; de Jong, Mook, and Becker, 1979; Pearson, Pilcher, and Baillie, 1983; Stuiver, 1982). ^{14}C measurement in the Belfast laboratory was carried out on dendrochronologically dated Irish oak divided to give decade or bi-decade samples of contiguous growth rings. The Irish oak chronology is absolute over the period presented and together with the ^{14}C measurements will provide a high-precision timescale calibration. For any calibration to have integrity it must carry appropriate error bands that are shown to be realistic. All parameters likely to give rise to errors must be investigated, corrections derived and their uncertainty included in the final error estimate (Pearson, 1979; 1980).

DENDROCHRONOLOGY

During the construction of the Belfast chronology every effort was made to ensure that the overlaps between successive ring patterns were replicated to a degree at which the chronology could stand independently (Baillie, 1973; 1977; 1982). In the final analysis it is useful to seek further and preferably independent support for the chronologies. Such support is available in Europe in a series of German chronologies, by comparison with which it is possible to demonstrate the integrity of the complex of Irish and Scottish chronologies.

The comparisons are step-wise and involve dating English chronologies against both the Irish and German chronologies. Such dating exercises were made for the later medieval, medieval, and early medieval periods and the consistency of these matches between the independent Irish and German chronologies removes any doubt about the placement of the chronologies in time (Baillie, 1982; Baillie, Pilcher, and Pearson, 1983).

^{14}C MEASUREMENT

The method used for the ^{14}C measurement of the samples presented in this paper was described in Pearson et al (1977; Pearson 1979; 1980). The system has been operative for measuring "calibration samples" since 1975. Quality controls were kept since the method was established involving the continuous monitoring of some 12 counting parameters additional to the measurement of samples, oxalic acid reference standard, and background. More than 60,000 parameter measurements were graphically displayed as a continuous quality control and used to determine instrument reliability over this whole period. Variation in overall gain during the 7 years of operation was kept within a range of ± 4½% from the balance point operating position. Pearson (1979) showed a change in gain of ± 4½% is equivalent to a change in ^{14}C efficiency of ca 0.03% which is further decreased by a correction based on an external source channels ratio measurement. Each sample was measured for sufficient time to accumulate at least 300,000 counts, ie, better than ± 1.8°/oo (≈ ± 14 years). The errors associated with the oxalic-acid reference standard and background measurement is 0.05% and 0.003 counts per minute, respectively. The additional errors associated with applied corrections are propogated in Pearson (1979; 1980) giving an overall error of approx ± 2.1°/oo, ie ca ± 17 years. All samples including those previously published (Pearson et al, 1977; Pearson, 1980) were recalculated using the most accurate information presently available before being incorporated in this series of measurements.

VALIDITY AND ACCEPTABILITY OF CALIBRATION CURVES

Many factors should be considered before a calibration curve is universally acceptable; some of these are discussed by Stuiver (1982) and Pearson, Pilcher, and Baillie (1983). The accuracy of ^{14}C measurement is perhaps the most important single factor that is entirely dependent upon laboratory technique and method of operation. Comparing Belfast and Seattle data provides an opportunity to examine all these factors in detail - the technique, methods, species measured, and origin of sample material, all being completely different. Seattle measurements (Stuiver, 1982) were made on Pacific Northwest Douglas Fir and California Sequoia using a gas proportional counting system to measure CO_2 from sample cellulose. The Belfast data was obtained from the liquid scintillation counting of benzene synthesized from Irish oak sample carbon. The Belfast laboratory is at ground level and the Seattle laboratory underground.

Similar dendro-age decades were measured from the different species by the Belfast and Seattle laboratories for the time period AD 950 to 1270 (only three decades centered on 1185, 1205, and 1245 were omitted by Belfast due to insufficient material). The results are given in figure 1 (Seattle results were taken from Stuiver, 1982 from fig 2 and can only be calculated to the nearest five years). The agreement between these data sets indicates that continental differences and species variability is negligible. If it is accepted that variations outside of laboratory-induced errors are negligible, as our operation illustrates, then an averaging of such data will provide an international calibration curve, at least for the temperate parts of the northern hemisphere.

Comparison of the Seattle measurement with other calibration curves, namely La Jolla Bristlecone Pine (Suess, 1978) and Heidleberg German Oak (Bruns, Munnich, and Becker, 1980) were adequately discussed in Stuiver,(1982) and because the agreement between the Belfast and Seattle measurements is very close, a further analysis of the Belfast data against these calibration curves would contribute little additional information. The calibration proposed by Klein et al (1982) is illustrated with the combined averaged data of Pearson and Stuiver over bi-decade intervals in figure 2. Very little similarity exists between the two curves and even with the very wide band width of the Klein et al curve, the two band widths are completely separate over significant periods. Furthermore, a distinct bias over extensive periods exists where the two overlap, and would result in the converted dates giving quite a different range of calendar years depending on the particular curve used.

INTER-LABORATORY COMPARISON

The Belfast laboratory has participated in a number of inter-laboratory comparisons during the last 3-4 years. The Harwell/British Museum benzene measurement UK study (Otlet et al, 1980) showed the Belfast results (Pearson, 1980) to be within the errors quoted from the weighted mean value of all the participating laboratories. In 1979 the Belfast laboratory measured four samples of the new oxalic acid reference standard on behalf of the National Bureau of Standards, USA. Each sample was measured to a precision of better than ± 2‰ (± 16 years) and all were found to be within ± 5 years of the mean value obtained from the 9 participating laboratories (W D Mann, pers commun) showing a bias of less than 0.16‰, ie < 2 years.

The Belfast laboratory recently participated in the Glasgow inter-laboratory calibration project involving 20 ^{14}C laboratories (Scott, Baxter, and Aitchison, 1981). The measurement of eight identical wood samples supplied by A Hayworth Aberystwyth, was made by each of the participating laboratories and the results presented by Stenhouse and Baxter (ms, Proc: ^{14}C and Archaeology, Groningen 1981). All eight samples were measured by Belfast to a precision of ± 18-20 years and showed a mean bias of four years from the weighted average of all the results. However, the study suggested that the Belfast quoted error should be multiplied by 1.27 which would change our average quoted error ± 17 years to that of ± 21 years, but did not rule out the possibility that unity is still valid since the number of samples measured was small. The reproducibility of measurements in the Belfast laboratory indicates that 1.27 would be a maximum error multiplication factor. Internal duplication of analysis would be consistent with an error multiplier of unity.

In addition to the above inter-laboratory comparisons, especially with Seattle, the Belfast laboratory also measured 18 samples of Irish oak covering > 360 years over the period previously measured by de Jong and Mook (de Jong, Mook, and Becker 1979). These results agree with de Jong's measurements (Pearson, Pilcher, and Baillie, 1983) and show a bias of < 20 years. From the above comparisons and interlaboratory checks it seems reasonable that any bias on the results presented here is small in relation to the mean error quoted of ± 17 years.

DECADE OR BI-DECADE CALIBRATION

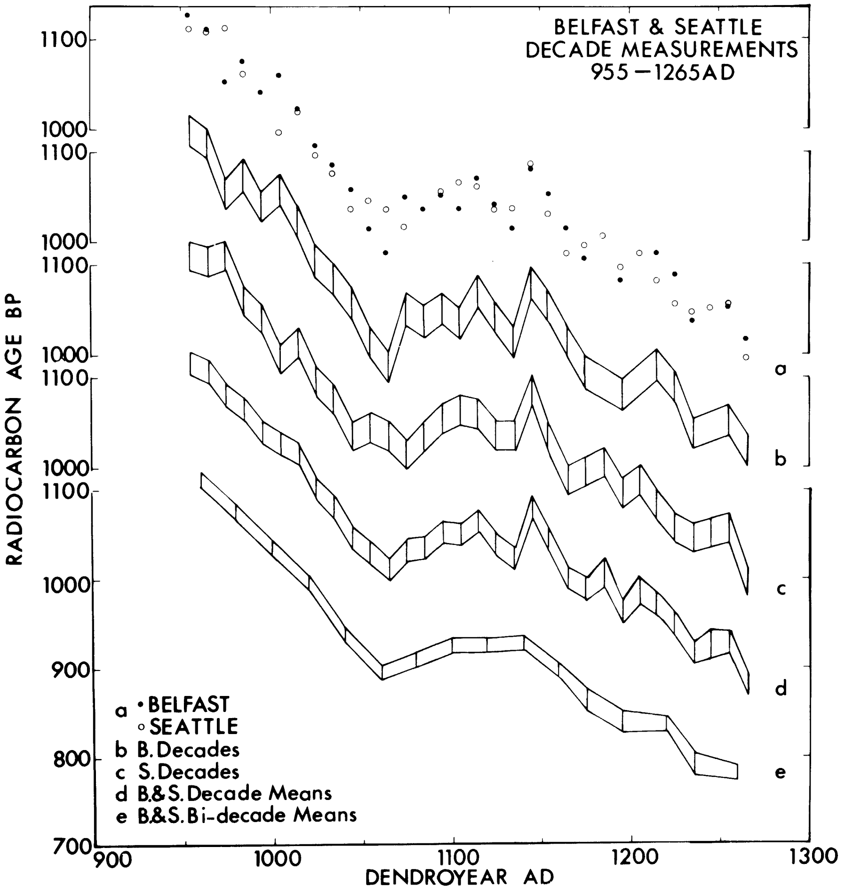

Fig 1 Comparison of data between Belfast and Seattle

Stuiver, 1982 concluded from his measurement of single-year samples over time periods AD 1510-1625 and AD 1820-1952 that the scatter of single-year data around the decade average trend is entirely compatible with the scatter expected solely from the quoted errors in the single-year measurements. He also concludes that any calibration made from decade measurements could be used by both single-year samples and decade samples to give equally accurate dendro-ages.

Figure 1b and c, show the decade measurements with 1σ band widths of Belfast and Seattle data, respectively. The decade measurement variations are also compatible to the normal statistical variations expected around a smooth trend curve. Many decade variations on one curve are canceled when averaged with the other laboratory's data, supporting the hypothesis of a smooth curve (fig 1, e). The decade at 1140 and 1150 dendro-age do show agreement on significant variations in the decade calibrations of each laboratory and are completely canceled out when averaged as bi-decade samples (fig 1, e). While these decade variations may be due to a random statistical coincidence like the decade variations that cancel each other out, this cannot be assumed. Some smoothing is bound to occur with any calibration that exceeds one year interval measurement; thus, for samples that have growth periods of less than the calibration interval, a corresponding increase in the calibration error will have to be made to allow for this smoothing factor. Although smoothing errors are significant for short-lived samples, unless the sample is measured to a high-precision, ie ca ± 20 years, the effect of such additional error is small.

The above arguments for a bi-decade calibration and additional error requirement for short-lived samples is supported by the successive averaging of 20 single-year measurements from the single-year series (Stuiver, 1982) and 4 of the 5-year separated annual growth rings given by de Jong (1982, pers commun).

TIME-SCALE CALIBRATION

The ^{14}C time-scale calibration curve AD 50-1840 is presented in figure 3, drawn from the high-precision measurement ($\sigma = \pm 17$ years which includes all correction errors) of some 74 bi-decade and 33 decade samples of Irish oak. Duplicate measurements are represented as mean values with appropriate reduction of precision. All ^{14}C ages were calculated using a 5568-year half-life and are measured directly against NBS oxalic acid reference standard in which zero in ^{14}C years BP is equal to the calendar year of AD 1950. If it is assumed that the dendro-age is without error, then the ^{14}C measurement will provide an accurate calendrical age conversion. Figure 2 shows the variation in calendar age band width and growth period > 20 years, when a comparison is made between the averaged Belfast and Seattle curve and the ± 20 year limits proposed by Klein et al (1932).

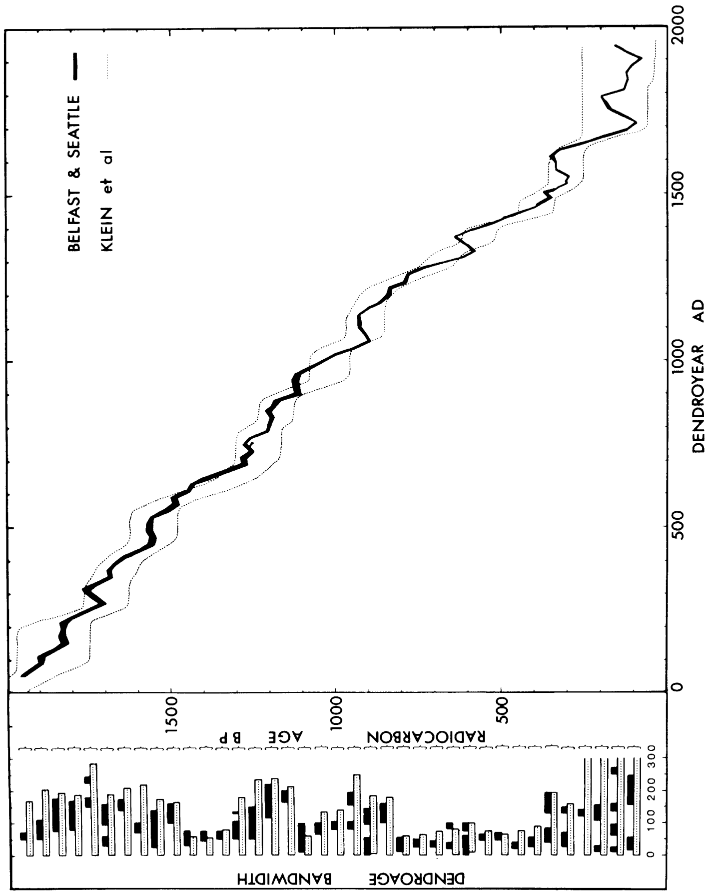

Fig 2 Comparison of combined Belfast and Seattle data (bi-decade intervals) with proposed curve of Klein et al (1932)

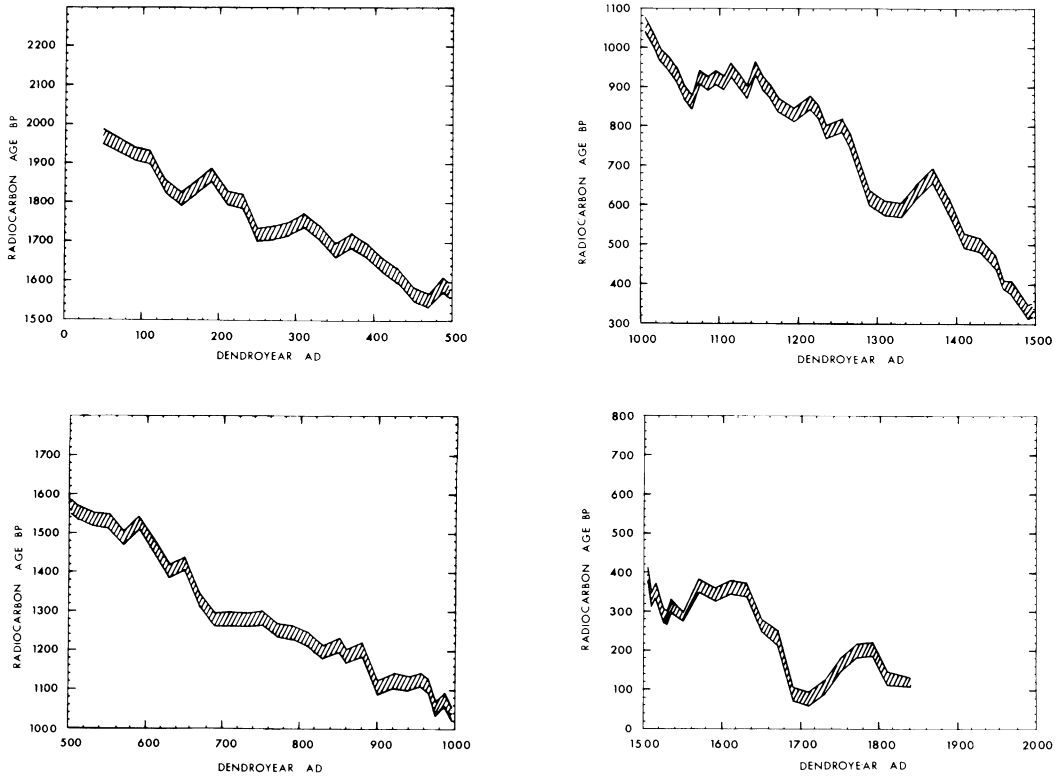

Fig 3 Bi-decade/decade interval measurements of Irish oak. Shaded area is ± 1σ error band.

CONVERSION OF ^{14}C AGE TO DENDRO-AGE

Details for conversion of ^{14}C age to dendro-age are given in Stuiver (1982) and Pearson, Pilcher, and Baillie (1983) and suffice for the calibration data presented here. For samples of short growth, an additional error should be added into the date error equation to compensate for the smoothing factor of bi-decade measurement. This value (σ_3) would be ca 15 years for a single-year growth, to zero for 20-years growth sample

$$\sigma_0 = \sqrt{\sigma_1^2 + \sigma_2^2 + \sigma_3^2}$$

where σ_0 = final error estimate, σ_1 = error on date,
σ_2 = error on calibration.

CONCLUSION

It has been shown that good agreement is possible between laboratories and that error estimates can be close to those quoted. A claim to accuracy can be made for the measurements presented in this paper. It is important for the acceptance of ^{14}C dating that the accuracy of routine dating is continuously assessed and improved.

ACKNOWLEDGMENTS

G W Pearson would like to thank all members of staff past and present of the ^{14}C laboratory who have participated in this research. Particular thanks are given to F Qua for the support and complete dedication to this project over many years, and to Y McCartney and E Glass who have been responsible for the routine analysis of samples. Many additional hours of hard work were given freely by the above members of staff and also our secretary, J Brown. Thanks are also given to the SERC for a grant to G W Pearson to carry out this research.

REFERENCES

Baillie, M G L, 1973, A recently developed Irish tree-ring Chronology: Tree-ring Bull 33, p 15-28.

___ 1977, The Belfast oak chronology to AD 1001: Tree-ring Bull 37, p 1-12.

___ 1982, Tree ring dating and archaeology: London, Croom-Helm.

Baillie, M G L, Pilcher, J R, and Pearson, G W, 1983 Dendrochronology at Belfast as a background to high-precision calibration, in Stuiver, Minze, and Kra, Renee, eds, Internatl radiocarbon conf, 11th Proc: Radiocarbon, v 25.

Bruns, M, Munnich, K O, and Becker, B, 1980, Natural radiocarbon variations from AD 200 to 800, in Stuiver, Minze, and Kra, Renee, eds, Internatl radiocarbon conf, 10th, Proc: Radiocarbon, v 22, no 2, p 273-377.

de Jong, A F M, Mook, W G, and Becker, B, 1979, Confirmation of Suess wiggles 3200-3700 BC: Nature, v 280, p 48-49.

Klein, J, Lerman, J C, Damon, P E, and Ralph, E K, 1982 , Calibration of radiocarbon dates: Tables based on the consensus data of the Workshop on Calibrating the Radiocarbon Time Scale: Radiocarbon, v 24, p 103-150.

Otlet, R L, Walker, A J, Hewson, A D, and Burleigh, Richard, 1980, ^{14}C Interlaboratory Comparison in the UK: Experiment design, preparation, and preliminary results, in Stuiver, Minze, and Kra, Renee, eds, Internatl radiocarbon conf, 10th Proc: Radiocarbon, v 23, no 3, p 936-946.

Pearson, G W, 1979, Precise ^{14}C measurement of liquid scintillation counting: Radiocarbon, v 21, p 1-21.

____ 1980, High-precision radiocarbon dating by liquid scintillation counting applied to radiocarbon time-scale calibration in Stuiver, Minze, and Kra, Renee, eds, Internatl radiocarbon conf, 10th Proc: Radiocarbon, v 22, no 2, p 337-345.

Pearson, G W, Pilcher, J R, and Baillie, M G L, (1983) High-precision ^{14}C measurement of Irish oaks to show the natural ^{14}C variations over the period 200 BC - 4000 BC, in Stuiver, Minze, and Kra, Renee, eds, Internatl radiocarbon conf, 11th Proc: Radiocarbon, v 25.

Pearson, G W, Pilcher, J R, Baillie, M G L, and Hillam, J, 1977, Absolute radiocarbon dating using a low altitude European tree-ring calibration: Nature, v 270, no 5632, p 25-28.

Scott, E M, Baxter, M S, and Aitchison, T C, in press, ^{14}C dating reproducibility. Evidence from a combined experimental and statistical programme, in Internatl symposium on ^{14}C and archaeology, 1st Proc: Groningen, 1981, in press.

Stuiver, Minze, 1982, A high-precision calibration of the AD radiocarbon timescale: Radiocarbon, v 24, p 1-26.

Suess, H E, 1978, La Jolla measurements of radiocarbon in tree-ring dated wood: Radiocarbon, v 20, p 1-18.

[Radiocarbon, Vol 25, No. 2, 1983, P 197-203]

THE LONG-TERM RADIOCARBON TREND OF THE ABSOLUTE GERMAN OAK TREE-RING CHRONOLOGY, 2800 TO 800 BC

BERND BECKER

Institut für Botanik 210, Universität Hohenheim
Postfach 700562, D-7000 Stuttgart 70, FRG

INTRODUCTION

The Hohenheim Tree-Ring Laboratory has extended the Holocene oak tree-ring chronology back to prehistoric times by analyses of subfossil tree trunks from gravel deposits along the rivers of central Europe. Hundreds of subfossil oaks can be collected each year because of widespread gravel quarrying. Despite this nearly continuous source of samples (at present, 2200 trees are analyzed), even within these deposits some limitations do exist in linking together a Holocene tree-ring sequence.

The main problem is the relatively short growth period of the Holocene valley oaks, reaching only 100 to 400 tree-rings. This requires a close temporal sequence of tree trunk deposits over thousands of years. However, while phases of increased flooding accumulated large numbers of eroded trees, there also have been periods of low fluvial activity, which left only few buried wood remains. Unfortunately, such a phase of reduced floodings occurred during the first millennium BC, a period from which wood samples from prehistoric settlement constructions, the other source of dendrochronology, are rarely found in southern Germany. A comprehensive study of Holocene riverine oak forests and their inter-relation with the fluvial regime will soon be published (Becker, in press).

These remarks explain why bridging of the remaining gaps in the extended floating Holocene oak chronologies became increasingly difficult. To overcome this problem, we have established an exchange of chronologies with Burkhard Schmidt at the Köln Tree-Ring Laboratory. This cooperation has closed one of the long-standing gaps in the Hohenheim master chronology by crossmatches of Roman and Pre-Roman oak series from northwest Germany, recently established by Schmidt in Köln (Becker and Schmidt, 1982). Recently collected subfossil oaks from the Danube River have bridged the next gap in our oak chronology, at 1500 BC. At its present stage, the absolute Hohenheim master is extended continuously back to the year 2804 BC.

REPLICATION OF THE GERMAN ABSOLUTE OAK MASTER CHRONOLOGY

The implications of this absolute tree-ring calendar for dendrochronologic dating of an increasing number of prehistoric lake dwellings as well as for calibration of the ^{14}C time scale demand a very careful presentation of the significance of the crossmatches within this sequence. This applies particularly at the points where there is little replication.

The present configuration of the Hohenheim oak chronology is given in figure 1 where all established south central European chronologies are listed, together with the resulting master curve, showing the minimum number of crossdated trees per century. This method shows up the parts of the dendrochronology where links are based on a low number of individual tree-ring curves.

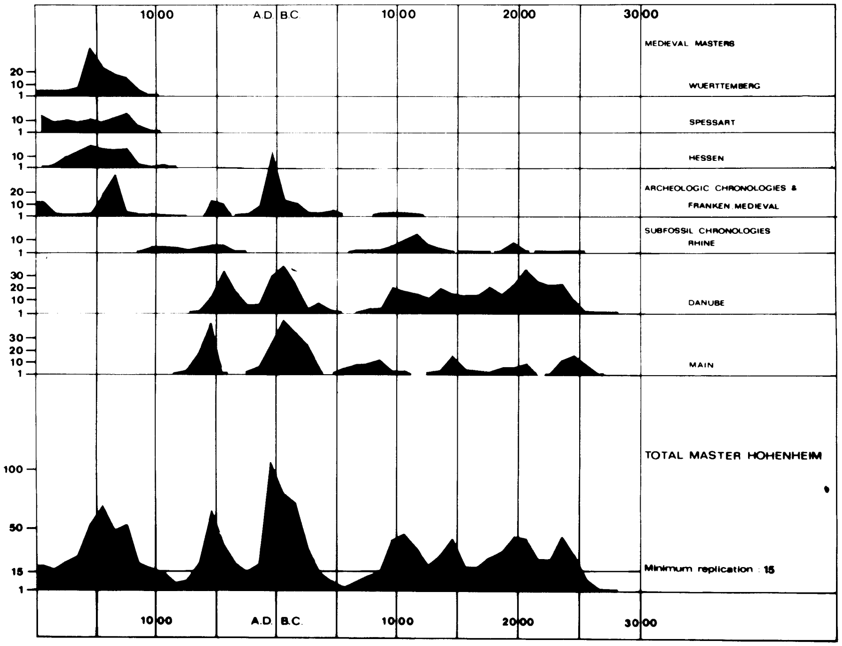

Fig 1. Replication of the south German absolute oak tree-ring chronology. Plotted are the <u>minimum replications</u> (per century) of the existing regional chronologies (upper part). These series are linked together to the absolute Hohenheim master reaching continuously back from the present to 2804 BC (lower part).

Comparison of all 18 independently established regional chronologies clearly demonstrates that only two periods in the first five millennia are replicated by a minimum number below 15 trees. The first occurs from AD 800 to 1000, the second, from 800 to 400 BC. Of these, the overlap between the Medieval chronologies (back to AD 744) and the Early Medieval sequences (Rhine River, AD 254 to 1162) is problem-free. This crossmatch covers 419 years and is additionally confirmed by a significant cross-correlation with the western German oak chronology developed by Hollstein (1980) in Trier (Becker, 1981).

The second critical link occurs between 600 to 400 BC. Our Pre-Roman series, which was the beginning of the absolute master before its recently achieved extension, starts at 546 BC. The earlier floating well-replicated Late Bronze Age masters end at 469 BC. The existing 87-year overlap was recognized by crossmatching the northwest German archaeologic site chronologies, mentioned above, and the earliest part of the western German chronology of Hollstein together with both Hohenheim series (Becker and Schmidt, 1982). These three independent masters have a significant overlap of at least 223 years.

The older section of the Hohenheim master, from 800 to 2500 BC, is replicated at every point by more than 15 trees. In addition, the chronology is represented by independent regional series of subfossil oaks from the Rhine, Main, and Danube valleys, together with various chronologies of prehistoric Swiss lake dwelling sites (Becker et al, 1979).

To summarize, there is only one period (600 to 400 BC) in the south central European oak chronology when linking of all the Hohenheim data is not independently replicated. For this portion, the linking of our series relies on crossmatches with tree-ring chronologies from neighboring regions.

THE LONG-TERM RADIOCARBON TREND OF THE OAK CHRONOLOGY

Several laboratories have studied the ^{14}C content of our oak sequences which include the absolutely-dated sections (Bruns, Münnich, and Becker, 1980) and the older floating series (Suess and Becker, 1977; Suess, 1978, 1980; deJong, Mook, and Becker, 1979; Bruns et al, in press; Rehin, 1982). In particular, Suess has analyzed the ^{14}C activity from earlier floating oak series which can now be crossdated to our absolute master. From this study, the first independent comparison can be made between the ^{14}C variations of European oak and the bristlecone-pine calibration.

The result is shown in figure 2 where the La Jolla oak data are plotted against the bristlecone-pine data for the period, 2800 to 700 BC. The graph points out an obvious long-term trend in European oak which is very similar to that of bristlecone pine of the southwest United States. In the oak, the first deviation of the ^{14}C ages from the appropriate dendro-dates becomes evident from 1000 to 1400 BC (the recently established overlap to the Bronze Age series, 1400 to 1600 BC, has not yet been analyzed).

Between 1550 and 1700 BC, the ^{14}C ages are too young by ca 100-150 years, increasing more or less steadily at 2200 BC to ca 250 years. During the third millennium BC, this difference reaches a maximum value of ca 600 calendar years. This

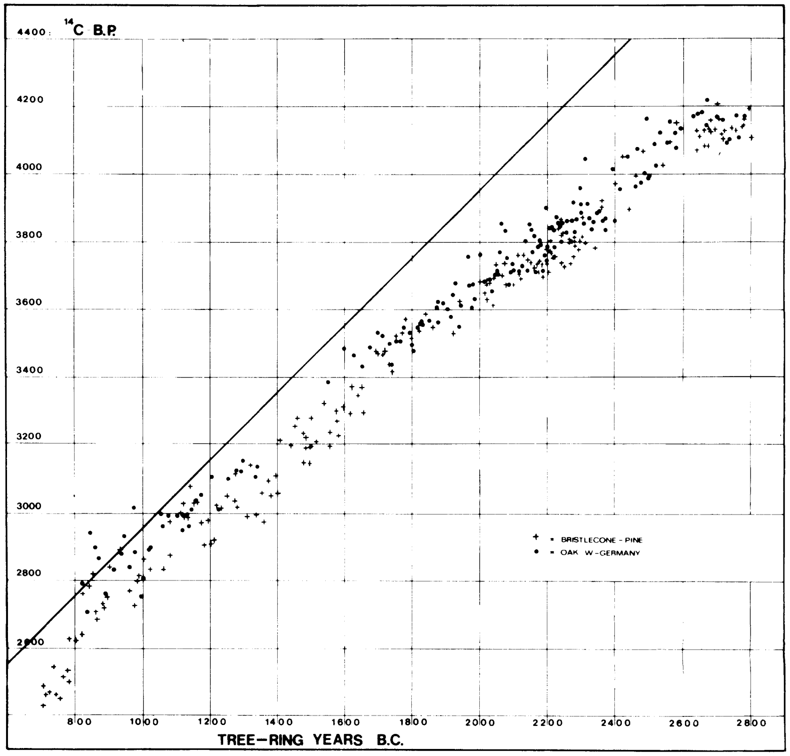

Fig 2. Comparison between the long-term ^{14}C variation of the bristlecone pine (crosses) and the German oak (dots) from 2800 to 700 BC, according to analyses of HE Suess, La Jolla (Suess, 1978). Within both series, a systematic long-term offset between the dendro-ages and the appropriate ^{14}C ages starts at ca 1200 BC and, during the 27th and 28th century BC, reaches a maximum value of ca 600 calendar years.

offset is almost the same as that observed in the La Jolla bristlecone-pine data for the same period.

Despite the general coincidence of increasing ^{14}C activity between bristlecone pine and German oak during the 2nd and 3rd millennia BC, a systematic offset occurs between the two series if one compares their medium-term variations. Wiggle matching of the earlier floating Late Bronze Age and Bronze Age masters of the bristlecone-pine calibration curve provided corrected zero-points of 1535 BC (dendro-age: 1462 BC) and 2871 BC (dendro-age: 2804 BC). This calibration placement had been based on a 300-year (Late Bronze Age series Donau 15 and Zug/Sumpf) and a 1250-year (Bronze Age master, Donau 3/10) measured tree-ring series and was statistically significant (Kruse et al, 1980). However, this calibration placement differs for both series from their dendro-dated zero-points by almost identical figures of 73 and 67 years, respectively.

If an error should exist within the Hohenheim dendrochronology, it very probably would not have occurred in the crossmatch between the Late Bronze Age and the Bronze Age series, since they both show the same offset as the bristlecone pine calibration curve. The German oak series 500 BC to present, on the other hand, is independently replicated by the significant cross-correlation with the western German master of Hollstein, as mentioned before. The only hypothetical mistake that could be considered is the link within the master between 600 and 400 BC. Nevertheless, it must be stressed that the crossmatches of the Trier, Köln, and Hohenheim series of that period are also significant as can be seen from the curves published by Becker and Schmidt (1982).

To check the offset between the German oak and the bristlecone pine wiggles definitively, the ^{14}C content of our sequence of the first millennium BC will be measured by Minze Stuiver in Seattle. Further conclusions relating to this offset should not be discussed until these results are available.

RADIOCARBON CALIBRATION OF THE GERMAN OAK CHRONOLOGIES, 2800 to 7600 BC

During the 11th International Radiocarbon Conference, a committee for high-precision calibration of tree-ring chronologies was formed. Therefore, it is relevant to include here an outline of the pre-existing calibrations of the older Holocene oak chronologies from Hohenheim.

Before 2800 BC, the south central European oak chronology consists of four large floating series. These have already been calibrated by conventional (La Jolla) and high-precision

(Heidelberg, Groningen) ^{14}C analyses. As shown in table 1, the older parts of the Hohenheim tree-ring chronology cover the period, 2600 to 7600 BC. It is evident that there are no major gaps remaining within the sequence.

TABLE 1. ^{14}C calibrated Holocene oak chronologies of the Hohenheim Laboratory

Chronology name	Ring-numbers	Calibrated age (BC)	Analyzed sections	Laboratory
Donau 7	1425	4058-2632	3970-3260	La Jolla
			3920-3220	Groningen
Donau 8	737	4850-4114	4420-4130	La Jolla
Main 6/13	1623	6515-4893	6450-5920	Heidelberg
			5960-5390	La Jolla
			5380-5020	Heidelberg
Main 4/11	846	7200-6355	7190-6370	Heidelberg
Main 9*	497	7600-7104*	7580-7190	Heidelberg

* Not calibrated

The earliest calibrated series (Main 4/11) extends beyond the beginning of the bristlecone-pine calibration curve (up to 7200 BC, Bruns et al, in press; Rhein, 1982). The Main 9 chronology must be even older. This can be derived from the comparison of the high-precision analyses of the Main 4/11 to the Main 9 series.

A further extension of the absolute master (starting at 2804 BC) is to be expected by the calibrated Neolithic master, Donau 7, which overlaps on its younger end (up to 2634 BC). In addition, this sequence, as well as the next older floating master, Donau 8, must already be covered by the four-millennia floating chronology from Northern Ireland. This chronology is calibrated to 5300-900 BC (Baillie, Pilcher, and Pearson, 1983).

The exchange of tree-ring data by Belfast, Köln, and Hohenheim and the projected intercalibration of the Holocene oak series from Northern Ireland and Germany should soon extend the European tree-ring standard further back into prehistory.

REFERENCES

Baillie, MGL, Pilcher, JR, and Pearson, GW, 1983, Dendrochronology at Belfast as a background to high-precision calibration, in Stuiver, M and Kra, RS, eds, Internatl ^{14}C conf, 11th, Proc: Radiocarbon, v 25.

Becker, B, 1981, Fällungsdaten römischer Bauhölzer anhand einer 2360- jährigen süddeutschen Eichen-Jahrring-chronologie: Fundberichte aus Baden Württemberg, v 6, p 369-386.

_________ in press, Dendrochronologie und Paläoökologie subfossiler Baumstämme aus Flußablagerungen. Ein Beitrag zur nacheiszeitlichen Auenentwicklung im südlichen Mitteleuropa: Mitt Komm fur Quartärforschung der Österr Akad der Wiss, in press.

Becker, B, Orcel, Chr, Egger, H, and Ruoff, U, 1979, Drei Beiträge zur Chronologie des Neolithikums in der Schweiz: Zeitschr Schweiz Archäol Kunstgesch, v 36, H 2, p 91-96.

Becker, B and Schmidt, B, 1982, Verlängerung der mitteleuropäischen Eichen-Jahrringchronologie in das zweite vorchristliche Jahrtausend (bis 1462 v Chr): Archäol Korrespondenzbl, v 12, p 101-106.

Bruns, M, Munnich, KO, and Becker, B, 1980, Natural radiocarbon variations from AD 200 to 800, in Stuiver, M and Kra, RS, eds, Internatl ^{14}C conf, 10th, Proc: Radiocarbon, v 22, no. 2, p 219-226.

Bruns, M, Rehin, M, Linik, TW, and Suess, HE, in press, The atmospheric carbon 14 level in the 7th millennium BC, in Mook, WG and Waterbolk, HT, eds, Conf on 14-C and Archaeology, 1st, Proc: Groningen, in press.

Hollstein, E, 1980, Mitteleuropäische Eichenchronologie; Trierer Grabungen Forschungen, v 11, 273 p, Mainz, Verlag Philipp von Zabern.

Kruse, HH, Linik, TW, Suess, HE, and Becker, B, 1980, Computer-matched radiocarbon dates of floating tree-ring series, in Stuiver, M and Kra, RS, eds, Internatl ^{14}C Conf, 10th , Proc: Radiocarbon, v 22, no. 2, p 260-266.

Rhein, M, ms, 1982, Schwankungen des atmosphärischen Kohlenstoff-14 Pegels im sechsten bis achten Jahrtausend v Chr: PhD dissert, Inst Umweltphysik, Univ Heidelberg, 62 p.

Suess, HE, 1978, La Jolla measurement of radiocarbon in tree-ring dated wood: Radiocarbon, v 20, p 1-18.

_________ 1980, Radiocarbon geophysics: Endeavour, v 4, p 113-117.

Suess, HE and Becker, B, 1977, Der Radiokarbongehalt von Jahrringproben aus postglazialen Eichenstämmen Mitteleuropas, in Frenzel, B, ed, Erdwiss Forschung: Wiesbaden, Steiner Verlag, v 12, p 156-170.

[Radiocarbon, Vol 25, No. 2, 1983 P 205-212]

RADIOCARBON ACTIVITY VARIATION IN DATED TREE RINGS GROWN IN MACKENZIE DELTA

C Y FAN*, CHEN TIE-MEI**, YUN SI-XUN**, AND DAI KAI-MEI†

ABSTRACT. Forty-five tree rings (1881-1925) were taken from a white spruce grown near Campbell River in Mackenzie Delta, Canada, for the measurement of ^{14}C activity variation. Because of the narrowness of the rings, 2 and sometimes 3 rings were combined to yield a total of 21 specimens. The ^{14}C content in these specimens was measured with a liquid scintillation-PM tube counter system of the History Department of Peking University. The data points exhibit a 10‰ variation, anti-correlated with sunspot numbers. The physical implication is discussed.

INTRODUCTION

Since Forbush (1954) discovered solar modulation of cosmic ray intensity, it has been assumed that there is a corresponding variation in the ^{14}C content in the earth's stratosphere. Lingenfelter and Ramaty (1970) calculated the production rates for 1953-1954 (solar activity minimum) and 1957-1958 (solar activity maximum) at various geomagnetic latitides; the difference between the average rates in these two periods was ca 22%. The question frequently asked was whether such a variation could cause a fluctuation in the ^{14}C concentration in the troposphere large enough to be measurable. Baxter and Walton (1971) reported an ∿ 30‰ $\Delta^{14}C$ variation from 1890-1950, and later, Baxter and Farmer (1973) reported a 10 to 20‰ variation from 1829-1865, both with an 11-year periodicity, anti-correlated with sunspot numbers. But the $\Delta^{14}C$ values in tree-ring samples from the same period measured by others (Broecker, Olson, and Bird, 1959; Cowan, Atluri, and Libby, 1965; Suess, 1965; Lerman, Mook, and Vogel, 1967; Damon, Long, and Wallick, 1973a; Tans, DeJong, and Mook, 1979; Burchuladze et al., 1980; Stuiver and Quay, 1980, 1981) do not show any large amplitude fluctuations, although some of them also exhibit 11-year periodicity. Since Baxter and Walton used grains grown in Scotland at latitudes ∿ 54°N, higher than that of most other sample locations, the disagreement may be due to

---

*Department of Physics, University of Arizona, Tucson
**Radiocarbon Laboratory, Archaeological Section, History Department, Peking University, Beijing, China
†Department of Physics, Nanjing University, Nanjing, China

the difference in latitudes as well as in the time and duration of photosynthetic assimilation of CO_2 by plants (Baxter and Farmer, 1973). Lerman, Mook, and Vogel (1970), in their thorough study of the variation of the ^{14}C content in the 19th- and 20th-century tree rings with geographic locations, found that, at 42°S latitude, contemporaneous tree rings contain $4.5 \pm 1‰$ less ^{14}C than those at 42°N latitude. Doubt persists as to whether the large amplitude reported by Baxter and Walton (1971) was partly real and partly due to a biased treatment of the measurements and selection of data (Damon, Long, and Wallick, 1973b). We describe here the results of our measurements of $\Delta^{14}C$ variation in 1881-1925 rings of a white spruce grown near Campbell River in Mackenzie Delta, Canada (68°N, 130°W). The data clearly exhibit a fluctuation with a periodicity of 11 years, anticorrelated with sunspot numbers. A plausible explanation is suggested.

SELECTION OF TREE RING SAMPLES

To study the possible latitudinal effect, we looked for trees from the utmost northerly region. We obtained two sections of dated white spruce from Dr ML Parker, Canadian Forestry Service, Vancouver; one of the sections contains 463 rings from AD 1510 to 1972. This sample enabled us to study the $\Delta^{14}C$ variation systematically over ca 40 solar cycles. We selected rings from AD 1881 to 1925 because 1) a number of existing $\Delta^{14}C$ measurements ca AD 1900 on tree rings from locations with a latitude spread from 32° to 63°N in the northern hemisphere can be compared with our result, 2) the AD 1908 ring permits re-examination of the anti-matter hypothesis of the Tunguska event (Cowan, Atluri, and Libby, 1965). The widths of the rings are narrow. Except for the AD 1925 ring, we had to combine 2 and sometimes 3 rings to yield enough carbon for one measurement. We obtained 22 samples but one (1917-1919) was contaminated by an accident.

EXPERIMENTAL METHOD

Measurements were made at the History Department of Peking University, using a liquid scintillation photomultiplier tube device. After being treated with routine HCl-NaOH-HCl procedure to remove resin, the samples, ca 10g each, were converted to CO_2 by burning and then to benzene by the following steps: $CO_2 \rightarrow CaC_2 \rightarrow C_2H_2 \rightarrow$ benzene. In the last step, $CrO_3 \cdot Al_2O_3 \cdot SiO_2$ was used as the catalyst.

For one measurement, 5cc synthesized benzene was used. For smaller samples, we added background benzene to make up 5cc so that all samples were measured under the same experimental conditions. The samples were then sealed in a low potassium glass vial. After storing for ten days to allow for radon decay, ^{14}C activity was counted with two GDB-52L photomultiplier tubes in coincidence. The system was shielded against cosmic ray secondaries by 5 to 10cm of lead and a special circuit for pulse height discrimination was used to reduce cross-talk between the two photomultipliers. The net count rate for a 5cc modern sample was 39cpm; the background was 6cpm.

Precaution was taken to reduce uncertainties. Reliability and precision of the measuring system were checked by repeated preparation and counting of a ^{14}C calibration standard. An overall precision, which was defined as the standard deviation, was better than 5‰, including a pure statistical uncertainty of ca 3‰. Every run of the measurements was statistically tested. For each sample, we measured ^{13}C/^{12}C for fractionation correction.

EXPERIMENTAL RESULTS

Table 1 is a list of 21 tree-ring samples and their corresponding δ^{13}C, Δ^{14}C (uncorrected) and Δ'^{14}C values

Table 1. Radiocarbon content in tree rings

Sample no.	Tree-ring dates	δ^{13}C ‰	Δ^{14}C ‰ (uncorrected)	Δ'^{14}C ‰ (corrected)
81301	1925	-26.05	-10.7 ± 4.4	- 2.6
81302	1923-1924	-26.40	+ 1.3 ± 4.7	+ 9.1
81303	1920-1922	-26.42	- 6.1 ± 3.8	+ 1.2
81304	1915-1916	-26.87	-10.4 ± 4.6	- 4.4
81305	1912-1914	-26.01	- 8.6 ± 4.4	- 3.2
81306	1910-1911	-25.57	- 1.0 ± 4.5	+ 3.9
81307	1908-1909	-26.01	-19.4 ± 4.2	-14.9
81308	1906-1907	-25.66	-16.9 ± 4.7	-12.8
81309	1904-1905	-26.45	- 1.5 ± 4.8	+ 2.2
81310	1902-1903	-26.25	+ 2.5 ± 4.4	+ 5.8
81311	1901-1902	-26.47	+ 1.7 ± 2.8	+ 4.8
82306	1899-1900	-26.75	+ 4.3 ± 3.0	+ 7.0
81313	1897-1898	-26.17	+ 2.8 ± 3.4	+ 5.1
81314	1895-1896	-26.18	+ 2.3 ± 2.8	+ 4.2
81315	1893-1894	-26.32	- 7.2 ± 3.1	- 5.7
81316	1891-1892	-25.90	- 6.4 ± 2.7	- 5.3
81301	1889-1890	-26.28	+ 3.8 ± 2.4	+ 4.5
82303	1887-1888	(-26.23)*	- 0.2 ± 2.9	+ 0.1
82304	1885-1886	(-26.23)*	+ 4.7 ± 3.6	+ 4.7
82305	1883-1884	(-26.23)*	- 0.8 ± 3.4	- 0.8
82302	1881-1882	-26.53	- 5.7 ± 3.0	- 5.7

*Estimated

(corrected for the Suess effects, linearly interpolated between 0‰ in 1885 and 8‰ in 1925). $\Delta^{14}C$ values were calculated according to Stuiver and Polach (1977):

$$\Delta^{14}C = \left\{ \frac{A_{sn} \exp[\lambda(1981 - x)]}{A_{abs}} - 1 \right\} \times 1000 ‰$$

As a limited amount of oxalic acid SRN-4990 was available, A_{abs} was measured with Chinese sucrose charcoal standard which had been precisely intercalibrated against the international standard.

The data points are plotted in figure 1 along with other published $\Delta^{14}C$ values for comparison. To show the correlation with solar activity, we plotted, in the upper panel of figure 2, the sunspot numbers with the ordinates inverted and in the lower panel, $\Delta'^{14}C$ values. The cross-correlation coefficients with time differences -2, -1, 0, +1, and +2 years (- stands for a delay, + for an advance) are -0.26, -0.53, -0.58, -0.42, and -0.09, respectively. In view of the fact that sunspot numbers and the modulation of cosmic-ray intensity are only loosely correlated, the anti-correlation indicated in figure 2 is convincing.

We did not observe any measurable increase in $\Delta^{14}C$ in 1908, which might be caused by the Tunguska event. This agrees with the results of Lerman, Mook, and Vogel (1967).

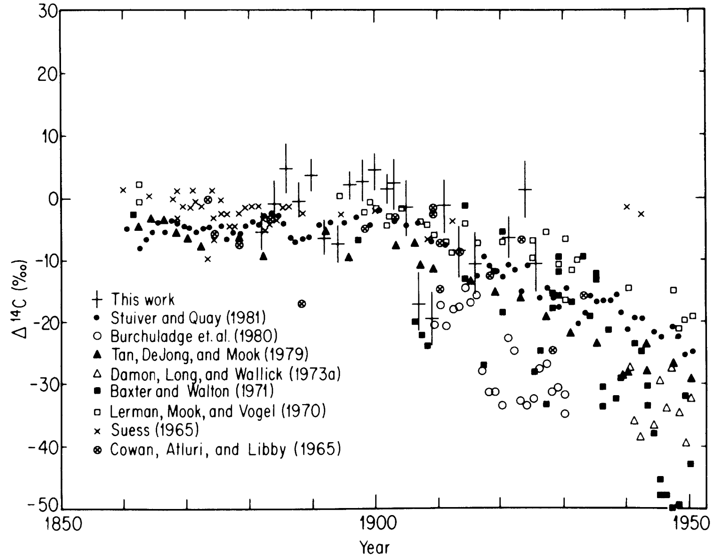

Fig 1. $\Delta^{14}C$ (uncorrected for the Suess effect)

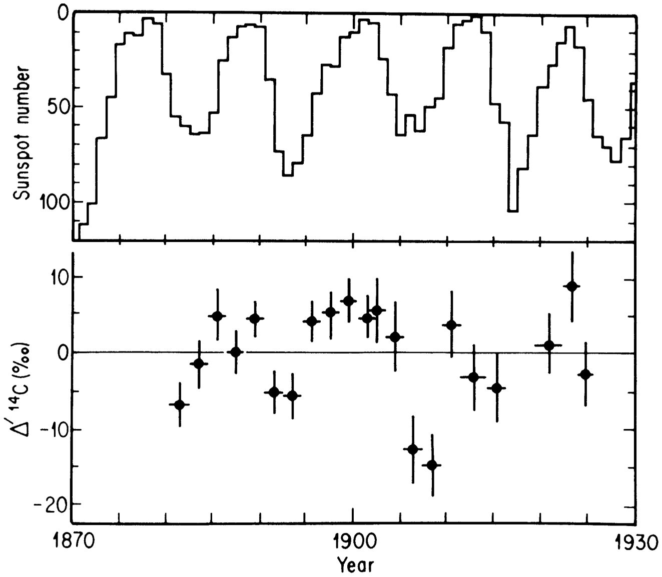

Fig 2. Upper panel: sunspot numbers
Lower panel: Δ'^{14}C (corrected for the Suess effect)

DISCUSSION

To explain the observation by de Vries (1958) of the variations of Δ^{14}C with time and location, Stuiver (1961) was the first to suggest that they are caused by the solar modulation of the ^{14}C production in the upper atmosphere. While the long-term Δ^{14}C change attributed to a variable sun has been studied by many investigators and the correlation established beyond any doubt (e g, Stuiver and Quay, 1980 and references therein), the puzzle remains as to why trees grown in high latitudes seem to respond to the 11-year cycle of cosmic-ray intensity change with higher sensitivity than those of lower latitudes. We have made the following observations: 1) The amplitude of the variation in ^{14}C production rates in a solar cycle increases with geomagnetic latitudes. Table 2 lists the ^{14}C production rates calculated by Lingenfelter and Ramaty (1970) in 1953-54 and 1957-1958 at various latitudes. The weighted averages of the amplitudes over the latitude ranges 0-60° and 60-90° are 11% and 33%, respectively. 2) After the last and most powerful high-altitude atomic bomb test in 1962, atmospheric ^{14}C concentration measured at latitudes 28-71°N were higher than those at latitudes 9-15°N, for almost three years (Nydal, 1968). This indicates that the time scale for the transport of ^{14}C across latitudes in the stratosphere is much longer than that in the troposphere. 3) The ocean surface area in the latitude range 60-70°N is only ca 30% of that of the land mass; beyond 70°N, it is frequently covered with ice. These physical conditions would cause the mixing rate of CO_2 with sea water to be much lower in this region than in lower latitudes.

Table 2. ^{14}C production rate by cosmic ray

Geomagnetic latitude	1953-1954 ^{14}C production rate (per cm^2 sec)	1957-1958 ^{14}C production rate (per cm^2 sec)
0°	0.91	0.86
10°	0.94	0.89
20°	1.13	1.07
30°	1.70	1.51
45°	2.80	2.27
50°	4.20	3.19
60°	4.88	3.50
70-90°	4.99	3.50

We suggest that the atmosphere of the northern hemisphere can be divided into two boxes, 60-90°N (box 1) and 0-60°N (box 2), and the transport of ^{14}C may be approximately represented as follows:

Q_1, stratosphere ^{14}C source $\rightarrow$ ^{14}C(box 1) $\rightarrow$ ^{14}C(box 2) $\rightarrow$ ocean

Q_2, stratosphere ^{14}C source $\rightarrow$ ^{14}C(box 2) $\rightarrow$ ocean
↳ ^{14}C(box 1)

with $\delta Q_1 \sim 3\delta Q_2$. A preliminary calculation indicated that this model seems to explain the observed 10‰ fluctuation and the difference reported by Lerman, Mook, and Vogel (1970) and by Baxter and Farmer (1973) between the northern and southern hemispheres. We are presently continuing our measurements and working out the details of the proposed model.

ACKNOWLEDGMENTS

Dr ML Parker of Canadian Forestry Service kindly supplied us with the two sections of dendrochronologically calibrated white spruce which made this study possible. We are grateful to the Department of History, Peking University, and the Department of Physics, Nanjing University, for their support. Special thanks from two of us (CYF and DKM) to Prof Shi Shi-Yuan for his interest and guidance. The contribution of Ma Li and Wang Bai-Zhen in processing the specimens was invaluable. This project is partially supported by NASA Grant NGR 03-002-107 and subcontract R 277664 from the University of Maryland.

REFERENCES

Baxter, MS and Farmer, JG, 1973, Radiocarbon: Short term variations: Earth Planetary Sci Letters, v 20, p 295-299.

Baxter, MS and Walton, A, 1971, Fluctuations of atmospheric carbon-14 concentrations during the past century: Royal Soc [London] Proc, Ser A, v 321, p 105-127.

Broecker, WS, Olson, EA, and Bird, J, 1959, Radiocarbon measurements on samples of known age: Nature, v 183, p 1582-1584.

Burchuladze, AA, Pagava, SV, Povinec, P. Togonidze, GI, and Usačev, S, 1980, Radiocarbon variations with the 11-year solar cycle during the last century: Nature, v 287, p 320-322.

Cowan, C, Atluri, CR, and Libby, WF, 1965, Possible anti-matter content of the Tunguska Meteor of 1908: Nature, v 206, p 861-865.

Damon, PE, Long, A, and Wallick, EI, 1973a, On the magnitude of the 11-year radiocarbon cycle: Earth Planetary Sci Letters, v 20, p 300-306.

____________ 1973b, Comments on "Radiocarbon: Short term variations," by MS Baxter and JG Farmer: Earth Planetary Sci Letters, v 20, p 311-314.

de Vries, HL, 1958, Variation in concentration of radiocarbon with time and location on earth: Proc Koninkl Ned Akad Wet, B61, no 2, p 1-9.

Forbush, SE, 1954, World-wide cosmic-ray variations, 1937-1952: Jour Geophys Research, v 59, p 525-542.

Lerman, JC, Mook, WG, and Vogel, JC, 1967, Effect of the Tunguska Meteor and sunspots on radiocarbon in tree rings: Naure, v 216, p 990-991.

____________ 1970, C14 in tree rings from different localities, in Olsson, IU, ed, Radiocarbon variations and absolute chronology: New York, John Wiley & Sons, p 275-301.

Lingenfelter, RE and Ramaty, R, 1970, Astrophysical and geophysical variations in C14 production, in Olsson, IU, ed, Radiocarbon variations and absolute chronology: New York, John Wiley & Sons, p 513-537.

Nydal, Reidar, 1968, Further investigation on the transfer of radiocarbon in nature: Jour Geophys Research, v 73, p 3617-3635.

Stuiver, M, 1961, Variation in radiocarbon concentration and sunspot activity: Jour Geophys Research, v 66, p 273-276.

Stuiver, M and Polach, HA, 1977, Discussion: Reporting of ^{14}C data: Radiocarbon, v 19, p 355-363.

Stuiver, M and Quay, PD, 1980, Changes in atmospheric carbon-14 attributed to a variable sun: Science, v 207, p 11-19.

____________ 1981, Atmospheric ^{14}C changes resulting from fossil fuel CO_2 release and cosmic ray flux variability: Earth Planetary Sci Letters, v 53, p 349-362.

Suess, HE, 1965, Secular variations of the cosmic-ray produced carbon-14 in the atmosphere and their interpretations: Jour Geophys Research, v 70, p 5937-5952.

Tans, PP, DeJong, AF, and Mook, WG, 1979, Natural atmospheric ^{14}C variation and the Suess effect: Nature, v 280, p 826-828.

[Radiocarbon, Vol 25, No. 2, 1983, P 213-218]

^{14}C VARIATIONS DURING THE UPPER PLEISTOCENE

J C VOGEL

CSIR, Box 395, Pretoria, South Africa

ABSTRACT. Parallel determinations of ^{14}C and ionium dates on a stalagmite from the Cango Caves provide evidence of variations in the ^{14}C content of the atmosphere beyond the range of the California tree-ring sequence. During the Holocene growth period the ^{230}Th dates are compatible with the tree-ring calibrated ^{14}C dates. At 18,000 BP and between 30,000 and 40,000 BP the ^{14}C ages are markedly younger than the ^{230}Th ages, suggesting that the ^{14}C level of the atmosphere was considerably higher at these times. Between the ^{230}Th ages of 35,000 and 29,000 BP the ^{14}C ages remain nearly constant at 29,500 BP, indicating that ^{14}C production must have been drastically reduced during this period. The ^{14}C fluctuation is greater than that predicted by Barbetti (1980) but it may be explained by postulating a substantial increase in the geomagnetic dipole field, for which there is mounting evidence.

INTRODUCTION

Several attempts have been made to establish the constancy of the ^{14}C content of the atmosphere in the period beyond the current range of the California tree-ring sequence, without thus far producing conclusive results. ^{14}C dates in the range of 23,000 to 32,000 BP were compared with ionium (uranium series) dates in the same sedimentary sequence, but no discrepancy could be detected (Peng, Goddard, and Broecker, 1978; Stuiver, 1978). However, some indication of considerable deviations between 17,000 and 40,000 BP were reported (Vogel, 1980), and Barbetti and Flude (1979) and Barbetti (1980) showed that the available paleomagnetic data may point to substantial fluctuations in the dipole field of the earth. These, in turn, would have produced significant distortions in ^{14}C dates during this period

In order to investigate this possibility further, a stalagmite, 2.8m high, was secured from the Cango Caves near Oudtshoorn in the Cape Province of South Africa. It stood some 1000m from the mouth of the cave, and since water still dripped onto it at times, we thought it could still be growing. The stalagmite consists of large calcite crystals and is virtually impervious and nearly transparent. Thus, it is ideally suited for both ionium and ^{14}C dating, since it is unlikely that either uranium or ^{14}C could have been adsorbed from percolating water after initial precipitation of the calcium carbonate, or that the uranium could have been leached out at a later stage. The surface shows no signs of re-solution so that it was probably never submerged under the groundwater table.

CALIBRATION

At ca 95cm from the top of the stalagmite, a discontinuity could be discerned, in that the lower part is slightly yellow-brown, while the upper 95cm are completely colorless. In the event there was a break of some 10,000 years in the growth of the speleothem at this point, the purer calcite accumulating during the past 6000 years. Both the ^{14}C and ionium age measurements for the upper section are shown in figure 1.

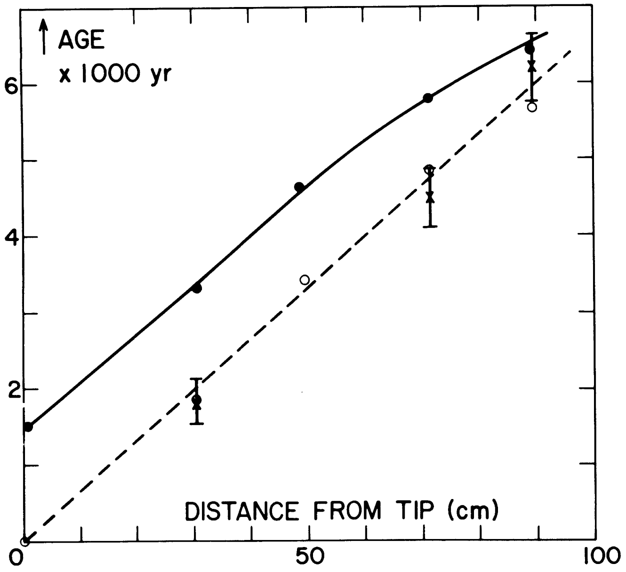

Fig 1. Growth curve for the upper 97cm of the stalagmite
- ● apparent ^{14}C ages of the samples
- o ages after correction for the apparent initial age (-1500 yr) and calibration for variation in the atmospheric ^{14}C content
- x associated ionium ages

As expected, the apparent ^{14}C ages are higher than the ionium ages due to the apparent age of the groundwater dripping into the cave. Excellent conformity of the two sets of data is obtained if the apparent initial age of the calcite is taken to be 1500 years and if the ages thus deduced are calibrated according to the curve of Suess (1970). As far as the ionium ages are concerned, all the samples reported on in this paper contained very little or no ^{232}Th. Where measurable amounts were present, the ages were adjusted for initial ^{230}Th, assuming a ^{230}Th/^{232}Th ratio of (1 ± 0.5). The maximum correction was 230 years, which is well within the uncertainty of the measurements. Both the ionium dates and the corrected ^{14}C dates show a uniform rate of growth of 15mm/century over the past 6000 years.

UPPER PLEISTOCENE PERIOD

With initial relative ^{14}C content of the speleothem established, an appropriate adjustment (1500 yr) can be made to the ^{14}C ages of the older sections. In addition to the correction for the apparent initial age, the ^{14}C dates are calculated using the more correct half-life of 5730 yr. The results are shown in figure 2 together with the ionium ages obtained for the same samples. The correction of 1500 yr need not necessarily apply to the older section, but an error in this figure would not change the conclusions presented below.

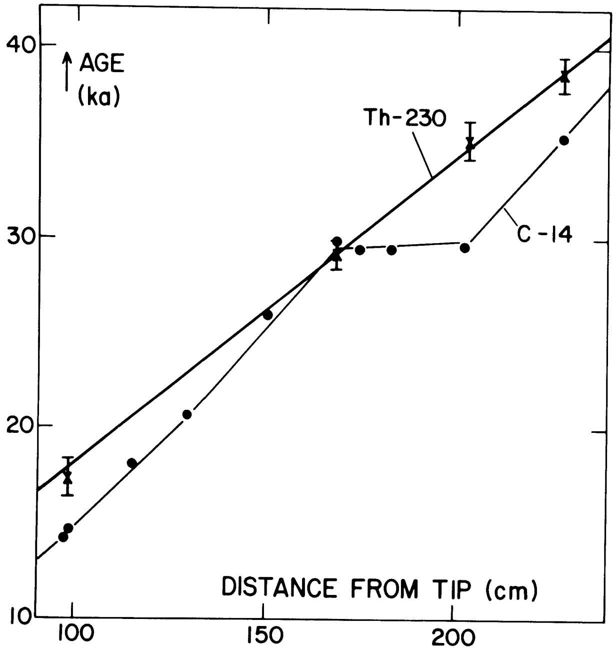

Fig 2. Growth curve for the lower section of the stalagmite. The ionium dates (x) show a linear rate of growth. The ^{14}C ages (●) are corrected for apparent initial age by subtracting 1500 yr and calculated using a half-life of 5730 yr for ^{14}C.

The first point to note is the abrupt jump in age between 90cm from the tip (6000 BP, fig 1) and 97cm (ca 16,000 BP, fig 2). This discontinuity represents a period during which the stalagmite did not grow at all, possibly because there was insufficient seepage at this time.

The ionium dates for the section 230cm to 97cm from the tip indicate a practically constant growth rate of 6.2mm/century between 39,000 BP and 18,000 BP. The ^{14}C dates, on the other hand, are substantially younger for much of the period, excepting those for the section between 205 and 166cm which remain virtually constant at ca 29,500 BP.

The discrepancy between the ^{14}C and ionium dates at 19,000, 35,000, and 39,000 BP (ionium ages) may most logically be interpreted to mean that the ^{14}C level in the atmosphere was then significantly higher than it is today. The alternative explanation that the accepted half-life of ^{230}Th (75,200 yr) is at least 10% too great, seems less likely at this stage. The observed discrepancy further confirms the previously reported suspicion of deviating ^{14}C ages at these dates (Vogel, 1980).

The second feature revealed in figure 2 is the substantial kink in the ^{14}C growth curve at ca 29,500 yr BP. This can be explained in two ways: either the growth rate of the stalagmite was at least 10 times greater during this period (60mm/century) <u>and</u> one or both the ionium dates at 167cm and 204cm are in error, or the rate of ^{14}C production in the atmosphere was drastically decreased for about 6000 yr after 35,000 BP. The second possibility seems more probable, especially in view of the very high paleomagnetic field strengths at ca 29,500 ^{14}C yr BP reported by Barbetti and McElhinny (1976) for the Lake Mungo site in Australia. If these magnetic field intensities represent an increase in the geomagnetic dipole moment, they would indicate that the dipole strength changed from as little as 2 to nearly $50 \times 10^{22} AM^2$ between 32,000 and 29,500 ^{14}C yr BP. This, in turn, could have reduced the production rate of ^{14}C by a factor of 5 (Barbetti, 1980; Lingenfelter and Ramaty, 1970). If such high values of the dipole field of the earth were maintained for several thousand years, it would have had the effect that apparent ^{14}C ages changed very slowly throughout the period. It appears, therefore, that the constancy of the ^{14}C ages observed between 165 and 205cm in the stalagmite could be explained by changes of the strength of the geomagnetic dipole alone.

The atmospheric ^{14}C concentration derived from the four pairs of ^{14}C and ^{230}Th dates are plotted in figure 3.

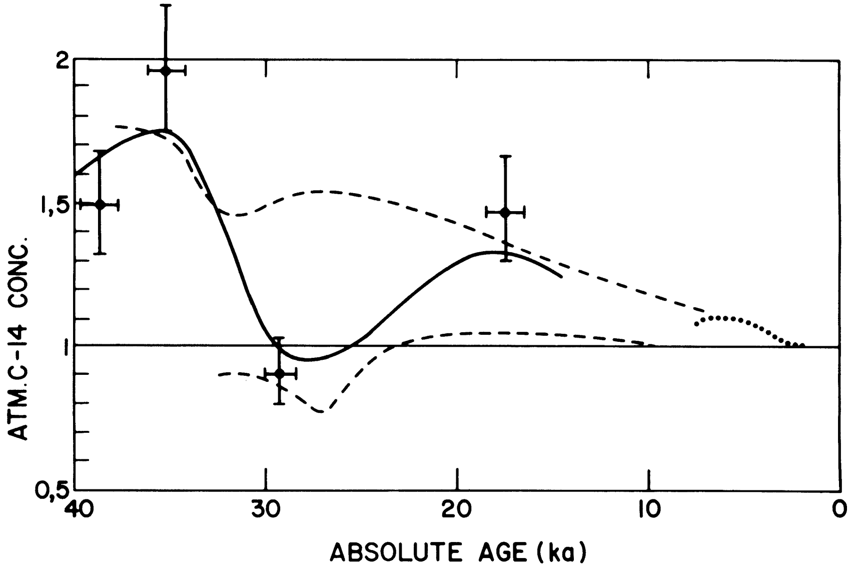

Fig 3. Relative atmospheric ^{14}C content deduced from the differences between the ^{14}C and ^{230}Th ages of the samples dated by both methods. The dashed lines are the extreme possible values calculated by Barbetti (1980) from geomagnetic data. The dotted line is the variation derived from dendrochronology.

The values lie within the limits calculated by Barbetti (1980) from the known data on magnetic field intensities (dashed lines). The results reported here are not at variance with other published pairs of dates summarized by Barbetti (1980), although the uncertainties associated with the existing measurements between 30,000 and 40,000 BP are too large to permit a meaningful comparison.

CONCLUSIONS

Evidence is presented that ^{14}C ages may be several thousand years too young at some stages during the Upper Pleniglacial and that they remain nearly constant between 29,000 and 35,000 BP. The latter finding suggests that the production of ^{14}C in the atmosphere was drastically decreased during this period. These observations need to be substantiated by further precise measurements on other samples from different regions before they can be accepted with confidence. The main problems in this regard are those of obtaining datable material in the relevant age range and of attaining sufficient accuracy in the ionium measurements.

ACKNOWLEDGMENTS

Michael Schultz, town clerk of Oudtshoorn, is especially thanked for the permission to remove the stalagmite from a remote part of the Cango Caves for scientific investigation, and J Blacquiere for his invaluable assistance in effecting the removal. H Deacon provided considerable help in initiating the project, and J Kronfeld helped me in setting up the ionium dating facility. G Sartory, E Visser, and T Bubenzer assisted with the laboratory analyses.

REFERENCES

Barbetti, M, 1980, Geomagnetic strength over the last 50,000 years and changes in atmospheric ^{14}C concentrations: emerging trends, in Stuiver, Minze and Kra, Renee, eds, Internatl radiocarbon conf, 10th, Proc: Radiocarbon, v 22, no. 2, p 192-199.

Barbetti, M and Flude, K, 1979, Geomagnetic variation during the late Pleistocene period and changes in the radiocarbon time scale: Nature, v 279, p 202-205.

Barbetti, MF and McElhinny, MW, 1976, The Lake Mungo geomagnetic excursion: Phil Trans Royal Soc, A, v 281, p 515-542.

Lingenfelter, RE and Ramaty, R, 1970, Astrophysical and geophysical variations in C 14 production, in Olsson, I U, ed, Radiocarbon variations and absolute chronology: New York, John Wiley & Sons, p 513-535.

Peng, T-H, Goddard, JG, and Broecker, WS, 1978, A direct comparison of ^{14}C and ^{230}Th ages at Searles Lake, California: Quarternary Research, v 9, p 319-329.

Stuiver, M, 1978, Radiocarbon timescale tested against magnetic and other dating methods: Nature, V 273, p 271-274.

Suess, H, 1970, Bristlecone-pine calibration of the radiocarbon time-scale 5200 BC to the present, in Olsson, I U, ed, Radiocarbon variations and absolute chronology: New York, John Wiley & Sons, p 303-311.

Vogel, JC, 1980, Accuracy in the radiocarbon time scale beyond 15,000 BP, in Stuiver, Minze and Kra, Renee, eds, Internatl radiocarbon conf, 10th, Proc: Radiocarbon, v 22, no. 2, p 210-218.

[Radiocarbon, Vol 25, No. 2, 1983, P 219-228]

STATISTICS OF THE AD RECORD OF CLIMATIC AND CARBON ISOTOPIC CHANGE

Minze Stuiver

Quaternary Isotope Laboratory and Geological Sciences
University of Washington, Seattle, Washington 98195

ABSTRACT. The AD time series of $\Delta^{14}C$, $\delta^{13}C$, and cosmic ray fluxes, Q, were analyzed for similarities. Two cases of significant correlation between Q and tree-ring $\delta^{13}C$ were encountered, for which up to 25% of the variance can be attributed to changes in the tree's isotope fractionation that related to solar induced climatic changes. However, it is possible that the demonstrated correlation is fortuitous because actual climate proxy records generally do not correlate significantly with the Q record.

The history of $^{13}C/^{12}C$ and $^{14}C/^{12}C$ ratios in atmospheric CO_2 can be obtained from tree-ring cellulose because the carbon of the ring's cell walls is derived from the atmospheric CO_2 source. Isotope fractionation in the photosynthetic process adds another signal, and the measured carbon isotopic record in tree rings gives the sum-total of the isotope variations in atmospheric CO_2 (which can be of global and local origin), and the variability in isotope fractionation of the plant. By normalizing on a constant $^{13}C/^{12}C$ ratio a $^{14}C/^{12}C$ record can be derived independently of the tree's variability in isotope fractionation. However, the derivation of a $^{13}C/^{12}C$ record solely reflecting atmospheric change is more difficult because here the factors influencing the plant's isotope fractionation have to be known in detail (Stuiver, 1982).

Our research has yielded time series of $\delta^{13}C$ and $\Delta^{14}C$ change in tree rings during the AD interval. The ^{14}C record appears to reflect upper atmospheric ^{14}C production rate changes that are related to changes in magnetic properties of the solar wind and the earth's geomagnetic wind. From the $\Delta^{14}C$ record the production rate changes can be calculated through the use of carbon reservoir models (Stuiver and Quay, 1980; 1981a). The resulting record of solar variability, as reflected in cosmic-ray intensity change, has been compared with the available proxy data of climatic change without finding significant overall correlation (Stuiver, 1980).

As discussed, the $\delta^{13}C$ record reflects global changes in $\delta^{13}C$ ratios of atmospheric CO_2 on which are superimposed the changes induced by isotope fractionation, and possibly, by the changes in isotope ratio of the CO_2 in the local environment. The global, as well as the non-global isotope changes in the $\delta^{13}C$ record may be related to climatic change, eg, favorable growing conditions of <u>Sequoia</u> <u>giganteum</u> resulting in wide rings also yield high $\delta^{13}C$ values, and vice versa. If these growth changes are climatically related (as is often the case, see Fritts, 1976) then the $\delta^{13}C$ record includes a climatic signal. This raises the question whether there is any degree of similarity between the $\Delta^{14}C$ record (which is tied to solar variability and possibly climatic change) and the $\delta^{13}C$ records which may reflect climatic change. In the following discussion only the pre-AD 1850 portions of the isotope records are used, thus restricting the comparisons entirely to natural variation.

The power spectrum analysis employed here evaluates the non-randomness of the time series. The spectral estimates in the figures are the amplitudes of the cosine transforms of the serial correlation coefficients for the time series that have been smoothed by a 3-term weighted moving average with weights equal to ¼, ½, and ¼, respectively. The null spectrum is the Markov "red noise," the shape of which depends on the lag-one correlation coefficient (Mitchell, 1966). The 95 and 5% confidence limits are multiples of the "red noise" spectrum obtained from the percent points of χ^2/ν distribution for the calculated degrees of freedom ν.

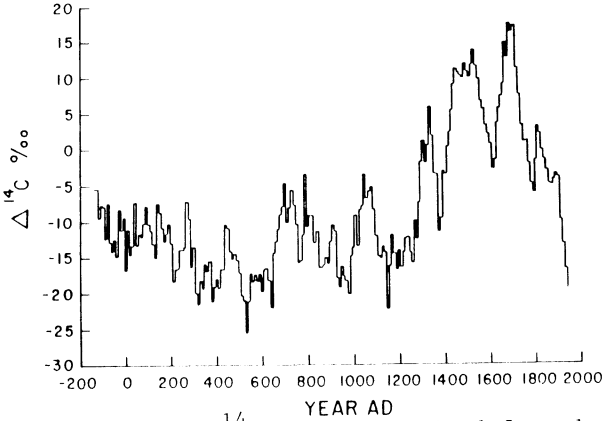

Fig 1. Atmospheric $\Delta^{14}C$ values, derived from decadal tree-ring samples from the Pacific Northwest and California.

The spectral properties of the $\delta^{13}C$ and $\Delta^{14}C$ time series vary with the time interval selected for each isotope, eg, the spectral distributions of the 1st and 2nd $\Delta^{14}C$ millennium AD record (fig 1) differ drastically. Whereas the AD 1000-1850 interval has two periodicities at ca 200 and 120 yr much beyond the 2σ level, the AD 1-1000 interval has significant power only at 105 and 42 yr (fig 2). The complete AD atmospheric $\Delta^{14}C$ record (AD 1-1850) has a periodicity that approaches the 2σ level at 42 yr only (fig 2). When extended to the BC period, there is again good evidence for a non-random 200-yr periodicity (Neftel, Oeschger, and Suess, 1981).

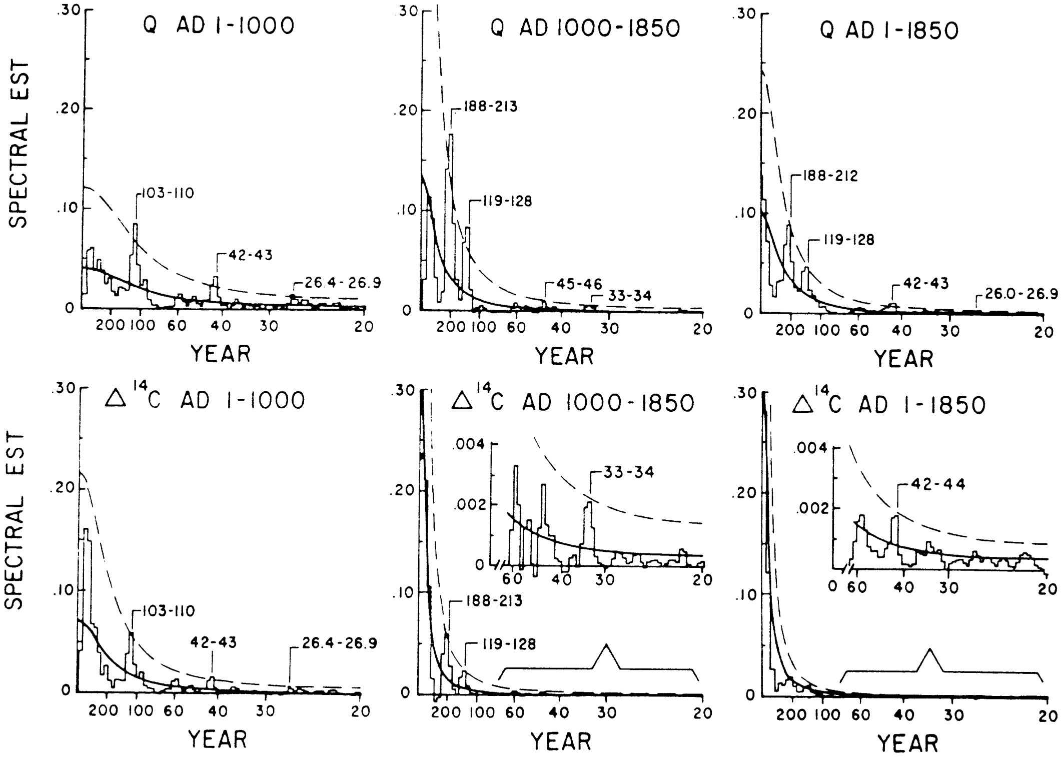

Fig 2. Spectral distribution of the decadal ^{14}C production rate record (Q) and Δ^{14}C. The dashed line gives the 2σ confidence limit; the solid line gives the red noise continuum.

The records of production rate changes, Q, in the upper atmosphere, and the corresponding atmostpheric $\Delta^{14}C$ change, differ in spectral composition because the transport of ^{14}C between the various carbon reservoirs transforms the time-dependent properties. The calculated Q record, as obtained from carbon reservoir modeling (Stuiver and Quay, 1980; 1981b) with an oceanic eddy diffusion coefficient of 2.2cm^2/sec, yields the spectral distribution given in upper portion of figure 2. This spectral distribution depends somewhat on the model parameters, eg, a biospheric residence time of 20 yr instead of 60 yr would change the attenuation of the higher frequencies.

Whereas the tree-ring $\Delta^{14}C$ record for the complete AD period shows spectral power at 42 yr only, the Q record of solar change exhibits periodicities of ca 200, 120, and 42 yr. The actual Q record (fig 3) shows that the various maxima in ^{14}C production rate (isotope stages) are related to the sunspot minima some of which were named previously (ie, M-1 is the Maunder, S-1 the Sporer, M-2 the Wolf, and M-3 the Oort minimum).

From our stable isotope studies, the average $\delta^{13}C$ value of 10-yr samples relative to PDB is available for several trees (Stuiver, 1982; Stuiver et al, in press). Figures 4 and 5 give the longer $\delta^{13}C$ records and their spectral distributions. The four trees and the lengths of the records analyzed are: 1) a Bristlecone Pine (BP) from the ancient Bristlecone Pine Forest botanical area in Inyo National Forest, California (37° N Lat) for the AD 180 - 1850 interval; 2) two Sequoia trees, RC and CS, from the Sequoia National Park (RC) and the University of California Whittaker Forest (CS), both (37°N Lat). The RC tree spans the AD 230 - 1850 interval, and the CS tree, the AD 1280 - 1850 interval; 3) a Sitka Spruce from

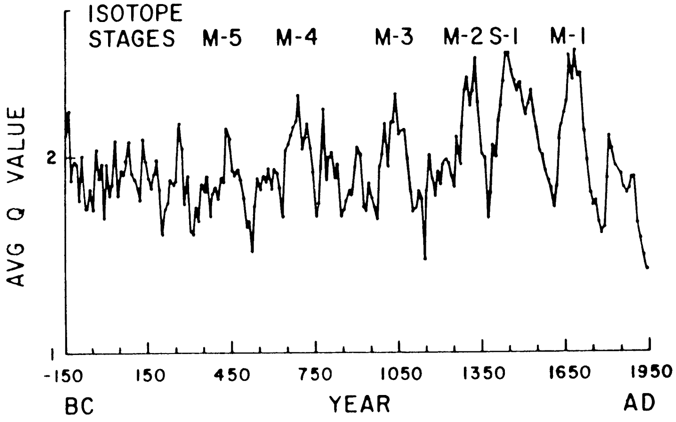

Fig 3. Calculated ^{14}C production rate Q of each decade in ^{14}C atoms/sec cm^2 (earth).

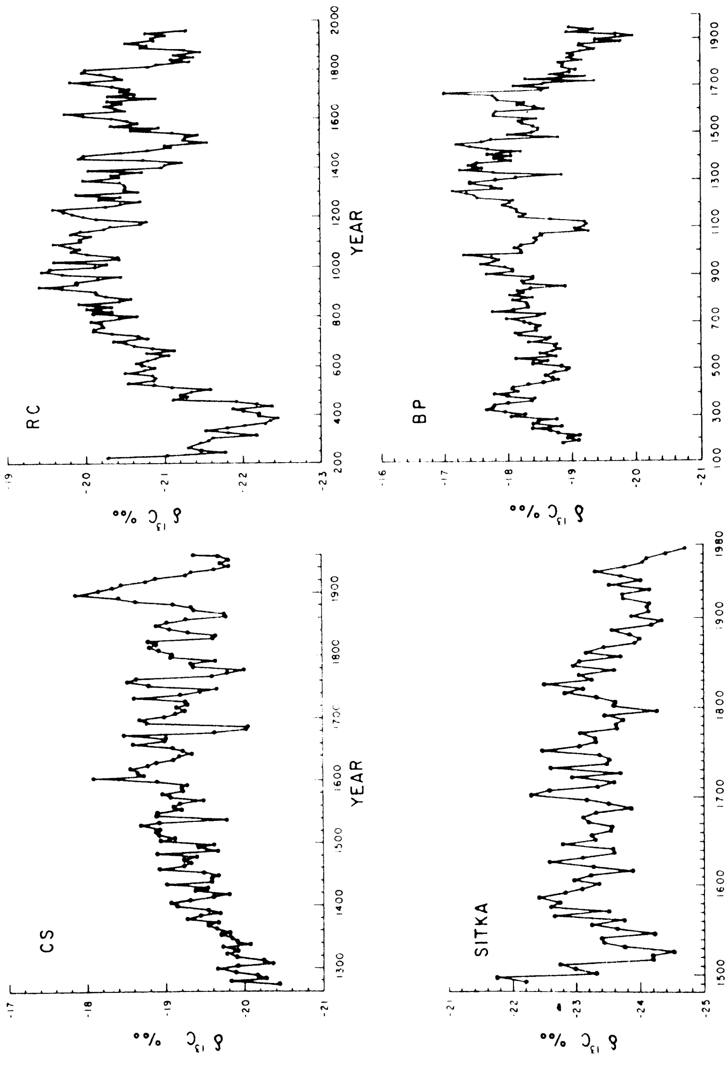

Fig 4. $\delta^{13}C$ decadal values, relative to PDB, of 2 sequoia's (CS and RC), a Sitka Spruce, and Bristlecone Pine (BP).

Bjorka Island, Alaska (57°N Lat) spanning the AD1490-1850 interval.

The spectra of the $\delta^{13}C$ time series (fig 5) contain few distinct features. The only statistically significant periods are 25 yr for Bristlecone Pine, and 30 yr for CS Sequoia. Evidently, common frequencies are absent in the $\delta^{13}C$ and $\Delta^{14}C$, or Q records.

The Q-$\delta^{13}C$ climate relationships can also be studied for randomness vs low frequency changes. The Q record, eg, is not a random series even though the properties are different for the two millennia. Randomness vs slow change was studied by analyzing auto-correlation coefficients. When a variable is generated entirely at random (in our case, by computer) the correlation coefficient of such a series when compared with itself is, of course, 1.0. However, when the series is compared with a lagged version of itself, the auto-correlation coefficients approach zero because the two compared series are not correlated. Figure 6A gives the auto-correlation record of a computer-generated random series, Figure 6b gives the auto-correlation plot of the Q data of the entire AD interval and figure 6c, of the current millennium. These Q auto-correlation diagrams differ strongly from the 6a curve, because the Q record contains an important non-random component.

Comparison of climate and Q records (Stuiver, 1980) revealed that only the oxygen isotope record of Camp Century, and the record of winter severity indexes in Russia, correlated at the 2 to 4% significance level with the Q record of the current millennium. Figures 6d and f give the auto-correlation diagrams of these climate records for the current millennium. The Russian winter severity index auto-correlation diagram shows much more randomness than the Q diagram, whereas the oxygen isotope auto-correlation diagram has similar features. Thus, the correlation between the record of solar variability, Q, and the Russian winter severity index may be coincidental.

Extending this analysis to $\delta^{13}C$ records yields figure 6e, g-i diagrams. Here Sitka Spruce and Bristlecone Pine $\delta^{13}C$ auto-correlation diagrams have features similar to the Q diagrams c and b that cover similar intervals. The Sequoia RC and CS auto-correlation plots are much broader because the $\delta^{13}C$ records of these trees include substantial long-term changes.

Correlation coefficients, r, were derived from cross-correlating the Q-record of solar variability and the $\delta^{13}C$ records (table 1). Correlation coefficients were also calculated by assuming a time lag between the Q and $\delta^{13}C$ curves of 100 yr or less. The maximum r values of this 100-yr interval are at time lags of 10 to 30 yr (table 1). These r_{max} values are not substantially different from the r values calculated through direct cross-correlation. If any relationship would exist between the Q and $\delta^{13}C$ curves, then a phase shift is restricted to a few decades only.

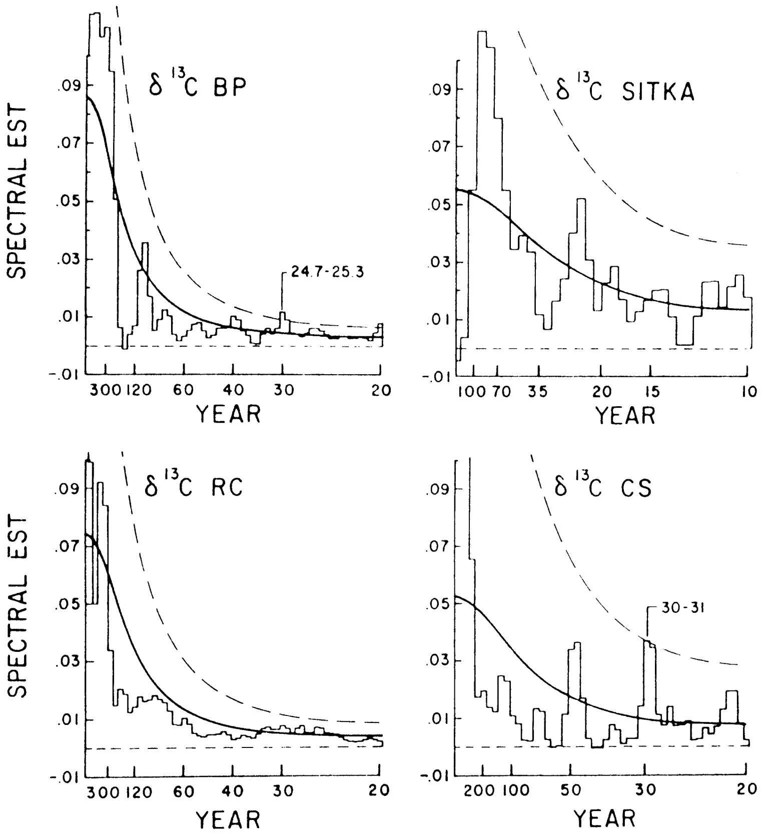

Fig 5. Spectral distribution of $\delta^{13}C$ records of figure 4. The dashed line gives the 2σ confidence level; the solid line gives the red noise continuum.

Because the Q record has substantial auto-correlation (it takes a 50 yr time lag for the auto-correlation coefficient to approach zero) the normal test of significance is no longer applicable. Auto-correlation reduces the number of independent observations used in interpreting the derived cross-correlations coefficients. The effective number N, of independent observations was calculated according to Quenouille (1952). N was subsequently used in deriving the probabilities of exceeding the values in table 1.

The r values derived from cross-correlating the $\delta^{13}C$ time series of Bristlecone Pine, and RC Sequoia, with the Q series are small despite the similar auto-correlation plot of BP (table 1), and indicate lack of relationship between global ^{14}C production and the $\delta^{13}C$ records of these trees. The correlation does not improve when the more recent AD 1400 - 1850

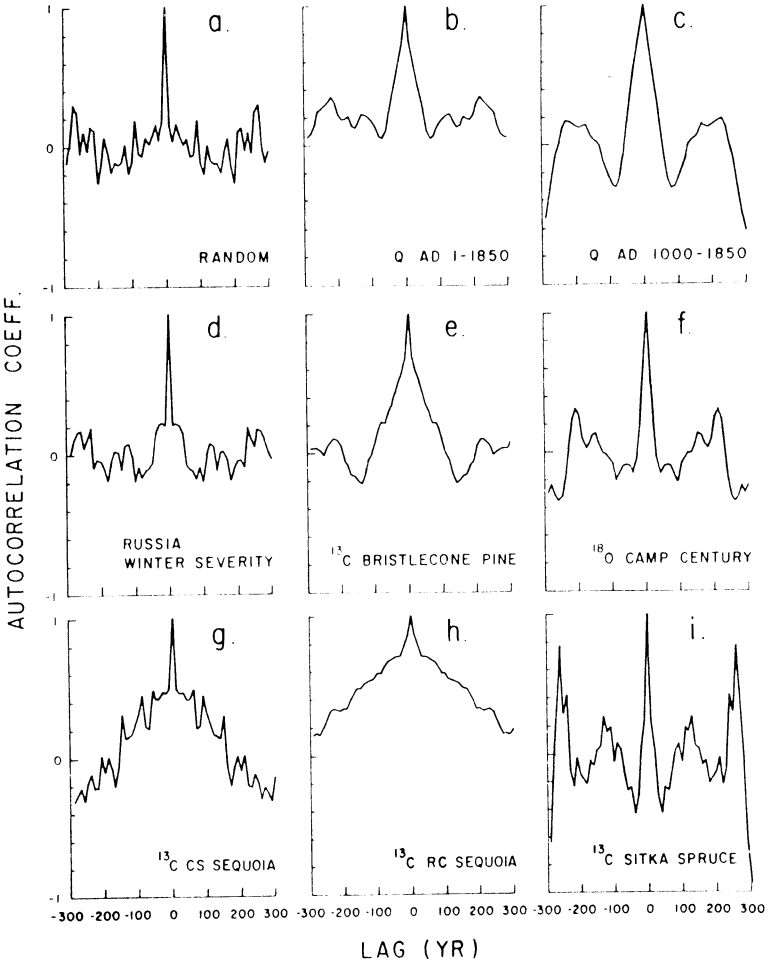

Fig 6. Autocorrelation coefficients of a. a random series, b-c. the ^{14}C production rate Q, d. Russian winter severity index (AD 1100-1850, e. decadal $\delta^{13}C$ values of Bristlecone Pine, f. $\delta^{18}O$ values of the Camp Century core (AD 1200-1850), and g-i. decadal $\delta^{13}C$ values of 2 sequoia's and a Sitka spruce.

TABLE 1. Correlation coefficients, r, derived from cross-correlating ^{14}C production rate, Q, record (fig 3) with $\delta^{13}C$ records listed below. All records have one measured (or calculated for the Q record) value per decade.

Locality, age	Species	r	Δt (yr)	r_{max}*	Δt (yr)	r_{max}*
Inyo Natl Forest (37°N Lat) AD 180-1850	Pinus aristata	0.117 (44%)	20	0.13 (39%)	-20	0.122 (42%)
Sequoia Natl Park, (37°N Lat) AD 230-1850	Sequoiadendron giganteum	0.15 (39%)	10	0.15 (39%)	-30	0.20 (25%)
Whittaker Forest (37°N Lat) AD 1280-1850	Sequoiadendron giganteum	0.39 (12%)	20	0.52 (3%)	0	0.39 (12%)
Bjorka (57°N Lat) AD 1490-1850	Picea sitchensis	0.38 (3%)	0	0.38 (3%)	0	0.38 (3%)

* Values are obtained by assuming 1) $\delta^{13}C$ variables precede Q changes, 2) Q changes precede $\delta^{13}C$ changes. The probabilities of exceeding the r values in a random series are in parenthesis. r_{max} values are only listed for time lags of 100 yr or less.

interval is considered for the above trees (significance levels respectively, 51 and 76% for zero lag).

The two remaining $\delta^{13}C$ records, of CS Sequoia and Sitka Spruce appear to correlate with the Q record at the 12 and 3% significance levels. While lagging the ^{13}C record by 20 yr, the significance level of the CS correlation also approaches 3% (table 1). This suggests, at least for two of our $\delta^{13}C$ records, a relationship between $\delta^{13}C$ change and ^{14}C production rate Q for the AD 1300 - 1850 interval.

The r value of global atmospheric $\Delta^{14}C$ and tree-ring $\delta^{13}C$ are 0.06 and 0.30 for Sitka Spruce and CS Sequoia, respectively. For a ±100 yr lag interval, the r values are, respectively, in the -.26 to .22 and -.41 to .24 range. Significant correlations are absent, especially since the $\Delta^{14}C$ record has substantial auto-correlation.

The absence of a direct tie between global $\Delta^{14}C$ and tree-ring $\delta^{13}C$ furthers the idea that the $\Delta^{14}C$ changes are not caused by large changes in carbon reservoir parameters, eg, changes caused by ocean-atmosphere exchange rate changes should influence the distribution of both isotopes in a similar manner.

The 3% significance level correlation of the $\delta^{13}C$ Sitka and CS record (for the latter, admittedly, with a 20-yr lag) and the Q record is interesting. For random time series, 1 in 20 comparisons should yield by chance alone a 5% or better significance level. Of actual comparisons, 2 out of 4 are beyond the 5% level. Evidently, for Sitka Spruce and CS Sequoia, a relationship between climatically controlled $\delta^{13}C$ and the global record of solar change, as found in the Q change, appears possible. Such an imprint of solar-induced climatic change could explain 16 to 25% of the variance in the δ^{13}C record of Sitka Spruce and CS Sequoia, respectively. Whether such a climatic change tied to solar variability is indeed possible remains to be seen. More direct comparisons with climate proxy records (Stuiver, 1980) generally do not favor a relationship between the Q record and climate.

ACKNOWLEDGMENTS

PD Quay was responsible for carbon reservoir modeling and PM Reimer assisted with spectral analysis. The ^{13}C research of the Quaternary Isotope Laboratory was supported by DOE contract 19X - 43303 - C of the Carbon Dioxide Research Division. The ^{14}C and climate aspects were supported by NSF grant ATM 8022240 of the Climate Dynamics Program.

REFERENCES

Fitts, HC, 1976, Tree rings and climate: New York Academic Press, 567 p.

Mitchell, JM, 1966, Climatic change: Technican note no. 79, World Meteorol Org no. 195 TP 100, Geneva, Switzerland.

Neftel, A, Oeschger, H, and Suess, HE, 1981, Secular non-random variations of cosmogenic carbon-14 in the terrestrial atmosphere: Earth Planetary Sci Letters, v 56, p 127-147.

Quenouille, MH, 1952, Associated measurements, vol 68: London, Butterworths.

Stuiver, M, 1980, Solar variability and climatic change during the current millennium: Nature, v 286, p 868-871.

___________ 1982, The history of the atmosphere as recorded by carbon isotopes, in Goldberg, ED, ed, Dahlem Workshop on Atmospheric Chemistry, Proc: Berlin, Springer Verlag, p 159-179.

Stuiver, M, Burk, RL, Quay, PD, and Ferguson, CW, ms, ^{13}C time variations of atmospheric CO_2: Jour Geophys Research.

Stuiver, M and Quay PD, 1980, Changes in atmospheric carbon-14 attributed to a variable sun: Science, v 207, p 11-19.

_______________________ 1981a, Atmospheric ^{14}C changes resulting from fossil fuel CO_2 release and cosmic ray flux variability: Earth Planetary Sci Letters, v 53, p 349-362.

_______________________ 1981b, A 1600 year long record of solar change derived from atmospheric ^{14}C levels: Solar Physics, v 74, p 479-481.

[Radiocarbon, Vol 25, No. 2, 1983 P 229-238]

^{14}C DATING AND MAGNETOSTRATIGRAPHY

ROY THOMPSON

Department of Geophysics
University of Edinburgh
James Clerk Maxwell Building
Mayfield Road, Edinburgh EH9 3JZ
Scotland

ABSTRACT. The history of the earth's magnetic field is preserved in the fossil magnetism of archaeologic specimens, natural rocks and sediments. Samples such as lava flows and baked sherds that acquired a thermoremanent magnetization on cooling can be used to estimate ancient geomagnetic field intensities and directions. Paleofield directions can also be obtained from fine-grained sediments that acquired detrital magnetic remanence when deposited. Study of the earth's magnetic field over the last few tens of thousands of years yields information on geomagnetic dynamo theories, causes of fluctuations in cosmic-ray activity, and the formulation of a new regional chronologic tool.

INTRODUCTION

Both the intensity and shape of the geomagnetic field change with time. Over 1000 paleo-intensity determinations have been made on materials covering the last 10,000 years. These determinations show that the global mean dipole moment during this time was 9×10^{22} Am^2 and that it varied from a broad minimum of 6.5×10^{22} Am^2 ca 6500 years BP to a maximum of 11.5×10^{22} Am^2 near 2700 years BP (McElhinny and Senanayake, in press). Superimposed on this overall trend are more rapid intensity fluctuations, such as those observed in the last century. Since AD 1850 the axial dipole has been decreasing at an average rate of 5% per century, the rate dropping for a few years ca AD 1950 to almost zero. Variations of even higher frequency have recently been observed. In AD 1970 the earth's magnetic field underwent a jerk (Malin and Hodder, 1982) which noticeably altered the rate of secular variation at many localities of the world. Sustained intensity changes causing the local field to vary by a factor of 2 or 3 in 100 years were suggested on the basis of a sequence of archaeomagnetic results from Greece (Walton, 1979). The general pattern of field intensity changes summarized above largely confirms that discussed by Smith (1966) and Bucha (1970) and reinforces the possibility of important global intensity changes occurring in only a few hundred years.

Detailed information about the evolution of the shape of the geomagnetic field over the last 10,000 years recently became available through paleomagnetic studies of lake sediment cores (Mackereth, 1971) from different regions of the world. Two key advances made the acquisition of global paleolimnomagnetic data possible. The first advance was the development of piston corers, such as Mackereth's (1958) pneumatic 6m corer which allowed multiple, long, undisturbed sediment cores to be collected from a lake during one day's fieldwork. The second advance was the computerization of fluxgate and cryogenic magnetometers which permitted the magnetic remanence of hundreds of fragile, weakly magnetized samples to be measured during one day's laboratory work. Following these technical developments, much of the paleomagnetic data synthesized below were collected from lake deposits. In Europe, e g, well over 50,000 samples from tens of lakes have been subjected to paleomagnetic measurements.

DATA QUALITY

PALEOMAGNETIC DATA. As most natural materials do not hold a reliable paleomagnetic record of ancient geomagnetic field changes, it is very important to demonstrate the credibility of the data before accepting them for magnetostratigraphic or geophysical work. The standard approach for such an assessment is to use minimum reliability criteria. In this approach practical quantitative criteria are used in order to reject results that are unlikely to be reliable indicators of the paleomagnetic field. In paleolimnomagnetic studies the most important criteria concern 1) reproducibility between samples, cores and lakes, and 2) independence from sediment lithology. Unusual paleomagnetic results from only one sediment sampling site should be viewed with great caution.

^{14}C DATA. Most paleolimnomagnetic records have been dated directly by the ^{14}C method. A limited number of key magnetic records have also been dated using a pollen biostratigraphy or tephra chronology, tied to the ^{14}C time scale. Sediments dated by yearly laminations are now beginning to yield reliable paleomagnetic records.

Contamination of lake sediments by old carbon (Olsson, 1979) is a recurrent problem in dating lake sediments. Natural carbon contamination due to either erosion of materials such as graphite, coal, or old soils in the catchment, or to the redeposition of old sediments cannot, at present, be dealt with satisfactorily by either laboratory pretreatment or modelling procedures. Particularly pronounced natural contamination can lead to out-of-sequence dates. Such highly aberrant ages can of course be easily discarded. More commonly, however, natural contamination leads to subtle systematic errors that can be difficult to detect unless the ^{14}C dates from lake sediments can be compared with dates from materials such as peat and charcoal.

A second problem concerns hard-water corrections. In regions of carbonate-rich bedrock or glacial deposits, ages can again be systematically old. The usual method of correcting hard-water errors is to extrapolate the ^{14}C age/depth relationship to the mud/water interface in order to estimate the present day hard-water error. This error is then assumed constant and all the ^{14}C ages are then reduced by the amount of the present hard-water error. Constant hard-water correction errors of several 100 years have had to be applied to the South Australian, North American, and Near Eastern master sediments. The need for duplicate dating techniques such as tephra or pollen zonation combined with ^{14}C dates is apparent. In this paper all ^{14}C dates were calibrated to calendar dates using Clark's (1975) tree-ring curve. Dates older than 6500 years (the limit of Clark's curve) were modified using an extension to Clark's calibration curve that decreases smoothly to zero correction at 10,000 years BP.

REGIONAL GEOMAGNETIC MASTER CURVES

Regional master curves (fig 1) were derived by analyzing high quality paleomagnetic results from lake sediments. The curves plot the variation of declination and inclination with calibrated ^{14}C age. All the directional records were confirmed by stacking results from more than one lake or from multiple samples. Stacking, however, was not used in constructing the master curves because of signal attenuation. Each curve consists of a cubic spline fitted to the sequential directional data of a type section. The type lakes and cores selected for the six regions are: South Australia, Bullenmerri core BC extended by Keilambete core KF (Barton and McElhinny, in press); North America, St Croix core 75 (Banerjee, Lund and Levi, 1979); western Europe, Lomond core LLRPI extended by Windermere core W3 (Thompson and Turner, 1979); eastern Europe, Paajarvi core P4 (Huttonen and Stober, 1980) extended by Lovojarvi core D (Tolonen, Siiriainen and Thompson, 1975); Near East, Kinneret core K8 (Thompson and Stiller, ms in preparation); East Asia, Kizaki core K3 (Horie et al, 1981). The North Pacific curve of fig 1 is based on the paleomagnetic results from ^{14}C dated lava flows of McWilliams, Holcomb and Champion (1982).

SECULAR VARIATION MAGNETOSTRATIGRAPHY

The regional master curves form a basis for dating Holo-

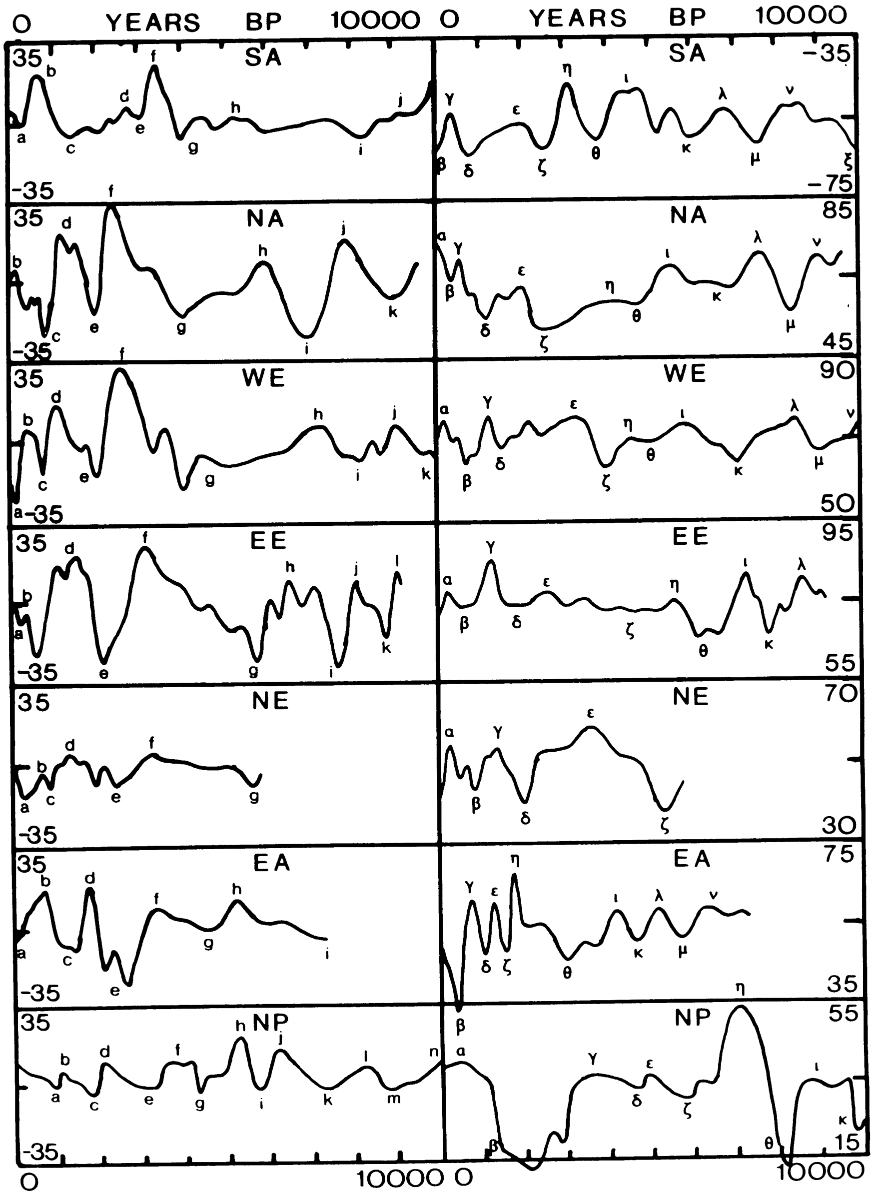

Fig 1. Regional declination (left) and inclination (right) master curves for South Australia, SA; North America, NA; West Europe, WE; East Europe, EE; Near East, NE; East Asia, EA; North Pacific, NP. Tree ring calibrated time scale in calendar years BP (O BP = AD 1950).

cene sediments. By matching paleomagnetic features from new sedimentary sequences with those of the curves, dates can be transferred to the new materials under investigation. Turning points of the direction variations prove to be the clearest features to recognize; thus, they are labelled (Fig 1). Some turning points are poorly developed; others, eg, WEe and WEg, have double peaks. Both of these are difficult to label. Bearing in mind difficulties discussed above, the typical uncertainty in the estimated ages of the secular variation features (Table 1) is probably ca 5%. Dominant errors relate to natural carbon contamination problems and not to paleomagnetic or isotopic laboratory experimental precision limitations. Geographic areas over which the regional magnetostratigraphy master curves will apply can best be judged from a study of the historic magnetic field.

Table 2 summarizes global Holocene geomagnetic field changes. The main geomagnetic variation is the fluctuation of the axial dipole intensity (g_1^o). The magnitude and timing of these variations can be used to account for a large proportion of the changes in ^{14}C production through a shielding modulation of the flux of galactic cosmic rays. Spherical harmonic analyses of the paleomagnetic data plotted in Figure 1 reveal slow changes in the axis of the geomagnetic dipole about the earth's spin axis (Table 2). The analyses indicate that the dipole axis was markedly tilted away from the rotation axis around 7500 and 2500 years ago as well as during the last few hundred years. An estimate of the relative importance of the non-dipole field has been made through the residual errors (RSS) to the best fitting dipole (Table 2). The non-dipole field appears to have been relatively strong around 7500 years BP and relatively weak around 5000 years BP.

THE HISTORICAL FIELD

Spherical harmonic analyses of historic and archaeomagnetic data provide a consistent set of harmonic coefficients at 50-year intervals since AD 1600 (Thompson and Barraclough, in press). By taking differences between these coefficients, global maps of magnetic field changes can be constructed. Two maps are shown in Figure 2A and B for the North Atlantic region. These illustrate the change in position of the westerly declination maxima WEa (Fig. 1) and the inclination maxima WEα (Fig 1) between AD 1625 and 1975. The maps were prepared by calculating and contouring the zero isopores of the rate of change of declination (D) and inclination (I). The zero isopores, in common with many features of the non-dipole field, exhibit a general westward drift. Their drift rate varied markedly from place to place, eg, compare the AD 1675 and 1875

Table 1. Ages of magnetostratigraphic features

Declination

Turning points	SA	NA	WE	EE	NE	EA	NP
a	300	-	140	160	220	0	900
b	680	100	450	300	700	700	1100
c	1300	750	600	600	850	1200	1800
d	2000	1200	1000	1400	1300	1650	2150
e	2800	2000	2000	2200	1900	2200	3200
f	3500	2400	2600	3100	2100	3100	3900
g	4500	4000	4900	5700	2400	4400	4400
h	5500	5900	7100	6500	3200	5100	5300
i	8300	7000	8300	7600	5600	7300	5600
j	9000	7900	9100	8000	-	-	6000
k	-	9000	10000	8700	-	-	7300
l	-	-	-	9000	-	-	8350
m	-	-	-	-	-	-	8900

Inclination

Turning points	SA	NA	WE	EE	NE	EA	NP
α	-	50	240	300	300	-	200
β	0	420	650	600	550	400	2150
γ	400	750	1150	1300	700	760	3500
δ	900	1200	1650	1900	900	1000	4700
ε	1900	2300	3100	2600	1400	1300	5100
ζ	2600	2900	3800	4600	2000	1550	5800
η	3200	3700	4300	5500	3600	1750	7000
θ	3600	4400	5000	6400	5300	2800	8200
ι	4600	5300	6000	7200	-	4100	8950
κ	6000	6600	7100	7800	-	4600	9800
λ	6800	7700	8300	8600	-	5100	-
μ	7900	8400	8800	-	-	5600	-
ν	8600	9600	9700	-	-	6600	-
ξ	10000	-	-	-	-	-	-

SA	South Australia	(35°S 140°E)
NA	North America	(45°N 90°W)
WE	Western Europe	(55°N 05°W)
EE	Eastern Europe	(60°N 30°E)
NE	Near East	(30°N 35°E)
EA	Eastern Asia	(35°N 140°E)
NP	North Pacific	(20°N 155°W)

Ages tabulated in calibrated ^{14}C years BP. The pre-2000 BP EA magnetostratigraphic features are taken from Horie et al (1981). The EA ages are rather poorly known, based here on a linear interpolation between the basal tephra layer and the archaeomagnetic features in the upper sediments. The NP turning points are based on the ^{14}C dated lava flow palaeomagnetic data of McWilliams et al (1982).

Table 2 Geomagnetic coefficients and parameters

Epoch BP	g_1^o μT	λ_c	ϕ_c	g_2^o/g_1^o	RSS	Regions
Present	-30.5	79°N	070°W	+0.05	-	>100
0	-30.5	81	087 W	+0.02	0.011	7
500	-37.6	83	086 W	-0.02	0.009	7
1000	-40.9	89	041 W	+0.04	0.014	7
1500	-41.8	85	163 E	+0.03	0.008	7
2000	-42.0	87	165 W	+0.07	0.018	7
2500	-44.0	80	155 E	+0.04	0.019	7
3000	-40.2	85	121 E	+0.02	0.011	7
3500	-33.9	89	110 W	-0.04	0.023	7
4000	-32.5	88	001 E	+0.00	0.015	7
4500	-32.6	88	008 E	-0.01	0.004	7
5000	-30.0	86	020 W	-0.02	0.003	7
5500	-26.9	84	080 W	-0.02	0.004	7
6000	-25.4	86	090 W	-0.01	0.008	6
6500	-25.2	86	015 W	+0.02	0.005	6
7000	-25.5	82	004 W	-0.06	0.019	6
7500	-27.1	80	054 W	+0.13	0.036	5
8000	-30.2	87	155 W	-0.01	0.004	5
8500	-32.8	88	113 E	-0.09	0.011	5
9000	-33.0	88	023 W	-0.04	0.011	5

g_1^o is the strength of the axial dipole. This is the dominant term in the spherical harmonic expansion of the earth's internal magnetic field and is the main parameter to be considered in assessing the influence of geomagnetic field variations on ^{14}C production. λ_c is the latitude of the north magnetic pole. ϕ_c is the longitude of the north magnetic pole. g_2^o/g_1^o is the ratio of the axial quadrupole to the axial dipole and is an important geomagnetic parameter in assessing asymmetry between the northern and southern hemispheres. RSS is the mean residual sum of squares, here presented as a proportion of the axial dipole (i e, with $g_1^o = 1.0$), to the palaeolimnomagnetic direction data when fitted by a 'tilted' geocentric dipole. RSS is a measure of the non-dipole field. Large values indicate times of high non-dipole to dipole field ratio. The right hand column notes the number of regions used in the calculations. The data used are shown in Fig 1. The effect of data distribution can be judged by comparing the 0 BP parameters with those of the present field. The small number of regions available for analysis and the lack of absolute orientation of the palaeomagnetic records can lead to systematic errors in spherical harmonic analyses.

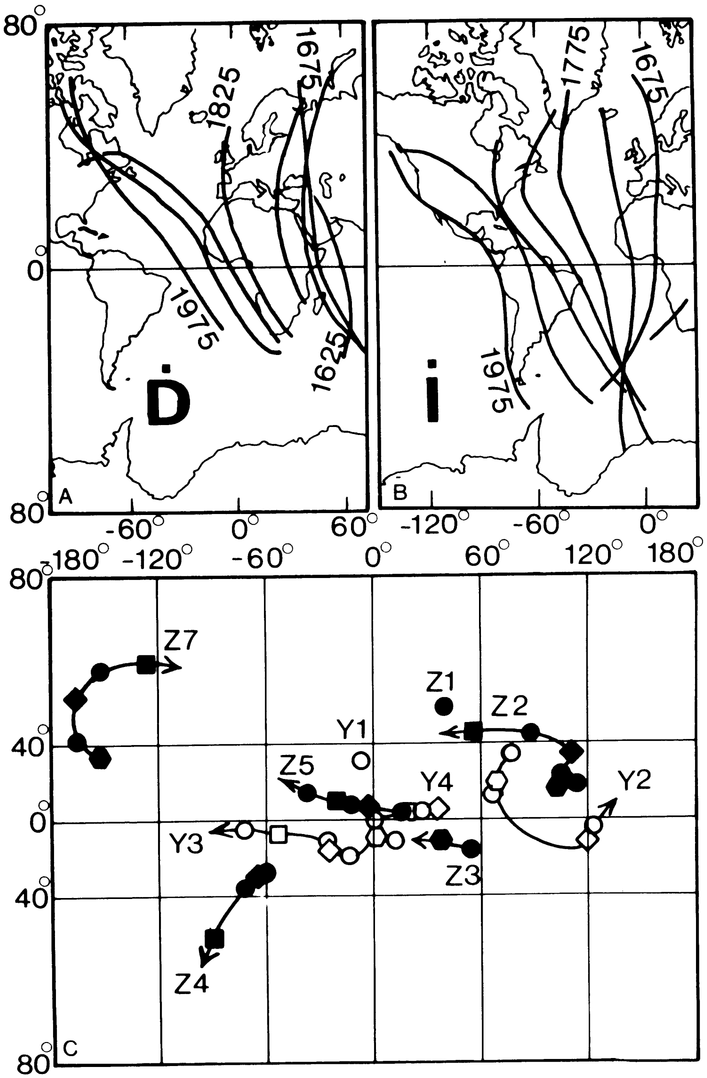

Fig 2. Examples of geomagnetic changes between AD 1625 and 1975. A. Location of the isopore D = 0. B. Location of the isopore I = 0. C. Major foci of changes in Y (open symbols) and Z (closed symbols) at 50-year intervals. Positive anomalies have even codes (eg, Y2), negative anomalies have odd codes. Hexagons, diamonds, and squares correspond to epochs AD 1725, 1825 and 1925, respectively.

positions of the zero D isopore at the equator and at the latitude of Britain in Figure 2A. These differences and the overall changes can be understood in terms of the growth, movement, and decay of local centers of secular change. Figure 2C shows the location of isoporic foci of the field elements Y and Z calculated from Thompson and Barraclough's coefficients. Changes in the easterly horizontal element (Y) and the vertical element (Z) are closely related to changes in declination and inclination, respectively. The 17th century pattern of North Atlantic declination changes was dominated by the foci Y1 and Y2. The change in location of the westerly declination turning point WEa (ie zero D isopore) has been controlled partly by the establishment of the new foci Y3 and Y4 and partly by the movement of all four foci. The change in position of the zero I isopore (WEα) was controlled by the evolution and movement of the minimum focus Z5 gradually replacing the foci Z1 and Z3, (Fig 2C).

SUMMARY

Holocene field intensities have varied by a factor of 2 or 3 due to fluctuations in the geomagnetic dipole moment, whereas field direction changes have been dominated by the turbulent evolution of the non-dipole field with short-lived foci of secular change. The foci have combined, largely at random, to produce the field variations of Figure 1. Analysis of historic field variations reveals regions of similar field changes several thousand kilometers in extent. The boundaries between such regions undoubtedly alter along with the field changes; nevertheless, the regional master curves (Fig 1) are likely to be useful over distances of several hundred kilometers and possibly a few thousand kilometers. The age differences of turning points, due to source drift, across such distances is only ca 100 years. When dating older Holocene sediments, such differences are not of critical importance, and for younger historic materials, the turning point chronology has now been mapped (Fig 2A, B).

ACKNOWLEDGMENTS

I thank C Barton, M Hyodo, and M O McWilliams for providing listings of their paleomagnetic data.

REFERENCES

Banerjee, SK, Lund, SP and Levi, S, 1979, Geomagnetic record in Minnesota lake sediments - Absence of the Gothenburg and Erieau excursions: Geology, v 7, p 588-591.

Barton, CE and McElhinny, MW, 1981, A 9000 year geomagnetic secular variation record from three Australian Maars: Geophys Jour Royal Astron Soc, v 67, p 465-485.

Bucha, V, 1970, Influence of the Earth's magnetic field on radiocarbon dating, in Olsson, IU, ed, ^{14}C variations and absolute chronology: New York, John Wiley & Sons, p 501-511.

Clark, RM, 1975, A calibration curve for radiocarbon dates: Antiquity, v 49, p 251-266.

Horie, S, Yaskawa, K, Yamamoto, T and Hyodo , M, in press, Paleolimnology of Lake Kizaki: Archives Hydrobiol, in press.

Huttonen, P and Stober, J, 1980, Dating of palaeomagnetic records from Finnish lake sediment cores using pollen analysis: Boreas, v 9, p 193-202.

Mackereth, FJH, 1958, A portable core sampler for lake deposits: Limnol Oceanogr, v 3, p 181-191.

Mackereth, FJH, 1971, On the variation in direction of the horizontal component of remanent magnetization in lake sediments: Earth Planetary Sci Letters, v 12, p 332-338.

Malin, SRC and Hodder, BM, 1982, Was the 1970 geomagnetic jerk of internal or external origin?: Nature, v 296, p 726-728.

McElhinny, MW and Senanayake, WE, in press, Variations in the geomagnetic dipole 1: The past 50,000 years: Jour Geomagnetism Geoelectricity.

McWilliams, MO, Holcomb, RT and Champion, DE, 1982, Geomagnetic secular variation from ^{14}C dated lava flows on Hawaii: Royal Soc [London] Philos Trans, v A306, p 211-222.

Olsson, IU, 1979, Radiometric dating in palaeohydrobiological changes in the temperate zone in the last 15000 years, in Berglund, BE, ed, IGCP 158, Lund.

Smith, PJ, 1966, Ancient geomagnetic field intensities, I Historic and archaeological data: Sets H1-H9: Geophys Jour Royal Astron Soc, v 13, p 417-419.

Thompson, R and Barraclough, DR, in press, Geomagnetic secular variations based on spherical harmonic and cross validation analyses of historical and archaeomagnetic data: Jour Geomagnetism Geoelectricity, in press.

Thompson, R and Turner, GM, 1979, British geomagnetic master curve 10,000 - 0 yr BP for dating European sediments: Geophys Research Letters, v 6, p 249-252.

Tolonen, K, Siiriainen, A and Thompson, R, 1975, Prehistoric field erosion sediment in Lake Lojarvi, S Finland and its palaeomagnetic dating: Ann Bot Fenn, v 12, p 161-164.

Walton, D, 1979, Geomagnetic intensity in Athens between 2000 BC and 400: Nature, v 272, p 643-644.

[Radiocarbon, Vol 25, No. 2, 1983, P 239-248]

ATMOSPHERIC RADIOCARBON: IMPLICATIONS FOR THE GEOMAGNETIC DIPOLE MOMENT

R S STERNBERG* and P E DAMON
Laboratory of Isotope Geochemistry
Department of Geosciences
University of Arizona
Tucson, Arizona 85721

INTRODUCTION

The geomagnetic field is one of the major physical fields of the earth. Because its source is fluid motion in the outer core, it exhibits temporal changes, called secular variation, which are quite rapid compared to most geologic phenomena. The prehistoric secular variation is usually inferred from paleomagnetic data. We will discuss here how changes in the atmospheric ^{14}C content can be used to gain additional insight into the behavior of the dipole moment over the past 8500 years. By rewriting the differential equations representing the ^{14}C geochemical cycle in finite-difference form, we are able to convert the atmospheric ^{14}C activity record into an equivalent radiocarbon dipole moment.

DIPOLE MOMENT AND ^{14}C FLUCTUATIONS

The changing strength of the geomagnetic dipole moment is one of the fundamental modes of secular variation of the recent geomagnetic field. Spherical harmonic analyses of geomagnetic field strength measurements since 1835 reveal a 6% linear decrease of the dipole moment (McDonald and Gunst, 1967). Syntheses of paleomagnetic field strengths (paleointensities) covering the last few millennia (Barton, Merrill, and Barbetti, 1979) show a quasi-sinusoidal oscillation of the dipole moment, subsuming the more recent linear decrease. This oscillation has a period of 8000 to 10,000 years, a mean moment of ca 8 x 10^{22} Am^2 (equal to present-day value), and maximum moment of ca 12 x 10^{25} Am^2 occurring 2000 to 2500 years ago. More attention has recently been given to the possibility that dipole moment fluctuations occur with periods less than the long-term 8000 to 10,000-year oscillations. Rapid paleointensity fluctuations on the order of 1000 years or less have been found at several different localities (see Games, 1980). Spectral analysis of dipole moment data by Champion (1980) revealed small concentrations of power at periods of 575,

---

*Now at Department of Geology, Franklin and Marshall College, P O Box 3003, Lancaster, Pennsylvania 17604

750, 950, and 2060 years (besides the predominant periodicity at 8700 years). Burlatskaya et al (1970) found a statistically significant dipole moment periodicity of 1000 years, and possibly significant peaks at 350 and 500 years. Yukutake's (1971) analysis of the magnetic field for the 17th and 18th centuries suggested a dipole moment fluctuation with a characteristic time of ca 350 years.

The nature of the paleointensity experiment, other modes of secular variation, and the poor temporal and spatial distribution of the paleointensity data make it difficult to conclusively infer these shorter periodicities from the paleomagnetic data (Barton, Merrill, and Barbetti, 1979). Holocene paleointensities become increasingly sparse prior to 2500 years BP due to the scarcity of well-dated archaeologic materials and igneous rocks. The geographic distribution of the Holocene data is poor for the entire record. Most of the data are from Europe and Asia; 98% are from the northern hemisphere. The current magnetic field shows an asymmetry between the northern and southern hemispheres (McDonald and Gunst, 1967). It is clearly risky to infer global magnetic field behavior from the primarily northern hemisphere archaeomagnetic data base.

^{14}C is created in the atmosphere when neutrons generated by cosmic ray interactions combine with ^{14}N. The flux of the charged cosmic rays into the atmosphere and the consequent ^{14}C production rate is modulated by the changing strength of the dipole moment (Elsasser, Ney, and Winckler, 1956; Lingenfelter and Ramaty, 1970). Thus, ^{14}C production is a global integrator of the magnetic field. As the production rate changes, ^{14}C activity in the various geochemical reservoirs will exhibit corresponding changes. A detailed 7300-year record of atmospheric activity fluctuations was determined from ca 1200 ^{14}C measurements on dendrochronologically dated tree-ring samples (Klein et al, 1980). This record can be used as a proxy indicator of dipole moment changes. The predominant long-term trend in ^{14}C activity with a peak-to-peak amplitude of ca 90 ‰ and a period of 8000 to 10,000 years is accepted to be due to the dipole moment oscillation with the same characteristic periodicity. Smaller wiggles (Suess, 1970; de Jong, Mook, and Becker, 1979) are superimposed upon this trend. Houtermans (ms) showed amplitude spectra peaks in the ^{14}C data at periods of 1000, 400, and 200 years. The 200-year periodicity has been confirmed by Neftel, Oeschger, and Suess (1981). Although these higher frequency fluctuations are generally assumed due to heliomagnetic modulation of ^{14}C production, there remains the possibility of dipole moment oscillations of similar frequency. Damon, Lerman, and Long (1978) reviewed the general problem of temporal fluctuations of ^{14}C.

RADIOCARBON DIPOLE MOMENT

The relationship between dipole moment changes and ^{14}C activity has been examined by several investigators (see references in Sternberg and Damon, 1979). The general approach has been to model the ^{14}C geochemical cycle as a system of connected reservoirs. There is input to the system through ^{14}C production, loss from the system through radioactive decay, and first-order exchange of ^{14}C between the different reservoirs, or elements, of the system. The model can then be represented by a set of linear differential equations. Model parameters are selected. A sinusoidal dipole moment model consistent with the paleomagnetic data is chosen, and a corresponding production function calculated. Predicted ^{14}C fluctuations are then compared to the activity record.

Libby (1967) explicitly suggested that "the agreement of radiocarbon dates with historical records up to 3500 to 4000 years ago within 1 or 2% places a serious restriction on the types of variation which the earth's effective dipole moment could have undergone." Kigoshi and Hasegawa (1966), Ramaty (1967), and Sternberg and Damon (1979) explored the sensitivity of the predicted ^{14}C activity to different magnetic field models. Nonetheless, the forward modeling problem has only been used (and is most convenient) with dipole moments having the single, characteristic long-term periodicity.

Barton, Merrill, and Barbetti (1979) perceived that the tree-ring record of ^{14}C activity was more complete than the paleointensity data. They assumed that all ^{14}C fluctuations are due to geomagnetic modulation, "and that the production and decay of ^{14}C instantaneously balanced so that the atmospheric concentration varies linearly with production." The shape of their computed radiocarbon dipole moment (RCDM) showed a broad maximum between 1500 and 3000 BP, agreeing with the modeling of Sternberg and Damon (1979) and the compiled paleomagnetic data of Champion (1980). However, both the average RCDM ($\sim 7.5 \times 10^{22}$ Am^2) and the amplitude of the RCDM oscillation ($\sim 0.7 \times 10^{12}$ Am^2) were too low to be consistent with the paleomagnetic data.

We have improved upon the efforts of Barton, Merrill, and Barbetti (1979) by explicitly accounting for the effects of the carbon reservoir system (Sternberg and Damon, 1981). We used a two-box model with sedimentary sink (see Sternberg and Damon, 1979, Fig 2). One box represents the rapidly exchanging ambient reservoirs -- the atmosphere, biosphere, and mixed layer of the ocean. The other box represents the deep-sea. The system is represented by a pair of first-order linear differential equations:

$$\frac{dn_a(t)}{dt} = -(k_{as} + \lambda)\, n_a(t) + k_{sa} n_s(t) + Q(t) \qquad (1)$$

$$\frac{dn_s(t)}{dt} = k_{as}\, n_a(t) - (k_{sa} + k_{ds} + \lambda)\, n_s(t), \qquad (2)$$

where n_a and n_s are the ^{14}C contents of the ambient and deep-sea reservoirs; Q is the production rate; λ is the radioactive decay constant; and k_{as}, k_{sa}, k_{ds} the first-order exchange rates between the ambient reservoirs and deep-sea, deep-sea and ambient reservoir, and from the deep-sea to the sedimentary sink, respectively.

The forward modeling problem is done by inputting Q(t) and calculating the response, $n_a(t)$ and $n_s(t)$. However, we wish to do the converse. We followed the approach of Stuiver and Quay (1980b), who applied a finite-difference approximation to their linear differential equations to back-calculate the heliomagnetic production rate for 860 years of ^{14}C data. Using first-order backward differences, equations 1 and 2 become

$$\frac{n_a(t) - n_a(t - \Delta t)}{\Delta t} = -(k_{as} + \lambda) n_a(t) + k_{sa} n_s(t) + Q(t) \quad (3)$$

$$\frac{n_s(t) - n_s(t - \Delta t)}{\Delta t} = k_{as}\, n_a(t) - (k_{sa} + k_{ds} + \lambda)\, n_s(t) \quad (4)$$

These equations can be manipulated to obtain

$$n_s(t + \Delta t) = \frac{n_s(t) + k_{as}\, n_a(t + \Delta t)\, \Delta t}{1 + \Delta t\, (k_{sa} + k_{ds} + \lambda)} \qquad (5)$$

$$Q(t + \Delta t) =$$

$$(k_{as} + \lambda + 1/\Delta t)\, n_a(t + \Delta t) - \frac{n_a(t)}{\Delta t} - k_{sa}\, n_s(t + \Delta t). \quad (6)$$

The ^{14}C contents n_a and n_s then can easily be converted to activities.

Klein et al (1980) applied a multistage linear regression technique to derive annual per mil atmospheric activities from the 7300-year tree-ring record. This can be converted to the series $n_a(t)$. Once k_{as} has been selected, equation 5 will generate the time series $n_s(t)$ if $n_s(t{=}0)$ is known. This initial condition was calculated from equation

2 by assuming steady state. Once the time series $n_s(t)$ was generated, it was used along with $n_a(t)$ in equation 6 to generate the series $Q(t)$. To convert the production into an equivalent dipole moment, M, a relation of the following form was used:

$$Q = CM^{-\alpha} \tag{7}$$

where C is a constant of proportionality and $\alpha \approx 0.5$ (Elsasser, Ney, and Winckler, 1956; Ramaty, 1967). The constant C was calculated to set the dipole moment at AD 1950 to 8.065×10^{22} Am^2, the value given by McDonald and Gunst (1967).

RESULTS AND DISCUSSION

Three independent model parameters must be set. In equations 3 and 4, these are k_{as}, k_{sa}, and k_{ds}. For our initial parameter set, we used the following: $k_{as} = 1/50$ yr^{-1}, $k_{sa} = 1/1250$ yr^{-1}, $k_{ds} = 5 \times 10^{-6}$ yr^{-1}, $\alpha = 0.45$, and $\Delta t = 10$ yr. These values are in accord with others suggested in the literature for the two-box model (eg, Houtermans, Suess, and Oeschger, 1973). They also were successful in predicting a good fit to the ^{14}C data using a sinusoidal dipole moment in the forward problem (Sternberg and Damon, 1979).

The resulting raw RCDM is shown in Figure 1. The anticipated long-term quasi-sinusoidal variation is evident. However, the superimposed high-frequency variations are too large and rapid to represent real geomagnetic behavior. These fluctuations are an artifact of the modeling procedure. The ^{14}C system represented by equations 1 and 2 acts as a low-pass filter, causing this effect.

The amplitude response spectrum for fluctuations of ^{14}C in the atmosphere for the two-box model is show in Figure 2. It is compared with similar spectra for the three-box model, the five-box model, and the box diffusion model (see Damon, Sternberg, and Radnell, 1983). These plots show

$$\frac{n_a(\omega)}{Q(\omega)} \div \frac{n_a(0)}{Q(0)} ,$$

the normalized response (or attenuation) of atmospheric ^{14}C to a harmonic production rate. Changes in the activity of the reservoirs are attenuated relative to changes in the production rate. Because the system is a low-pass filter, high frequencies in the activity data will be amplified in the calculation of the RCDM.

Normalization of the amplitude spectra is by the DC gain (Lazear, Damon, and Sternberg, 1980), which is essentially a scaling factor relating $Q(0)$ to $n_a(0)$. The DC gains for the 3B, 5B, and BD have been adjusted downwards to values of

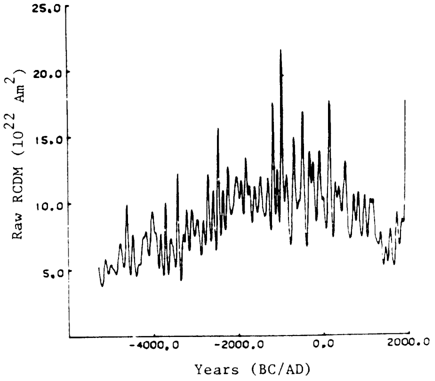

Fig 1. The raw radiocarbon dipole moment vs time. Calculated from the tree-ring activity record using a finite-difference representation of the two-box model.

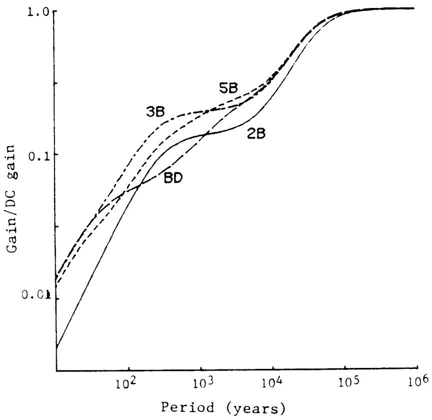

Fig 2. Amplitude spectra of reservoir models for atmospheric ^{14}C fluctuations. 2B, two-box model used in this study; 3B, three-box model; 5B, five-box model; BD, box diffusion model.

111 yr by the addition of sedimentary sinks (Damon, Sternberg, and Radnell, 1983). The DC gain for the two-box model is 352 yr. This is because the two-box model incorporates the mixed layer and biosphere into the ambient reservoir (Houtermans, Suess, and Oeschger, 1973) while the more complex models retain a separate mixed layer.

Much of the higher frequency content of the RCDM either represents noise in the activity data or heliomagnetic modulation. Sunspots are one manifestation of solar activity. Spectral analysis of post-AD 1750 sunspot numbers (Cohen and Lintz, 1974) shows that power is concentrated at a periodicity of 10.9 years corresponding to the well-known sunspot cycle. A smaller spectral peak exists at 110 years, and the longest periodicity of 179 years is due to a beating effect. Longer periodicities cannot be inferred from the extant sunspot record. Considering that the shorter periodicities noted for the dipole moment are $\geq$ 350 years, it may be possible to separate geomagnetic from heliomagnetic (and other high-frequency) effects.

To effect this separation, the raw RCDM was smoothed by convolution with a Gaussian smoothing function. Weights of this filter and the amplitude response have the shape of a normal distribution. The filter weights can be determined by specifying the response at a particular frequency. Furthermore, no phase-shifting is introduced. The filter used was designed to have a response of 10% for a period of 200 years since this periodicity seems to represent a breakpoint between geomagnetic and heliomagnetic effects. Some higher frequency information is inevitably admitted and some

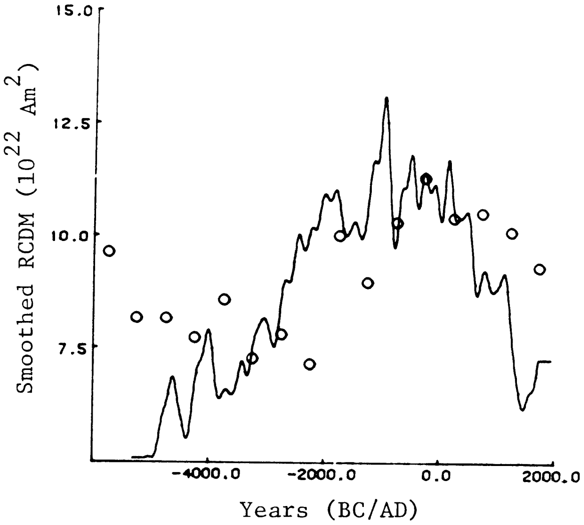

Fig 3. The smoothed ^{14}C dipole moment vs time. The circles are 500-yr averages for the dipole moment from paleomagnetic data (Champion, 1980).

lower frequency information is filtered. The response at periods of 10, 500, 1000 and 10,000 years is 0.01%, 69%, 91% and 99.9%, respectively.

The resulting smoothed RCDM is shown in Figure 3. The long period quasi-sinusoid is still evident, with an average moment of ca 9 x 10^{22} Am^2, an amplitude of 3 x 10^{22} Am^2, and a broad maximum lasting from ca AD 200 to 1100 BC. This is different than the earlier paleomagnetic syntheses which placed the dipole maximum early in AD times. However, Sternberg and Damon (1979) concluded from forward modeling that a sinusoidal dipole moment model should peak closer to 500 BC. This conclusion is also consistent with the recent paleomagnetic summary of Champion (1980). His 500-year interval average dipole moments are plotted as circles in Figure 3. These data show the peak dipole moment occurring at 300 BC.

The smoothed RCDM agrees quite well with the paleomagnetic data between 3000 BC and AD 1 with the exception of two points. However, the paleomagnetic results are consistently higher during the intervals 6000 to 4000 BC and AD 500 to 1900. There are three possible reasons for these discrepancies. First, the paleomagnetic results may not properly reflect the dipole moment due to their poor geographic distribution and their sparseness prior to 500 BC. The strength of the magnetic field is currently stronger in the northern hemisphere than at corresponding latitudes in the southern hemisphere (McDonald and Gunst, 1967). Since most archaeomagnetic data are from the northern hemisphere, this is in the right sense to account for the discrepancies.

A second possible problem is with the modeling. This could result from using an oversimplified model or from incorrect parameterization of the model. Figure 2 shows that there are differences in the amplitude spectra for the periodicities of interest, 10^2 to 10^4 years. Thus, these models as parameterized are not completely compatible with one another. Also, the two-box model parameters were assumed to be constant. However, reservoir sizes and exchange rates could vary over time in response to climatic change. These effects have probably been minor since the transition to the Holocene (Damon, 1970; Siegenthaler, Heimann, and Oeschger, 1980; Stuiver and Quay, 1980a), but might be significant for the calculations ca 7500 BP.

A third possible cause for the discrepancies between the RCDM and the paleomagnetic data is the choice of a proper filter. The final frequency content of the smoothed RCDM depends on the response functions of both the model and the filter. While the filter used was designed in accord with the general spectra of geomagnetic and heliomagnetic fluctuations, the final choice of response function and filter weights was somewhat arbitrary. Also, longer records of heliomagnetic activity might reveal lower frequencies that would overlap with geomagnetic frequencies.

In conclusion, the radiocarbon dipole moment successfully reflects the general pattern of recent variation of the dipole moment. The RCDM complements the paleomagnetic data, and may allow inferences to be made on north-south asymmetry of the magnetic field or variations of the reservoir parameters over time. Our future work will concentrate on refinement of the modeling (different parameter sets and more complex models) and further investigation of the nature of the discrepancies between the RCDM and the paleomagnetic data. We will also extend the RCDM back to 8550 BP, based on new ^{14}C measurements of older bristlecone pine samples.

ACKNOWLEDGMENTS

We thank Juan Carlos Lerman and Jeff Klein for supplying the ^{14}C data base. The work was supported by National Science Foundation grant EAR-8116196.

REFERENCES

Barton, D E, Merrill, R T, and Barbetti, M, 1979, Intensity of the earth's magnetic field over the last 10 000 years: Physics Earth Planetary Interiors, v 20, p 96-110.

Burlatskaya, S P, Nachasova, I E, Uechaeva, T B, Rusakov, O M, Zagniv, G F, Tarhov, E N, and Tchelidze, Z A, 1970, Archaeomagnetic research in the U S S R: Recent results and spectral analysis: Archaeometry, v 12, p 73-85.

Champion, D E, 1980, Holocene geomagnetic secular variation in the western United States: Implications for the global geomagnetic field: U S Geol Survey open-file rept 80-824, Denver, Colorado.

Cohen, T J and Lintz, P R, 1974, Long term periodicities in the sunspot cycle: Nature, v 250, p 393-399.

Damon, P E, 1970, Climatic versus magnetic perturbation of the atmospheric C14 reservoir, in Olsson, I U, ed, Radiocarbon variations and absolute chronology: John Wiley and Sons, New York, p 571-593.

Damon, P E, Lerman, J C, and Long, A, 1978, Temporal fluctuations of atmospheric ^{14}C: Causal factors and implications: Ann Rev Earth Planetary Sci, v 6, p 457-494.

Damon, P E, Sternberg, R S, and Radnell, C J, 1983, Modeling atmospheric radiocarbon fluctuations for the past three centuries in Stuiver, Minze and Kra, Renee eds, Internatl radiocarbon conf, 11th, Proc: Radiocarbon, v 25.

Elsasser, W, Ney, E P, and Winckler, J R, 1956, Cosmic-ray intensity and geomagnetism: Nature, v 178, p 1226-1227.

Games, K P, 1980, The magnitude of the archaeomagnetic field in Egypt between 3000 and 0 BC: Geophys Jour Royal Astron Soc, v 63, p 45-56.

Houtermans, J C, ms, 1971, Geophysical interpretations of bristlecone pine radiocarbon measurements using a method of Fourier analysis of unequally spaced data: unpub PhD dissert, Univ Bern.

Houtermans, J C, Suess, H E, and Oeschger, H, 1973, Reservoir models and production rate variations of natural radiocarbon: Jour Geophys Research, v 78, p 1897-1908.

deJong, A F M, Mook, W G, and Becker, B, 1979, Confirmation of the Suess wiggles: 3200-3700 BC: Nature, v 280, p 48-49.

Kigoshi, K and Hasegawa, H, 1966, Secular variation of atmospheric radiocarbon concentration and its dependence on geomagnetism: Jour Geophys Research, v 71, p 1056-1071.

Klein, J, Lerman, J C, Damon, P E, and Linick, T W, 1980, Radiocarbon concentration in the atmosphere: 8000 year record of variations in tree rings: first results of a U S A workshop, in Stuiver, Minze and Kra, Renee, eds, Internatl radiocarbon conf, 10th, Proc: Radiocarbon, v 22, no 3, p 950-961.

Lazear, G, Damon, P E, and Sternberg, R, 1980, The concept of DC again in modeling secular variations in atmospheric ^{14}C, in Stuiver, Minze, and Kra, Renee, eds, Internatl radiocarbon conf, 10th, Proc: Radiocarbon, v 22, no 2, p 318-327.

Libby, W F, 1967, Radiocarbon and paleomagnetism, in Hindmarsh, W R, Lowes F J, Roberts, P H, and Runcorn, S K, eds, Magnetism and the cosmos: New York, Am Elsevier, p 60-65.

Lingenfelter, R E and Ramaty, R, 1970, Astrophysical and geophysical variations in C14 production, in Olsson, I U, ed, Radiocarbon variations and absolute chronology: New York, John Wiley and Sons, p 513-537.

McDonald, K and Gunst, R, 1967, An analysis of the earth's magnetic field from 1835 to 1965: ESSA tech rept IER 46-IFS 1, Washington, US Govt Printing Office, 87 p.

Neftel, A, Oeschger, H, and Suess, H E, 1981, Secular non-random variations of cosmogenic carbon-14 in the terrestrial atmosphere: Earth Planetary Sci Letters, v 56, p 127-147.

Ramaty, R, 1967, The influence of geomagnetic shielding on C^{14} production and content, in Hindmarsh, W R, Lowes, F J, Roberts, P H, and Runcorn, S K, eds, Magnetism and the cosmos: New York, Am Elsevier, p 66-78.

Siegenthaler, U, Heimann, M, and Oeschger, H, 1980, ^{14}C variations caused by changes in the global carbon cycle, in Stuiver, Minze, and Kra, Renee, eds, Internatl radiocarbon conf, 10th, Proc: Radiocarbon, v 22, no 2, p 177-191.

Sternberg, R S and Damon, P E, 1979, Sensitivity of radiocarbon fluctuations and inventory to geomagnetic and reservoir parameters, in Berger, Rainer and Suess, E, eds, Radiocarbon dating, Internatl radiocarbon conf, 9th, Proc: Berkeley, Univ California Press, p 691-717.

________________ 1981, A finite-difference solution for the radiocarbon dipole moment: EOS, v 62, p. 272

Stuiver, Minze and Quay, P D, 1980a, Patterns of atmospheric ^{14}C changes, in Stuiver, Minze and Kra, Renee, eds, Internatl radiocarbon conf, 10th Proc: Radiocarbon, v 22, no 2, p 166-176.

________________ 1980b, Changes in atmospheric carbon-14 attributed to a variable sun: Science, v 207, p 11-19.

Suess, H E, 1970, The three causes of the secular C14 fluctuations, their amplitudes and time constants, in Olsson, I U, ed, Radiocarbon variations and absolute chronology: New York, John Wiley and Sons, p 595-605.

Yukutake, T, 1971, Spherical harmonic analysis of the earth's magnetic field for the 17th and 18th centuries; Jour Geomagnetism Geoelectricity, v 23, p 11-31.

[Radiocarbon, Vol 25, No. 2, 1983, P 249-258]

MODELING OF ATMOSPHERIC RADIOCARBON FLUCTUATIONS FOR THE PAST THREE CENTURIES

P E DAMON*, R S STERNBERG**, and C J RADNELL†

INTRODUCTION

Relatively precise quantitative observations of geophysical parameters are available to evaluate the fluctuations of atmospheric ^{14}C activity during the past three centuries. As reviewed by Damon, Lerman, and Long (1978), these fluctuations seem to result from three factors: 1) changes in the earth's dipole magnetic field intensity, which has been decreasing since the first measurements by Gauss (McDonald and Gunst, 1968); 2) solar modulation of the cosmic-ray production, which has been correlated with the sunspot record of Waldmeier (1961), and more recently, to the Aa geomagnetic index by Stuiver and Quay (1980); and 3) the combustion of fossil fuels (Suess, 1955). A relationship between the climatic time series and the ^{14}C-derived record of solar change has not yet been demonstrated (Stuiver, 1980).

To relate ^{14}C fluctuations to geophysical parameters, we must use reservoir models as analogues to the ^{14}C cycle. We have investigated four models of the ^{14}C exchange system (Lazear, Damon, and Sternberg, 1980), a 1-box model (Grey and Damon, 1970), 3-box first-order exchange model (eg, Houtermans, Suess, and Oeschger, 1973), 5- and 6-box first-order exchange models (eg, Bacastow and Keeling, 1973; Ekdahl and Keeling, 1973), and a box-diffusion model (Oeschger et al, 1975). We will concentrate here primarily on the multibox and box-diffusion models that are more or less adequate analogues to nature.

None of the originally parameterized models included a sedimentary sink, which we added to all of the models because it significantly decreases the DC gain and improves their performance as natural system analogues. We suggested that the DC gain (Lazear, Damon, and Sternberg, 1980) and ^{14}C inventory (Sternberg and Damon, 1979) are useful boundary conditions that models and production functions should satisfy to be adequate natural analogues. We make use of these boundary conditions to evaluate both the production function and the amount of carbon entering into the sedimentary reservoir. Walsh et al (1981) indicate that the flux of carbon into the sedimentary sink may

---

*Laboratory of Isotope Geochemistry, Department of Geosciences, University of Arizona, Tucson, Arizona 85721

Department of Geology, **Franklin and **Marshall** College, P O Box 3003, Lancaster, Pennsylvania 17604

†College of Earth Sciences, Australian National University, P O Box 4, Canberra, ACT 2600, Australia

provide the missing carbon in the global CO_2 cycle required to account for fossil-fuel emission and the pioneer effect (ie, clearance of forests for agriculture).

INVENTORY (I) AND DC GAIN ($\bar{g}$)

One method of determining the total amount of ^{14}C in the geochemical cycle is to inventory the carbon reservoirs. Table 1 is an inventory modified from Damon, Lerman, and Long (1978). The modifications were to reduce the carbon content of the atmosphere to the pre-industrial level and to increase the activity of carbon entering the sedimentary sink to the level of the mixed layer rather than the deep sea because most of the carbon in sediments was derived from the mixed layer rather than the deep sea. The total carbon in the inventory sums to 9.65 g cm_e^{-2} and the decay rate is ca 120 dpm cm_e^{-2}.

TABLE 1. Radiocarbon inventory

Reservoir	C in reservoir (N) g cm_e^{-2}	^{14}C activity* in reservoir (A) dpm g^{-1} C	Decay rate in reservoir dpm cm_e^{-2}
Atmosphere	0.121	14.1	1.85
Terrestrial biosphere	0.108	13.6	1.47
Humus (dead terrestrial organic matter)	0.206	13.5	2.78
Hydrosphere (fresh water)	0.088	8.2	0.72
Hydrosphere (mixed layer of oceans)	0.180	13.6	2.44
Hydrosphere (deep sea)	7.386	12.3	90.85
Biosphere (marine)	0.001	14.2	0.01
Oceans (dead organic matter)	0.588	12.3	7.23
Sediments	0.972	13.6	13.22
	$\Sigma = 9.650$ g cm_e^{-2}	$\bar{A} = 12.3$ (dpm g^{-1})	$\Sigma = 120.5$ dpm cm_e^{-2}
			$= 2.01$ dps cm_e^{-2}

*Modified from Damon et al (1978).

The inventory (I) of radiocarbon decay rates in all reservoirs should have been balanced by past production:

$$I = -\lambda \int_{\infty}^{0} Q(t)e^{-\lambda t}dt \qquad (1)$$

where Q(t) is the production as a function of time (t), where t is measured from the present to the past, and λ is the decay constant of ^{14}C. This was evaluated by Sternberg and Damon (1979) for a sinusoidal dipole moment using the production function of Lingenfelter and Ramaty (1970) and the assumption that the average long term heliomagnetic activity has remained constant. The result was that I, calculated from equation 1, was ≥ 122 dpm cm_e^{-2} with a most probable value of 124 dpm cm_e^{-2}. This is not significantly different that the value of 120 dpm cm_e^{-2} obtained from the reservoir inventory.

O'Brien (1979) obtained a much lower production function than we calculated using a linear approximation relating Lingenfelter and Ramaty's production data to the Zurich sunspot numbers. The two production functions are:

$$Q = 2.434 - 0.00264\ S \text{ dps } cm_e^{-2} \quad \text{(Lingenfelter \& Ramaty, 1970)} \tag{2}$$

$$Q = 1.937 - 0.00242\ S \text{ dps } cm_e^{-2} \quad \text{(O'Brien, 1979)} \tag{3}$$

These two production functions were evaluated for different years and compared with other ^{14}C production calculations. Light et al (1973) agree with Lingenfelter and Ramaty (1970) and O'Brien's values are ca 30% lower. According to Lingenfelter (pers commun, 1982), O'Brien's calculations are theoretically correct but not adequately related to measurements of the neutron flux. Also, the inventory for O'Brien's production function calcuated from equation 1 yields a value that is ca 20% lower.

Lazear, Damon, and Sternberg (1980) state that the observed DC gain (g_{obs}) is equal to the ratio of the steady state ^{14}C content of the atmosphere ($\bar{N}_a^*$) to the steady-state production rate ($\bar{Q}$) which they approximated by mean values for the observed record and evaluated at 111 ± 22 years.

Using the standard parameters of the authors, we obtained the DC gain of the 3-box, 5-box, and box-diffusion model (table 2).

TABLE 2. Standard model DC gain ($\bar{g}$), steady-state atmospheric ^{14}C activities ($\bar{A}_a^*$), transfer constants (K_{sed}), ratios of mixed layer to atmospheric carbon contents (N_m/N_a), and required flux to the sedimentary sink (ϕ)

Model	$\bar{g}$ yr	$\bar{A}_a$* dpm g^{-1}	$\bar{A}_a$** dpm g^{-1}	K_{sed} yr^{-1}	N_m/N_a	ϕ† $\times 10^{15}$ g yr^{-1}
3-box	151	19.9	14.6	2.07×10^{-1}	1.3	1.66
5-box	150	19.8	14.5	1.28×10^{-3}	2.0	1.58
box-diffusion	142	18.7	13.7	1.73×10^{-3}	1.3	1.39

*Standard model with Lingenfelter and Ramaty (1970) production function and no sedimentary sink

**Standard model with O'Brien (1979) production function and no sedimentary sink

†Flux to the sedimentary sink required to reduce $\bar{g}$ to 111 yr

The model DC gains are high by ca 30%. Consequently, if the Lingenfelter and Ramaty (1970) production function is used, the models generate a high steady-state atmospheric ^{14}C content and high steady-state ^{14}C activities ($\bar{A}_a$):

$$\bar{N}_a^* = \bar{g}\,\bar{Q} \qquad (4) \qquad\qquad \bar{A}_a = \frac{\bar{N}_a^*}{N_a \bar{T}} \qquad (5)$$

where N_a is the pre-industrial atmospheric carbon content and $\bar{T}$ is the mean life of ^{14}C. Table 2 shows that the model-generated ^{14}C activities are unacceptably high (18.7 to 19.9 dpm $g^{-1}C$).

This problem can be rectified by using the lower production function of O'Brien (1979) or by adding a sedimentary sink to the standard models. Table 2 also shows that the O'Brien production function generates acceptable atmospheric ^{14}C activities. We believe this is fortuitous because the carbon inventory demands a sedimentary sink and O'Brien's production function yields a lower inventory and production rates compared to all other calculations. Inclusion of a sedimentary sink predicts sedimentary fluxes that are acceptably close to values required by inventories of the carbon cycle. The carbon in the sedimentary reservoir in table 1 is based on a flux (ϕ) of 0.6×10^{15} g yr^{-1} (Damon and Wallick, 1972). Hay and Southam (1977) estimated the minimum Holocene flux to the sedimentary reservoir at 0.43×10^{15} g yr^{-1} and the maximum Holocene sedimentary flux at 0.86×10^{15} g yr^{-1}. Walsh et al (1981) require a post-industrial flux of 1.8×10^{15} g yr^{-1}, with up to 0.75×10^{15} g yr^{-1} due to increased eutrophication since the industrial revolution, and 1.05×10^{15} g yr^{-1} entering the sedimentary sink prior to the industrial revolution. Thus, the sedimentary sink flux required by the models when evaluated with the Lingenfelter and Ramaty (1970) production function agrees reasonably well with independent estimates. Both Hay and Southam (1977) and Walsh et al (1981) emphasize the importance of the flux to shelf sediments. The latter authors suggest that this flux may account for the missing carbon in the global cycle that is required when the pioneer-effect emission is added to the fossil fuel emission. Use of the DC gain and inventory as boundary conditions also suggests that the surplus carbon produced by the pioneer effect can be accounted for by the flux to the sedimentary sink.

As suggested by Houtermans, Suess, and Oeschger (1973), the DC gain acts as a scaling factor because of its effect on the apparent ^{14}C activity of the atmosphere. Thus, the high ^{14}C activities produced by neglect of the sedimentary sink in table 2 will reduce ^{14}C fluctuations (Δ ‰) by 36% in all three models. We will demonstrate this in the model of the ^{14}C fluctuations observed during the past three centuries.

COMPARISON OF MODELS

We used a general-purpose electrical-circuit analysis program (SPICE, University of California) for evaluation of the 3-box, 5-box, and box-diffusion models and trapezoidal method of numerical integration. The program is convenient and useful for ac, dc, and transient analysis. We accepted the standard parameters used by the authors, modifying only the production function and adding a sedimentary sink when required by the DC gain. We were concerned with only the past three centuries for which sunspot data are available. We used Waldmeir (1961) sunspot numbers (S) as modified for the Maunder minimum by Eddy (1976). Fine tuning of the models was not necessary because performance of the models is insensitive to small changes in initial conditions after the first 100 years; we limited our comparisons to the 19th and late 18th centuries. We raised the atmosphere and mixed layer by ca 1.5% at AD 1650 to simulate the Maunder minimum while leaving the deep sea unchanged. For the box-diffusion model, we also assumed a 1.5% increase for the uppermost part of the ocean immediately below the mixed layer, exponentially decreasing to standard deep sea values with depth. We approximated the variation [Q(t)] resulting from the decreasing geomagnetic dipole field intensity [M(t)] using the geomagnetic field intensities from McDonald and Gunst (1968) and the relationship between Q(t) and M(t) derived by Elsasser, Ney, and Winckler (1956).

Figure 1 shows that the transfer functions are the same below periods of 1000 years for the standard models with high DC gain (~150) as for the models with DC gain adjusted to 111 by adding a sedimentary sink. Figure 2 shows the resulting response of the models with sedimentary sinks to the sunspot record using the Lingenfelter and Ramaty (1970) production function (eq 2). The response curve compares favorably with measured data after the reservoirs adjust to the initial conditions (see Damon, Lerman, and Long, 1978, fig 2; Stuiver and Quay, 1980, fig 5). There is a minimum, eg, at AD 1790 and a maximum at AD 1825 which also occur in the measured data (table 3), but, with a

TABLE 3. Comparison of model predictions with measurement

	Lingenfelter and Ramaty (1970) with sedimentary sink			O'Brien (1979) without sedimentary sink			Measured values Stuiver & Quay (1980)
	3B*	5B	BD	3B	5B	BD	
Min (°/oo) (AD 1790)	-6.26 (-4.52)	-3.22	-3.33	-5.83	-3.23	-2.87	-7
Max (°/oo) (AD 1825)	+0.33 (+0.20)	+0.58	+0.97	+0.27	+0.46	0.94	+3
Peak to peak (°/o)	6.59 (4.52)	3.80	4.30	6.10	3.69	3.81	10 (11)**
Phase lag (yr)	15	14	14	14	14	14	15
Sunspot min (°/oo) (AD 1856)	-0.87 (-0.64)	-0.94	-0.69	-0.71	-0.76	-0.72	?
Sunspot max (°/oo) (AD 1848)	-2.60 (-1.94)	-2.30	-2.40	-2.34	-2.02	-2.28	?
Peak to peak (°/o)	1.73 (1.30)	1.36	1.71	1.63	1.26	1.56	?
Phase lag (yr)	3	2	3	3	2	3	?

*Number in parentheses corresponds to Lingenfelter and Ramaty (1970) production function and 3B model without sedimentary sink

**Number in parentheses is from figure 2 of Damon, Lerman, and Long (1978)

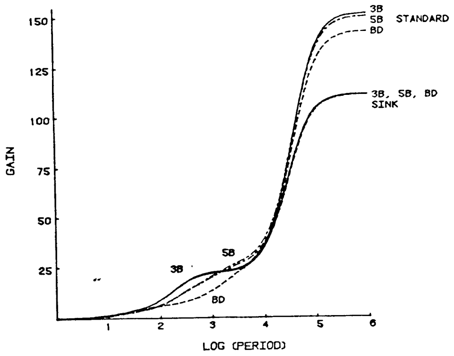

Fig 1. Transfer functions for 3-box (3B), 5-box (5B), and box-diffusion models (BD) with and without sedimentary sink.

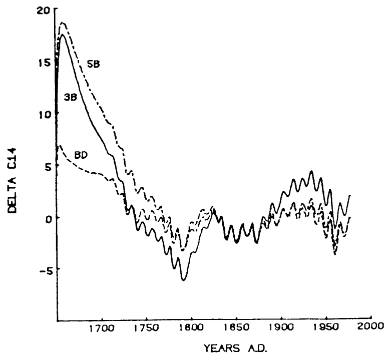

Fig 2. Response of 3B, 5B, and BD models with sedimentary sink to the Lingenfelter and Ramaty (1970) production function.

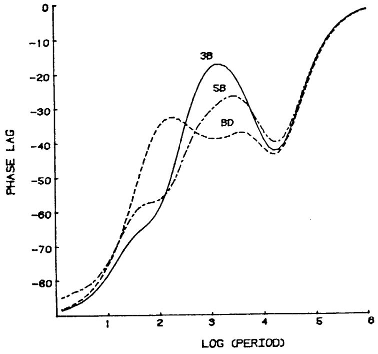

Fig 3. Phase lag of the 3B, 5B, and BD models with sedimentary sink.

greater amplitude. Amplitudes from the models are only 38% to 66% of the measured values but the phase lag corresponds to theory (fig 3). The standard models without sedimentary sink and using O'Brien's (1979) production function yield slightly lower amplitudes. The models also predict a peak-to-peak variation of 1.3‰ to 1.7‰ for the sunspot cycle with a minimum at AD 1856 (S = 4) and a maximum at AD 1848 (S = 125). Annual measurements at ± 2‰ for an entire sunspot cycle should be able to resolve a variation of that magnitude.

If the standard models without sedimentary sink are evaluated with Lingenfelter and Ramaty's (1970) production function, the "wiggles" are further reduced by the expected amount (eg, see the numbers in parentheses for 3B model in table 3. However, unreasonably high steady-state ^{14}C activities are generated compared to natural values (table 2) and initial ^{14}C activities must be increased to match the steady-state values. If the modeler is not aware of the high steady-state ^{14}C activities generated by the model and inputs reasonable ^{14}C activities for the natural environment, the ^{14}C activity and Δ values will start low and steadily climb to the steady-state value. The modeler may then be tempted to avoid the catastrophe of apparent atmospheric ^{14}C buildup by lowering the production rate to values that correct the problem at the expense of unacceptably low production rates relative to the natural environment. The modeler might also ignore the importance of the sedimentary sink in reducing the DC gain and, hence, the steady-state atmospheric ^{14}C activity. Thus, an important source of information would be lost.

DISCUSSION AND CONCLUSIONS

O'Brien's (1979) production function yields rates of production that are low compared to other independent estimates. It also yields an inventory that is 20% lower than that obtained by summing the disintegration rates in all reservoirs (table 1), whereas Lingenfelter and Ramaty's (1970) production function predicts an inventory (124 dpm cm_e^{-2}) very close to the estimate from table 1 (120 dpm cm_e^{-2}). We did not include ^{14}C dissolved in the water content of sediments in table 1 (Lazear, Damon, and Sternberg, 1980) which would raise the inventory and provide a source of ^{14}C-depleted carbon resulting from diagenesis and consequently, lower the ^{14}C activity of deep water. O'Brien's production function does not require a sedimentary sink to lower the DC gain. This further suggests that his estimates of ^{14}C production are too low because independent estimates demonstrate that the flux of carbon to sediments is very significant and, indeed, may account for the "missing" carbon in the carbon cycle.

In contrast, the production function that we obtain from Lingenfelter and Ramaty (1970) agrees reasonably well with estimates other than O'Brien's (1979) and predicts an acceptable inventory. Coupled with a sedimentary sink, it produces a reasonable response with standard values in qualitative agreement with measurements. Both production functions predict amplitudes for "wiggles" that are lower than indicated by measurements. This may be a difficiency in the models as natural analogues (Lazear, Damon, and Sternberg, 1980) or an inadequacy of a production function based on a sunspot vs neutron flux relationship derived solely from three 20th-century sunspot cycle (Stuiver and Quay, 1980). The one-box model does predict the correct amplitude for the AD 1790 - AD 1825 "wiggle" because its gain is 1.5 times the gain of the 3B model at that frequency. However, this is fortuitous because the 1B model is not an adequate natural analogue and it would predict gains that are too high for periods above 200 years.

Based upon experience with multibox models, we do not expect that reasonable manipulation of the model parameters will yield a sufficiently high gain at periods between 50 and 200 years. Rather, as Stuiver and Quay (1980) suggest, a production function based upon modulation during the 11-year cycle is probably not adequate for longer periods. Thus, the solar modulation process, like the ^{14}C reservoir system, may also be acting as a low pass filter or, perhaps, it is affected by cosmic-ray drift in the interplanetary field (Shea and Smart, 1981; Jokipii, 1981). Shea and Smart (1981) showed that the correlation between the Mt Washington neutron monitor counting rate and the geomagnetic Aa index significantly changes from one solar cycle to the next. Jokipii (1981) demonstrated that cosmic-ray drifts can produce the sense of the observed shift in correlation. Also, Stuiver and Quay (1980) suggest modulation of cosmic-ray intensities probably continues beyond zero sunspot number.

The Lingenfelter and Ramaty (1970) production function does predict an inventory and a sedimentary flux that are in reasonable agreement with independent estimates. Thus, their average production rate for the three 20th-century solar cycles, when corrected for past changes in the geomagnetic dipole field intensity (Sternberg and Damon, 1979), appears also to be about the average for the past eight millennia. If so, the ^{14}C flux to the sedimentary sink may account for all or a large part of the missing anthropogenic carbon.

An 11-year cycle in ^{14}C must exist and should be measurable at the 2‰ (sd) precision level. Failure to observe it may be due either to measurement error, or, most probably, to a combination of geographic effects, suggested by Baxter and Farmer (1973 and Damon (1982), solar flare production of ^{14}C (Lingenfelter and Ramaty, 1970), and the annual injection of stratospheric ^{14}C into the troposphere. We note in this regard that the annual injection of artificial ^{14}C into the troposphere still persists at measurable levels long after cessation of major tests in the early 1960's (Nydal, Lövseth, and Gulliksen, 1979).

ACKNOWLEDGMENT

This work was supported by NSF Grant No. EAR-8116196 and the State of Arizona.

REFERENCES

Bacastow, R and Keeling, C D, 1973, Atmospheric carbon dioxide and radiocarbon in the natural carbon cycle. II. Changes from AD 1700 to 2070 as deduced from a geochemical model, in Woodwell, G M, and Pecan, E V, eds, Carbon and the biosphere, Brookhaven symposium in biol, 24th, Proc: Upton, New York, USAEC Conf 720510, p 86-135.

Baxter, M S and Farmer, J G, 1973, Radiocarbon: Short term variations: Earth Planetary Sci Letters, v 20, no. 3, p 295-299.

Damon, P E, 1982, Fluctuation of atmospheric radiocarbon and the radiocarbon time scale, in Currie, L A, ed, Nuclear and chemical dating techniques: Interpreting the environmental record: Am Chem Sos symposium ser, no. 176, p 233-244.

Damon, P E, Lerman, J C, and Long, Austin, 1978, Temporal fluctuations of atmospheric ^{14}C: causal factors and implications, in Annual review of earth and planetary sciences: Ann Rev Inc, Palo Alto, California, p 457-494.

Damon, P E and Wallick, E I, 1972, Changes in atmospheric radiocarbon concentration during the last eight millennia, in Contributions to recent geochemistry and analytical chemistry, Moscow: Nauka Publ Office, p 441-452 (in Russian; preprints in English).

Eddy, J A, 1976, The Maunder Minimum: Science, v 192, p 1189-1202.

Ekdahl, C A and Keeling, C A, 1973, Atmospheric carbon dioxide and radiocarbon in the natural carbon cycle: I. Quantitative deductions from records at Mauna Loa observatory and at the South Pole, in Woodwell, G M, and Pecan, E V, eds, Carbon and the biosphere, Brookhaven symposium in biol, 24th, Proc: Upton, New York, 1972: USAEC Conf 720510, p 51-85.

Elsasser, W E, Ney, E P, and Winckler, J R, 1956, Cosmic ray intensity and geomagnetism: Nature, v 178, p 1226-1227.

Grey, D C and Damon, P E, 1970, Sunspots and radiocarbon dating in the Middle ages, in Berger, Rainer, ed, Scientific studies in Medieval archaeology: Berkeley, Univ California Press, p 167-182.

Hay, W W and Southam, J R, 1977, Modulation of marine sedimentation by the continental shelves, in Anderson, N R and Malahoff, Alexander, eds, The fate of fossil fuel CO_2 in the oceans: New York, Plenum Press, p 569-604.

Houtermans, J C, Suess, H E, and Oeschger, Hans, 1973, Reservoir models and production rate variations of natural radiocarbon: Jour Geophys Research, v 79, no. 12, p 1897-1908.

Jokipii, J R, 1981, Correlation of the cosmic-ray intensity with solar-terrestrial parameters: Geophys Research Letters, v 8, no. 7, p 837-839.

Lazear, Gregory, Damon, P E, and Sternberg, R S, 1980, The concept of DC gain in modeling secular variations in atmospheric ^{14}C, <u>in</u> Stuiver, Minze and Kra, Renee, eds, Internatl radiocarbon conf, 10th, Proc: Radiocarbon, v 22, no. 2, p 318-327.

Light, E S, Merker, M, Verschell, H J, Mendell, R B, and Korff, S A, 1973, Time dependent worldwide distribution of atmospheric neutrons and of their products, 2, calculation: Jour Geophys Research, v 78, no. 16, p 2741-2762.

Lingenfelter, R E and Ramaty, R, 1970, Astrophysical and geophysical variations in C^{14} production, <u>in</u> Olsson, I U, ed, Radiocarbon variations and absolute chronology: New York, John Wiley & Sons, p 513-537.

McDonald, K L and Gunst, R H, 1968, Recent trends in the earth's magnetic field: Jour Geophys Research, v 73, no. 6, p 2057-2067.

Nydal, R, Lövseth, K, and Gulliksen, S, 1979, A survey of radiocarbon variation in nature since the Test Ban Treaty, <u>in</u> Berger, Rainer and Suess, H E, eds, Radiocarbon dating, Internatl conf on radiocarbon dating, 9th, Proc: Berkeley, Univ California Press, p 313-321.

O'Brien, K J, 1979, Secular variations in the production of cosmogenic isotopes: Jour Geophys Research, v 84, p 423-431.

Oeschger, H, Siegenthaler, U, Schotterer, U, and Gugelmann, A, 1975, A box diffusion model to study the carbon dioxide exchange in nature: Tellus, v 27, no. 2, p 168-192.

Shea, M A and Smart, D F, 1981, Preliminary search for cosmic radiation and solar terrestrial parameters correlated with the reversal of the solar magnetic field: Advances in Space Research, v 1, no. 3, p 147-150.

Sternberg, R S and Damon, P E, 1979, Sensitivity of radiocarbon fluctuations and inventory to geomagnetic and reservoir parameters, <u>in</u> Berger, Rainer and Suess, H E, eds, Radiocarbon dating, Internatl conf on radiocarbon dating, 9th, Proc: Berkeley, Univ California Press, p 691-720.

Stuiver, Minze, 1980, Solar variability and climatic change during the current millennium: Nature, v 286, p 868-871.

Stuiver, Minze and Quay, P D, 1980, Changes in atmospheric ^{14}C attributed to a variable sun: Science, v 207, p 11-19.

Suess, H E, 1955, Radiocarbon concentration in modern wood: Science, v 122, p 415-417.

Waldmeier, M, 1961, The sunspot activity in the years 1610-1960: Zurich, Schulthess.

Walsh, J F, Rowe, G T, Iverson, R L, and McRoy, C P, 1981, Biological export of shelf carbon is a sink of global CO_2 cycle: Nature, v 291, p 196-201.

[Radiocarbon, Vol 25, No. 2, 1983 P 259-266]

SHORT-TERM VARIATIONS IN RADIOCARBON CONCENTRATION WITH THE 11-YEAR SOLAR CYCLE

PAVEL POVINEC

Department of Nuclear Physics Comenius University,
842 15 Bratislava, Czechoslovakia

A A BURCHULADZE, and S V PAGAVA

Department of Nuclear Physics, Tbilisi State
University, Tbilisi, USSR

ABSTRACT. Previous investigations on short-term ^{14}C variations in tree rings are compared with ^{14}C measurements in wine samples. The comparison is made for 4 solar cycles (1903-1944) with the same method of statistical evaluation of measured results. The average amplitude of $\Delta^{14}C$ variations as observed by various authors in tree-ring samples is ca 2 ± 1 ‰; however, wine samples show an average amplitude of 4.3 ± 1.6 ‰. The anticorrelation dependence of $\Delta^{14}C$ on Wolf sunspot numbers was observed with a time shift between W maxima and $\Delta^{14}C$ minima of 3-5 yr for different solar cycles.

INTRODUCTION

Stuiver (1961) was first to point out an inverse correlation between ^{14}C concentration in tree rings and sunspot numbers. He found a ^{14}C cycle with a period of ca 100 years. More recently, Lin et al (1975) and Kocharov, Dergachev, and Gordeichik (1975) reported ^{14}C variations in tree-rings with a period of 80-90 years. The well-known Suess wiggles (de Jong, Mook, and Becker, 1979; Suess, 1980) have a characteristic time scale of ca 200 years. The amplitude of these ^{14}C variations is from 1 to 2%. It is believed that this effect is due to a modulation of galactic cosmic rays by solar wind (Stuiver and Quay, 1980; 1981).

The most prominent cycle in the solar activity observed till now is the 11-year solar cycle. Thus, it seems reasonable to investigate if the 11-year solar cycle has a similar influence on ^{14}C production as the 80-year solar cycle.

Calculations of ^{14}C production rate performed by Lingenfelter and Ramaty (1970) for the 19th solar cycle has shown that a global average ^{14}C production rate during solar minimum (1953), which corresponds to the maximum cosmic ray flux, was 2.4×10^4 ^{14}C atoms.m^{-2}.s^{-1}, while during solar maximum (1957) it decreased to 1.9×10^4 ^{14}C atoms.m^{-2}.s^{-1}. This points to variations in the ^{14}C production rate during the 19th solar cycle of ca 25%. Similar calculations (Povinec, 1977) performed for the 20th solar cycle showed that ^{14}C production rate during solar minimum (1965) was 2.6×10^4 ^{14}C atoms.m^{-2}.s^{-1} and for solar maximum (1968), 2.1×10^4 ^{14}C atoms.m^{-2}.s^{-1}. This was confirmed by calculation of ^{14}C production rate based on measurements of neutron fluxes in the atmosphere by the Deep River neutron monitor (Korff and Mendell, 1980).

However, short-term ^{14}C variations are difficult to observe because a change in the ^{14}C production rate may not give a measurable change in atmospheric ^{14}C concentration. This is because atmospheric carbon dioxide which is labeled with cosmogenic ^{14}C is in equilibrium with a large oceanic reservoir of CO_2, acting as a buffer against changes of atmospheric ^{14}C concentrations.

Houtermans (1966) showed that the amplitude of a ^{14}C variation with a period of 10 years is attenuated by a factor of ca 100, while ^{14}C variations with a period of the order of 100 years show an attenuation only by a factor of ca 10. More recent calculations by Siegenthaler, Heimann, and Oeschger (1980) who used the more sophisticated box-diffusion model (Oeschger et al, 1975) yielded an attenuation factor of 90.

Taking into account calculations of ^{14}C production rates based on the measured cosmic ray data for the 19th and 20th solar cycles and their approximation for previous solar cycles, as well as recent calculations on exchange rates between carbon reservoirs, a variation in the ^{14}C activity during an 11-year solar cycle may be expected to have an average amplitude of ca 1 ‰ to 2 ‰.

Experimental results on ^{14}C variations with the 11-year solar cycle have been scarce. The first ^{14}C results were reported for annual tree-ring samples ca 1910, in connection with the effect of the Tunguska meteor on the ^{14}C concentration of the atmosphere (Covan, Atluri, and Libby, 1965). Venkatavaradan (1965) compared these data with sunspot record; however, a definite conclusion was not obtained as only 2 to 3 ^{14}C values per solar cycle were available. Suess (1965) measured ^{14}C concentrations in single annual tree rings for the period 1860-1888 but did not observe short-term ^{14}C variations. Lerman (1970) analyzed tree-ring results of Lerman, Mook, and Vogel (1967) from 1894 to 1917. These results indicated some periodicity in ^{14}C concentration during the 11-year solar cycle with an amplitude of ca 2 ‰ and a phase shift of 4 years. Baxter and Farmer (1973) and Baxter, Farmer, and Walton (1973) reported an average amplitude of ca 10 ‰ in tree rings for the period 1829-1865. On the other hand, Damon, Long, and Wallick (1973a,b) reported ^{14}C tree-ring data which show only ca 1.5 °/oo amplitude variations with the 11-year solar cycle for the period 1940-1954. For the interval 1900-1916, Lavrukhina et al (1973) obtained for the average amplitude a value of ca 10 °/oo, but the same authors (Alekseev, Lavrukhina, and Milnikova, 1975) reported the average amplitude of 3 °/oo for 1810-1900. Povinec (1977) reported a 3 °/oo amplitude oscillation over the 11-year solar cycle for the interval 1932-1952. Very precise ^{14}C tree-ring measurements reported more recently (Tans, de Jong, and Mook, 1979; Stuiver and Quay, 1980; 1981; Stuiver, 1982) show only minor short-term ^{14}C variations.

All the ^{14}C measurements mentioned above were made on tree-ring samples. However, Baxter and Walton (1971) measured ^{14}C in samples of whiskies, wines, and plant seeds from the period 1890-1950, observing fluctuations with an average amplitude of ca 15 °/oo. On the other hand, Burchuladze et al (1980) found 4.3 ± 1.1 °/oo average amplitudes of ^{14}C variations in Georgian wine samples from the period 1909-1952.

This short review shows that different groups obtained contradictory results, even for the same solar cycle. A comparison of results obtained by Stuiver (1978) and Baxter, Farmer, and Walton (1973) suggests that the larger ^{14}C fluctuations found by the latter group may be due to a lower precision of their ^{14}C measurements. Generally, larger amplitudes observed with wine samples are poorly understood. One purpose of this paper is to compare ^{14}C results obtained by various authors for the same solar cycles and to perform a similar statistical evaluation of obtained results. A direct comparison of ^{14}C data from different groups was not possible before, as different methods of statistical analysis were used for the evaluation of ^{14}C variations.

RESULTS AND DISCUSSION

Spectral analysis, correlation analysis, and harmonic analysis of $\Delta^{14}C$ values were performed together with similar analyses of sunspot numbers. The most precise tree-ring ^{14}C data (Stuiver and Quay, 1981) and wine ^{14}C data (Burchuladze et al, 1980) covering 3 and 4 solar cycles (1903-1944), respectively, were used for the analyses. We excluded the 18th solar cycle (1944-1954), as $\Delta^{14}C$ values for this cycle have been disturbed by nuclear bomb effects. Figure 1 shows the results of spectral analysis, ie, the autocorrelation functions $r(U)$ of stationary time rows $\Delta^{14}C(t)$ and the Wolf sunspot numbers, $W(t)$. It can be seen that for both types of samples the autocorrelation functions have a quasiperiodical behavior with the

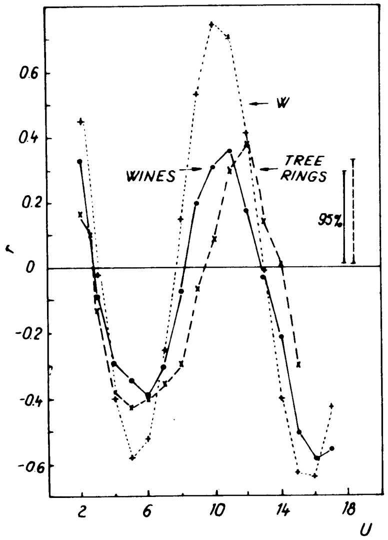

Fig 1. Autocorrelation functions r(U) of stationary time rows $\Delta^{14}C(t)$ (wine and tree-ring samples) and W(t) for argument values $U_{wines} = 11 \pm 1$ yr, $U_{trees} = 12 \pm 1$ yr and $U_W = 10 \pm 1$ yr.

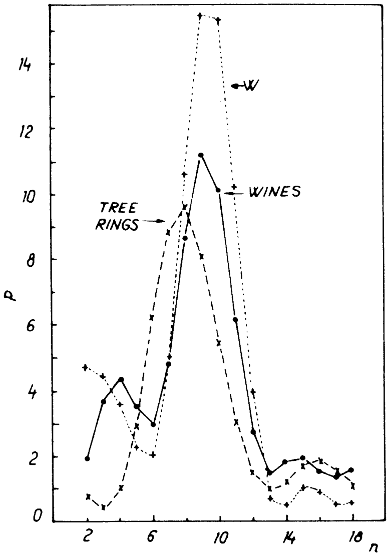

Fig 2. Spectrum estimation of stationary time rows $\Delta^{14}C(t)$ and W(t).

11-year period at the 95% confidence interval. The spectrum estimation of $\Delta^{14}C(t)$ and W(t) rows is shown in figure 2. The basic power of the spectra is concentrated at the period, 11 years. The existence of anticorrelation between the sunspot function and ^{14}C function has been confirmed by correlation analysis. Correlation coefficients have been obtained of more than - 0.6.

The results of the harmonic analysis are given in table 1. Harmonic analysis enables the determination of the amplitude and the phase of $\Delta^{14}C$ variations for different solar cycles, as well as the time shift between W and $\Delta^{14}C$. The amplitude of $\Delta^{14}C$ variations in wines ranged from (4.0 ± 0.8)‰ to (4.5 ± 0.9)‰ and from (1.5 ± 0.5)‰ to (2.1 ± 0.5)‰ for tree-ring samples for different solar cycles. The amplitude varies from cycle to cycle, but its dependence on sunspot numbers for the investigated solar cycles is within the error of analysis. The average amplitude for wines is (4.3 ± 1.6) ‰ and (1.9 ± 0.8)‰ for tree-ring samples.

Table 2 lists the results of the spectral analysis, the

TABLE 1. Amplitude of Δ^{14}C variations (in ‰) calculated for different solar cycles from wine samples (Burchuladze et al, 1980) and tree-ring samples (Stuiver and Quay, 1981) using harmonic analysis

Samples	14th solar cycle 1903-1913	15th solar cycle 1913-1923	16th solar cycle 1923-1933	17th solar cycle 1933-1944
Wines	4.0 ± 0.8	4.3 ± 0.8	4.5 ± 0.9	4.3 ± 0.8
Tree Rings		1.5 ± 0.5	2.1 ± 0.5	2.0 ± 0.5

TABLE 2. Comparison of data on Δ^{14}C variations with the 11-yr solar cycle as obtained by different groups

Reference	Samples	Investigated time interval	Periodicity (yr)	Average time shift (yr)	Average Δ^{14}C amplitude (‰)
Baxter & Walton (1971)	Whiskies	1925-1954	11±1	4	7.2±4.9
Damon, Long & Wallick (1973a)	Tree rings	1940-1954	10±1	4	2.1±1.0
Povinec	Tree rings	1932-1952	10±1	3	3.1±1.2
Burchuladze et al (1980)	Wines	1909-1952	11±1	4	4.3±1.6
Stuiver and Quay (1981)	Tree rings	1916-1954	12±1	4	1.9±0.8

correlation analysis, and the harmonic analysis of annual Δ^{14}C data reported by different groups. It can be seen that results obtained with tree rings are comparable, although only 1 to 2 solar cycles have been investigated. Tree-ring data of Tans, de Jong, and Mook (1979) were not used for comparison as the ^{14}C measurements were not performed on an annual basis. Results of Baxter and Walton (1971) on whiskies, wines, and seeds showed an average Δ^{14}C amplitude larger than by factor 2 in comparison with results on wines of Burchuladze et al (1980). All compared results showed the basic power of the spectra concentrated at the period ca 11 years. The calculated average time shifts between W maxima and Δ^{14}C minima for the different solar cycles are ca 4 years, indicating an anticorrelation dependence of Δ^{14}C on W.

A comparison of previous studies on short-term ^{14}C variations with the 11-year solar cycle revealed discrepancies that may be partly due to insufficient precision of ^{14}C measurements. This can also be seen from table 2, where calculated average Δ^{14}C amplitudes are well within 2 sigma. However, we can not entirely exclude the possibility of differences caused by sample location, such as local variations of stratospheric input and the time lag between input and growth season.

In conclusion, we want to stress that although our study demonstrated the existence of the 11-year ^{14}C variations at least for 4 solar cycles (1903-1944), more high-precision ^{14}C measurements in annually-dated samples are needed for a better understanding of short-term ^{14}C variations.

REFERENCES

Alekseev, V A, Lavrukhina, A K, and Milnikova, Z K, 1975, Radiocarbon variations in annual tree rings of the sequoia 1890-1916 : Geokhimia, no.5, p 667-675.

Baxter, M S and Farmer, J G, 1973, Radiocarbon: short term variations: Earth Planetary Sci Letters, v 20, p 295-299.

Baxter, M S, Farmer, J G, and Walton, A, 1973, Comments on "On the magnitude of the 11-year radiocarbon cycle": Earth Planetary Sci Letters, v 20, p 307-310.

Baxter, M S and Walton, A, 1971, Fluctuations of atmospheric carbon-14 concentrations during the past century: Royal Soc London Proc ser A, v 321, p 105-127.

Burchuladze, A A, Pagava, S V, Povinec, P, Togonidze, G I, and Usačev, S, 1980, Radiocarbon variations with the 11-year solar cycle during the last century: Nature, v 287, p 320-322.

Covan, C, Atluri, C R, and Libby, W F, 1965, Possible antimatter content of the Tunguska meteor of 1908: Nature, v 206, p 861-865.

Damon, P E, Long, A, and Wallick, E I, 1973a, On the magnitude of the 11-year radiocarbon cycle: Earth Planetary Sci Letters, v 20, p 300-306.

——————————————————— 1973b, Comments on "Radiocarbon: short term variations": Earth Planetary Sci Letters, v 20, p 311-314.

Houtermans, I C, 1966, On the quantitative relationship between geophysical parameters and the natural carbon-14 inventory: Zeitschr Physik, v 193, p 1-12.

Jong, A F M, de, Mook, W G, and Becker, B, 1979, Confirmation of the Suess wiggles: 3200-3700 B C: Nature, v 280,p 48-49.

Kocharov, G E, Dergachev, V A, and Gordeichik, N I, 1975, Rate of production of cosmogenic isotopes in the past and solar activity *in* Internatl conf on cosmic rays, 14th, Proc: München, Max Planck Inst.,p 1001-1013.

Korf, S A and Mendell, R B, 1980, Variations in radiocarbon procuction in the earth's atmosphere, *in* Stuiver, Minze and Kra, Renee eds, Internatl radiocarbon conf, 10th Proc: Radiocarbon, v 22, no.2, p 159-165.

Lavrukhina, A K, Alekseev, V A, Galimov, E M, and Sulerzickii, L D, 1973, Radiocarbon in tree rings of sequoia: Dokl Akad Nauk, v 210, p 941-943.

Lerman, J C, 1970, Discussion of causes of secular variations, *in* Olsson, I U, ed, Radiocarbon variations and absolute chronology: New York, John Wiley Sons, p 609-610.

Lerman, J C, Mook, W G, and Vogel, I C, 1967, Effect of the Tunguska meteor and sunspots on radiocarbon in tree rings: Nature, v 216, p 990-991.

Lin, Y C, Fan, C Y, Damon, P E, and Wallick, E I, 1975, Long term modulation of cosmic-ray intensity and solar activity cycle *in* Internatl conf on cosmic rays, 14th, Proc: München, Max Planck Inst., p 995-999.

Lingenfelter, R E and Ramaty, R, 1970, Astrophysical and geophysical variations in ^{14}C production, *in* Olsson, I U, ed, Radiocarbon variations and absolute chronology: New York, John Wiley Sons, p 513-537.

Oeschger, H, Siegenthaler, U, Gugelmann, A, and Schotterer, U, 1975, A box-diffusion model to study the carbon dioxide exchange in nature: Tellus, v 27, p 168-192.

Povinec, P, 1977, Influence of the 11-yr solar cycle on the radiocarbon variations in the atmosphere: Acta Physica Comeniana, v 18, p 139-149.

Siegenthaler, U, Heimann, M, and Oeschger, H, 1980, ^{14}C variations caused by changes in the global carbon cycle, *in* Stuiver, Minze and Kra, Renee ids, Internatl radiocarbon conf, 10th, Proc: Radiocarbon, v 22, no.2, p 177-191.

Stuiver, Minze, 1961, Variations in radiocarbon concentration and sunspot activity: Jour Geophys Research, v 66, p 273-276.

———— 1978, Radiocarbon timescale tested against magnetic and other dating methods: Nature, 273, p 271-274.

———— 1982, A high-precision calibration at the AD radiocarbon time scale: Radiocarbon, v 24, p 1-26.

Stuiver, Minze and Quay, P D, 1980, Changes in atmospheric carbon-14 attributed to a variable sun: Science, v 207, p 11-19.

———————— 1981, Atmospheric ^{14}C changes resulting from fossil fuel CO_2 release and cosmic ray flux variability: Earth Planetary Sci Letters, v 53, p 349-362.

Suess, H E, 1965, Secular variations of the cosmic ray produced carbon-14 in the atmosphere and their interpretations: Jour Geophys Research, v 70, p 5937-5952.

———— 1980, The radiocarbon record in tree rings of the last 8000 years, in Stuiver, Minze and Kra, Renee eds, Internatl radiocarbon conf, 10th, Proc: Radiocarbon, v 22, no.2, p 200-209.

Tans, P P, Jong, A F M, de, and Mook, W G, 1979, Natural atmospheric ^{14}C variation and the Suess effect: Nature, v 280, p 826-828.

Venkatavaradan, V S, 1965, Antimatter and tree rings: Nature, v 208, p 772.

[Radiocarbon, Vol 25, No. 2, 1983, P 267-268]

ON A 50-YEAR "CLIMATE-FREE" $\delta^{13}C$ RECORD FROM JUNIPER TREE RINGS

STEVEN W LEAVITT and AUSTIN LONG

Department of Geosciences, University of Arizona
Tucson, Arizona 85721

When used with ^{14}C records, an accurate reconstruction of the $^{13}C/^{12}C$ changes of atmospheric CO_2 may be a key constraint to determining the historic activity of the biosphere as CO_2 source or sink. We recently detailed the derivation of an atmospheric $\delta^{13}C$ record for 1930-1979 from Arizona juniper tree rings (Leavitt and Long, 1983). Each tree was close to a weather station, allowing us to account for the effects of climate on the tree-ring $\delta^{13}C$ records. The resulting atmospheric $\delta^{13}C$ trend shows an overall decrease of ca 1.3°/oo, but instead of decreasing exponentially over the whole 50-year period, the best-fit curve decreases exponentially to ca 1960 and then flattens out. The drop from 1956 to 1978 was ca 0.55°/oo, still very similar to the measured atmospheric drop over that period of 0.65 ± 0.13°/oo (Keeling, Mook, and Tans, 1979).

Although this $\delta^{13}C$ trend is not reproduced in other tree-ring studies, it suggests a change in the biosphere from net CO_2 source to sink in the early 1960's. Other studies offer evidence of the important and/or increasing role of biospheric sink activity which may support our $\delta^{13}C$ trend. Seiler and Crutzen (1980) discuss an elemental carbon (charcoal) sink from forest and grassland burning, and Walsh et al (1981) describe a primary production detrital sink on continental shelves. Lugo and Brown (1982) found undisturbed tropical forest lands are potentially a significant sink, enough so, that tropical forests may be in balance or even a slight CO_2 sink.

The decelerating $\delta^{13}C$ trend may be interpreted differently. If the biosphere has been approximately in balance, either this $\delta^{13}C$ trend is not globally representative or, if the trend is representative, another mechanism would have to decelerate the decreasing trend. More time and research will judge the former possibility. For the latter, we speculate on the existence of "light-carbon (^{12}C) sinks" which may increase $\delta^{13}C$ of atmospheric CO_2 and the tree-ring $\delta^{13}C$ records. Four ^{12}C sinks are: 1) Net increase of organic soils (Bohn, 1978) could lead to accumulation of relatively decay-resistant lignins and lipids which are isotopically lighter by ca 1 to 3°/oo relative to their original whole tissue (Park and Epstein, 1961); 2) The early years of tree growth (ca 50 years) are often characterized by ^{13}C depletion, ca 2°/oo less ^{13}C than that of later years (eg, Craig, 1954). With significant forest regrowth in previously-cleared areas, this young regrowth could also represent a ^{12}C sink; 3) Pyrolysis experiments (Leavitt, Donahue, and Long, 1982) indicate the char residue may be enriched in ^{12}C by ca 2.5°/oo relative to the original wood. An elemental carbon sink from forest fires may also be a potentially active light-carbon sink; 4) An increased proportion of C_3 to C_4 plants would yield a ^{12}C sink even without biomass changes. Deforestation and replacement by agriculture should generally be the reverse of such a trend: C_3 trees would be removed, and in some cases, be replaced with C_4 crops (eg, corn and sugar cane). Where fields were cleared for farming and then abandoned, "old-field succession" may take place with the opposite transition of C_4 to C_3.

The impact of the first three sinks would probably be insignificant because, 1) the carbon stored is only ca 2 to 3‰ lighter than the average biospheric composition of ca -25‰, and 2) these carbon sinks are limited in size. The large difference in $\delta^{13}C$ of C_3 and C_4 plants (C_3 plants ca 14‰ lighter) indicates a potentially more significant light-carbon sink. Per cent changes in the proportion of C_3 to C_4 plants could translate to atmospheric changes in tenths of a ‰.

Representative or not, the unusual $\delta^{13}C$ trend should stimulate closer examination of biospheric carbon sources and sinks, including the potential influence of light-carbon sinks.

REFERENCES

Bohn, HL, 1978, On organic soil carbon and CO_2: Tellus, v 30, p 472-475.

Craig, Harmon, 1954, Carbon-13 variations in Sequoia rings and the atmosphere: Science, v 119, p 141-143.

Keeling, CD, Mook, WG, and Tans, PP, 1979, Recent trends in the $^{13}C/^{12}C$ ratio of atmospheric carbon dioxide: Nature, v 277, p 121-123.

Leavitt, SW, Donahue, DJ, and Long, A, 1982, Charcoal production from wood and cellulose: implications to radiocarbon dates and accelerator target production: Radiocarbon, v 24, p 27-35.

Leavitt, SW and Long, A, 1983, An atmospheric $^{13}C/^{12}C$ reconstruction generated through removal of climate effects from tree-ring $^{13}C/^{12}C$ measurements: Tellus, v 35, p 000-000.

Lugo, AE and Brown, S, 1982, The role of tropical forests in the global carbon cycle: state of understanding, in Brown, S, ed, Global dynamics of biospheric carbon: Washington, D C, U S Dept Energy, Publ No. CONF-8108131, p 115-130.

Park, R and Epstein, S, 1961, Metabolic fractionation of $^{13}C/^{12}C$ in plants: Plant Physiol, v 36, p 133-138.

Seiler, W and Crutzen, PJ, 1980, Estimates of growth and net fluxes of carbon between the biosphere and the atmosphere from biomass burning: Climatic Change, v 2, p 207-247.

Walsh, JJ, Rowe, GT, Iverson, RL, and McRoy, CP, 1981, Biological export of shelf carbon is a sink of the global CO_2 cycle: Nature, v 291, p 196-201.

[Radiocarbon, Vol 25, No. 2, 1983 P 269-278]

TEMPORAL ^{10}BE VARIATIONS IN ICE

JUERG BEER, MICHAEL ANDREE, HANS OESCHGER
AND BERNHARD STAUFFER

Physics Institute, University of Bern
Sidlerstrasse 5, 3012 Bern, Switzerland

and

RICHARD BALZER, GEORGES BONANI, CHRISTIAN STOLLER,
MARTIN SUTER AND WILLY WOELFLI

Laboratorium für Kernphysik
Swiss Federal Institute of Technology ETHZ
8093 Zürich, Switzerland

and

ROBERT C FINKEL

Mt Soledad Laboratory
Scripps Institution of Oceanography S - 002
La Jolla, California 92093, U S A

INTRODUCTION

^{10}Be ($T_{1/2} = 1.5 \cdot 10^6$y) is mainly produced in the atmosphere by cosmic ray spallation reactions on nitrogen and oxygen. About 70 % of the production takes place in the stratosphere. ^{10}Be becomes attached to aerosols within a very short time. If ^{10}Be is produced in the stratosphere some latitudinal mixing occurs. Most of the ^{10}Be is transferred to the troposphere during spring and early summer when, mainly at median latitudes, large stratospheric air masses enter the troposphere. Tropospheric ^{10}Be is deposited rapidly on the earth's surface by precipitation. The mean residence time of ^{10}Be in the atmosphere is ca 1 to 2 years. ^{10}Be removed from the atmosphere by precipitation is either preserved in snow and ice layers, in the topsoil and the biosphere, or it enters the hydrosphere (oceans and lakes), where it is transported to the sediments.

Many precise ^{14}C measurements on tree rings covering the last 8000 years (Suess, 1980; Stuiver and Quay, 1980) clearly show that atmospheric ^{14}C concentration has not been constant. Possible causes of these variations with amplitudes of 1 to 2 % are 1) changes of the production rate due to changes of the galactic cosmic ray intensity. Incoming cosmic ray flux is modulated by the magnetic properties of the solar wind plasma and the intensity of the geomagnetic field; 2) changes of the global carbon cycle (Siegenthaler, Heimann, and Oeschger, 1980). Reservoir sizes and exchange fluxes can be influenced by changes of environmental conditions.

Fluctuations of the ^{14}C production rate are strongly dampened due to the large size of the atmospheric CO_2 reservoir and the exchange processes with the ocean. Model calculations show that, eg, the production variation induced by the 11-year solar cycle is attenuated by a factor of 100. Because of its rapid transfer from the atmosphere to the geosphere ^{10}Be responds with a much greater amplitude to changes of the production rate. The 11-year production variation is attenuated only by ca 20 %.

Until 1977 only a few ^{10}Be measurements were made mainly on ocean sediments (Somayajulu, 1977; Finkel, Krishnaswami, and Clarck, 1977). Because of its $\sim$ 100 times smaller global production rate compared to ^{14}C and its $\sim$ 300 times larger half-life, the detection of ^{10}Be by conventional low-level counting techniques is very difficult. For the first ^{10}Be measurement on polar ice which represents the best record of precipitation, $1.2 \cdot 10^6$kg of meltwater were processed (McCorkell, Fireman, and Langway, 1967). Since the development of accelerator mass spectrometry in 1977, samples of ca 1kg containing $\sim 10^7$ ^{10}Be atoms are sufficient for a measurement. The first sets of ^{10}Be measurements in ice cores from Antarctica using the accelerator technique show very promising results (Raisbeck *et al*, 1981). To study ^{10}Be variations in ice cores for at least the last 10^5 years, we started with two sets of samples drilled at Dye 3, Greenland. The main goal of set A for 1900 - 1976 is to study short-term fluctuations caused by changes of solar activity, ie, the 11-year solar cycle. Set B contains 14 samples distributed over the depth range 1300 to 1950m corresponding to a period from 3600 BP to $\sim$ 30,000 BP. These samples should provide some information on long-term fluctuations and on the changing conditions during the transition from glacial to postglacial times (10,000 - 13,000 BP).

SAMPLE PREPARATION

Samples were prepared from two ice cores drilled at Dye 3, Greenland (65° 11' N, 43° 50'W) for GISP (Greenland Ice Sheet Project) an American-Danish-Swiss collaboration. Samples of set A were prepared from a 70m shallow firn core. The $\delta^{18}O$

profile (*ca* 8 samples per year) measured by the Danish group was used to cut the core into pieces containing the precipitation of one year. Each sample was mechanically cleaned and melted. Aliquots for tritium and chemical analysis were taken. Before adding Be- (1.18 mg Be) and Cl-carrier (2 mg Cl) the precipitation of two years was combined to one sample to increase the ^{10}Be concentration. First, the water volume (2 to 6kg, cf table 1) was reduced by evaporation to ca 30ml. Then the chlorine was separated by precipitation of AgCl and purified as described elsewhere (Nishiizumi et al, 1979). After an additional volume reduction to 2ml, the samples were analyzed by gamma spectroscopy. Beryllium acetylacetonate in the presence of EDTA was extracted into $CHCl_3$ and evaporated after adding HCl. The organic material was oxidized with aqua-regia. $Be(OH)_2$ was precipitated with NH_4OH and converted to BeO by ignition at 950°C in a quartz crucible. The 14 samples of set B were prepared from ice of the 2037m long deep core, reaching bedrock. Depending on the depth, one sample represents the precipitation of ca 10 to 250 years. The samples were processed in the same way as the samples of set A.

MEASUREMENTS

The ^{10}Be concentrations were measured using the EN-tandem accelerator facility of the ETH Zürich. This system was designed in 1978 to detect, in a first step ^{14}C and ^{10}Be, and in a second step, ^{36}Cl and ^{26}Al in natural samples. The Cs sputter ion source produced BeO currents of up to 1 μA leading to count rates of up to 10^3 cph for a typical ^{10}Be/^{9}Be ratio of $5 \cdot 10^{-13}$. The background is of the order of 10^{-14} depending on the boron content of the sample. The accelerator mass spectrometer is described in more detail by Woelfli et al (1983). The gamma activity of the samples was measured with a 64cc Ge(Li) detector. The tritium content was determined by a commercial liquid scintillation counter. Both counters were operated in a well-shielded underground laboratory (Oeschger et al, 1981).

RESULTS

The shape and the maximum of the nuclear bomb pulses of ^{3}H and ^{137}Cs were used to confirm the dating of the ice core based on $\delta^{18}O$ variations. The ^{10}Be concentrations and the weights of set A and B are given in tables 1 and 2. All samples (except 2) were measured twice, at different times. The measuring time (20-30 min) was divided into intervals of

TABLE 1. ^{10}Be concentrations in the Dye 3 firn core

Year	Sample weight (g)	^{10}Be concentration 10^4 atoms/g
1900-1901	3853	1.11 ± 0.05
1902-1903	3192	0.91 ± 0.05
1904-1905	3354	1.09 ± 0.06
1906-1907	2295	1.27 ± 0.07
1908-1909	4236	0.79 ± 0.05
1910-1911	2970	0.81 ± 0.06
1912-1913	4623	0.87 ± 0.05
1914-1915	3558	1.10 ± 0.10
1916-1917	3460	0.85 ± 0.05
1918-1919	3584	0.77 ± 0.09
1920-1921	3255	0.98 ± 0.14
1922-1923	3892	0.74 ± 0.09
1924-1925	3028	1.01 ± 0.20
1926-1927	3853	0.85 ± 0.14
1928-1929	4604	0.57 ± 0.07
1930-1931	2836	0.98 ± 0.13
1932-1933	3230	0.97 ± 0.09
1934-1935	3392	0.86 ± 0.10
1936-1937	2941	0.97 ± 0.13
1938-1939	6559	0.72 ± 0.05
1940-1941	4493	
1942-1943	3401	0.74 ± 0.11
1944-1945	2821	0.80 ± 0.12
1946-1947	4274	0.90 ± 0.08
1948-1949	2387	0.93 ± 0.11
1950-1951	2673	0.98 ± 0.08
1952-1953	2538	1.40 ± 0.12
1954-1955	3652	0.81 ± 0.12
1956-1957	2660	0.83 ± 0.11
1958-1959	3560	0.62 ± 0.06
1960-1961	3573	
1962-1963	2256	0.57 ± 0.15
1964-1965	3199	1.41 ± 0.12
1966-1967	2140	1.17 ± 0.17
1968-1969	2843	1.10 ± 0.10
1970-1971	3105	0.93 ± 0.08
1972-1973	3629	0.78 ± 0.07
1974-1975	3118	0.78 ± 0.07
1976-1977	3026	1.47 ± 0.10

TABLE 2. ^{10}Be concentrations in the Dye 3 deep core

Depth (m)	Sample weight (g)	^{10}Be concentration (10^4 atoms/g)
1314-1315	1856	0.59 ± 0.10
1397-1398	1701	1.16 ± 0.14
1517-1517.5/1537-1537.5	1932	1.20 ± 0.15
1636-1636.5/1657-1657.5	1842	0.72 ± 0.13
1714.5-1715.5	2175	1.05 ± 0.12
1775.5-1776.5	1837	1.11 ± 0.12
1800.5-1801.5	1687	1.60 ± 0.15
1810.5-1811.5	1781	0.86 ± 0.09
1832.5-1833.5	1200	2.45 ± 0.13
1852.5-1853.5	1445	2.87 ± 0.14
1873.5-1874.5	1804	2.43 ± 0.16
1895.5-1896.5	1272	1.43 ± 0.11
1913.5-1914.5	1689	1.93 ± 0.12
1930-1931	2004	1.52 ± 0.15

50 sec. The final result was obtained by calculating the weighted mean value of the two measurements. For absolute calibration the measurements were periodically compared to a ^{10}Be standard with a known ^{10}Be/^{9}Be ratio.

The data of set A are plotted together with the sunspot numbers and the Δ^{14}C data of the period 1915-1940 (Stuiver and Quay, 1981) in figure 1. A comparison of the ^{10}Be spline function fit with the sunspot curve shows general agreement. The maximum of the spectral density function is at 13 ± 3 years. The cross-correlation between the Be data and the sunspot numbers yields a phase lag of the ^{10}Be variations of 1.5 years which is consistent with the mean atmospheric residence time of ^{10}Be. Model calculations of the variation of the ^{10}Be production rate induced by the 11-year solar cycle predict changes of ca 60 % (Oeschger et al, 1970) in agreement with the variations shown in figure 1.

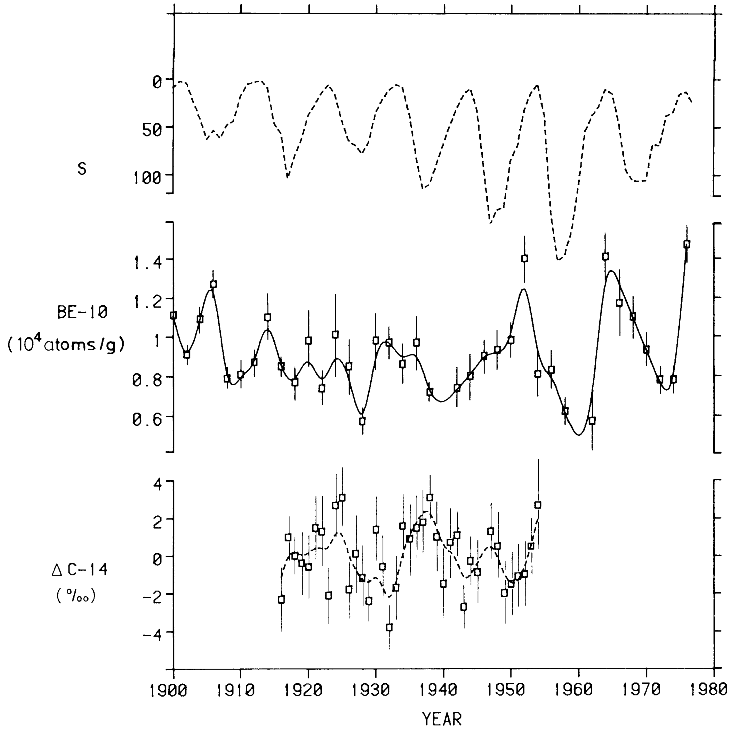

Fig 1. Comparison of ^{10}Be concentrations (two-year means) in the Dye 3 firn core with sunspot numbers and Δ^{14}C variations

Between 1900 and 1960 the ^{10}Be concentration shows a slight decreasing trend which could be explained by the observed slow rise of the solar activity. After 1960 the ^{10}Be concentration rises again with greater amplitudes. There is no clear indication of a bomb peak due to nuclear weapon tests as observed for ^{137}Cs, T and ^{36}Cl (Elmore et al, 1982). The mean value between 1900 and 1976 is (0.93 ± 0.22) 10^4 atoms per gram of ice. The $\Delta^{14}C$ values shown in figure 1 were obtained by subtracting the Suess effect using linear regression. Data before 1915 were not used, since according to Stuiver, contamination cannot be excluded. The cross-correlation with the ^{10}Be curve reaches a maximum of 0.4 when ^{14}C lags 4 ± 2.5 years behind ^{10}Be while CO_2 model calculations predict a lag of 3 years between the solar activity and the atmospheric ^{14}C concentration.

Table 2 and figure 2 give the results of the samples from the deep core. Because there is no general agreement about the age below 1780 m (corresponding to 10,000 BP) the data are listed as a function of depth. The time scale added in figure 2 is based on an ice flow model (Hammer et al, 1978). The ^{10}Be concentration changes dramatically between 1810 and 1830m corresponding to the end of the last ice age.

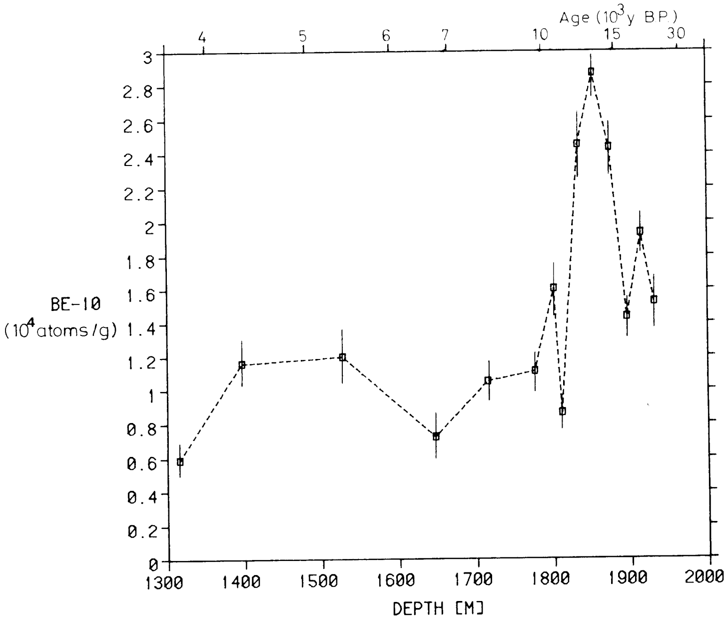

Fig 2. ^{10}Be concentration in the deep ice core from Dye 3

The mean value of the first 6 points above 1780m is (0.97 ± 0.25) 10^4 atoms/g concurring with the value found for the 20th century (0.93 ± 0.22) 10^4 atoms/g.

DISCUSSION

The ^{10}Be concentration of the time period 1900 to 1976 reflects, to some extent, the 11-year solar cycle. This conclusion is supported by the size of the amplitude, the spectral density function, and the phase lag. Since measurements of ^{10}Be concentration in monthly rainwater in France (Raisbeck, 1979) show variations of a factor of 3, it is not surprising to find some "meteorological noise" in the two-year mean vaules. Absence of a clear nuclear bomb peak is expected because the environmental ^{9}Be concentration and the n-activation cross-section are small.

Using the fallout pattern of Lal and Peters (1967) and the average rainfall for the latitude of Dye 3 (Moller, 1951) the mean ^{10}Be concentration of (0.93 ± 0.22) 10^4 atoms/g corresponds to a global deposition rate of 0.016 $cm^{-2}sec^{-1}$, which agrees well with the value 0.018 $cm^{-2}sec^{-1}$ derived by Amin, Lal, and Somayajulu (1975). In spite of a general similarity between the ^{10}Be and the $\Delta^{14}C$ curve, the number of data points is not sufficient for a clear correlation. More measurements covering longer periods are needed.

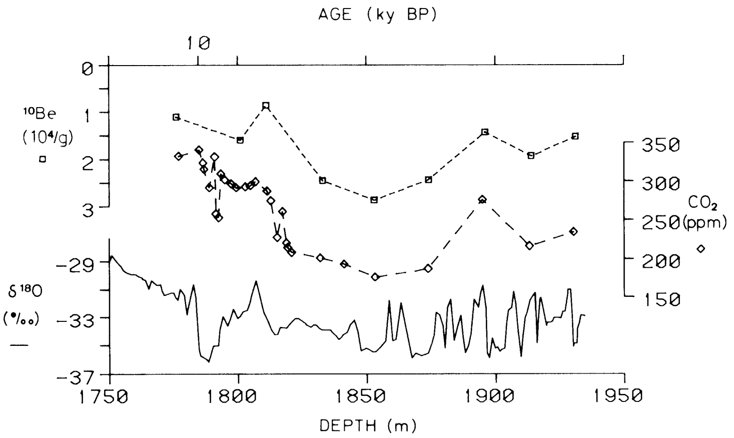

Fig 3. Comparison of the ^{10}Be concentrations around the transition from glacial to postglacial time (∿ 10,000 BP) with $\delta^{18}O$ values and CO_2 concentrations

There are three possible explanations for the significant change of ^{10}Be concentration at the transition from Wisconsin to Holocene. The increase by a factor of 2.5 to 3 can be caused by an enhanced production rate, by changes of atmospheric circulation and mixing processes, or by changes of precipitation rates. Other parameters like δ^{18}O, CO_2 content, anion and dust concentration which have been measured on the same ice core also show significant variations at this depth. In figure 3 the ^{10}Be values around the transition are plotted together with Danish δ^{18}O data and the CO_2 concentration (Stauffer et al, 1982). The correlation between these three data sets is surprisingly good. Raisbeck et al (1981) found the same features in an ice core from Dome C, Antarctica; an increase by a factor of 2 to 3 between 10,000 and 15,000 BP and a good correlation with the δ^{18}O curve. Considering that the increase of ^{10}Be concentration coincides with a strong climatic change, it is very probable that this effect can be attributed to serious changes of atmospheric circulations and precipitation rates. Herron and Langway (1982) find that, based on sulfate measurements, precipitation during the last ice age at Dye 3 was lower by a factor of 2 to 3. However, there are indications that the deposition rate in Antarctica was rather constant during this time. With the present information it is difficult to decide if the production rate of ^{10}Be was higher during Wisconsin. Figure 1 and results deduced from ice samples of the Maunder minimum (Raisbeck et al, 1981) show that the production rate during periods of very low solar activity is increased by $<$ 100 %. Thus, it seems improbable that changing solar magnetic properties alone could account for the observed threefold higher ^{10}Be concentrations.

CONCLUSIONS

Despite some meteorologic disturbances, the ^{10}Be data seem to reflect solar activity as well as climatic changes. If confirmed by more measurements from other sites, this observation has important implications. Records of solar activity provide basic information for understanding the solar cycle mechanism. Comparisons of ^{10}Be and ^{14}C data sequences enable us to distinguish variations due to fluctuations of the global carbon cycle. The correlation of the ^{10}Be concentration with δ^{18}O values and other climatic parameters could be very helpful in studying not only the climate of the last 10^5 to 10^6 years but also the extent to which climatic changes are influenced by the sun.

ACKNOWLEDGMENTS

We thank A Salem for help in preparing the BeO samples, U Schotterer for the preparation of the tritium samples, and M Heimann for assistance in the analysis of the results. Further thanks are due the US NSF for continuing support, especially for logistic help during field seasons at Dye 3, and to the Commission for Scientific Research in Greenland supporting the development of the Danish drill. We are indebted to all members of the American-Danish-Swiss group who contributed to the successful deep drilling at Dye 3. This work was financially supported by the Swiss National Science Foundation.

REFERENCES

Amin, BS, Lal, D, and Somayajulu, BLK, 1975, Chronology of marine sediments using the ^{10}Be method: intercomparison with other methods: Geochim et Cosmochim Acta, v 39, p 1187-1192.

Elmore, D, Tubbs, LE, Newman, D, Ma, XZ, Finkel, R, Nishiizumi, K, Beer, J, Oeschger, H, and Andrée, M, in press, The ^{36}Cl bomb pulse measured in a 100 m ice core from Dye 3, Greenland: submitted to Nature.

Finkel, R, Krishnaswami, S, and Clarck, DL, 1977, ^{10}Be in arctic ocean sediments: Earth Planetary Sci Letters, v 35, p 199-204.

Hammer, CU, Clausen, HB, Dansgaard, W, Gundestrub, N, Johnsen, SJ, and Reeh, N, 1978, Dating of Greenland ice cores by flow models, isotopes, volcanic debris and continental dust: Jour Glaciol, v 20, p 3-26.

Herron, MM, and Langway CC, 1982, Chloride, nitrate and sulfate in the Dye 3 and Camp Century, Greenland, ice cores: Am Geophys Union mtg, Philadelphia, May 31-June 14, 1982.

Lal, D, and Peters, B, 1967, Cosmic ray produced radioactivity on the earth, in Flügge, S, ed, Handbuch Physik: Berlin, Springer, v 462, p 551-612.

McCorkell, R, Fireman, EL, and Langway, CC, 1967, Aluminum-26 and Beryllium-10 in Greenland ice: Science, v 158, p 1690-1692.

Moller, F, 1951, Vierteljahreskarten des Niederschlages für die ganze Erde: Petermanns Geog Mitt, v 95, p 1-7.

Nishiizumi, K, Arnold, JR, Elmore, D, Ferraro, RD, Gove, HE, Finkel, RC, Beukens, RO, Chang, KH, and Kilius, LR, 1979, Measurements of ^{36}Cl in antarctic meteorites and antarctic ice using a van de Graaff accelerator, in Earth Planetary

Sci Letters, v 45, p 285-292.

Oeschger, H, Beer, J, Loosli, HH, and Schotterer, U, 1981, Low level counting systems in deep underground laboratories, in Methods of low-level-counting and spectrometry: IAEA symposium, Berlin 1981, Proc: p 459-474.

Oeschger, H, Houtermans, J, Loosli, HH, and Wahlen, M, 1970, The constancy of cosmic radiation from isotope studies in meteorites and on the Earth, in Olsson, IU, ed, Radiocarbon variations and absolute chronology: New York, John Wiley + Sons, p 471-498.

Raisbeck, GM, Yiou, F, Fruneau, M, Loiseaux, JM, Lieuvin, M, and Ravel, JC, 1979, Cosmogenic ^{10}Be; mean deposition rate and seasonal concentration variations in precipitation: Nature, v 282, p 279-280.

Raisbeck, GM, Yiou, F, Lieuvin, M, Ravel, JC, Fruneau, M, and Loiseaux, JM, 1981, ^{10}Be in the environment: some recent results and their applications, in Kutschera, W, ed, Symposium on accelerator mass spectrometry, Proc: Argonne, Illinois, p 228-243.

Siegenthaler, U, Heimann, M, and Oeschger, H, 1980, ^{14}C variations caused by changes in the global carbon cycle: in Stuiver, Minze and Kra, Renee, eds, Internatl radiocarbon Conf, 10th, Proc: Radiocarbon, v 22, no. 2, p 177-191.

Somayajulu, BLK, 1977, Analysis of causes for the beryllium-10 variations in deep sea sediments: Geochim et Cosmochim Acta, v 41, p 909-913.

Stauffer, B, Neftel, A, Oeschger, H, and Schwander, J, 1982, CO_2 concentration in air extracted from Greenland ice samples: Am Geophys Union mtg, Philadelphia, May 31 - June 14, 1982.

Stuiver, Minze, and Quay, PD, 1980, Changes in atmospheric carbon-14 attributed to a variable sun: Science, v 207, p 11-19.

Stuiver, Minze, and Quay, PD, 1981, Atmospheric ^{14}C changes resulting from fossil fuel CO_2 release and cosmic ray flux variability: Earth Planetary Sci Letters, v 53, p 349-362.

Suess, HE, 1980, The radiocarbon record in tree rings of the last 8000 years, in Stuiver, Minze and Kra, Renee, eds, Internatl radiocarbon Conf, 10th, Proc: v 22, no. 2, p 200-209.

Woelfli, W, Bonani, G, Suter, M, Balzer, R, Nessi, M, and Stoller, Ch, 1982, Radioisotope dating with the ETHZ-EN-tandem accelerator, in Stuiver, Minze and Kra, Renee, eds, Internatl radiocarbon Conf, 11th, Proc: Radiocarbon, v 25.

[Radiocarbon, Vol 25, No. 2, 1983, P 279-286]

CALIBRATED ^{14}C DATES IN CENTRAL EUROPE - SAME AS ELSEWHERE?

J C FREUNDLICH and BURGHART SCHMIDT

^{14}C -Laboratorium and Labor fuer Dendrochronologie, Univ Koeln
Weyertal 125, D-5000 Koeln 41, Germany (Fed Rep)

ABSTRACT. ^{14}C dating results derived from an absolutely-dated 471-year tree-ring sequence from central European oak show a trend towards somewhat older dates than those for bristlecone-pine tree rings of the same age, but similar to those for Egyptian historical samples. Differences visible between these trend lines are not relevant considering the standard errors proposed by Clark (1975).

INTRODUCTION

From the beginning, the ^{14}C dating method has been extensively checked (Arnold and Libby, 1949) by testing samples of known age. Subsequently, many more known-age samples were cross-dated by ^{14}C, (1) mostly tree-rings from California long-lived trees (more than 1000 dates; Clark, 1975; Klein et al, 1982) and (2) Egyptian historically dated materials (about 50 dates; Olsson, 1970; Clark and Renfrew, 1973). From these measurements it was concluded that ^{14}C dates generally deviate from known ages by determinable amounts of time and that recalibration is needed before comparing ^{14}C dates with historical dates.

CALIBRATION FUNCTIONS

For this "calibration," 16 tables or graphs were prepared by a variety of interpolation methods: (1) free-hand line drawing, (2) Fourier analysis, (3) polynomial regression, (4) averaging methods, and (5) spline functions. McKerrell (1975) compiled ^{14}C analyses on Egyptian historically dated samples for comparison with the results gained on bristlecone-pine tree rings. Figure 1 shows that there is no contradiction between calibration functions as long as realistic allowance is made (Clark, 1975) for measurement scatter.

EUROPEAN OAK CHRONOLOGIES

A third path towards known-age material was opened by Huber (1941) inaugurating dendrochronology of the European oak. Seven laboratories in Germany reported on progress of dendrochronology in central Europe (Frenzel, 1977), other laboratories are active in Northern Ireland, Belgium, and Switzerland. Close cooperation recently resulted in an absolute oak chronology

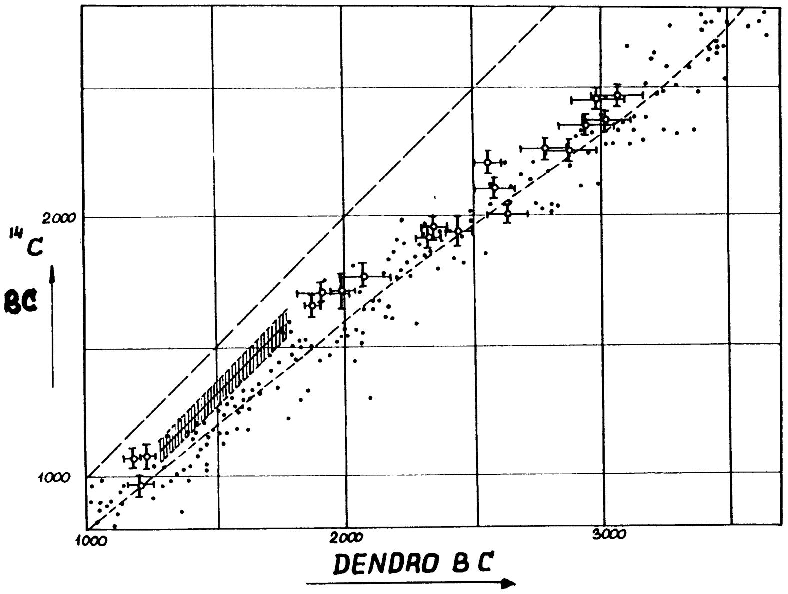

Fig 1. Comparison of ^{14}C measurements on samples of precisely known age from Egyptian history and from bristlecone-pine tree rings.

● = bristlecone-pine tree rings (after McKerrell, 1975, fig 5, p 73)

⊢ϕ⊣ = Egyptian samples (with error range after McKerrell, 1975, fig 11, p 77)

----- = 6th order regression polynomial

covering the last four millennia (Schmidt and Schwabedissen, 1982) and offered promise for a connection with the 4000-yr chronology of the Irish oak (Pearson, Pilcher, and Baillie, 1983; Becker, 1983).

RESULTS

A tree-ring sequence of nearly 500 years close to the oldest part of our chronology was analyzed in our laboratory (table 1). Figure 2A shows the results as well as those of contemporaneous bristlecone-pine tree rings (Suess, 1978). Measurements were made in our CO_2-filled proportional counters containing ca 1g of carbon accumulating ca 150,000 to 300,000 counts. Tree-ring samples were pretreated by the acid/alkali/acid (AAA) method described earlier (Freundlich, 1973); results were measured to a counting statistic precision of 2.4‰ (±19 yr) to 3.5‰ (±28 yr). Estimating a set of additional error sources equivalent to Pearson et al (1977) increases these standard errors by a factor of nearly 1.3.

TABLE 1. Koeln ^{14}C measurements on absolutely-dated tree rings from European oak

					^{14}C Date			
^{14}C sample	Tree-ring sample	No. annual rings	Dendro-date* BC	Dendro-date* BP	^{13}C corrected	BP	1σ error	$\delta^{13}C$ ‰
KN-2800	Ram 5/ 36	16	1732	3681	1507	3456	21	-25.8
-2799	Ram 5/ 69	11	1699	3648	1597	3546	19	-25.8
-2798	Ram 5/ 95	8	1673	3622	1492	3441	22	-24.2
-2797	Ram 5/125	8	1643	3592	1436	3385	28	-24.3
-2796	Ram 5/155	5	1613	3562	1394	3343	23	-24.4
-2795	Ram 5/185	7	1583	3532	1450	3399	25	-24.5
-2429	IpM370/ 18	4	1559	3508	1403	3352	27	-25.0
-2794	Ram 5/215	8	1553	3502	1293	3242	22	-25.4
-2430	IpM370/ 38	4	1539	3488	1343	3292	28	-24.6
-2793	Ram 5/247	12	1521	3470	1320	3269	26	-24.9
-2431	IpM370/ 58	4	1519	3468	1336	3285	27	-24.8
-2432	IpM370/ 78	4	1499	3448	1384	3333	28	-24.6
-2792	Ram 5/275	8	1493	3442	1334	3283	28	-24.8
-2433	IpM370/ 98	4	1479	3428	1366	3315	27	-24.2
-2791	Ram 5/305	12	1463	3412	1288	3237	25	-25.0
-2434	IpM370/118	4	1459	3408	1236	3185	28	-24.5
-2435	IpM370/138	4	1439	3388	1256	3205	27	-25.0
-2790	Ram 5/335	7	1433	3382	1212	3161	26	-24.5
-2436	IpM370/158	4	1419	3368	1191	3140	25	-25.1
-2437	IpM370/178	4	1399	3348	1249	3198	27	-25.4
-2438	IpM370/198	4	1379	3328	1231	3180	28	-24.4
-2439	IpM370/218	4	1359	3308	1163	3112	28	-25.1
-2440	IpM370/238	4	1339	3288	1158	3107	27	-24.5
-2441	IpM370/258	4	1319	3268	1104	3053	28	-24.5
-2442	IpM370/278	4	1299	3248	1134	3083	27	-24.6

* From middle tree ring

Statistical approximation by a weighted least squares regression line yields a slope ($\Delta^{14}C/\Delta$dendro) = 1.0138 and least squares standard deviation of ±43.3 years (fig 2B). The calibration curve of Clark (1975) is included for reference (including Clark's standard error of ± 112 years). Figures 2A and 2B show a trend similar to that found by comparing Egyptian historical samples with bristlecone-pine tree rings. Our ^{14}C dates for central European tree rings lie fairly close to bristlecone-pine tree rings of the same dendrochronologic age, almost within the 1σ statistical range. (The same is evident by entering our regression line in figure 1 - shaded band).

WIGGLES. Our results show "wiggles" although not very conspicuously. It seems that we are in a relatively quiet period similar to that of Pearson et al (1977). Perhaps the wiggles structure will become more evident upon subsequent reduction of standard errors. The average standard deviation, ± 43.3 years as derived from our least squares approximation is comparable to the adjusted average precision figure, ± 33 years, especially when visualizing the observable wiggles structure.

FHS DATE. Besides the absolute dendrochronologic date of our analyzed tree rings, a "wiggle-matching" date has also been tentatively determined by a method similar to the one proposed by FHS (Ferguson, Huber, and Suess, 1966) (table 2; fig 3).

TABLE 2. Comparison of dendrochronologic and FHS dates for the first tree ring of our 471-year sequence.

FHS date (fig 3)	1830 ± 40	BC
Dedrochronologic date	1737	BC

The resulting difference, 63 ± 40 years, closely resembles the "off-set" figures quoted for bristlecone pine by Stuiver (1982, table 2, p 18). Possible reasons for this off-set may be attributed to 1) in situ ^{14}C production (Suess and Strahm, 1970, p 94,95; Radnell, Aitken, and Otlet, 1979), 2) younger ^{14}C transported by mobile organic constituents (Suess, 1978, p 4, legend, App 1; Long et al, 1979).

CONCLUSION

There has been considerable unrest about calibrated ^{14}C dates from the Old World Bronze age, presumably because inherent precision questions had not been adequately assessed. Even McKerrell's (1975) alternate list of "Egyptian historical" calibration figures lying almost halfway between bristlecone-pine calibration figures and zero calibration, does not lie off further than permissible by statistics (!). Our results fit this quite well (fig 1). They are somewhat different from formerly accepted bristlecone-pine based calibration figures; they do not give completely new figures, but rather form a narrower band of somewhat revised calibration figures for the time period mentioned (table 3).

ACKNOWLEDGMENTS

Thanks are due Hermann Schwabedissen for his invaluable assistance, Hajo Hayen, Oldenburg/O, and Friedrich Hohenschwert, Detmold, and many others for cooperation in field work; U Jux, N Zygojannis, and S Strecker, Geol Inst, Univ Koeln, for ^{13}C analyses, and Roland Aniol, for computer programming. Our work was partly funded by Deutsche Forschungsgemeinschaft, Bonn, and by Stiftung Volkswagenwerk, Hannover. We were assisted by H Grützmacher, E Norkus, and P Velicky.

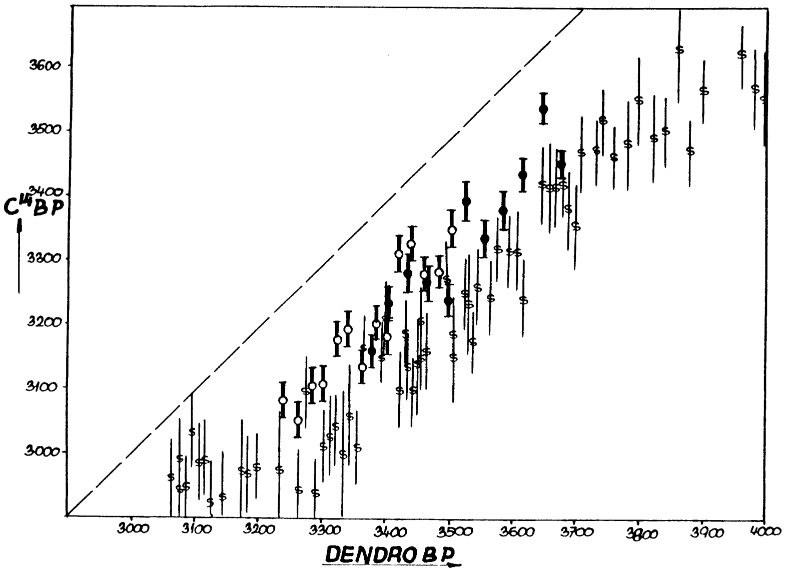

Fig 2A. ^{14}C measurement on absolutely dated tree rings from European oak. Chart of individual dates with 1σ counting error.

○; ● = this paper (IpM370; Ram5 tree-ring series)

$ = bristlecone-pine dates (after Suess, 1978)

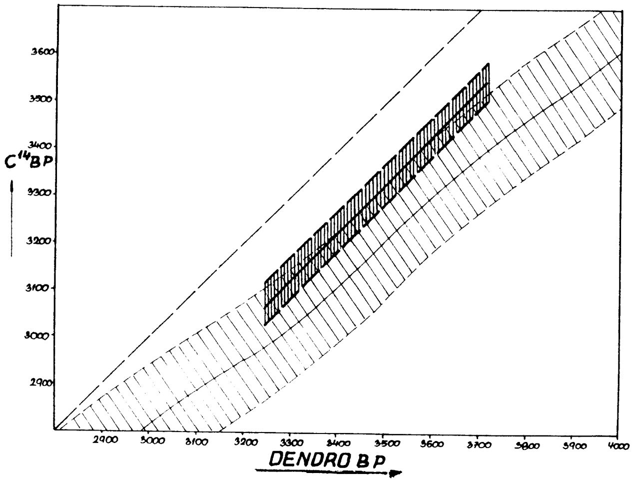

Fig 2B. Trend lines (with band giving average 1σ statistical error)

▥ = this paper; least squares regression line

▨ = bristlecone pine: spline functions (after Clark, 1975)

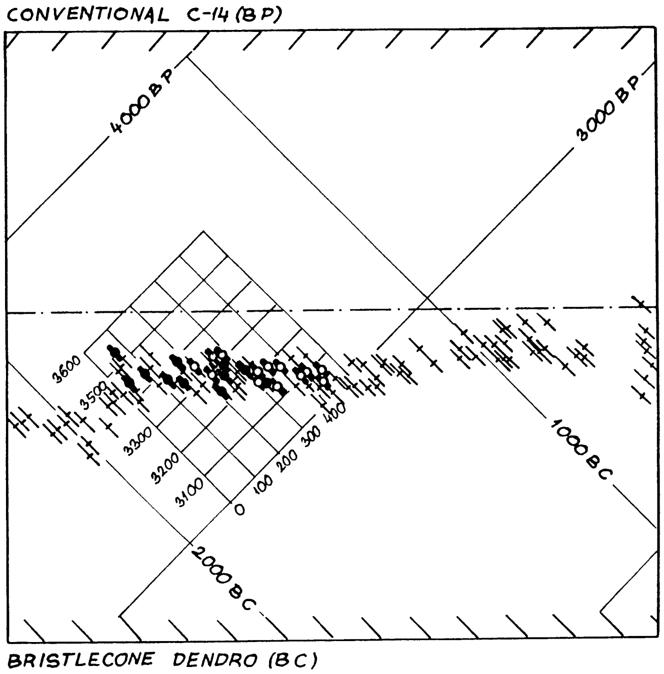

Fig 3. Tentative bristlecone-pine calibration with method proposed by Ferguson, Huber, and Suess (1966)

o: ● = this paper (only relative year rings used)

+ = bristlecone-pine date (after Suess, 1970)

TABLE 3. Comparison between calibration figures from various sources (calendrical minus ^{14}C dates in years)

Calibration figure (years) as quoted from \ Conventional ^{14}C date (5568)	1050 3000	1250 3200	1450 3400	1650 B C 3600 B P
Damon, Long, and Wallick (1972)	275±125	325±103	380±103	440± 63
Switsur (1973)	280±125	310±103	375±103	445± 63
Ralph, Michael, and Han (1973)	250	270/340	270/420	460
Clark (1975 (1 σ standard error)	270±112	300±112	320±112	385±112
McKerrell (1975) ("Egyptian historical")	80/170	90/180	120/230	200/320
("50-year average")	210/320	270/310	250/430	430/460
Suess (1979)	260/340	270/330	290	310/450
Freundlich and Schmidt (1983) (least squares fit)	(184± 43)	181± 43	179± 43	(176± 43)

REFERENCES

Arnold JR and Libby, WF, 1949, Age determinations by radiocarbon content: Checks with samples of known age: Science v 110, p 678-680.

Becker, B, 1983, Long-term radiocarbon trends of the absolute Central-European tree-ring sequence, in Stuiver, M and Kra, RS, eds, Internatl ^{14}C conf, 11th, Proc: Radiocarbon, v 25.

Clark, RM, 1975, A calibration curve for radiocarbon dates; Antiquity, v 49, p 251-266.

Clark, RM and Renfrew, C, 1973, Tree-ring calibration of radiocarbon dates and the chronology of ancient Egypt: Nature, v 243, p 266-270.

Damon, PE, Long, A, and Wallick, EI, 1972, Dendrochronologic calibration of the carbon-14 time scale, in Rafter, TA and Grant-Taylor, T, eds, Internatl conf on ^{14}C dating, 8th, Proc: Wellington, Royal Soc New Zealand, v 1, p A29-A43.

Ferguson, CW, Huber, B, and Suess, HE, 1966, Determination of the age of Swiss lake dwellings as an example of dendrochronologically-calibrated radiocarbon dating: Zeitschr Naturforsch, ser a, v 21, p 1173-1177.

Frenzel, B, ed, 1977, Dendrochronologie and postglaziale Klimaschwankungen in Europa: Wiesbaden, F Steiner Verlag.

Freundlich, JC, 1973, Die Altersbestimmungen nach der Radiokohlenstoffmethode: Archäol Korrespondenzblatt, Mainz, von Zabern Verlag, v 3, p 159-162.

Huber, B, 1941, Aufbau einer mitteleuropäischen Jahrringchronologie: Mitt Akad Deutsch Forstwiss, v 1, p 110-125 (after Frenzel, ed, 1977, p 8).

Klein, J, Lerman, JC, Damon, PE, and Ralph, EK, 1982, Calibration of radiocarbon dates: Tables based on the consensus data of the workshop on calibrating the radiocarbon time scale: Radiocarbon, v 24, p 103-150.

Long, A, Arnold, LD, Damon, PE, Ferguson, CW, Berman, JC, and Wilson, AT, 1979, Radial translocation of carbon in bristlecone pine, in Berger, Rainer and Suess, HE, eds, Radiocarbon dating, Internatl ^{14}C conf, 9th, Proc: Berkeley, Univ California Press, p 532-537.

McKerrell, H, 1975, Correction procedures for C-14 dates, in Watkins, T, ed, Radiocarbon: Calibration and prehistory: Edinburgh, Univ Press, p 47-100.

Olsson, IU, ed, 1970, Radiocarbon variations and absolute chronology: Stockholm, Almqvist & Wiksell.

Pearson, GE, Pilcher, JR, Baillie, MGL, and Hillam, J, 1977, Absolute radiocarbon dating using a low altitude European tree-ring calibration: Nature, v 270, p 25-28.

Pearson, GW, Pilcher, JR, and Baillie, MGL, 1983, High-precision ^{14}C measurement of Irish Oaks to show the natural ^{14}C variations from 200BC to 4000BC, in Stuiver, M and Kra, RS, eds, Internatl ^{14}C conf, 11th, Proc: Radiocarbon, v 25.

Radnell, CJ, Aitken, MJ, and Otlet, RL, 1979, In-situ production of ^{14}C in wood, in Berger, Rainer and Suess, HE, eds, Radiocarbon dating, Internatl ^{14}C conf, 9th, Proc: Berkeley, Univ California Press, p 543-657.

Ralph, EK, Michael, HN, and Han, MC, 1973, Radiocarbon dates and reality: Masca Newsletter, v 9, p 1-20.

Schmidt, B and Schwabedissen, H, 1982, Ausbau des mitteleuropäischen Eichenjahrringkalenders bis in neolithische Zeit (2061 v Chr): Archäol Korrespondenzblatt, Mainz, von Zabern Verlag, v 12, p 107-108.

Stuiver, M, 1982, A high-precision calibration of the AD radiocarbon time scale: Radiocarbon, v 24, p 1-26.

Suess, HE, 1978, La Jolla measurements of radiocarbon in tree-ring dated wood: Radiocarbon, v 20, p 1-18.

______ 1979, A calibration table for conventional radiocarbon dates, in Berger, Rainer and Suess, HE, eds, Radiocarbon dating, Internatl ^{14}C conf, 9th, Proc: Berkeley, Univ California Press, p 777-784.

Suess, HE and Strahm, C, 1970, The Neolithic of Auvernier, Switzerland: Antiquity, v 44, p 91-99.

Switsur, VR, 1973, The radiocarbon calendar recalibrated: Antiquity, v 37, p 131-137.

[Radiocarbon, Vol 25, No. 2, 1983, P 287-288]

DENDROCHRONOLOGY OF BRISTLECONE PINE: A PROGRESS REPORT

C W FERGUSON and D A GRAYBILL

Laboratory of Tree-Ring Research
University of Arizona
Tucson, Arizona 85721

ABSTRACT. Dendrochronological studies of bristlecone pine, *Pinus longaeva*, have produced a continuous tree-ring sequence back to 6700 BC for the White Mountains of California and to 3258 BC for east-central Nevada.

Dendrochronological studies of bristlecone pine, *Pinus longaeva*, at 10,000 feet in the White Mountains of east-central California, have resulted in the establishment of a continuous tree-ring sequence back to 6700 BC, a total of 8681 years. This represents a 1576-year extension of the chronology since it was last published (Ferguson, 1969;1970).

Given the quality and length of series of specimens that have recently been dated in the 5500-6500 BC range, we are cautiously optimistic that the chronology may eventually reach back at least 10,000 years. This thought is buttressed by the presence of a 500-year "floating" sequence in the range of 9000 years BP (Ferguson, 1968). Current ^{14}C analysis seems to indicate that another remnant, collected in 1981, again with ca 500 rings, may be over 10,000 years old (H N Michael, pers commun, 1982). Continuing tree-ring and ^{14}C studies will further define the temporal relationship of these two specimens.

One other long bristlecone-pine chronology was recently developed. Collections at a site in the White Pine Range, east-central Nevada, have provided excellent material for a chronology back to 3258 BC, a total of 5238 years. This provides the second longest continuous record of isotopic and paleoclimatic variation at the lower, rainfall dependent range of the species.

The historic development of the bristlecone-pine project, a general overview of its relation to other scientific activity and a summary of the inventory of prepared samples was recently presented by Ferguson (1979). The primary focus of the project -- to provide dendrochronologically-dated decade samples for an interlaboratory calibration of the ^{14}C time scale (Klein *et al*, 1982) -- continues as bulk material for selected time periods becomes available.

Another focus of the project is to attempt paleoclimatic inference with the long bristlecone-pine tree-ring series (Ferguson and Graybill, 1981). The primary climatic signal that can be isolated in both the California and Nevada series is annual moisture variability. Current efforts are directed at calibration of the tree-ring series with instrumented climatic series.

ACKNOWLEDGMENTS

We would like to thank the National Science Foundation for their support, since 1956, of the bristlecone-pine project through various grants, most recently EAR 78-04436 and EAR-8018687. The US Department of Energy should also be acknowledged for their recent support of the bristlecone-pine project with Contracts EE-78-A-28-3274 and DEC-AC02-81EV10680.

Field work has been in cooperation with divisions of the US Forest Service, especially the Inyo National Forest, Bishop, California, the Humboldt National Forest, Elko, Nevada, and the Toiyabe National Forest, Reno, Nevada.

REFERENCES

Ferguson, CW, 1968, Bristlecone Pine; Science and Esthetics: Science, v 159, no. 3817, p 839-846.

________ 1969, A 7104-year annual tree-ring chronology for bristlecone pine, Pinus aristata, from the White Mountains, California: Tree-Ring Bull, v 29, no. 3-4, p 1-29.

________ 1970, Dendrochronology of bristlecone pine, Pinus aristata: establishment of a 7484-year chronology in the White Mountains of eastern-central California, in Olsson, I U, ed, Radiocarbon variations and absolute chronology: New York, John Wiley & Sons, p 237-245.

________ 1979, Dendrochronology of bristlecone pine, Pinus longaeva: Environment Internat, v 2, no. 4-6, p 209-214.

Ferguson, CW and Graybill, DA, 1981, Dendrochronology of bristlecone pine: Terminal rept NSF Grant EAR-78-04436 and DOE no. EE-78-A-28-3274.

Klein, Jeffrey, Lerman, JC, Damon, PE, and Ralph, EK, 1982, Calibration of radiocarbon dates: Tables based on the consensus data of the Workshop on Calibrating the Radiocarbon Time Scale: Radiocarbon, v 24, p 103-150.

II. HYDROLOGY

[Radiocarbon, Vol 25, No. 2, 1983, P 291-300]

MATHEMATICAL MODELING OF THE DISTRIBUTION OF NATURAL ^{14}C, ^{234}U, and ^{238}U IN A REGIONAL GROUND-WATER SYSTEM

F J PEARSON, JR, C J NORONHA, and R W ANDREWS
INTERA Environmental Consultants, Inc
11999 Katy Freeway, Suite 610, Houston, Texas 77079

Increasing concern with nuclear waste isolation technology is leading to additional studies of naturally occurring isotopes in ground water. Such studies provide information on 1) the use of radionuclides to estimate ground-water travel times and/or residence times. This information can be an extremely useful adjunct to conventional hydrologic data in developing the understanding of regional hydrology needed in the site selection process, and 2) the use of natural radionuclides as analogues to the behavior of radionuclides of concern in nuclear waste.

Many waste isolation decisions will be based on the results of digital models simulating the performance of proposed repositories. It is important not only that such models be demonstratably valid representations of the phenomena they are meant to simulate, but also, that the parameters used in them for specific performance assessments be correct within known limits. A simulation of the measured behavior of naturally occurring radionuclides on a regional scale can serve to validate simulation models themselves or, for models known to be valid, can serve as calibration in a given site situation.

In this paper we will describe the use of a digital ground-water flow and radionuclide transport model to simulate the behavior of ^{14}C and ^{234}U and ^{238}U in the Carrizo Aquifer of south Texas. The hydrology and distribution of ^{14}C in the system have been described by Pearson and White (1967) and the uranium isotope data are from Cowart and Osmond (1974) and Osmond (written commun 1981).

Enough is known about Carrizo hydrology and carbonate geochemistry to permit the calculation of ^{14}C concentrations in the aquifer. Agreement of the calculated values with the measured values validates the model. The validated model is then used to simulate uranium transport and to determine uranium retardation in the system from comparison between calculated and measured $^{234}U/^{238}U$ ratios.

NUCLIDE TRANSPORT MODEL. A solute moving in a ground-water system can be described by the conservation of mass equation (written here for one-dimensional transport):

$$\frac{\partial}{\partial t}\left[\phi C_f + \rho_s (1-\phi)\, C_s\right] = -\frac{\partial}{\partial x}\left(V_D C_f - \phi D \frac{\partial C_f}{\partial x}\right) - \lambda\left[\phi C_f + \rho_s (1-\phi)\, C_s\right] \pm I \qquad (1)$$

On the left of the equal sign is an accumulation term. The first term on the right represents transport of the solute both by convection (the first term in parenthesis) and dispersion (the second term in parenthesis). The second term on the right is a chemical reaction term, and is written here as a simple first order decay, as appropriate for radioisotopes. The third term is a source (+) or sink (-) term. The parameters in the equation are:

C_f, C_s = solute concentration in the moving fluid (f) and on the stationary solid (s), (mass/mass)

ρ_s = solid grain density (mass/volume)

ϕ = porosity (volume/volume)

λ = first order decay constant (time^{-1})

I = source/sink term (mass/time)

V_D = specific discharge (length/time). The magnitude and direction of this term depends on ground-water flow in the system. It equals the discharge (volume/time) per area of flow (length^2) and is often called the Darcy velocity. It should not be confused with the actual velocity of water movement through the pores of the aquifer which is the interstitial velocity, V_i, and equals V_D/ϕ.

D = $\alpha \dfrac{V_D}{\phi} + \dfrac{D_m}{\phi\tau}$;

α is the hydrodynamic dispersivity (length) and is an aquifer property the value of which tends to increase with the scale of the modeled system (Pickens and Grisak, 1981). D_m is the conventional molecular diffusion coefficient (length^2/time), and τ

> the tortuosity (length/length). Typically, the dispersivity term is several orders of magnitude larger than the diffusion term.

Evaluation of the transport equation (1) is greatly simplified by expressing the solid phase concentration (C_s) in terms of concentration in the fluid phase (C_f). Most transport models are intended for use with trace solute concentrations and include the assumption that the solid and fluid concentrations are linearly related by: $C_s = k_d C_f$. The proportionality constant k_d is known as the distribution coefficient.

With this assumption, the terms in brackets in equation (1) can be written:

$$\left[\phi C_f + \rho_s(1-\phi)C_s\right] = \left(1 + \frac{(1-\phi)}{\phi}\,\rho_s k_d\right)\,\phi\,C_f \qquad (2)$$

The term in parenthesis in (2) equals the retardation coefficient, R_d, which is the ratio of the interstitial fluid velocity, V_i, to the rate of movement of the solute itself, V_c. The total mass of solute present in a given volume of aquifer equals that present in the fluid phase (ϕC_f) plus that associated with the solid ($\rho_s(1-\phi)C_s$). The rate of movement of the dissolved nuclide equals the interstitial velocity of the fluid itself, while the nuclide associated with the solid is stationary. The apparent velocity of the nuclide in the given aquifer volume is then:

$$V_c = \frac{V_i\,\phi\,C_f}{\phi C_f + \rho_s(1-\phi)C_s}, \text{ and, } R_d = \frac{V_i}{V_c} = 1 + \frac{(1-\phi)}{\phi}\,\rho_s k_d \qquad (3)$$

While some closed-form solutions to Equation (1) are available, numerical solution techniques have certain advantages. For adequate simulations in many natural environments, it is necessary to consider spatial variation of the hydraulic properties of the aquifer system, and the consequent variations in the flow field. It is also not uncommon that chemical variability in a flow system effects solute transport in a way that can be simulated only by permitting spatial variation in the distribution coefficients. Finally, while for simplicity only the one-dimensional form of a solute transport equation has been considered here, transport in two or even three dimensions must normally be treated in order to simulate real field problems. Multi-dimensional solute transport equations can only be evaluated numerically except for a few very highly idealized physical situations useful only in relatively few real situations.

Digital models for solute transport simulation are complex and require validation before they can be applied with confidence to performance assessment problems. An appropriate validation test is to show that a given model is capable of adequately simulating the behavior of a system similar in such respects as time and distance scale and radioisotope identity to the systems that are to be assessed. The simulation of the ^{14}C distribution in the Carrizo described here was made using the finite-difference model SWENT (Simulator for Water, Energy and Nuclide Transport).

FIELD SETTING AND DATA. The Carrizo formation of south Texas is an Eocene coastal plain sandstone which crops out nearly parallel to the coast and dips toward the Gulf of Mexico. In the area of interest in Atascosa and counties to the south, the aquifer is used for water supply at depths to over 1500m. Because of its importance as a water supply, the Carrizo has been intensely studied for over 50 years. A comprehensive report on its hydrology together with a numerical model of its regional flow was made by the Texas Water Development Board (Klempt, Duffin and Elder, 1976). The data required to calculate the ground-water flow term V_D in equation (1) were taken from Klempt's report.

For this report, a vertical cross-section of the Carrizo was modeled, extending from its outcrop in northern Atascosa County down-gradient to the southeast for 100km. The finite difference model comprised 100 blocks of 1km each in the horizontal (x) direction and with vertical (z) dimensions ranging from 45.7 to 243.8m to match the varying aquifer thickness.

To model nuclide transport in the Carrizo requires values of the parameters in the solute transport equation (1) in addition to V_D. The values used and the rationale behind their selection are as follows:

ϕ 35%. Many Carrizo porosity measurements have been made, most between 30 and 40%. The central value was chosen (Pearson and White, 1967).

α 500m. This value was chosen to satisfy constraints imposed by the finite difference procedure used. While it is, perhaps, 10 or 20 times larger than values determined in other aquifer systems (Anderson, 1979, table 4), these determinations were made in systems at least a factor of 10 smaller than that described here. Because of the scale dependence of dispersivity mentioned above, the value chosen is probably not inappropriate.

ρ_s 2.6 gm/ml. The Carrizo is composed mostly of quartz sand with only minor amounts of other minerals (Pearson and White, 1967). The density chosen is that of quartz.

λ $^{14}C = 1.210 \times 10^{-4} yr^{-1}$;
$^{238}U = 1.551 \times 10^{-10} yr^{-1}$;
$^{234}U = 2.841 \times 10^{-6} yr^{-1}$.

C_f mass nuclide/mass water. Values of this parameter as a function of space were calculated using the model and compared with measured ^{14}C and $^{234}U/^{238}U$ data for model validation and uranium retardation determination, respectively. The transformation of measured carbon and uranium isotope data to mass fractions and the methods for selecting source rates (I) and distribution coefficients (k_d) are described below.

^{14}C DATA AND SIMULATION RESULTS. A number of measurements of the ^{14}C content of Carrizo water in the region modeled are available. They include both total dissolved carbonate contents ($C_{tot} = H_2CO_3 + HCO_3^- + CO_3^{-2}$) and the ^{14}C content of the dissolved carbonate as pmc (per cent modern carbon). From pmc and C_{tot} values, ^{14}C mass fractions can be calculated using:

$$\frac{gm\ ^{14}C}{gm\ H_2O} = pmc \times C_{tot} \left(\frac{mMol}{kg\ H_2O}\right) \times 1.64 \times 10^{-19}$$

In calculating this constant, the molecular weight of carbon is taken as 12gm, the specific activity of modern carbon (pmc = 100) as 13.56dpm/gmC and the ^{14}C half-life as 5730 years. 100pmc corresponds to 1.37 x 10^{-12}gm ^{14}C/gm C. Table 1 gives the ^{14}C mass fractions for Carrizo waters calculated from the pmc and C_{tot} values of Pearson and White (1967).

The ^{14}C mass fraction in recharge to the Carrizo given in table 1 is based on 100pmc and a C_{tot} value of 2.21 ± 0.12mMol/kg H_2O. The C_{tot} is that determined by Pearson and White (1967) using the relationship between the C_{tot} values of Carrizo samples and their stable ^{13}C isotope contents. The recharge mass fraction value can be combined with the recharge rate from the flow calculations (14.2kg $H_2O/m^2/yr$) to yield the value of 5.14 x 10^{-13}gm $^{14}C/m^2/yr$, the source term, required for the transport equation (1).

The measured ^{14}C mass fractions are shown in figure 1 along with the simulation modeling results. Those obtained using $\phi = 0.35$ are in excellent agreement with the field data, except for samples from two wells in the up-gradient part of the system. These wells are not directly on the modeled cross-section and are in areas of less regular distribution of hydraulic conductivities than elsewhere in the system (Klempt, Duffin, and Elder, 1976). These points do not detract from the overall agreement between field and simulation results which serves to validate the model.

To illustrate the sensitivity of the system to parameter variability, results of a simulation made using $\phi = 0.30$ are also shown in figure 1. The lower porosity leads to slightly higher interstitial water velocities and, hence, to higher ^{14}C mass fractions. The measured ^{14}C data, though, are more consistent with the higher porosity value.

URANIUM DATA AND SIMULATION RESULTS. Many measurements of dissolved uranium concentrations and of ^{234}U activity ratios have been reported for Carrizo samples and are also given in table 1.

Uranium solubility is strongly dependent on its oxidation state. Under oxidizing conditions, as occur near the Carrizo outcrop, the relatively soluble uranyl (UO_2^+) ion is stable, and uranium concentrations in the 1 - 10^2 parts per billion (ppb) range occur. Under reducing conditions, as prevail down-gradient, U^{+4} and its complexes are dominant and uranium concentrations of only 1 - 10 x 10^{-3} ppb occur (table 1).

^{234}U is a daughter of the much longer-lived ^{238}U. In a sufficiently old, closed system the two isotopes will be in secular equilibrium and their activity ratio (AR) will equal one. As figure 2 and table 1 show, at distances from 0 to ca 20km, where the Carrizo is oxidizing the uranium dissolution is occurring, AR values of 1.0 ± 0.3 are found. Between ca 20 and 33km, uranium concentrations drop dramatically (table 1), and AR values concentrations as high as 9 occur. Below ca 33km, low dissolved uranium persists, accompanied by a regular decrease in the AR toward the secular equilibrium value of 1. This decrease can be used as a measure of the rate of uranium movement in the Carrizo, which is related, in turn, to the rate of groundwater via the R_d and k_d factors defined above.

The numerical transport model validated using the ^{14}C data was used to simulate ^{234}U and ^{238}U movement in the reducing part of the Carrizo. The simulation began at a distance of 33km where a constant flux of uranium into the solution with an activity ratio of 9 was assumed. The transport of uranium down-gradient from this source was modeled, using several k_d values to account for reaction between dissolved uranium and the aquifer framework which retards the rate of uranium movement relative to that of the water, itself.

The simulation results are compared with the measured uranium AR values in figure 2. The line of $k_d = 0$ shows how the AR would decrease if uranium behaved like ^{14}C in this system and did not react with the aquifer. Uranium transport in the Carrizo is best simulated using a k_d of 6.0. From equation (3), this indicates that the uranium velocity in the Carrizo is only 1/30 of the insterstitial velocity of water.

The agreement between the calculated and measured AR values throughout the system down-gradient of 33km attests to the validity of choosing a simple linear relationship between C_f and C_s. It also supports the use of a constant k_d value throughout a large part of a regional aquifer system, provided that the geochemical behavior of the element of interest is constant throughout the region being simulated.

ACKNOWLEDGMENTS

Discussions over the years with Ken Osmond and Jim Cowart helped lead to the present interpretation of uranium isotope data. Expressing ^{14}C analyses per unit water rather

TABLE 1. ^{14}C Mass fractions, calculated from data of Pearson and White (1967, table 1) and dissolved uranium concentrations and activity ratios from Cowart and Osmond (1974) and Osmond (written commun., 1981). Errors are of counting and chemical analyses, ± 2 standard deviations.

Sample no.		^{14}C mass fractions x 10^{18}	Uranium concentration x 10^3 ppb	$^{234}U/^{238}U$ activity ratio
Uranium	^{14}C			
Recharge		36.2 ± 2.0		
414	TX - 91	35.6 ± 3.3	202 ± 6	0.90 ± 0.04
469			629 ± 16	1.03 ± 0.03
471			2560 ± 55	.77 ± 0.03
467			29 ± 3	1.09 ± 0.16
	TX-91	32.7 ± 2.5		
2113			7400	0.87
	TX-92	22.8 ± 1.8		
2114			18	1.3
472			8 ± 1	1.77 ± 0.29
	TX-210	29.2 ± 1.9		
468			4 ± 1	5.48 ± 1.63
413	TX-93	16.5 ± 1.0	21 ± 3.5	1.63 ± 0.33
465			3 ± 1	9.02 ± 1.03
466			4 ± 1	6.36 ± 1.68
2105			5	6.7
2115			2.7	7.9
	TX-94	6.4 ± 0.8		
422	TX-226	4.8 ± 0.4	3 ± 1	5.14 ± 1.87
2107			3	5.2
	TX-96	3.5 ± 0.6		
421	TX-216	3.0 ± 0.2	1 ± 4	3.44 ± 1.20
	TX-214	2.1 ± 0.3		
411			4 ± 2	3.93 ± 1.57
	TX-215	2.6		
	TX-92	4.8		
2102			3	4.7
	TX-217	1.1 ± 0.2		
2101			1.1	2.5
	TX-219	< 1.8		
417	TX-218	< 1.1	2 ± 1	2.71 ± 1.00
2104			6	2.80
476			2 ± 4	2.08 ± 0.51

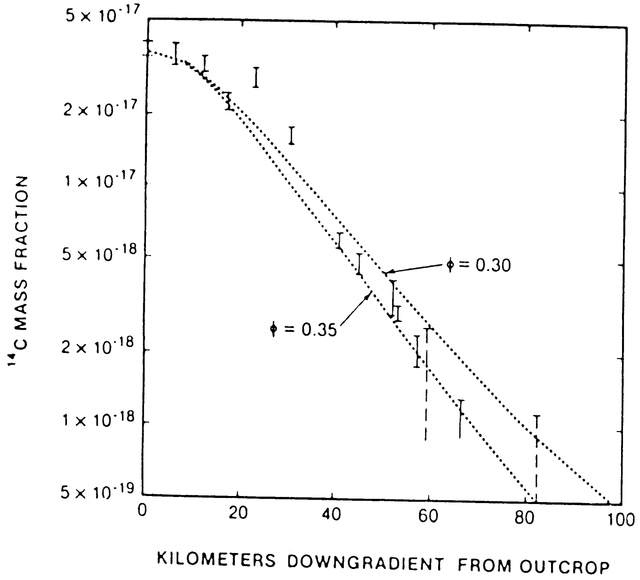

Fig. 1. Measured and simulated ^{14}C contents with distance down-gradient from outcrop

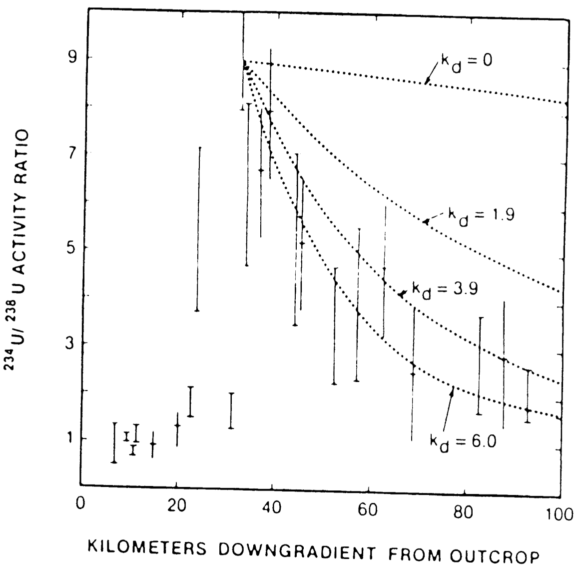

Fig. 2. Measured and simulated uranium activity ratios with distance down-gradient from outcrop

than per unit carbon was required by the transport model used. Oeschger (1974) pointed out that the same approach would also be useful for general ground-water ^{14}C interpretations. These model validation calculations were made as part of the SCEPTER program being carried out by INTERA Environmental Consultants, Inc for the Battelle Projects Management Division, Office of Nuclear Waste Isolation as prime contractor to the U S Department of Energy.

REFERENCES

Anderson, M P, 1979, Using models to simulate the movement of contaminants through groundwater flow systems: CRC Critical Rev Environmental Control, v 9, p 97-156.

Cowart, J B and Osmond, J K, 1974, ^{234}U and ^{238}U in the Carrizo Sandstone aquifer of south Texas, in Isotope Techniques in Groundwater Hydrology 1974: IAEA, Vienna, v 2, p 131-149.

Klempt, W B, Duffin, G L, and Elder, G R, 1976, Ground-water resources of the Carrizo Aquifer in the Winter Garden area of Texas: Texas Water Development Bd Rept 210, v 1, 73 p.

Oeschger, Hans, 1974, Discussion in Isotope Techniques in Groundwater Hydrology 1974: IAEA, Vienna, v 2, p 91.

Pearson, F J, Jr and White, D E, 1967, Carbon-14 ages and flow rates of water in Carrizo sand, Atascosa County, Texas: Water Resources Research, v 3, p 151-161.

Pickens, J F and Grisak, F E, 1981, Modeling of scale dependent dispersion in hydrogeologic systems: Water Resources Research, v 17, p 1701-1711.

[Radiocarbon, Vol 25, No. 2, 1983, P 301-314]

$^{13}CO_2$ AND $^{14}CO_2$ MEASUREMENTS ON SOIL ATMOSPHERE SAMPLED IN THE SUB-SURFACE UNSATURATED ZONE IN THE WESTERN GREAT PLAINS OF THE US

HERBERT HAAS*, DW FISHER**, DC THORSTENSON**, AND EP WEEKS+

ABSTRACT. Soil gas samples were obtained from the unsaturated zone at eight sites in the Great Plains. Three of these sites were sampled extensively for gas composition and carbon isotopes. Sampling equipment consisted of a nest of gas probes vertically spaced by roughly 3m at most sites, generally approaching the water table. Water wells, 10cm in diameter, were screened in the topmost layer groundwater. Inverted cattle tanks were used to collect CO_2 samples from the soil surface. The major gas components were analyzed with emphasis on CO_2, $\delta\,^{13}C$, and ^{14}C measurements. The same components were studied in groundwater samples. Higher than atmospheric CO_2 concentrations were found in all soil samples. Root respiration and oxidation of organic matter were sources for the additional CO_2. When lignite was present in the unsaturated zone, gaseous oxygen reacted almost completely, and CO_2 levels rose to 19%. Near the surface, annual cycles in total CO_2, $\delta\,^{13}C$, and ^{14}C were observed. ^{14}C activities were close to present post-bomb levels at the surface and generally declined with depth. At some sites, oxidation of lignite caused decline of ^{14}C levels to 1 or 2% of their surface value at 8m depth. Without lignite, the ^{14}C activity remained above 50% at all depths. Concentrations of total carbon and its isotopes in ground water remained very stable throughout the study. This implies that geochemical processes in the aquifer vary on time scales longer than the seasonal effects observed in the near-surface unsaturated zone.

INTRODUCTION

The chemistry of CO_2 in soil above the groundwater table has been the subject of several publications. These can be grouped according to the following criteria: 1) depth and number of sampling points in a vertical profile, 2) number

---

* Southern Methodist University, Dallas, Texas 75275
** US Geological Survey, Reston Virginia 22092
+ US Geological Survey, Denver Colorado 80225

of collections made to detect seasonal variation, 3) measurement of stable isotopes $^{13}C/^{12}C$, 4) ^{14}C determination, 5) oxygen concentrations, and 6) the nature of soil gas transport through soil layers.

Seasonal CO_2 variation was studied by Atkinson (1977), Enoch and Dasberg (1971), Miotke (1974), Rightmire (1978), and Reardon, Allison, and Fritz (1979). Galimov (1966), Kunkler (1969), Reardon, Allison, and Fritz (1979), Reardon, Mozeto, and Fritz (1980) and Kunkler (1969) are of particular interest here because they record measurements made with deep probes (5m and 290m, respectively) and theorize on diffusion as a transport model for soil gases.

This study is based on measurements that include all of the above criteria. Also, two selected examples show how stratigraphic differences in the depth profile lead to distinctly different behavior of all soil gas components. Field measurements were made in the Great Plains, at 2 sites in the Texas Panhandle and at 6 sites in southwestern North Dakota. Data are presented here for 3 of the North Dakota sites; 2 of these, near a lignite mine at Gascoyne, North Dakota, were extensively studied. Additional data appear in Thorstenson et al (1983). This paper includes site descriptions, sampling methods and analytical techniques, and inferences drawn from the data. The companion paper (Thorstenson et al, 1983) attempts to model the vapor-phase transport of $^{12}CO_2$, $^{13}CO_2$, and $^{14}CO_2$.

COLLECTION TECHNIQUES

Soil gas pumped from the gas probes and dissolved gas extracted from groundwater samples were analyzed by gas chromatography at the U S Geological Survey laboratory in Reston. The analyzed gas species were CO_2, O_2, N_2, and Ar. CO_2 contained in soil gases and bicarbonate and CO_2 dissolved in the groundwater samples were extracted and analyzed for ^{14}C activity at SMU ^{14}C laboratory. $^{13}C/^{12}C$ stable isotope ratios were measured for all samples.

During the sampling procedure for ^{14}C in the field, the CO_2 in soil gases was absorbed in a 5-molar solution of carbon-free KOH. In the laboratory, this solution was acidified whereby the CO_2 was released, then isolated and converted into benzene for ^{14}C analysis by scintillation counting. Fractionation was avoided during these chemical conversions by ensuring high reaction yields, ie, between 99 and 100%. During collection, similar yields were achieved with a suitable collector flask design (fig 1). The flow of sample gas was dispersed through a fritted glass plate. The fine stream of bubbles rose through 8cm of 5-molar KOH solution. Collected CO_2 was released in the same vessel; no transfer of the

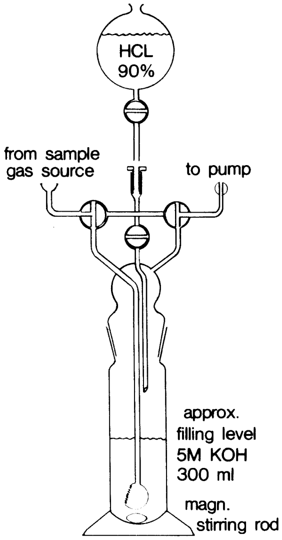

Fig 1. Soil gas collector

solution was necessary. The required amount of acid was introduced through a separate inlet; a built-in small stirring rod assured steady progress of this reaction. Laboratory tests demonstrated a collection efficiency of 99.8% and no detectable fractionation. The NBS oxalic acid standard was used. The collectors contained 300ml of 5-molar KOH solution which can theoretically absorb 15.8L of CO_2 if only the efficient "hydroxide-to-carbonate" reaction is considered. We planned to collect between 7 and 8L of CO_2 from each soil gas probe. We made rapid assessment of the CO_2 concentration in the soil gases by measuring the weight gain of a small ascarite [1] -filled glass tube through which the dried gas was pumped at a flow-gauge-monitored rate of 0.5L per minute. Figure 2 schematically depicts field equipment. The valves on top of the collector flask allow the bypass flow of the gas during initial cleanout of the well and during the ascarite test. Not shown on this drawing are heating tapes around the hoses and collectors to make the field work possible during the hard winter months in North Dakota.

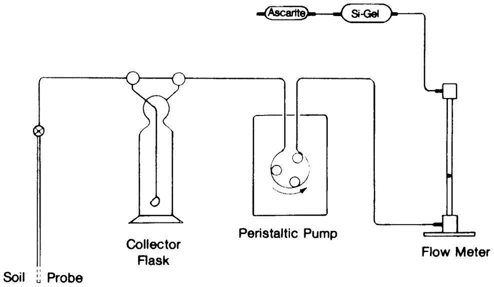

Fig 2. Field installation for soil gas collection

---

[1] Brand name for NaOH-coated asbestos; used for identification purposes only

Water was pumped from the water table wells with a Middelburg pump, consisting of a metal tube equipped with check valves at the top and bottom and a pulsating silicone rubber bladder inside the tube. The pumped water was fed into a 25L plastic carboy. KOH (in pellet form), $SrCl_2$, and $FeSO_4$ were added to the filled carboy. The dissolved CO_2 and HCO_3^- in the water reacts to $SrCO_3$, which flocculates readily in the presence of $FeSO_4$ and settles rapidly in the neck of the inverted carboy. A faucet attached to the cap allowed draining of the sediment into 0.5L bottles. In the laboratory, the sediment was transferred into a hydrolysis system where it was acidified under vacuum. The released CO_2 was processed as above. We also sampled the surface layer of the soil gas at both sites. An inverted cattle tank 2m in diameter was sealed tightly to the ground. Above-ground vegetation was removed from the site, but no attempt was made to remove the roots. Inside the tank, six shallow glass trays filled 1cm deep with 5-molar KOH solution served as CO_2 collectors. Since no pumping was done, no atmospheric air was drawn through the soil into the tank, and CO_2 reached the collector trays only through diffusion from the root zone.

DESCRIPTION

Most of the data presented in this paper were collected from sites in southwestern North Dakota and near the Gascoyne lignite mine in Bowman County. Two of these sites (unmined) were extensively studied and provide the basis for the models proposed by Thorstenson et al, (1983). The intensity of sampling at the other North Dakota sites has been variable.

The Gascoyne area of North Dakota has been under study by the Water Resources Division of the U S Geological Survey since the early 1970's. The early investigations are reported in Fisher and Thorstenson (1983).

Samples for ^{14}C analysis were collected at some sites as early as 1977. The water table wells at Sites 1, 4, and 6 were drilled in the summer of 1980. The general stratigraphic relationship between the lignite, water table, ground surface, and sampling nests for the two intensive-study sites (4 and 6) are shown in figure 3. These sites are discussed in some detail below; shorter descriptions of the other sites follow.

NORTH DAKOTA SITE 4 (T131N, R099 W, sec 33DCD) This site is located on a local topographic high (ca 15m) accompanied by a local high in the water table, at 17.4m below ground surface. Recharge at this site must therefore be vertical. From the surface to a depth of ca 8m, the rocks consist of siltstone and claystone. A thin stringer of lignite may be present at ca 5m. Bulk x-ray diffraction (XRD) of core samples showed

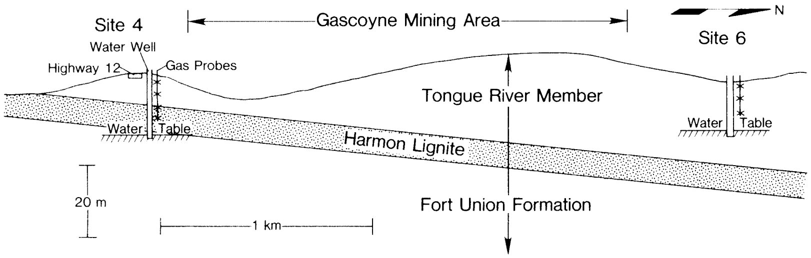

Fig 3. Cross section through Gascoyne mining area

abundant quartz, kaolinite, chlorite, illite, and smectite in the sites and clays. Dolomite ranges from 15 to 20%; calcite is absent. Abundant gypsum (15%) is present in the upper part of the lignite; sulfides are absent. Harmon lignite is present from 8 to 16m, underlain to the water table (17m) by mudstone and siltstone. The bottom two gas probes were screened in the lignite, which is sufficiently close to ground surface to be strongly oxidized. Except for the gypsum near its top, the only XRD-identifiable minerals in the lignite are small amounts of quartz, feldspar, and clays. The lignite is eroded away south of Site 4. The top two gas probes were screened above the Harmon lignite, and the two lower probes were screened in it.

NORTH DAKOTA SITE 6 (T131N, R099W, sec 21CCB) Site 6 is located between two wheat fields just north of the mine, in a very slight topographic low that will temporarily pond water after heavy rains. The water table is at ca 14.3m, ca 5m above the top of the Harmon lignite. Bulk x-ray diffraction on cores showed abundant quartz, kaolinite, chlorite, illite, and smectite. Both pyrite and gypsum are present at and below the water table. Calcite and dolomite (10%-20% each) are present throughout the unsaturated zone and just into the water table, but disappear below it. Groundwater was sampled at two wells that reach depths of 15.9m and 17.4m. Thus, water was sampled at depths of 1.2m and 2.7m, respectively, below the water table.

NORTH DAKOTA SITE 1 (T131N, R099W, sec 36 BCC) At Site 1, an unmined area east of the mine, a 1m stringer of lignite is present just above the water table at ca 13m. Also, a perched water table (the gas probes pumped water) was present at depths of 3m to 9m until at least 1977. Prior to this, the deep samples at Site 1 resembled samples from similar depths at Site 4 in both CO_2 and $^{14}CO_2$ content. The perched water lens disappeared sometime between 1977 and 1980. From 1980 to the present, the data from all depths show extreme variability; it was initially believed that the grouting had cracked or that some other sampling problem existed. However, more recent analysis of the data shows that the partial pressure of $^{14}CO_2$ is generally (not always) nearly constant, suggesting a lack of atmospheric influence. No plausible model for processes at this site is available.

DISCUSSION OF THE RESULTS

Our measurements are discussed and interpreted in Thorstenson et al (1983). Measurement of the CO_2 concentration in each soil gas well provides the fundamental data. The gas analyses are presented in Thorstenson et al (1983, Table 2); CO_2 data are plotted in figures 4 and 5. Figure 4 shows results for Site 6. All data points are plotted in a

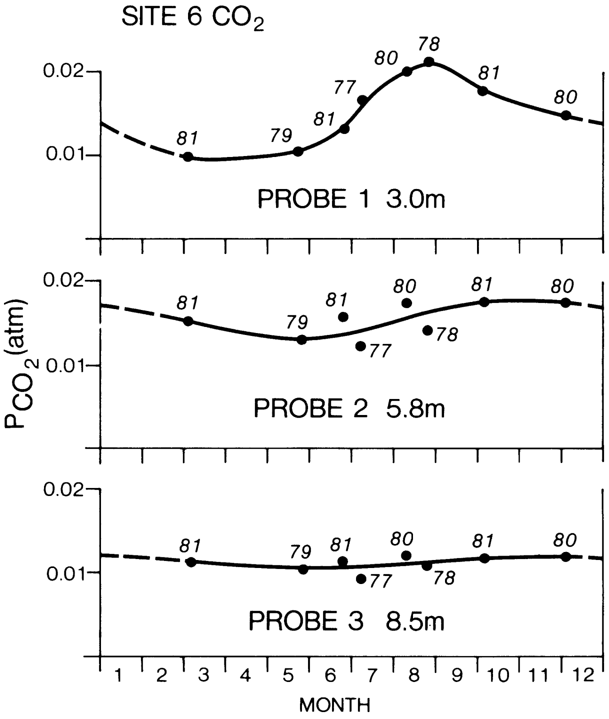

Fig 4. Gascoyne, North Dakota Site 6, CO_2 concentrations

one-year cycle according to the month and day on which they were obtained, independent of the year of measurement. The observed CO_2 concentrations at all depths vary between 1 and 2% of the total gas volume. The pronounced seasonal variation (100%) observed at the first probe (3m deep) correlates with the annual fluctuation of plant growth but is delayed by approximately two months (the peak of vegetation growth is in June, and the observed peak at Probe 1 is in August). A further delay of two months is observed at Probe 2 at 5.8m depth. Variation dropped to 30%. At 8.5m depth, 10%

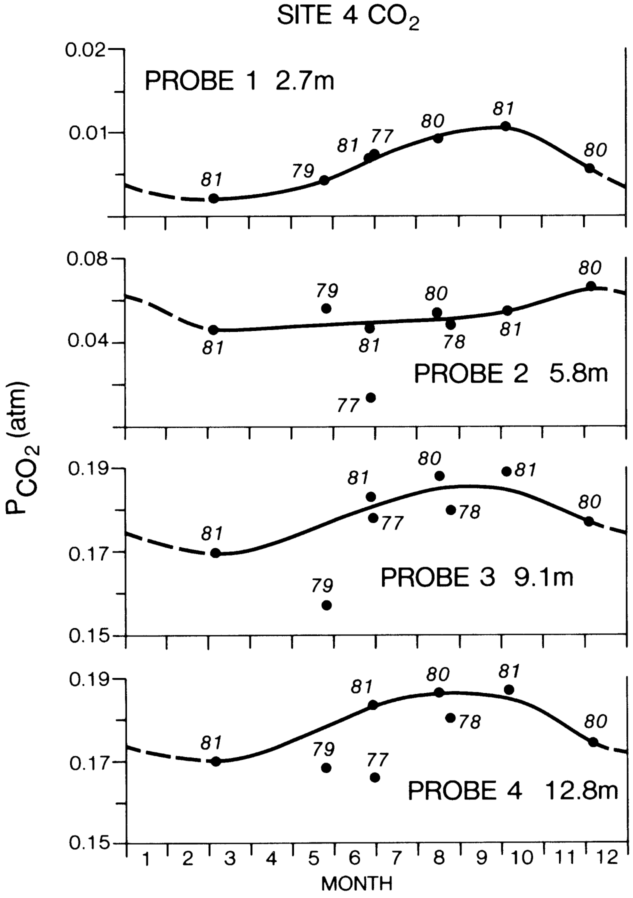

Fig 5. Gascoyne, North Dakota Site 4, CO_2 concentrations: note changes of scale

variation is observed, but the peak is not well defined.

Entirely different observations were made at Site 4 (fig 5). Here the observed concentrations increase strongly with depth and reach 19% at 9.1m. This depth corresponds roughly to the top surface of the lignite which, through oxidation, acts as a strong source for CO_2. The seasonal variation is evident in the most shallow probe but is almost imperceptible at 5.8m. The deeper probes again show a distinct seasonal variation. Oxygen, although present at these depths in concentrations $\leq$ 0.3%, shows a definite minimum corresponding to the CO_2 maximum (see Thorstenson et al, 1983, tables 1 and 2). This suggests a possible control of CO_2 concentrations by O_2 availability, although the nature of processes that show seasonal effects at this depth is unclear.

Oxidation of lignite or of more recent organic matter has been observed at all test sites in the Gascoyne area. This process shows great variability and is limited in extreme cases by the oxygen supply. Oxygen concentration at these sites varies inversely with CO_2 concentration (fig 6). The linear regression of 84 O_2-CO_2 data pairs gave 20.912% oxygen at 0% CO_2 which compares well with 20.946% for atmospheric air.

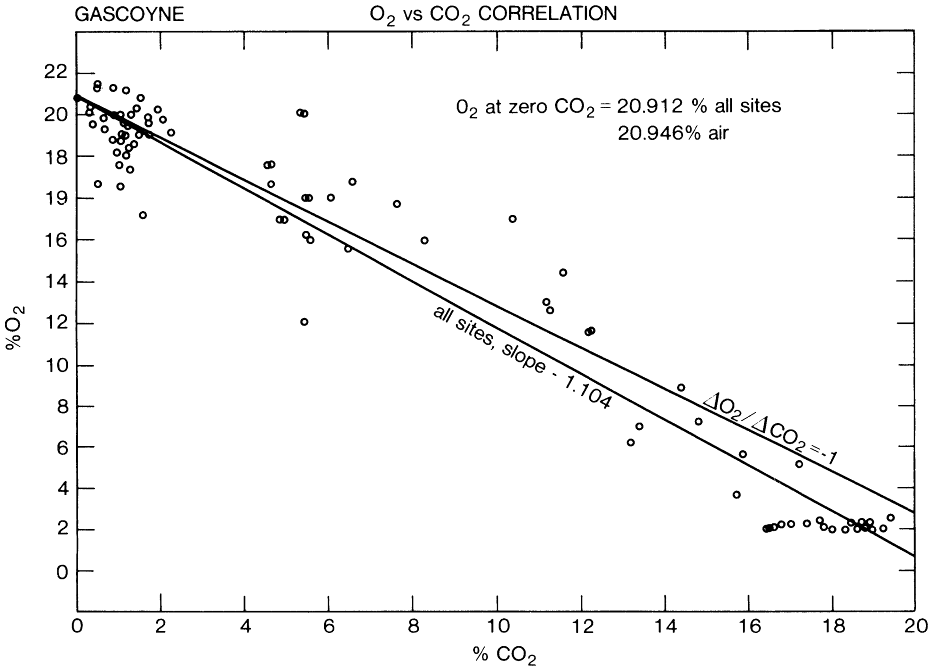

Fig 6. Gascoyne, North Dakota all sites

The correlation factor of the data is .974, and the slope of the regression line is -1.104 which indicates an oxygen deficiency assuming a 1:1 mole ratio of oxygen consumed to CO_2 produced. This deficiency could result from more complex reactions between the lignite and oxygen, or from oxidation of inorganic soil components such as pyrite.

The ^{14}C data are presented in table 1 and figures 7 and 8. In addition to the data from soil gas probes are also given the measurements of atmospheric air, surface soil gas, and water samples. In tabular form, the data show small variations in the range of a few per cent of modern ^{14}C activity, which can not be seen in figures.

Seasonal variations occur at the soil surface level. A lower percentage of ^{14}C during the winter might be due to oxidation of older organic matter in the absence of significant root respiration. Thus, surface ^{14}C level cannot reach the post-bomb ^{14}C level in the atmosphere, which decreased in 1980/81 to 136% modern. Our free atmospheric air measurements were made with air intake 1.8m above the soil surface, at the edge of a wheat field. Our measurements of 126 and 129% modern are slightly below the value of the well-mixed atmosphere in 1981.

The absolute concentration of the subsurface ^{14}C data reflects the stratigraphic difference between the two sites. Remarkable at both sites is the constant level of ^{14}C activity through the seasonal cycles which strongly affected the total CO_2 concentration in the shallow probes. At Site 6 (fig 7),

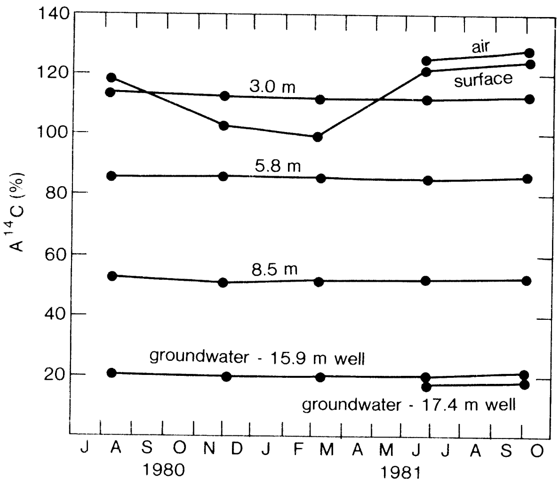

Fig 7. Gascoyne, North Dakota Site 6, ^{14}C concentrations

TABLE 1. GASCOYNE, NORTH DAKOTA: ^{14}C ACTIVITIES IN % MODERN

Modern is 95% activity of old NBS standard. Data are not corrected for $\delta^{13}C$.

Site/Well	May 1979	Aug 80	Dec 80	March 81	June 81	Oct 81
No. 6						
Air					125.99	129.05
Surface		118.08	103.62	99.07	122.67	124.83
3.0m	114.13	113.26	112.79	112.18	112.52	112.33
5.8m	90.90	86.24	86.29	86.02	85.47	86.84
8.5m	51.16	53.07	51.28	52.45	52.30	52.96
Water 15.9m					17.95, 16.64	18.84
Water 17.4m		21.24	20.33	20.10	19.21,21.31,19.45	20.41
No. 4						
Surface				115.17	123.64	116.77
2.7m	103.00	95.13	83.72	81.52	87.38	91.70
5.8m	10.00	10.92	8.79	8.82	9.29	10.71
9.1m	1.75	1.43	2.35	2.72	2.22	1.81
12.8m	2.09	2.08	2.32	2.82		2.40
Water 19.4m		6.73	6.51	6.26	5.89	5.01
No. 1						
Surface					121.50	117.95
3.0m				3.21	2.99	5.46
5.2m						6.03
10.9m		1.85	1.81	2.06	1.57	1.45
13.7m		20.35	9.04	3.65	3.12	
Water 16.5m				38.06, 37.89		

In June 1981, 2 or 3 subsequent water samples were pumped on Sites 1 and 6..

the 3m probe shows a ^{14}C activity of 112% modern with a maximal seasonal variation of 2%; the deeper probes steadily decline in ^{14}C activity from 5 to 8% per meter depth. The shallow water table was sampled at two different levels. A lower activity was observed closer to the surface; 1.5m lower in the groundwater reservoir, the activity was greater by 2% at 20% of modern. All seasonal changes are minimal and vary by < 2%. The water was pumped at a rate of < 20L per hour. Even this slow rate caused a water level drawdown of 1m. Water levels recovered within 24 hours, apparently without changing the isotopic composition either systematically or significantly. Subsequent samplings from both wells at Site 6 and from a well at Site 1 were made in June 1982 (table 1). The 1σ sample error of these tests is ± .65%. The ^{14}C data are within 1σ for all sample groups except for the second of the three where the 2σ error ranges overlap. Thus, the results are valid for a substantial volume of water surrounding each well. An alternative assumption of rapid achievement of a local equilibrium is less probable since all data on carbon isotopes show values different from the corresponding soil gas data. This is consistent with the assumption of a zero-flux lower boundary for the unsaturated zone used in diffusion models (Thorstenson et al, 1983).

At Site 4 (fig 8), the 2.7m probe shows a relatively slight seasonal ^{14}C trend reflecting the surface variation. The ^{14}C activity averages 91% of modern, and the variation lies within ± 12%. All deeper probes and the water at the

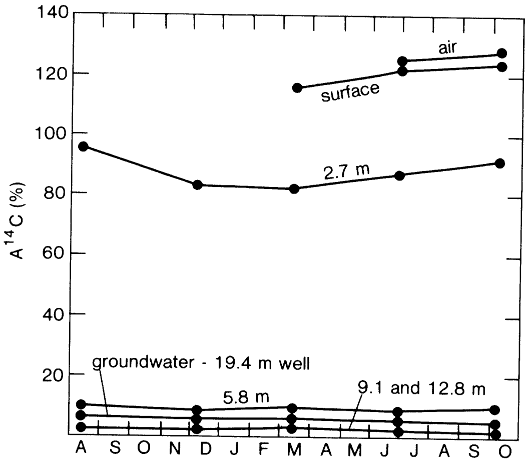

Fig 8. Gascoyne, North Dakota Site 4, ^{14}C concentrations

phreatic surface show ^{14}C activities of < 10% and no seasonal variation. This is consistent with the position of these probes close to or within the lignite beds.

The accuracy of the tabulated ^{14}C data is a function of counting time and sample size. Except for the small free-air samples, we worked with 3cc benzene samples for liquid scintillation counting. Counting time varied between 1400 min for samples in the 85 to 125% modern range to 3000 min for samples in the 1 to 2% modern range. The resulting 1σ errors average ± .6% for modern samples and ± .25% for low-level samples. The free-air samples have 1σ errors of 1.9% for the June 1981 and 1.4% for the October 1981 measurements.

^{13}C data are shown in table 2. We have not attempted a detailed explanation of the data, which have been included to provide a complete data set. A point worth mentioning is that detectable methane (limit ∿ .01%) was observed only once (Site 4, probes in the lignite - May 1979). Surface samples show a strong seasonal variation in $\delta\ ^{13}C$ which is similar to that observed by Rightmire and Hanshaw (1973). More negative values in spring and summer reflect the influx of biogenic CO_2 during the growth season; a negative peak of -24.6‰ is compatible with the Calvin cycle vegetation in the area (van der Merwe, 1982). As shown with the ^{14}C data, oxidizing lignite causes a distinctly different distribution of carbon isotopes with increasing depth. At Site 6, where there is no lignite in the unsaturated zone, the $\delta^{13}C$ values increase with depth and lie close to -17‰ at 8.5m below surface. The June measurement for the 3m probe was lost and we are not certain whether the annual cycle is reflected at this depth. The two deeper probes and the groundwater samples show variations within 2‰. These variations cannot be related with certainty to an annual cycle. The free-air measurements are lower than the typical -7.5‰ value for the well mixed atmosphere. As indicated earlier, we suspect that the samples may have been collected too close to ground surface.

Data from Site 4 strongly reflect the presence of lignite. The two deepest gas probes (9.1m and 12.8m) give results in the -24‰ range, which is close to an estimated value of -26‰ for lignite. The series of successive water measurements performed in June 1981 yield very constant $\delta\ ^{13}C$ values for each well. This supports the conclusions derived from the ^{14}C data. The data presented here are expressed in standard form as ratios of $^{14}C/^{12}C$ (expressed as pmc) or $^{13}C/^{12}C$ (expressed $\delta\ ^{13}C$). Thorstenson et al (1983) demonstrate the importance of considering $^{12}CO_2$, $^{13}CO_2$, and $^{14}CO_2$ as separate entities, which behave according to their own partial pressures, reacting and diffusing independently of each other.

TABLE 2. GASCOYNE, NORTH DAKOTA: $\delta^{13}C$ IN ‰ RELATIVE TO PBD STANDARD

Site/Well	May 1979	Aug 80	Dec 80	March 81	June 81	Oct 81
No. 6						
Air					-8.1	-7.8
Surface		-23.5	-18.3	-18.1	-24.6	-24.0
3.0m	-24.2	-22.6	-22.6	-22.5		-22.5
5.8m	-21.8	-20.1	-20.0	-20.8	-21.7	-20.9
8.5m	-18.5		-18.2	-17.1	-17.8	-17.9
Water 15.9m					-6.7, -6.8	-7.3
Water 17.4m		-5.3	-6.7	-6.2	-6.4, -6.4, -6.4	-6.4
No. 4						
Surface				-19.7	-23.9	-22.6
2.7m	-27.9	-20.3	-20.8	-21.5	-20.8	-21.3
5.8m	-27.9		-22.2	-23.3	-23.9	-22.8
9.1m	-29.4	-24.0	-24.0	-24.0	-23.7	-23.2
12.8m		-24.1	-24.0	-23.8	-23.1	-23.9
Water 19.4m		-17.1	-16.7	-16.8	-16.6	
No.1						
Surface					-23.4	-19.4
3.0m				-18.1		-17.9
5.2m						-17.5
10.9m		-17.0	-18.9	-17.5	-17.6	-17.5
13.7m		-16.6	-15.4	-17.4	-16.0	
Water 16.5m					-11.0, -11.7	-11.3

In June 1981, 2 or 3 subsequent water samples were pumped on Sites 1 and 6.

REFERENCES

Atkinson, T C, 1977, Carbon dioxide in the atmosphere of the unsaturated zone: An important control of groundwater hardness in limestone: Jour Hydrol, v 35, p 111-123.

Enoch, H and Dasberg, S, 1971, The occurrence of high CO_2 concentrations in soil air: Geoderma, v 6, p 17-21.

Fisher, D W and Thorstenson, D C, 1983, Geochemical processes in the Gascoyne lignite mining area, Bowman County, N D: US Geol Survey, Water Resources Inv, 90p.

Galimov, E M, 1966, Carbon isotopes of soil CO_2: Geokhimiya, no. 9, p 1110-1118.

Kunkler, J L, 1969, The sources of carbon dioxide in the zone of aeration of the Bandelier tuff, near Los Alamos, New Mexico: US Geol Survey, Prof Paper 650B, p 185-188.

Miotke, F-D, 1974, Carbon dioxide and the soil atmosphere: Karst-u Höhlenkunde Abh, v 9, p 1-49.

Reardon, E J, Allison, G B, and Fritz, P, 1979, Seasonal chemical and isotopic variations of soil CO_2 at Trout Creek, Ontario: Jour Hydrol, v 43, p 355-371.

Reardon, E J, Mozeto, A A, and Fritz, P, 1980, Recharge in northern clime calcareous sandy soils: soil water chemical and carbon-14 evolution : Geochim et Cosmochim Acta, v 44, p 1723-1735.

Rightmire, C T, 1978, Seasonal variation in P_{CO_2} and ^{13}C content of soil atmosphere: Water Resources Research, v 14, p 691-692.

Rightmire, C T, and Hanshaw, B B, 1973, Relationship between the carbon isotope composition of soil CO_2 and dissolved carbonate species in groundwater: Water Resources Research v 9, p 958-967.

Thorstenson, D C, Weeks, E P, Haas, Herbert, and Fisher, D W, 1983, Distribution of gaseous $^{12}CO_2$, $^{13}CO_2$, and $^{14}CO_2$ in the sub-soil unsaturated zone of the western US great plains: Radiocarbon, v 25.

van der Merwe, N J, 1982, Carbon isotopes, photosynthesis, and archaeology: Am Scientist, v 70, p 596-606.

[Radiocarbon, Vol 25, No. 2, 1983, P 315-346]

DISTRIBUTION OF GASEOUS $^{12}CO_2$, $^{13}CO_2$, AND $^{14}CO_2$ IN THE SUB-SOIL UNSATURATED ZONE OF THE WESTERN US GREAT PLAINS

DC THORSTENSON*, EP WEEKS**, HERBERT HAAS†, and DW FISHER*

ABSTRACT. Data on the depth distribution of the major atmospheric gases and the abundance of gaseous $^{12}CO_2$, $^{13}CO_2$, and $^{14}CO_2$ in the subsoil unsaturated zone have been obtained from several sites in the western Great Plains of the United States. Sample profiles range from land surface to depths of 50m. Although each site must be considered on an individual basis, several general statements can be made regarding the profiles. 1) Diffusion of these gaseous molecules through the unsaturated zone is an important transport mechanism. 2) As predicted by diffusion theory, depth profiles of the various isotopic species of CO_2 differ substantially from one another, depending on individual sources and sinks such as root respiration and oxidation of organic carbon at depth. 3) In general, post-bomb (> 100% modern) ^{14}C activities are not observed in the deep unsaturated zone, in contrast to diffusion model predictions. 4) In spite of generally decreasing ^{14}C activities with depth, absolute partial pressures of $^{14}CO_2$ in the subsoil unsaturated zone are 1-2 orders of magnitude higher than the partial pressure of $^{14}CO_2$ in the atmosphere.

INTRODUCTION

JL Kunkler (1969) performed the first ^{14}C analyses of CO_2 gas from the deep unsaturated zone in the Bandelier Tuff at the Los Alamos National Laboratory. His data showed ^{14}C activities > 100% modern carbon (pmc) at depths of 24m and 86m, indicating that post-bomb CO_2 had penetrated the tuff to at least that depth. Kunkler's research remained unique until recent studies on the unsaturated zone by Reardon, Allison, and Fritz (1979) and Reardon, Mozeto, and Fritz (1980). Data are presented here on the abundance and distribution of unsaturated-zone $^{12}CO_2$, $^{13}CO_2$, and $^{14}CO_2$ from several sampling sites in North Dakota and Texas.

---

* US Geological Survey, Reston, Virginia 22092
** US Geological Survey, Denver, Colorado 80225
† Southern Methodist University, Dallas, Texas 75275

Three of the North Dakota sites were sampled repetitively over a five-year period; two of these sites are discussed in a preliminary attempt to evaluate the role of gaseous diffusion in unsaturated zone processes at these locales. All of the unsaturated zone CO_2 data collected to date by the authors are presented. Although site-specific process models have not been formulated for each site, some important geochemical generalizations can be made.

PHYSICO-CHEMICAL PRINCIPLES

For chemical modeling and equilibrium calculations involving gases, the gas partial pressure is the most useful variable. Alternatively, transport modeling and calculation of diffusive fluxes from Fick's laws require the abundance of diffusing species to be expressed in units of mass/volume (generally mol-cm^{-3}). These statements hold for any isotopic species of the same gas, as well as for different gases, eg, $^{14}CO_2$ will diffuse in response to its own concentration gradient regardless of the distribution of $^{12}CO_2$ and $^{13}CO_2$ in the gas mixtures*. Outlined below are the methods for calculating partial pressures and concentrations from the original analytical data. For purposes of this paper, the behavior of all gases can be assumed to be ideal.

MAJOR GASES. The analytical data for the unsaturated zone gases are available as volume percent for N_2, O_2, Ar, and CO_2**, as $\delta^{13}C$(‰) for $^{13}CO_2$, and as $A^{14}C$ in percent modern carbon (pmc) for $^{14}CO_2$. Dissolved CO_2 is initially reported as partial pressure. For N_2, O_2, Ar, and CO_2 the volume percent equals mol percent, and the mol fraction of a given gas, X_i, is simply $X_i = (\text{vol}\%_i/100)$.

---

* The fact that different isotopes of a single chemical species must respond only to their own concentration gradients is perhaps best visualized through the random-walk model for diffusive processes (Feynman, Leighton, and Sands, 1963, Chap 43). The independence of isotopic diffusion is the basis for tracer diffusion experiments and is implicit in the general equations for calculating the self-diffusion coefficients of one isotopic species in another (Bird, Stewart, and Lightfoot, 1960; Jost, 1960; Li and Gregory, 1974).

** For simplicity, we use CO_2 to refer to $^{12}CO_2 + {}^{13}CO_2 + {}^{14}CO_2$ (there is no isotopic separation in the gas chromatograph columns).

The partial pressure of i is given by

$$P_i = X_i\, P_{total}{}^{\dagger}. \tag{1}$$

Then, from the ideal gas law $n_i/V = P_i/RT$,

$$C_i(\text{mol-cm}^{-3}) \equiv \frac{n_i(\text{mol})}{V(\text{cm}^3)} = \frac{X_i P_{total}(\text{atm})}{R(\text{cm}^3\text{-atm-K}^{-1}\text{-mol}^{-1})T(\text{K})} . \tag{2}$$

^{13}C. The molar ratio, R, of $^{13}CO_2$ to CO_2 in the PDB standard ($\delta^{13}C \equiv 0$) is 0.0111 (Landgren, 1954). Given this value, concentrations of $^{13}CO_2$ can be calculated from $\delta^{13}C$ values and total CO_2 concentrations as follows:

$$\delta^{13}C \equiv \left\{ \frac{R_{sample}}{R_{reference}} - 1 \right\} 1000 = \left\{ \frac{R_{sample}}{0.0111} - 1 \right\} 1000. \tag{3}$$

Rearranging,

$$R_{sample} = \frac{C(^{13}CO_2)}{C(CO_2)} = 0.0111 \{ 1 + (\delta^{13}C/1000) \} , \tag{4}$$

and

$$C(^{13}CO_2) = [C(CO_2)](0.0111) \{ 1 + (\delta^{13}C/1000) \} . \tag{5}$$

The relative gradients of $^{13}CO_2$ and CO_2 will therefore differ only by the factor $(1+\delta^{13}C/1000)$. Total variation of this factor through the range of $\delta^{13}C$ values observed in this study amounts to < 2%, which is of about the same magnitude as the uncertainty in CO_2 collection and analysis. Therefore, transport modeling of $^{13}CO_2$ will produce results essentially identical to those for CO_2, with calculated fluxes multiplied by 0.0111. The utility of the ^{13}C signature as a means of identifying sources of carbon in the system remains undiminished, although the ^{13}C variations are not emphasized in this report.

---

† For the North Dakota sites, $P_{total} = 0.91$ atm; at the Texas sites $P_{total} = 0.88$ atm; and at Los Alamos, $P_{total} = 0.77$ atm

^{14}C. For ^{14}C, the ratio $R_{^{14}CO_2}$ = (moles $^{14}CO_2$)/(moles CO_2) must be obtained from analytical values of $A^{14}C$ (pmc)*. The quantity $R_{^{14}CO_2}$ can be obtained from the decay equation $-dN/dt = \lambda N$ where N is the number of ^{14}C atoms per gram of carbon, and the decay constant λ has the value 3.84×10^{-12} sec^{-1}.

For a 100 pmc sample, the decay rate is 0.226 dps/g-C. In this case

$$N = \frac{-dN/dt}{\lambda} = \frac{0.226}{3.84 \times 10^{-12}} = 5.89 \times 10^{10} \text{ atoms } ^{14}C/\text{g-C}, \qquad (6)$$

or, introducing Avogadro's number and the atomic weight of carbon,

$$R_{^{14}CO_2} = \frac{5.89 \times 10^{10}/6.023 \times 10^{23}}{1\ /\ 12.011} = 1.17 \times 10^{-12} \frac{\text{mol}\,^{14}C}{\text{mol C}} \text{ at 100pmc.} \qquad (7)$$

Then for a 1 pmc sample, $R_{^{14}CO_2}$ would be 1.17×10^{-14} mol ^{14}C per mol C, and for an arbitrary ^{14}C activity

$$R_{^{14}CO_2} = (\ 1.17 \times 10^{-14}\ )(\ A^{14}C(\text{pmc})\ )\text{mol}\,^{14}C/\text{mol C}\ . \qquad (8)$$

The mole fraction of $^{14}CO_2$ in the original gas sample is then

$$X_{^{14}CO_2} = (R_{^{14}CO_2})(X_{CO_2}) = (1.17 \times 10^{-16})\ (A^{14}C(\text{pmc}))(\text{vol\% } CO_2). \qquad (9)$$

---

* Reardon, Mozeto, and Fritz (1980) discussed the distribution of $^{14}CO_2$ in the unsaturated zone as a function of $R_{^{14}CO_2}$. Their conclusions will be correct to the extent that the CO_2 content of the gas phase is constant.

Partial pressures will be given by

$$P_{^{14}CO_2} = X_{^{14}CO_2}\, P_{total} \, . \qquad (10)$$

Concentrations of $^{14}CO_2$ will be given by combining equations (2) and (9), with $R = 82.05$ atm-cm^3-mol^{-1}-K^{-1}:

$$C_{^{14}CO_2} = \frac{X_{^{14}CO_2} P_{total}}{RT} = \qquad (11)$$

$$= \frac{(1.43\text{x}10^{-18})(A^{14}C(\text{pmc}))(\text{Vol}\%CO_2)(P_{total}(\text{atm}))}{T(K)} \text{ in } \frac{\text{mol}^{14}CO_2}{\text{cm}^3} .$$

The values of $A^{14}C$(pmc) to be used in equation (11) must be uncorrected because no age estimation is intended, and the chemical parameters of interest require only raw data on the isotopic abundances.

DIFFUSION MODELING

As mentioned above, each isotopic species of CO_2 within the soil gas diffuses through the unsaturated zone according to its own concentration gradient as described by Fick's Second Law. However, for movement in the unsaturated zone, Fick's Second Law must be modified to account for the effects of the porous medium structure on the rate of diffusion and for reactions between the gas and the liquid and solid phases of the medium. With these modifications, the Law becomes

$$\tau \Theta_D D_{AB} \frac{\partial^2 C_A}{\partial x^2} = \Theta_D \frac{\partial C_A}{\partial t} + \rho_w(\Theta_T - \Theta_D) \frac{\partial C_A^{\dagger}}{\partial t} + \frac{\partial \bar{C}_A}{\partial t} + \alpha_T \, , \qquad (12)$$

where

τ = a tortuosity factor accounting for the added resistance to diffusion imposed by the structure of the porous medium (dimensionless);

Θ_D = drained or gas-filled porosity (dimensionless);

D_{AB} = molecular diffusion constant for diffusion of gas A into gas B (cm^2/sec);

C_A = concentration of gas A (mol/cm^3);

x = dimension increasing with depth; $\equiv 0$ at land surface (cm);

t = time (sec);

ρ_w = density of soil water (g/cm^3);

Θ_T = total porosity (dimensionless);

$C_A^{\dagger}$ = concentration of gas A transferred to the soil water (mol/g of water);

$\bar{C}_A$ = concentration of substance A transferred to the solid phase (mol/[cm^3 of medium], where [cm^3 of medium] refers to the space occupied by solids + liquids + gases);

and α_T = a production term for substance A [mol/(cm^3 of medium)/sec].

Equation (12) states that the rate of one-dimensional diffusion of gas A toward a given point minus the rate of diffusion from the point is equal to the combined rate of change in concentration in 1) the gas phase, 2) the liquid phase, as dissolved gas and any dissolved chemical species containing the gas molecule, 3) in the solid phase, plus 4) the amount of the gas produced or consumed at that point per unit time.

THE DIFFUSION COEFFICIENT. The diffusivity of CO_2 in free air has been measured to be 0.144 cm^2/sec at STP (Bird, Stewart, and Lightfoot, 1960), which is corrected within the program to ambient conditions by the equation

$$D_{AB} = D^{\circ}_{AB} (P_o/P)(T/T_o)^{1.823} \, *, \qquad (13)$$

---

* Equation (13) is based on Bird, Stewart, and Lightfoot (1960), p 505, eq 16.3-1.

where $D°_{AB}$ = diffusion constant at STP (cm^2/sec);

P_o = standard atmospheric pressure (one atmosphere);

P = mean atmospheric pressure at site (atmospheres);

T = mean annual air temperature at site (K);

and T_o = temperature at standard conditions (273.2 K).

EVALUATION OF $\partial C_A^\dagger/\partial t$ AND $\partial \bar{C}_A/\partial t$. To evaluate the partitioning of CO_2 between the gas and liquid phase requires a functional relationship between P_{CO_2} and the total dissolved CO_2. A simple function that can be used in the transport program becomes available if the aqueous chemistry in the unsaturated zone can be ascribed to few or one reaction. For this model, it is assumed that calcite is present throughout the unsaturated zone, and that carbonate chemistry in the water is governed by CO_2 - calcite equilibria via reaction (14):

$$CaCO_{3(s)} + CO_{2(g)} + H_2O_{(\ell)} = Ca^{2+}_{(aq)} + 2HCO^-_{3(aq)}. \qquad (14)$$

The equilibrium constant for this reaction is

$$K_{eq} = \frac{a_{Ca^{2+}}\, a^2_{HCO_3^-}}{P_{CO_2}} , \qquad (15)$$

and if this is the only reaction considered,

$$m_{Ca^{2+}} = \frac{1}{2}\, m_{HCO_3^-} . \qquad (16)$$

If we assume ideality ($a_i = m_i$),

$$K_{eq} = \frac{m^3_{HCO_3^-}}{2\, P_{CO_2}} , \qquad (17)$$

or,

$$m_{HCO_3^-(aq)} = (2\, K_{eq} P_{CO_2})^{1/3} = 1.260\, K_{eq}{}^{1/3}\, P_{CO_2}{}^{1/3} , \quad (18)$$

where

m_i = molality and P_{CO_2} = partial pressure of CO_2 in atm * .

Use of the partitioning coefficient concept to model transport in the gas phase relies on determining the amount of the subject gas going into solution due to a change in concentration in the gas phase. In reaction (14) 1/2 of the aqueous CO_2 comes from solid-phase carbonate dissolution, and the other half by solution from the gas phase. Thus, in equation (12),

$$\frac{\partial \overline{C}_A}{\partial t} = - \frac{1}{2} \rho_w (\Theta_T - \Theta_D) \frac{\partial C_A^{\dagger}}{\partial t} , \quad (19)$$

where the minus sign indicates that $CaCO_{3(s)}$ decreases as $CO_{2(g)}$ increases. The relation $\partial C_A^{\dagger}/\partial t = (\partial C_A^{\dagger}/\partial C_A)(\partial C_A/\partial t)$, in conjunction with equation (19), allows equation (12) to be expressed only in terms of C_A, as derived below. From equation (18),

$$m_{HCO_3^-} = (2\, K_{eq} P_{CO_2})^{1/3} . \quad (20)$$

However, the concentration in mol/cm^3 is essentially equal to $m_{HCO_3^-}/1000$. Thus,

$$C_A^{\dagger} = 10^{-3}\, (2\, K_{eq}\, P_{CO_2})^{1/3} . \quad (21)$$

To express all terms as a function of C_A, rather than P_{CO_2}, the gas law is employed as in equation (2):

---

* This model is a simplified version of the calculation of carbonate equilibria at a given P_{CO_2} (see, eg, Garrels and Christ, 1965, p 81-83).

$$C_A = \frac{n}{V} = \frac{P_{CO_2}}{RT} ,$$

or

$$P_{CO_2} = RT\ C_A \quad .$$

With P in atm, C_A in mol/cm^3, and T in kelvins, R = 82.05 atm-cm^3-mol^{-1}-K^{-1}. Therefore

$$C_A^\dagger = 10^{-3} (2K_{eq})^{1/3} (82.05TC_A)^{1/3}, \tag{22}$$

$$C_A^\dagger = 5.475\text{x}10^{-3} (K_{eq}T)^{1/3} C_A{}^{1/3} \quad , \tag{23}$$

and thus

$$\frac{\partial C_A^\dagger}{\partial C_A} = 1.825\text{x}10^{-3} (K_{eq}T)^{1/3} C_A{}^{-2/3} \ . \tag{24}$$

Combining equations (24) and (19), expressing the fact that only 1/2 of the change in $C_A^\dagger$ is due to CO_2 from the gas phase, equation (12) becomes

$$\tau\Theta_D D_{AB} \frac{\partial^2 C_A}{\partial x^2} =$$

$$= \{\Theta_D + 9.125\text{x}10^{-4}(\Theta_T - \Theta_D)(K_{eq}T)^{1/3} C_A{}^{-2/3}\} \frac{\partial C_A}{\partial t} + \alpha_T . \tag{25}$$

The same equation can be expressed in terms of P_{CO_2} by substituting P_{CO_2}/RT for C_A (from the gas law) in equation (25) and multiplying by RT to give

$$\tau\Theta_D D_{AB} \frac{\partial^2 P_{CO_2}}{\partial x^2} = \tag{26}$$

$$= \{\Theta_D + 9.125\text{x}10^{-4}(\Theta_T-\Theta_D)(K_{eq}T)^{1/3}[P_{CO_2}/RT]^{-2/3}\} \frac{\partial P_{CO_2}}{\partial t} + RT\alpha_T,$$

or

$$\tau\theta_D D_{AB} \frac{\partial^2 P_{CO_2}}{\partial x^2} = \tag{27}$$

$$= \{\Theta_D + 0.01723T(\Theta_T-\Theta_D)K_{eq}{}^{1/3}P_{CO_2}{}^{-2/3}\} \frac{\partial P_{CO_2}}{\partial t} + 82.05T\alpha_T.$$

Either equation (25) or equation (27) may be used for modeling purposes, depending on convenience or preference.

THE PRODUCTION TERM. The high concentration of CO_2 in the unsaturated zone relative to that in the atmosphere results from root respiration, microbial activity, and oxidation of organic carbon in the soil zone. All of these activities usually occur mainly near the surface, and in our model were assumed to occur uniformly with depth from land surface to a depth of 1m, but not to occur below that depth. Attempts to include additional CO_2 production at greater depths (see Site 4, fig 6) have not yet been made.

CO_2 production is seasonal, however, with annual production approximately constant, resulting in an essentially steady CO_2 partial pressure at depth. Both average and seasonal production rates were used in our modeling exercises. The average production rate was determined using an equation developed by van Bavel (1951), based on the root-zone production profile described above, a constant partial pressure of CO_2 in the atmosphere at land surface, and no diffusion of CO_2 across the water table. His equation is

$$\bar{\alpha} = \frac{2\Theta_D\tau D_{AB}(C_{depth} - C_{atm})}{a^2}, \tag{28}$$

where $\bar{\alpha}$ = the average production rate of CO_2 in the root zone (mol/cm^3 of medium/sec);

C_{depth} = CO_2 concentration at depth (mol/cm^3);

C_{atm} = CO_2 concentration in the atmosphere (mol/cm^3);

a = depth of root zone (cm);

and other symbols are defined above.

To model seasonal variations in P_{CO_2} with depth, it is assumed that the CO_2 production rate in the root zone is proportional to that given by a sine curve during the growing season, and that the rate is zero during the rest rest of the year. The amplitude of the production curve is calculated to provide the same total production for the year as that determined from the average production rate. Based on integration of the area under the sine curve, this amplitude is

$$\Omega = \frac{\pi}{2}\,(T_{tot}/T_P)\,\bar{\alpha} \quad , \tag{29}$$

where

Ω = the maximum rate of CO_2 production, (mol/cm^3 of medium/sec);

T_{tot} = total time (one year);

T_P = time of CO_2 production (in fraction of a year);

and other symbols are as defined above. Thus, the seasonal production rate may be expressed in equation form

$$\alpha_T = \frac{\pi\,T_{tot}}{2\,T_P}\,\bar{\alpha}\sin\left[\frac{\pi\,(T - T_o)}{T_P}\right] , \quad T_o \leqslant T \leqslant (T_o + T_P); \tag{30}$$

and

$$\alpha_T = 0, \quad T < T_o \text{ or } T > (T_o + T_P); \tag{31}$$

where

α_T = production rate at time T (mol/cm^3 of medium/sec);

T = time (years);

T_o = time at which seasonal production starts (years).

DATA PRESENTATION

Table 1 presents the various derived parameters P_{CO_2}, X_{CO_2}, and $P_{^{14}CO_2}$ for all samples collected. The more standard $\delta^{13}C$ and $A^{14}C$ data are provided for comparison. $P_{^{13}CO_2}$ was not tabulated because for all practical purposes $P_{^{13}CO_2} \cong 10^{-2} P_{CO_2}$. Table 2 includes additional compositional data for the principal atmospheric gases. Seasonal variations of P_{CO_2} in individual probes are shown in figure 1, seasonal variation of $P_{^{14}CO_2}$ in figure 4, and depth profiles of P_{CO_2} and $P_{^{14}CO_2}$ in figure 6.

MODEL APPLICATION

Only two sites provide sufficient data to attempt seasonal modeling (North Dakota Sites 4 and 6); only Site 6 contains calcite throughout the unsaturated zone. The modeling efforts presented here are thus limited to North Dakota Site 6. The location and hydrogeologic characteristics of this site are described in Haas et al (1983). Models are presented first for the time and depth distribution of CO_2, then for the time and depth distribution of $^{14}CO_2$.

CO_2 concentrations in the unsaturated zone were modeled for this study using a numerical solution to the finite-difference form of equation (27), as described by Weeks, Earp, and Thompson (1982). Briefly, for modeling purposes, the entire unsaturated zone is divided into equal nodal increments, and a finite-difference equation is written for each node. Variations in media properties are accounted for

TABLE 1. Carbon dioxide and carbon isotopes at various depths from sites in southwestern North Dakota, west Texas, and New Mexico

Date of collection	Vol % CO_2	P_{CO_2} a/ atm x 10^2	$\delta^{13}CO_2$ b/ °/oo	$A^{14}CO_2$ pmc	$X^{14}CO_2$ c/ x 10^{14}	$P^{14}CO_2$ d/ atm x 10^{14}	$C^{14}CO_2$ e/ x 10^{20}
Site 6, ND							
Air f/							
6/30/81	0.033	0.030	-8.1	125.99	0.049	0.045	1.91
10/07/81	0.033	0.030	-7.8	129.05	0.050	0.046	1.96
Surface g/							
8/10/80	-	-	-23.5	118.08	-	-	-
12/04/80	-	-	-18.3	103.62	-	-	-
3/04/81	-	-	-18.1	99.07	-	-	-
6/25/81	-	-	-24.6	122.67	-	-	-
10/06/81	-	-	-24.0	124.83	-	-	-
Probe 1 (3.0m)							
7/06/77	1.63	1.48	-	-	-	-	-
8/23/78(8b)	2.3	2.09	-	-	-	-	-
5/22/79	1.08	0.98	-24.2	114.13	1.44	1.31	56.7
8/10/80(8a)	2.00	1.82	-22.6	113.26	2.65	2.41	104.2
12/04/80	1.48	1.35	-22.6	112.79	1.95	1.77	76.8
3/04/81	0.98	0.89	-22.5	112.18	1.29	1.17	50.6
6/25/81	1.28	1.16	-	112.52	1.68	1.53	66.3
10/06/81	1.79	1.63	-22.5	112.33	2.35	2.14	92.5
Probe 2 (5.8m)							
7/06/77	1.23	1.12	-	-	-	-	-
8/23/78(8b)	1.42	1.29	-	-	-	-	-
5/22/79	1.32	1.20	-21.8	90.90	1.40	1.28	55.2
8/10/80(8a)	1.74	1.58	-20.1	86.24	1.76	1.60	69.0
12/04/80	1.74	1.58	-20.0	86.29	1.76	1.60	69.1
3/04/81	1.54	1.40	-20.8	86.02	1.55	1.41	60.9
6/25/81	1.56	1.42	-21.7	85.47	1.56	1.42	61.3
10/06/81	1.77	1.61	-20.9	86.84	1.80	1.64	70.7
Probe 3 (8.5m)							
7/06/77	0.95	0.86	-	-	-	-	-
8/23/78(8b)	1.09	0.99	-	-	-	-	-
5/22/79	1.04	0.95	-18.5	51.16	.62	0.56	24.5
8/10/80(8a)	1.21	1.10	-	53.07	.75	0.68	29.5
12/04/80	1.20	1.09	-18.2	51.28	.72	0.66	28.3
3/04/81	1.15	1.05	-17.1	52.45	0.71	0.65	27.7
6/25/81	1.14	1.04	-17.8	52.30	0.70	0.64	27.4
10/06/81	1.20	1.09	-17.9	52.96	.74	0.67	29.2
Site 6 (continued)							
Water table ≅ 14.5m							
South 4" well (15.9m) h/							
6/28/81		2.3	-6.8	17.29	- h/	0.47 h/	- h/
10/04/81		2.2	-7.3	18.84	-	0.48	-
North 4" well (17.4m) h/							
8/17/80		2.4	-5.3	21.24	- h/	0.60 h/	- h/
12/04/80		1.9	-6.7	20.33	-	0.45	-
3/05/81		2.1	-6.2	20.10	-	0.49	-
6/25/81		2.2	-6.4	19.99	-	0.51	-
10/06/81		2.2	-6.4	20.41	-	0.53	-
Site 4, ND							
Surface g/							
3/05/81	-	-	-19.7	115.17	-	-	-
6/26/81	-	-	-23.9	123.64	-	-	-
10/05/81	-	-	-22.6	116.77	-	-	-
Probe 1 (2.7m)							
6/29/77(6b)	0.73	0.66	-				
5/23/79	0.44	0.40	-27.9	103.00	0.53	0.48	20.8
8/16/80(8a)	0.92	0.84	-20.3	95.13	1.02	0.93	40.3
12/05/80	0.56	0.51	-20.8	83.72	0.55	0.50	21.6
3/05/81	0.40	0.36	-21.5	81.52	0.38	0.35	15.0
6/26/81(6a)	0.71	0.65	-20.8	87.38	0.73	0.66	28.5
10/05/81	1.09	0.99	-21.3	91.70	1.17	1.06	46.0
Probe 2 (5.8m)							
6/29/77(6b)	1.32	1.20	-	-	-	-	-
8/23/78(8b)	4.90	4.46	-	-	-	-	-
5/23/79	5.63	5.12	-27.9	10.00	0.66	0.60	25.9
8/16/80(8a)	5.34	4.86	-	10.92	0.68	0.62	26.8
12/05/80	6.69	6.09	-22.2	8.79	0.69	0.63	27.0
3/05/81	4.63	4.21	-23.3	8.82	0.48	0.43	18.8
6/26/81(6a)	4.66	4.24	-23.9	9.29	0.51	0.46	19.9
10/05/81	5.53	5.03	-22.8	10.71	0.69	0.63	27.2
Probe 3 (9.1m)							
6/29/77(6b	17.8	16.2	-	2.4	.50	0.45	19.6
8/23/78(8b)	18.0	16.4	-	-	-		
5/23/79	15.7	14.3	-29.4	1.75	.32	0.29	12.6
8/16/80(8a)	18.8	17.1	-24.0	1.43	.31	0.29	12.4
12/05/80	17.7	16.1	-24.0	2.35	.49	0.44	19.1
3/05/81	17.0	15.5	-24.0	2.72	.54	0.49	21.3
6/26/81(6a)	18.3	16.7	-23.7	2.22	.48	0.44	18.7
10/05/81	18.9	17.2	-23.2	1.81	.40	0.36	15.7

(Table 1 cont'd)

Date of collection	Vol % CO_2	P_{CO_2} a/ atm x 10^2	$\delta^{13}CO_2$ b/ $^o/_{oo}$	$A^{14}CO_2$ pmc	$X_{14}CO_2$ c/ x 10^{14}	$P_{14}CO_2$ d/ atm x 10^{14}	$C_{14}CO_2$ e/ x 10^{20}
Site 4 (continued)							
Probe 4 (12.8m)							
6/29/77(6b)	16.6	15.1	-	-	-	-	-
8/23/78(8b)	18.0	16.4	-	-	-	-	-
5/23/79	16.8	15.3	-	2.09	.41	0.37	16.1
8/16/80(8a)	18.6	16.9	-24.1	2.08	.45	0.41	17.8
12/05/80	17.4	15.8	-24.0	2.32	.47	0.43	18.6
3/05/80	17.0	15.5	-23.8	2.82	.56	0.51	22.0
6/26/81(6a)	18.3	16.7	-23.1	-	-	-	-
10/05/81	18.7	17.0	-23.9	2.40	.53	0.48	20.6
Water table ≅ 17.5m							
4" well (19.4m) h/							
8/16/80	-	9.0	-17.1	6.73	- h/	0.71 h/	- h/
12/05/80		8.1	-16.7	6.51	-	0.62	-
3/05/81		8.1	-16.8	6.26	-	0.59	-
6/26/81		8.3	-16.6	5.89	-	0.57	-
10/05/81		10.0	-16.6	5.01	-	0.57	-
Site # 1, ND							
Surface g/							
6/28/81	-		-23.4	121.5	-	-	-
10/08/81	-		-19.4	117.95	-	-	-
Probe 1 (3.0m)							
9/10/76	0.056	0.051	-	-	-	-	-
6/28/77	0.080	0.073	-34.8	(small isotope sample)		-	
8/13/80	11.3	10.3	-	-	-	-	-
3/06/81	13.4	12.2	-18.1	3.21	0.50	.46	19.8
6/28/81	10.4	9.46	-	2.99	0.36	0.33	14.3
10/08/81	7.71	7.01	-17.9	5.46	0.49	0.45	19.3
Probe 2 (5.2m)							
9/10/76	0.56	0.51	-	-	(gas sample pumped water)		
6/28/77	7.01	6.38	-	-	-	-	
6/28/81	11.6	10.6	-	-	-	-	-
10/08/81	6.10	5.55	-17.5	6.03	0.43	0.39	16.9
Probe 3 (7.6m) i/							
Probe 4 (10.9m)							
9/10/76	16.4	14.9	-	-	-	-	-
6/28/77	18.5	16.8	-17.68	2.1	0.45	.41	17.9
8/13/80	17.2	15.7	-17.0	1.85	0.37	0.34	14.6
12/06/80	14.8	13.5	-18.9	1.81	0.31	0.29	12.3
3/06/81	15.9	14.5	-17.5	2.06	0.38	0.35	15.1
6/28/81	14.4	13.1	-17.6	1.57	0.26	0.24	10.4
10/08/81	12.3	11.2	-17.5	1.45	0.21	0.19	8.2
Site 1 (continued)							
Probe 5 (13.7m)							
9/10/76	18.9	17.2	-	-	-	-	-
6/28/77	13.2	12.0	-17.28	2.1	0.32	0.30	12.8
8/13/80	1.59	1.45	-16.6	20.35	0.38	0.34	14.9
12/06/80	1.27	1.16	-15.4	9.04	0.13	0.12	5.3
3/06/81	8.31	7.56	-17.4	3.65	0.35	0.32	13.9
6/28/81	5.49	4.09	-16.0	3.12	0.20	0.18	7.9
10/08/81	1.33	1.21		-			
Water table ≅ 14.0m							
4" well (16.5m) h/							
8/18/80	-	6.0	-	-	- h/	-	- h/
3/07/81	-	6.3	-	-	-	-	
7/01/81		5.9	-11.7	37.98	-	2.62	
10/05/81		4.4	-11.2	-	-	-	
Site 2, ND							
Probe 1 (2.7m)							
9/13/76	5.42	4.93	-	-	-	-	-
6/28/77	6.51	5.92	-21.64	-	-	-	-
Probe 2 (5.8m)							
9/13/76	5.81	5.28	-	-	-	-	-
6/28/77	7.93	7.22	-21.63	18.1	1.67	1.52	65.8
Probe 3 (8.8m)							
9/13/76	11.3	10.3	-	-	-	-	-
8/10/80	11.6	10.6	-	-	-	-	-
Site 3, ND							
Probe 1 (1.2m)							
9/13/76	11.2	10.2	-	-	-	-	-
7/03/77	12.2	11.1	-12.01	20.6	2.94	2.68	116.
Probe 2 (3.4m)							
9/13/76	25.2	22.9	-	-	-	-	-
7/03/77	19.4	17.7	-11.68	12.2	2.77	2.52	109.
Probe 3 (6.1m)							
9/13/76	24.2	22.0	-	-	-	-	-
7/03/77	19.2	17.5	-	13.2	2.96	2.70	117.
Lamb Site j/							
10/23/78							
#5 (5.8m)	1.89	1.66	-	-	-	-	-
#4 (11.0m)	1.08	0.95	-	-	-	-	-
#3 (17.1m)	0.09	0.08	-	-	-	-	-
#2 (21.4m)	0.14	0.12	-	-	-	-	-
#1 (26.5m)	0.03	0.03	-	-	-	-	-

(Table 1 cont'd)

Date of collection	Vol % CO_2	P_{CO_2} a/ atm x 10^2	$\delta^{13}CO_2$ b/ °/oo	$A^{14}CO_2$ pmc	$X_{^{14}CO_2}$ c/ x 10^{14}	$P_{^{14}CO_2}$ d/ atm x 10^{14}	$C_{^{14}CO_2}$ e/ x 10^{20}
Lamb Site (continued)							
4/11/79							
#5 (5.8m)	2.91	2.65	-20.6	113.1	3.85	3.39	143.
#4 (11.0m)	1.74	1.53	-22.9	111.5	2.27	2.00	84.4
#3 (17.1m)	2.10	1.85	-18.7	108.4	2.66	2.34	99.0
#2 (21.4m)	2.22	1.94	-21.2	108.6	2.82	2.48	106.
Glenn Site j/							
5/79							
#5 (13.4m)	0.57	0.50	-	-	-	-	-
#3 (25.3m)	1.01	0.89	-	-	-	-	-
#2 (36.3m)	0.86	0.76	-	-	-	-	-
#1 (44.5m)	0.06	0.05	-	-	-	-	-
10/79							
#6 (7.0m)	0.36	0.32	-16.03	97.18	0.41	0.36	15.2
#5 (13.4m)	0.68	0.59	-25.3	62.91	0.50	0.44	18.6
#4 (19.8m)	-	-	-17.3	60.22	0.48	0.42	17.8
#3 (25.3m)	1.13	0.99	-23.1	63.71	0.84	0.74	31.3
#2 (36.3m)	0.59	0.52	-27.7	62.45	0.43	0.38	16.0
#1 (44.5m)	0.98	0.86	-25.9	56.18	0.64	0.57	23.9
Kunkler (1969) k/							
8/24/67							
TA-52-22 83.0-88.8m	0.47	0.36	-18.5	101	0.56	0.43	18.3
8/5/67							
TA-52-23 23.8-25.3m	0.89	0.69	-17.9	115	1.20	0.92	39.4
Reardon et al (1980) l/							
3-7m	0.4	0.4	- k/	~ 110	0.51	0.51	22.

Footnotes to Table 1

a. Calculated from eq (1), with X_{CO_2} = vol % CO_2/100. P_{total} = 0.91, 0.88, and 0.77atm at North Dakota, Texas, and New Mexico sites, respectively.

b. PDB standard

c. Calculated from eq (9)

d. Calculated from eq (10); P_{total} as in footnote a

e. Calculated from eq (11); " " ";

$T_{North\ Dakota} = 283K$, $T_{Texas} = 289K$, $T_{New\ Mexico} = 283K$

f. The inlet for the air sample was 2m above land surface.

g. Volume % CO_2 (and thus, P_{CO_2}) were not measured in the soil zone. The surface samples represent CO_2 that diffused out of the soil zone.

h. These analyses represent dissolved gases in shallow groundwater. The values reported for P_{CO_2} represent the partial pressure of dissolved CO_2, $P_{CO_2(aq)}$. It can be shown that $P_{^{14}CO_{2(aq)}} = (R_{^{14}CO_2})(P_{CO_{2(aq)}})$. Because there is no gas phase present, $X_{^{14}CO_2}$ and $C_{^{14}CO_2}$ are not relevant for these samples.

i. No samples were obtained; periodic attempts produced a vacuum whenever this probe was pumped.

j. For additional data on CO_2 contents of the Texas sites, see Petraitis (1981).

k. These data (Kunkler, 1969) are from the unsaturated zone in the Bandelier Tuff near Los Alamos, New Mexico.

l. These data are from the unsaturated zone in a forested area underlain by calcareous sand at Trout Creek, Ontario, Canada. The numbers cited are estimated average values. For further details, see Reardon et al (1979; 1980).

TABLE 2. Nitrogen, argon, and oxygen contents of unsaturated-zone and dissolved gases from sites in southwestern North Dakota and in west Texas

Date of collection	N_2	Ar	O_2
Site 6, ND	Volume %		
Probe 1 (3.0m)			
7/06/77	82.1	1.1	15.2
8/23/78(8b)	77.6	1.0	19.1
5/22/79	81.3	1.1	16.6
8/10/80(8a)	76.8	1.0	20.2
12/04/80	77.3	.9	20.3
3/04/81	78.1	.9	20.0
6/25/81	78.3	.9	19.5
10/06/81	78	1.0	19
Probe 2 (5.8m)			
7/06/77	79.5	1.0	18.1
8/23/78(8b)	78.9	1.0	18.1
5/22/79	80.2	1.0	17.4
8/10/80(8a)	77.4	1.0	19.9
12/04/80	77.6	1.0	19.7
3/04/81	78.6	.9	19.0
6/25/81	78.4	1.0	19.0
10/06/81	78	1.0	19
Probe 3 (8.5m)			
7/06/77	79.2	1.0	18.8
8/23/78(8b)	80.4	1.0	17.6
5/22/79	79.7	1.0	18.2
8/10/80(8a)	78.2	1.0	19.6
12/04/80	78.2	.9	19.6
3/04/81	79.2	1.0	18.7
6/25/81	78.8	1.0	19.0
10/06/81	79.	1.0	19
South 4" well (15.9m)	Pressure, atmospheres		
6/28/81	.92	.010	< .001
10/04/81	.97	.011	.001
North 4" well (17.4m)			
8/17/80	1.11	.011	< .001
12/04/80	.94	.010	.002
3/05/81	.99	.012	.002
6/25/81	1.16	.012	.012
10/06/81	1.01	.011	.020
Site 4, ND	Volume %		
Probe 1 (2.7m)			
6/29/77	79.0	1.0	19.3
5/23/79	79.0	1.0	19.5
8/16/80	76.8	1.0	21.3
12/05/80	77.2	1.0	21.3
3/05/81	78.5	1.0	20.0
6/26/81	78.4	1.0	19.8
10/05/81	78	1.1	20
Probe 2 (5.8m)			
6/29/77	79.2	1.0	18.4
8/23/78(8b)	79.0	1.1	15.0
5/23/79	79.4	1.0	14.0
8/14/80	73.5	1.0	20.1
12/05/80	75.6	.9	16.8
3/05/81	76.8	.9	17.6
6/26/81	77.6	1.1	16.7
10/05/81	77	1.1	16
Probe 3 (9.1m)			
6/29/77	81.0	1.1	.15
8/23/78(8b)	80.9	1.1	.06
5/23/79	81.4	1.1	1.9
8/16/80(8a)	80.1	1.1	.09
12/05/80	80.8	1.0	.5
3/05/81	81.7	1.0	.3
6/26/81	80.7	1.0	<.06
10/05/81	80	1.0	.34
Probe 4 (12.8m)			
6/29/77	82.2	1.1	.11
8/23/78(8b)	80.9	1.1	.06
5/23/79	81.8	1.1	.3
8/16/80(8a)	80.3	1.0	.06
12/05/80	81.2	1.0	.3
3/05/81	81.7	.9	.3
6/26/81	80.8	1.0	< .06
10/05/81	80	1.1	.35
4" well (19.4m)	Pressure, atmospheres		
8/16/80	.97	.012	< .001
12/05/80	.94	.011	.002
5/05/81	.93	.011	.003
6/26/81	.98	.011	< .001
10/05/81	.98	.012	.002
Site 1, ND	Volume %		
Probe 1 (3.0m)			
7/10/76	96.8	1.3	1.8
6/28/77	78.1	1.0	20.8
8/13/80	77.1	1.0	10.6
3/06/81	80.7	.9	5.0
6/28/81	73.5	1.0	15.0
10/08/81	76	1.0	15.7
Probe 2 (5.2m)			
9/10/76	81.7	1.1	16.7
6/28/77	89.7	1.9	1.4
6/28/81	74.9	1.0	12.5
10/08/81	77	1.0	16.0
Probe 4 (10.9m)			
9/10/76	82.1	1.4	.06
6/28/77	80.1	1.1	.3
8/13/80	78.6	1.0	3.2
12/06/80	79.0	1.0	5.2
3/06/81	79.5	1.0	3.7
6/28/81	77.7	1.1	6.9
10/08/81	78	1.1	9.7
Probe 5 (13.7m)			
9/10/76	79.9	1.1	.04
6/28/77	81.4	1.1	4.2
8/13/80	76.6	1.0	20.8
12/06/80	76.5	1.0	21.2
3/06/81	76.8	.9	14.0
6/28/81	79.3	1.1	14.2
10/08/81	78	1.0	20
4" well (16.5m)	Pressure, atmospheres		
8/18/80	1.22	.009	<.001
3/07/81	1.04	.008	.003
6/28/81	1.07	.007	<.001
10/03/81	.99	.008	.002
Site 3, ND	Volume %		
Probe 1 (1.2m)			
9/13/76	75.5	1.0	11.1
7/03/77	77.7	1.0	9.6
Probe 2 (3.4m)			
9/13/76	72.6	1.0	.96
7/03/77	79.7	1.1	.6
Probe 3 (6.1m)			
9/13/76	73.0	1.0	.31
7/03/77	79.0	1.1	.03
Site 2, ND			
Probe 1 (2.7m)			
9/13/76	82.9	1.0	10.1
6/28/77	79.2	1.0	13.6
Probe 2 (5.8m)			
9/13/76	86.7	1.1	6.2
6/28/77	79.5	1.1	11.6
Probe 3 (8.8m)			
7/04/76	87.0	1.2	.43
9/13/76	87.7	1.2	.15

(Table 2 cont'd)

Date of collection	N_2	Ar	O_2
Lamb site, TX			
10/23/78			
Probe 4 (11.0m)	86.6	1.2	11.1
Probe 3 (17.1m)	77.6	1.0	20.7
Probe 2 (21.4m)	77.3	1.1	20.8
Probe 1 (26.5m)	80.9	1.1	17.8
4/79			
Probe 5 (5.8m)	78.8	1.0	17.5
Probe 4 (11.0m)	80.5	1.0	16.5
Probe 3 (17.1m)	80.5	1.1	15.6
Probe 2 (21.4m)	81.1	1.1	15.5

Date of collection	N_2	Ar	O_2
Glenn site, TX			
4/11/79			
Probe 5 (13.4m)	77.8	1.0	20.6
Probe 3 (25.3m)	78.4	1.1	19.5
Probe 2 (36.3m)	78.6	1.0	19.5
Probe 1 (44.5m)	76.8	1.0	22.1
10/79			
Probe 6 (7.0m)	77.7	1.0	21.5
Probe 5 (13.4m)	78.1	1.0	20.8
Probe 4 (19.8m)	78.9	1.0	19.7
Probe 3 (25.3m)	79.1	1.0	20.0
Probe 2 (36.3m)	78.7	1.1	19.4

by dividing the unsaturated zone into layers, each containing several nodes and within which the properties of the medium, including its tortuosity, drained porosity, and total porosity, are assumed constant. Each screened interval is considered to comprise a layer.

GAS AND MEDIA PROPERTIES. Application of the model requires the input of various parameters to describe the diffusive properties of the gas and medium; the interaction of CO_2 among the gas, liquid, and solid phases within the medium; the production term; boundary conditions at the top and bottom of the unsaturated zone column; and initial conditions at the start of the transient simulation. The values of the parameters used to model North Dakota Site 6 are described below.

Based on observed groundwater temperatures, the mean annual temperature at Gascoyne, North Dakota, is approximated as 10°C. The total pressure is 0.91 atm. The diffusion coefficient of CO_2 in air is calculated internally in the computer program (equation (13)) with these parameters. The equilibrium constant for equation (15) has the value log $K_{eq}(10°C) = -5.65$*. At 283 K, equation (27) thus reduces to

$$\tau \Theta_D D_{AB} \frac{\partial^2 P_{CO_2}}{\partial x^2} =$$

$$= \{\Theta_D + 0.0638(\Theta_T - \Theta_D) P_{CO_2}^{-2/3}\} \frac{\partial P_{CO_2}}{\partial t} + 2.322\text{x}10^4 \alpha_T \ . \qquad (32)$$

The dependence of the rate of mass transfer of CO_2 between the gas and liquid phases upon the gas-phase partial pressure of CO_2 makes equation (32) nonlinear. However, because the value of $P_{CO_2}^{-2/3}$ varies relatively slowly with P_{CO_2}, no particular problems arise in the numerical solution of the equation. For this study, $P_{CO_2}^{-2/3}$ for a given time step was evaluated from the concentration at the previous time step. Small enough time steps (3 days) were used to

---

* Calculated from the data of Plummer and Busenberg (1982)

ensure that the largest error was $\leqslant$ 1%, as determined by trial and error.

The materials comprising the unsaturated zone at North Dakota Site 6 include sandy clay from a depth of 0 to 10m, and fine-grained sand below that depth. Based on these textural descriptions, the total porosity was assumed to be 0.35 for the entire profile, as this is a common value for unconsolidated sediments. Drained porosity was assumed to be 0.15 above 10m, and 0.20 below that depth. Tortuosities for the two layers were computed from the relationship (Lai, Tiedje, and Erickson, 1976)

$$\tau = \Theta_D^{4/3} \quad , \tag{33}$$

resulting in a value of .08 for the upper layer and of .12 for the lower layer.

THE CO_2 MODEL. Boundary and initial conditions: The concentration of CO_2 at land surface (the upper boundary) is assumed to be specified as a function of time. For the seasonal modeling, P_{CO_2} was assumed constant at .0003 atm, and the water table, which is at a depth of ca 15m at Site 6, was assumed to be a no-diffusion boundary. Assumed initial conditions are that the partial pressure of CO_2 is 0.014 atm throughout the profile.

Assuming that the average P_{CO_2} at depth is 0.014 atm as measured at 6m at Site 6, that P_{CO_2} in the atmosphere is .0003 atm, and that the root zone depth is 1m, the average rate of production in the root zone at Site 6 is 2.4×10^{-13} mol/cm^3 of medium/sec, a value that is calculated internally in the computer program from user-supplied data. The variation of P_{CO_2} with depth is based on a seasonal production rate (equations (29) to (31)) that assumes a five-month growing season that begins on May 1 each year.

RESULTS. The most important influence on CO_2 chemistry in the unsaturated zone at Site 6 appears to be chemical reactions in the soil zone with downward propagation of CO_2 by vapor phase diffusion. The well defined annual cycles of P_{CO_2} at the 3m probe, the attenuation of the cycles with depth, and the shifts of the maxima and minima to later dates with depth are all consistent with downward diffusion

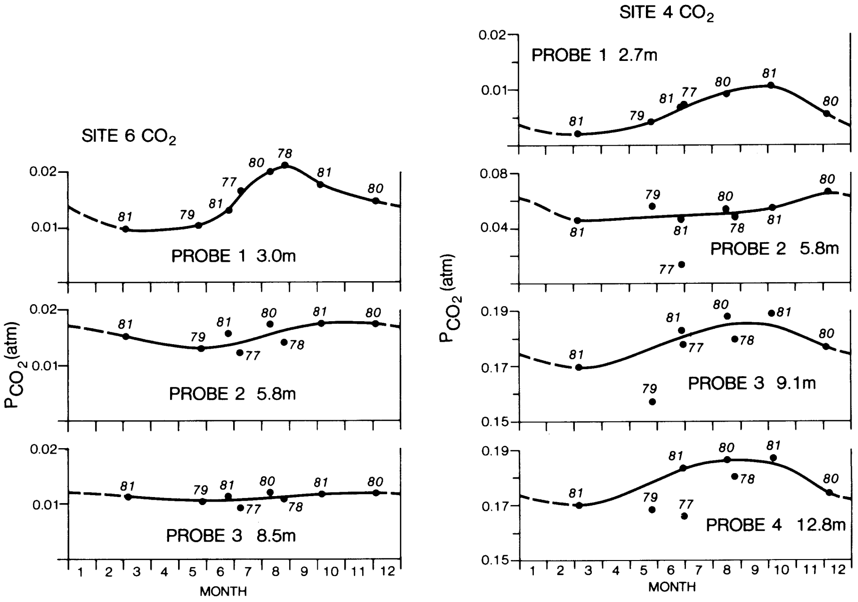

Fig 1. Seasonal variation of P_{CO_2} at North Dakota Sites 6 and 4. Data are plotted by collection date, independent of year, with the year of collection noted at each data point. Data from table 1.

from a seasonally varying source of CO_2 in the soil zone (fig 1). Some details of the modeling results are described below.

Once specific data for Site 6 were incorporated into the mathematical model, the seasonal distribution of P_{CO_2} with depth was computed, based on the assumption that the CO_2 production history exactly repeats itself every year, an assumption that appears well-justified based on the seasonal cycles in the shallow probes at both Site 6 and Site 4 (fig 1). Five years were simulated to ensure steady cyclic conditions for the final year of simulation. Results, in terms of P_{CO_2} vs depth during each month of the growing season, are shown in figure 2. These curves are compared (fig 2) with the detailed depth-time CO_2 data from Trout Creek, Ontario (Reardon, Allison, and Fritz, 1979). Qualitative

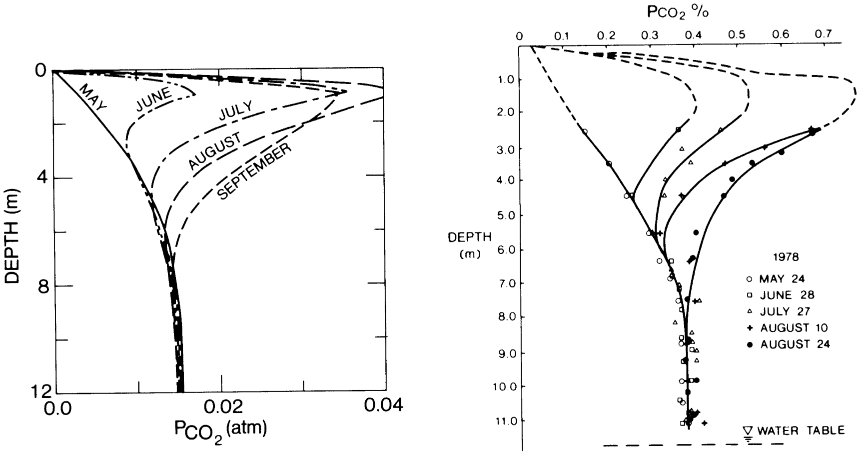

Fig 2. Seasonal profiles of P_{CO_2} vs depth in the unsaturated zone. A. Model calculated for North Dakota Site 6 B. Data from Trout Creek, Ontario; from Reardon, Allison, and Fritz (1979).

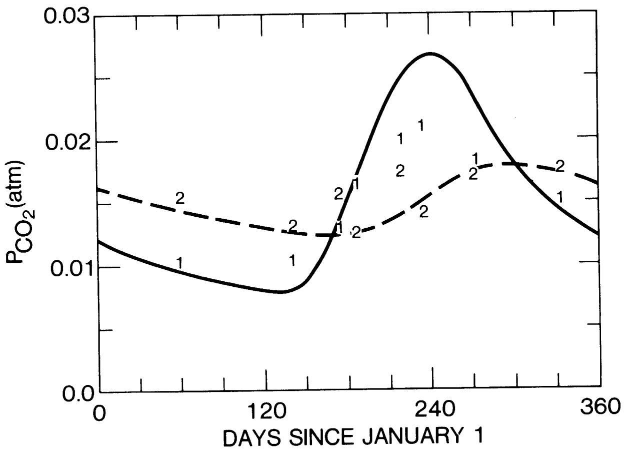

Fig 3. Comparison of calculated seasonal variation of P_{CO_2} at North Dakota Site 6 with observed data. Solid line: probe 1 model; dashed line: probe 2 model. Numbers are measured P_{CO_2}'s for probes 1 and 2, respectively. Probe 1 is screened at 3.0m, probe 2 at 5.8m.

agreement is quite good, indicating that diffusion theory adequately explains the Trout Creek data, even without incorporating site-specific parameters for their site.

The time variation of P_{CO_2} at the depths of probes 1 and 2, Site 6, from this simulation were also calculated and are compared with the measured values for Site 6 in figure 3. The comparison shows slightly less predicted seasonal variation for probe 1 than was observed; for probe 2, the predicted seasonal variation is somewhat greater than observed. Trial-and-error simulations (not shown) made by varying the tortuosity indicate that the amplitude and timing of the measured P_{CO_2} seasonal pattern for probe 1 can be very well simulated using a tortuosity of 0.07 ($\tau = 0.08$ is used in fig 3). Alternatively, an excellent match between measured and simulated results can be obtained for probe 2 using a tortuosity of 0.09. These tortuosities are both well within the plausible range for Site 6. However, an implausibly large value for tortuosity is required to force a simultaneous good fit to the data for both probes.

The inability to obtain a satisfactory simultaneous fit to the measured values for probes 1 and 2 at Site 6 suggests that the actual diffusion process may not be truly one-dimensional. A plausible explanation is that CO_2 moves by a somewhat less tortuous path from land surface to probe 2 than from land surface to probe 1, possibly due to a very local clay lens in the top three meters. However, the goodness of fit is adequate to strongly suggest that mainly vertical diffusion and calcite equilibrium are indeed the dominant mass-transport and mass-transfer mechanisms affecting the CO_2 distribution in the unsaturated zone at Site 6.

THE $^{14}CO_2$ MODEL. Boundary and initial conditions: The well-defined seasonal variation of $P_{^{14}CO_2}$ in the shallow probes at Sites 6 and 4 (fig 4) suggests that diffusion is also important in the transport of $^{14}CO_2$. However, unlike CO_2, atmospheric $P_{^{14}CO_2}$ has shown dramatic changes during the last 30 years as a result of atmospheric nuclear testing in the 1950's and 1960's. Because each species diffuses according to its own gradient, this post-bomb ^{14}C should have migrated at least tens of meters into the unsaturated zone by now. To test this idea, an attempt was made to simulate $P_{^{14}CO_2}$ at Site 6, with the same media parameters used to simulate the seasonal effects described above.

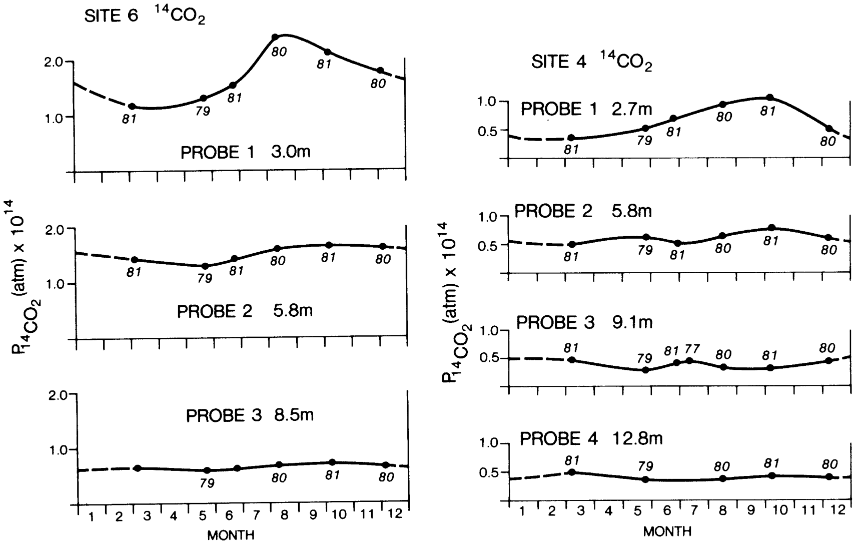

Fig 4. Seasonal variation of $P_{^{14}CO_2}$ at North Dakota Sites 6 and 4. Data are plotted by collection date, independent of year, with the year of collection noted at each data point. Data from table 1.

To model $^{14}CO_2$, information is needed regarding the production of $^{14}CO_2$ in the root zone. $^{14}CO_2$ production was calculated from equation (34):

$$\bar{\alpha}_{^{14}CO_2}(t) = [\ \bar{\alpha}_{^{14}CO_2}(1981)\ ] \times \frac{A^{14}C(t)}{A^{14}C(1981)} \qquad (34)$$

where t = time;

$\bar{\alpha}_{^{14}CO_2}(t)$ = average production rate of $^{14}CO_2$ in the root zone at time t, mol/cm^3 of medium/sec;

and $A^{14}C(t)$ = activity (pmc) of ^{14}C in the atmosphere at time t (fig 5A).

The atmospheric ^{14}C activity through 1975 was estimated from data presented in figure 4 of Broecker, Peng, and Engh (1980), and was then extrapolated to our measured values in 1981. $\bar{\alpha}_{14_{CO_2}}$ (1981) was computed to produce an average $P_{14_{CO_2}}$ of 1.6 x 10^{-14} atm, the average Site 6 value measured at 3m. A 30-year period, starting in 1951, was simulated. Seasonal effects were ignored and 30-day time steps were used in the simulation. The proportionality postulated between atmospheric ^{14}C activity and soil-zone ^{14}C activity represents a major assumption that cannot be rigorously documented at present; the assumption is supported by the near-atmospheric ^{14}C activities in most of the surface CO_2 collections.

The mass transfer of $^{14}CO_2$ between the gas and liquid phases was also handled differently in this simulation. The ^{14}C mass transfer was assumed to occur at a rate proportional to that of CO_2*. The soil gas was assumed to have an average partial pressure throughout the column of .014 atm. Using this value, the partitioning term in equation (32) reduces to $\{\Theta_D + 1.10(\Theta_T - \Theta_D)\}$, thus linearizing equation (32) and making large time steps possible.

The lower boundary condition was also modified for this simulation. Diffusion in the liquid phase could be significant during the long time span covered; hence, another layer was added to represent the saturated material from 15m to 25m. As a mathematical artifice, these materials were assumed to have total and drained porosities of 0.35, and the tortuosity was assumed to be .0001. This approach allows gas diffusion through the fully-saturated medium to be approximated without reprogramming.

---

* This is not an obvious assumption. It is derived from a chemical model developed by the authors, the presentation of which is beyond the space limitations of this paper. The fundamental assumption is that dissolution and precipitation of calcite is governed by changes in P_{CO_2}.

This, in turn, leads to aqueous dilution or enrichment factors that overshadow the changes in $P_{14_{CO_2}}$.

Hence, the dependence on P_{CO_2}, rather than $P_{14_{CO_2}}$.

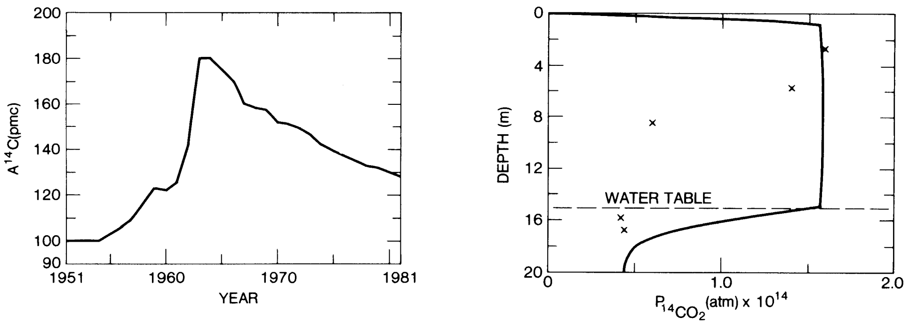

Fig 5. A. Atmospheric ^{14}C activity, adapted from Broecker, Peng, and Engh (1980); see text for discussion. B. Calculated depth profile for $P_{^{14}CO_2}$ at North Dakota Site 6; see text for discussion.

Initial conditions to be assumed in the simulation of $^{14}CO_2$ are problemmatical, as the $^{14}CO_2$ profiles themselves suggest that they cannot be adequately explained by diffusion theory alone. For this simulation, it was assumed that $P_{^{14}CO_2}$ in 1951 was equal to 0.48 x 10^{-14} atm, which is the same as that measured in the ground water in 1981.

RESULTS. The long-term ^{14}C simulation is shown in figure 5B. The calculated profile is almost vertical, with a slight bulge about mid-depth in the unsaturated zone arising from the effect of currently declining production rates following the 1964 peak in ^{14}C activity in the atmosphere. Note that the curve departs radically from the average measured partial pressures, symbolized by X's in the figure. The measured values show a sharp dropoff that cannot be explained by the gaseous diffusion-calcite equilibrium model. Moreover, according to theory, the dissolved $^{14}CO_2$ should have established a steep gradient to a depth of ca 3m into the water table during the 30-year period. The near equality of $^{14}CO_2$ partial pressures in the lower gas probes and groundwater samples at different depths (fig 6) shows that this has not been the case.

In spite of the clearly defined seasonal profile in the shallow probes (fig 4) application of diffusion theory to measured $^{14}CO_2$ profiles in the deep unsaturated zone indicates that some as yet unexplained mechanisms severely retard the migration of $^{14}CO_2$ with depth in the deep unsaturated zone. The general decreases in CO_2 and $^{14}CO_2$ cannot be readily explained with a steady state diffusion model because of the relatively large fluxes that can be achieved with gaseous diffusion. The depth distribution of CO_2 suggests transient processes on a fairly short time scale - not exceeding a few tens of years. The $^{14}CO_2$ is more rapidly attenuated with depth and shows a greater overall decrease than does CO_2, suggesting a selective sink for $^{14}CO_2$ at Site 6. A time lag might also exist between changes in atmospheric ^{14}C activity and the ^{14}C activity in the root zone. However, if this were the only faulty assumption in the model, the decrease in $P_{^{14}CO_2}$ from 3m to 9m should not exceed ~30%, rather than the observed decrease of a factor of 2.

A particularly interesting observation is that soil gas-shallow groundwater $^{14}CO_2$ pressures approach equilibrium more closely than do the corressponding total P_{CO_2}'s, despite the selective attenuation of $^{14}CO_2$ with depth in the unsaturated zone at Site 6. No obvious processes to account for this phenomenon are apparent. However, whatever these mechanisms are, they can profoundly affect the ^{14}C activity of recharged ground water, and suggest that conclusions concerning the residence time of ground water in the unsaturated zone based solely on ^{14}C activities are extremely suspect.

An estimate of the relative magnitudes of diffusive and advective fluxes of CO_2 is needed. The following example, based on North Dakota Sites 4 and 6, provides a numerical comparison that might approximate Great Plains environments. Groundwater alkalinities in the area average ~ 10 meq/l; recharge in Bowman County is estimated as ~ 1 cm/yr (Croft, 1978). A recharge rate of 1ml H_2O/cm^2-yr (ignoring media effects) yields a CO_2 flux to the water table of 10μmol/cm^2-yr. In the gas phase a gradient of 1% CO_2 over 10m, including the moderating effects of porosity and reaction, provides a calculated diffusive flux of ~ 15μmol/cm^2-yr. It thus appears that the diffusive fluxes due to the large, rapidly changing gradients associated with near-surface seasonal CO_2 fluctuations should overshadow recharge effects, while if smaller gradients occur in the deeper unsaturated zone the fluxes might approach each other in magnitude. Rough estimates suggest that sub-soil diffusion should pre-

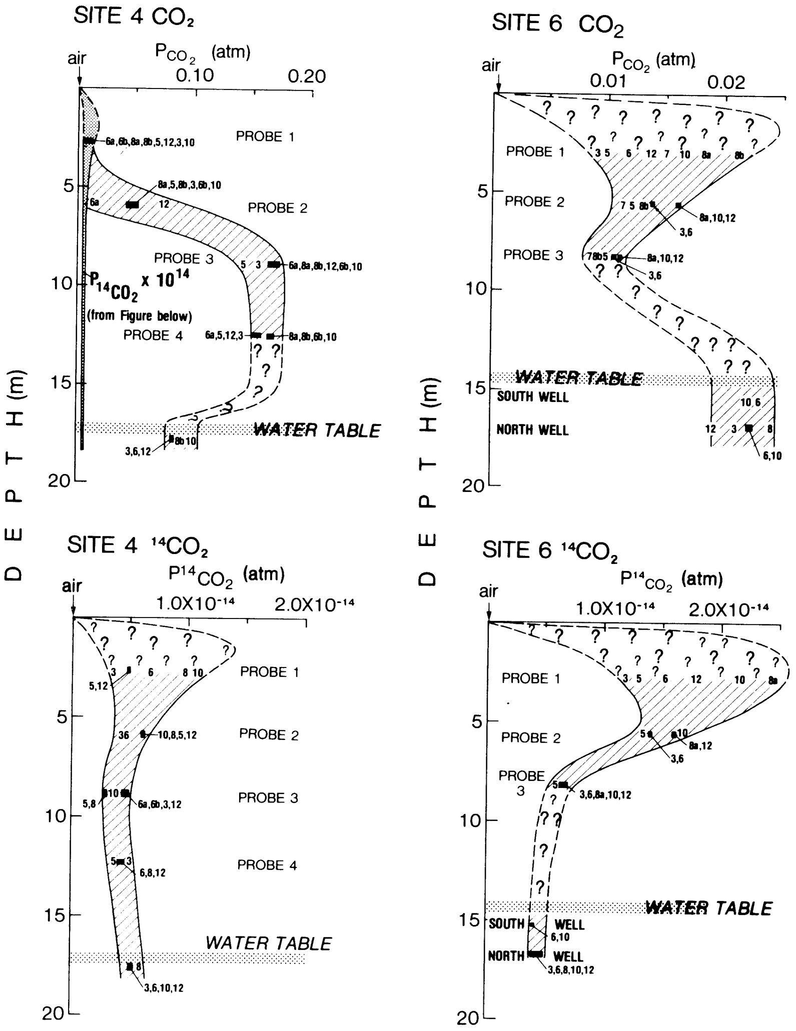

Fig 6. P_{CO_2} and $P_{^{14}CO_2}$ vs depth at North Dakota Sites 4 and 6. Numbers refer to month of collection date, independent of year, and correspond to entries in table 1.

dominate for CO_2 and $^{14}CO_2$ at Sites 6, and CO_2 at Site 4; the relative magnitude of $^{14}CO_2$ diffusion below ~ 5m at Site 4 is much less.

The data tables show that a wealth of information is available in the accumulated ^{13}C data for the unsaturated zone gases at all sites, both in terms of inter-site comparisons and in the differences between gases and the water table wells. No attempt has been made in this paper to incorporate these ^{13}C data into chemical models of unsaturated zone process. Also, no quantitative transport modeling for the other sites has yet been attempted. In the following discussion, important general aspects of the data at other sites are briefly pointed out.

DESCRIPTION OF OTHER SITES

NORTH DAKOTA SITE 4. (See Haas et al, 1983, for detailed description). This site provides an excellent example of the independent behavior of $^{12}CO_2$, $^{13}CO_2$, and $^{14}CO_2$. The major source of ^{12}C and ^{13}C in the system occurs at a depth of 7.5 to 9.5m, where oxidation in the upper portion of the lignite reduces oxygen pressure to near zero and produces CO_2 contents approaching 20 volume%. This CO_2 then diffuses upward, and masks the seasonal cycle in P_{CO_2} in all but the shallowest probe. The observed gradient in P_{CO_2} suggests that the CO_2 produced in this zone also diffuses downward towards the water table, which appears to be acting as a sink for CO_2 at this site.

In spite of P_{CO_2} -depth variation greater than an order of magnitude in the unsaturated zone, and three orders of magnitude difference relative to the atmosphere, the partial-pressure depth profiles of $^{14}CO_2$ are the most uniform observed in this study. The $^{14}CO_2$ depth profile is a better approximation to the elementary diffusion model (compare fig 6B with fig 1A) than either CO_2 or $^{14}CO_2$ from any other North Dakota sampling site. The surprising observation is again made that partial pressure equilibrium between the gas phase and the water table is approached more closely for $^{14}CO_2$ than for CO_2. Note that here the partial pressure of CO_2 is lower in the water - opposite the situation present at North Dakota Site 6. The existence of the CO_2 gradient from the base of the lignite to the water table-if steady state-implies a large flux of $^{12}CO_2$ and $^{13}CO_2$ to the ground water.

NORTH DAKOTA SITES 2 AND 3. Both of these sites are located in lignite-rich spoils, and both show some of the general characteristics of North Dakota Site 4 - namely high and variable CO_2 contents due to lignite oxidation, and relatively uniform $^{14}CO_2$ profiles. Although an investigation of these sites was originally one of the motivations for this work, because of their hydrologic variability due to mine pumpage, we decided early to concentrate on natural processes in the undisturbed sites.

NORTH DAKOTA SITE 1. At Site 1 a stringer of lignite is present just above the water table and a perched water table (the gas probes pumped water) was present at depths of 3m to 8m until at least 1977. Prior to this, the deep samples at Site 1 resembled samples from similar depths at Site 4 in both CO_2 and $^{14}CO_2$ content. The perched water lens disappeared sometime between 1977 and 1980. From the latter date to the present the data at all depths show extreme variability; it was initially believed that the grouting had cracked or that some other sampling problem existed. However, more recent analysis of the data shows that the partial pressure of $^{14}CO_2$ is generally (not always) nearly constant, suggesting a lack of atmospheric influence. No plausible model for processes at this site is available at present.

THE TEXAS SITES. The sampling nests at both Texas sites were constructed as part of an artificial recharge study in the Ogallala aquifer conducted by the US Geological Survey (Weeks, 1978). At the Glenn and Lamb sites, located near Lubbock, Texas, the Ogallala formation consists of interbedded sands, silts, and clays, with local development of massive caliche. The water tables at the sites are at depths of 51m (Glenn) and 77m (Lamb). For additional geologic and hydrologic information, see Weeks (1978) and Petraitis (1981); much additional CO_2 and $\delta^{13}C$ data for these sites are presented in Petraitis (1981).

THE GLENN SITE. Two sets of samples were collected from this site (table 1). CO_2 partial pressures are 0.01 atm or less; highest CO_2 pressures occur at intermediate depths. In the single set of $^{14}CO_2$ samples collected, the relative variation of $P_{^{14}CO_2}$ is less than that of P_{CO_2}, but the greatest value is found at an intermediate depth. The partial pressure of $^{14}CO_2$ at this site is quite similar in magnitude to the values observed at North Dakota Site 4. No $^{14}CO_2$ data are available at the water table.

THE LAMB SITE. Two sets of CO_2 data are available, but in this case, they are quite dissimilar; only the shallow probes show fairly consistent values of P_{CO_2}. If the variation is due to sampling error, it is most likely that the initial samples were collected without sufficient initial pumping.

This site is quite interesting in that it is the only site for which our data definitively show post-bomb $^{14}CO_2$ activities in deep samples, in spite of a perched water table at 28m. Combined with the relatively high CO_2 partial pressures, the resulting $^{14}CO_2$ partial pressures at the Lamb site are equalled only by the lignite spoils at North Dakota Site 3. The $^{14}CO_2$ partial pressures are nearly constant in the deeper probes.

GENERAL OBSERVATIONS

A number of general observations can be made regarding the behavior of $^{14}CO_2$ in the unsaturated zone that are independent of sampling location or date.

1) The geochemistry of $^{14}CO_2$ in the unsaturated zone must be evaluated in terms of both the partial pressure of $^{14}CO_2$ and the ^{14}C activity of the CO_2 gas samples. A value of $A^{14}C > 100$pmc still remains the only unequivocal signature of post-bomb carbon. However, the general lack of correlation between the $A^{14}C$ and $P_{^{14}CO_2}$ depth profiles emphasizes the need for evaluation of both parameters in unsaturated zone ^{14}C studies.

2) Diffusion is a major mechanism of gas transport in the sub-soil unsaturated zone. The various isotopes of CO_2 each diffuse in response to their own sources and sinks, as best illustrated by the data from North Dakota Site 4. The diffusion models must consider individually the absolute concentration of each isotopic species in units of mass/-volume or the corresponding gas partial pressures. Diffusive fluxes of CO_2 and its isotopes appear to predominate over advective fluxes in the shallow (< 5m) unsaturated zone. No generalizations regarding greater depths can be made.

3) $^{14}CO_2$ and $^{12}CO_2$ are biologically generated in the shallow soil zone. Penetration of the $^{14}CO_2$ into the unsaturated zone and observed activities >100pmc in surface samples imply relatively rapid diffusion of this species in the subsurface. Considering the relatively large fluxes that can be generated by diffusive transport of gases, the variable

shapes of the P_{CO_2}- and $P_{^{14}CO_2}$ depth profiles and the partial pressure disequilibrium between the gas and aqueous phases suggest that steady-state processes are very unlikely at any of the sites studied.

4) The measured concentration, in mass/volume of gas, of $^{14}CO_2$ in the unsaturated zone is without exception 10 to 100 times greater than the concentration of $^{14}CO_2$ in the atmosphere.

ACKNOWLEDGMENTS

This has been a long and collective effort; however, some mention of individual areas of expertise seems warranted. DW Fisher was responsible for collection, analysis, and interpretation of the gas analyses; the very precise ^{14}C work is due to Herbert Haas; DC Thorstenson provided geochemical modeling concepts and ballast during field work in the high winds of the northern Great Plains; EP Weeks provided the transport modeling capability and the crucial initial observation that $^{14}CO_2$ must be dealt with in terms of partial pressures, and not simply in terms of ^{14}C activities. The manuscript was much improved as a result of discussion and review from Eric Sundquist and Ike Winograd. A number of people in the North Dakota District, Water Resources Division, US Geological Survey, willingly contributed many hours of help and support during the course of this project.

Finally, the existence of much of the data is due in large part to the continual good humor and competence--sometimes under extreme conditions--of Dave Stannard, whose help in the field is much appreciated.

REFERENCES

Bavel, CHM van, 1951, A soil aeration theory based on diffusion: Soil Sci, v 72, p 33-46.

Bird, RB, Stewart, WE, and Lightfoot, EN, 1960, Transport phenomena: New York, John Wiley and Sons, 780 p.

Broecker, WS, Peng, T-H, and Engh, R, 1980, Modeling the carbon system, in Stuiver, M, and Kra, RS, eds, Internatl ^{14}C Conf, 10th, Proc: Radiocarbon, v 22, no. 3, p 565-598.

Croft, MG, 1978, Ground-water resources of Adams and Bowman Counties, North Dakota: North Dakota Geol Survey Bull, 165 (III), 54 p.

Feynman, RP, Leighton, RB, and Sands, M, 1963, The Feynman lectures on physics, vol 1, chap 43: Reading, Mass, Addison-Wesley Pub Co, Inc.

Garrels, RM and Christ, CL, 1965, Solutions, minerals, and equilibria: New York, Harper & Row, 450 p.

Haas, H, Fisher, DW, Thorstenson, DC, and Weeks, EP, 1983, $^{13}CO_2$ and $^{14}CO_2$ measurements on soil atmosphere sampled in the sub-surface unsaturated zone in the western great plains of the US: Radiocarbon, v 25.

Jost, W, 1960, Diffusion in solids, liquids, gases: New York, Academic Press, 3rd printing with addendum, 652 p.

Kunkler, JL, 1969, The sources of carbon dioxide in the zone of aeration of the Bandelier Tuff, near Los Alamos, New Mexico: US Geol Survey Prof Paper 650-13, p B185-B188.

Lai, S-H, Tiedje, JM, and Erickson, AE, 1976, In situ measurement of gas diffusion coefficient in soil: Soil Sci Soc America, v 40, no. 1, p 3-6.

Landergren, S, 1954, On the relative abundance of the stable carbon isotopes in marine sediments: Deep Sea Research, v 1, p 98-120.

Li, YH, and Gregory, S, 1974, Diffusion of ions in sea water and in deep-sea sediments: Geochim et Cosmochim Acta, v 38, p 703-714.

Petraitis, MJ, 1981, Carbon dioxide in the unsaturated zone of the southern high plains of Texas: Unpublished master's thesis, Lubbock, Texas, Texas Tech Univ, 134 p.

Plummer, LN, and Busenberg, E, 1982, The solubilities of calcite, aragonite, and vaterite in CO_2-H_2O solutions between 0 and 90°C, and an evaluation of the aqueous model for the system $CaCO_3$-CO_2-H_2O: Geochim et Cosmochim Acta, v 46, p 1011-1040.

Reardon, EJ, Allison, GB, and Fritz, P, 1979, Seasonal chemical and isotopic variations of soil CO_2 at Trout Creek, Ontario: Jour Hydrology, v 43, p 355-371.

Reardon, EJ, Mozeto, AA, and Fritz, P, 1980, Recharge in northern clime calcareous sandy soils: soil water chemical and carbon-14 evolution: Geochim et Cosmochim Acta, v 44, p 1723-1735.

Weeks, EP, 1978, Field determination of vertical permeability to air in the unsaturated zone: US Geol Survey Prof Paper 1057, 41 p.

Weeks, EP, Earp, DE, and Thompson, GM, 1982, Use of atmospheric fluorocarbons F-11 and F-12 to determine the diffusion parameters of the unsaturated zone in the southern High Plains of Texas: Water Resources Research, in press.

[Radiocarbon, Vol 25, No. 2, 1983, P 347-356]

A CONTRIBUTION TO THE INTERPRETATION OF ^{14}C GROUNDWATER AGES CONSIDERING THE EXAMPLE OF A PARTIALLY CONFINED SANDSTONE AQUIFER

LORENZ EICHINGER

GSF, Institut für Radiohydrometrie, D-8042 Neuherberg,
West Germany

ABSTRACT. Previously described models and a new model were compared to determine the initial ^{14}C content of groundwater in a partially-confined and unconfined sandstone aquifer (Fränkisches Albvorland, Germany). Isotope and chemical data were derived from samples of water, soil-CO_2, and solid carbonates. The various ^{14}C models lead to important differences in resulting groundwater ages.
From the relationship between ^{14}C and ^{2}H or ^{18}O concentrations of groundwater, it must be assumed that chemical and/or physical carbon isotope exchange between the DIC and the solid carbonate has occurred provided the groundwater with lower ^{18}O and ^{2}H concentrations was generated during the Pleistocene. Groundwater ages deduced from ^{14}C and ^{39}Ar concentrations showed discrepancies which can be explained if carbon isotope exchange between DIC and solid carbonate as well as mixing of recent and fossil waters is considered.

TEST SITE

The area under study lies south of Nuremberg, southern Germany. The unconfined area is in the northwest (Fränkisches Albvorland) where sandstone layers of Keuperage crop out, partially interrupted by discontinuous clay lenses "Zwischenletten". Nearly all surface waters receive discharging Keuper groundwater (Andres and Geyh, 1970; Rietzler, ms). The confined area is in the Frankenalb and its foreland where the sandstones are entirely covered by thick clay layers of the upper "Mittlere Keuper" (Feuerletten), Lias and Dogger. The Danube and Altmühl rivers receive the discharge from this area.

MODEL CONSIDERATIONS FOR DETERMINING INITIAL ^{14}C CONCENTRATION

In humid climates ^{14}C produced and oxidized in the atmosphere is introduced via soil-CO_2 into groundwater which dissolves ^{14}C free carbonate (Münnich, 1957). This concept led to the chemical mixing model (equation 1) and the isotope mixing model for calculating the initial ^{14}C concentration, A_o (Ingerson and Pearson, 1964):

$$A_{o,1}=(N_{CO_2}+0.5\ N_{HCO_3})\ A_g{}^{*)} \tag{1}$$

$$A_{o,2}=\frac{\delta^{13}C_{DIC}-\delta^{13}C_s}{\delta^{13}C_g-\delta^{13}C_s}\ A_g \tag{2}$$

A_o can be subsequently increased if the soil carbonates contain ^{14}C or if carbon isotope exchange takes place between DIC and soil-CO_2 in the unsaturated zone of the groundwater recharge area. Vogel (1970) deduced empirically an initial ^{14}C concentration of $A_o=(85+5)$%modern. The simple models described by equation 1 and 2 were further developed by considering additional carbon isotope exchange

---

*)	Symbols:
A_o:	initial ^{14}C concentration
$A_{o,1}$, $A_{o,2}$:	initial ^{14}C concentration calculated by the chemical mixing model respectively isotope mixing model
A_g:	^{14}C concentration of soil-CO_2
B:	calculated carbon exchange factor
$\delta^{13}C_g$, $\delta^{13}C_s$:	$\delta^{13}C$ value of soil-CO_2 and solid carbonate
$\delta^{13}C_{DIC}$, $\delta^{13}C_{b\ ex}$, $\delta^{13}C_{s\ eq}$:	measured $\delta^{13}C$ value of DIC, calculated $\delta^{13}C$ values of DIC before carbon exchange takes place, and $\delta^{13}C$ of DIC in equilibrium with the solid carbonate
$\varepsilon_{g/aq}$, $\varepsilon_{g/s}$, ε_{s/HCO_3^-}:	carbon isotope fractionation between gaseous CO_2 - dissolved CO_2, gaseous CO_2 - solid carbonate, and solid carbonate - bicarbonate
N_{CO_2}, $N_{HCO_3^-}$:	mol-fraction of aqueous CO_2 and HCO_3^-
DIC:	Dissolved Inorganic Carbon

in an open or closed system, and dissolution precipitation reactions (Mook, 1976; Fontes and Garnier, 1979; Reardon and Fritz, 1978; Wigley, Plummer, and Pearson, 1978; Mozeto, 1981). The temporal alteration of $A_{o,1}$, if recognizable by changes of the ^{13}C concentrations, can be expressed approximately by a factor B in equation 1 (Eichinger, ms):

$$A_o = B \cdot A_{o,1} \tag{3}$$

In B, the measured δ^{13}C value is related to calculated δ^{13}C values obtained without isotope exchange and with isotope exchange under the condition of isotope equilibrium between DIC and solid carbonates:

$$B = \frac{\delta^{13}C_{DIC} - \delta^{13}C_{s\ eq}}{\delta^{13}C_{b\ ex} - \delta^{13}C_{s\ eq}} \tag{4}$$

δ^{13}C can be derived from the stoichiometric formation of DIC, considering isotopic fractionation during CO_2 dissolution in water (for fractionation factors, see Mook, 1980):

$$\delta^{13}C_{b\ ex} = N_{CO_2}(\delta^{13}C_g - \varepsilon_{g/aq}) + 0.5\ N_{HCO_3^-}(\delta^{13}C_g - \varepsilon_{g/aq} + \delta^{13}C_s) \tag{5}$$

If a carbon isotope equilibrium is established between DIC and solid carbonate, then $\delta^{13}C_{DIC} = \delta^{13}C_{s\ eq}$ and

$$\delta^{13}C_{s\ eq} = N_{CO_2}\ (\delta^{13}C_g - \varepsilon_{g/s}) + N_{HCO_3^-}\ (\varepsilon_{s/HCO_3^-}) + \delta^{13}C_s \tag{6}$$

ISOTOPE HYDROLOGY AND HYDROCHEMISTRY

A_o can be obtained from equation 3 if the originally existing initial ^{14}C concentration $A_{o,1}$ was changed through carbonate reactions, ion exchange, carbon isotope exchange between DIC and solid carbonates, and/or outgassing of CO_2 accompanied by carbonate precipitation. The conditions for the use of equation 3 (as well as for all the other models) are:

δ^{13}C values of soil-CO_2 and reacting solid carbonates must be known; the groundwater under investigation does not originate from surface water recharge, i e, surface water that underwent carbon isotope exchange with atmospheric CO_2; outgassing of CO_2 did not take place without accompanying carbonate precipitation; no admixture of CO_2 of magmatic or fossil organic origin occurred.

^{13}C IN SOIL-CO_2. Most published $\delta^{13}C$ values of soil-CO_2 from humid climates lie between -28 and -19‰. For the area here under study, a $\delta^{13}C$ value of ca (-23 ± 1)‰ can be deduced for modern soil-CO_2. Taking into account the influence of fossil fuel combustion since the beginning of industrialization, a $\delta^{13}C$ value of ca (-21 ± 1)‰ is assumed for old groundwater and the pertinent soil-CO_2.

^{13}C IN SOLID CARBONATE. ^{13}C concentrations were measured on 62 samples of rock from 6 deep cores and 9 samples from surface outcrops. The samples from the "Mittleren Keuper" and "Oberen Keuper" gave $\delta^{13}C$ values between -14 and -3‰ with a mean value of -7.9‰; those from Jurassic formations range from 0 to +2‰ with a mean of +1‰, which means that an uniform $\delta^{13}C$ value for the solid carbonate cannot be assumed.

SPRINGS AND WELLS.The investigation, made between May 1979 and September 1980, included many spring and well waters. From the unconfined towards the confined area, the water in deep wells shows increasing concentrations of Ca^{2+}, Mg^{2+}, HCO_3^-, Na^+, K^+, as well as increasing pH-values, and saturation indices for calcite, dolomite, and gypsum.

The following relationships between isotope concentrations and hydrochemical parameters are evident:

1) $\delta^{18}O$ and $\delta^{2}H$ values show a clear tendency towards lower values for those groundwaters with ^{14}C concentrations below 10% modern. If we assume that these waters infiltrated ca 10 000 to 13 000 years ago at the end of the last glacier time (Rudloff, 1980), the measured ^{14}C concentrations of 10% modern would indicate that initial ^{14}C concentrations were in the range of 33 to 48% modern, considering only decay. In contrast, the chemical mixing model yields an $A_{o,1}$ value of < 50% modern. These differing initial concentrations lead to the assumption, that carbon isotope exchange may have affected ^{14}C concentrations.

2)The change from alkaline earth to alkali bicarbonate groundwaters is caused by cation exchange whereby a decrease in alkaline earth ions parallels a decrease of ^{14}C

concentration in the confined aquifer.

A clear relationship also exists between ^{14}C and ^{13}C concentrations of the DIC, or bicarbonate whereby the $\delta^{13}C$ values become more positive with decreasing ^{14}C concentrations. This change cannot be explained by increasing calcite dissolution alone. Therefore carbon isotope exchange between DIC and solid carbonate was also taken into account.

CALCULATION OF THE INITIAL ^{14}C CONCENTRATIONS

YOUNG GROUNDWATER (WITH ^{3}H, > 10 TU). The only possibility for determining initial ^{14}C concentration independent of chemical or biologic reactions, is to measure ^{3}H (Geyh, 1972) or ^{85}Kr concentrations (Salvamoser, ms). In this case, applicability of the hydrologic exponential model is assumed and permits the determination of A_o and mean residence time of groundwater (Eichinger, ms). Figure 1 compares initial ^{14}C concentrations for young spring and well waters obtained from the hydrologic exponential model (EM) and the chemical mixing model (CMM). Compared to the hydrologic exponential model, the CMM shows, on the average, a 5% modern higher initial ^{14}C concentration for 18 wells and 11 springs (table 1). However, this difference is not significant. Regarding well waters alone, the average difference is 3% modern, and, if spring waters are compared, the difference amounts to 6% modern (table 1). A difference of at most 20% modern is observed among well waters (see fig 1, sample 6.64).This great variation of A_o is possibly related to infiltration of surface waters which had undergone carbon exchange with the atmosphere. For spring waters, only samples from aquifers with an estimated $\delta^{13}C_s$ value of ca 1‰ (Malm) were used and differences of at most 14% modern were observed.

Almost equal A_o values are found for the model described in equation 3 and for the isotope mixing model; for the Fontes-Garnier model, A_o is determined to be ca 5% modern higher, for the Mook model, ca 17% modern higher, and for the Reardon-Fritz model, ca 18% modern higher. The A_o values calculated with the Reardon-Fritz model assumed a carbonate controlled pH range of 6.3 to 7.0 and PCO_2 range of $10^{-1.7}$ to $10^{-1.5}$ atm for the recharge area (table 1).

Those models in which the carbon isotope of the DIC is assumed to be in equilibrium with the soil-CO_2 in the unsaturated zone of the recharge area, show considerably higher A_o values compared with the hydrologic exponential and other models.

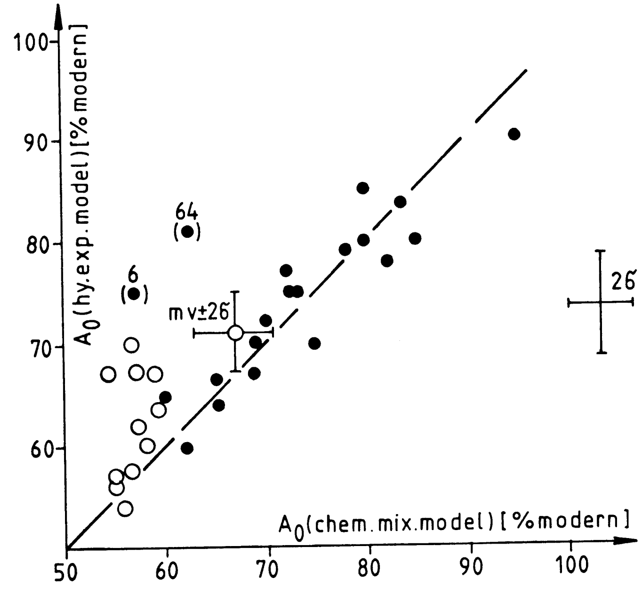

Fig 1. Initial ^{14}C concentration calculated by the hydrologic exponential model (Salvamoser, ms) and the chemical mixing model. Samples are from wells(●) and springs (o). Numbers 6 and 64 have not been considered. mv=mean value of the mean with 95% confidence level.

OLD GROUNDWATER (^3H CONTENT LOW OR UNDETECTABLE, < 1 TU). The initial ^{14}C concentrations in relatively old groundwaters with low or undetectable ^3H concentrations can only be determined by hydrochemical models. The Fontes-Garnier model and especially the Mook model show a very strong dependence of A_0 of $\delta^{13}C$ values of soil-CO_2 and of solid carbonate. Further, the Mook model shows, in some of the in-

TABLE 1. Initial ^{14}C concentration estimated from different models for young groundwater samples (95% confidence level)

		Initial ^{14}C concentration calculated from						
	No of samples	Hydrologic exponential model	Chemical mixing model	^{13}C isotope exchange model	Isotope mixing model	Fontes-Garnier model	Mook model	Reardon-Fritz model
Springs	11	63 ± 3	57 ± 1	60 ± 2	62 ± 2	68 ± 4	80 ± 10	81 ± 1
Wells	18	77 ± 4	74 ± 2					
Both	29	72 ± 4	67 ± 4					

vestigated cases an unrealistic decrease of A_o with increasing $\delta^{13}C$ values of the solid carbonate and realistic $\delta^{13}C$ values of soil-CO_2. Both models result in incorrect values for A_o, if the $\delta^{13}C_g$ values approximate $(\varepsilon_{g/s} + \delta^{13}C_s)$ or $(\varepsilon_{g/HCO_3^-} + \delta^{13}C_s)$.

The described model (equation 3) mostly results in somewhat smaller A_o values than those from the isotope mixing model.

Because of the difficulties in the determination of the $\delta^{13}C$ values of groundwaters, soil-CO_2, and solid carbonate, the calculated ^{14}C concentrations often have such a wide range that the derivation of groundwater ages becomes meaningless.

PROFILE OF THE AREA

Initial ^{14}C concentrations calculated from different models were used to deduce flow velocities of the ground water, given in table 2. The first profile leads from the unconfined to the confined area, while the second profile only belongs to the deep wells in the unconfined area. Assuming that maximum isotope exchange ($\delta^{13}C_s = -8‰$) has occurred, calculated groundwater ages (equation 3) are lower than those obtained from the empirical model ($A_o = (85\pm10)\%$ modern) or the chemical mixing model. However, flow velocities (table 2) calculated from the differences in the groundwater ages prove to be independent from the type of model. They agree well with distance velocities calculated from hydraulic considerations in the first profile, while in contrast the distance velocities in the second profile show remarkably higher results.

TABLE 2. Groundwater flow velocities deduced from radiometric ages calculated with different ^{14}C models and from "Darcy's Law"

Groundwater flow [km]		Groundwater flow velocities [m/a]						
Model		^{14}C Measured values	Chemical mixing	Isotope mixing		^{13}C isotope exchange		"Darcy"
$\delta^{13}C_s$ [‰]				1	-8	1	-8	
confined	7	0.9 ± 0.1	1.1 ± 0.1	1.8	7	1.4 ± 0.3	-	1.4 ± 0.4
area	26	1.0 ± 0.1	1.1 ± 0.1	1.1	1.4	1.1 ± 0.1	1.6 ± 0.4	
unconfined	3.5	1.8 ± 0.5	1.6 ± 0.2	5.8	-	$5.8^{+13.1}_{-5.8}$	$1.8^{+2.0}_{-1.8}$	9.1 ± 4.0
area	13	0.9 ± 0.1	1.0 ± 0.1	1.1	1.9	1.0 ± 0.2	2.4 ± 1.0	

COMPARISON OF THE GROUNDWATER AGES DERIVED FROM THE ^{14}C AND ^{39}Ar CONCENTRATION

^{39}Ar measurements were made in some well waters in this area for the comparison with ^{14}C groundwater ages (Loosli and Oeschger, 1979). In most cases, the calculated values of the groundwater ages were much smaller than the ^{14}C ages (fig 2 A). The reasons for these discrepancies could be underground production of ^{39}Ar or gas exchange with the atmosphere through the aquiclude (Loosli and Oeschger, 1979). In addition, the ^{14}C concentration of the DIC decreases through carbon isotope exchange with the solid carbonate and the calculated groundwater ages with A_o = 85% modern are too high.

In figure 2 A the calculated correlation between ^{14}C and ^{39}Ar concentrations are plotted for three different mixing models. All measuring points should be on the right

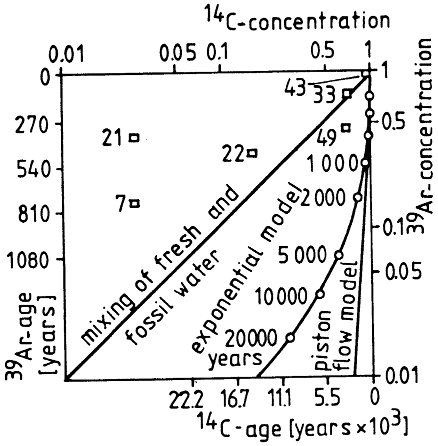

Fig 2 A. Theoretical correlation between ^{39}Ar and ^{14}C concentration for three different mixing models. Data (□) are given for the test side (Fränkisches Albvorland). The ^{14}C groundwater ages are calculated with an initial ^{14}C concentration of 85% modern (Loosli, 1980).

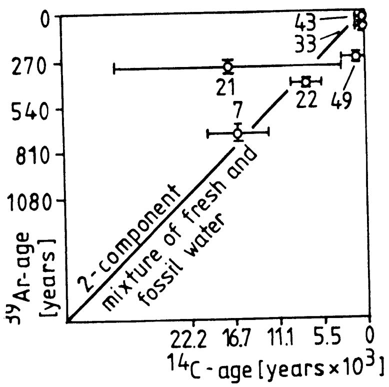

Fig 2B. ^{39}Ar and ^{14}C groundwater ages. Initial ^{14}C concentration is calculated from equation 3 with $\delta^{13}C_g$=-21‰ and $\delta^{13}C_s$=-8‰. ^{39}Ar groundwater ages from Loosli, (1980).

of the straight line for a mixing of recent and fossil waters. This is not the case, but when the ^{14}C groundwater ages are calculated from equation 3, they then agree with the ^{39}Ar groundwater ages (fig 2 B). With this interpretation, the results of both dating methods could be explained if mixing of water of different ages had occurred. However, it would have to be assumed that substantial amounts of groundwater leak through the nearly impermeable layers of the Lias and that the ^{14}C concentrations of the younger water decreased through geochemical processes.

CONCLUSIONS

The interpretation of isotope data from the unconfined and confined aquifers in the project area clearly documents the dependance of model calculations on the exact determination of input parameters. It is also possible that isotope exchange between aqueous and solid carbonate modifies the ^{14}C concentrations in these systems. However, comparison with ^{39}Ar data suggests that mixing of different waters may occur even in the confined aquifer which would invalidate the application of most model considerations on a regional basis.

ACKNOWLEDGMENTS

For helpful discussion respectively for the translations I thank H Moser, W Rauert, P Fritz, J Salvamoser, M Forster and M Wolf. For typing I thank Mrs K Kufner.

REFERENCES

Andres, G and Geyh, M A, 1970, Untersuchungen über den Grundwasserhaushalt im überdeckten Sandsteinkeuper mit Hilfe der ^{14}C- und ^{3}H-Wasseranalysen: Wasserwirtschaft, 60, no 8, p 259-263.

Eichinger, L, 1981, Bestimmung des Alters von Grundwässern mit Kohlenstoff-14: Messung und Interpretation der Grundwässer des Fränkischen Albvorlandes: Ph D, Univ Munich, 193 p.

Fontes, J C and Garnier, J M, 1979, Determination of the initial ^{14}C activity of the total dissolved carbon: a review of the existing models and a new approach: Water Resources Research, v 15, p 399-413.

Geyh, M A, 1973, On the determination of the initial ^{14}C content in groundwater in Rafter, T A and Grant-Taylor, T, eds, International Radiocarbon Conf, 8th, Wellington, Royal Soc, New Zealand, p 369-380.

Ingerson, E and Pearson, F J jr, 1964, Estimation of age and rate of motion of groundwater by the ^{14}C method, in Recent researches in the fields of hydrosphere, atmosphere and nuclear geochemistry: Tokyo, Maruzen, p 263-283.

Loosli, H H and Oeschger, H, 1979, Argon-39, carbon-14 and krypton-85 measurements in groundwater samples, in Isotope Hydrology: Vienna, IAEA, p 931-947.

Mook, W G, 1976, The dissolution-exchange model for dating groundwater with carbon-14, in Interpretation of environmental and hydrochemical data on groundwater hydrology: Vienna, IAEA, p 213-225.

---------- 1980, Carbon-14 in hydrological studies, in Fritz, P and Fontes, J Ch, eds, Handbook of environmental isotope geochemstry, Vol 1: Amsterdam, Elsevier Sci, p 49-74.

Mozeto, A A, 1981, Carbon isotope exchange in aqueous systems: A field and laboratory investigation: Ph D, Univ Waterloo, Canada, 185 p.

Münnich, K O, 1957, Messung des ^{14}C-Gehalts von hartem Grundwasser, Naturwissenschaften v 44, p 32-39.

Reardon, E J and Fritz, P, 1978, Computer modelling of groundwater ^{13}C and ^{14}C isotope composition: Jour Hydrol, v 36, p 201-224.

Rietzler, J, 1979, Zur Hydrogeologie des Raumes südöstlich von Nürnberg unter besonderer Berücksichtigung der Gradabteilungsblätter 6533 Röthenbach, 6633 Feucht und 6733 Allersberg: Ph D, Univ Munich, 183 p.

Rudloff, H v, 1980, Die Klima-Entwicklung in den letzten Jahrhunderten im mitteleuropäischen Raum (mit einem Rückblick auf die postglaziale Periode), in Oeschger, H, Messerli, B, and Svilar, M, eds, Das Klima, Berlin, Springer Verlag, p 125-148.

Salvamoser, J, 1982, ^{85}Kr im Grundwasser-Meßmethodik, Modellüberlegungen und Anwendungen auf natürliche Grundwassersysteme:Ph D, Univ Munich, 126 p.

Vogel, J C, 1970, ^{14}C-Dating of groundwater, in Isotope Hydrology: Vienna, IAEA, p 225-240.

Wigley, T M L, Plummer, L N and Pearson, F J, 1978, Mass transfer and carbon isotope evolution in natural water systems: Geochim et Cosmochim Acta, v 42, p 117-1139.

[Radiocarbon, Vol 25, No. 2, 1983, P 357-372]

GROUND-WATER CIRCULATION IN THE MEADE THRUST ALLOCHTHON EVALUATED BY RADIOCARBON TECHNIQUES

AB MULLER
Sandia National Laboratories, Albuquerque, New Mexico

and

AL MAYO
University of Colorado, Colorado Springs, Colorado

ABSTRACT. The Meade thrust, in southeastern Idaho, is a major element of the Western Overthrust Belt. The allochthon is of geo-economic importance both as a potential hydrothermal area and as the principal mining area within the Western Phosphate Field. To assist in the development of these two resources, an understanding of the regional ground-water circulation was sought. Geologic and hydrologic data from boreholes in this area are virtually nonexistent. Waterwell development in the area has not occurred because of the abundance of springs and only a few hydrocarbon exploration boreholes have been drilled. Thus, the problem lends itself to evaluation by isotope hydrologic and geochemical methods. Ten springs from within the thrust block and around its periphery were sampled for major ions, $^2H/^{18}O$, and $^{14}C/^{13}C$ analysis. Data from these analyses and from field geologic evidence have identified two distinct flow regimes within the Meade thrust allochthon. Shallow flow systems lie above the impermeable Phosphoria Formation, usually within a few hundred meters of the surface. Most of the spring waters from this system are recent and cool. In all cases, they have mean subsurface residence times of less than a few hundred years. The deeper flow systems which lie below the Phosphoria formation are hydraulically isolated from the shallow system. Warm waters from these springs have ^{14}C contents suggesting mean ground-water residence times on the order of 15,000 years. Although these waters could have circulated to as deep as 1900m, $^2H/^{18}O$ results show that high temperatures were never reached. There is no evidence to suggest that water from beneath the Meade thrust has contributed to the circulation in the allochthon.

INTRODUCTION

The Meade thrust allochthon (Fig 1) is a major segment of the Idaho-Wyoming thrust belt, covering ca 3700km^2, includes most of the Western Phosphate Field, and is a potential source of geothermal energy and of hydrocarbons. Our aim was to understand the ground-water circulation patterns for the development of the phosphate and geothermal resources.

The relationships between ground-water flow patterns and the structures involved in thrust and block faulting in the

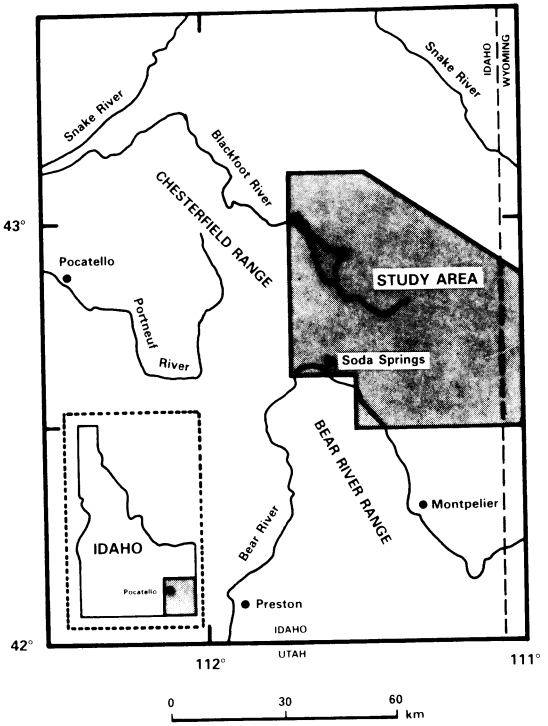

Fig 1. Index map of southeastern Idaho showing the location of the study area. Shaded region in the Idaho map inset shows location of index map.

allochthon have been poorly understood. Faults, particularly along the periphery of the allochthon, appear to be significant factors controlling the discharge from many of the aquifers within the allochthon. The larger springs and the thermal springs are concentrated along the periphery extension and thrust faults. Springs in the interior of the allochthon have smaller discharges and lower discharge temperatures. Deep drilling in the area has been limited to a few oil/gas exploration boreholes. Water wells have not been developed because of the abundance of springs. Evaluating the ground-water flow pattern lends itself readily to isotope hydrologic and geochemical methods.

THE SETTING

GEOLOGY. The Meade thrust allochthon is a body of upper Paleozoic and lower Mesozoic marine strata underlain by the Meade thrust fault. The upper Paleozoic formations are predominantly carbonate and sandy strata which have a maximum aggregate thickness of ca 2000m. The lower Mesozoic formations consist of carbonate and sandy, shaly strata which are generally less massively bedded. The Phosphoria Formation, the uppermost Paleozoic formation, is of particular importance to this investigation because it contains siliceous mudstones, cherts, and phosphate rocks which have significantly lower hydraulic conductivities than the underlying strata. The Phosphoria Formation, 150m-thick, forms a hydraulic barrier between the Paleozoic aquifers below it and the Mesozoic aquifers above it.

The allochthon is up to 40km wide in an east-west direction and up to 80km long in a north-south direction. The major structural features of the allochthon are shown on the generalized geologic map (Fig 2) and on an east-west structure section (Fig 3). The sole of the Meade thrust is thought to be continuous under the allochthon (Mansfield, 1927; Royse, Warner, and Reese, 1975). Structure sections by Mansfield (1927) and Cressman (1964) show the depth of the generally flat-lying thrust sole to 2200m below land surface. The Meade thrust fault surfaces as a series of steeply inclined thrust splays along the eastern and southern borders of the allochthon. The

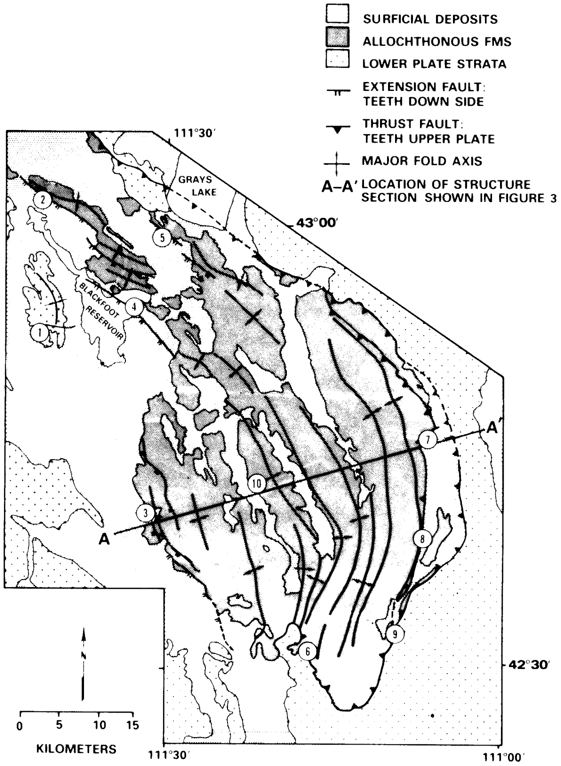

Fig 2. Generalized geologic map of the Meade thrust area showing the location of the structural section in Figure 3. Modified after Mansfield (1927).

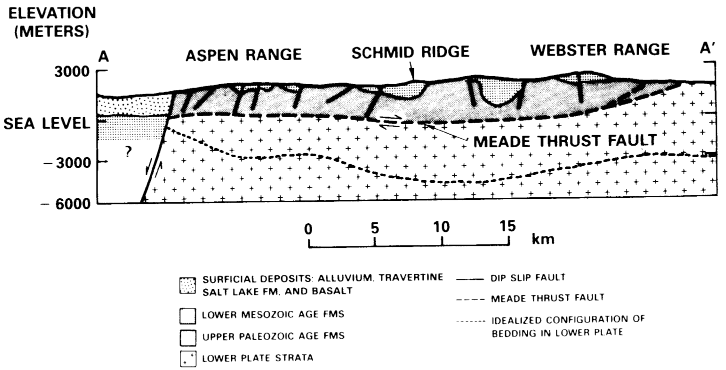

Fig 3. Generalized east-west structural section through the Meade thrust area, southeastern Idaho. The section is approximately perpendicular to the trend of the major folds in the allochthon. Modified after Mansfield (1972) and Royse, Warner, and Reese (1975). Note that minor faults not extending to the thrust fault are not shown in this figure.

eastern thrust zone is 1.5 to 4.5km wide and extends for a distance of 70km. The western portion of the allochthon is abruptly truncated by a major extension fault zone > 40km long, forming the border separating the allochthon to the east from the Blackfoot Reservoir and the Bear River Valley grabens to the west. Armstrong (1969) suggests that there is at least 910 to 1500m of stratigraphic throw along the frontal fault zone. Mabey and Oriel (1970) identified up to 1500m of Teritary sediments in the adjacent grabens.

Normal faults with throws of 200m or less (Mansfield, 1927; Cressman and Gulbrandsen, 1955) have cut the allochthonous strata in many locations. The limited stratigraphic throws suggest the faults are restricted to the allochthonous strata and do not displace lower plate rocks. Strata below the Meade thrust fault are believed to be continuous and nearly horizontal (Cressman, 1964; Royse, Warner, and Reese, 1975). Strata within the allochthon have been folded into broad and open, northerly trending anticlines and synclines, eroded into a ridge and valley system in which narrow, linear features dominate the topography of the allochthon's interior. The system extends almost the entire surface of the allochthon. Shallow seated extension faults commonly parallel the fold axes.

HYDROGEOLOGY. Springs in the Meade thrust area can be assigned to three classes: the Periphery extension group, the Periphery thrust group, and the Interior group. Periphery extension springs discharge from the extension faults forming the western periphery of the allochthon. These springs have nearly constant discharges, have water temperatures in the low thermal range and are associated with massive deposits of travertine. Periphery thrust springs discharge from splays of the Meade thrust fault along the southern and eastern periphery of the allochthon and generally have lower discharge temperatures and are not associated with travertine deposits. The Periphery groups appear to be the discharge locations of major aquifer systems which have not yet been described. The hydrostratigraphy and ground-water flow patterns in the interior of the allochthon were investigated by several researchers (eg, Ralston et al, 1977). They concluded that 1) the formations above and below the Phosphoria Formation are capable of containing major ground-water flow systems, 2) the Phosphoria Formation forms a regional barrier between these systems, and 3) ground-water flow systems in the lower Mesozoic formations are mostly of the local and intermediate types, and ground-water flow systems in the upper Paleozoic formations are presumably regional. Flow paths in the interior of the Allochthon are fracture dominated, tend to follow bedding planes, and are perpendicular to the trend of the fold axial traces. Flow paths are also perpendicular to the trend of the ridge and valley system, since topographic trends are coincident with fold trends. Interior fold-patterns are either intrabasin or interbasin. Intrabasin systems occur along the flanks of ridges where the strata are folded so that they form the upper and lower flanks of the ridge. Interbasin systems develop where the folded strata are continuous under a ridge and form a hydraulic conduit to the opposite ridge flank or adjacent valley.

Many valley floors in the interior of the allochthon are underlain by upper Paleozoic formations which receive significant amounts of recharge waters from snow melt and stream flows. Spring discharges from these formations usually do not occur in the interior of the allochthon. The Periphery springs are the suspected discharge locations of the system. The relationships between extension and thrust fault structures and the flow patterns of these suspected regional aquifers are uncertain, and the occurrence of ground-water circulation across the sole of the Meade thrust fault is also unknown.

GEOTHERMAL STUDY. A geothermal survey was conducted by Mitchell (1976). He found that most discharge temperatures of springs and wells in the western portion of the study area are in the low thermal range (10 to 40°C). He concluded that the thermal waters are probably shallowly circulating meteoric waters moving along normal faults. These waters may have the potential for small-scale domestic and commercial applications.

DATA COLLECTION

The periphery of the Meade thrust allochthon is outlined by approximately 40 springs and the interior of the block contains > 100 points of discharge. A survey of the Periphery springs led to the selection of four from both the Periphery extension and the Periphery thrust groups for detailed isotopic and geochemical analysis. Also selected was a spring from the Interior group and a flowing artesian well from an adjacent thrust block.

The flowing artesian well at Corral Creek (1)[1] was selected because its discharge temperature is considerably greater than those found in the Meade thrust allochthon and yet it has many geologic similarities with springs in the Periphery extension group. The Corral Creek system is actively depositing travertine and is associated with a tear fault. Corral Creek could provide additional insight into circulation patterns in the Meade thrust allochthon.

Sampling sites from the Periphery extension and Periphery thrust groups were selected to represent the springs in the groups and for their spacing along the periphery faults. Periphery extension springs are indicated in table 1. Except for Chubb (5), these springs are associated with massive deposits of travertine. Of the Periphery thrust group, Auburn Fish Hatchery (1) is the northernmost spring. Only one sample was taken from the Interior group because recession characteristics of these springs demonstrated recent recharge. The spring at Knudsen Ranch (10) was sampled to confirm this conclusion since it discharges from a flow system which is well understood. The Knudsen Ranch system circulates to ca 750 to 1000m below land surface and has a travel distance of 4 to 5km.

The discharge temperature, pH, carbonate, and bicarbonate content of the waters were determined in the field. Samples taken for later major ion analysis were passed through 0.45μ filters and stabilized with concentrated nitric acid. Previous analyses showed only trace concentrations of NO_3 in the spring waters of this area. Separate 100ml samples were taken in paraffin sealed glass bottles for deuterium and ^{18}O analysis. ^{14}C samples were collected using standard IAEA (1981) procedures. Sodium-carbonate-free sodium hydroxide was used to adjust the pH of the sample to above 11.5 and reagent grade barium chloride was used to precipitate the barium carbonate. Exposure of the treated sample to atmospheric CO_2 was minimized, and particulate carbonate was excluded from the sample by filtration when appropriate. Table 1 shows the results of the physical, chemical,[2] and isotopic[3] analyses.

---

[1] Numbers in parentheses indicate sample numbers in table 1.

[2] Chemical analyses were made at the University of Idaho.

[3] Isotopic analyses were made at the Laboratory of Isotope Geochemistry, University of Arizona.

DISCUSSION

Regardless of their ionic strength and discharge temperatures, the waters from all three spring groups fall within a calcium bicarbonate geochemical facies. The chemical similarity of these waters is further emphasized by the ^{18}O and deuterium data obtained. Figure 4 shows that all these data fall near the continental meteoric water line (Craig, 1961). Although quite low in both ^{18}O and deuterium, the isotopic compositions observed do not disagree with expectations for such a cold climate and high altitude. No ^{18}O shift is observed as it would be if the waters had exchanged at high temperature with the oxygen of aquifer materials while maintaining constant deuterium content. This would indicate that the waters have not cooled from some high temperature at depth. Rather, these data show that the waters have not been exposed to aquifer temperatures above ca 80°C for any appreciable time. Knowledge of the maximum possible aquifer temperature, when combined with estimates of the regional geothermal gradient and the mean annual air temperature, can be used for estimating maximum ground-water circulation depths. A maximum possible circulation depth of ca 1900m below land surface was calculated by dividing the maximum possible aquifer temperature minus the mean annual air temperature by the geothermal gradient. This result is based on a geothermal gradient of 40°C km^{-1} (Mitchell, 1976) and a mean annual air temperature of 5°C.

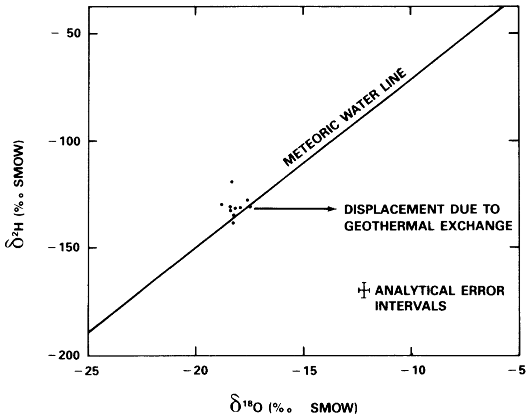

Fig 4. δ^2H vs $\delta^{18}O$ of the 10 waters reported, showing no displacement due to geothermal exchange

TABLE 1.Data summary and results

Sample number	Spring (well) name (Lat, Long)	Spring (flowing well) description	Spring group(1)
1	Corral Creek (42°52'30"N, 111°42'20"W)	Artesian flow from phosphate test holes	
2	Sinkhole (43°02'05"N, 111°41'05"W)	Flows from Wells(2) Formation along the Enoch Valley fault; associated with Wells Formation	PE
3	Formation (42°41'55"N, 111°32'30"W)	Flows up an unnamed extension fault along the front of the northern Aspen Range; associated with Wells Formation	PE
4	Henry Warm #2 (42°54'40"N, 111°32'50"W)	Discharges on the Henry travertine terrace which conceals the intersection of the Henry and Slug Valley faults	PE
5	Chubb (42°50'40"N, 111°30'20"W)	Flows from Monroe Canyon Limestone along the Chubb Springs fault	PE
6	Georgetown Canyon (42°30'15"N, 111°16'35"W)	Flows from the Wells Formation along a splay of the Meade thrust	PT
7	Auburn Fish Hatchery (42°46'20"N, 111°06'20"W)	Flows from Meade thrust and the Thaynes Formation	PT
8	Sage Valley (42°38'10"N, 111°06'45"W)	Flows from the Meade thrust and Wells (?) Formation	PT
9	Crow Creek Ranch (42°33'25"N, 111°11'00"W)	Flows from the Wells Formation at the contact with Monroe Canyon Limestone	PT
10	Knudsen Ranch (42°41'55"N, 111°21'10"W)	Flows from Dinwoody Formation after passing under Schmid Ridge via Schmid Syncline	I

(1) PE: Periphery Extension group; PT: Periphery Thrust group; I: Interior group

(2) The Thaynes and Dinwoody Formations lie above the Phosphoria Formation while the Wells and the Monroe Canyon Formations lie below it

	Major ion concentrations in meq ℓ^{-1} (mg ℓ^{-1})							
Field pH	Ca^{+2}	Mg^{+2}	Na^{+}	K^{+}	SO_4^{-2}	Cl^{-}	F^{-}	HCO_3^{-}
6.6	44.9 (900)	22.6 (275)	3.8 (89)	6.4 (250)	18.7 (900)	1.1 (39)	0.10 (1.9)	46.4 (2830)
6.8	7.3 (147)	2.4 (29)	1.2 (27)	0.10 (3)	0.7 (33)	0.8 (29)	0.03 (0.6)	8.3 (505)
6.6	9.5 (190)	2.4 (29)	trace	0.03 (1)	1.2 (57)	0.2 (6)	0.02 (0.3)	10.2 (620)
6.3	14.2 (284)	3.6 (44)	1.1 (25)	0.20 (8)	3.0 (145)	0.9 (32)	0.05 (1.0)	14.3 (870)
7.5	3.0 (61)	1.6 (20)	1.0 (24)	0.05 (2)	1.3 (61)	0.7 (26)	0.02 (0.3)	3.0 (240)
7.4	3.1 (63)	1.2 (15)	trace	0.01 (0.5)	1.4 (69)	trace	0.01 (0.1)	3.2 (195)
7.5	3.9 (58)	1.7 (21)	0.3 (6)	0.03 (1)	0.3 (16)	0.1 (2)	0.01 (0.1)	3.8 (232)
7.5	3.2 (64)	1.7 (21)	0.3 (6)	trace	0.8 (38)	0.2 (7)	0.02 (0.4)	3.8 (232)
7.4	2.9 (59)	1.2 (14)	0.1 (2)	0.01 (0.5)	0.5 (22)	0.1 (2)	0.01 (0.1)	3.7 (226)
7.5	3.1 (63)	1.2 (15)	0.3 (8)	0.05 (2)	0.4 (17)	0.1 (5)	trace	3.9 (238)

TABLE 1.(cont)

Sample number	Spring (well) name	Discharge ℓs^{-1}	Temperature (°C)	Specific conductance (μmho cm^{-1})	log P_{CO_2} (atm)	SI_c(3)
1	Corral Creek	5	40	n/a	-0.2	17.90
2	Sinkhole	290	19	n/a	-0.2	1.13
3	Formation	490	11	920	-0.9	0.82
4	Henry Warm #2	55	20	1410	-0.6	1.31
5	Chubb	45	12	545	-2.2	1.04
6	Georgetown Canyon	410	7	n/a	-2.2	0.57
7	Auburn Fish Hatchery	140	9	440	-2.3	0.97
8	Sage Valley	245	12	460	-2.2	1.04
9	Crow Creek Ranch	160	7	360	-2.2	0.67
10	Knudsen Ranch	100	12	360	-2.2	1.13

(3)Saturation index of calcite (IAP/K_{eq}) at the measured temperature

$\delta^{2}H$ (vs SMOW ‰)(4)	$\delta^{18}O$ (vs SMOW ‰)(5)	$\delta^{13}C$ (vs PDB ‰)	$A^{14}C$ (pmc)	Estimated mean subsurface residence time (years BP)
-119	-18.4	2.2	0.80 ±0.14	$\left(36{,}500^{+4000}_{-3000}\right)^{(6)}$
-132	-18.2	-3.1	13.9 ±0.2	$12{,}500^{+2000}_{-1000}$
-139	-18.3	-1.7	12.2 ±0.1	$14{,}500^{+2000}_{-1000}$
-133	-18.4	-2.4	6.19±0.23	$20{,}500^{+5000}_{-2000}$
-136	-18.3	-9.0	44.1 ±0.6	1900±500
-131	-18.0	-9.6	59.87±0.63	Recent
-131	-18.5	-10.2	52.7 ±0.9	Recent
-130	-19.0	-10.0	52.7 ±0.9	450±200
-128	-17.6	-10.4	61.3 ±0.8	Recent
-131	-17.5	-11.2/ -11.3	61.7 ±0.8	Recent

(4) Analytical error interval for ^{2}H is ±3 ‰

(5) Analytical error interval for ^{18}O is ±0.2 ‰

(6) Maximum, see text

The concept, ground-water "age," is a difficult one. A volume of water issuing from a spring is the product of the admixture of many waters of diverse origins and histories. The water has no unique age. When differences between the chemical behavior of dissolved carbonates and the water have been accounted for, the ^{14}C in solution can give an idea of the integrated mean subsurface residence times of the water. Fontes and Garnier (1979) outline methods used to account for these differences. The mean subsurface residence time of a spring water is determined from the difference between the ^{14}C activity measured in the sample and the initial activity (A_o). The water derived its dissolved carbonate either from the absorption of CO_2 in the atmosphere or in the soil zone, or from the dissolution of mineral carbonates in the soil or in the aquifer. One method (Ingerson and Pearson, 1964) of estimating the fraction (F) of carbon derived from the gaseous reservoir is based on stoichiometry. Half the bicarbonate content and all the aqueous CO_2 content can be taken to be derived from that source according to the reaction

$$CO_{2(aq)} + H_2O + MeCO_3 \rightleftarrows Me^{2+} + 2HCO_3^-$$

Another method (Pearson and Hanshaw, 1970) depends on the similarity in ^{13}C and ^{14}C chemical behavior. When isotopic fractionation differences are accounted for, only the decay of ^{14}C differentiates between the behavior of these isotopes. Since ^{13}C must reflect all changes in ^{14}C content from recharge to sampling, it may be used to reconstruct the changes in ^{14}C activity due to all mechanisms except decay. These two methods estimate A_o using independent sets of variables to calculate F. If both approaches are valid, the equations for F may be set equal to each other and be solved for the variable known with least certainty. The carbonic acid (a), bicarbonate (b) and ^{13}C contents (δ_m) of the sample are measured. The $\delta^{13}C$ of the mineral reservoir presumably has not changed since the recharge occurred and therefore can be measured from well cuttings or outcrops. This leaves the ^{13}C of the soil gas at the time of recharge (δ_g) to be estimated by the relationship

$$\delta_g = \frac{a + b}{a + 1/2b} (\delta_m - \delta_c) + \delta_c$$

Calcium carbonate mineral samples at the springs at Sinkhole, Chubb and Sage Valley had δ_c values of 4.0, 2.6, and 3.3‰ respectively. These values, having a relatively small spread of 1.4‰, provided the data base for δ_c in δ_g and A_o calculations. The δ_g values estimated for Chubb Springs, the Periphery thrust springs sampled and Knudsen Ranch fall in the range of -19 to -24‰, which is consistent with the temperate forest environment of the area. The estimates of A_o obtained by the two methods converged at these values, suggesting the mean subsurface residence times of these springs as quite short. Chubb and Sage Valley Springs were calculated at 1900±500 and 450±200 years, respectively, while the other springs could be reconciled only with a modern gaseous carbon reservoir, possibly containing some anthropogenic ^{14}C from the bomb test era.

Similar convergence of modeled A_o values did not occur at realistic values of δg for the remaining four springs because of the remarkably high ^{13}C contents measured. These values suggest the evolution of a light gaseous component leaving isotopically heavy residual bicarbonate in solution. This is consistent with the evolution of $CO_{2(g)}$ at these springs, driven by the precipitation of travertine or with the evolution of methane. The values are consistent with observations made in other waters from carbonate terrains. Corral Creek and the remaining Periphery extension springs show high discharge temperatures and are near saturation or are supersaturated in calcite. Although some of the other spring waters are also near calcite saturation, they are cooler, have appreciably lower bicarbonate concentrations, and do not precipitate travertine. The initial ^{14}C activities of these four springs were modeled with only the stoichiometric approach modified to account for fractionation. The Periphery extension springs showed mean ground-water residence times of $12{,}500\pm^{2000}_{1000}$ to $20{,}500\pm^{5000}_{2000}$ years, while Corral Creek showed a value of $36{,}500\pm^{4000}_{3000}$ years. This last result can only be interpreted as very old water, since assigning a numerical age to water with measured ^{14}C activity of 0.80±0.14 pmc is very uncertain due to potential contamination and to the extreme sensitivity of the radioactive decay equation at this activity range. The evolution of $CO_{2(g)}$ from these waters will cause an increase in ^{14}C as well as in ^{13}C. This can be on the order of 2 pmc, which would correspond to an underestimate of residence times on the order of 3000 years. This is reflected in the error intervals assigned in the table. Another potential source of error is the possible introduction of ^{14}C-free bicarbonate into solution from the thermal decomposition of mineral carbonates. The low maximum water temperatures indicated by the $^{2}H/^{18}O$ data suggest that this has not occurred in these waters, although the possibility of this mechanism cannot be ruled out.

PROPOSED FLOW MODEL

The geologic, chemical, and isotopic data collected during this investigation may be used to help define the nature of ground-water flow patterns in the Meade thrust allochthon. A preliminary three-tier ground-water flow model is proposed. Possible flow patterns are illustrated in figure 5.

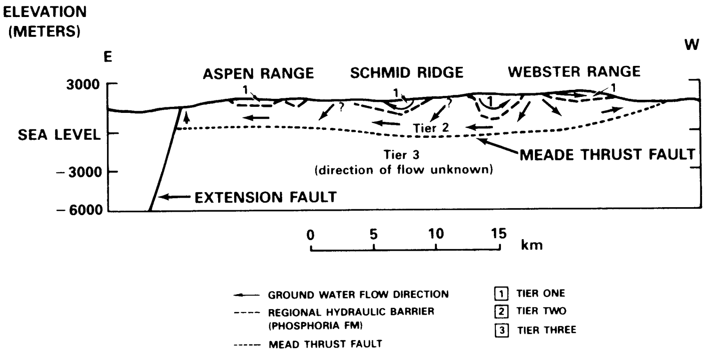

Fig 5. Postulated three-tier ground-water flow model in the Meade thrust area

1) The very short residence times of ground-water flow systems which are contained in the formations above the hydraulic boundary created by the Phosphoria Formation have been confirmed by ^{14}C methods. Such residence times are consistent with the shallow, intra- and inter-basin flow systems in the interior of the allochthon. These systems constitute the first tier.

2) Short mean residence times were determined for ground-water flow systems which discharge from Periphery thrust springs. These springs occur at the base of the Webster Range and appear to be recharged in the higher elevations of the range. Most of those systems constitute the eastern lobe of the second tier. The northernmost springs of this group are part of the first tier.

3) Long mean residence times were determined for ground-water flow systems discharging from major exterior faults which truncate the western periphery of the allochthon. These hot, carbonate-laden waters appear to be contained in the formations below the hydraulic barrier created by the Phosphoria Formation, and constitute the western lobe of the second tier. An apparent ground-water divide separates those lobes. The appreciably different ground-water residence times in the lobes result from the much greater distance from the recharge area in the western lobe (see Fig 5).

4) A maximum circulation depth of ca 1900m below land surface is suggested by the ^{18}O data and the regional geothermal gradient. Thus, circulation of ground water in the second tier probably is restricted to the allochthonous strata. Possible circulation in the lower plate is designated as the third tier. There is no evidence to suggest that water from the third tier is contributing to circulation in the overlying tiers.

ACKNOWLEDGMENTS

This research was funded primarily by grants from the Idaho Mining and Mineral Resources Research Institute. The authors would like to express their thanks to Jean-Charles Fontes of the Laboratoire d'Hydrologie et de Géochimie Isotopique, Université de Paris-Sud, for his critical review and suggestions.

REFERENCES

Armstrong, FC, 1969, Geologic map of the Soda Springs quadrangle, southeastern Idaho: US Geol Survey Misc Geol Inv Map I-557.

Craig, H, 1961, Isotopic variations in meteoric waters: Science, v 133, p 1702-1703.

Cressman, ER, 1964, Geology of the Georgetown Canyon-Snowdrift Mountain area, southeastern Idaho: US Geol Survey Bull 1153, 105 p.

Cressman, ER and Gulbrandsen, RA, 1955, Geology of the Dry Valley quadrangle, Idaho: US Geol Survey Bull 1015-I, 18 p.

Fontes, JC and Garnier, JM, 1979, Determination of initial ^{14}C activity of the total dissolved carbon: A review of the existing models and a new approach: Water Resources Research, v 15, no. 2, p 399-413.

IAEA, 1981, Sampling of water for ^{14}C analysis, Isotope Hydrology Lab, Vienna, IAEA.

Ingerson, E and Pearson, FJ, Jr, 1964, Estimation of age and rate of motion in ground-water by the carbon-14 method, in recent research in the fields of hydrosphere, atmosphere and nuclear geochemistry: Tokyo, Maruzen, p 263-283.

Mabey, DR and Oriel, SS, 1970, Gravity and magnetic anomalies in the Soda Springs region, southeastern Idaho: US Geol Survey Prof Paper 646-E, 15 p.

Mansfield, GR, 1927, Geography, geology, and mineral resources of part of southeastern Idaho, with description of carboniferous and Triassic fossils, by GH Girty: US Geol Survey Prof Paper 152, 453 p.

Mitchell, JC, 1976, Geothermal investigations in Idaho, Pt 6, Geochemistry and geologic setting of the thermal and mineral waters of the Blackfoot Reservoir area, Caribou County, Idaho: Idaho Dept Water Resources, Water Info Bull No. 30, 47 p.

Pearson, FJ, Jr and Hanshaw, BB, 1970, Sources of dissolved carbonate species in ground water and their effects on carbon-14 dating, in Isotope Hydrology: Vienna, IAEA, p 271-285.

Ralston, DR, Omj, M, Robinette, MJ, and Edwards, TK, 1977, Solutions of water resource problems associated with open-pit mining in the phosphate area of southeastern Idaho: Completion rept, Ground water study contract no. 50-897, US Dept Agric, Forest Service, 125 p.

Royse, F, Jr, Warner, MA, and Reese, DC, 1975, Thrust belt structural geometry and related stratigraphic problems Wyoming-Idaho-Northern Utah, in Bolyard, DW, ed, Deep drilling frontiers of the central Rocky Mountains: Denver, Colorado, Rocky Mountain Assoc Geol, p 41-54.

III. ^{14}C APPLICATIONS

[Radiocarbon, Vol 25, No. 2, 1983 P 375-379]

RADIOCARBON PROFILES OF ROCKY ISLET, XI-SHA ISLANDS: EVIDENCE OF RECENT CRUSTAL MOVEMENTS IN THE SOUTH CHINA SEA

CHEN YEE-CHEIN and JIAO WEN-QIANG

Radiocarbon Dating Laboratory, Institute of Geology
National Bureau of Seismology, Beijing, China

The Xi-Sha Islands comprise 35 coral reefs, cays, and islets lying to the northwest of the South China Sea. Since Miocene time, > 1200m of bioherms developed on slowly subsiding granite-gneiss bed rock. These sediments provide evidence for sea-level changes and crustal movements in the South China Sea.

GEOLOGIC SETTING

According to an echo sounding survey, the Xi-Sha Islands consist of eight coral reefs scattered regularly around a northeast to northwest trend line. This suggests that the growth of these reefs is tied to the regional tectonic trend and relates to the evolution of the South China Sea.

Rocky Islet and Yong-Zing Islet lie on the same reef flat in the Xuan-Dei Islands to the north of the Xi-Sha Islands. The distance between both islets is only ca 1000m, but the geomorphology of both islets are quite different. Rocky Islet consists of cemented bioclastic limestone and its maximum elevation is 15m, the highest of the Xi-Sha Islands. Rocky Islet is surrounded with cliffs except in the southeast. An unconformity boundary exists in the strata at 8 to 10m elevation. The Yong-Xing Islet is a sandy cay with vegetation, consisting of uncemented coral-shell sands 20 to 22m thick. At the center of the islet the elevation is only +3 to +5m. These factors suggest that an active fault existed between both islets under the reef flat. Due to the vertical movements of this fault, Rocky Islet was uplifted and emerged, as illustrated in figure 1.

RADIOCARBON AGE DETERMINATIONS

Thirty samples obtained from three profiles of Rocky Islet have been ^{14}C dated, using the ^{14}C half-life of 5568 years. The first results were rather surprising because the ^{14}C age of the profiles were reversed, ie, the lower strata were younger than the upper strata (fig 2). Such an anachronism can be explained by the depositional process, as illustrated in figure 3.

The bioclastic limestone on the Rocky Islet seems to be lithified under air and has been dissolved and leached by rain

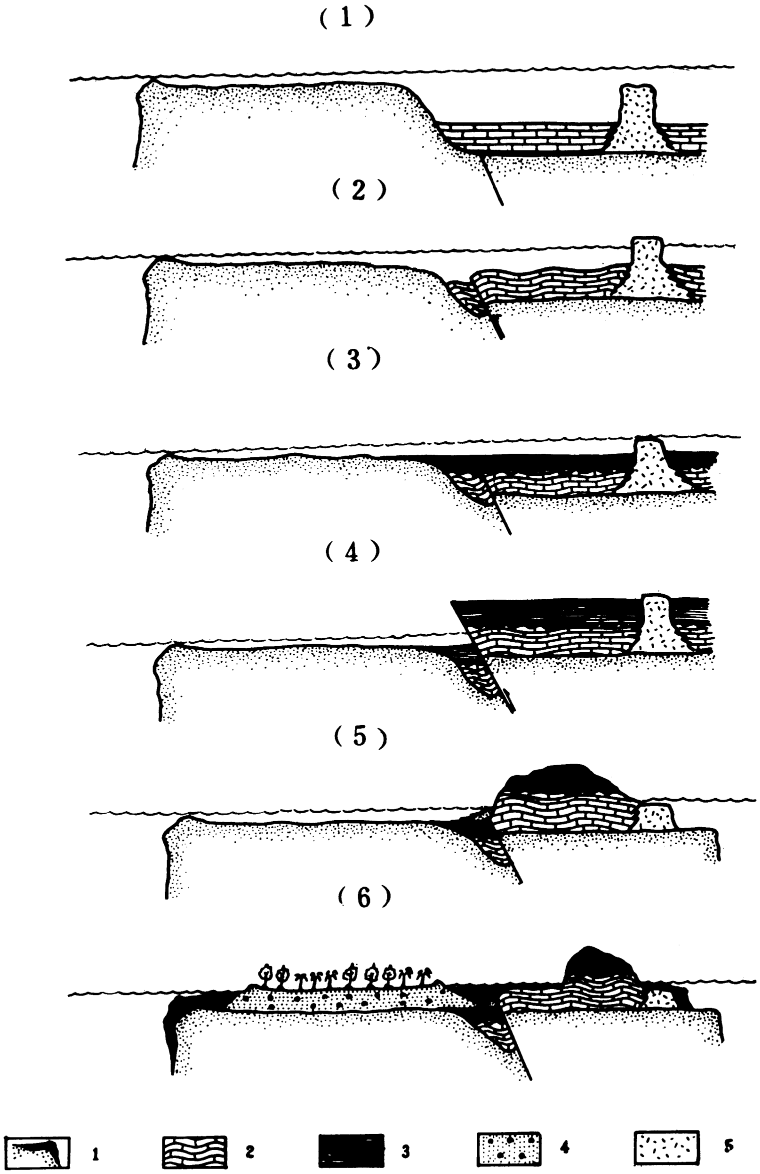

Fig 1. Stages of development of Rocky and Yong-Xing Islets. Key: 1) reef limestone and modern reef flat; 2) lower bioclastic limestone; 3) upper bioclastic limestone; 4) coral-shell sand; 5) reef patch

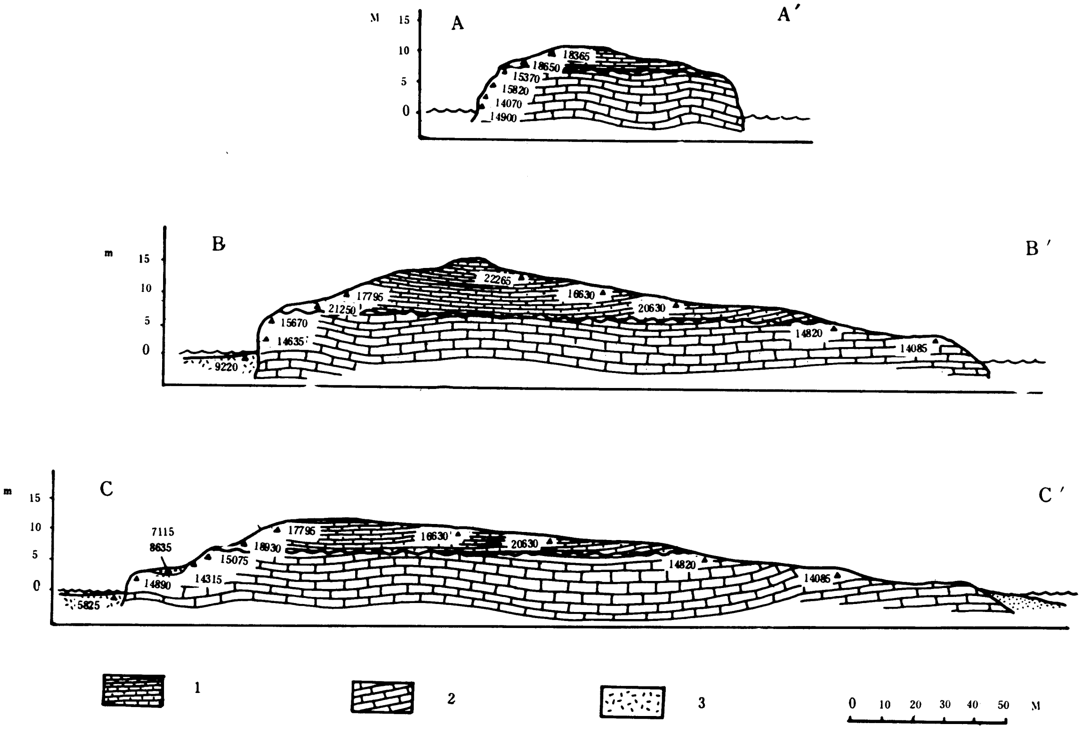

Fig 2. ^{14}C profiles of Rocky Islet.
Key: 1) upper bioclastic limestone;
2) lower bioclastic limestone;
3) coral conglomerate and reef limestone

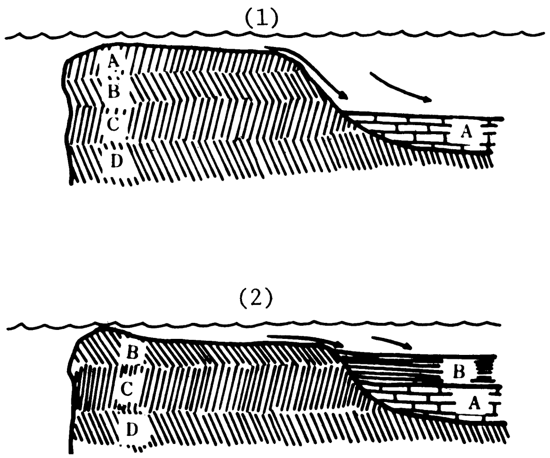

Fig 3. Deposition in a lagoon showing the formation of an anachronistic profile

water. Based on the proportion of cements within the samples, we assume that the maximum proportion of contamination by modern carbon was possibly up to 20%. Thus, we must add 7000 years to the ^{14}C ages for 16,000-year-old samples. Thus, the corrected ages of the lower strata should be 21,000-23,000 yr BP. If the upper strata were deposited 2000 yr after the former, then the ages of the upper strata should be 19,000- 21,000 yr BP.

ESTIMATE OF UPLIFT RATES

In order to estimate the uplift rates, we must establish the position of sea level during the deposition of sediments. From the echo-sounding data, two submarine terraces were recognized at depths of 20 to 25m and 50 to 60m. We deduce that both submarine terraces were probably formed during a time when glacially-lowered sea level transformed these atolls into temporary high islands. We believe that the submarine terraces of 20 to 25m were formed during the Würm glaciation, ie, the level of the sea, while depositing bioclastic limestone, was 20m below the present level. If the depth of the lagoon where bioclastic limestone was deposited is assumed to be 10m, the range of uplift of Rocky Islet would be 45m and the mean uplift rate, ca 2.25m/1000 yr.

DEVELOPMENT STAGES

Stages of development on Rocky Islet and Youn-Xing Islet are illustrated in figure 1. Because the atolls that had developed were destroyed by submarine volcanoes and faulting during the Pleistocene, the ring feature of the atoll seems to have disappeared in the Xuan-Dei and Eastern Islands although it remained in the other islands. From AD 1605 to 1969, five earthquakes approaching magnitude six occurred along the littoral extent of South China. We conclude that recent crustal movements in this region have been rapid since the late Pleistocene.

REFERENCES

Chappell, J and Polach, HA, 1976, Holocene sea-level changes and coral-reef growth at Huon Peninsula, Papua New Guinea: Geol Soc America Bull v 87, p 235-240.

Curray, JR, 1970, Late Quaternary sea-level studies in Micronesia; CARMARSEL expedition: Geol Soc America Bull, v 81, p 1865-1880.

Easton, WH and Olson, EA, 1976, Radiocarbon profile of Hanauma reef, Oahu, Hawaii: Geol Soc America Bull v 87, p 711-719.

Polach, HA et al, 1978, Radiocarbon ages from the northern Great Barrier Reef: Royal Soc [London] Philos Trans, v A 291, p 139-158.

Tracey, JI et al, 1974, Quaternary history of Eniwetok and Bikini atolls, Marshall Islands: Coral reef symposium, 2nd, Proc, v 2, p 537-550.

[Radiocarbon, Vol 25, No. 2, 1983, P 381-391]

MID-WISCONSINAN RADIOCARBON DATES FROM MASTODON- AND MAMMOTH-BEARING SPRINGS, OZARK HIGHLAND, MISSOURI

C V HAYNES*, MINZE STUIVER**, HERBERT HAAS†,
J E KING‡, F B KING‡, and J J SAUNDERS‡

From 1966 to 1979, the University of Missouri, the University of Arizona, and the Illinois State Museum conducted extensive interdisciplinary investigations of Late Pleistocene peat deposits associated with springs, some extinct, in the Pomme de Terre River Valley of the Ozark Highland, Missouri (fig 1). Most of the sites are now beneath the waters of the Harry S Truman reservoir. Archaeologic investigations in the area produced a remarkably long sequence of cultural change and development during the Holocene but produced no evidence of human presence in the area prior to 11,000 years ago despite diligent excavation of favorable bone-bearing deposits.

The chronosequence (fig 2) determined by detailed lithostratigraphic and geomorphic studies in conjunction with ^{14}C dating, consists of 7 alluvial terrace deposits of which 4 contain buried lenses of bone-, plant-, and pollen-bearing peat associated with ancient springs (Haynes, 1976; in press; Brakenridge, 1981). The Holocene alluvium consists of the Pippins formation of late prehistoric to historic age and the Rodgers formation containing evidence of as many as six cut and fill cycles. The earliest deposition (R_1) contains Paleo Indian artifacts and is dated to as early as 10,500 BP in Rodgers Rock Shelter which has yielded the most complete archaeologic record in the region (McMillan, 1976a). The next older alluvium is the Boney Spring formation with a date of 13,000 BP at the top, the 13,500-year-old Boney Spring fauna below this (Saunders, 1977), and an organic deposit near the base > 27,000 BP.

The Koch formation contains the Koch spring site where, in 1840, A C Koch recovered one of the best-preserved mastodon skeletons known (McMillan, 1976a). The assembled skeleton now resides in the British Museum of Natural History. The peat lens that contained the bones is between 30,000 and > 32,000 years old, based upon ^{14}C dating of Koch Spring, as discussed below. The Trolinger formation contains three spring sites, all of which have buried peat lenses and complex stratigraphy

---

*University of Arizona, Tucson, Arizona 85721
**University of Washington, Seattle, Washington 98195
†Southern Methodist University, Dallas, Texas 75222
‡Illinois State Museum, Springfield, Illinois 62706

ranging in age from 32,000 to > 57,000 years old. The springs originated by water erupting through several meters of fine-grained floodplain sediments overlying aquifers composed of basal alluvial gravels (Haynes, in press). Loci of the springs appear to be controlled by topographic highs on top of the gravels and/or by fault-controlled feeders.

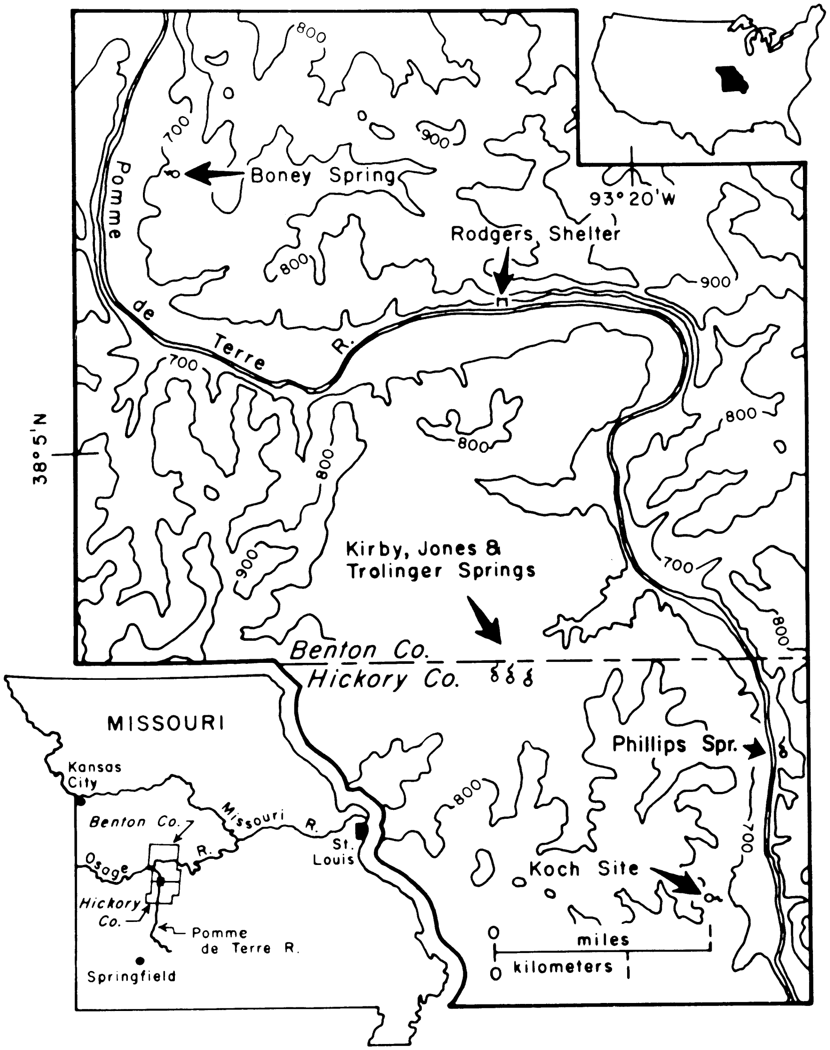

Fig 1. Spring locations, lower Pomme de Terre River, Benton and Hickory counties, Missouri

Hydrostatic pressure causing initial eruption seems to have been due to increased recharge associated with the more mesic parts of the late Pleistocene climatic cycles. Fossil pollen and plant macrofossils indicate that all of the peat lenses formed during the more xeric parts of the cycles when spring discharge was low. ^{14}C dating of the peat deposits or wood contained therein provides a discontinuous time calibration for the alluvial deposits. There appears to be general correlation between the peat deposits and the late Pleistocene interstadials.

TROLINGER SPRING. Previous studies at Trolinger Spring (Wood, 1976; King and Lindsay, 1976) revealed a bone-bearing peat lens overlying white, well-sorted quartz feeder sand, overlain by gray to brown alluvial silty clay, probably of the Boney Spring formation. The peat was subdivided into older (d_3) and younger (e) parts on the basis of sharp but discontinuous contacts within it (Haynes, 1976). ^{14}C dates within both parts ranged from 14,450 ± 500 BP (Gx-1318) to 34,300 ± 1200 BP (A-1080) but were not stratigraphically consistent. This made interpretations of the pollen and faunal data somewhat equivocal (Mehringer et al, 1968; King and Lindsay, 1976; King, 1973). Another potential problem might be churning of the peat by mastodons and other large animals entrapped in the spring as well as by a farm tractor that some local residents claimed had become stuck in the spring bog. Further, humic acids extracted from two peat samples yielded apparent ages much younger than the peat residue fractions, thus raising the question of adequate pretreatment before ^{14}C analysis.

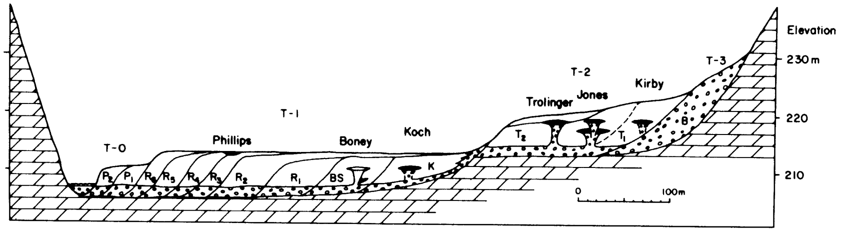

Fig 2. Generalized geologic cross section of alluvial terraces of the Pomme de Terre River valley showing the stratigraphic relationship of the spring sites with peat deposits (black lenses) to the terraces (T-0, T-1, T-2, and T-3). Geologic formations are Pippin (P), Rodgers (R), Boney Spring (BS), Koch (K), Trolinger (T), and Breshears (B).

Renewed excavations in 1978 and 1979 provided a new opportunity to perform ^{14}C dating with microstratigraphic control (fig 3). A third subdivision (d_3b) was recognized in the peat as well as what appear to be fragments of older peat incorporated as irregular masses in and below its basal part. Samples, carefully collected to obtain representative portions of each subunit, were rigorously pretreated by repeated digestion with hot HCl solution followed by NaOH extraction of humic acids and thorough washing with distilled water. Complete absence of humic acids is indicated when the base extractions become essentially colorless. This required as many as five cycles for some samples, resulting in smaller samples than desired by the Southern Methodist University Radiocarbon Laboratory. The standard deviations are, therefore, larger than desired, but adequate.

The five ^{14}C dates are all between 32,000 and 39,000 years old (table 1), indicating that all of the previous ^{14}C dates on Trolinger peat may have been too young. The five mean values are essentially in reverse stratigraphic order. They fall, however, into two distinct groups (fig 4): one between 32,270 ± 920 BP (SMU-931) and 32,950 ± 1040 BP (SMU-932), the other between 38,020 ± 2850 BP (SMU-935) and 38,880 ± 3750 BP (SMU-934) with an intermediate value of 38,200 ± 1680 BP (SMU-933). The two groups do not overlap at 1 σ, suggesting that the stratigraphic contact between them represents a significant hiatus. The sloping contact suggests that units e and d_3b were deposited after unit d_3a but the ^{14}C dates indicate that the reverse is true. Haynes (1976) suggested that the peaty organic matter around the eye of a cauldron type spring might be expected to accumulate inward as the discharge declined. It is possible that this happened at Trolinger Spring but more samples will have to be dated to substantiate it. Fortunately, more undated samples exist. If this turns out to be the case, the sloping contacts within the peat may be microfaults caused by disturbance and/or compaction rather than depositional contacts.

The presence of 22,000-year-old mastodon bones at the base of the peat (d_3) indicates the probability of some mixing. These are experimental dates on bone collagen and apatite, but they are probably correct (Hassan, ms). They support the suggestion (Haynes, 1976) that, in late Wisconsinan time, one or more mastodons, while seeking water, sank through a peat mat overlying the edge of a pool of water that formed the eye of the spring.

In addition to the peat at Trolinger Spring, we also collected fragments of wood that were encountered during excavation of the outer conduit gravels surrounding the feeder sand (fig. 3). These were possibly swept up during the initial period of spring eruption from the basal gravel and organic layer known to underlie the Breshears Valley in the area of Trolinger, Jones, and Kirby springs (Haynes, in press). ^{14}C analysis of one of these wood fragments (4 Mo 79, oak) in the University of Washington's subterranean counter after rigorous pretreatment at the University of Arizona produced a minimum age of > 55,000 BP (QL-1428) (table 1). This date is presumably associated with the grassland or savanna fauna from the conduit gravels including bear (Ursus), mammoth, horses (Equus, 2 species), extant deer (Odocoileus), and bison (Bison) (Saunders, 1981). A cool interstadial period, dominated by pine and herbs, is indicated by the fossil pollen from the peat at Trolinger Spring (King, 1973; King and Lindsay, 1976; Mehringer, King, and Lindsay, 1970). This is also consistent with the associated fauna of mastodon (Mammut), extinct deer (Sangamona), and woodland muskox (Symbos) (King and Lindsay, 1976; Saunders, 1977; 1981).

KOCH SPRING. Our previous investigations at Koch's original 1840 excavations demonstrated that the mastodon remains came from a buried peat lens (b_2) that dated 31,880 ± 1340 BP (Tx-1412) and 30,880 ± 1320 BP (Tx-1455) (Haynes, 1976). Concern about possibly incomplete humic-acid-removal from these samples prompted us to re-expose the peat lens at Koch Spring in 1978 to recollect large volume samples for analysis by the high-precision counting system at the University of Washington. Bulk samples of the upper and lower halves of the brown peat were collected. The peat contained abundant wood and

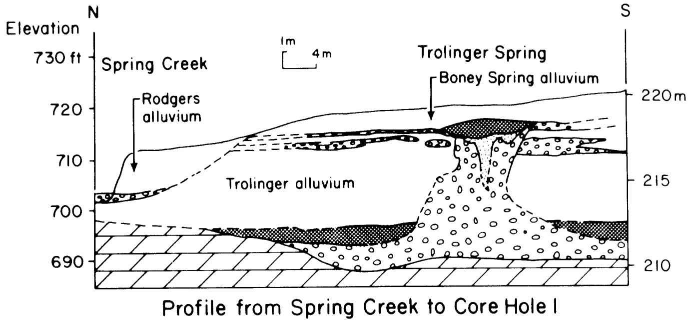

Fig 3. Geologic cross section (length 63m) of Trolinger Spring showing stratigraphic relationship of peat lens (dark stippling), feeder sand (light stippling), and conduit gravel (irregular circles) to alluvium. Lower organic ("peat") layer is an ancient slough.

plant fragments concentrated by screen washing and flotation set up by Illinois State Museum archaeologists at nearby Philips Spring (Kay, 1980). At the University of Arizona these concentrations were given the same pretreatment as described for the Trolinger samples. The stratigraphically consistent results of 30,530 ± 200 BP (QL-1427) over 31,090 ± 150 BP (QL-1429) for these samples (fig 4 and table 1) confirmed the previous dates for the peat lens and presumably, for the Koch mastodon in the British Museum. The lack of apparent mixing of the Koch peat in contrast to the Trolinger peat is perhaps due to the greater distance of the sampling sites from the central area or eye where the maximum concentration of bones and presumably disturbance occurred.

JONES SPRING. Excavations at Jones Spring from 1973-1977 revealed two superimposed lenses of bone-bearing peat (fig 5). The stratigraphy and the mixed and abraded faunal remains and fossil pollen indicate that the upper peat was in part derived from the lower lens when the latter was penetrated and disrupted by conduit sands and gravels during a renewed eruption of spring activity (Haynes, in press). The first generation of ^{14}C dates indicated an age of > 40,000 years for the lower lens and > 35,000 years for the upper lens. A younger age for the upper peat can probably be precluded despite its mixed nature because it is stratigraphically the same age as or older than the peat at Trolinger Spring, < 150m to the northeast.

Table 1. ^{14}C dates from the Pomme de Terre valley

Sample No.	^{14}C date; yrs BP (lab no)	Unit	Spring Location
	<u>Koch Formation</u>		
47 Mo 78	30,530±200 (QL-1427)	Brown peat b_2	Koch
48 Mo 78	31,090±150 (QL-1429)	" " "	"
	<u>Trolinger Formation</u>		
5 Mo 78	32,270±920 (SMU-931)	Black peat d_3a	Trolinger
6 Mo 78	32,950±1040 (SMU-932)	" " "	"
9 Mo 78	38,020±2850 (SMU-935)	" " e	"
8 Mo 78	38,880±3750 (SMU-934)	" " e	"
7 Mo 78	38,200±1680 (SMU-933)	" " d_3b	"
11 JEK 76	48,900±900 (QL-962)	Gray clay	Jones
4 Mo 79	> 55,000 (QL-1428)	Conduit gravel	Trolinger
45 Mo 78	> 57,000 (QL-1426)	Brown peat	Kirby

The basal portion (c_1) of the lower peat lens at Jones Spring is pebbly and contains different ecologic indicators than the overlying portion (c_2). A small log of red cedar (Juniperus virginiana) at the basal contact of the lower peat dated 48,900 ± 900 BP (QL-962) (fig 4 and table 1) and applies

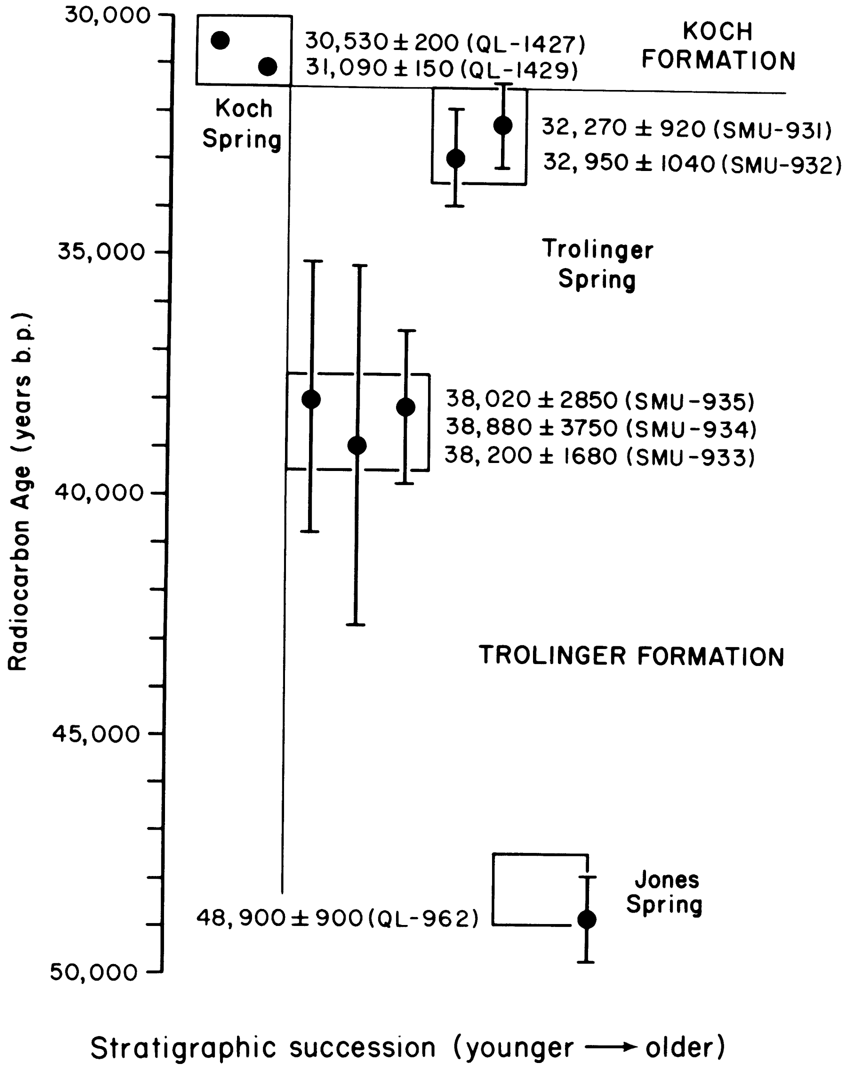

Fig 4. ^{14}C age determinations versus stratigraphic succession for the Koch and Trolinger formations

to a warm c_1 fauna including mastodon, grazers such as mammoth (*Mammuthus*), camel (*Camelops*), and giant bison (*Bison latifrons*), as well as alligator (*Alligator*) and large turtles. The associated plant macrofossils reflect warmer interstadial vegetation. A change to cooler interstadial conditions in the overlying c_2 is indicated by a fauna containing a smaller bison (*B antiquus*) and woodland muskox (*Symbos* or *Bootherium*). The upper peat lens at Jones is too mixed to provide a reliable faunal assemblage or a reproducible pollen record.

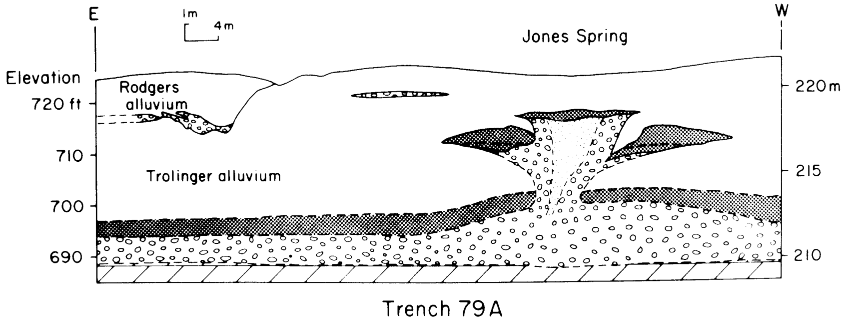

Fig 5. Geologic cross section (length 81m) of Jones Spring showing stratigraphic relationship of peat lenses (dark stippling), feeder sand (light stippling), and conduit gravel (irregular circles) to alluvium. Lower organic ("peat") layer is an ancient slough.

KIRBY SPRING. The oldest ^{14}C date from this region is > 57,000 BP (QL-1426) (table 1) for a brown peat layer at Kirby Spring occurring 300m west of Jones Spring. The date agrees with previous dates in excess of 25,000 (Gx-2720), 27,000 (Gx-2719, and 37,000 BP (Tx-2719) (Haynes, 1976). Fossil bones including those of probosicideans are thought to have been removed from here in the late 1800's, but the character of the fauna is unknown (McMillan, 1976b). Fossil pollen, on the other hand, provided a useful record of herbaceous pollen dominance and more xeric conditions than those of today. We believe this deposit is interglacial, probably Sangamon, or stage 5e of the sea floor oxygen isotope record (Shackleton and Opdyke, 1973).

CONCLUSIONS

Correlations of the Pomme de Terre paleoecologic record with the glacial chronologies of the Great Lakes areas is frustrated by the lack of ecologic indicators and ^{14}C dates from the deposits occurring between the peat lenses. Only the alluvium at Boney Spring proved adequate in this regard and revealed an obvious correlation of alluvial clays (C_4 and D, Haynes, 1976) with the Woodfordian Substage of the Wisconsinan Stage of Frye, Willman, and Glass (1968). The underlying peat (C_3) is a logical correlative of the Farmdalian Substage, based on both age (22,000 - 27,000 BP) and interstadial pollen record.

If we consider the previous ^{14}C dates from the Trolinger peat too young, then the Koch peat provides the next younger dates of 30,000 to 31,000 BP for an interstadial interval. This could be equivalent to the last part of the Plum Point interstade of Dreimanis and Goldthwait (1973). Possibly, the entire interval, 22,000 BP - 31,500 BP, in the Ozark Highland is one of interstadial climatic conditions and thus coincides with the Plum Point of the eastern Great Lakes region. The pollen record from Boney Spring indicates gradual rise in the spruce maximum ca 20,000 BP whereas pollen profiles from both Trolinger and Koch peats show a very abrupt spruce appearance at their tops. A possible explanation is that the spruce pollen in the latter two deposits is intrusive into the top of the peats and actually reflects the vegetation at the beginning of deposition of the overlying clays. The accessibility of Trolinger peat to animals 22,000 years ago is demonstrated by the age of the ^{14}C-dated mastodon bones. The overlying clay (f_2) is considered to be backwater deposits of the Boney Spring formation carried into the abandoned meander of the Breshears Valley by flood waters from the Pomme de Terre River.

The next oldest ^{14}C dates are from 32,000 to 39,000 BP from the Trolinger Spring peat with a possible intermediate hiatus. Again, the pollen and fauna indicate cool interstadial conditions. This chronology leaves little room for significant cold stadials between 22,000 and 39,000 years ago, and leads to the possibility that this period represents the intermediate climate indicated by the early part of Stage 2 and the later part of Stage 3 of the sea floor oxygen isotope record (Shackleton and Opdyke, 1973). Episodes of renewed spring discharge indicated within the microstratigraphy of the spring sediments, such as subfeeders, may represent the smaller climatic fluctuations in the oxygen isotope curve.

The initial eruption of Jones and Trolinger Springs may have occurred during Stage 4 when a cold episode almost as severe as that of Stage 2 occurred. If this correlation is correct, the basal fauna and pollen record from the lower peat at Jones Springs would fall somehwere in Stage 5 after 5e, which, as already suggested, is the likely correlative of the pollen record from Kirby Spring and possibly represents a Sangamonian flora.

ACKNOWLEDGMENTS

This work was supported by the National Science Foundation and the U S Army Corps of Engineers, Kansas City, Missouri. The cooperation of the people of the lower Pomme de Terre Vally is appreciated.

REFERENCES

Brakenridge, G R, 1981, Late Quaternary floodplain sedimentation along the Pomme de Terre River, Southern Missouri: Quaternary Research, v 15, p 62-76.

Dreimanis, A and Goldthwait, R P, 1973, Wisconsin glaciation in the Huron, Erie, and Ontario Lobes, in Black, R F, Goldthwait, R P, and Willman, H B, eds, The Wisconsinan Stage: Geol Soc America Mem 136, p 71-105.

Frye, J C, Willman, H B, and Glass, H D, 1968, Correlation of Midwestern loesses with the glacial succession, in Schultz, C B and Frye, J C, Loess, eds, Loess and related eolian deposits of the world, 7th Proc: INQUA cong, Lincoln, Univ Nebraska Press, v 12, p 3-21.

Hassan, A A, (ms), 1976, Geochemical and mineralogical studies on bone material and their implications for radiocarbon dating: PhD dissert, Southern Methodist Univ, Univ Micro films, Ann Arbor, Michigan.

Haynes, C V, 1976, Late Quaternary geology of the lower Pomme de Terre Valley, in Wood, W R and McMillan, R B, eds, Prehistoric man and his environments: a case study in the Ozark Highland: New York, Academic Press, p 47-61.

-- in press, Geochronology of mastodon-bearing springs and the lower Pomme de Terre River, Missouri: Geol Soc America spec paper.

Kay, M, 1980, Stratigraphic studies at Rodgers Shelter, in Kay, M, ed, Holocene adaptations within the Lower Pomme de Terre River Valley, Missouri: Rep U S Army Crops Engineers

Kansas City Dist, p 81-106.

King, J E, 1973, Late Pleistocene palynology and biogeography of the Western Missouri Ozarks: Ecol Mon, v 43, p 539-565.

King, J E and Lindsay, E H, 1976, Late Quaternary biotic records from spring deposits in western Missouri, in Wood, W R, and McMillan, R B, eds, Prehistoric man and his environments: a case study in the Ozark Highland: New York, Academic Press, p 65-78.

McMillan, R B, 1976a, Rodgers Shelter: a record of cultural and environmental changes, in Wood, W R and McMillan, R B, eds, Prehistoric man and his environment: a case study in the Ozark Highland: New York, Academic Press, p 111-122.

-- 1976b, Man and mastodon: a review of Koch's 1840 Pomme de Terre expeditions, in Wood, W R and McMillan, R B, eds, Prehistoric man and his environments: a case study in the Ozark Highland, New York, Academic Press, p 82-96.

Mehringer, P J, Jr, Schweger, C E, Wood, W R, and McMillan, R B, 1968, Late-Pleistocene boreal forest in the western Ozark Highlands?: Ecology, v 49, p 567-568.

Mehringer, P J, Jr, King, J E, and Lindsay, E H, 1970, A record of Wisconsin-age vegetation and fauna from the Ozarks of western Missouri, in Dart, W, Jr, and Jones, J K, Jr, eds, Pleistocene and recent environments of the central Great Plains, Lawrence, University of Kansas Press, p 173-183.

Saunders, J J, 1977, Late Pleistocene vertebrates of the Western Ozark Highland, Missouri: Illinois State Mus Repts Inv no. 33, 118 p.

-- 1981, Mitigation of the adverse effects upon the local paleontological resources of the Harry S Truman Dam and Reservoir, Osage River Basin, Missouri: Rept US Army, Corps Engineers, Kansas City Dist.

Shackleton, N J and Opdyke, N D, 1973, Oxygen isotope and paleomagnetic stratigraphy of equatorial Pacific Core V28-238: Oxygen isotope temperatures and ice volumes on a 10^5 year and 10^6 year scale: Quaternary Research, v 3, p 39-55.

Wood, W R, 1976, Archaeological investigations at the Pomme de Terre Springs, in Wood, W R and McMillan, R B, eds, Prehistoric man and his environments: a case study in the Ozark Highland, New York, Academic Press, p 97-107.

[Radiocarbon, Vol 25, No. 2, 1983, P 393-394]

RADIOCARBON DATING IN THE ARCTIC REGION

INGRID U OLSSON

Institute of Physics, Uppsala University
Box 530, S-751 21 Uppsala, Sweden

The Landnám of Iceland is usually dated too early by the ^{14}C dating method, at least to judge from the tradition according to the *Landnámabók*. Various sources of error are considered. One, the use of driftwood, can be excluded in many cases, since birch is often selected for dating purposes. Second, the settlers may have brought wood with them. A third obvious source of uncertainty is the age of a tree before felling. It is difficult to explain the seemingly too early results by secular global variations of ^{14}C content. A regional low level of ^{14}C may result from volcanic activity or the small size of the land areas in the Arctic region.

The release of old CO_2 by volcanoes during eruptions is proven, as is a continuous local supply emitted by hot springs. The activity of the atmosphere was measured by means of numerous samples, the majority from Iceland — mostly collected in 1978. Some plant samples were obtained in 1980 in connection with the YMER-80 Expedition.

The measurements so far completed indicate that the decrease of the activity from 1978 to 1980 is equal to about 4% of the standard. The excess activity over Iceland is close to, although probably slightly less than that over Sweden, whereas that over Svalbard seems to be some 2% lower. The reduced activity earlier observed on Svalbard (Olsson and Karlén, 1965; Stenberg and Olsson, 1967; Olsson and Klasson, 1970) from 1962 to 1964 was attributed to diffusion from lower latitudes where the mixture occurs between the stratosphere and troposphere.

Early studies of tree-ring dated wood do not include geographic variations. The results presented by Robinson (1982) from samples from Hawaii and sites close to the coast of California, however, reveal an increase of ^{14}C with elevation. Robinson's findings and our present results, together with some earlier measurements, suggest that the putative island effect (Olsson, 1979), as a permanent phenomenon, must be further considered.

Measurements of ^{14}C activity of deep water from the Arctic Ocean, collected in 1980, indicate a deficiency, compared with the standard, of less than 8%.

ACKNOWLEDGMENTS

This work was supported by grants from the Swedish Natural Science Research Council. The author would like to thank all persons involved in the work, from the collection of the samples to the measurements of the activities.

REFERENCES

Olsson, IU, 1979, The radiocarbon contents of various reservoirs, in Berger, Rainer and Suess, HE, eds, Radiocarbon dating, Internatl radiocarbon Conf, 9th, Proc: Berkeley, Univ California Press, p 613-618.

Olsson, IU and Karlén, Ingvar, 1965, Uppsala radiocarbon measurements VI: Radiocarbon, v 7, p 331-335.

Olsson, IU and Klasson, Martin, 1970, Uppsala radiocarbon measurements X: Radiocarbon, v 12, no. 1, p 281-284.

Robinson, SW, 1982, Vertical variations of Δ^{14}C in the contemporary troposhpere (abs): Abstracts, Internatl radiocarbon Conf, 11th, June 20-26, 1982, Seattle, Washington, p 70.

Stenberg, Allan and Olsson, IU, 1967, Uppsala radiocarbon measurements VIII: Radiocarbon, v 9, p 471-476.

[Radiocarbon, Vol 25, No. 2, 1983 P 395-408]

STUDIES ON HOLOCENE GEOCHRONOLOGY OF THE COASTAL REGION OF SOUTHERN FUJIAN, CHINA

CHEN CHENGHUI

Third Institute of Oceanography
National Bureau of Oceanography, China

HUANG BAOLIN and WANG MINGLIANG

Institute of Geochemistry, Academia Sinica, China

ABSTRACT. Our studies on ^{14}C chronology and palynology of Holocene sediments in southern Fujian along the western coast of the Taiwan Straits show that the natural environment has undergone three stages of development during the Holocene. From Early Holocene (ca 10,000-8000 yr ago) to Middle Holocene (8000-2500 yr ago) and then to Late Holocene (2500 yr ago), sediments varied from land-sea transitional to marine and then to terrigenous; vegetation altered from mixed forest to evergreen broad-leaf forest and then steppe; climate fluctuated from temperate to hot and then to warm. The sea-level maximum in the post-glacial period occurred at 5000-6000 yr ago, at 5 to 10m elevation. During the subsequent regression, two stable stages of sea-level dated at >3000 and ca 2000 yr ago. The climatic drying and eolian sand deposit began at 700 yr ago. The results agree with our previous studies in southern Liaoning.

INTRODUCTION

The history of climatic fluctuation, land-sea change, and sedimentary development since Late Glaciation can be explained as well as geologic events chronologized and stratigraphic subdivisions and correlations made by ^{14}C dating and palynologic analysis of sediments. These are important aspects of Quaternary and especially of Holocene research. Some significant results of Holocene geochronologic studies on the coastal region of China have been obtained. A Holocene geologic time scale has been established for southern Liaoning (Chen, Lu, and Shen, 1978). The marine strata and shell banks along the western coast of the Pohai Sea (Lab Quaternary Geol, 1980; Zhao et al, 1978), as well as the continental sediments in the Yellow Sea and East China Sea (Geng, 1981) have also been chronologically studied.

Holocene sediments in the coastal region of southern Fujian are well-developed and mainly distributed on coastal and estuarine plains, in which marine, alluvial, and eolian deposits predominate. They commonly contain materials suitable for ^{14}C

dating such as shells, peat, wood, and mud, and are rich in pollen and spores all of which are advantageous for Holocene geochronologic study.

Based on a geologic survey of the adjacent area of Xiamen (Amoy) Harbor made by the Third Institute of Oceanography during 1978-79, further studies of several sedimentary profiles in the Longhai estuarine plain and Zhangpu coastal plain were made. More than a dozen ^{14}C dates were determined and palynologic associations of three profiles were analyzed. Thus, a fundamental outline of the history of Holocene environmental evolution of the coastal region of southern Fujian was tentatively drawn.

PROFILES AND ^{14}C DATES

Seven sedimentary profiles were studied (fig 1,2). ^{14}C dates were determined at The Institute of Geochemistry by the liquid-scintillation counter technique. The half-life of ^{14}C used was 5568 years and the ages given are before AD 1950. Table 1 lists the ^{14}C dates.

TABLE 1. ^{14}C dates from the coastal region of southern Fujian

Site	Sample No.	Depth (m)	Sample	^{14}C date (yr BP)
Gaobiantou, Longhai	GC-310	2.8	Shell	3150±150
Xulintou, Longhai	GC-376	1.2	Shell	3330±150
Chonglong, Longhai	GC-313	0.6	Shell	1870±100
	GC-314	1.3	Shell	2350±120
	GC-315	1.6	Shell	3800±150
Tangnei, Longhai	GC-305	0.9-1.0	Mud	2000±120
	GC-308	1.3	Peat	2450±120
	GC-307	1.45	Mud	2760±150
Xiacai, Zhangpu	GC-316	1.0-1.2	Peat	700±50
You'ao, Zhangpu	GC-318	0.5-0.6	Shell	1400±90
	GC-319	2.6-2.7	Shell	1980±100
	GC-320	2.8-3.0	Shell	2600±120
	GC-321	3.5-3.8	Shell	3100±150
Tangbian, Xiamen (Amoy)	GC-369	2.2	Mud	>35,000

THE GAOBIANTOU MARINE-ALLUVIAL PROFILE IN LONGHAI PLAIN. Longhai Plain, ca 300km^2, is an estuarine plain formed by the comprehensive action of the dynamics of the Jiulongjiang River and sea waters. The Quaternary sediments, 81m in maximum thickness, mainly belong to the Late Pleistocene and Holocene. The Upper Pleistocene series is pluvial-alluvial and consists of interbedding yellow or gray-white clay and sand-gravel, 10 to 58m thick. The Holocene series is marine-alluvial, 10 to 20m

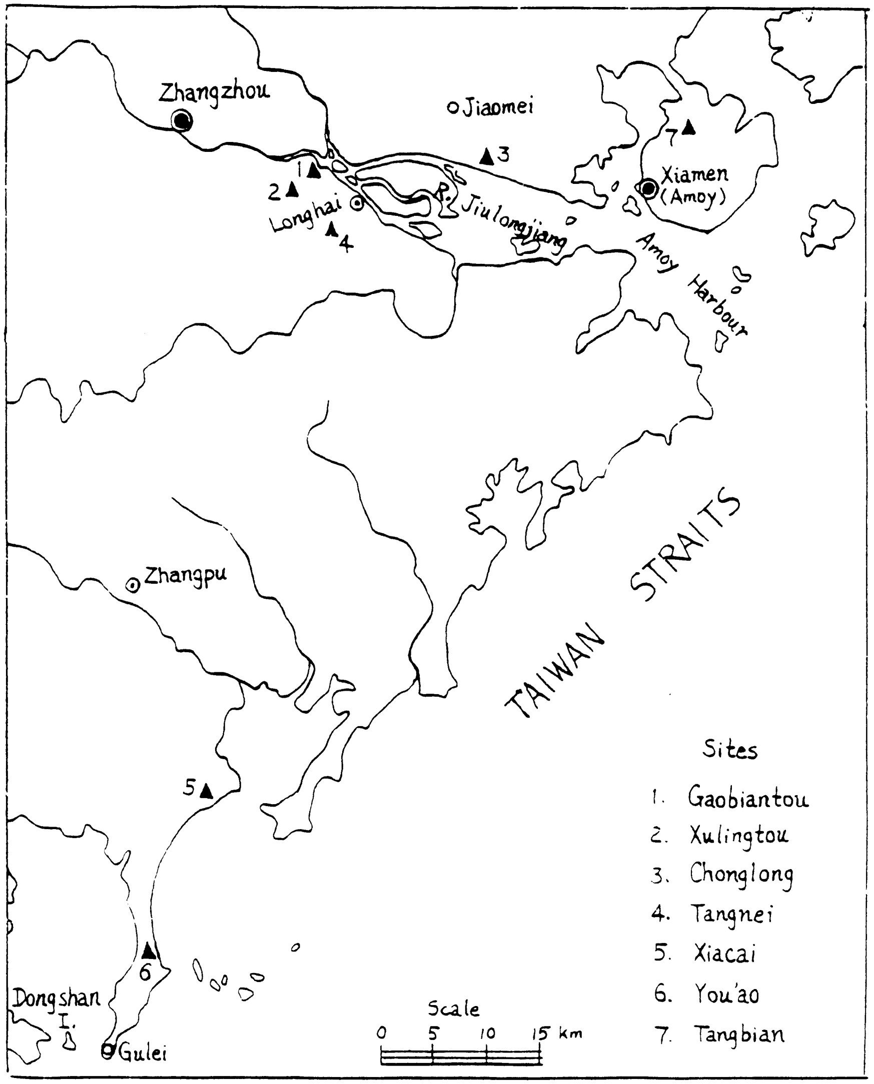

Fig 1. Sampling site for ^{14}C dating of southern Fujian

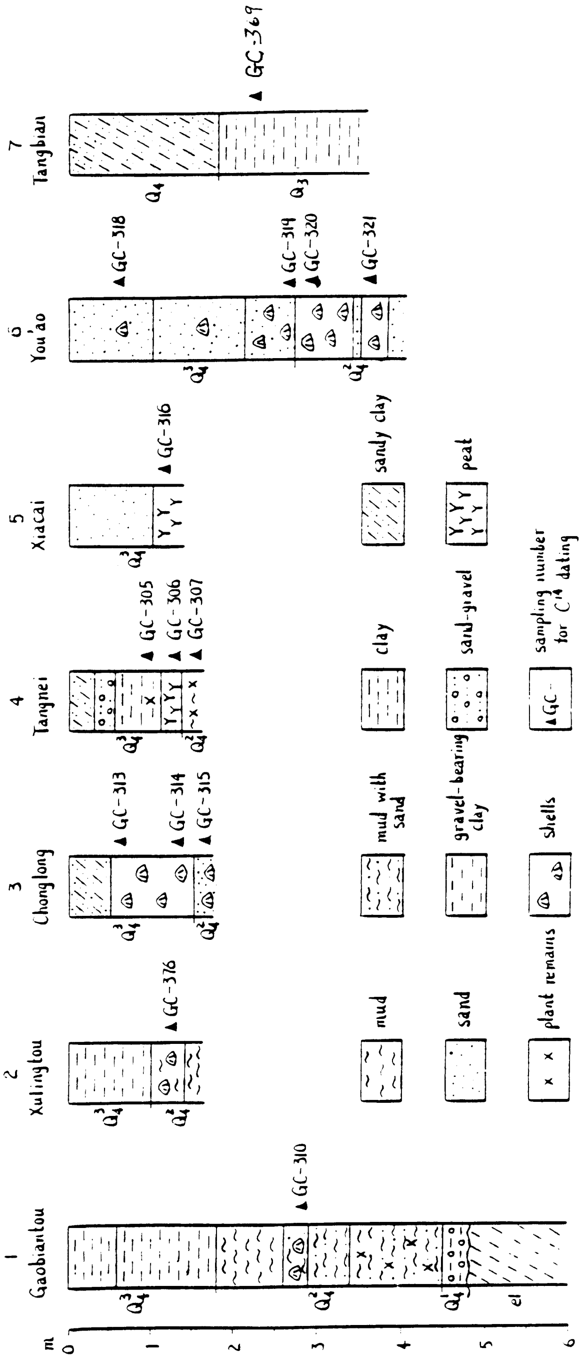

Fig 2. Diagrams of sampling profiles of southern Fujian

thick, and can be divided into three parts. The lower part is land-sea transitional deposits, consisting of gray sand with thin mud beds. The Middle part is marine, consisting of dark gray mud with many shells and plant remains, with a layer of oyster shells at 1 to 3m depth. The upper part is alluvial, consisting of yellow-gray clay.

The Gaobiantou profile is from the eastern side of Guanyin Hill in the western part of Longhai Plain. Holocene sediments, 4.8m thick, overlying the weathering crust of Upper Jurassic Changlin sandstone, from the top downwards (at +5m) are as follows: 0 to 1.8m, yellow-gray to gray clay; 1.8 to 4.5m, dark-gray mud with shells and plant remains, thin layers of fine sand, interbedded in the middle with a layer of abundant oyster shells at 2.6 to 2.9m depth dated at 3150±150 yr ago; 4.5 to 4.8m, gray gravel-bearing clay with plant remains. This profile is roughly the same as the three parts of the Holocene mentioned above, but the lower part here is thinner and shows different lithologic characteristics.

XULINTOU MARINE-ALLUVIAL PROFILE IN LONGHAI PLAIN. The profile is at the northwest side of Xulintou hillock in the western part of Longhai Plain. The sediments, from the top downwards (at ca +4m) are as follows: 0 to 2m, gray clay; 1 to 1.6m (basal), dark-gray to gray-black mud with shells, with a layer of oyster shells at 1 to 1.4m depth dated at 3330±150 yr ago.

This profile corresponds to the upper and middle parts of the Gaobiantou profile. The oyster beds of both profiles, the dates of which are quite close, corresponding to the later Middle Holocene, can be considered diagnostic of Holocene stratigraphic subdivision and correlation.

THE CHONGLONG SHELL BANK PROFILE IN LONGHAI PLAIN. This shell bank is at the northern border of Longhai Plain, 1km from the northern bank of the Jiulongjiang River to the south, >10km from the coastline to the east. It extends in a NE-SW direction, 180m long, 50 to 60m wide, ca +5m. On the southeast or seaward side, is a cliff 2 to 3m above the plain with abundant shells. On the northwest is a smooth slope consisting mainly of sandy loam without shells, 1.5m above the ancient bay surface. Sediments of the cliff profile from the top downwards are as follows: 0 to 0.5m, yellow-brown sandy loam with shell debris; 0.5 to 1.5m, semi-consolidated shell layer, dated at 1870±100 for its upper part and 2350±120 yr ago for its lower part; 1.5 to 1.8m (basal), loose shelly sand bed, with mixed shell debris and fine sand dated at 3800±150 yr ago. The shelly sand bed in the lower part of the profile may be beach deposit below the high-tide line, the formative age of which is a little earlier than the oyster bed in the plain and corresponds to the later Middle Holocene. The shell bed in the upper part is shell-bank deposit that accumulated at a constant rate around the high-tide line through wave and tide action during a period of little change in sea level and coastline, the formative age of which corresponds to an earlier stage of the Late Holocene. A sedimentary interruption between the layers represents an interval of regression.

TANGNEI PEAT PROFILE IN LONGHAI PLAIN. This profile is in the foothills of the western border of Longhai Plain. The sediments, from the top (+7m) downwards are as follows: 0 to 0.55m, gray-yellow sandy clay and yellow-brown clayey sand-gravel; 0.55 to 1.1m, gray to dark-gray muddy clay with abundant plant remains, dated at 2000±120 yr ago at its base; 1.1 to 1.35m, yellow-brown peat of low decomposition, dated at 2450±120 yr ago at its base; 1.35 to 1.5m (basal), brown-gray mud with abundant plant remains, dated at 2760±150 yr ago. The brown-gray mud below the peat is dated between the lower and middle parts of Chonglong shell bank, corresponding to the latest stage of the Middle Holocene, and belongs to the lagoonal deposit laid down during the regression process. The peat and muddy clay are products of swamping of the lagoon and are contemporary with the upper part of Chonglong shell bank, the earlier stage of the Late Holocene. The sand-gravel and sandy clay are alluvial-pluvial deposits of a rivulet and belong to the later stage of the Late Holocene.

THE XIACAI PEAT PROFILE OF THE ZHANGPU COAST. The peat beds of Zhangpu coast, commonly underlie eolian sand, with maximum thickness reaching 1.5m. The peat is gray-brown, highly decomposed, and dated at 700±50 at the top. In the vicinity, the peat bed is gradually thinned out and embedded in eolian sand. In view of its greater thickness, the peat may have accumulated from the formation of Tangnei peat 700 years ago, covering the whole earlier and middle Late Holocene. The different decomposition of the peat beds is due to the diverse overlying sediments. Tangnei peat, underlying the muddy clay, is basically sealed off which is unfavorable for peat composition. Xiacai peat, underlying the loose permeable eolian sand, is subjected to oxidation and decomposition.

THE YOU'AO BEACH ROCK PROFILE IN GULEI PENINSULA, ZHANGPU. The beach rocks of Gulei Peninsula extend in a NE-SW direction, and consist mainly of consolidated to semi-consolidated shelly sand beds. Eolian sand is also widely distributed over the peninsula, overlying the marine sediments and reaching a height of 20 to 30m. The sediments of the You'ao profile, from the top (+4m) downwards are as follows: 0 to 1m, loose gray-yellow middle to fine sand with shell debris; the surface layer is wind-blown and reworked; the shells are dated at 1400±90 yr ago;

1 to 2.1m, consolidated to semi-consolidated gray-yellow middle to coarse sand with shell debris; 2.1 to 2.7m, loose gray-yellow shelly sand, consisting of middle to fine sand and varied shells such as clam and oyster, dated at 1980±100 yr ago at its base; 2.7 to 3.4m, consolidated gray-white shell layer, dated at 2600±120 yr ago at its top; 3.4 to 3.5m, loose brown-yellow fine sand without shells; 3.5 to 3.8m, loose to semi-consolidated gray-yellow shell bed, dated at 3100±150 yr ago; from 3.8m downwards, loose fine sand without shells. The lower gray-yellow shell bed is contemporary with the oyster bed in Longhai Plain, formed in the later stage of the Middle Holocene. There is a sedimentary interruption of ca 600 years between the top of the middle gray-white shell bed and the bottom of the upper gray-yellow shelly sand, corresponding to the boundary of the Middle and Late Holocene. The upper part of the profile is contemporary with the upper part of the Chonglong shell bank, deposited in the Late Holocene.

THE TANGBIAN SEDIMENTARY PROFILE IN XIAMEN (AMOY) ISLAND. Abrasion-denudation terraces, on which alluvial laterite develops, are widely distributed along the coast of southern Fujian. The three terraces of Xiamen (Amoy) Island are 5 to 10m, 10 to 20m, and 30 to 45m in elevation. The lacustrine deposit filled in the depression on the third terrace at ca 30m elevation near Tangbian is gray-black muddy clay, dated at >35,000 yr ago. The age cannot be exactly determined as it is older than our dating limit. Since the sediments of the Middle Pleistocene are generally laterized, the lacustrine deposit may be of the Late Pleistocene and the third terrace may have been formed in the Middle Pleistocene. The overlying gray-yellow sandy clay, 1.8m thick, is a Holocene alluvial-pluvial deposit.

VEGETATION ALTERNATION AND CLIMATIC FLUCTUATION

The samples from Gaobiantou, Tangnei, and Xiacai profiles were palynologically analyzed. Six sporo-pollen zones can be distinguished (Chen, 1982) (fig 3), representing the different stages of vegetation alternation and climatic fluctuation during the Holocene correlated to the climatic periods of Scandinavia. The palynologic composition of the earliest postglacial stage, the Pre-boreal, was not found. According to the characteristics of the subsequent zone VI of the Boreal, the Pre-boreal vegetation can be interpreted to be mainly coniferous and deciduous broad leaf trees, and the climate to be rather cool.

The VI Castanopsis-Castanea zone of arboreal palynologic association found in gravel-bearing clay in the lower part of the Gaobiantou profile shows deciduous and evergreen broad-leaf mixed forest which was quite open with poor development of

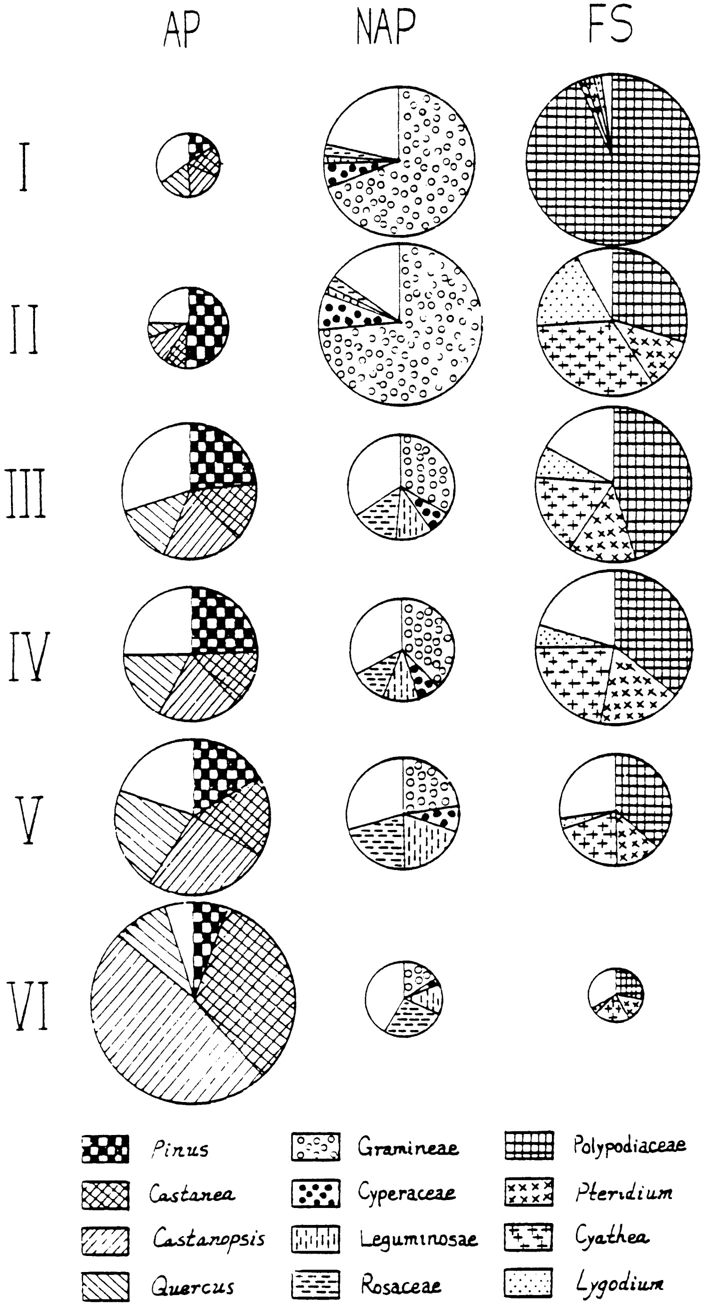

Fig 3. Schematic sporo-pollen diagram of Holocene sediments of southern Fujian

plant cover. The climate was temperate and dry, corresponding to the Boreal.

The V Castanopsis, Quercus- Polypodiaceae zone of arboreal palynologic composition found in dark-gray in the lower-middle part of the Gaobiantou profile shows evergreen broadleaf forest which flourished with abundant shrubs and herbs. The climate was wettest and hottest then, a little more than at present, corresponding to the postglacial climatic optimum, the Atlantic.

The IV Polypodiaceae, Cyathea-Pinus, Castanopsis, Quercus zone of fern-aboreal palynologic composition found in dark-gray mud with sand in the upper-middle part of Gaobiantou profile and in brown-gray mud in the lower part of Tangnei profile shows evergreen broad-leaf forest with some coniferous and deciduous broad-leaf trees. The forest and plant cover flourished less than in the preceding stage. The climate was still hot, but much drier, corresponding to the Sub-boreal.

The III Polypodiaceae- Pinus, Castanopsis zone of fern-arboreal palynologic composition in gray clay in the upper part of the Gaobiantou profile and in peat and dark-gray muddy clay in the middle part of the Tangnei profile shows coniferous and broad-leaf mixed forest. In view of the increase of the coniferous and deciduous broad-leaf components and the development of peat, the temperature was lower and the humidity higher than in the preceding stage. This indicates warm and wet climate, corresponding to the Sub-atlantic.

The II Gramineae- Cyathea, Polypodiaceae- Pinus zone of nonarboreal-fern palynologic composition found in yellow-gray clay of the uppermost part of the Gaobiantou profile and gray clay of the upper part of the Tangnei profile shows forested steppe. The expansion of newly deposited land and effects of human activities facilitated the alteration of vegetation from forest to steppe. A small number of trees, in which coniferous were more abundant than broad-leaf, were distributed on the border of or scattered on the plain, forming sparse forested steppe landscape. Herbage was mostly Gramineae, a large portion of which might have been cultivated. This implies that cultivation of the region began at this stage. The climate was the same as the preceding stage, warm and wet, with slight fluctuation in temperature and humidity, corresponding to "Scandic" and "New-Atlantic" stage (Wendland and Bryson, 1974).

The I Polypodiaceae-Gramineae zone of the fern-nonarboreal palynologic composition found in the uppermost part of Xiacai peat shows steppe-type vegetation. The trees are mainly broadleaf and scattered. The climate turned dry and warm, corresponding to the "Pacific" stage. The forest retreated, the steppe cultivated. swamps dried, and native vegetation transformed into planted crops on fields and herbs on wasteland because of the drier climate and the effects of human activities. Eolian sand prevailed along the coast. According to the ^{14}C date for the top of the Xiacai peat underlying the sand, drier climate began ca 700 yr ago, which concurs with the results of our previous research in southern Liaoning (Chen, Lu, and Shen, 1978). Arid conditions occurred as a result of both climate change and human activities.

SEA-LEVEL CHANGE AND COASTLINE DISPLACEMENT

Ancient shell banks and beach rocks line the coast and provide records on sea-level change and coastal displacement. Some research has been done on shell banks in Tianjin (Tientsin) (Lab Quaternary Geol, 1980) and southern Liaoning (Chen, Lu, and Shen, 1978) and on beach rocks in the South China Sea (Zeng, 1980). Unlike the parallel shell banks of Tianjin, there is only one aggradational shell bank in southern Fujian. As mentioned above, a sedimentary interruption occurred between the lower and upper parts of the Chonglong shell bank and the You 'ao beach rock extending >1000 and ca 600 yr, respectively. They are superimposed sediments of two stages corresponding to both the Jugezhuang-Shajingzi and Nigu-Shanggulin shell banks of Tianjin (Lab Quaternary Geol, 1980).

Holocene sea level changes are global and can be approximately correlated for various regions, although elevations may vary because of neo-tectonic and sedimentation processes. The lowest sea level in the latest stage of the Late Pleistocene is at 150 to 160m below present sea level in the East China Sea. Taiwan was then connected to Fujian. Sea level continuously rose during the Early Holocene, submerging the Taiwan Straits and part of the Jiulongjiang estuary, causing land-sea transitional sedimentation in the Lower Holocene. Transgression reached its maximum during the highest sea level dated at ca 5000-6000 yr ago. The whole Longhai Plain was submerged and a thick layer of marine mud was deposited. The first abrasion terrace, at 5 to 10m elevation, was formed along the coast. Sea level was then located at ca 5 to 10m elevation and water depth was ca 10m. Later sea level fell gradually and regression began. The location of sea level and the coastline were relatively stable 3800-3150 yr ago forming deposits of the lower part of the Chonglong shell bank and oyster bed in the plain. During another stable sea level stage, 2350-1870 yr ago, the upper part of the Chonglong shell bank was deposited. The lowered sea level and aggradation of sediments caused the Longhai Plain to emerge. Sea level has been basically stable, sedimentation in the Jiulongjiang estuary strengthening and the area of the plain expanding rapidly for 700 yr.

As for the Gulei Peninsula, the maximum transgression changed Gulei Hill into an island. During the subsequent regression two relatively stable stages of sea level dated at 3100-2600 and 1980-1400 years ago, formed a tombalo or bar connecting Gulei Hill with the continent. As the formative dates of cementing materials in the beach rock may be younger than those of the deposits themselves, the ^{14}C dates may be younger than the real ages and the beach rock considered contemporary with the shell bank in the estuarine plain.

STRATIGRAPHICAL SUBDIVISION AND SEDIMENTARY HISTORY

In China, the Holocene is divided into three periods according to palynologic composition, ^{14}C dates, and sedimentary lithofacies. On the coast of China during the Early Holocene (Q_4^1, 10,300-8000 years ago) (table 2) following the end of the Late Plestocene glaciation, the climate gradually warmed, the sea constantly rose from the low level of the Late Glaciation and sediments were generally coarse and terrigenous. The Middle Holocene (Q_4^2, 4000-2500 years ago) experienced climatic optimum and sea-level maximum, in which sediments were generally fine-grained and marine. In the Late Holocene (Q_4^3, for the last 2500 years), the climate turned mild, the sea level fell or was close to present, and sediments were mainly terrigenous.

Holocene sediments of the coastal region of southern Fujian also show the same characteristics. As mentioned above, the Holocene series of the Longhai Plain can be subdivided into three sections, corresponding to Lower, Middle, and Upper Holocene. The Lower Holocene Gaobiantou Formation is characterized by land-sea transitional deposits consisting of gray sand with a thin layer of mud or gravel-bearing clay. With the rise in sea level, the estuary of the Jiulongjiang River was gradually transgressed and the silt washed down by the river was continuously accumulated over the alluvial-pluvial beds of the Upper Pleistocene Longhai Formation.

The Middle Holocene Xulintou Formation marine sediments consist of dark-gray mud and can be further subdivided into two sections, the lower being deposited during the warmest climate, with maximum transgression and highest sea level during the Holocene. Wet, hot climate and flourishing vegetation provided the sediments with abundant plant remains such as the wood in the mud layer from Jiaomei in the northern Longhai Plain dated at 5660±95 yr ago (Zhang, Li, and Zhao, 1980). The upper part was deposited during regression. Because of the aggradation of sediments and the lowered sea level, sea water shallowed and shell deposits developed in a suitable environment such as the lower parts of the Chonglong shell bank and the You 'ao beach rock as well as the oyster layer in the plain.

The Upper Holocene Tangnei Formation is mainly terrigenous. Following the continual fall in sea level, the plain began to emerge, alluvial clay, 1 to 2m thick, accumulated, and rivulets formed in former tidal channels. Peat developed in ancient bays and lagoons such as the peat beds of Tangnei and Xiacai. The upper parts of the Chonglong shell bank and the You 'ao beach rock were also formed during this stage. According to the ages of the peat and underlying gray-brown mud in the Tangnei profile, the boundary date between the Middle and Upper Holocene is ca 2500 yr ago. As the age of the top of the Xiacai peat bed is 700 years old and it lies under eolian sand, the Upper Holocene can be subdivided into two sections: the clay, peat, and shell deposits mentioned above belong to the lower part, and the overlying eolian sand, alluvial-pluvial deposit on the border of the plain as well as the present valley and shoal deposits belong to the upper part.

CONCLUSION

Our studies on the ^{14}C chronology and palynology of Holocene sediments of the coastal region of southern Fujian indicate the following (table 2):

1) The natural environment underwent three stages of development during the postglacial; thus the Holocene can be divided into three stages: Early Holocene, ca 10,000-8000 yr ago, Middle Holocene, 8000-2500 yr ago, and Late Holocene, from 2500 yr ago.

2) The Holocene series can be divided into three parts: the Lower Holocene Gaobiantou Formation (land-sea transition), the Middle Holocene Xulintou Formation (marine), and the Upper Holocene Tangnei Formation (terrigenous).

3) From Early to Middle and then to Late Holocene, ancient vegetation changed from mixed forest to evergreen broad leaf forest and then to mixed forest and steppe; ancient climate changed from temperate to hot and then to warm. The earlier stage of the Middle Holocene, the Atlantic, had the hottest and wettest climate of the postglacial. During the later stage of the Late Holocene, the "Pacific," the climate dried and eolian sands developed.

4) The highest sea level of the postglacial period occurred at ca 6000-5000 yr ago, at 5 to 10m elevation. During the subsequent regression, two relatively stable stages of sea level occurred at >3000 and ca 2000 yr ago.

Our studies of the Middle and Late Holocene are detailed, but we lack ^{14}C dates of the Early Holocene.

ACKNOWLEDGMENTS

This research was done under the direction of Liu Dongsheng Thanks go to our colleagues at the Institute of Geochemistry, Academia Sinica and the Third Institute of Oceanography, National Bureau of Oceanography, for their support and help.

TABLE 2. Outline of Holocene geochronology of the coastal region of southern Fujian, China

Geologic age	Stratigraphy	Sediment	Palynologic Composition	Vegetation	Climate	Sea Level	Correlation			Boundary date (yr ago)
							Tiajin coastline (2)	S Liaoning stratigraphy (1)	Scandinavian climatic period (6)	
Late Holocene Q_4^3	Upper Tangnei Formation	Eolian sand, fluvial deposit	I zone FS-NAP	Steppe	Warm-dry	Basically stable	Basically stable Shell bank I	Upper Zhuanghe Formation	Pacific	700
	Lower Tangnei Formation	Alluvial clay and peat	II zone NAP-FS	Forested steppe	Mild-wet	Fall	Regression	Lower Zhuanghe Formation	Scandic New-Atlantic	1600
			III zone FS-AP	Mixed forest	Warm-wet	Stable (upper shells)	Shell bank II		Sub-atlantic	2500
Middle Holocene Q_4^2	Upper Xulintou Formation	Marine mud with sand and peat	IV zone FS-AP	Evergreen broad leaf forest	Hot-dry	Fall Stable (lower shells) Fall	Regression Shell bank III Regression	Upper Dagushan Formation	Sub-boreal	5000
	Lower Xulintou Formation	Marine mud	V zone AP	Evergreen broad leaf forest	Hot-wet	Highest (5-10m) (I marine terrace)	Huanghua transgression	Lower Dagushan Formation	Atlantic	8000
Early Holocene Q_4^1	Gaobiantou Formation	Marine-alluvial, clayey sand-gravel	VI zone AP	Deciduous evergreen broad leaf forest	Mild-dry	Rise		Pulandian Formation	Boreal	9500
					Cool				Pre-boreal	10,300
Late Pleistocene	Longhai Formation	Alluvial-pluvial			Cold	Lowest (-150-160m)			Late Glaciation	

REFERENCES

Chen, C, 1982, Sporo-pollen associations of some Holocene profiles in the coastal region of southern Fujian. Taiwan Strait, v 1, no. 1, p 45-53.

Chen, C, Lu, Y, and Shen, C, 1978, Development of natural environment in the southern part of Liaoning Province during the last 10,000 years: Sinica, v 21, no. 4, p 516-532.

Geng, X, 1981, Transgressions and regressions in East China during Late Pleistocene: Acta Oceanologia, v 3, no. 1, p 114-130.

Lab Quaternary Geol and Lab Radiocarbon, Inst Geochemistry, Acad Sinica, 1980, Holocene coastline changes on the west bank of Pohai Gulf; Quaternaria Sinica, v 5, no. 1, p 64-69.

Wendland, WM and Bryson, RA, 1974, Dating climatic episodes of the Holocene; Quaternary Research, v 4, no. 1, p 9-24.

Zeng, Z, 1980, A short review on beach rocks in China: Quaternaria Sinica, v 5, no. 1, p 14-19.

Zhang, J, Li, G, and Zhao, X, 1982, Chronological studies on the Late Quaternary stratigraphy and neotectonic movement along the coastal area of South Fujian and East Guangdong: Seismology and Geology, v 4, no. 3, p 27-36.

Zhao, S, Xia, D, et al, 1978, Marine strata and coastline on the west coast of the Pohai Gulf: Oceanologia et Limnologia, v 9, no. 1, p 15-25.

Zu, Y, Li, G, Zeng, C, and Li, B, 1979, Lowest sealevel of Late Pleistocene in the continental shelf of the East China Sea: Science Bull, v 24, no. 7, p 317-320.

[Radiocarbon, Vol 25, No. 2, 1983, P 409-416]

THE UNRELIABILITY OF ^{14}C DATES OBTAINED FROM BURIED SANDY PODZOLS

MEBUS A GEYH, GÜNTER ROESCHMANN,
Niedersächsisches Landesamt für Bodenforschung
D 3000 Hannover, Federal Republic of Germany

T A WIJMSTRA, and A A MIDDELDORP
Universiteit van Amsterdam, Hugo de Vries Laboratorium
NL 1018 BX Amsterdam, The Netherlands

ABSTRACT. A test for the reliability of ^{14}C dating of soil was made at two sites with buried, autochthonous, and in parts, allochthonous sandy podzols, dated either litho- and pedostratigraphically or palynologically. The differences between the age ranges obtained and the apparent mean residence times (AMRT) calculated from the ^{14}C content of alkaline extracts from fossil soil layers and horizons lean in organic matter exceed 10,000 years, corresponding to a maximum contamination with recent carbon of up to 50 %. The use of correction factors for the apparent mean residence times of podzols is not valid, not even for climate zones, because these values have a broad scatter for the same profile.

INTRODUCTION: EXPERIENCES GATHERED IN SOIL ^{14}C DATING

Dating of soils is of general geoscientific interest because their formation depends upon climate, vegetation, lithologic environment, and topography. However, there is general agreement (Scharpenseel and Schiffmann, 1977) that ^{14}C dating of alkaline extracts of soils only yields apparent mean residence times (Geyh, Benzler, and Roeschmann, 1971; Scharpenseel, 1971). These are lower than the corresponding true ages, which start with the beginning of humus formation in the regolith. The best agreements have been obtained with the residue remaining after successive hydrolyses with 6N HCl (Scharpenseel, 1979; Gilet-Blein, Marien, and Evin, 1980). This residue may consist mainly of biologically inert carbon (Gerasimov, 1971; 1974), assuming such carbon exists in soils at all. It should be remembered that "soil dating" is a questionable attempt to date only a small part of the total humic matter of a soil horizon and to interpret the result as representative of the whole sample.

The discrepancy between ^{14}C soil dates and true ages results from the complexity of soil genesis, which is a continuous process of accumulation and decomposition of organic substances. Penetration of rootlets, bioturbation, and percolation of soluble humic substances (ie, chelates) cause rejuvenation, and the admixture of allochthonous plant residues (Schoute et al, 1981) may cause apparent aging. As a result, the organic matter in a soil is a mixture of an unknown number of compounds (Paul et al, 1964) of unknown chemical composition, concentration, and age. Therefore, the various classical humus extracts (fulvic acid, hymatomelanic acid, brown humic acid, gray humic acid, humin, humus coal) do not show the anticipated relationship of ^{14}C ages, carbon content, mean molecular weight, and the number of peripheral functional groups. Moreover, the ^{14}C/depth distribution cannot be deciphered in terms of a paleorecord of dynamic processes in a soil due to many factors that influence carbon transport in different soil profiles. The ^{14}C/depth gradients that have been postulated as characteristic for various soil types may not be usable without finer differentiation, eg, in primarily- and secondarily-formed podzols, as well as autochthonous and allochthonous podzol horizons and layers (Scharpenseel, 1972; Matthews, 1981).

Despite the now generally accepted discrepancy between AMRT and true ages, the deviation is often greater than assumed. Scharpenseel et al, (1980) believe they can determine rather reliable time marks for humid climatic periods with ^{14}C soil dates and carry out dendrochronologic corrections (Scharpenseel and Zakosek, 1979), which are theoretically unacceptable for such complex mixtures of old constituents. Matthews (1981) seeks reliable ^{14}C gradients in soil profiles in order to correct radiometric data, goals that conflict with the present uncertainty in ^{14}C soil dating.

CASE STUDIES

INVESTIGATION SITES. To estimate maximum rejuvenation and its scattering in a soil profile, two sites were chosen at which buried, sandy podzols of differing genesis occur. These podzols were dated roughly by geologic, paleopedologic, and geomorphologic field studies or by palynologic analyses. Podzols are formed in a relatively cool and moderately humid climate and show percolation of organic substances but little or no bioturbation.

The first site is 6 km northwest of Rotenburg/Wümme (53° 7'N, 9°0'W). As in another case study by Roeschmann (1975), 3 m of niveofluviatile stratified sands of Late Pleistocene age overlie a sandy fossil podzol profile from which four separate, allochthonous, redeposited A_h-horizon layers were dated. The originally autochthonous B horizon is disturbed by glacial cryoturbation. The soil profiles are several meters above the groundwater table (fig 1). A pine forest grows at the surface. Living roots penetrate all soil layers. Pollen grains are not preserved, but the ^{14}C ages were high enough to yield good estimates of maximum contamination. Depths of the sampling points below surface, relative carbon contents of the alkaline extract (mg/g of sample), and total quantity of carbon (g) used for dating are compiled in table 1.

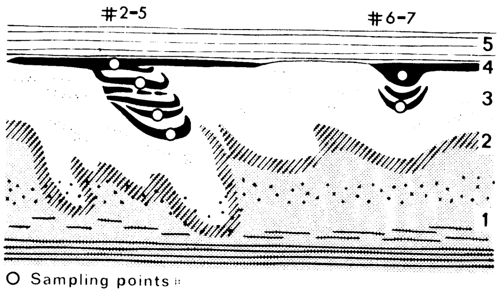

Fig 1. Fossil podzol from glacio-fluviatile sands of the Saale Glacial beneath niveo-fluviatile sands of the Weichsel Glacial in the Rotenburg sand pit in Lower Saxony. 1 = laminated, and in the upper parts, cryoturbated sands with gravel layers from the Saale Glacial. 2 = secondarily cryoturbated podzol B horizon. 3 = secondarily cryoturbated, bleached podzol horizon, in the upper part reworked by solifluction. 4 = reworked humus material. 5 = laminated niveo-fluviatile Weichselian sands.

Table 1. Results of the profile "Rotenburg"

No.	Profile	Depth	C content		$\delta^{13}C$	Hv	Conventional ^{14}C age yr BP	q*	
		m	mg/g	g	‰			%	ppm
1	IV 4	3.80	0.14	0.21	-26.8	8913	19,640 ± 1330	17.3	24
2	VI 10	2.80	0.91	1.54	-27.6	8901	27,415 ± 325	6.6	60
3	VI 10	2.90	0.86	1.69	-27.6	8903	41,200 ± 3160	1.2	10
4	VI 10	3.00	0.71	1.07	-24.2	8905	25,350 ± 450	8.5	60
5	VI 10	3.10	0.41	0.62	-26.0	8907	25,950 ± 980	7.9	32
6	VI 11	2.80	1.56	1.85	-27.5	8909	24,350 ± 395	9.7	151
7	VI 11	2.90	1.28	1.35	-26.8	8911	33,940 ± 1460	2.9	37
8	IX	7.80	1.68	2.70	-28.4	8915	39,500 ± 2150	1.5	25

* - contamination according to Eq 1

Along the eastern bank of the Dinkel river (52°23'N, 7° 0'W), samples were taken from several podzol horizons and peaty layers in four stratified profiles (fig 2). Roots from the forest were present in all of the samples. From previous pollen analyses (van der Hammen and Wijmstra, 1971) we know that soils were formed during late glacial and postglacial periods. The deepest, partly redeposited peaty layers and podzol horizons are probably seasonally inundated when the groundwater table rises in the springtime. The podzol horizons, classified according to Kuntze et al, (1981), depths below the surface, lithostratigraphically (S) or palynologically (P) estimated ages, relative carbon content of the alkaline extracts (‰), as well as the total quantity of carbon (g) used for dating are compiled in table 2.

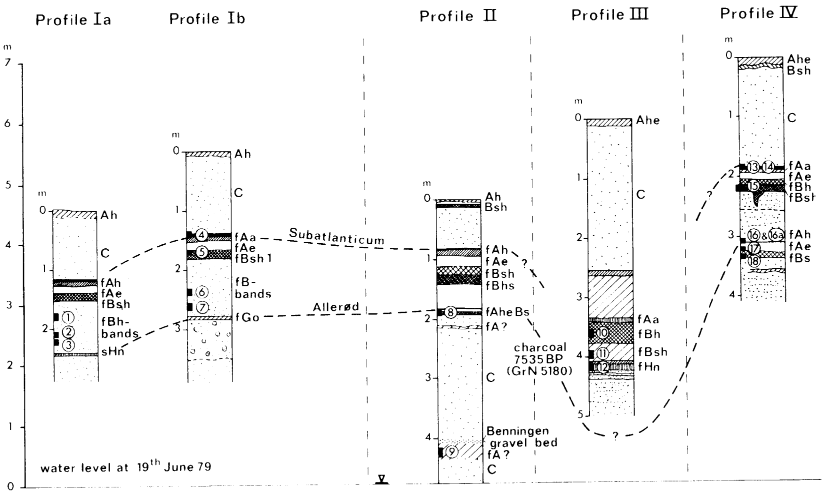

Fig 2. Five exposures with fossil soils in Weichselian sands at the Dinkel Valley near Denekamp. The Netherlands. Sampling sites are shown as circles with reference numbers. The symbols of the soil horizons follow the scheme given by Kuntze et al (1981).

Table 2. Field data and analysis results from Dinkel profiles

No.	Pro-file	Pedol horizon	Depth m	Stratigraphic and palynologic age estimates yr BP		C content alkaline extract		Hv	$o^{13}C$ PDB ‰	Conventional ^{14}C age yr BP	Contamination recent carbon	
						‰	g				%	ppm
1	I a	fBtBs	1.80	S-LD*	11500-10200	0.63	0.89	9783	-27.6	6325± 135	24-28	165-194
2	I a	fBt	2.10	S-LD*	11500-10200	0.36	0.39	9782	-28.1	6970± 175	19-24	70- 86
3	I a	fBht	2.25	S-LD*	11500-10200	0.42	0.63	9781	-28.4	7740± 225	14-19	60- 79
4	I b	fAa	1.30	P-Sa*	2500- 0	2.76	2.47	9787	-29.7	2145± 45	-	-
5	I b	fBsh1	1.60	P-Pb*	10200- 8900	1.63	1.48	9786	-28.8	3935± 110	42-46	687-752
6	I b	fBtBs	2.30	S-LD*	11500-10200	0.17	0.36	9784	-29.1	5230± 250	33-37	57- 63
7	I b	fBt	2.55	S-LD*	11500-10200	0.10	0.14	9785	-27.5	6145± 400	26-30	25- 29
8	II	AheBs	1.80	P-Al*	12000-11500	0.67	0.91	9789	-28.3	4125± 570	47-48	20
9	II	fA(?)	4.20	S-UP*	28000-13000	0.75	1.20	9788	-26.5	7580± 95	24-37	179-278
10	III	fBh	3.50	P-At*	7800- 5000	1.07	2.01	9791	-29.0	3060± 100	32-49	338-525
11	III	fBhs2	3.80	P-Bo*	8900- 7800	0.22	0.33	9792	-28.0	4245± 145	34-39	76- 87
12	III	peat	4.00	P-Pb*	10200- 8900	4.16	0.48	9790	-29.3	7850± 255	7-13	287-553
13	IV	charc	1.70	P-Sa*	2500- 0	220	2.74	9799	-24.9	8585± 110	?	?
14	IV	peat	1.70	P-Sa*	2500- 0	18	2.26	9800	-29.8	9205± 85	?	?
15	IV	fBsh	7.00	P-At*	7800- 5000	0.30	0.47	9797	-28.8	4225± 200	12-34	35-102
16	IV	fAh	2.95	S-Al*	12000-11500	0.13	0.25	9798	-27.2	5280± 510	37-38	47- 48
16a	IV	pom	2.95	S-Al*	12000-11500	0.57	0.16	11262	-25.8	1855± 235	73	415-418
17	IV	fAe	3.10	S-Al*	12000-11500	0.05	0.09	9795	-27.2	4800±1560	41-42	22
18	IV	fBs	3.20	S-Al*	12000-11500	0.03	0.08	9794	-	6320±1125	28-30	23- 24

* UP - upper pleniglacial; Al - Allerød; LD - Late Dryas; Pb - Preboreal; Bo - Boreal; At - Atlantic; Sa - Subatlantic; S - stratigraphic age; P - palynologic age; pom - NaOH-insolulable organic matter

SOIL SAMPLE PREPARATION FOR ^{14}C DATING

Recommended fractions for routine dating of soils are humic acids and humins extracted with hot sodium hydroxide solution (SCHARPENSEEL, 1971; 1972; 1979; Schoute et al, 1981) from organic complexes bound in clay if successive hydrolyses with 6N HCl cannot be done due to a small carbon content (Gilet-Blein, Marien, and Evin, 1980). In our laboratory macroscopic, light-colored rootlets, as well as particulate organic matter were removed by course-sieving and flotation. Then, humic acids were dissolved in 2 % NaOH during 20 min of boiling and reprecipitated with concentrated HCl. The alkaline extract was washed until neutral, dried, burned, and transformed into acetylene, which serves as a counting gas in low-level proportional counters. With this treatment the bulk of extremely young organic substances (fulvic and hymatomelanic acids) is removed. The remaining humic acids are only a very small part of the total organic matter in the soil (table 2).

RESULTS

ROTENBURG PROFILES. Table 1 lists results of the isotope analyses and the estimated maximum contamination. Only alkaline extracts were analyzed since none of the samples contained sufficient NaOH-insoluble organic matter for dating. The conventional ^{14}C ages exceed 20,000 yr BP (table 1). ^{14}C results for stratigraphically co-eval samples, eg, #2 and #6, as well as #3 and #7, do not agree within the range of their standard deviations. Moreover, there is no trend in the ^{14}C ages with depth. The pedologic explanation is that the organic matter of the humic layers probably stems from redeposited A_h horizons of adjacent soils. However, the soils might also have been contaminated during the Holocene and the actual soil ages may exceed the maximum conventional ^{14}C age of 41,000 yr BP obtained. In order to estimate the maximum degree of carbon contamination we assumed that the alkaline extract of soil with a ^{14}C content A_a is contaminated with q % organic matter of a ^{14}C content A_c. Then, the measured ^{14}C content A_m of this sample is given by

$$A_m = q / 100 * (A_c - A_a) + A_a \qquad (1)$$

The ^{14}C content A can be calculated from the conventional ^{14}C age T by

$$A = 100 * e^{-T/8033} \qquad (2)$$

In the Rotenburg case, the ^{14}C content of the admixed Holocene organic matter is assumed to be 50 %. Then, the maximum degree of contamination q amounts to ≤17 % according to Eq 1 or ≤125 μg of ca 5000-yr-old carbon per gram sample (ppm). Contamination of this amount could have easily occurred and it is obvious that the use of "age correction factors" (Scharpenseel, 1971) for at least such sites would be incorrect.

DINKEL PROFILES. The results of the pollen and isotope analyses, as well as of their interpretation as a measure of contamination, are compiled in table 2. The relative carbon content of the alkaline extracts of the samples (‰), and the carbon quantities (g) used for dating are in the same range as those from the Rotenburg profiles. However, the conventional ^{14}C ages are much lower ($\leq$ 9200 yr BP) although litho-, pedostratigraphic, and palynologic age estimates range up to 28,000 yr BP. Thus, contamination with very young carbon must have occurred (A_c is assumed to be 100 %).

For samples containing little organic matter, the relative and absolute contamination with recent carbon ranges from 15 - 55 % (Eq 1) or 20 to 750 ppm, respectively. Rapid decrease in contamination and carbon content with depth is obvious. This is due to blocking of the fine pores in the fossil soil by organic matter during podzolization, thus reducing carbon transport with increasing depth. Rejuvenation of the organic matter may be even so great that samples older than 20,000 yr BP appear younger than 10,000 yr BP.

Three exceptional results must be interpreted separately: the NaOH-insoluble fraction of sample #16a contained sufficient carbon for dating. The low age and the relatively large carbon content are explained by the presence of rootlets, the ^{14}C dates of peat and charcoal samples #13 and #14 from profile IV are very much greater then the pollen ages. Geomorphologically, the samples may be redeposited organic sediments. The results emphasize the fact that the interpretation of ^{14}C soil dates must consider not only the soil profiles, but also the paleorelief. Only in this way can autochthonous and allochthonous soil horizons and sediments be distinguished and the primary origin of the organic matter at the time of soil formation (ie, before any contamination with younger material) be reliably recognized.

CONCLUSIONS

The results of our study show that, 1) ^{14}C dating of fossil podzol horizons yield AMRT values which may differ from the true ages by 10,000 years and even more. Therefore, Pleistocene and Holocene soils cannot always be distinguished, 2) the degree of particularly contemporaneous contamination (rootlets, humic acids) may cover at least one order of magnitude in the same podzol profile and does not justify the use of "age correction factors" for humid areas, 3) conventional ^{14}C data obtained from fossil podzol soils of different profiles will not be comparable as time marks in any case, even if they were obtained from the same laboratory, and 4) soil dating demands a detailed description of the soil with primary and secondary soil types as well as autochthonous and allochthonous soil features dependent on the paleorelief (Roeschmann, 1971).

REFERENCES

Gerasimov, I P, 1971, Nature and originality of paleosols, in Yaalon, D H, ed, Paleopedology - origin, nature and dating of paleosols: Jerusalem, Israel Univ Press, p 15 - 27.

---------- 1974, The age of recent soils: Geoderma, v 12, p 17 - 25.

Geyh, M A, Benzler, J H, and Roeschmann, G, 1971, Problems of dating Pleistocene and Holocene soils by radiometric methods, in Yaalon, D H, ed, Paleopedology - origin, nature and dating of paleosols: Jerusalem, Israel Univ Press, p 63 - 75.

Gilet-Blein, N, Marien, G, and Evin, J, 1980, Unreliability of ^{14}C dates from organic matter of soils, in Stuiver, Minze and Kra, Renee, eds, Internatl radiocarbon conf, 10th, Proc: Radiocarbon, v 22, no. 3, p 919 - 929.

Kuntze, H, Niemann, J, Roeschmann, G, and Schwerdtfeger, G, 1981, Bodenkunde: Stuttgart, Verlag Eugen Ulmer, 407 p.

Matthews, J A, 1981, Natural ^{14}C age/depth gradient in a buried soil: Naturwissenschaften, v 68, p 472 - 474.

Paul, E A, Campbel, C A, Rennie, D A, and McCallum K J, 1964, Investigations of the dynamics of soil humus utilizing carbon dating techniques: Internatl cong soil sci, 8th, Trans, v 3, p 201 - 208.

Roeschmann, G, 1971, Problems concerning investigations of paleosols in older sedimentary rocks. Demonstrated by the example of Wurzelböden of the carboniferous system, in Yaalon, D H, ed, Paleopedology - origin, nature and dating of paleosols: Jerusalem, Israel Univ Press, p 311 - 320.

---------- 1975, Zur Untersuchungsmethodik, pedogenetischen Deutung und Datierung fossiler Sandböden des Pleistozäns in Norddeutschland: Deutsch Bodenkundl Gesell Mitt, v 22, p 581 - 590.

Scharpenseel, H W, 1971, Radiocarbon dating of soils - problems, troubles, hopes, in Yaalon, D H, ed, Paleopedology - origin, nature and dating of paleosols: Jerusalem, Israel Univ Press, p 77 - 87.

---------- 1972, Natural radiocarbon measurement on soil organic matter fractions and on soil profiles of different pedogenesis, in Rafter, T A and Grant-Taylor, T L, eds, Internatl radiocarbon conf, 8th, Proc: Wellington, p 382 - 393.

Scharpenseel, H W and Schiffmann, H, 1977, Radiocarbon dating of soils: Pflanzenernähr Bodenkunde Zeitschr, v 140, p 159 - 174.

Scharpenseel, H W, 1979, Soil fraction dating, in Berger, Rainer and Suess, H E, eds, Radiocarbon dating, Internatl radiocarbon conf, 9th, Proc: Los Angeles, Univ Calif Press, p 277 -283.

Scharpenseel, H W and Zakosek, H, 1979, Phasen und Bödenbildung in Tunesien: Geomorph N F Zeitschr, v 33, p 118 - 126.

Scharpenseel H W, Zakosek, H, Neue, U, and Schiffmann, H, 1980, Search for pedogenic phases during younger Pleistocene and Holocene (Soltanien and Rharbien) of Tunesia, in Stuiver, Minze and Kra, Renee, eds, Internatl radiocarbon conf, 10th, Proc: Radiocarbon, v 22, no. 3, p 879 - 884.

Schoute, J F Th, Griede, J W, Mook, W G, and Roeleveld, W, 1981, Radiocarbon dating of vegetation horizons, illustrated by an example from the Holocene coastal plain in the northern Netherlands: Geol Mijnbouw, v 60, p 453 - 459.

Van der Hammen, T and Wijmstra, T A, 1971, The Upper Quaternary of the Dinkel Valley (Twente, Eastern Overijssel, The Netherlands): Rijks Geol Dienst Medd, ns, v 22, p 55 - 213.

[Radiocarbon, Vol 25, No. 2, 1983, P 417-420]

POSSIBLE DEPLETION IN ^{14}C IN TREES GROWING IN CALCAREOUS SOILS

HENRIK TAUBER

^{14}C Dating Laboratory, National Museum,
Ny Vestergade 10, Copenhagen, Denmark

ABSTRACT. ^{14}C activities of decadal samples from beech trees growing under extreme calcareous conditions were compared to ^{14}C activities of decadal samples of the same age from a beech tree growing in a normal mold soil in order to see whether part of the carbon assimilated during photosynthesis might originate from ^{14}C-deficient carbonates in the soil. The calcareous soils contained from 18 to 52% calcium carbonate, and this carbonate had a mean ^{14}C age of 10,200 to 17,600 years BP. A comparison was also made with the ^{14}C activity of contemporaneous samples from Douglas Fir from the US North Pacific (Stuiver, 1982).

No significant depletion in ^{14}C activity in beech trees growing in the highly calcareous soils was detected. The measured mean difference in ^{14}C activity in beech trees from calcareous and non-calcareous sites corresponds to an uptake of 0.12 ± 0.3% carbon from soil carbonates in the calcareous sites.

INTRODUCTION

It is a prerequisite for a universal ^{14}C time scale that regional variations in the ^{14}C content of suitable organic materials are minimal compared to dating errors. A large number of comparisons between the ^{14}C activity of wood grown in North America and in Europe between AD 950 and the present have shown that regional or continental variations in the atmospheric ^{14}C levels of the northern hemisphere have indeed been small (Stuiver, 1982). The application of a universal calibration curve for the whole northern hemispfere, therefore, seems justified.

However, this concordance may be upset in specific cases if soil CO_2 and soil carbonate, deficient in ^{14}C, could enter via the root system into the photosynthetic pathways and be assimilated together with atmospheric CO_2 during photosynthesis. This mechanism might be considered because inorganic minerals from the soil are known to take part in the intermediate photosynthetic processes.

In order to investigate this possibility, which does not seem to have attracted much attention, neither from ^{14}C laboratories nor from plant physiologists, the ^{14}C activity of annual rings of a known age from two beech trees which had grown in extremely calcareous soils was measured and compared to the ^{14}C activity of annual rings of the same age from a beech tree which had grown in a normal mold soil. The distance between the calcareous and the non-calcareous sites was only ca 20km. The ^{14}C activity was further compared to the supposed mean hemispheric ^{14}C activity of tree rings from the northern hemisphere as given by Stuiver (1982).

DENDROCHRONOLOGIC MATERIAL

Extreme calcareous conditions prevail in a small protected test forest at Allindelille in the middle of Zealand, Denmark. In parts of the forest, pre-Quaternary carbonates crop up to the surface or are covered only by a thin layer of mold soil which, itself, contains up to 50% carbonates. Beech trees growing in this soil are chlorotic and develop light yellow leaves because the strongly alkaline conditions inhibit an uptake of iron from the soil.

Two beech trees (Fagus sylvatica) from such a chlorotic grove were felled and the annual rings were counted dendrochronologically and divided into decadal samples. The first beech tree, Al I, was ca 160 years old and mold soil taken 5 to 15cm below the surface, directly at the stub, contained ca 18% $CaCO_3$ relative to the dry weight of the soil. This carbonate had a mean ^{14}C age of 10,260 ± 155 years BP ($\delta^{13}C$ = -2.4 ^{o}/oo PDB). The second beech tree, Al II, was 75 years old and grew in a soil that contained ca 52% carbonates of a mean ^{14}C age of 17,620 ± 310 BP ($\delta^{13}C$ = +1.3^{o}/oo PDB).

For comparison, decadal samples of ages identical to those from Allindelille were taken from a third beech tree (Fagus sylvatica) that had grown in a normal mold soil with < 1% carbonate. The beech tree, So I, grew in wooded grounds at the outskirts of a minor town, Sorø, ca 20km from Allindelille.

^{14}C ACTIVITIES

All the tree-ring samples were extracted with diluted acid and hydroxide (de Vries pretreatment), and the ^{14}C activities were measured in a CO_2 gas counter. All measurements were corrected for isotopic fractionation and normalized to $\delta^{13}C$ = -25.0^{o}/oo PDB. $\delta^{13}C$ values ranged from -24.9 to -26.0 ^{o}/oo for the chlorotic beech trees (lowest for Al II which had grown in the most alkaline soil), and from -23.3 to -24.0^{o}/oo for the normal beech tree.

The measured activities are listed in table 1 as conventional and normalized ^{14}C ages. The very precise ^{14}C ages measured by Stuiver (1982) on decadal samples of similar ages taken from Douglas Fir (Pseudotsuga menziesii) from the Paci-

TABLE 1. ^{14}C activity of tree rings from calcareous and non-calcareous sites

Annual rings	Conventional ^{14}C years BP			
AD	Beech calcareous Al I	Beech calcareous Al II	Beech non-calcareous So I	Douglas Fir US Pacific (Stuiver,1982)
1850-1860	29 ± 35		48 ± 40	116 ± 10
1870-1880	61 ± 40		43 ± 40	113 ± 10
1890-1900	149 ± 40		70 ± 40	82 ± 10
1900-1910		143 ± 40*	62 ± 40	75 ± 10
1910-1920		122 ± 40	133 ± 40	114 ± 10
1920-1930		141 ± 40	164 ± 40	132 ± 10
1930-1940		123 ± 40	126 ± 40	150 ± 10

Mean of paired differences:

Al I and Al II minus So I : +8 ± 20 ^{14}C years
Al I and Al II minus Douglas Fir: -7 ± 15 ^{14}C years
So I minus Douglas Fir : -20 ± 16 ^{14}C years

---

*Represents only annual rings 1903-1910

fic Northwest of the US are also listed in table 1. These ^{14}C ages are supposed to be close to the mean ages of contemporaneous wood from the northern hemisphere.

Table 1 shows that no significant systematic deviations between the ^{14}C activities of contemporaneous samples from the chlorotic beech trees (Al I and Al II) and from trees growing in normal soils could be found. Paired differences between the ^{14}C ages of Al I or Al II and So I (8 pairs) have a mean value of +8 ± 20 years, and the paired differences between Al I or Al II and the Douglas Fir (8 pairs) have a mean value of -7 ± 15 years. It may also be noted that the paired differences between the ^{14}C ages of contemporaneous samples from the normal beech tree from Denmark (So I) and from Douglas Fir from the US (7 pairs) have a mean value of -20 ± 16 years. This is an approximate measure of either the difference in atmospheric ^{14}C levels between Denmark and the US Pacific coast, or of the laboratory bias of the Copenhagen ^{14}C lab relative to the Seattle ^{14}C laboratory.

CONCLUSION

The mean difference between ^{14}C ages of contemporaneous decadal samples from beech trees growing in highly calcareous soils and in a normal mold soil was measured to +8 ± 20 years. Hence, a significant assimilation of soil CO_2 or soil carbonate during photosynthesis could not be detected. If the ^{14}C ages of the soil carbonate (ca 10,200 to 17,600 BP) are taken into consideration, the measured mean difference in ^{14}C ages correspond to an uptake in tree rings of 0.12 ± 0.3% carbon from soil carbonate in the beech trees growing in highly calcareous soils. Only in very special cases could a possible assimilation of this magnitude constitute a source of error in ^{14}C dating.

ACKNOWLEDGMENTS

Knud Jakobsen, Institute of Systematic Botany, University of Copenhagen, kindly supplied disks of the investigated beech trees from the University research estates.

REFERENCE

Stuiver, Minze, 1982, A high-precision calibration of the AD radiocarbon time scale: Radiocarbon, v 24, p 1-26.

[Radiocarbon, Vol 25, No. 2, 1983, P 421-427]

RADIOCARBON DATING OF TUFA IN PALEOCLIMATIC STUDIES

DUŠAN SRDOČ, NADA HORVATINČIĆ, and BOGOMIL OBELIĆ

Rudjer Bošković Institute, Zagreb, Yugoslavia, PO Box 1016

and

ADELA SLIEPČEVIĆ

Faculty of Veterinary Science, University of Zagreb,
Zagreb, Yugoslavia

ABSTRACT. Calcareous deposits known as tufa or travertine contain biogenic carbon and are a potential source of geochronologic information. Many dated samples from Karstic regions in Yugoslavia proved that ^{14}C analyses of tufa can provide reliable data reflecting climatic conditions in the past. Systematic dating of tufa samples revealed two distinct groups of deposits: recent tufa deposits, with a sharp age limit of ~6000 ± 500 years BP, and old tufa deposits with ^{14}C age ranges from 25,000 ± 2300 years BP to the lowest limit of our ^{14}C dating system (~37,000 years). A histogram based on the initial activity $A_o = 0.85$ shows the age distribution of randomly sampled tufas vs sample frequency. A time gap between ~6000 BP and ~23,000 BP is evident, reflecting cooler climatic conditions. The start of peat deposition is coincident with that of tufa growth in the Holocene.

Paleoclimatic implications of tufa growth periods obtained by ^{14}C dating are as follows: climatic conditions that favor tufa formation at least in karstic regions, are very stringent. Therefore, climatic conditions, such as mean annual temperature and humidity, as well as hydrologic and vegetational conditions, must have been very similar in periods of tufa growth. While recent tufa deposits are coincident with the warm Holocene period, old tufa can be associated with warm interstadials in the Würm.

INTRODUCTION

Tufa concretions are found in predominantly karstic

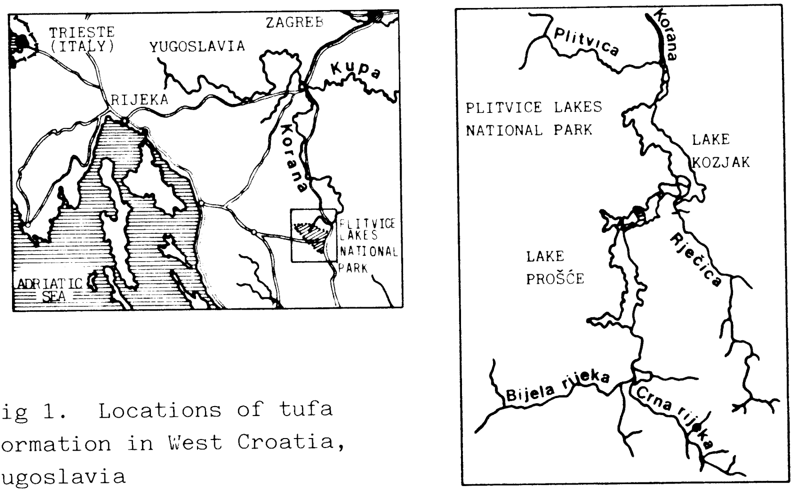

Fig 1. Locations of tufa formation in West Croatia, Yugoslavia

areas in Yugoslavia, always associated with present or past surface water flow. Tufa is usually deposited as a crust on aquatic plants near cascades and waterfalls or finely dispersed in lakes, forming thick basal sediments. Tufa deposits range in thickness from several centimeters to tens of meters, usually preserving the structure of objects on which it was originally deposited. Since tufa contains carbon of biogenic origin it can be used, in principle, for ^{14}C dating. We carried out ^{14}C measurements of tufa deposits from Plitvice Lakes National Park, Central Croatia (fig 1). This is a typical karst area where tufa formations are dominant in an area of $2km^2$ along the Korana River and its tributaries.

According to Polšak (1979), the entire Park area ($200km^2$) consists of Mesozoic carbonate beds of folded and faulted structures. Faults run in a NW-SE direction which is typical of Dinarides. The Upper Triassic dolomites form impermeable beds which influence surface flow and karst spring locations. Recent tufa is found along streams and lakes, whereas old tufa outcroppings emerge from alluvial deposits, or are preserved on top of present-day hills or gorge rims.

^{14}C DATING OF TUFA

Several factors influence the accuracy of the age of ^{14}C-dated tufa samples. Some preliminary values were encouraging (Srdoč et al, 1980); we continued ^{14}C dating a substantial number of randomly selected samples of tufa in the Plitvice Lakes National Park area. The following factors play an important role in measuring and calculating the age of tufa: 1) initial ^{14}C activity of groundwater or, more specifically, the activity of dissolved bicarbonates, which precipitate in the form of calcium carbonate (tufa) following the loss of CO_2 after surfacing and warming up of groundwater 2) contamination of old tufa beds by recent calcareous material and/or bomb-test-produced ^{14}C.

Initial groundwater activity was measured at several karst springs, and surface water activity along the creeks, lakes, and the Korana River. An increase of ^{14}C activity A_o was observed from 60% modern at the karst spring, Crna Rijeka, to 92% modern in the Korana River. The large difference between the groundwater activity and the subsequently increased activity of river water introduces a large error in calculating tufa age unless a proper value of A_o is associated with every tufa sample, depending on the sampling location. Fortunately, tufa is precipitated for a very short stretch (6 to 7km) of the Korana River where the surface water attained a practically constant ^{14}C activity equal to 85% modern. A more serious problem is contamination of recent groundwater with bomb-test-produced ^{14}C. A relatively short mean residence time makes groundwater in karstic areas susceptible to bomb-test contamination, proven by a high tritium concentration of groundwater. Use of the present-day initial activity of groundwater introduces another error in age calculation of pre-bomb-test tufas which cannot be easily estimated. Thus, we sought "pre-war" samples of tufa of known age, associated with organic material (wood, moss, etc). These measurements gave a mean initial activity A_o = 85% modern, which is in accordance with the expected values for karst areas (Geyh, 1973). It should be emphasized that groundwater activity has not followed the sharp increase of atmospheric CO_2 activity after nuclear weapon tests of 1953 and after.

Contamination of old tufa beds through exposure to atmospheric CO_2 or seepage of precipitation water is another potential source of error in dating tufa. However, we found tufa layers that had been exposed to rain and snow or even surface water, which were "dead", ie, their ^{14}C concentration was below the detectable limit of our system. This indicates that exposure to recent surface or precipitation water does not necessarily result in contamination.

RESULTS

The following were measured: 146 samples of tufa, 32 samples of peat, 10 samples of ground and surface water, and 20 samples of various organic materials (wood, plants, etc). A complete list appears elsewhere (Srdoč et al, 1982), whereas data relevant to paleoclimatic studies are presented in figure 2. The ^{14}C age of tufa and peat samples is calculated using 5730±40 years for the half-life of ^{14}C; it is assumed that the initial activity of tufa samples was 85% of modern standard. All Holocene samples are dendrochronologically-corrected using MASCA curves (Ralph, Michael, and Han, 1973).

PALEOCLIMATIC IMPLICATIONS

The coincident start of tufa and peat formation shown in figure 3 is certainly not fortuitous. A relatively thick layer of organic detritus plays a decisive role in aquatic chemistry through enrichment of seeping water with CO_2, which in turn dissolves $CaCO_3$ in karstic areas. Under favorable conditions, the excess of dissolved calcium bicarbonate is precipitated in the form of tufa in a relatively short period which makes the organic material (peat, gyttja, humus) and tufa practically contemporaneous on the ^{14}C time scale. However, the dissolution of limestone by groundwater introduces an uncertainty in the initial ^{14}C activity of tufa which must be considered when comparing the ^{14}C age of these materials, as explained previously.

The environmental conditions under which tufa precipitates are very stringent. The list of parameters that determines the environmental conditions favorable for tufa formation is not yet complete, but the most important parameters are climatic, hydrogeologic, limnologic, and biologic factors. There is, of course, a strong interplay among these factors. Groundwater alkalinity, temperature, an increase of

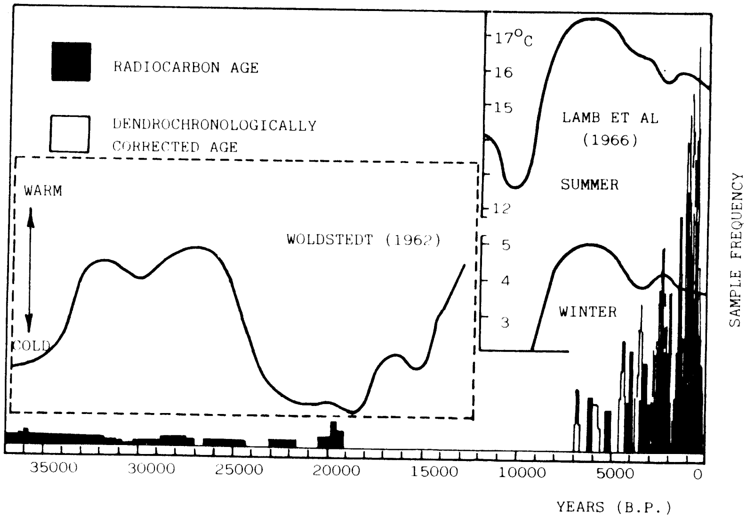

Fig 2. Frequency of randomly collected tufa samples (62) vs ^{14}C age. The general trend of mean annual temperature in the Würm is according to Woldstedt (1962) and summer and winter temperatures in England during the Holocene (Lamb, Lewis, and Woodroffe, 1966).

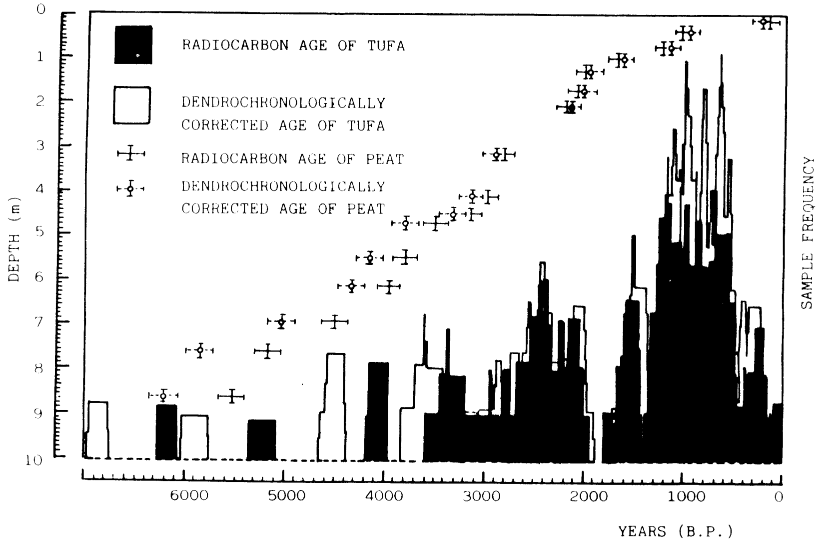

Fig 3. Expanded histogram showing frequency of randomly selected tufa samples (48) vs ^{14}C age. The age of peat found in the same area is shown vs depth. Very abundant recent tufa deposits (age <200 yr) are not included.

surface water temperature, and a drop of hardness due to tufa precipitation are of primary importance. They all depend on the mean annual temperature and precipitation. Consequently, periods of tufa formation in a specific area must have had very similar climatic conditions. Thus, ^{14}C dating of tufa (or associated organic material such as embedded wood) provides a useful tool in paleoclimatic studies. In our case, the climate that favors tufa precipitation in karstic areas, is close to or identical with the present climate. The mean annual temperature curve for the past 7000 years (Lamb, Lewis, and Woodroffe, 1966) supports our reasoning, even though the curve is given for England which has a different climate.

Our ^{14}C measurements of tufa in Plitvice National Park revealed two distinct groups of beds belonging to two geologic epochs. Whereas ^{14}C dates of Holocene tufa beds, tested by measuring organic material (wood) found in tufa beds and pollen analysis, are quite reliable, the dating of old tufa (~30,000 years) is less reliable. Some contamination of very old tufa samples with recent calcareous material will result in an error or shifting the age of old tufa. The ^{14}C date will be too young. Thus, we seek other dating methods to compare with the old dates shown in figure 2. These dates are close to the lower limit of the ^{14}C method. It should be noted, however, that contamination with recent tufa probably does not exceed 1 or 2% in well-preserved samples of old tufa, which introduces a shift of 1000 to 1800 years for tufa that is ca 23,000 years old (Olsson, 1980). This is an error comparable to that due to the uncertainty of the initial groundwater activity A_o. Consequently, the total inherent error of ^{14}C dates of tufa samples in the range between 20 and 25,000 years is ca ±2300 years. Continuity of tufa ages stretches from 25,000±2300 years BP down to the lowest limit of our ^{14}C measurements with the exception of two samples, 19,000 and 20,000 years old, as shown in figure 2. This implies a warm climate, like the present, from 25,000±2300 years BP extending at least to the limit of our measurements, $37,000^{+3500}_{-2500}$ years. This period coincides with the warm interstadial often referred to in older literature as Paudorf-Arcy (Woldstedt, 1962), and more recently, as Denekamp and Hengelo interstadials in the Weichselian period in Central Europe (Geyh and Rohde, 1972).

REFERENCES

Geyh, MA, 1973, On the determination of the initial ^{14}C content in groundwater, in Rafter, TA and Grant-Taylor, T, eds, Internatl radiocarbon conf, 8th, Proc: Wellington, Royal Soc New Zealand, p D58-D69.

Geyh, MA, Rohde, P, 1972, Weichselian chronostratigraphy, ^{14}C dating and statistics, in Internatl geol cong, 24th, Proc: Montreal, sec 12, p 26-36.

Lamb, HH, Lewis, R, and Woodroffe, A, 1966, Atmospheric circulation and the main climatic variables, in Internatl symposium world climate from 8000 to 0 BC, Proc: London, Royal Meteorol Soc, p 174.

Olsson, IU, 1980, Progress in radiocarbon dating, promising techniques and trends in the research, in Srdoč, D, Obelić, B, Sliepčević, A, eds, Regional conf on the application of isotope analyses in archaeology, geology, and hydrology, Proc: Fizika, v 12 (S2), p 37-68.

Ralph, EK, Michael, HN, and Han, MC, 1973, Radiocarbon dates and reality: MASCA Newsletter, v 9, 1, p 1-20.

Srdoč, D, Horvatinčić, N, Obelić, B, and Sliepčević, A, 1982, Rudjer Bošković Institute radiocarbon measurements VII: Radiocarbon, v 24, p 352-371.

Srdoč, D, Obelić, B, Horvatinčić, N, and Sliepčević, A, 1980, Radiocarbon dating of calcareous tufa; how reliable results can we expect?, in Stuiver, M and Kra, R, eds, Internatl radiocarbon conf, 10th, Proc: Radiocarbon, v 22, p 858-862.

Woldstedt, P, 1962, Ueber die Gliederung der Quartärs und Pleistozäns: Eiszeitalter u Gegenwart, Oehringen/Württ, v 13, p 115.

[Radiocarbon, Vol 25, No. 2, 1983, P 429-439]

A SYSTEM FOR STUDYING CARBON ALLOCATION IN PLANTS USING ^{11}C-LABELED CARBON DIOXIDE

YOUHANNA FARES*, JD GOESCHL*, CE MAGNUSON**, CE NELSON+
BR STRAIN**, CH JAEGER**, AND EG BILPUCH‡

INTRODUCTION

The effects of environmental factors such as water stress, elevated CO_2, or temperature on carbon assimilation and allocation in plants have been studied extensively (Gifford and Evans, 1981; Loomis, Rabbinge, and Ng, 1979; Neales and Incoll, 1968). However, the interactions of these processes are not well understood and cannot be predicted with any degree of confidence. Continuous and simultaneous measurements of photosynthesis, transport, and sink activity have never been made during the short- and long-term responses of live, intact plants to step changes in environmental factors. Thus, direct environmental effects and adaptive responses of plants are generally not distinguished. This results in part from limitation in experimental techniques and protocol used in past studies and the lack of experimental validation of hypotheses and models (eg, Goeschl _et al_, 1976; Magnuson _et al_, 1979; Smith _et al_, 1970) dealing with these problems. This paper describes in detail the components of an integrated technique for studying carbon assimilation, transportation, and allocation in intact live plants under any set of environmental conditions, using continuously produced $^{11}CO_2$.

EXPERIMENTAL DESIGN

The central theme of the experimental component of the integrated approach is the utilization of CO_2 labeled with the radioactive isotope ^{11}C. There are three main reasons for the use of ^{11}C as tracer (Fares _et al_, 1978; Magnuson _et al_. 1982). As a tracer, ^{11}C has several advantages. 1) It decays by positron (β^+) emission followed by a subsequent emmision of two oppositely-directed gamma rays. These γ-rays have

---

* Biosystems Research Division, Industrial Engineering Department,
Texas A&M University, College Station, Texas 77843

** Botany Department and Phytotron, Duke University, Durham, North Carolina 27706

\+ Department of Radiology and Physics, Duke University

‡ Physics Department, Duke University

sufficient energy (0.511MeV) to be detected through several cm of tissue in vivo and in time coincidence which makes it possible to localize the source and to reduce undesired background activity. 2) The short half-life of ^{11}C (20.3 min) makes it possible to perform several experiments on the same plant under the same set of environmental conditions. 3) Its half-life is comparable with turnover times of the photosynthetic pool and the velocity of transport, making possible dynamic measurements which cannot be done with long-lived tracers.

SYSTEMS COMPONENTS

The integrated system is made up of six components as shown in figure 1.

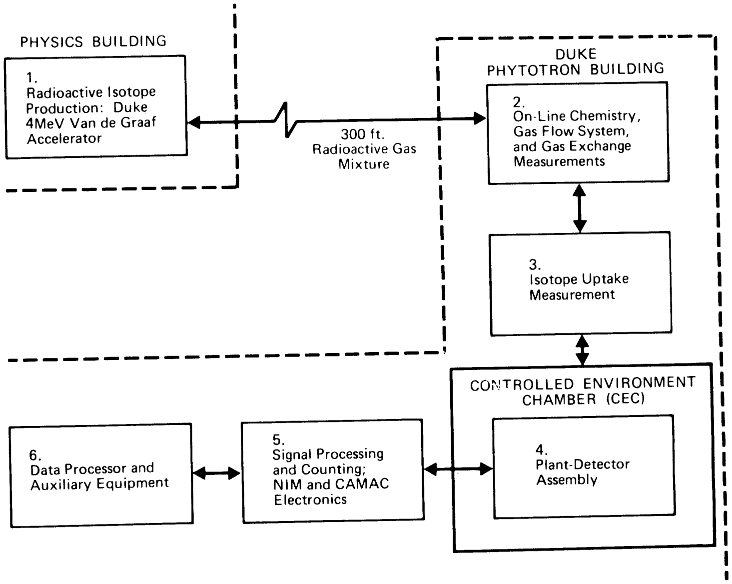

Fig 1. Outline of the integrated system for studying the carbon allocation in plants using radioactive tracers under controlled environment conditions

1. RADIOACTIVE ISOTOPE PRODUCTION. ^{11}C is produced by bombarding $^{12}CO_2$ gas flowing through a target chamber mounted on the beam line of the 4MeV Van de Graaff of Duke University. The nuclear reaction $^{12}C(^{3}He, ^{4}He)^{11}C$ is used (Cirilov *et al*. 1966). The activity produced flows through a 100m capillary tube to the nearby Duke Phytotron where the plants are grown under controlled environmental conditions.

To eliminate contaminant isotopes, the transport time of activity from the target chamber to the phytotron is adjusted to be longer than six half-lives of the longest lived of the two contaminant isotopes, ^{15}O. In an earlier study with 35MeV protons, of a total of 100% ^{11}C activity, 98% was in the form of ^{11}CO and 2% $^{11}CO_2$, which made it possible to separate the activity from the target with only 2% loss (Fares *et al*, 1978). The separation of ^{11}CO from the target $^{12}CO_2$ and $^{11}CO_2$ is necessary to control the specific activity. In the present study, with 4MeV ^{3}He, the composition of the effluent gas is 10% ^{11}CO and 90% $^{11}CO_2$. However, the cross-section of the ^{3}He reaction is 3 to 4 times that of the proton reaction, which compensated for some of the loss of activity to the target material and produced enough ^{11}CO to carry out the experiments without difficulty. An attempt to increase the recovery of ^{11}CO was done by mixing the target, $^{12}CO_2$, with some H_2 gas. The attempt worked by reducing some $^{11}CO_2$ to ^{11}CO, but at the same time, it reduced $^{12}CO_2$ to ^{12}CO, so the overall recovery of ^{11}C was increased but the specific activity did not change (results of this study will be reported elsewhere). What happens in the target chamber can be summarized as follows:

Without hydrogen

$$^{12}CO_2 \longrightarrow \boxed{\begin{array}{l}\text{Target}\\ \text{chamber}\end{array}} \longrightarrow {}^{12}CO_2 + {}^{11}CO_2\ 90\% + {}^{11}CO\ 10\% \tag{1}$$

With hydrogen

$$\begin{aligned} ^{12}CO_2 + H_2 \longrightarrow \boxed{\begin{array}{l}\text{Target}\\ \text{chamber}\end{array}} \longrightarrow {}^{12}CO_2 + {}^{11}CO_2\ 10\% + {}^{11}CO\ 90\% \\ + {}^{12}CO + H_2O + H_2 \end{aligned} \tag{2}$$

The ratio of $^{11}CO_2$ to ^{11}CO will depend on the amount of H_2 added. The production rate as monitored at the entry station in the phytotron (see fig 2) is, after correcting for the decay in transport, $0.12 \mu ci\ sec^{-1}\ \mu A^{-1}$.

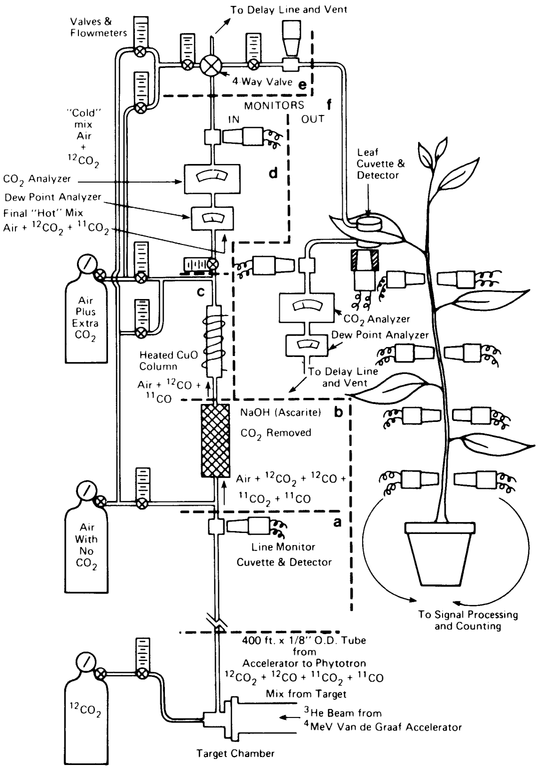

Fig 2. The experimental layout. a. Line Monitor. b. Removal of target material. c. Oxidation of ^{11}CO. d. In Line Monitor, CO$_2$ analyzer and dew point analyzer. e. Final In Monitor. f. Out Monitor, leaf cuvette, and plant and detector assembly in the controlled environment chamber (CEC).

2. ON-LINE CHEMISTRY, GAS FLOW SYSTEM, AND GAS EXCHANGE MEASUREMENTS. The objective of the on-line chemistry station, positioned in the phytotron, is to separate ^{11}CO from the target material and any other contaminants. It then oxidizes it to ^{11}CO$_2$ so that when mixed with CO$_2$-free air and the right amount of ^{12}CO$_2$ is added, air with the desired concentration of CO$_2$, and known specific activity will be presented to the plant leaf. The effluent gases from the target chamber are transported 100m (in 14 min) to the phytotron via a 2.5mm id teflon tube. The following sequence of steps takes place in the chemistry station as shown in figure 2, a,b,c, and d.

a) On arrival at the phytotron, the gases flow at a known rate, through a spiral plastic cuvette of known volume positioned in front of a γ-ray detector at a given, fixed detection geometry. The detection efficiency of every detector in the given geometry is calibrated for every experiment with a standard γ-ray source. This station that monitors the activity of the incoming gases is called the "Line Monitor." Profile #1 (fig 4B) gives the production rate of the radioactive isotope.

b) As the gases exit from the cuvette of the line monitor, they flow through an ascarite column. The ascarite column, being sodium hydroxide impregnated into asbestos, removes all the $^{11}CO_2$ and $^{12}CO_2$ gases. The small volume of ^{11}CO left (or ^{11}CO, ^{12}CO, H_2) is purged from the column by CO_2-free air added to the gases as they enter the ascarite column.

c) The next step is to oxidize ^{11}CO to $^{11}CO_2$ by flowing the exiting mixture of gases over a CuO bed heated to 600°C in a quartz tube in a horizontal muffle as shown in figure 2c. Oxygen in the air recovers the used CuO.

d) To the effluent gases from the CuO bed, ie, air + $^{11}CO_2$ or air + $^{11}CO_2$ + $^{12}CO_2$, either $^{12}CO_2$-free air or air + a controlled amount of $^{12}CO_2$ is added to bring the concentration of total CO_2 in the so-called "Hot Mix" to the desired value. The gases then flow through a dew point analyzer to determine the total concentration of CO_2 in ppm as shown in figure 2d. As the gases exit from the CO_2 analyzer, they flow through a spiral cuvette positioned in front of a γ-ray detector to determine the specific activity of the gas mixture that will be presented to the leaf.

e) Finally, adjustment of the gas flow to be comparable to field flow rates is made via a 4-way valve which allows for venting unwanted gases to the absorbers. If adjustment is needed, the activity and the final flow rate are re-measured as shown in figure 2c.

3. ISOTOPE UPTAKE. The net isotope uptake by that portion of the leaf exposed to the final Hot Mix in the leaf cuvette is determined. It is simply a station where the specific activity of the input and output gas mixtures into and out of the leaf cuvette is measured. The flow rate and specific activity of the input gas mixture are measured in station (e) above and called the "In-Monitor." Similarly, the specific activity of the output gas mixture is measured in the "Out-Monitor." The effluent gases from the Out-Monitor flow through a CO_2 analyzer, then through a dew point analyzer before they are vented to the absorbers as shown in figure 2f. Thus, net photosynthetic rates can be calculated as well. The final flow rate of the gases is also monitored to adjust for the Out-Monitor measurement in case there is a perceptable reduction

of flow. Signals from the CO_2 and dew point analyzers are either recorded by multipen strip chart recorder or digitized and input into the computer as described below.

4. PLANT DETECTOR ASSEMBLY. The plant and the detectors are positioned in the controlled environment chamber. The radioactive gas mixture is presented to a portion of the leaf through a cuvette which consists of a Plexiglas^{R} water jacket on the top and bottom of the leaf. The cuvette is created by a 2mm-thick closed-cell form neoprene gasket on each water jacket. The cuvette is clamped to the leaf in such a way that the gas mixture coming out of the In-Monitor flows across the upper surface of the leaf, around the edge, and back across the lower surface. Immediately below the leaf cuvette, a γ-ray detector is positioned to monitor the tracer build-up in the leaf. This detector is shielded with a lead collar.

In order to monitor the movement of the labeled photosynthates in the phloem, 4 to 6 pairs of detectors are positioned on either side of the plant stem above and below the labeled leaf. The detector pairs are operated in time coincidence at 180° with respect to each other (see fig 2f). The distances between the detector pairs and their geometry with respect to the stem and to one another are carefully assigned.

Each detector is made of 5 x 2.8cm NE102^{R} plastic scintillator crystal light-coupled to a photomultiplier-voltage divider system capable of producing fast and slow output signals. The front end of the detector assembly facing the source of activity, is collimated with a lead collar to give a desired window. A highly stabilized high-voltage power supply is used to bias the detectors.

The controlled environment room CER in which the plant detector station is located is a typical chamber of type B of the Duke Phytotron (see eg, Kramer, Hellmers, and Downs, 1970; Downs, Hellmers, and Kramer, 1972). In such a chamber, temperature, humidity, light intensity, light cycle, and CO_2 concentration and flow speed of air are controlled. The light cycle and CO_2 concentration are adjusted to the conditions of growth of the plant under study.

5. SIGNAL PROCESSING AND COUNTING. We have standard NIM electronics for processing the signals from the detectors for counting and CAMAC electronics for data acquisition and interfacing with the data processor. The fast signal from each detector is processed by the NIM electronics and then presented to the scalars in the CAMAC crate to be counted under the command of the CAMAC unit controller. The CAMAC unit is under control of the processor (fig 3) through the general purpose interface bus (GPIB). Standard LeCroy fast electronics modules are used in the NIM system and Kinetic System CAMAC

units are used in the CAMAC system. The CAMAC crate provides the physical mounting, power, cooling, and dataway connections for the modules. A normal crate has 25 stations of which station 25 is assigned to the crate controller and the remaining slots are normal stations for modules such as scalars, digitizers, etc. The system works by commands and responses from the controller to the modules and back and from the controller to the computer and back as shown in figure 3. The controller is the traffic director of the systems signals. All systems parameters are carefully defined within the IEEE CAMAC specifications 583.

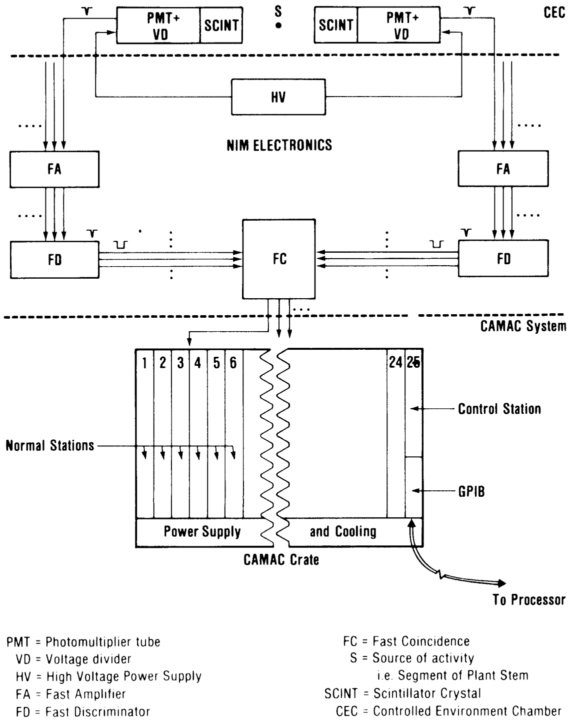

PMT = Photomultiplier tube
VD = Voltage divider
HV = High Voltage Power Supply
FA = Fast Amplifier
FD = Fast Discriminator

FC = Fast Coincidence
S = Source of activity
i.e. Segment of Plant Stem
SCINT = Scintillator Crystal
CEC = Controlled Environment Chamber

Fig 3. Signal processing and counting using NIM and CAMAC systems.
NIM = Nuclear Instrumentation Electronic Modular
CAMAC = Computer Automated Measurement and Control.

6. THE PROCESSOR. For the above system to be an integrated on-line facility, a processor that can handle the following

functions is needed: 1) to communicate with the CAMAC system, ie, send commands to and receive responses from it; 2) to implement routines such as calibration and background corrections; 3) for on-line data acquisition, reduction, and storage; 4) for on-line data display; 5) for on-line and off-line testing of acquired data; 6) for utility programs.

In this system, an HP 9845 B (option 250) minicomuter is used. This computer has 186K byte memory expandable to 500K and uses the extended basic language. It has the additional advantage of graphic capabilities and a large CRT for visual display. It can drive the following accessories: two magnetic tape drives, floppy disk drives, thermal printer, multipen multicolor recorders, and extra CRT's for display or monitoring. Figure 4 is a copy of the graphic display on the CRT of this computer of an on-line real-time experiment described in the protocol below.

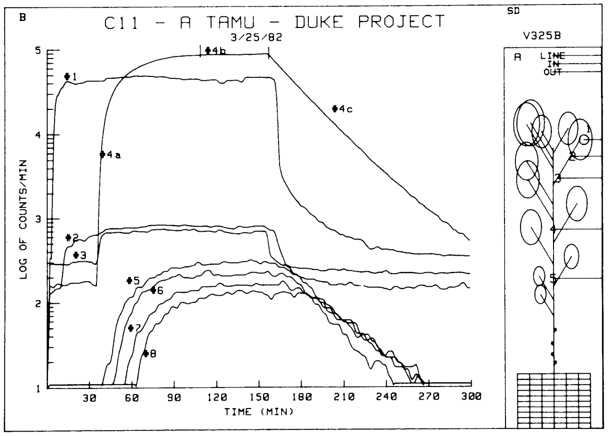

Fig 4. Live-time display of tracer profiles of Velvet Leaf (Abutilon theophrastic Medic). A. Plant geometry with detectors #1 monitoring the leaf and detector pairs #2, #3, #4, and #5 monitoring the phloem activity. B. Profile #1 shows the line activity as recorded by the Line Monitor, #2 and #3, the input and output activities as recorded by the Input and Output Monitors, respectively. Profile #4-a, #4-b, and #4-c show the time-dependent, the steady-state, and the washout behavior of the leaf, respectively. Profiles 5, 6, 7, and 8 show the tracer profiles in the phloem as monitored by detector pairs #2, #3, #4, and #5 (fig 4A).

EXPERIMENTAL PROTOCOL

Described here are some simple experiments, which we call "step input," to illustrate our daily experimental protocol. Figure 4 shows the on-line real-time computer output of the data obtained from this experiment for rates of net photosynthesis, carbon storage (eg, starch) and export (eg, sucrose) from a given area of a leaf and the velocity of translocation of Velvet Leaf (Abutilon theophrasti Medic).

The plant of choice, grown under the environmental conditions chosen for a particular study is moved into the controlled environment chamber, CEC, 24-48 hours before the start of the experiment. A portion of one of the leaves of the plant is enclosed within a cooled cuvette and is supplied with a continuous flow of air at a given, steady-state concentration of $^{12}CO_2$ (eg, 400ppm at a flow which will maintain 350ppm in the cuvette). Net photosynthesis, transpiration, and other biologically related functions are monitored continuously as explained above. The detectors are arranged on the plant at the desired positions and the geometry of the leaves and the petiole of the leaf on which the experiment is conducted is measured and entered into the computer (see fig 4A). On the morning of the experiment, as soon as the lights in the CEC come on, the background activity at each detector is determined and the detectors are calibrated with a standard ^{22}Na source. This information is automatically entered and stored in the computer. An updated listing of data by the thermal printer displays the information at a predetermined interval. Radioactive gases flow from the target chamber in the accelerator laboratory to the phytotron and the activity is monitored by the line monitor as explained above (profile #1, fig 4B) until a steady-state level is reached. The gases then flow through the chemical processing station and are monitored for steady-state level of specific activity (profile #2, fig 4B). At the appropriate time, the 4-way valve is turned to divert the flow of unlabeled air and substitute an identical flow of the Hot Mix at the same total CO_2 concentration as the original. The build-up of activity in the leaf and its movement in the transport stream are continuously measured and updated in the computer. A real-time continuous display of that behavior is shown in figure 4B, profile 4 for the leaf, and profiles 5,6,7,8 in the phloem. The specific activity of the gases exiting the leaf cuvette is shown in profile #3. All data input into the computer is stored on cassette tapes as well as listed in the updated printout.

Tracer studies of this type must be conducted when the leaf has reached, and is expected to maintain steady-state rates of photosynthesis and carbon allocation, because of the implicit assumption of steady state in tracer data analysis.

These conditions tend to be reached mid-morning in most plants grown in growth chambers. However, step input experiments early in the morning or late afternoon when the rates of carbon metabolism are changing with time are also possible, but require non-steady-state data analysis.

Two hours after stopping the tracer input in the leaf only ca 1.5% of the activity is left in the plant and the same experiment (or other experiments) can be repeated on the same plant under the same environmental conditions. However, it is not necessary to wait that long, since corrections by the computer for residual activity can be made at the same time data is acquired.

A host of ecologically-related environmental and biological factors can be tested with this technique which should lead to improved qualitative and quantitative understanding of plant responses to environmental stimuli.

CONCLUSION

An integrated approach to studying the effects of environmental factors on plants is described. Though the tracer described is ^{11}C, ^{13}N can be used for nitrogen fixation studies with minor changes in the system. ^{11}C and ^{13}N seem to provide very convenient tracers that are natural constituents of plants and their environments. A host of ecologically, agriculturally, and genetically important questions can be answered using this technique. The consequences of elevated CO_2 concentration in the atmosphere, the effects of water stress on growth rates of plants and the information required to genetically engineer a plant to suit our needs, are but a few of the major scientific questions that can be studied by this method.

ACKNOWLEDGMENTS

Research was supported jointly by the National Science Foundation Ecosystem Studies Program (DEB-22165) and the US Department of Energy Office of Carbon Dioxide and Climate Research (DEA 101-81ER60012). We also acknowledge the NSF Biological Research Resources Program (DEB80-21312) for support of the Duke University Phytotron.

REFERENCES

Cirilov, SD, Newton, JD, and Schapira, JP, 1966, Total cross sections for the reaction ^{12}C (^{3}He, ^{4}He) ^{11}C and ^{12}C (^{3}He, n) ^{14}O: Nuclear Physics, v 77, p 472-476.

Downs, RJ, Hellmers, H, and Kramer, PJ, 1972, Engineering problems in the design and operation of phytotrons: Am Soc of Heating Refrig and Air Conditioning Engineers Jour, June

1972, p 47-55.

Fares, Y, DeMichele, DW, Goeschl, JD, and Baltuskonis, DA, 1978, Continuously produced, high specific activity ^{11}C for studies of photosynthesis, transport and metabolism: Internatl Jour Appl Radiation Isotopes, v 29, p 431-441.

Gifford, RM, and Evans, LT, 1981, Photosynthesis, carbon partitioning, and yield: Ann Rev Plant Physiol, v 32, p 485-509.

Goeschl, JD, Magnuson, CE, DeMichele, DW and Sharpe, PJH, 1976, Concentration dependent unloading as a necessary assumption for a closed-form mathematical model of osmotically driven pressure-flow in phloem: Plant Physiol, v 58, p 556-562.

Kramer, PJ, Hellmers, H, and Downs, RJ, 1970, SEPEL: New phytotrons for environmental research: Bioscience, v 20, no. 22, p 1201-1208.

Loomis, RS, Rabbinge, R, and Ng, E, 1979, Explanatory models in crop physiology: Ann Rev Plant Physiol, v 30, p 339-367.

Magnuson, CE, Goeschl, JD, Sharpe, PJH and DeMichele, DW, 1979, Consequences of insufficient equations in model of the Munch hypothesis of phloem transport: Plant Cell and Environm, v 2, p 181-188.

Magnuson, CE, Fares, Y, Goeschl, JD, Nelson, CE, Strain, DR, Jaeger, CH and Bilpuch, EG, 1982, An integrated tracer kinetics system for studying carbon uptake and allocation in plants using continuously produced $^{11}CO_2$: Rad and Environm Biophys, in press.

Neales, TF, and Incoll, LD, 1968, The control of leaf photosynthesis rate by level of assimilate concentration in the leaf: A review of the hypothesis: Bot Rev, v 34, p 107-125.

Smith, KC, Magnuson, CE, Goeschl, JD and DeMichele, DW, 1980, A time-dependent mathematical expression of the Munch hypothesis of phloem transport: Jour Theor Biol, v 86, p 493-505.

[Radiocarbon, Vol 25, No. 2, 1983, P 441-446]

MEASUREMENT OF CARBON FIXATION AND ALLOCATION USING ^{11}C-LABELED CARBON DIOXIDE

Boyd R Strain*, John D Goeschl**, Charles H Jaeger*,
Youhanna Fares**, Charles E Magnuson**,
and Charles E Nelson+

INTRODUCTION

The real-time measurement of net photosynthesis and dark respiration of plants has been possible since the development of the infra-red analyzer and its application in the 1940's. This technique has allowed intensive investigations of the mechanisms and dynamics of carbon dioxide assimilation by green plants (Sestak, Catsky, and Jarvis, 1971). As a result, physiologic and ecologic aspects of net carbon dioxide exchange are the subject of much research (eg, Osmond, Bjorkman and Anderson, 1980).

Comparable research on the movement of carbon within the plant has been hindered, however, by the lack of a technique which would allow real-time observation of carbon translocation. Much tracer work with the radioisotope ^{14}C has been accomplished (Sestak, Catsky, and Jarvis, 1971), but it has not been generally possible to closely link carbon dioxide uptake and carbon movement using ^{14}C.

This β-emitting long-lived isotope has two primary drawbacks. 1) The low energy emission makes it necessary to destructively harvest tissues and to quantify radioactivity by scintillation counting of prepared samples. Thus, carbon translocation has to be determined by time-series and statistical procedures. Physiologic variability requires several to many replicates for each measurement.

---

*Botany Department and Phytotron, Duke University,
Durham, North Carolina 27706

**Biosystems Division, Industrial Engineering
Department, Texas A & M University, College Station,
Texas 77840

+Departments of Physics and Radiology, Duke University

2) The long half-life of ^{14}C prevents repeated and long-term measurements on a given individual. Once the radioisotope is applied to the plant, it is difficult or impossible to know how the isotope is moving internally. Biochemical conversions of carbohydrates following the initial labeling confuse the issue.

Since the 1930's (Fares *et al*, 1978) we have known that ^{11}C could be used as a carbon tracer. This short half-lived isotope has several advantages. 1) It decays by positron (+) emission followed by positron-electron annihilation with the emission of two oppositely-directed gamma rays. These rays have sufficient energy (0.511Mev) to be detected through several cm of living tissue. Thus, real-time movement of ^{11}C can be detected from outside of the plant without destructive harvesting. In fact, sensors can be located close to, but not touching the plant and carbon movement observed without disturbing the plant at all (Fares *et al*, 1978; Minchin and Troughton, 1980).

This paper describes the use of continuously produced and applied ^{11}C in measurements of carbon dioxide assimilation and C movement in plant research. This technique differs from the pulsing type ^{11}C research underway in other laboratories by being continuous and on-line with computer analysis making steady-state measurements of carbon fixation and movement possible. The studies to be described here will make clear the advantages of using continuously produced and applied short half-lived isotopes.

METHODS AND MATERIALS

The details of this technique have been previously described (Fares *et al*, 1978; Magnuson *et al*, 1982; Fares *et al*, 1983). It is not necessary to redescribe the hardware and the technical details here. It is, however, necessary to briefly describe the experimental protocol and the specific experimental methods employed.

Plants were grown in controlled environments of the Duke University Phytotron. Day/night temperature conditions were 28/20 ^{o}C with a 16-hour photoperiod. Light intensity was 600 mol m^{-2}s^{-1} (400-700nm). Relative humidity was 75% during the day and near 95% at night. Plants were grown in a standard 1:1:1 mixture by volume of vermiculite: gravel: turface (Jaeger, Hellmers and Teare, 1981). The plants were 8 weeks old when the measurements were made.

The plants used were cotton and velvet leaf. The latter plant is a weed in cotton fields throughout the southern United States. Both species are in the same plant family and they have similar environmental requirements for growth. It is known, however, that cool nights during the active growing season will damage the crop more than the weed. Just one seasonally cool night will decrease growth in cotton significantly more than the weed. This study compares the phloem transport of the two plant species to chilling of the conduction tissue.

One plant of each species was conditioned to the 28/20 day/night temperature. They were then moved into position for labeling with $^{11}CO_2$. The radioactive gas was passed through a leaf cuvette in a gas stream of $^{11}CO_2 + {}^{12}CO_2 = 400\ \mu l \cdot l^{-1}$. The plant photosynthesized the $^{11}CO_2$ into ^{11}C carbohydrates (alcohol soluble sugars and starch).

RESULTS

The labeled leaf on both species reaches ^{11}C steady state within 30 min after the initiation of the measurement. The activity in the phloem tissues of the stem 5cm below the petiole insertion of the labeled leaf reached steady state within 90 min.

Figure 1 is a representative on-line display of tracer profiles on a velvet leaf plant. Profile #7 shows the line activity of the $^{11}CO_2$ coming to the system. Line #10 is the activity in the labeled leaf. This detector-pair monitors the carbohydrates at the site of carbon fixation by the leaf. Lines #8 and #9 show activity of the $^{11}CO_2$ gas stream before and after the photosynthesis cuvette, respectively. The difference between these two lines #2, 3, and 4 show the ^{11}C activity at successively lower points on the stem. Line #1 shows the activity in the stem slightly above the petiole attachment.

After the plants reached radioactive steady state (Ca 90 min) the responses to 2-min temperature chills were recorded. Table 1 is a representative time series of such a treatment on one plant of each species. Relative values are shown so the responses can be directly compared. It is clear from table 1 that velvet leaf responded faster and to a greater extent than cotton.

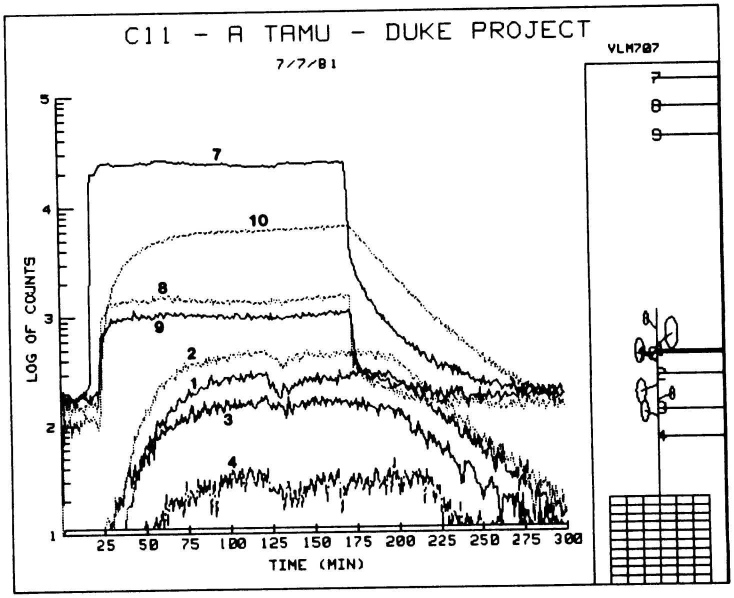

Fig. 1. Line-time display of tracer profiles of velvet leaf. On the right is a diagram of plant geometry showing detector location, leaf number, and relative leaf area. The numbered tracer lines are described in the text.

TABLE 1. Representative results in a test of the effect of temperature chilling on phloem transport rates in cotton and in velvet leaf. A 5° chill was applied for 2 min beginning at 90 min.

Time (min)	Relative activity (% cpm)* Cotton	Velvet Leaf
0	0	0
5	0	0
15	3	1
30	12	19
60	50	81
90	100	100
100	83	62
105	85	81
110	92	100
115	98	100
120	100	100

*Each column is the percent of the steady-state value.

DISCUSSION

Table 1 presents one set of measurements to show the application of the technique described in Fares et al (1983). The effect of a slight (5 °C) temperature chill on phloem transport kinetics is shown for cotton and one of its most serious weed species, velvet leaf.

Farmers have long observed that aseasonal cool nights in the height of the growing season will impede cotton growth more than the velvet leaf weed. This test shows a basic difference in the way these phylogenetically closely related species respond to temperature chilling. It is our hypothesis that carbon allocation is seriously impeded by cool temperatures in the cotton but recovers quickly in the velvet leaf. Thus, velvet leaf recovers quickly from the occasional cool night whereas cotton requires much longer to recover.

The steady-state ^{11}C technique clearly showed a possible mechanism for such a difference. Additional research is now underway to examine this hypothesis in more detail.

ACKNOWLEDGMENTS

Research was supported jointly by the National Science Foundation, Ecosystems Program (DEB80-22165), and the US Department of Energy, Office of Carbon Dioxide and Climate Research (DEA 101-31ER60012). We also acknowledge the NSF Biological Research Resources Program (DEB80-12312) for support of the Duke University Phytotron.

REFERENCES

Fares, Y, Demichele, DW, Goeschl, JD, and Baltuskonis, DA, 1978, Continuously produced ^{11}C for studies of photosynthesis, transport and metabolism: Internatl Jour Appl Radiation Isotopes, v 29, 431-441.

Fares, Y, Goeschl, JD, Magnuson, CE, Nelson, CE, Strain, BR, and Jaeger, CH, 1983, A system for studying carbon translocation in plants using ^{11}C labeled carbon dioxide: Radiocarbon, v 25.

Jaeger, CH, Hellmers, H, Teare, ID, 1981, An improved medium fonutriculture incorporating arcillite: Horticultural Sci, v 16, 176-177.

Magnuson, CE, Fares, Y, Goeschl, JD, Nelson, CE, Strain, BR, Jaeger, CH, and EC Bilpuch, 1982, An integrated tracer kinetics system for studying carbon uptake and allocation in plants using continuously produced $^{11}CO_2$: Radiation Environmental Biophys, v 21, 51-65.

Minchin, PEH and Troughton JH, 1980, Quantitative interpretation of phloem translocation data: Ann Rev Plant Physiol, v 31, 191-215.

Osmond, CB, Bjorkman, O, and Anderson, DJ, 1980, Physiological processes in plant ecology: Toward a synthesis with Atriplex: Ecol studies vol 36, New York, Springer-Verlag, 468 p.

Sestak, Z, Catsky, J, and Jarvis, PG, 1971, Plant photosynthetic production: Manuel of methods: Dr W Junk Publs, The Hague, 818 p.

IV. OCEANOGRAPHY

[Radiocarbon, Vol 25, No. 2, 1983, P 449-458]

LONG-TERM VARIABILITY OF TEMPERATURE AND ^{14}C IN THE GULF STREAM: OCEANOGRAPHIC IMPLICATIONS

ELLEN M DRUFFEL
Department of Chemistry, Woods Hole Oceanographic Institution
Woods Hole, Massachusetts 02543

ABSTRACT. Variability in temperature and ^{14}C levels are recorded in coralline aragonite that grew in the Gulf Stream during the past four centuries. In particular, $^{18}O/^{16}O$ ratios reflect a decrease of ca 1°C in surface water temperature during the latter part of the Little Ice age. ^{14}C levels also rose in the surface waters of the Gulf Stream and in atmospheric CO_2 during the Maunder minimum. These observations indicate that ocean circulation may have been significantly different in the North Atlantic around the beginning of the 18th century.

INTRODUCTION

^{14}C levels were especially high during 3 distinct periods of the 2nd millenium AD (Stuiver and Quay, 1981). These intervals are known as the Wolf minimum (AD 1300), Sporer minimum (AD 1500) and Maunder minimum (AD 1700), when solar activity was especially low (Waldmeier, 1961; Eddy, 1976). The galactic cosmic ray flux responsible for ^{14}C production is modulated by changes in solar wind magnetic fields. When the intensity of the solar wind decreases, as in a time of low sun spot numbers, more galactic cosmic rays are admitted to the earth's atmosphere, causing increased ^{14}C production. The three periods of unusually high ^{14}C production were coincident, though not directly correlated (Stuiver, 1980), with recorded intervals of especially severe winters in Europe (Suess, 1980), a period known as the Little Ice age. Whether the Little Ice age was a direct result of low solar activity or a coincidence has not yet been resolved.

One possibility not yet investigated is that which could involve the oceans as the cause of the increase in atmospheric ^{14}C levels. It is conceivable that decreased vertical mixing in the upper few hundred meters of the water column could have induced this rise in ^{14}C. In order to eliminate this possibility, however, it is necessary to acquire ^{14}C and temperature records for this period in the oceans. Banded, hermatypic corals are useful for recovering valuable information on past surface ocean water character (Druffel and Linick, 1978; Nozaki et al, 1978; Druffel, 1982). Coral records can be correlated with atmospheric ^{14}C records to determine the causal relationship and timing of ^{14}C variations observed in these two reservoirs during the past, and they can also yield important information about changes in ocean circulation during the Little Ice age.

Within the aragonitic skeleton, corals record the $^{14}C/^{12}C$ ratio of the dissolved inorganic carbon (DIC) in sea water at the time of formation (Druffel and Linick, 1978). Temperature records can also be reconstructed for waters at the time of formation using the $^{18}O/^{16}O$ ratio of calcium carbonate in corals (Fairbanks and Dodge, 1979). As the world's surface oceans are saturated with respect to aragonite, hermatypic coral skeletons do not dissolve with time. Nor does aragonite exchange with any other source of carbon. Coralline aragonite is a permanent, unaltered record of the $^{14}C/^{12}C$ and $^{18}O/^{16}O$ ratios that existed in past surface sea waters.

A morphologic characteristic that make reef-building corals so useful as geochemical probes is the annual density variation of the accreted aragonite. These 'bands' are primary skeletal features exhibited as seasonal variations in the bulk density of the secreted skeleton (Buddemeier, Maragos, and Knutson, 1974). The growth bands are discernible by X-ray (some by the naked eye) of a thin slab of coral skeleton (4 to 10mm thick). Many authors have confirmed the annual nature of coral banding by using various techniques such as in situ alizarin staining, densiometry, autoradiography, and direct field observations (Knutson, Buddemeier and Smith, 1972; MacIntyre and Smith, 1974; Hudson et al, 1976). Various radioisotopes, such as bomb-produced ^{14}C, ^{90}Sr, and ^{228}Ra have also corroborated the annual nature of growth bands in corals (Druffel, 1980; Toggweiler, 1980; Moore and Krishnaswami, 1974).

PROCEDURE

The coral cores used in this project were collected from "The Rocks" reef off the Florida Keys. They were laved by waters flowing through the Florida Straits, a part of the Gulf Stream System, which originates in the Caribbean Sea. Hudson et al (1976) used corals of the same species (Montastrea annularis) from the Florida Straits to illustrate a second type of high density banding, stress bands, that occur during periods of extreme cold on the reef. These workers observed an excellent correlation between Cold Fronts recorded in southern Florida and the appearance of unusually high density bands in the coral record spanning the past 50 years.

Examination of the stress banding in two cores reveals an excellent correlation with Cold Fronts recorded as far back as 1856. This indicates that Montastrea annularis do not eliminate growth bands, nor do they accrete extra bands.

The coral cores were X-rayed (fig 1) and sectioned in the manner described elsewhere (Druffel, 1982). ^{14}C measurements were made on samples representing one to ten years' growth. Gas proportional counting techniques were used with acetylene as the counting gas. ^{14}C values are

TR II CORAL CORE

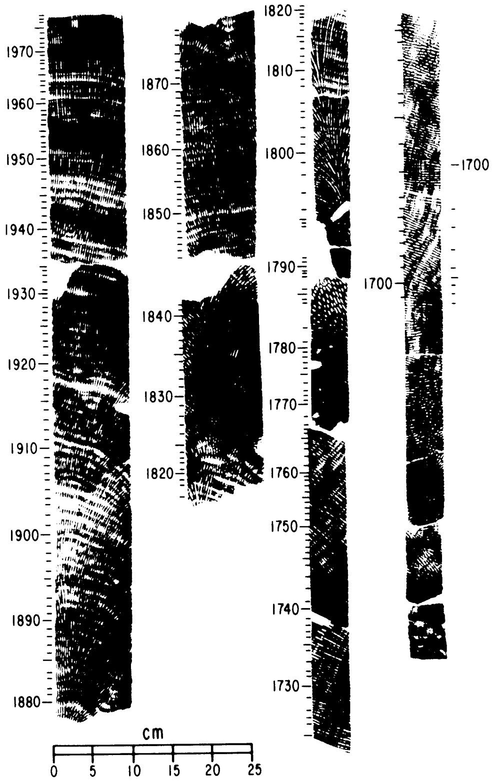

Fig 1. X-radiographs of the coral slabs from the core of Montastrea annularis (TRII) collected in July, 1978. A core collected in June 1975 (TRI) was also used in this project. Dark, dense bands represent growth during warm water months (July through September). Thus, TRII represents coral growth from AD 1694 to 1978.

reported in the standard Δ notation (Broecker and Olson, 1961) and were corrected for decay from the time of formation to AD 1950. Precision of these measurements ranged from 3^{o}/oo to 6^{o}/oo. $^{18}O/^{16}O$ ratios were performed by W G Mook at the University of Groningen on samples of one year's growth (Druffel, 1982). Results are reported in the standard δ (^{o}/oo) notation relative to the PDB-1 standard. Precision for isotopic measurements was ±0.05^{o}/oo.

RESULTS

^{14}C measurements were made on two Florida coral cores (TRII shown in Figure 2) for the period AD 1642-1952. Several trends are apparent in this time series. First, the baseline $\Delta^{14}C$ value is ca $-48^o/oo$. A deviation from this trend occurred ca AD 1710, when values rose sharply by $7^o/oo$ in about ten years and then slowly decayed back to $-50^o/oo$ by 1750. Second, $\Delta^{14}C$ values decreased slowly during the early to mid-1800's by $4-5^o/oo$, and then returned to the ambient level ($-50^o/oo$) rather quickly. Third, a decrease of $11^o/oo$ is noticed from AD 1900-1952, and is attributed to the dilution of existing ^{14}C levels by the input of fossil fuel CO_2 to the oceans (Druffel and Linick, 1978; Nozaki et al, 1978). Estimates for the Suess effect in the atmosphere range from $-18^o/oo$ to $-25^o/oo$.

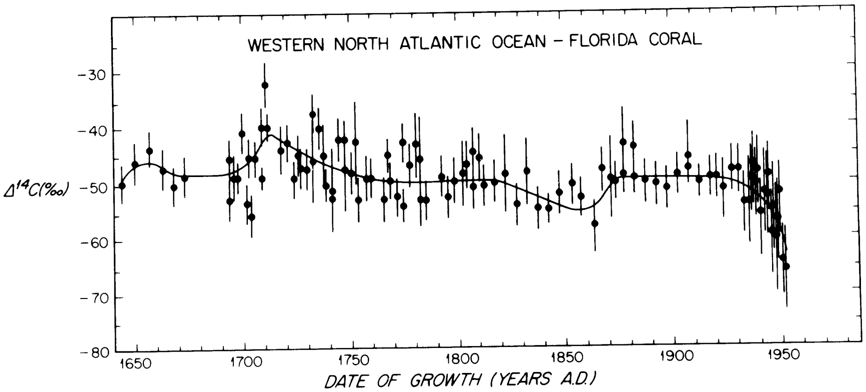

Fig 2. $\Delta^{14}C$ measurements of Florida coral cores (1642-1952). Three long-term trends are apparent: 1) 1710-1750: Little Ice age effect seen as a $7^o/oo$ rise in $\Delta^{14}C$ and subsequent decrease. This is probably the result of increased ^{14}C levels in the atmosphere during this time; 2) 1820-1870: $4^o/oo$ to $5^o/oo$ decrease in $\Delta^{14}C$, which may be the result of decreased ^{14}C levels in the atmosphere during the 19th century; 3) 1900-1952: Suess effect is ca $-12^o/oo$ in the Gulf Stream surface ocean waters (Druffel and Linick, 1978).

To interpret this oceanic ^{14}C record, it must be correlated with the ^{14}C record in the atmosphere obtained from tree rings (Stuiver and Quay, 1981). Line drawings representing both of these ^{14}C records appear in Figure 3. As CO_2 is exchanged between atmosphere and ocean, a rise in the atmospheric $^{14}CO_2$ concentration would also be

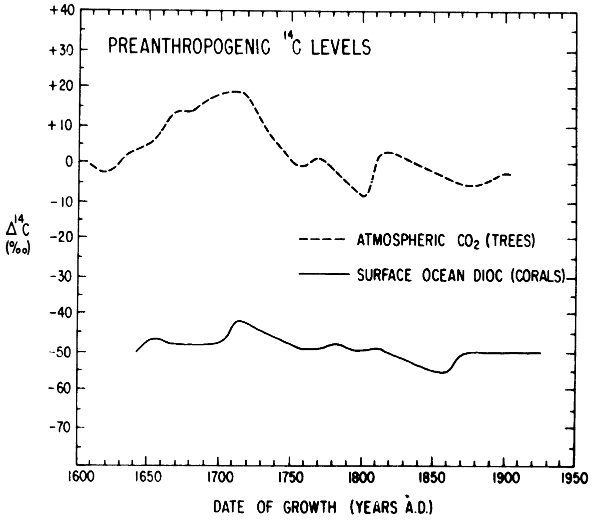

Fig 3. Average pre-anthropogenic ^{14}C levels in tree rings and coral rings that grew from AD 1600-1900. The $\Delta^{14}C$ trend for trees is based on data from numerous areas in North America (Stuiver and Quay, 1980; Tans, de Jong and Mook, 1979). The $\Delta^{14}C$ trend for corals is a spline curve fitted to data from Montastrea annularis collected from the Florida Straits (Druffel, 1982).

expected in the DIC of the surface ocean. Such is the case with the ^{14}C peak ca 1700. There is a lag time of 3 to 4 decades between the onset of the rise in the atmosphere and in the ocean. Part of this delay can be attributed to the long residence time of 10-15 years for $^{14}CO_2$ in the atmosphere (Druffel and Suess, in press). The rise probably originates in the atmosphere due to solar modulation of the cosmic-ray flux. The overall ^{14}C rise in the atmosphere was ca 20‰, whereas that in the oceans was only 7‰. The signal was attenuated in the oceans due to vertical exchange of older subsurface waters (which contain less ^{14}C due to *in situ* decay) with surface waters.

During the 19th century, ^{14}C levels in both the atmosphere and ocean decreased substantially. Again, the amount of decrease in the ocean (4-5‰) was attenuated in comparison to that in the atmosphere (9‰). This change in the ^{14}C level is also believed to have been caused by variation in solar activity; the decrease in ^{14}C originated in the atmosphere and then filtered into the surface ocean by gas exchange.

An alternative explanation for the rise in ^{14}C ca AD 1700 involves the role of the oceans during this period. A decrease in the rate of vertical mixing in the upper few hundred meters of the water column could conceivably have caused a rise in ^{14}C levels in both the surface ocean and atmosphere. This scenario would also be accompanied by higher surface water temperatures, a phenomenon not expected during a small ice age.

Stable isotopic measurements of yearly samples from the Florida cores, however, indicate that the water temperature in the Gulf Stream was slightly lower during the early 1700's and increased ca 1°C by 1800 (fig 4). Superimposed on this trend toward lighter (warmer) $\delta^{18}O$ values with time, is a fine structure that illustrates variations on a decade time scale. Cooler surface water temperatures during the early 1700's implies that there was an increase in vertical mixing between surface and subsurface waters, not a decrease as would have been the case had changes in ocean circulation been the cause of the ^{14}C rise in the atmosphere during this period.

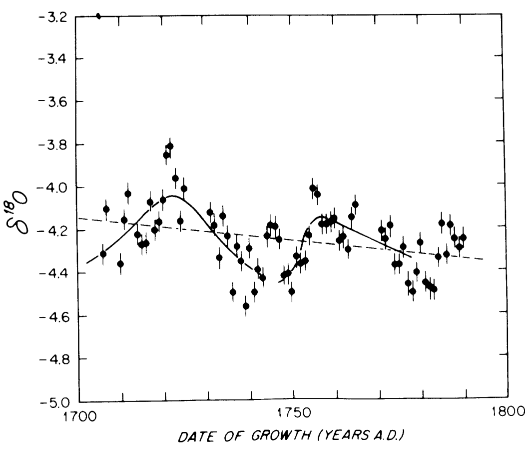

Fig 4. $\delta^{18}O$ measurements (made by W G Mook) for annual coral samples from the TRI core, relative to the Chicago PDB standard. A least squares fit of the individual measurements (dashed line) reveals a 0.2°/oo decrease from AD 1700-1790. Using the calibration curve of Dunbar and Wellington (1981) this decrease represents an overall rise in seawater temperature of ca 1°C from 1700-1790. There also appears to be two maxima in $\delta^{18}O$ ca 1720 and 1760, representing periods of lower seawater temperature.

OCEANOGRAPHIC IMPLICATIONS

The Gulf Stream originates in the Sargasso Sea, an anticyclonic, subtropical gyre in the North Atlantic (fig 5).

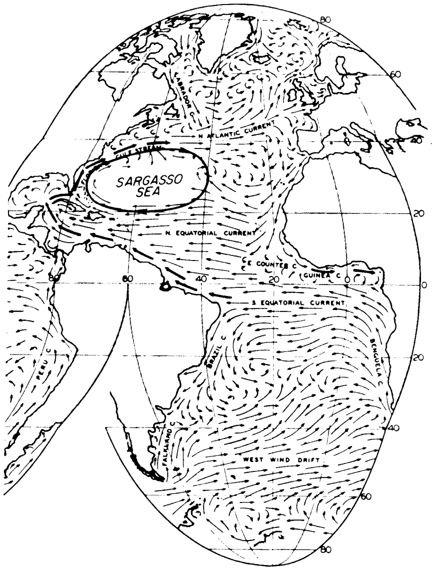

Fig 5. Surface currents of the Atlantic Ocean. The Sargasso Sea, a subtropical gyre in the northwestern Atlantic, circulates in an anticyclonic (clockwise) direction and is the main source of water for the Gulf Stream.

The circulation in the surface mixed layer is wind-driven (Ekman transport) and that in the deep water is powered by geostrophic forces. Ekman transport is convergent in a subtropical gyre, which forces water downward from the mixed layer (fig 6). There is a complex process at work that selects only late winter water for actual net downward pumping, called Ekman pumping, into the geostrophic regime below (Stommel, 1979). As the surface waters in the Gulf Stream were 1°C cooler during the early 1700's, the Sargasso Sea surface waters were probably also cooler during this period as well. It is likely that cooler surface water temperatures during the latter part of the Little Ice age promoted enhanced downward penetration of waters in the Sargasso Sea during the late winter, and perhaps induced prolonged convection that extended from early winter to

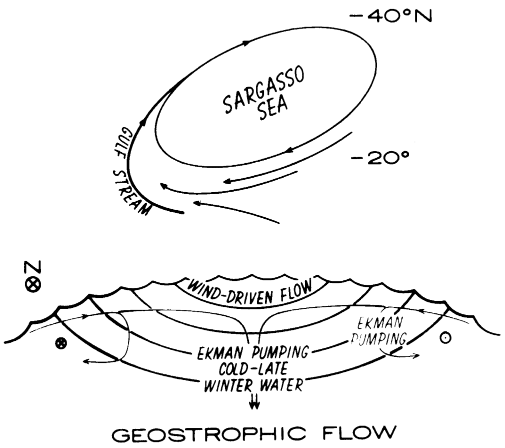

Fig 6. Areal view of the circulation of the Sargasso Sea (upper portion). Schematic representation of isopycnals and circulation within the gyre along 30°N (lower portion). Water is carried downward by Ekman transport (downwelling) and is incorporated into the deeper geostrophic flow only during late winter, when water is cold and dense.

spring.

Variations in temperature on decade time scales in Gulf Stream surface waters (fig 4) also have important implications for our understanding of ocean circulation. Jenkins (1982) calculated a factor of two variation in the shallow water mass renewal rates from 1954-1980 based on oxygen, salinity, and ^3H-^3He data from the Sargasso Sea. The data presented here also imply that long-term variations in circulation have occurred in the ocean and cannot be ignored when modeling geochemical quantities such as Lagrangian tracers.

CONCLUSIONS

The ^{14}C rise in surface waters of the Florida Straits and in atmospheric CO_2 during the Little Ice age was probably the result of reduced solar activity during the Maunder minimum. Stable isotopic analyses ($\delta^{18}O$) of these corals show that slightly cooler surface water temperatures (by 1°C) were present in the Gulf Stream during the latter part of the Little Ice age. This cooling suggests that ocean mixing patterns may have been different in the Gulf Stream during this period. A likely scenario may have included enhanced convection in the Sargasso Sea that consisted not only of late winter water (Stommel, 1979) but also the downward penetration of cooler spring and early winter water into the geostrophic regime below.

ACKNOWLEDGMENTS

My thanks go to J H Hudson and E A Shinn for providing the coral cores. The technical expertise of Sheila Griffin, Paul Yeager, Donald Sullivan, Carol Hutto, and Timothy Linick is greatly appreciated. I am particularly grateful to Willem Mook, who measured the $\delta^{18}O$, and Peter Williams, Joe Reid, Hans Oeschger, Peter Brewer, Werner Deuser, Lloyd Keigwin, J Hudson, Bob Michel, Stephen Rodriguez, Bill Jenkins, Peter Rhines, Hans Suess, and Henry Stommel for enlightening discussions. I also thank Margaret Harvey and Ted Velasquez for their help in preparing the manuscript. Financial support from the National Science Foundation through grants EAR-78-15183 and OCE-79-17652, and from the Woods Hole Oceanographic Industries Program (No. 4470) is gratefully acknowledged. This paper is contribution No. 5191 from the Woods Hole Oceanographic Institution.

REFERENCES

Broecker, W S and Olson, E A, 1961, Lamont radiocarbon measurements VIII: Radiocarbon, v 3, p 176-204.

Buddemeier, R W, Maragos J E, and Knutson, D W, 1974, Radiographic studies of reef coral exoskeletons: rates and patterns of coral growth: Jour Experimental Marine Biol Ecol, v 14, p 179-200.

Druffel, E M, 1980, Radiocarbon in annual corals rings from Belize and Florida, in Stuiver, Minze and Kra, Renee, eds, Internatl radiocarbon conf, 10th, Proc: Radiocarbon, v 22, no 2, p 363-371.

------------ 1982, Banded corals: Changes in oceanic carbon-14 levels during the Little Ice Age: Science, v 218, p 13-19.

Druffel, E M and Linick, T W, 1978, Radiocarbon in annual coral rings from Florida: Geophys Research Letters, v 5, p 913-916.

Druffel, E M and Suess, H E, in press, On the radiocarbon record in banded corals: Exchange parameters and net transport of $^{14}CO_2$ between atmosphere and surface ocean: Jour Geophys Research.

Dunbar, R B, and Wellington, G M, 1981, Stable isotopes in a branching coral monitor seasonal temperature variation: Nature, v 293, p 453-455.

Eddy, J A, 1976, The Maunder minimum: Science, v 192, p 1189.

Fairbanks, R G and Dodge, R E, 1979, Annual periodicity of the $^{18}O/^{16}O$ and $^{13}C/^{12}C$ ratios in the coral Montastrea annularis: Geochim et Cosmochim Acta, v 43, p 1009-1020.

Hudson, J A, Shinn, E A, Halley, R B, and Lidz, B, 1976, Sclerochronology: a tool for interpreting past environments: Geology, v 4, p 361-364.

Jenkins, W J, 1982, On the climate of a subtropical ocean gyre: Decade time-scale variations in water mass renewal in the Sargasso Sea, Jour Marine Research, v 40, p 265-290.

Knutson, D W, Buddemeier, R W, and Smith, S V, 1972, Coral chronometers: seasonal growth bands in reef corals: Science, v 177, p 270-272.

MacIntyre, I G, and Smith, S V, 1974, X-radiographic studies of skeletal development in modern coral colonies, in Internatl symposium coral reefs, 2nd, Proc: Brisbane, p 277-287.

Moore, W S and Krishnaswami, S, 1974, Correlation of x-radiography revealed banding in corals with radiometric growth rates, in Internatl coral reef Symposium, 2nd, Proc: Brisbane, p 269-276.

Nozaki, Y, Rye, D M, Turekian, K K, and Dodge, R E, 1978, A 200-year record of carbon-13 and carbon-14 variations in a Bermuda coral: Geophys Research Letters, v 5, p 825-828.

Stommel, H, 1979, Determination of water mass properties of water pumped down from the Ekman layer to the geostrophic flow below: Natl Acad Sci, 76th, Proc: Washington, DC, p 3051-55.

Stuiver, M, 1980, Solar variability and climatic change during the current millennium: Nature, v 286, p 868-871.

Stuiver, M and Quay, P M, 1980, Changes in atmospheric ^{14}C attributed to a variable sun: Science, v 207, p 11-19.

------------------------ 1981, Atmospheric ^{14}C changes resulting from fossil fuel CO_2 release and cosmic ray flux variability: Earth Planetary Sci Letters, v 53, p 349-362.

Suess, H E, 1980, The radiocarbon record in tree rings of the last 8000 years, in Stuiver, Minze and Kra, Renee, eds, Internatl radiocarbon conf, 10th, Proc: Radiocarbon, v 22, no 2, p 200-209.

Tans, P P, de Jong, A F M, and Mook, W G, 1979, Natural atmospheric ^{14}C variation and the Suess effect: Nature, v 280, p 826.

Toggweiler, J F, 1980, Time histories of Sr-90 in Pacific surface water as recorded by head forming corals: EOS, v 61, no. 46, p 984.

Waldmeier, M, 1961, The sunspot activity in the years 1610-1960: Zurich, Schultess.

[Radiocarbon, Vol 25, No. 2, 1983, P 459-471]

CARBON EXCHANGE BETWEEN ATMOSPHERE AND OCEANS IN A LATITUDE-DEPENDENT ADVECTION-DIFFUSION MODEL

GERHARD KRATZ, G H KOHLMAIER, E O SIRÉ, URSULA FISCHBACH and HORST BRÖHL

Institut für Physikalische und Theoretische Chemie
Universität Frankfurt, Robert-Mayer-Str 11
D-6000 Frankfurt/M, West Germany

ABSTRACT. Marine transport of inorganic and organic carbon is simulated by means of a computer model in which the oceans are divided into a high and low latitude region. Water transport (and with it carbon transport) is reproduced 1) as downwelling of surface waters at low latitudes, and 2) in general, as different depth-dependent turbulent diffusion in both deep-sea regions. The model is calibrated with pre-bomb ^{14}C and validated against perturbations of total carbon, $^{13}C/C$- and $^{14}C/C$-ratios; it is compatible with carbon release from fossil fuels and from biogenic sources.

INTRODUCTION

In view of possibly serious climatic consequences of increased atmospheric CO_2 (greenhouse-effect), efforts have been made to model the cycling of carbon through the global environment. The reliability of a simulation model is increased according to the number of independent observations it can verify. A major problem is whether the terrestrial biota are to be regarded as a source or a sink for additional atmospheric CO_2. The model presented here has been developed to account for at least part of an additional CO_2 input into the atmosphere resulting from forest destruction and desertification.

ATMOSPHERE AND BIOSPHERE

The model atmosphere is subdivided into tropospheric and stratospheric parts. The total atmospheric CO_2 content in the initial stationary state was taken to be 608Gt C (≙ 285ppm). Exchange between the two atmospheric compartments is linearly donor-controlled with a stratosphere-to-troposphere exchange time of 2 years (Machta, 1973). Data for fossil fuel input into the troposphere is taken from Rotty (1981) for the time period 1860-1978 (Fig 1). Natural production of ^{14}C in the stratosphere ($P^{14}_{nat}(t)$) is assumed time dependent according to the variation of Aa indices (Stuiver and Quay, 1980):

$$P^{14}_{nat}(t) = P^{14}_{o} + (0.43 - 0.024 \cdot Aa) \frac{O_e \cdot \theta}{N_A} \qquad (1a)$$

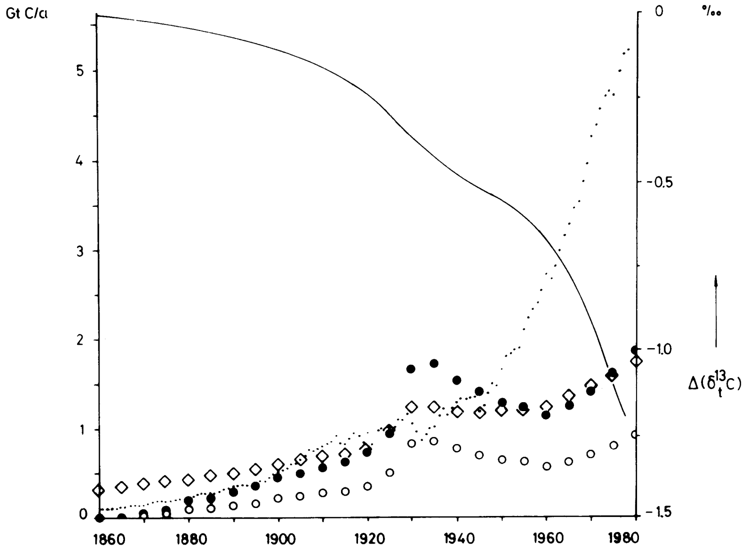

Fig 1. $\Delta(\delta_t^{13}C)$ in response to total carbon inputs into the troposphere (solid line)

.... = fossil fuel release

oooo = net biogenic input as introduced into the model calculations ($F_{b,net}$)

●●●● = total biogenic release ($F_{b,tot}$)

◇◇◇ = 2 · $F_{b,net}$ as estimated in Kohlmaier et al (1981)

O_e: earth's surface $5.1 \cdot 10^{18} cm^2$, θ: $31.6 \cdot 10^6$ sec/a, N_A: Avogadro's number, P_o^{14}: stationary ^{14}C production. The bomb ^{14}C production ($P_b^{14}(t)$) is taken from Killough (1980). The total ^{14}C production is then

$$P^{14}(t) = P_{nat}^{14}(t) + P_b^{14}(t) \qquad (1b)$$

Since the description of the oceanic part of the global carbon cycle is our primary concern here, only a summary of the terrestrial biosphere part will be given (see Kohlmaier et al, 1981, for details). The terrestrial biota are subdivided into five major biomes (tropical forests, tropical grasslands, extra-tropical forests, extra-tropical grasslands and deserts) each consisting of living biomass and humus. In order to model regrowth of cleared forest areas, the living biomass of these biomes was further subdivided into 20 compartments that extend over varying areas each representing a certain growth state. Under such assumptions we can model a steady state for a constant forest clearing rate. The total amount of CO_2 released through the perturbation of the biota is $F_{b,tot}$, the net flux to the atmosphere resulting from deforestation ($F_{b,net}$) is then given by the difference between $F_{b,tot}$ and the net ecosystem production ($F_{b,NEP}$) (fig 1).

Non-tropical forests are assumed to be affected by wildfires and clearings, whereas tropical forest areas are diminished by commercial clearings and increased permanent agriculture. Tropical forest areas cleared for shifting cultivation are assumed to be regrown, and soil erosion and charcoal formation are accounted for (Buringh, 1979; Seiler and Crutzen, 1980). Former model calculations (Kohlmaier et al, 1981) yielded a total net biospheric input of ca 2Gt C/a during 1980. Best agreement with the measured atmospheric ^{13}C data is obtained, if 50 % of this input is introduced into the model calculations.

OCEANS

The model ocean consists of two regions of high (c) and low (1) latitudes, respectively (fig 2).

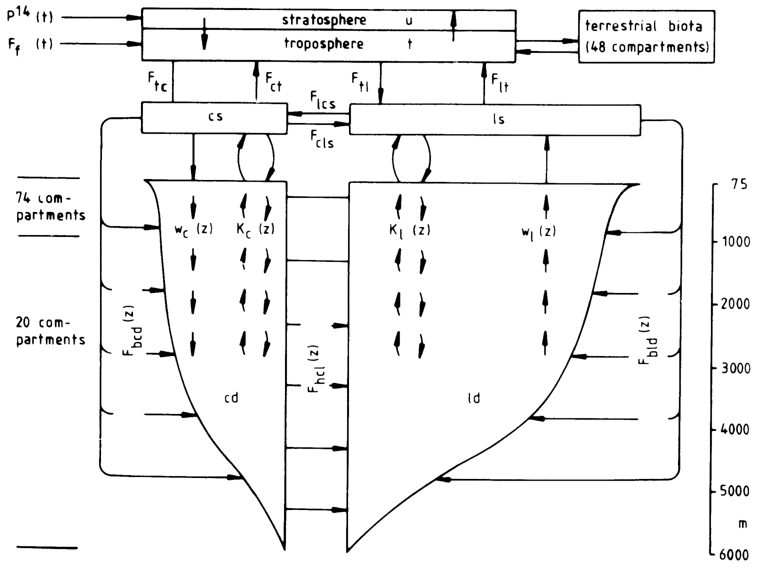

Fig 2. Compartments and fluxes in the atmosphere-ocean-sub-system of the carbon cycle model
l = ocean region of warm surface water or low latitudes
c = ocean region of cold surface water or high latitudes
s = surface ocean compartments
d = deep sea
F_{bcd}, F_{bld} = sinking of biogenic matter and dissolution in the high and low latitudes deep sea, respectively
F_{hcl} = horizontal flux due to water mass movement
w_c, w_l = sinking and upwelling velocities
K_c, K_l = eddy diffusion constants in the deep sea of high and low latitudes, respectively

The subdivision represents 1) different CO_2 uptake behaviors of cold and warm surface waters resulting in a net flux of CO_2 from equatorial oceans via the atmosphere to high latitudes surface waters, 2) different turbulent diffusivities in each deep sea region, 3) advection, i e, the sinking of cold surface water of high latitudes which spreads into low latitudes in the deep sea where it upwells. The surface water compartments are connected by fluxes in either direction, the difference of which corresponds to the net deep circulation of water masses. In the computer model it is possible to set the boundary latitude between the two ocean regions alternatively at either 40, 50, or 60°N and S, respectively, but only one model with an ocean subdivision at 40° is presented here. This model structure does not take into account that regions of deep water formation are rather restricted, nor does it show that at least part of the surface water that sinks is not derived from horizontally admixed surface water but from deeper layers and thus can only partially reach isotopic equilibrium with atmospheric $^{13}C/C$ and $^{14}C/C$.

The depth of both surface compartments is chosen as 75m. The depth interval from 75 to 1000m has been subdivided into 37 compartments in each region, each extending over a depth of 25m. The deep sea from 1000 to 6000 m is represented by 10 compartments 500m deep in each region (Oeschger et al, 1975). The volume of each compartment in either region is determined from the hypsometric curve according to Menard and Smith (1966).

Exchange between atmosphere and oceans is proportional to the respective CO_2 partial pressures:

$$F_{tc} = G_c/V_m \cdot p_t \qquad F_{ct} = G_c/V_m \cdot p_{cs} \tag{2a,b}$$

$$F_{tl} = G_l/V_m \cdot p_t \qquad F_{lt} = G_l/V_m \cdot p_{ls} \tag{2c,d}$$

V_m: molar volume, $0.0224 m^3/mole$, G_c, G_l: total gas exchange (in m^3/a) in either ocean region, where $G_c + G_l = G$.

The CO_2 partial pressures in the surface ocean compartments are calculated from the corresponding ΣC considering the chemical equilibria which determine the pH in surface waters (calculation procedure, see Bacastow, 1981). Temperatures of 11 and 25°C, respectively, in either surface compartment directly influence solubility and other equilibrium constants.

Fluxes of isotopes ^{13}C and ^{14}C from compartment i to j are generally formulated as

$$F_{ij}^{13} = \overline{\alpha_{ij}^{13}}\, Q_i^{13}\, F_{ij} \qquad F_{ij}^{14} = \overline{Q_i^{14}}\, F_{ij} \tag{3a,b}$$

$\overline{\alpha^{13}_{ij}}$ = corrected fractionation factor for ^{13}C; Q^{13} = isotopic ratio of mole numbers n^{13}/n or concentrations c^{13}/c (n and c refer to total carbon)

$\overline{Q^{14}}$ = isotopic ratio for $^{14}C/C$ from fractionation corrected $\Delta^{14}C$ values: $\overline{Q^{14}} = (\Delta^{14}C/1000 + 1)\cdot Q^{14}_{std}$

$Q^{14}_{std} = 1.176\cdot 10^{-12}$ (Karlén et al, 1964); F_{ij} = total carbon flux

$\overline{\alpha^{13}_{ij}}$ is derived from α^{13}_{ij} according to

$$\overline{\alpha^{13}_{ij}} = \alpha^{13}_{ij}/[1-(1-\alpha^{13}_{ij})\cdot Q^{13}_{i0}] \tag{4}$$

0 = stationary state. α^{13}_{tc} and α^{13}_{tl} are calculated according to Vogel, Grootes and Mook (1970), yielding corrected values of 0.99837 and 0.99842 for high and low latitudes, respectively. Considering isotopic equilibration among CO_2, HCO_3^- and CO_3^{2-}, as given by Emrich, Ehhalt and Vogel (1970), leads to values for $\overline{\alpha^{13}_{ct}}$ (0.98872) and $\overline{\alpha^{13}_{lt}}$ (0.99028).

Variation of total carbon content (in mole numbers n) in deep-sea compartment, i, of either region is described as:

$$\begin{aligned}\dot{n}_{cd}(i) &= F_{ad,c}(i) - F_{ad,c}(i+1) - F_{hcl}(i)\\ &\quad - F_{diff,c}(i) + F_{diff,c}(i+1) + F_{bcd}\end{aligned} \tag{5a}$$

$$\begin{aligned}\dot{n}_{ld}(i) &= F_{ad,l}(i+1) - F_{ad,l}(i) + F_{hcl}(i)\\ &\quad + F_{diff,l}(i+1) - F_{diff,l}(i) + F_{bld}(i)\end{aligned} \tag{5b}$$

Vertical advection fluxes are denoted by F_{ad}, horizontal fluxes being F_{hcl}; F_{diff} are turbulent diffusion fluxes and F_{bd} represent the transport of biogenic matter to the deep sea and its subsequent dissolution. Indices, i, refer to the upper boundary of compartment, i. The individual fluxes are

$$F_{ad,c}(i) = W_d(i)\ c_{cd}(i-1) \qquad F_{ad,l}(i) = W_d(i)\ c_{ld}(i) \tag{6a,b}$$

$$F_{hcl}(i) = [W_d(i) - W_d(i+1)]\ c_{cd}(i) \tag{6c}$$

$$F_{diff,c}(i) = \kappa\ O_s\ \overline{h}(i)\ K_c(i)[c_{cd}(i) - c_{cd}(i-1)]/\Delta z(i) \tag{6d}$$

$$F_{diff,l}(i) = (1-\kappa)O_s\overline{h}(i)\ K_l(i)[c_{ld}(i) - c_{ld}(i-1)]/\Delta z(i) \tag{6e}$$

$W_d(i)$ is the water mass passing through the upper boundary area $O_s\overline{h}(i)$, such that $W_d(i) = \kappa\ O_s\ \overline{h}(i)\ w_c(i) = (1-\kappa)\ O_s\ \overline{h}(i)\ w_l(i)$ where κ is the ratio of high latitudes region to total ocean surface area (0.332); $w_c(i)$ and $w_l(i)$ are downwelling and upwelling velocity, respectively. $K_c(i)$ and $K_l(i)$ are turbulent diffusion constants. The boundary conditions for the two bottom compartments are:

$$W_d(i+1) = 0, \quad K_c(i+1) = 0, \quad K_l(i+1) = 0 \tag{7a-c}$$

The related differential equations for ^{13}C and ^{14}C differ significantly in two ways: 1) for ^{14}C, the decay term $\lambda n^{14}_{cd}(i)$ and $\lambda n^{14}_{ld}(i)$ must be added, 2) the isotopic composition of the biogenic flux is always assumed proportional to the respective biotic isotopic ratios.

The time behavior of the surface compartments can now be described by:

$$\dot{n}_{cs} = F_{tc} - F_{ct} + F_{lcs} - F_{cls} - F_{ad,c}(1) + F_{diff,c}(1) - F_{csb}$$
$$\dot{n}_{ls} = F_{tl} - F_{lt} + F_{cls} - F_{lcs} + F_{ad,l}(1) + F_{diff,l}(1) - F_{lsb}$$

(8a,b)

where F_{cls} and F_{lcs} denote the horizontal fluxes connecting the surface compartments.

$$F_{cls} = W_{cls}\, c_{cs} \qquad F_{lcs} = W_{lcs}\, c_{ls} \tag{9a,b}$$

$$W_{lcs} - W_{cls} = W_d(1) \tag{9c}$$

$$F_{csb} = \sum_i F_{bcd}(i) \qquad F_{lsb} = \sum_i F_{bld}(i) \tag{9d,e}$$

According to equations (5a,b) and (6a-e), the concentrations for the stationary state ($\dot{n}_{cd0} = \dot{n}_{ld0} = 0$) in compartments (i-1) can be derived from the stationary concentrations in compartments i and (i+1). Under consideration of the additional decay term for ^{14}C analogue equations yield the stationary concentrations for the rare carbon isotopes. From boundary conditions (7) follows that, once a set of bottom concentrations for each of the state variables is given, all stationary deep-sea and surface-ocean compartment concentrations can be computed subsequently.

The calibration of the model deep-sea proceeds as follows:
1) Depth-dependent functions for $W_d(i)$ and $K_c(i)$ are assumed.
2) $\Delta^{14}_{cd0}C(47)$ is varied so that a certain value for $\Delta^{14}_{ls0}C$ results.
3) $F_{bcd}(i)$ is varied to reproduce data for $c_{cd0}(z)$.
4) $\delta^{13}_{cd0}C(47)$ is varied in such a way that the resulting $\delta^{13}_{cs0}C$ falls within the range of 1.5-2.5‰.

5) $K_l(i)$ is determined for each compartment separately by varying its numerical value to agree with a prescribed depth profile of $\Delta^{14}_{ld0}C(i)$ (fig 4).
6) $F_{bld}(i)$ is varied to approximately reproduce $c_{ld0}(i)$ which may lead to major changes in $\Delta^{14}_{ld0}C(i)$ so that 5) has to be repeated.
7) $\delta^{13}_{cd0}C(47)$ is varied to reproduce a prescribed $\delta^{13}_{ld0}C(i)$ depth profile.

1) $W_d(z)$ is assumed a function with two inflection points, one at 1000 and one at 4000m, reflecting both intermediate and deep water spreading into the low latitudes deep sea. Equal volumes of intermediate and deep water are formed per unit time. A value of 15Sv for the deep-water formation is adopted here which is on the low end of the respective estimation range (Dietrich et al, 1975; Arons and Stommel, 1967; Weiss, Östlund and Craig, 1979; Broecker, Peng and Engh, 1980). On the whole, 30Sv ($\cong 10^{15} m^3/a$) are assumed to sink down in high latitudes resulting in an upwelling velocity of ca 5m/a in low latitudes just below the surface compartment.

$K_c(z)$ is described by

$$K_c(z) = 10^5 m^2/a \cdot \exp(-z/500m) \qquad (10)$$

yielding a depth-averaged $\overline{K}_c = 8330\ m^2/a$,

2) As discussed below, the model requires the assumption of a value of $\Delta^{14}_{cs0}C = -35\%o$. This can be explained by the fact that the model does not allow for relatively "old" high-latitude deep water to upwell and become part of the surface water in this region.

3) $c_{cd0}(z)$ is taken from Takahashi, Broecker and Brainbridge (1981, table S-14, GEOSECS Antarctic data). A mean water density of 1.026g/cm^3 was used to convert mmoles/kg to moles/m^3. $F_{bcd}(i)$ and $F_{bld}(i)$ are normalized exponential functions (table 1).

4) A stationary value of $\delta^{13}_{bsc0}C = -20$ ‰ is used.

5) $\Delta^{14}_{ld0}C(i)$ for the depth range from 1000 to 6000m is calculated as an area weighted mean of the GEOSECS data (Stuiver, Östlund and McConnaughey, 1981) for the Atlantic and Pacific ocean (50°N to 50°S). These layers are probably left essentially unaffected by perturbations of the atmospheric $^{14}C/C$ ratio. From the pre-industrial values for $\Delta^{14}_{ls0}C$ estimated by Stuiver (1980) (-40%o) and determined from corals (Druffel and Linnick, 1978) (-50%o) the average of -45%o is adopted here. To obtain $\Delta^{14}_{ld0}C(i)$ for 75 to 1000m depth, a smooth curve connecting the

TABLE 1. Transfer coefficients of deep-sea model for 75 and 1000m

z (m)	K_c (m^2/a)	K_l (m^2/a)	w_l (m/a)
75	100,000	8000	5
1000	16,500	800	3.1

F_{csb} = 24Gt C/a — 75% NPP_{oc}

F_{lsb} = 8.4Gt C/a

$$\int_{z=1000m}^{6000m} F_{bcd}(z)dz = 1.25\text{Gt C/a}$$

3.3% NPP_{oc}

$$\int_{z=1000m}^{6000m} F_{bld}(z)dz = 0.18\text{Gt C/a}$$

NPP_{oc}: marine net primary production (De Vooys, 1979: 43.5GtC/a) 25% NPP_{oc} are dissolved in the surface ocean.

$\Delta^{14}_{ld0}C$ values of the lower layers with $\Delta^{14}_{ls0}C$ is constructed. This curve can be varied to obtain a $K_l(i)$ distribution that best reproduces the bomb ^{14}C input into the thermocline.

6) $c_{ld0}(z)$ is taken as an area weighted mean of the data of Takahashi, Broecker and Bainbridge (1981). As in 3), a mean water density of $1.026 g/cm^3$ is used. 7) According to Craig (1970), a mean $\delta^{13}_{bls0}C = -15‰$ is inserted, which means that ca 30% of the dissolved material is $CaCO_3$.

The stationary state assumption for the entire ocean with respect to ΣC and ^{14}C is then used in calibrating atmosphere ocean exchange:

$$0 = G/V_m \cdot p_{a0} - G_c/V_m \cdot p_{cs0} - G_l/V_m \cdot p_{ls0} \tag{11a}$$

$$0 = G/V_m \cdot \overline{Q^{14}_{t0}} \cdot p_{a0} - G_c/V_m \cdot \overline{Q^{14}_{cs0}} \cdot p_{cs0} - G_l/V_m \cdot \overline{Q^{14}_{ls0}} \cdot p_{ls0} - \lambda n^{14}_{oc,0} \tag{11b}$$

($n^{14}_{oc,0}$: total stationary ^{14}C inventory in the oceans)

Because of $G = G_l + G_c$, equations (11a,b) yield:

$$G = V_m \cdot \lambda \cdot n^{14}_{oc,0} \cdot \{\overline{Q^{14}_{t0}} \cdot p_{a0} - [\overline{Q^{14}_{cs0}} \cdot (p_{ls0} - p_{a0}) p_{cs0} + \overline{Q^{14}_{ls0}} \cdot (p_{a0} - p_{cs0}) p_{ls0}] / (p_{ls0} - p_{cs0})\}^{-1} \tag{12}$$

The water mass transport from low to high latitudes is calculated using a stationary state for n^{14}_{cs0}:

$$W_{lcs} = \{F^{14}_{ct0} - F^{14}_{tc0} - \kappa O_s \, \bar{h}(1)/\Delta z(1) \, K_c(1) \, [c^{14}_{cd0}(1) - c^{14}_{cs0}] + \lambda \, n^{14}_{cs0} + F^{14}_{csb}\}/(c^{14}_{ls0} - c^{14}_{cs0}) \qquad (13)$$

Since p_{cs0} and p_{ls0} are essentially unknown, an iterative procedure beginning with arbitrary values for p_{cs0} and p_{ls0} is employed to obtain stationarity for atmosphere and surface ocean compartments with respect to ΣC and ^{14}C. The entire atmosphere-ocean model is then run without perturbation for 360 years to yield stationary $^{13}C/C$ ratios which may also slightly shift p_{cs0}, p_{ls0}, and $\Delta^{14}_{0}C$ values.

The calculated atmosphere ocean exchange time $\tau_{as} = 6.7a$ corresponds to a stationary exchange flux of 90.9Gt C/a or a mean CO_2 exchange of 20.9 moles/m^2/a. The value for τ_{as} given here is to be compared with 5 to (15$\pm$5)a (Broecker and Peng, 1974; Oeschger et al, 1975; Peng et al, 1979), the center of estimates being between 6-8a. For the stationary state $F_{lt0} - F_{tl0} = 3.9$Gt C/a is calculated.

TABLE 2. Quantities related to atmosphere-ocean-exchange

$p_{cs0} = 242$ppm	$p_{lso} = 302$ppm
$F_{tc0} = 26$Gt C/a	$F_{tl0} = 64.9$Gt C/a
$F_{ct0} = 22.1$Gt C/a	$F_{lt0} = 68.8$Gt C/a
$\tau_{ts} = 5.7a$	$\tau_{as} = 6.7a$
$W_{cls} = 0.179\cdot10^{15}m^3/a$	$W_{lcs} = 1.309\cdot10^{15}m^3/a$

RESULTS AND DISCUSSION

As stated above, the atmospheric initial partial pressure and the biospheric input were chosen to reproduce the troposheric partial pressure and $\delta_t^{13}C$. The average CO_2 partial pressure as measured at Mauna Loa and at the South Pole (Bacastow and Keeling, 1981) was 316ppm in 1959 and 334.3ppm in 1978. The model calculations yield values of 314.2ppm for 1959 and 337.1ppm for 1978. Whereas the measured average airborne fraction with respect to fossil input was 49.3%, the airborne fraction as obtained from the model is 42.2%. For the entire calculation (1860-1980), an airborne fraction of 49.6% results.

$\delta_t^{13}C$ shows a difference of -0.57‰ between 1956 and 1978 which is within the uncertainty range of (-0.65 $\pm$ 0.13)‰ as obtained from atmospheric ^{13}C measurements (Keeling, Bacastow, and Tans, 1980). Clearly, the biogenic model input can be increased for $\Delta(\delta_t^{13}C)$ to closer approach -0.65‰ for the period in question, but then agreement with the atmospheric CO_2 par-

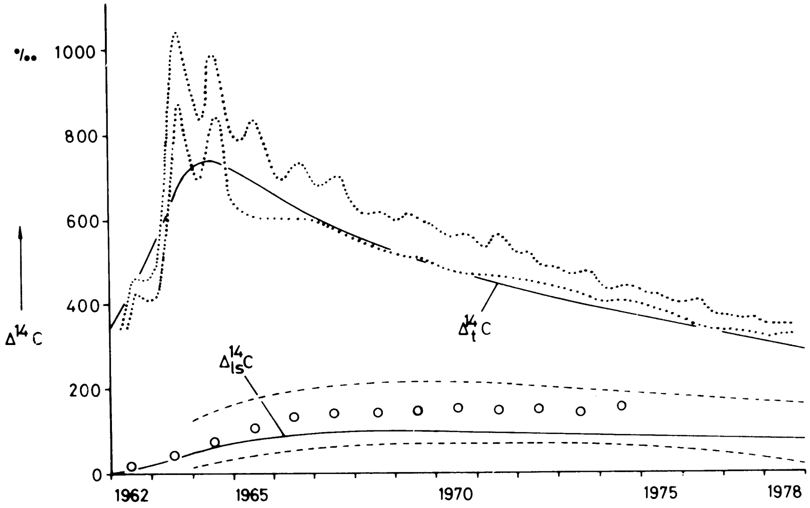

Fig 3. $\Delta^{14}C$ in troposphere ($\Delta_t^{14}D$) and low latitudes surface ocean ($\Delta^{14}_{ls}C$) in response to bomb ^{14}C input (solid lines); envelopes of significant data for the troposphere (....) and for surface ocean (- - - -) (Nydal, Lövseth, and Skogseth, 1980); ooo = coral measurements (Druffel and Linick, 1978).

tial pressure data would be decreased. The $\Delta(\delta_t^{13}C)$ for the period 1860 - 1940 is -0.48‰ which neither agrees with Freyer's (1979) tree-ring measurements (-1.6‰) nor with Francey's (1981) (0‰).

The model response to the ^{14}C bomb input is shown in figure 3, which shows $\Delta^{14}C$ in the troposphere and the low latitudes surface ocean as calculated. The agreement with data observed for the troposphere seems good although the calculated values lie at the lower end of the data range. $\Delta^{14}_{ls}C$ is significantly lower than the coral measurements. In view of the broad band of data, however, higher reliability cannot be expected. In general, the model response to ^{14}C perturbations is characterized by a more pronounced relaxation than is observed. This may be explained by, at least, one of the following: 1) K_c is assumed too large; 2) in contrast to the real ocean, cold surface water is described as attaining nearly perfect isotopic equilibrium with the atmosphere, thereby taking up more ^{14}C and ^{13}C than observed; 3) the ^{14}C bomb input, as estimated by Killough (1980), is too small. 1) and 2) lead to an overemphasized uptake capacity of the high latitudes deep sea.

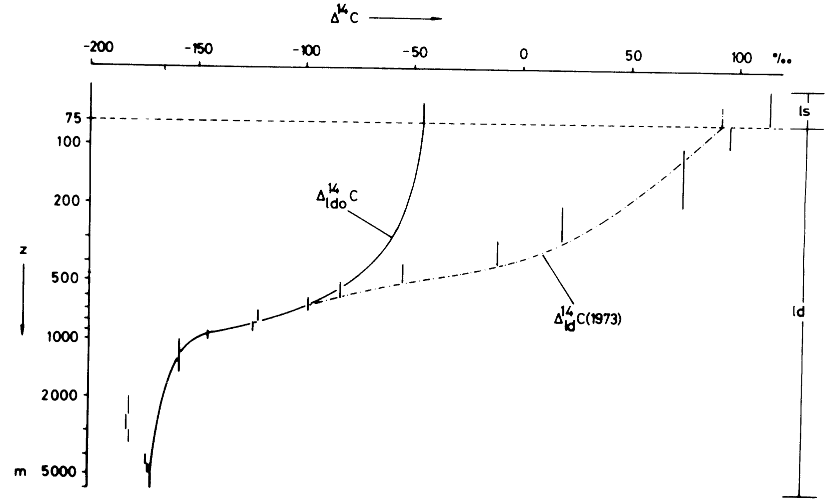

Fig 4. Depth distribution of $\Delta^{14}C$ in low latitudes for a stationary stage (solid line) and for the year 1973 (_._._.) as compared to averages of the GEOSECS data (Stuiver and Quay, 1980) (||||).

The behavior of bomb ^{14}C in the low latitudes deep sea as calculated from the model is given in figure 4; the agreement with the GEOSECS data for 1973 seems good. The Suess effect is calculated as $\Delta(\Delta_t^{14}C) = -18.6‰$ in 1950 ($\Delta_{t0}^{14}C = 0.6‰$) which should be compared to the results of tree-ring measurements of −21‰ (Lerman, Mook, and Vogel, 1970) and ca −23‰ (De Jong and Mook, 1982).

REFERENCES

Arons, AB and Stommel, H, 1967, On the abyssal circulation of the world ocean - III. An advection lateral mixing model of the distribution of a tracer property in an ocean basin: Deep-Sea Research, v 14, p 441-457.

Bacastow, R, 1981, Numerical evaluation of the evasion factor, in Bolin, B, ed, Carbon cycle modelling: New York, John Wiley & Sons, p 95-101.

Bacastow, R and Keeling, CD, 1981, Atmospheric carbon dioxide concentration and the observed airborne fraction, in Bolin, B, ed, Carbon cycle modelling: New York, John Wiley & Sons, p 103-112.

Broecker, WS and Peng, T-H, 1974, Gas exchange rates between air and sea: Tellus, v 26, p 21-35.

Broecker, WS, Peng, T-H, and Engh, R, 1980, Modelling the carbon cycle, in Stuiver, M and Kra, RS, eds, Internatl ^{14}C Conf, 10th, Proc: Radiocarbon, v 22, no 3, p 565-598.

Buringh, P, 1979, Decline of organic carbon in soils of the world, Paper SCOPE conf The role of the terrestrial vegetation in the global carbon cycle: Woods Hole, Massachusetts.

Craig, H, 1970, Abyssal carbon 13 in the south pacific: Jour Geophys Research, v 75, p 691-695

Dietrich, G, Kalle, K, Kraus, W, and Siedler, G, 1975, Allgemeine Meereskunde: Berlin, Borntraeger.

Druffel, EM and Linick, TW, 1978, Radiocarbon in annual coral rings of Florida: Geophys Research Letters, v 5, p 913-916.

Emrich, K, Ehhalt, DH, and Vogel, JC, 1970, Carbon isotope fractionation during the precipitation of calcium carbonate: Earth Planetary Sci Letters, v 8, p 363-371.

Francey, RJ, 1981, Tasmanian tree rings belie suggested anthropogenic ^{13}C/^{12}C trends: Nature, v 290, p 232-235.

Freyer, HD, 1979, On the ^{13}C record in tree rings I. ^{13}C variations in northern hemispheric trees during the last 150 years: Tellus, v 31, p 124-137.

de Jong, AFM, and Mook, WG, 1982, An anomalous Suess effect above Europe: Nature, v 298, p 641-644.

Karlén, I, Olsson, IU, Kallenberg, P, and Killici, S, 1964, Absolut determination of the activity of the two ^{14}C dating standards: Arkiv Geofysik, v 4, p 465-471.

Keeling, CD, Bacastow, RB, and Tans, PP, 1980, Predicted shift in the ^{13}C/^{12}C ratio of atmospheric carbon dioxide: Geophys Research Letters, v 7, p 505-508.

Killough, GG, 1980, A dynamic model for estimating radiation dose to the world population from releases of ^{14}C to the atmosphere: Health Physics, v 38, p 269-300.

Kohlmaier, GH, Kratz, G, Bröhl, H, and Siré, EO, 1981, The source-sink function of the terrestrial biota within the global carbon cycle, in Mitsch, WJ, Bossermann, RW, and Klopatek, JM, eds, Energy and ecological modelling: Amsterdam, Elsevier, p 57-68.

Lerman, JC, Mook, WG, and Vogel, JC, 1970, C14 in tree rings from different localities, in Olsson, IU, ed, Radiocarbon variations and absolute chronology, New York, John Wiley & Sons, Stockholm, Almqvist & Wiksell, p 257-299.

Machta, L, 1973, Prediction of CO$_2$ in the atmosphere, in Woodwell, GM, and Pecan, EV, eds, Carbon and the biosphere: US Atomic Energy Comm, NTIS, Springfield, Virginia, CONF-720510, p 21-30.

Menard, HW, and Smith, SM, 1966, Hypsometry of ocean basin provinces: Jour Geophys Research, v 71, p 4305-4325.

Nydal, R, Lövseth, K, and Skogseth, FH, 1980, Transfer of bomb ^{14}C to the ocean surface, in Stuiver, M and Kra, RS, eds, Internatl ^{14}C Conf, 10th, Proc: Radiocarbon, v 22, no 3, p 626-635.

Oeschger, H, Siegenthaler, U, Schotterer, U, and Gugelmann, A, 1975, A box diffusion model to study the carbon dioxide exchange in nature: Tellus, v 27, p 168-192.

Peng, TH, Broecker, WS, Mathieu, GG, and Li, YH, 1979, Radon evasion rates in the Atlantic and Pacific oceans as determined during the GEOSECS program: Jour Geophys Research, v 84, p 2471-2486.

Rotty, RM, 1981, Data for global CO_2 production from fossil fuels and cement, in Bolin, B, ed, Carbon cycle modelling: New York, John Wiley & Sons, p 121-125.

Seiler, W, and Crutzen, PJ, 1980, Estimates of gross and net fluxes of carbon between the biosphere and the atmosphere from biomass burning: Climatic Change, v 2, p 207-247.

Stuiver, M, 1980, ^{14}C distribution in the Atlantic ocean: Jour Geophys Research, v 85, p 2711-2718.

Stuiver, M, Östlund, HG, and McConnaughey, TA, 1981, GEOSECS Atlantic and Pacific ^{14}C distribution, in Bolin, B, ed, Carbon cycle modelling: New York, John Wiley & Sons, p 201-221.

Stuiver, M and Quay, PD, 1980, Changes in atmospheric carbon-14 attributed to a variable sun: Science, v 207, p 11-19.

Takahashi, T, Broecker, WS, and Bainbridge, AE, 1981, Supplement to the alkalinity and total carbon dioxide concentration in the world oceans, in Bolin, B, ed, Carbon cycle modelling: New York, John Wiley & Sons, p 159-199.

Vogel, JC, Grootes, PM, and Mook, WG, 1970, Isotopic fractionation between gaseous and dissolved carbon dioxide: Zeitschr. Physik, v 230, p 225-238.

de Vooys, CGN, 1981, Primary production in aquatic environments, in Bolin, B, Degens, ET, Kempe, S, and Ketner, P, eds, The global carbon cycle: New York, John Wiley & Sons, p 259-292.

Weiss, RF, Östlund, HG, and Craig, H, 1979, Geochemical studies of the Weddell Sea: Deep Sea Research, v 26a, p 1093-1120.

V. GENERAL ASPECTS OF ^{14}C TECHNIQUE

[Radiocarbon, Vol 25, No. 2, 1983, P 475-484]

INTERNATIONAL COMPARISON OF PROPORTIONAL GAS COUNTERS FOR ^{14}C ACTIVITY MEASUREMENTS*

WILLEM G MOOK

Isotope Physics Laboratory, University Groningen,
Westersingel 34, 9718 CM Groningen, The Netherlands

In early 1982 we attempted to compile information on ^{14}C counting equipment from all laboratories listed in RADIOCARBON. A gratifying number of laboratories cooperated in communicating their data: more than 65% of those in which proportional counters are in operation. Our compilation covers more than 80% of all gas counters used for ^{14}C dating. Unfortunately, the number of parameters determining counter quality as well as the spread in these factors is so large that their separate influence cannot be established beyond statistical doubt. Nevertheless qualitative and semi-quantitative trends are clearly observed. Laboratories are not identified in the data but the calculations and standardization procedures allow the laboratories to identify their own counter data in the graphs. Each plot does not contain a complete compilation of all counters. This is either because of lack of or internally inconsistent information.

COUNTER TYPES

Forty-nine laboratories reported use of 174 gas counters, and 32 laboratories employed liquid scintillation spectrometry. We have identified different types of counters according to construction material and type of filling gas. A survey is presented in figure 1. Most of the ^{14}C laboratories appear to apply CO_2 counting in proportional counters made of copper.

The largest single counter is a Cu/CO_2 counter with a volume of 7.5L. The smallest are Qu/CO_2 microcounters of 5mL. There are 15 Oeschger-type counters. The counter set-ups obtaining the high precision of ca 1 ‰ (2 x 22 hours counting period) consist of sets of counters connected in parallel.

EFFECTIVE VOLUME AND NORMALIZED COUNTING RATE

In order to compare counter performances, certain characteristics such as the recent counting rate, background and meson counting rate, are normalized to a standard volume of 1L. In so doing, the dead volume (= volume of the counter

---

* This paper is from an invited talk.

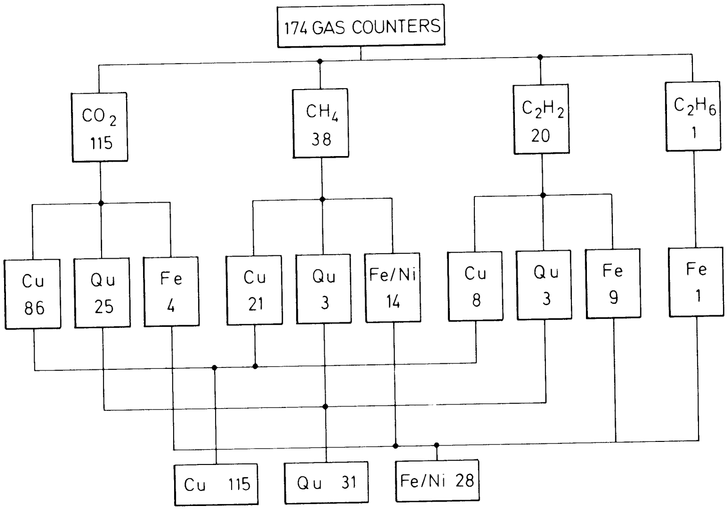

Fig 1. Survey of construction materials and counting gases used for ^{14}C proportional counters. This compilation represents > 80% of the ^{14}C counters in operation. Cu = copper, Qu = quartz, Fe = iron, Ni = nickel.

end pieces + tubing of the inlet system) has to be subtracted from the total volume. The resulting effective volume for each counter is more easily obtained by dividing the standard counting rate A_{ox} by 0.95 x the specific activity of NBS oxalic acid (= standard activity) and by the operating pressure of the counting gas, p. Further, we must consider the number of carbon atoms per molecule of counting gas, N_c. The normalized standard counting rate then is:

$$A_N = \frac{A_{ox}}{pN_c} \qquad (1)$$

and the effective volume:

$$V_e = \frac{A_N}{13.51} \times 2 \text{ (liters)} \qquad (2)$$

where 13.51 dpm is the standardized specific activity of 1g of recent carbon in 1981.

Comparing the effective volume with the counter volume as calculated from the dimensions reveals that the ratios observed for the large as well as the minicounters range between 0.65 and 0.95, with the majority between 0.85 and 0.95. This means that the wire connections in the counter can be made so that only minimal end effects occur.

MESON COUNTING RATE

To make an easy comparison between counters at ground surface and underground, the meson counting rate is normalized to the counting rate per cm^2 of effective horizontal counter cross-section, S_e. To obtain the latter, the effective length L_e, is multiplied by the inner diameter, D:

$$S_e = L_e . D = \frac{V_e}{\pi(D/2)^2} . D \qquad (3)$$

Figure 2 shows the thus obtained standardized meson counting rates per cm^2 as a function of the effective counter size (equivalent to the normalized standard counting rate). For ground-level counters, the spread is in the range of 0.8 to $1cpm/cm^2$, but within this range, it seems to hardly depend on the counter size.

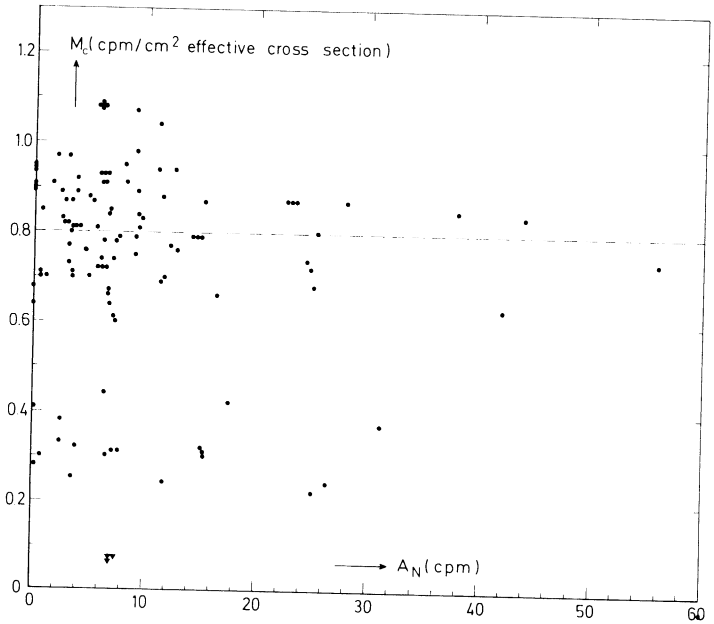

Fig 2. Meson counting rates of ^{14}C proportional counters per cm^2 of effective counter cross section (Eq 3) as a function of the effective counter size (normalized standard counting rate (Eq 1)). The triangular points are maximum counting rates.

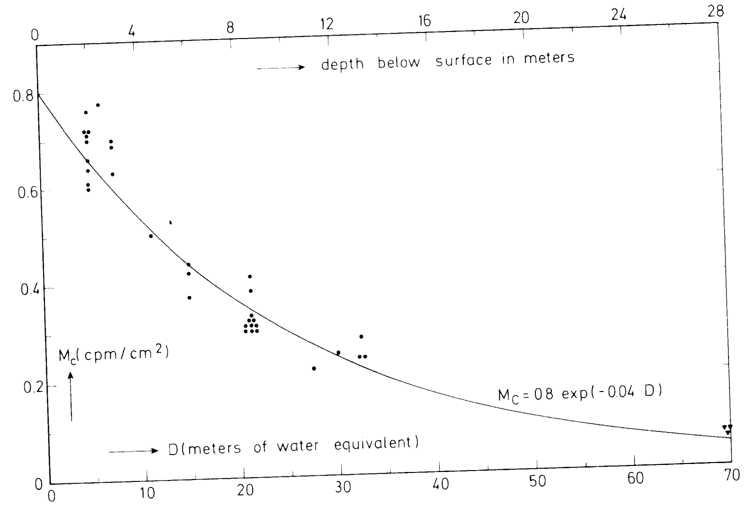

Fig 3. Meson counting rates of a number of ^{14}C proportional counters per cm^2 of effective counter cross-section as a function of the shielding. The shielding capacity of sand and concrete was transferred to meters of water equivalent by using an average specific gravity of 2.5g/cm^3. The shielding effect observed is 4%/m of water or ca 10%/m of depth (Eq 4).

In figure 3, the meson counting rate per cm^2 of effective counter cross-section is shown as a function of the amount of shielding. For a better comparison, the latter is given in meters of water equivalent, obtained by multiplying thickness by specific gravity. For earth and concrete we have used an average value of 2.5g/cm^3. This comparison only can be made on a limited number of counters because most are operated in basements with an unspecified shielding effect of the buildings above. Nevertheless, the results point to an absorption coefficient for water of 4%/m equivalent to ca 10%/m of sand or concrete:

$$M_c \simeq 0.8 \exp(-0.04\ D)\ (\text{cpm/cm}^2) \qquad (4)$$

where D is the depth in meters of water equivalent. The meson counting rate at the earth surface again is ca 0.8 cpm/cm^2.

COUNTER BACKGROUND

The background of the proportional ^{14}C counters originates from mesons and neutrons in cosmic radiation, from the radioactivity of the environment (building walls, paint, etc), and from the radioactivity incorporated in the materials of the counter itself and its surroundings (GM and anti-coincidence counters, shielding, etc). Shielding against the second component is simply obtained by some 15 to 30cm of lead or iron. The last component is minimized by selecting low-activity material as copper or quartz, and by including an inner shield of old lead or mercury. The meson/neutron component is dealt with by installing the counters as deep underground as possible, further shielding with heavy metals and a material of high hydrogen content such as paraffin or polyethylene for reducing neutron energies and boron (boric acid) for absorbing thermal neutrons. It is essential that an anti-coincidence shield of GM-counters or plastic scintillator surrounds the ^{14}C counter. Such shielding is also obtained by the concentric internal arrangement of anti-coincidence wires in Oeschger-type counters.

In order to study the shielding capacity of various counter set-ups, we will compare the background counting rate with the measured meson counting rate (fig 4). Distinction

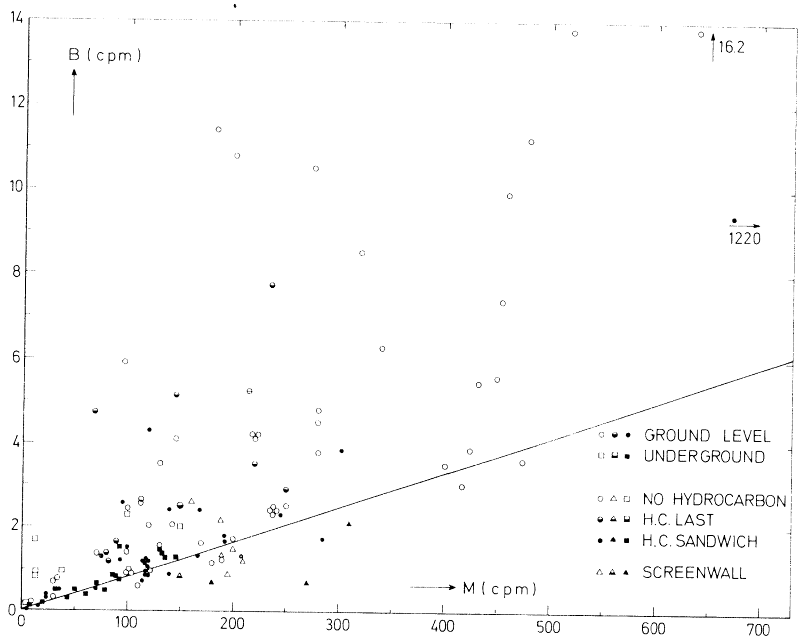

Fig 4. Background counting rate (B) as a function of meson counting rate (M). The underground laboratories (below 7m) are specifically indicated. Further identification was made for Oeschger-type counters and for the counter shielding: no neutron shielding by a layer of a hydrocarbon compound (HC), merely an inner layer of HC and a layer of HC between two layers of high specific density material (HC sandwich). The solid line indicates a favourable trend of B/M of 0.83% (2.5cpm/300cpm).

has been made between surface or basement level laboratories and those deeper underground. We also indicate the type of shielding applied with a neutron shield consisting of any form of hydrocarbon. High backgrounds seem to coincide with the absence of this HC shield. Further, it is our impression that shielding with HC is further improved by applying a heavy material inside the HC shield for the absorption of gamma rays or protons, originating in the neutron shield ("HC sandwich").

It appears that a background/meson ratio of:

$$B/M \simeq 0.8\text{cpm}/100\text{cpm} \tag{5}$$

is a favourable trend, although a theoretical justification for this number cannot be given. This trend also applies to the underground laboratories. It does not imply that the background is only determined by cosmic radiation. The meson counting rate is also proportional to the counter size and thus, more or less, to the amount of material used in the counter construction.

Although not indicated in figure 4, no significant difference is found among different counter materials. In practice, copper and quartz appear to be equally suitable, as well as steel which is generally used in Oeschger-type counters.

QUALITY OF COUNTERS

We must emphasize that good quality ^{14}C counters are not only characterized by high precision, which is, in turn, determined by the choice of counter size, depending on the amount of sample generally available.

Again, for counter comparison we have to normalize for filling pressure, using the normalized standard counting rate (A_N) defined by Eq (2). The counter background is normalized for a standard filling pressure of the counting gas of 1 atm. From the data reported by a few laboratories, we obtained a pressure dependence of the background of ca 0.2‰/Torr (= (dB/dp)/B). The normalized background then is:

$$B_N = B\left[1 - (p - 760)\,\frac{dB/dp}{B}\right] \tag{6}$$

(cf Grootes, 1977)

where the filling pressure, p, is in Torr.

The normalized values of the standard counting rate and the background are compiled in figure 5. Identifications have been made of the position of the counter with respect to ground level and the type of shielding (cf fig 4). Again, the HC sandwich shielding appears to be the most favourable. We present the same set of data in figure 6 according to counter

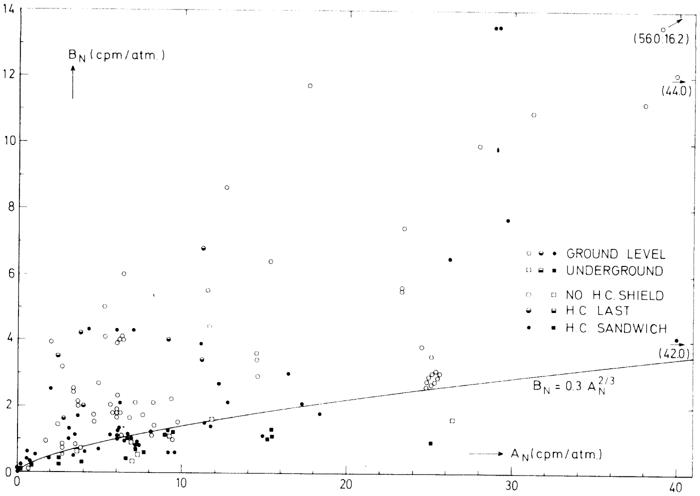

Fig 5. Relation between ^{14}C counter background, B_N, normalized to 1 atm (Eq 6) and the effective counter size, represented by the normalized standard activity, A_N (Eq 1). Identifications are made of the position of the counter with respect to ground level (underground = > 7m below ground level) and type of shielding.

material and filling gas. The plot does not show a generally lower background for one type of counter material. Comparing the two graphs of figures 5 and 6, however, reveals that a high background for a certain counter size is hardly observed for quartz counters that have been properly shielded by an HC sandwich.

A further striking point is that underground counters generally but not necessarily have a relatively low background. Also a proper neutron shield seems to reduce the background, which is confirmed by Stuiver et al (1979).

Assuming that the background is proportional to the counter surface, while the standard counting rate is proportional to the volume, a tentative favourable trend has been drawn in both figures 5 and 6 given by:

$$B_N = 0.3A_N^{2/3} \tag{7}$$

This is approximately equivalent to a ratio of

$$B_N/A_N \simeq 0.1\text{cpm/cpm} \tag{8}$$

Finally, figure 7 represents a compilation of all data on factors determining the quality of a counter. The figure of merit represents the dating limit of a counter. If this is

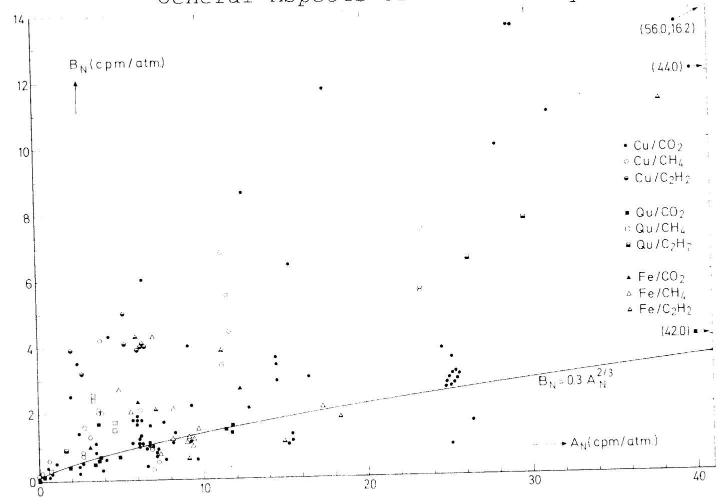

Fig 6. Relation between ^{14}C counter background and effective counter size, both normalized to 1 atm of filling pressure (cf fig 5). Identifications are made of the counter construction material and the type of filling gas. Fe refers to iron, nickel or steel. The same set of data is in figure 5.

conventionally defined as the measured activity, A_{min}, equal to twice the standard deviation in the background, σ_B, the age limit is:

$$T_{max} = -8033 \ln \frac{A_{min}}{A_{ox}} \tag{9}$$

where

$$A_{min} = 2\sigma_B = 2\sqrt{B/t_c} \tag{10}$$

and t_c is the counting time (taken as 2 x 22 hours = 2640min), resulting in:

$$T_{max} = 8033 \ln \left[\tfrac{1}{2}\sqrt{t_c} \cdot \frac{A_{ox}}{\sqrt{B}} \right] \tag{11}$$

The factor $A_{ox}/\sqrt{B}$ is the figure of merit.

The relative precision of the standard counting rate is:

$$\sigma_{A_{ox}}/A_{ox} = \sqrt{(A_{ox} + B)/t_c}/A_{ox} \tag{12}$$

To better understand this plot, a separate, similar graph is inserted showing the true standard counting rate, A_{ox}, and the measured background, B, deduced from chosen realistic values of the figure of merit and the standard precision.

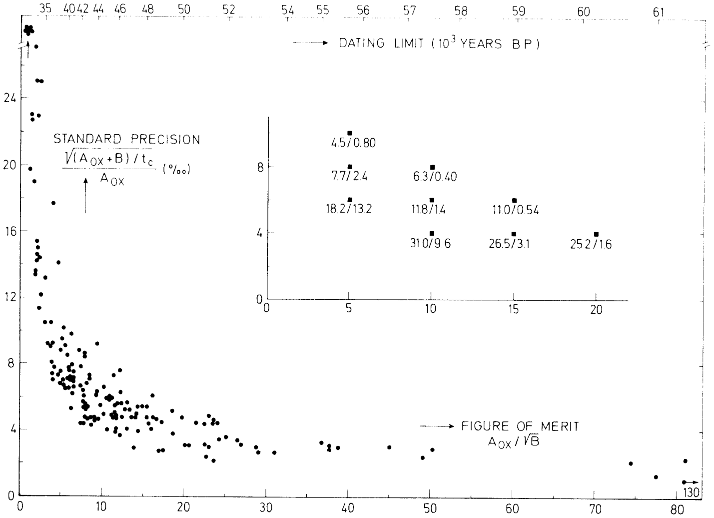

Fig 7. Compilation of the figure of merit and the precision of a two-day (2640 min) measurement of the standard activity in ^{14}C proportional gas counters. This plot merely presents a general view of the detection capacities of ^{14}C laboratories with regard to obtainable precision and dating limit (upper scale; Eq 11). The upper left hand corner shows that data on some mini- and microcounters with volumes below 100mL are beyond the scale. The similar, inserted graph shows A_{OX} and B values (given as A_{OX}/B) deduced from certain realistic values of the figure of merit and the standard, precision.

These values are given as A_{OX}/B. The inner curvature of the assembly of data points consists of the relatively small counters with low background, the outer curvature of the large counters with relatively high background.

SUMMARY AND CONCLUSIONS

From the compilation of data on the performance of 174 proportional gas counters for ^{14}C detection the following conclusions can be drawn:

1) the large number of, and variability in parameters allow only qualitative or semi-quantitative conclusions.

2) from 111 ^{14}C laboratories recently listed in RADIOCARBON, 32 use liquid scintillation counting; 49 use 174 proportional gas counters.

3) ca 50% of these counters are made of copper and are used with CO_2 as a counting gas (fig 1).

4) the volumes of the counters range from 7.5L to 5mL.

5) the effective volume of the counters (= counter volume - dead volume) ranges from 65 to 95% and generally is 90 ± 5%.

6) the meson counting rate per cm^2 of effective cross section ranges from 0.1 to 1cpm, whereas the ground-level laboratories generally detect 0.8 to $0.9cpm/cm^2$. The trend with increasing depth below ground level is a reduction of ca 4%/m of water, equivalent to roughly 10%/m of soil (figs 2 and 3).
7) in general, the lowest background is obtained if the shielding consists of a neutron shield containing a material with a high hydrogen density (paraffin + boric acid) between two layers of heavy metal. This also seems to apply to underground laboratories (figs 4 and 5).
8) generally, counters in underground laboratories (below 8m) have a relatively low background.
9) a favourable trend in the ratio between the background and the meson counting rate is ca 0.8% (= 0.8cpm/100cpm) (fig 4).
10) generally, copper, quartz, steel and nickel seem equally suitable for obtaining a low background although exceptions exist for copper and steel (fig 6). A favourable trend in the ratio between background, B_N, and standard activity, A_N, both normalized to 1 atm of filling pressure is observed of $B_N = 0.3\ A_N^{2/3}$ (figs 5 and 6).

ACKNOWLEDGMENTS

The author is grateful to the contributors for taking their time to complete my questionnaires. I hope that, on this occasion, they consider their efforts worthwhile.

REFERENCES

Grootes, PM, 1977, Thermal diffusion isotopic enrichment and radiocarbon dating beyond 50,000 years BP: Dissert, Univ Groningen.

Stuiver, M, Robinson, SW, and Yang, IC, 1979, ^{14}C dating up to 60,000 years BP with high efficiency proportional counters, in Berger, R and Suess, HE, eds, Radiocarbon dating, Internatl ^{14}C conf, 9th, Proc: Berkeley, Univ California Press, p 202-215.

[Radiocarbon, Vol 25, No. 2, 1983, P 485-492]

RADIOCARBON DATING OF MILLIMOLE-SIZED GASEOUS SAMPLES

DUŠAN SRDOČ, BOGOMIL OBELIĆ and NADA HORVATINČIĆ

Ruđer Bošković Institute, Zagreb, POBox 1016, Yugoslavia

ABSTRACT. As an alternative to the accelerator technique, a simple, compact, small counter system has been developed and tested for routine ^{14}C dating. Our small counter is an all-metal design made of the OFHC copper with quartz supports for the anode (25μm stainless steel). Careful selection of materials for the counter construction was made based on the measurements of the alpha contamination. Methane as the counter filling gave better resolution and gas gain stability, whereas CO_2 gave lower background counting rate and it was easier to prepare and to handle. The long term run using CH_4 showed that the gas gain remained stable within 1-2% for months after the initial drop which followed the counter filling. A 7-day counting period was sufficient to achieve a 3% relative standard deviation which was considered acceptable for routine dating of younger samples.

INTRODUCTION

^{14}C dating of small samples containing carbon in the millimole range (~12mg) is obviously needed (Sayre et al, 1981; Currie, Klouda, and Cooper, 1980). The very promising accelerator technique is presently in a developmental stage and an increasing number of ^{14}C laboratories are trying to cope with milligram-sized samples. The seemingly inherent drawbacks associated with the saml1 counter technique are 1) very long counting time, and 2) a poor sample-to-background count ratio. Whereas low counting rate is a direct result of reduced sample size which cannot be avoided, the sample-to-background count ratio can be improved. A better anticoincidence shield in the form of a large NaI crystal (Sayre et al, 1981) is one choice, although very expensive. Careful selection of counter construction materials, described here, also helps but the figure of merit S^2/B for small counters must still be made comparable to that for a standard counter.

The aim of this paper is to show that the construction and operation of a counting system capable of measuring small samples is within the reach of normally equipped ^{14}C laboratory. Several specific features pertinent to small counter technology are described as well as results of measurements.

THE SMALL COUNTER DESIGN

Our 5ml counter (fig 1) is an all-metal design made of OFHC copper with quartz supports for the anode (25µm stainless steel).

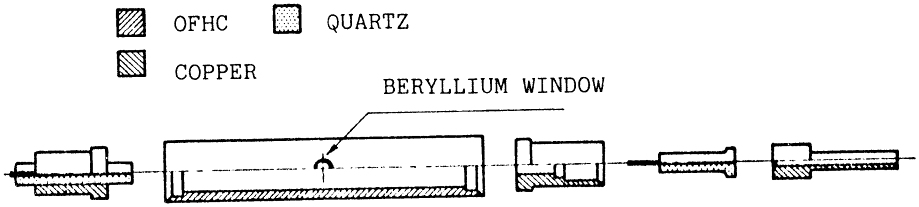

Fig. 1 Schematic of the small (5 ml) proportional counter. Anode: 25µm stainless steel wire; metal parts: OFHC copper; insulators: quartz; vaccum tight joints: Torr-seal.

Pumping and filling is performed via 2mm i d copper tubing which is permanently sealed after filling the counter. No valves or stopcocks are used to maintain the gas inside the counter at the required high-level purity over long counting periods. The counter can withstand a moderate bake-out as well as immersion in liquid N_2 to transfer the counting gas quantitatively from the mani-fold to the counter. The vacuum-tight joint between quartz insulators and metal parts of the counter is obtained by applying Torr-seal epoxy resin. No adverse effect on counter gas gain stability has been observed in counters assembled with the aid of Torr-seal resin. The counter design makes possible a direct noise-free coupling to the FET pre-amplifier. The negative voltage is applied to the counter cathode, ie, to the copper casing. The assembled counter and pre-amplifier make a compact unit which is positioned in the center of the shielding system consisting of the guard counter and a cylindrical lead shield, 25cm thick. The guard counter is made of 2 concentric steel tubings separated into 16 sections by metal sheets. Each section represents an individual Geiger counter. The guard counter is filled with 1.5atm of argon with 2% butane as a quenching admixture.

Materials for the counter construction were carefully selected to avoid natural or man-made radioactive contamination. Many materials were tested for alpha activity which indicates natural contamination. The results are presented elsewhere (Srdoč, in press). Construction materials included OFHC copper, mild steel, epoxy resin, and quartz as the radioactively cleanest material. Stainless steel and high-purity tin solder could not be avoided in small quantities even though their alpha activity was somewhat higher, although far from that of aluminium or commercial tin solder, which should be avoided in any case. Natural contamination of materials commonly used in the low level technique is presented in table 1.

SMALL COUNTER PERFORMANCES

We tested methane and carbon dioxide for small counter filling. Synthesis of methane requires an additional step in gas preparation. Methane is less susceptible to electronegative impurities and, thus, more convenient for prolonged measurements. However, methane gives higher background count due to proton recoils as opposed to CO_2, which is, on the other hand, more sensitive to gaseous impurities. The counter resolution for low-energy photons (5.9keV X-ray from ^{55}Fe) and the constancy of the peak position are excellent indicators of gas properties. The results of 1 1/2 months of testing the stability of the sealed-off counter are shown in figure 2 along with the spectrum of ^{55}Fe source (5.9keV) measured 47 days after sealing the counter.

The efficiency of the counter and the ratio S^2/B depend also on the lower and upper discriminator settings of the electronic counting system. A single-channel analyzer (SCA) with a wide-open window must be properly adjusted to obtain the optimal S^2/B ratio. The spectra shown in figure 3 implied the total and residual background pulse height

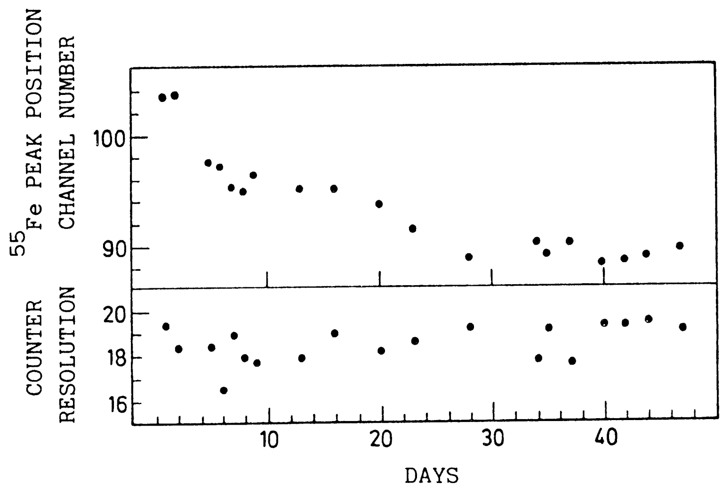

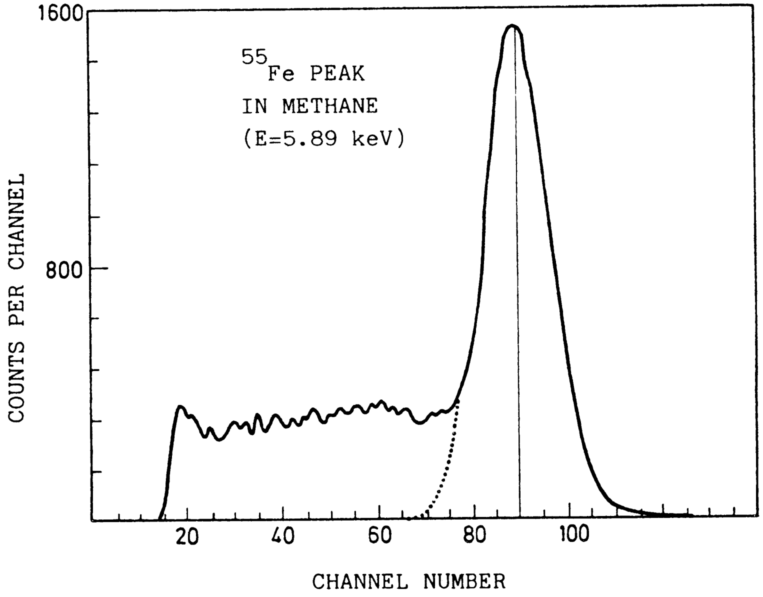

Fig. 2 Properties of small proportional counter: ^{55}Fe peak position and counter resolution vs time (top). ^{55}Fe spectrum 47 days after filling the counter (bottom). Counter gas: CH_4.

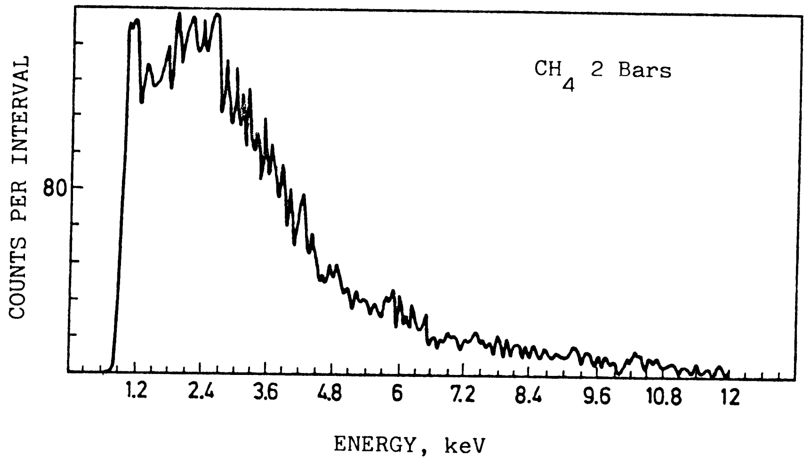

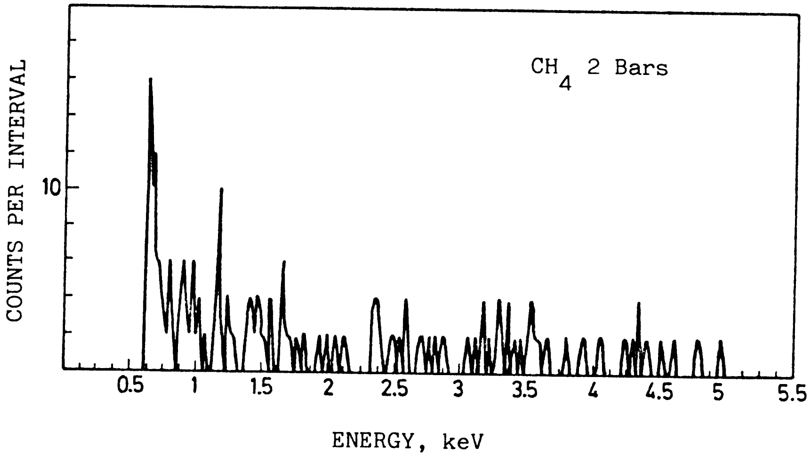

Fig. 3 Total (coincident) and residual (anticoincident) background pulse height distribution in small proportional counter filled with CH_4 (2 Bars). Top: Total background spectrum. Bottom: Residual background spectrum, after elimination of coincident pulses.

TABLE 1. Surface activity of various materials

Material	Technical description, source or/and provenience of samples	Alpha activity $dm^{-2} h^{-1}$ ± 10%
	Metals	
Aluminum	Foil, 25μm, Reynolds, Wrap	23.5
Brass	Sheet, 1mm, commercial, unknown origin	7.0
Copper	Cast metal, OFHC, J Mathey, London, UK	3.0
Lead	Sheet, 3mm, commercial, Mežice, YU	11.0
Old lead	Cast metal, Roman anchor, Adriatic Sea	2.2
Stainless steel	Rolled sheet, 0.5mm, Schoeller-Bleckmann, Vienna, Austria	6.0
Steel	Rolled sheet, commercial, Zenica, YU	2.6
Solder, soft	Tin-based soft solder, CN-7 Duduco, Pforzheim, W Germany	600
	Plastics	
Lucite	Clear tubing, Polypenco, London, UK	1.4
Teflon	Electrical grade, The Edison Swan Co, London, UK	1.6

distributions. The total (coincident) background spectrum has a peaked pulse-height distribution because most charged particles cross the counter volume. In such cases, the spectrum reflects counter geometry and gas density. The residual background (anticoincidence) spectrum is relatively flat, as is the sample plus residual background spectrum. However, the extremely low counting rate (~0.1CPM) hampers the pulse height analysis so badly that reliable spectra of ^{14}C beta particles in a small counter cannot be obtained without a much stronger ^{14}C source. Presently, we use the spectra calibrated with ^{55}Fe to set the lower discriminator level at 0.3keV, which is well above the electronic noise and the upper level at 20keV. Most truncated ^{14}C beta particle tracks are within these limits. Further optimization of discriminator settings will be possible upon more precise analysis of ^{14}C spectrum that we hope to measure soon.

Samples containing 10 to 100mg of carbon were combusted by the conventional technique used in organic chemistry. CO_2 was purified to a high degree, applying the technique developed in this laboratory (Srdoč and Sliepčević, 1963). Catalytic hydrogenation of CO_2 at 450°C cover Ru catalyst was applied to obtain methane. During the experimental stage, both were used for counting purpose. Most of our measurements consist of background and oxalic acid (NBS) standard samples as well as fractions of large samples measured by our conventional ^{14}C system, to check the reliability of the small counter. A 7-day counting period was sufficient to achieve 3% relative standard deviation which was considered acceptable for testing purposes. Table 2 shows the properties of our small volume counter.

TABLE 2. Properties of the 5ml counter

Counting gas	Millimoles of carbon	Oxalic (NBS) standard CPM (net)	Background CPM
CO_2	1	0.14 ± 0.04	0.084 ± 0.025
CH_4	1	0.15 ± 0.04	0.096 ± 0.030

Our goal is to replicate the small counter and set up a honeycomb-like structure with 7 counters in anticoincidence. Thus, the output of the small counter assembly would be comparable to the conventional ^{14}C dating system in terms of number of processed samples per year and the accuracy of measurement.

REFERENCES

Currie, LA, Klouda, GA, and Copper, JA, 1980, Mini-radiocarbon measurements, chemical selectivity and the impact of man on environmental pollution and climate, in Stuiver M and Kra, RS, eds, Internatl ^{14}C conf, 10th Proc: Radiocarbon, v 22, no. 2, p 349-362.

Sayre, EV, Harbottle, G, Stoenner, RW, Otlet, RL, and Evans, GV, 1981, Small gas proportional counters for the ^{14}C measurement of very small samples, in Methods of low-level counting and spectrometry, Proc: Berlin, IAEA, p 393-407.

Srdoč, D, in press, Surface emission of alpha particles from materials used in low-level radioactivity technique, in Internatl conf on low-level activity measurements and applications, 2nd Proc: High Tatras, Czechoslovakia.

Srdoč, D, and Sliepčević, A, 1963, Carbon dioxide proportional counter; effects of gaseous impurities and gas purification method: Jour Appl Radiation Isotopes, v 14, p 481-488.

[Radiocarbon, Vol 25, No. 2, 1983 P 493-500]

RADIOCARBON DATING ARCHAEOLOGIC AND ENVIRONMENTAL SAMPLES CONTAINING 10 TO 120 MILLIGRAMS OF CARBON

JOHN C SHEPPARD, J FRED HOPPER, and YVONNE WELTER

Department of Chemical Engineering
Washington State University
Pullman, Washington 99164

A conventional ^{14}C system with either a $15cm^3$ or a $100cm^3$ methane gas proportional counting tube, each constructed from high purity copper, has been used at the Washington State University ^{14}C laboratory for three years (Sheppard, Hopper, Westberg, 1981). The electronic components of this system included highly stable (John Fluke) power supplies, modified pre-amplifiers (Canberra), and NIM amplifiers, single channel analyzers, scalers, timers, etc, (ORTEC). Modules were selected for a highly stable low-noise system. The system was designed to minimize problems generated by ground-loops, electromagnetic noise pick-up, and line noise. It operates in a copper-lined basement room of a four-story brick and concrete building along with a second and older gas proportional system which has three $500cm^3$ copper counting tubes operated at 2 or 3 atmospheres of methane. Analysis of the older system's background data indicates that the background counting rate of 0.8 counts per minute is virtually independent of atmospheric pressure. It has not been possible to determine the pressure dependence of the small counting tubes.

During the past three years ca 40 samples were dated using the 15 and $100cm^3$ counting tubes and ca 10 samples, first prepared for the $500cm^3$ tubes, were counted in the larger and smaller counting tubes to calibrate the small tubes and to learn more about non-Poissonian errors believed to increase the actual standard deviation of a ^{14}C age measurement.

This analysis started with the assumption that the actual error associated with a ^{14}C age measurement is larger than the Poissonian error derived from the ^{14}C decay law and related counting statistics. Our experience with the updating of a marginal, lightly shielded system with noisy electronics, strongly suggested that non-statistical sources or error exist even for well-managed systems. Similarly, Currie (1973) found that such increased errors are likely, while Clark and Renfrew (1973) and Scott, Baxter, and Aitchison (1981) observed that the actual ^{14}C age error is likely to be twice the Poissonian value. The following observations were developed from an analysis of paired age data and series of partial counts for the 15, 100, and 500 cm^3 counting tubes.

COMPARISONS OF THE SMALL AND LARGE COUNTING TUBE DATA

Ten pairs of ^{14}C age measurements for the 100cm^3 counting tube age were compared to those obtained with large 500cm^3 counting tubes. Application of the F test to these data yielded an F value of 0.02. Since 0.02 is much less than the 1% critical value of F(0.01, 1, 18) = 8.28, the null hypothesis could not be rejected, indicating that the mean ^{14}C ages determined by the 100 and 500cm^3 tubes were not significantly different. Use of the F test for ten pairs of ^{14}C age measurements for the 15 and 500cm^3 counting tubes yielded the same conclusion--the ^{14}C ages were not significantly different.

The two sets of paired ^{14}C age determinations were then subjected to regression analysis, with and without weighting. Comparison of the 15 and 100cm^3 age measurements with those for the 500cm^3 counting tubes yielded correlation coefficients >0.96 and 0.90 for the 100 and 15cm^3 counting tubes, respectively. Both analyses indicated potential biases in the small tube measurements because non-zero intercepts of -260 and 600 years for the 100 and 15cm^3 counting tubes, respectively, but the intercept errors of 270 and 440 years do not strongly support this hypothesis. Paired t tests also support these conclusions. ^{14}C ages for the 15 and 500cm^3 tubes were recalculated using running averages for the backgrounds and oxalate counting rates, as well as those just before and after the sample count. There was a slight improvement with the before-after approach which we believe is preferable because small samples are counted much less frequently for the large system. Further analysis of the oxalate counting data for the 100cm^3 tube suggests a non-Poissonian component of 1.5, slightly lower than the factor of two observed by Scott, Baxter, and Aitchison (1981).

To summarize, this analysis suggests that the small counting tube age determinations are in statistical agreement with the large tube data. However, there is some evidence for a bias and variability that require further study. During the comparison occasional cable noise was observed, several NIM modules (ORTEC, mainly) malfunctioned, and some problems with gas purity were encountered. Just how these episodes influenced the small tube data is not clear, but they were probably adversely affected, at least slightly.

FURTHER ANALYSIS OF THE ^{14}C COUNTING DATA FOR NON-POISSONIAN BEHAVIOR

It has been evident from the beginning of the operation of the WSU system that various interferences adversely influence results. For example, the first counting tube had small Teflon gaskets that outgassed a volatile impurity that completely quenched impulses. Noise generated by a teletype of an adjacent ^{14}C system was eliminated by replacement of an ORTEC pre-amplifier with one built by Canberra. It is not clear why ORTEC pre-amplifiers behaved this way. Later, a more subtle problem emerged when chi-square values began to increase. A search revealed that ORTEC scalers were dropping digits as the data were transferred from scalers to the line printer. Thus, some of our dates were probably biased, but by how much is unclear. We found that cables occasionally generate significant noise and must be replaced. All sources of error were corrected but, more important, they do occur at various times. When the background is ca 1 count every 6 minutes and sample count rates of 1 count every 50 minutes are being measured, it is clear that 1 count every 100 minutes is very undesirable. Most of the time the spurious count rate is 1 per 1000 minutes.

In addition to these readily corrected errors, slight variations of the high voltage and discrimination level may cause fluctuations in the observed counting rate; further, gas impurities may cause subtle changes in counting efficiency. These perturbations are generally classified as non-Poisson errors (sometimes referred to as dead-time distorted Poisson processes). Excellent discussions of such non-Poissonian behavior were given by Müller (1973; 1974), Currie (1971), Hooton and Parsons (1973), Hilaire (1973), and Pazdur (1976). In various ways, all have attempted to extract the non-Poissonian error component from the observed counting data.

In our analysis of counting data for the WSU ^{14}C systems we used the approaches of Hooton and Parsons (1973), Hilaire (1976), and Pazdur (1976). Most days, every ^{14}C laboratory generates a series of partial counts, usually 100 minutes long, that last from 1 to 7 days. Thus, anywhere from 14 to 100 partial counts are available for analysis. Hooton and Parsons (1973) and Hilaire (1973) employed the mean-square successive difference (MSSD) method, first developed by Hart (1942) and expanded by Bennett and Franklin (1954), to analyze counting data for indications of instrumental drift.

We used the Hooton-Parsons method. The MSSD statistic ρ^2 is calculated as the mean of the squares of n-1 successive differences between n observations:

$$\rho^2 = \Sigma(x_{i+1} - x_i)^2/(n - 1) \quad i + 1, 2, \text{--} \; n - 1. \tag{1}$$

Further, the average value of

$$\rho^2 \approx 2S^2 \tag{2}$$

where

$$S^2 = \frac{\Sigma(x_i - \overline{x})^2}{n-1} = \text{the sample variance of a series of particle counts.} \tag{3}$$

Also, the a value of ρ^2 is less affected by a gradual drift than s^2 but is more influenced than s^2 by rapid oscillations. Thus, the ratio

$$\rho^2/s^2 = \eta \tag{4}$$

is a measure of departures from a normal distribution. Drifting counting systems, eg, will have η's significantly less than 2, while η's significantly greater than 2 characterize oscillating systems.

Another way of looking at the MSSD method is that it is a time-dependent chi-square test, where

$$x^2 = \frac{n - 1}{\eta} \cdot \frac{\rho^2}{\overline{x}} \approx \frac{n - 1}{2} \cdot \frac{\rho^2}{\overline{x}} \tag{5}$$

and $\overline{x}$ = the mean counting rate for n partial counts. It is important to note here that n refers to the number of counting intervals of 100 minutes.

Many MSSD analyses were done for the 15, 100, and 500cm^3 gas proportional counting tubes and results are summarized in table 1.

TABLE 1. MSSD of counting data for the WSU radiocarbon systems

Counting tube	Volume	Electronic system	Number of counts	η(ave)
2	500	Old	19	1.93 ± 0.43
3	500	Old	14	1.97 ± 0.59
T4	100	New	15	1.92 ± 0.30
T2	15	New	15	1.91 ± 0.33

Consider the data for the new system and small counting tubes. Since limiting values of η for $n = 15$ and a 95% confidence level are $1.21 < \eta < 2.79$, it can be assumed that the counting data are randomly distributed. None of the T2 or T4 data fell outside these bounds. Two of the MSSD analyses for counting tube 3 showed η's less than the lower bound for 14 counts. Subsequently, it was found that counting tube 3 had a leak. After a repair, the performance of counting tube 3 returned to normal. To summarize, application of the MSSD method to the WSU counting tubes indicated normal stable performance with the exceptions of two abnormal counts.

EXAMINATION OF THE LONG-TERM PERFORMANCE OF THE WSU COUNTING TUBES AND ELECTRONICS

Pazdur (1976) showed that a dead-time distorted distribution obeys the "negative binomial distribution" as developed by Greenwood and Yule (1920). Furthermore, Feller (1966) showed that such distributions belong to the class of compound Poisson distributions, which in the limit reduce to the ideal Poisson distribution. Pazdur (1976) also showed, for a series of counts with a partial counting time T, that the variance for a non-Poisson situation is

$$\sigma^2 = RT(1 + RT\delta^2) \qquad (6)$$

where R is the average counting rate and δ^2 = rms fluctuation of the detection efficiency. To further clarify δ^2, let $R = R_o\varepsilon$, where $\varepsilon = \varepsilon(\nu_B, \nu_D)$. R_o is the true ^{14}C disintegration rate and ε is a detection efficiency with a variable component ν_B due to fluctuations of bias voltage and another component ν_D which varies with the discriminator level. Of course, this is grossly over-simplified but it emphasizes that such variations of counting efficiency do occur.

To estimate these fluctuations, let $V = \sigma^2/\bar{m}$, remembering that $\bar{m} = RT$. With substitution and rearrangement equation 6 becomes

$$V = 1 + RT\delta^2 \qquad (7)$$

As Pazdur (1976) showed that values of V can be estimated from the ratio of the sample variance s^2 to the population or Poisson variance S_p^2, then

$$\hat{V} = S_s^2/S_p^2 \qquad (8)$$

For n partial counts of time T

$$\hat{V} = \frac{S_s^2 T}{R} \qquad (9)$$

Thus, values of $\hat{V}$ should be calculated for as many long counts as available to obtain an average, $\bar{V}$. Since S_s^2 and S_p^2 are both estimators of the true variance of the ^{14}C counting rate, values of $\hat{V}$ should scatter around unity. It can be argued that the larger of S_s^2 and S_p^2 should be used in ^{14}C age error calculations to obtain a conservative estimate. Table 2 contains an analysis of the two small counting tubes and two large (500cm^3) tubes of the WSU systems.

TABLE 2. Pazdur analysis of WSU counting tubes

Detector/ volume(cm^3)	Pressure atm	Number of counts*	Average cpm,R	$\bar{V}$	δ^2
T2/15	3.0	41	0.27	1.01 ± 0.24	4.8×10^{-4}
T4/100	3.0	20	1.21	1.06 ± 0.17	5.3×10^{-4}
2/500	2.0	45	3.74	1.03 ± 0.45	7.0×10^{-5}
3/500	3.0	45	4.77	1.04 ± 0.44	1.0×10^{-4}

*The partial counting time for all these counts was 100 minutes with the number of partial counts ranging from 10 to 14 for the large counting tubes to 10 to 50 for the smaller tubes.

The data in table 2 reveal that $\bar{V}$ does fluctuate about unity as predicted. More important, values of δ^2 for all counting tubes are rather small, which means that variations of detector-efficiency-related fluctuations in bias and discriminator levels and other sources of random instrumental error are negligible for the "small" and "large" systems.

CONCLUSIONS

Analyses applied to the small and large systems at the WSU ^{14}C laboratory suggest that electronic components of a well-managed system are minor sources of non-Poisson error. MSSD analysis indicated that short-term drift and oscillation of the order of day(s) was not significant. Similarly, application of the Pazdur (1976) test, which covers weeks or months of instrument operation, showed that instrumental fluctuations were negligible. While these tests provide bases for the elimination of instrument-based errors, they do not eliminate potential intra-latorabory or systematic errors that include pulse quenching, isotopic fractionation, use or non-use of running averages for backgrounds and oxalate standards, and other unnamed sources of error.

It seems unreasonable to assume that all the ^{14}C age errors of a small tube system, or even a large one, are due solely to counting errors. Thus, we are left with extra-instrumental error sources as mentioned above. The recent data of Scott, Baxter, an Aitchison (1981) strongly support the existence of such errors for large and small systems.

If ^{14}C age errors are actually larger than those obtained by Poisson statistics, perhaps this problem should be recognized. Müller (1979) suggested that it is legitimate to multiply an error by a factor of two or three, provided this arbitrary augmentation is applied at the very end of the age calculation and not at some intermediate stage. If the Scott, Baxter, and Aitchison (1981) data are used as a criterion, this factor should be two. However, before such an augmentation is made, there must be universal agreement among ^{14}C laboratories on 1) whether to do it at all and 2) the actual magnitude. The latter requires considerable study and research.

REFERENCES

Bennett, CA and Franklin, NL, 1954, Statistical analysis in chemistry and the chemical industry; New York, John Wiley & Sons, p 677-684.

Clark, RM and Renfrew, C, 1973, The tree-ring calibration of radiocarbon and the chronology of ancient Egypt: Nature, v 243, p 266-270.

Currie, LA, 1971, On the interpretation of errors in counting experiments: Anal Letters, v 4, p 777-784.

---------- 1973, The evaluation of radiocarbon measurements and inherent statistical limitations in age resolution, in Rafter, TA and Grant-Taylor, T, eds, Internatl conf on radiocarbon dating, 8th Proc: Wellington, Royal Soc New Zealand, p 598-611.

Feller, W, 1966, An introduction to probability theory and its applications, v II: New York, John Wiley & Sons, p 56-57.

Greenwood, M and Yule, GU, 1920, An inquiry into the nature of frequency distributions representative of multiple happenings: Jour Royal Stat Soc, v 83, p 255-279.

Hart, BI, 1942, Significance levels of the ratio of the mean square successive difference to the variance: Anal Math Statistics, v 12, p 1-13.

Hilaire, M, 1973, Treatment of errors in low-activity measurements: Nuclear Instruments Methods, v 112, p 385-390.

Hooton, KAH and Parsons, ML, 1973, Equipment stability in x-ray fluorescence spectrometry and radioactive counting--a statistical approach: Anal Chemistry, v 45, p 2218-2227.

Müller, JW, 1973, Dead-time problems: Nuclear Instruments Methods: v 112, p 47-57.

---------- 1974, Some formulae for a dead-time-distorted Poisson process: Nuclear Instruments Methods: v 117, p 401-404.

---------- 1979, Some second thoughts on error statement: Nuclear Instruments Methods: v 163, p 241-251.

Pazdur, MF, 1976, Counting statistics in low-level radioactivity measurements with fluctuating counting efficiency: Internatl Jour Appl Isotopes, v 20, p 179-184.

Scott, EM, Baxter, MS, and Aitchison, TC, 1931, An Assessment of variability in radiocarbon dating, in Methods of low-level counting and spectrometry: IAEA, Vienna, p 371-391.

Sheppard, JC, Hopper, JF, and Westberg, HH, 1981, Radiocarbon dating of milligram-sized archaeological and environmental samples, in Methods of low-level counting and spectrometry: IAEA, Vienna, p 409-416.

[Radiocarbon, Vol 25, No. 2, 1983, P 501-510]

THE RADON PROBLEM IN ^{14}C DATING

REIDAR NYDAL

Radiological Dating Laboratory, The Norwegian Institute
of Technology, Trondheim, Norway

ABSTRACT. Due to traces of radium and uranium in most ^{14}C samples, radon appears as a radioactive contamination in the CO_2 prepared by combustion. This contamination must be removed by an active purification prodecure or by storing the CO_2 prior to measurement. No effective electronic discrimination against radon and its daughter elements can be performed. The necessary storage time until radon has decayed varies widely, especially for marine shells. The latter material, collected from Norway and Svalbard, has been a main object for the present investigation. In a few cases, a measureable amount of radon may be left even after eight weeks. The behavior of radon and its daughter elements in a CO_2 proportional counter has been studied.

INTRODUCTION

From radium (^{226}Ra) incorporated in various kinds of material used for ^{14}C dating, it was early discovered that radon (^{222}Rn) appeared as a source of radioactive contamination. This must be removed before measurement, especially if CO_2 is directly used as a counting gas. De Vries (1957) made the first serious attempt to remove radon in CO_2 in a slow distillation process, but a common method is to store the gas samples for several weeks until radon disappears by natural decay.

This laboratory became interested in radon in the late 1950's when a trend of increasing radon content with age in marine carbonates was observed. A radon counting technique was then developed for seeking an independent time scale based on the radium-uranium ratio in marine calcium carbonate (Nydal, 1977). After the early successful Th/U dating of coral limestone (Sackett, 1958), it was hoped that the Th/U ratio (or Ra/U ratio) also could be applied for dating old marine shells. It turned out, however, that the method often failed for the latter material (Kaufman et al, 1971).

While studying the Ra/U ratio for a number of old shell samples from Norway and Svalbard (Andersen et al, 1981; Salvigsen and Nydal, 1981), our measurements yielded valuable information about their highly variable radium (and radon) content, especially about the necessary storage time and behaviour of radon and its daughter elements in a CO_2 proportional counter.

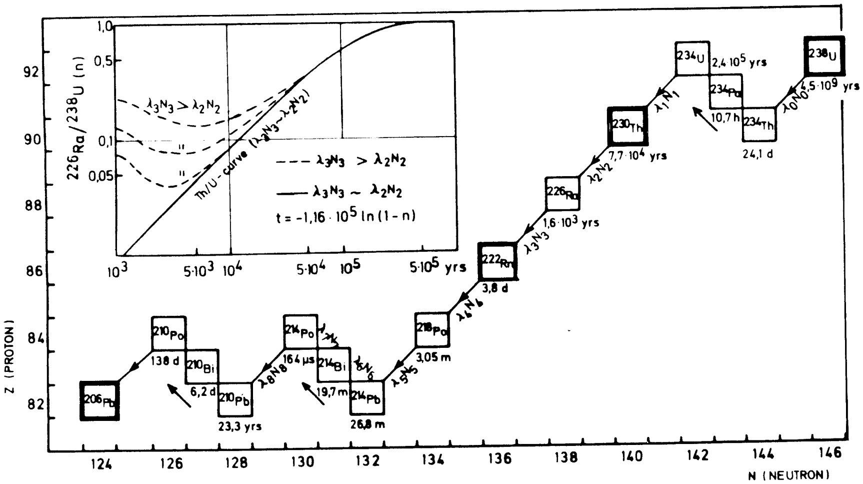

Fig 1. Uranium decay series

RADON AND ITS PROPERTIES

The important radon isotope is ^{222}Rn with a half-life of 3.8 days. It is the first daughter element of ^{226}Ra and belongs to the ^{238}U series (fig 1). Because of the larger half-life of ^{238}U (3.8 · 10^9 yr) the abundance of ^{226}Ra, and thus, of ^{222}Rn in nature is relatively high. ^{222}Rn is a noble gas and thus, the only radioactive element of importance which persists in CO_2 after combustion. Radon is normally conserved in unchanged concentration during a purification procedure of CO_2 (fig 2).

When CO_2 contains radon, four of its daughter elements are built up in the counter, contributing to the counting rate. Two of these are the α emitting elements, ^{218}Po and ^{214}Po, with respective half-lives of 3.05 min and 164 µsec. The other two are the β emitters ^{214}Pb and ^{214}Bi, with half-lives of 26.8 min and 19.7 min. The α particles from ^{222}Rn, ^{218}Po, and ^{214}Po (respectively, 5.8 MeV, 6.0 MeV, and 7.7 MeV) result in a separate α plateau where the high-energy α particles can be counted in a separate channel (fig 3). The α pulses can easily be subtracted by means of an anticoincidence unit. The β pulses from ^{214}Pb and ^{214}Bi, however, cannot be distinguished from the ^{14}C β pulses.

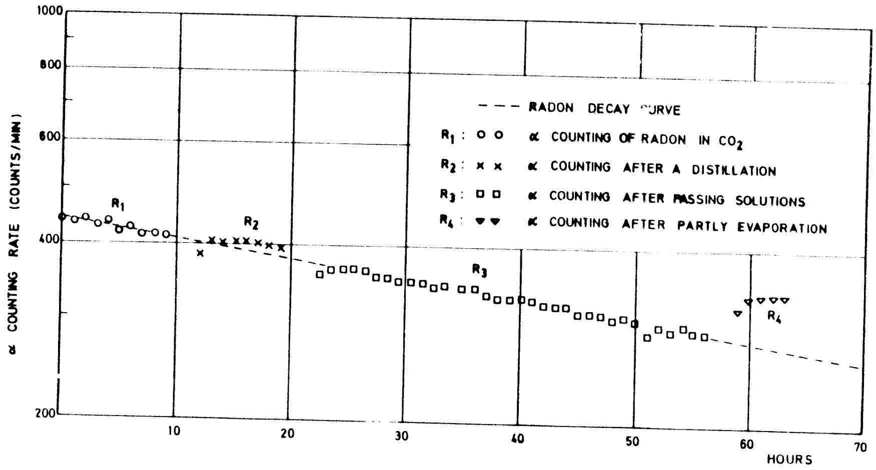

Fig 2. Conservation of radon during various treatments of CO_2. Radon is successively observed after an ordinary distillation process (R_2: Condensation of CO_2 under continuously pumping), and after passing through solutions (R_3: 0.3L, 50% HCl and 0.3L, 2% $KMnO_4$). Radon is slightly enriched in the CO_2 gas phase of partly evaporated CO_2 ice (R_4).

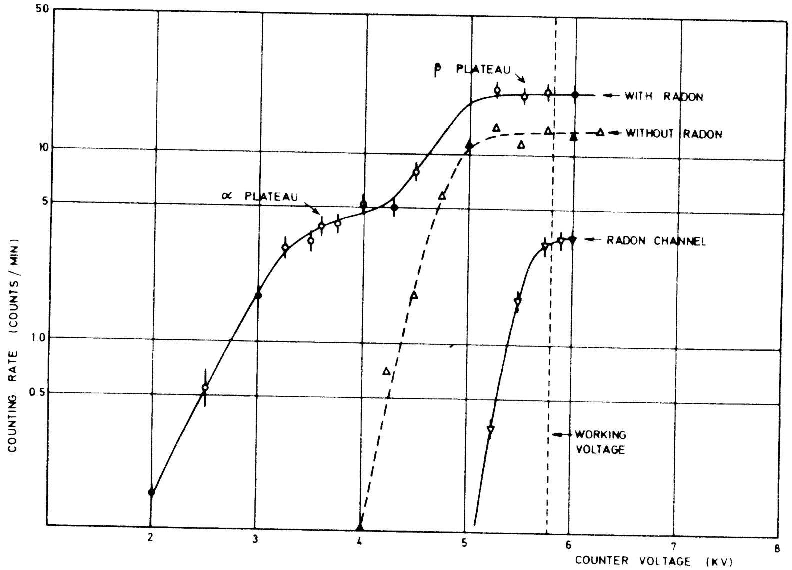

Fig 3. Characteristic curves for α and β counting in a CO_2 proportional counter.

DAUGHTER ELEMENTS ON THE COUNTER WALL

When radon is introduced in a gas proportional counter, the counting rate changes with time. The behavior of radon and the two α emitting daughter elements, ^{218}Po and ^{214}Po, was studied during two experiments in a special counter (Nydal, 1965). In the first experiment, CO_2 mixed with radon was introduced into the counter within 10 sec, and the α counting rate increased with time because of the build-up of ^{218}Po and ^{214}Po (fig 4). The first rapid increase is due to ^{218}Po with a half-life of 3.05 min. Further and slower increase is due to ^{214}Po with a half-life of 164 μsec. The apparent longer half-life of the latter is due to a delay through the intermediate β emitting elements, ^{214}Pb and ^{214}Bi. After 3.3 hours, an equilibrium (99.3%) between radon and the daughter elements is almost obtained. The curve has then reached its maximum and decreases later in accordance with the half-life of radon.

In the second experiment, radon gas in equilibrium with its daughter elements was quickly removed from the counter and replaced by a neutral CO_2 gas. The measurements now show the decay of ^{218}Po and ^{214}Po. The full curve (I_f) in figure 5 is calculated from the following set of decay equations:

$$^{218}Po: \quad dN_5/dt = -\lambda_5 N_5 + \lambda_4 N_4$$

$$^{214}Po: \quad dN_6/dt = -\lambda_6 N_6 + \lambda_5 N_5$$

$$^{214}Bi: \quad dN_7/dt = -\lambda_7 N_7 + \lambda_6 N_6$$

$$^{214}Po: \quad dN_8/dt = -\lambda_8 N_8 + \lambda_7 N_7$$

It is derived from the two experiments that the radon daughter elements ^{214}Po and ^{218}Po only contribute with 25 per cent each to the total α counting rate. This is because the elements, with a positive net charge just after formation, stick to the counter wall and thus, reduce their activity. One half of the α particles penetrate to the active volume of the counter while the other half is absorbed in the counter wall. The same is true for the β emitting elements ^{214}Pb and ^{214}Bi. In accordance with the observations, the total counting rate (without anticoincidence) on the β plateau is approximately three times that of pure radon.

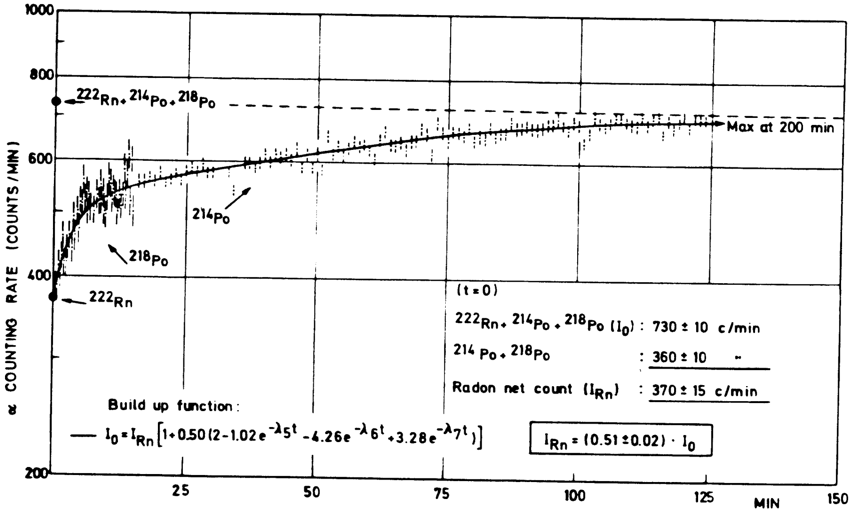

Fig 4. Build up of daughter elements from radon when radon is filled into a gas proportional counter

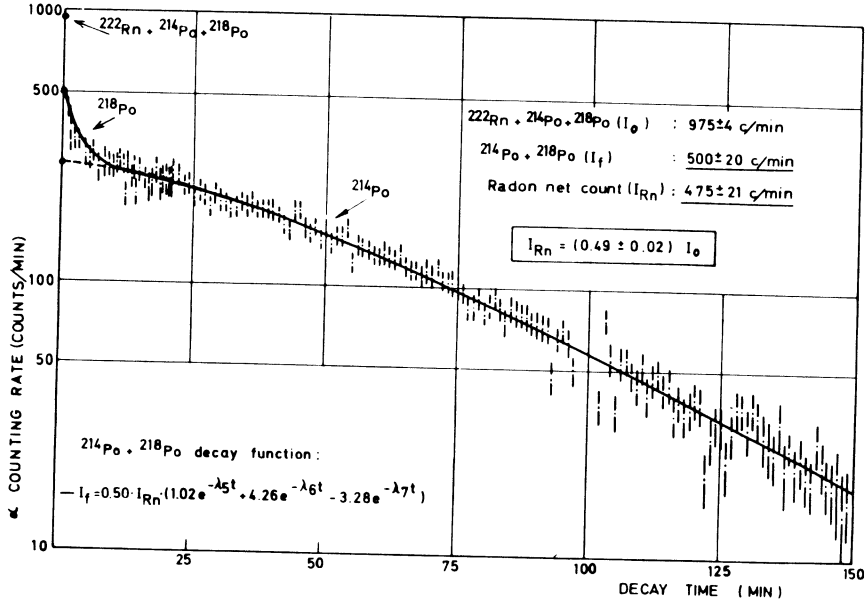

Fig 5. Decay of radon daughter elements on the counter wall when radon is removed from the counter

RADON FLUSHING SYSTEMS

The relativly thick center wire (0.1mm) of our radon counter and the low pressure (≤ 1 atm) greatly reduce the sensitivity for electronegative contamination. Radon can immediately be measured in the CO_2 evolved from the carbonate sample in system I (fig 6) without any distillation process. Prior to CO_2 preparation, the shells are surface treated and placed in the bulb, and the whole system is evacuated. A predetermined amount of HNO_3 is added to the shells, and the reaction allowed to proceed until neutralization. The total amount of CO_2 containing radon is transferred into the counter with liquid nitrogen. Radon can also be measured in an aliquot from the solution in the alternative system II (Nydal, 1977). Propane (C_3H_8) is presently applied as a flushing gas because it has slightly better counting properties than CO_2.

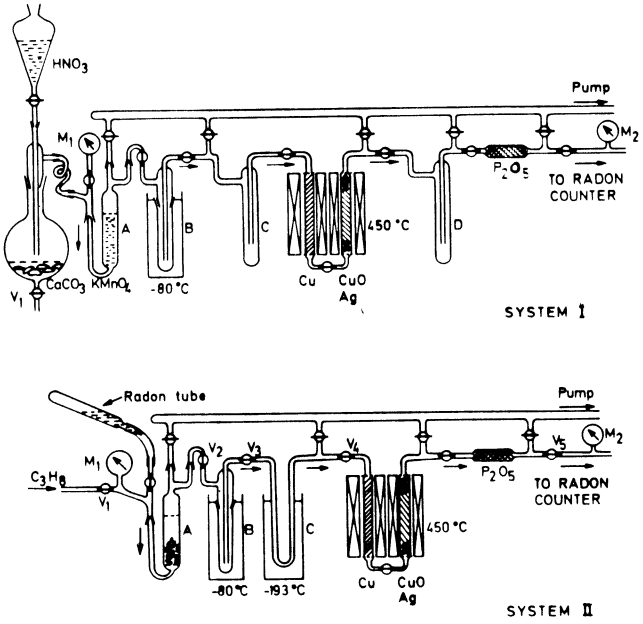

Fig 6. Radon flushing systems

RESULTS AND DISCUSSION

A search for a time scale based on the $^{226}Ra/^{238}U$ ratio in marine shells has provided valuable information about the actual radon content in this material. Because of the short

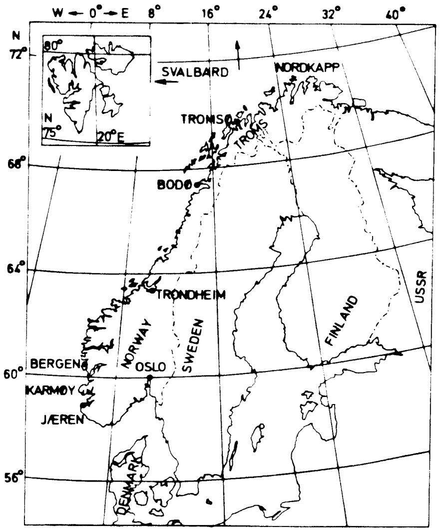

Fig 7. Map of Norway and locations for marine shells

half-life of radon (3.8 days) compared to radium (1600 yr), a radioactive equilibrium between these isotopes ($\lambda_3 N_3 = \lambda_4 N_4$) exists within the shells. The radium content (counts/min) given in tables 1-3 is the same as for radon, and is measured with an accurracy of 5-10 per cent (1σ). Th/U dating is based on the assumption that uranium is out of radioactive equilibrium with its daughter elements in living molluscs at the time of absorption. Shells must further act as a closed system prior to formation. Under these circumstances, ^{226}Ra, which is in equilibrium with ^{230}Th ($\lambda_2 N_2 = \lambda_3 N_3$), is built up from ^{238}U according to the time formula given in figure 1. Because of the long half-life of ^{230}Th (77,000 yr) the amount of radon (counts/min), deriving from incorporated uranium, increases slowly with time according to

$$^{222}\text{Rn} = 1.15\ ^{238}\text{U}(1 - e^{-t/1.16\cdot 10^5})$$

The factor, 1.15, is due to anomalous fractionation effect between the uranium isotopes in nature (Thurber et al, 1965: $^{234}\text{U}/^{238}\text{U} \sim 1.15$). Experience with marine shells shows, however, that the observed radon content does not always follow a simple time formula. In some cases, there is more radium than predicted by uranium decay, and in other cases, there is a deficit. It turns out that shells only exceptionally act as closed systems, and migration of uranium and daughter elements out and into the shells frequently occurs. In single cases, a strong accumulation of uranium is observed. The results presented in tables 1-3 should give a fairly good cross-section of radon content which may be expected in material from Norway and Svalbard (fig 7). The Th/U ages given in the tables are based on measurements of ^{226}Ra and ^{238}U and calculated in agreement with the above formula. A more accurate Th/U age should, however, be based on direct measurement of the $^{230}\text{Th}/^{234}\text{U}$ ratio.

Some former radium and uranium results for 6000 to 12,000

TABLE 1. ^{226}Ra and ^{238}U in shell samples from Norway

Sample no.	Sample	Loc	Fraction %	^{226}Ra c/min 10g	^{238}U c/min 10g	^{226}Ra/^{238}U	^{14}C age yr
T-119C	Mytilus edulis	Oslo	90	1.1	10.9	0.10	9450±250
T-180	Mytilus edulis	Oslo	90	5.2	85.0	0.06	9200±300
T-179	Pecten septemr	Oslo	90	9.6	4.6	2.03	9750±250
T-158	Pecten septemr	Oslo	85	1.9	8.4	0.23	6950±200
T-117B	Macoma calcarea	Fredrikstad	90	1.3	1.8	0.68	9950±300
T-121B	Isocardia cor	Fredrikstad	82	13.0	6.1	1.08	6570±150
T-123B	Littorina littorea	Kråkerøy	90	0.2	0.2	1.0	6850±170
T-178	Macoma calcarea	Tønsberg	90	1.1	4.1	0.27	10,200±200
T-229A T-229B	Mya truncata	Bergen	41 43	2.3 1.5	3.2 3.7	0.71 0.42	10,150±300
T-142B	Mya truncata	Bergen	95	0.6	0.5	0.12	11,500±300
T-139A T-139B	Mytilus edulis	Bergen		1.0 1.5	2.7 7.4	0.37 0.20	12,700±350
T-112	Mya truncata	Troms	93	1.4	6.8	0.20	11,500±300
T-125	Mya truncata	Troms	85	1.8	7.7	0.23	9880±240
T-214	Mya truncata	Troms	80	1.5	1.6	1.0	11,400±250
T-260	Mya truncata	Troms		1.7	4.8	0.34	ca 10,000

year old shells (Nydal, 1960; 1962) from various parts of Norway are shown in table 1. The uranium figures vary widely, from a negligible amount of 0.2 counts/min in 10g carbonates (T-123B) at the outer Oslofjord, to a relativly high value of 85.0 counts/min from Oslo (T-180). The uranium content at Oslo is known to be relativly high, which seems to be reflected in the material. The observed radon content in most shell samples is generally very low, partly because of the small contribution from uranium during a relativly short period. A few samples (T-179, -121B, -123B, and -114), however, show a radium and radon content which is much greater than could be predicted from a closed uranium system. Table 2 shows a fairly good agreement between Th/U age and ^{14}C age (for additional details, see Andersen et al, 1981), at least for the innermost fractions, and the measured radium and radon content largely agrees with that derived from incorporated uranium. The shells were well-preserved in hard clay, and the approach to a closed system seems to be satisfied. ^{226}Ra/^{238}U ratio has also been measured on a number of samples from Svalbard (Salvigsen and Nydal, 1981), and the most controversial results are shown in table 3. The series from Phippsøya demonstrate in an instructive way how uranium and radium migrate out and into the shell, and how the time formula based on the radium-uranium ratio has failed. For the fractions of samples T-3101 and T-3100, radium is either lost during the past, or more reasonably, a major portion of the uranium accumulates at a later stage. The radium and uranium content in sample T-3814 constitute, respectivly, 8 and 4 times the earlier ob-

TABLE 2. ^{226}Ra and ^{238}U in shell samples from southwestern Norway

Sample no.	Sample	Loc	Fraction %	^{266}Ra c/min 10g	^{238}U c/min 10g	^{226}Ra/^{238}U	Th/U age yr	^{14}C age yr
T-3422A	Mya truncata	Jæren	43	18.3	25.6	0.71	109,000	39,200
T-3422B			45	19.9	50.0	0.40	48,800	38,600
T-3423A	Mya truncata	Jæren	30	11.3	12.8	0.88	166,000	27,900
T-3423B			60	4.9	9.0	0.54	74,000	31,300
T-116	Arctica islandica	Jæren	98	1.9	5.1	0.37	46,000	>36,000 2σ
T-116B	Arctica islandica	Jæren	57	2.8	6.2	0.45	57,000	
T-116C			33	2.0	1.3?	1.50		
T-3631A	Arctica islandica	Jæren	43	2.9	8.7	0.33	39,400	46,700
T-3631B			44	1.8	3.7	0.49	58,000	
T-140	Mya truncata	Bø, Karmøy	95	4.5	13.4	0.34	40,400	34,000
T-2006A	Arctica islandica	Bø, Karmøy	11	8.3	20.1	0.41	50,800	
T-2006B			44	4.0	16.8	0.24	27,000	
T-2006C			45	3.8	12.8	0.30	36,200	37,500
T-2007A	Mya truncata	Bø, Karmøy	10	9.4	13.1	0.72	113,000	
T-2007B			45	3.7	11.3	0.33	38,900	
T-2007C			45	3.8	11.5	0.33	38,900	38,300
T-2953A	Mya truncata	Bø, Karmøy	23	7.1	41.6	0.17	18,600	38,500
T-2953B			30	4.6	21.9	0.21	23,100	39,200
T-2953C			22	4.5	11.8	0.28	46,100	42,200
T-2953D			24	3.1	6.1	0.53	63,600	43,000
T-2954A	Chlamys islandica	Bø, Karmøy	31	4.9	5.2	0.94	197,000	>46,500 2σ
T-2954B			58	1.2	2.6	0.62	88,000	

TABLE 3. ^{226}Ra and ^{238}U in shell samples from Svalbard

Sample no.	Sample	Loc	Fraction %	^{226}Ra c/min 10g	^{238}U c/min 10g	^{226}Ra/^{238}U	Th/U age yr	^{14}C age yr
T-3294II	Mya truncata	Phippsøya	11					
T-3294A		Sjuøyane	33	11.9	21.6	0.55	76,000	42,000
T-3294B			33	12.5	19.3	0.64	96,000	45,100
T-3294C			23	9.9	18.9	0.53	70,000	
T-3101	Mya truncata	Phippsøya	18					
T-3101A		Sjuøyane	22	14.1	97.3	0.15	15,000	41,200
T-3101B			22	12.7	122.8	0.10	11,000	38,000
T-3101C			38	12.5	149.7	0.08	8000	39,800
T-3614	Hiatella arct	Phippsøya	10					
T-3614A		Sjuøyane	31	155.8	231.5	0.68	102,000	38,100
T-3614B			31	130.6	285.5	0.46	58,000	42,200
T-3614C			28	137.4	324.2	0.43	53,000	
T-3102	Mya truncata	Phippsøya	10					
T-3102A		Sjuøyane	30	4.2	1.5	0.40	49,000	38,400
T-3102B			30	2.9	11.5	0.25	29,000	37,600
T-3102C			32	2.1	10.3	0.21	23,000	41,400
T-3100	Mya truncata	Phippsøya	10					
T-3100A		Sjuøyane	22	13.0	183.7	0.07	7400	9950
T-3100B			22	13.0	175.3	0.07	7600	
T-3100C			23	19.5	142.0	0.14	14,600	
T-3100D			23	19.5	150.0	0.13	13,800	

served maximum value. The total radon counting rate for this sample on the β plateau (radon + daughter elements) in a 2L CO_2 proportional counter (2 atm pressure) is ca 400 counts/min at the time of preparation, decreasing to 0.015 counts/min after a storage time of eight weeks.

However, it is not always practical to wait 6 to 8 weeks until radon is removed by natural decay. The first attempt at physical removal of radon by a slow distillation process (de Vries, 1957) was both critical and time consuming, and has only been used by a few laboratories. Another method, which now seems to be well-accepted, is a chromatographic process in which radon is absorbed in charcoal when CO_2 passes through.

Radon can be removed from the charcoal afterwards at a higher temperature. A method that indirectly removes radon is absorbing the CO_2 sample in ammonia and further precipitation as calcium carbonate. This procedure was introduced in our laboratory for most samples except shells, for removing electronegative impurities (eg,SO_2), but it also serves to remove radon.

No chemical or physical process for removal of radon may be absolutely complete, and a storage time of 1 to 2 weeks may still be necessary, especially for very old samples.

ACKNOWLEDGMENTS

I wish to thank Eiliv Steinnes and Oddvar Johansen, Institute of Atomic Energy, Kjeller, for performing uranium measurements, and Knut Berg, Instrument Center, The Norwegian Institute of Technology, for beautiful drawing of figures.

REFERENCES

Andersen, B G, Nydal, R, Wangen, O P, and Østmo, S, 1981, Weichselian before 15,000 years BP at Jæren-Karmøy in southwestern Norway: Boreas, v 10, p 297-314.

Kaufman, H, Broecker, W S, Ku, T L, and Thurber, D L, 1971, The status of the U-series methods of mollusc dating: Geochim et Cosmochim Acta, v 35, p 1155-1183.

Nydal, R, 1960, Trondheim natural radiocarbon measurements II: Radiocarbon, v 2, p 82-96.

——— 1962, Trondheim natural radiocarbon measurements III: Radiocarbon, v 4, p 160-181.

——— 1965, Ten years trial and error with the CO_2 proportional counting technique in Trondheim, in Chatters, R M and Olson, E A, eds, Internatl conf on radiocarbon and tritium dating, 6th, Proc: Washington DC, Clearinghouse for Fed Sci Tech Inf, NBS, p 1-16.

——— 1977, Thorium-uranium dating of marine deposited calcium carbonate, in Povinec, P and Usačev, S, eds, Low-radioactivity measurements and applications, Proc: Internatl conf, High Tatras, CSSR, p 345-349.

Sackett, W M, (ms) 1958, Ionium-uranium ratios in marine deposited calcium carbonates and related materials: PhD thesis, Washington Univ, St Louis, Missouri.

Salvigsen, O, and Nydal, R, 1981, The Weichselian glaciation in Svalbard before 15,000 BP: Boreas, v 10, p 434-446.

Thurber, D L, 1962, Anomalous $^{234}U/^{238}U$ in nature: J Geophys Res, v 62, p 4518-4520.

Vries, Hessel de, 1957, The removal of radon from CO_2 for use in ^{14}C age measurements: Appl Sci Research sec B, v 6, p 461-470.

[Radiocarbon, Vol 25, No. 2, 1983, P 511-518]

EVALUATION OF DIRECT-PRECIPITATION AND GAS-EVOLUTION METHODS FOR RADIOCARBON DATING OF GROUND WATER

IN CHE YANG

US Geological Survey, Mail Stop 407
PO Box 25046, Denver Federal Center
Denver, Colorado 80225

ABSTRACT. The extraction of dissolved carbonate species for age dating from a 100L water sample by the direct-precipitation method (DPM) and by the gas-evolution method (GEM) has been investigated. Stable carbon-isotope fractionation between initial and final carbon dioxide evolved was ca 11‰ by GEM and 1‰ by DPM. GEM will produce isotopically lighter carbon dioxide compared with DPM if carbonate recovery is low. Extraction efficiency of $>95\%$ can be achieved by GEM in 3 hours using nitrogen gas at a sweeping rate of 2000cc per minute. DPM requires precipitates to settle overnight to assure $> 95\%$ recovery. GEM is little affected by a high concentration of sulfate ions, whereas DPM is greatly affected by sulfate resulting in less yield.

Important in the correction of ^{14}C age for ground water is estimating the contributions of various sources of dissolved carbonate species based on measured $^{13}C/^{12}C$ ratios and total carbonate. Because large fractionations were observed with a large sample, a separate small aliquot of water sample (500ml) should be analyzed for stable carbon isotopes by DPM to assure complete extraction. For small samples ($<$ 1ml of benzene) gas counting is preferred over liquid-scintillation counting. A carbon dioxide-methane conversion can be accomplished in 3 hours with a 98% yield for a 4L sample.

INTRODUCTION

Groundwater samples for ^{14}C dating at the US Geological Survey water-quality laboratory, Denver, Colorado are either collected and returned to the laboratory for carbonate precipitation or precipitated at the sampling site and shipped back for ^{14}C analysis (Thatcher, Janzer, and Edwards, 1977). Precipitation at the sampling site has the advantage of shipping small containers although it yields less carbonate precipitate because of insufficient settling time. Laboratory precipitation costs more for sample shipment and dissolved carbon dioxide (CO_2) may be lost during transportation. The precipitation method gives low carbonate yields when sulfate ions are present in high concentration. Gleason, Friedman, and Hanshaw (1969) studied the effect of carbon-isotope fractionation by the gas-evolution method (GEM) and the direct-precipitation method (DPM) and found that the former technique seemed to give large fractionations. The present investigation further studies the two methods with an improved gas-evolution apparatus and aims at substituting the present DPM with GEM. This will enable us to obtain a greater CO_2 yield from carbonate species at the sampling site in less time, facilitate shipment of collected gas samples, and eliminate the problem of atmospheric CO_2 contamination. The scope of the studies includes CO_2 yield from carbonate species by GEM, and comparison of carbon-isotope fractionation by both methods in 100L samples.

GAS-EVOLUTION METHOD (GEM)

LABORATORY STUDIES OF THE CO_2 YIELD. Laboratory experiments were conducted with sodium bicarbonate ($NaHCO_3$) dissolved in de-ionized water and with calcium chloride ($CaCl_2$) and magnesium sulfate ($MgSO_4$) added to produce an artifical ground water. De-ionized water was purged with CO_2-free nitrogen (N_2) gas to expel any dissolved CO_2 in the water before dissolution of $NaHCO_3$. Complete evolution of CO_2 is achieved by addition of excess sulfuric acid (H_2SO_4). To produce 8L of CO_2 at 25°C and 760mm Hg, 28.7g of $NaHCO_3$, 7g of $MgSO_4 \cdot 7H_2O$, and 45g of $CaCl_2 \cdot 2H_2O$ are dissolved in 100L of water. The water was kept in two 60L carboys connected in series. CO_2 was collected in two liquid-nitrogen-cooled traps in the laboratory vacuum-line system. The N_2 sweep facilitates collection of CO_2. The exit gas was bubbled through a bottle containing saturated solution of barium hydroxide ($Ba(OH)_2$) to ensure no loss of CO_2. If CO_2 escapes, white precipitate will be formed in the bottle. Nitrogen flow rates were controlled at two speeds: one at 2000cm^3/min, and the other at 1000cm^3/min. The rate of CO_2 evolution was determined by measuring the incremental volume evolved vs elapsed time. Each volume measurement was done by expanding the CO_2 collected in two liquid-nitrogen traps into a known volume of reservoirs in the vacuum-line system. The time/yield relation is shown in table 1. The data indicate that 95% or more of CO_2 in water can be collected in < 2 hr at a sweep rate of 2000cm^3/min, and in 3 hr at a sweep rate of 1000 cm^3/min. Thus, if the CO_2 recovery is 95% or more, the occurrence of carbon-isotope fractionation should be negligible for our purpose.

LABORATORY STUDIES OF CARBON-ISOTOPE FRACTIONATION. Samples for fractionation studies were collected in five fractions of approximately equal volumes of CO_2 by adding theoretical amounts of acid required in each fraction. Carbon dioxide evolved in each fraction was precipitated separately in an

TABLE 1. Time vs CO_2 yield at two flow rates (carrier gas, N_2, sample size of 100L of water in 2 carboys, acidified, and total of 8L of CO_2 representing 100% yield)

Flow rate of N_2 (cm^3/min)	Elapsed time (min)	Accumulated CO_2 yield (%)
1000	20	11.5
	40	44.0
	80	63.0
	150	89.3
	180	95.0
	240	100.0
2000	10	4.9
	30	47.0
	50	66.1
	80	85.2
	110	96.0
	160	100.0

TABLE 2. Laboratory studies of carbon-isotope fractionation by GEM from artificial ground water. Each fraction contains ca 20% of the total carbon content of the water sample*

Water sample**	Fraction	$\delta^{13}C$ (‰) (fractional)	$\delta^{13}C$ (‰) (accumulated)
1	1st	-11.3	-11.3
	2nd	-12.0	-11.7
	3rd	-9.0	-10.8
	4th	-3.3	-8.9
	5th	-1.8	-7.5
2	1st	-9.2	-9.2
	2nd	-11.9	-10.6
	3rd	-9.7	-10.3
	4th	-6.5	-9.3
	5th	-2.1	-7.9

* Samples for fractionation studies were collected in five fractions of approximately equal volumes of CO_2 by adding theoretical volumes of acid required in each fraction.

**Water sample was prepared by dissolving 28g of $NaHCO_3$ in 100L of distilled water and adding $CaCl_2$ and $MgSO_4$ to simulate a natural ground water.

TABLE 3. Comparison of carbon-isotope fractionation by DPM and GEM methods for water from a limestone aquifer near Gillette, Wyoming. (The precision for $\delta^{13}C$ values is ±0.2%)

	DPM			GEM	
Sample	Fraction*		$\delta^{13}C$ (‰)	Cylinder**	$\delta^{13}C$ (‰)
PRB 6	1st		-12.5	1st(28%)	-19.0
	2nd		-13.1	2nd(1%)	-24.2
	3rd		-13.3	3rd(71%)	-14.8
	4th		-13.4		
		Average	-13.1	Weighted average	-16.1
PRB 11	1st		-11.2	1st(80%)	-13.3
	2nd		-11.2	2nd(20%)	-9.6
	3rd		-11.4		
	4th		-11.8		
		Average	-11.4	Weighted average	-12.6

*$\delta^{13}C$ samples were precipitated in four fractions of approximately equal volumes by adding ¼ of the required amount of $SrCl_2$-NH_4OH solution to the sample water each time.

**Gas evolved from two carboys (60L each) was collected in a Linde 5A molecular sieve contained in two $500cm^3$ stainless-steel cylinders connected in series (fig 1). For sample PRB 6, first two cylinders collected the dissolved CO_2 by direct purging of water sample without acidification for 30 min followed by replacing the first two cylinders with the third cylinder and collecting the remaining carbonate by acidification.

evacuated bottle (near vapor pressure of water) containing a saturated $Ba(OH)_2$ solution. The reaction proceeded instantaneously to form barium carbonate ($BaCO_3$) precipitate. A small portion of mixed, dry $BaCO_3$ was taken, acidified and analyzed for $^{13}C/^{12}C$. The results are shown in table 2. Values of $\delta^{13}C$ indicate that large fractionation occurred in both studies. The tendency, as expected, is to release the lighter carbon-isotope initially and the heavier carbon-isotope at the end of the studies. The maximum $\delta^{13}C$ difference between the initial and final fractions is 10.2‰ in the first study and 9.8‰ in the second study. The accumulated $\delta^{13}C$ difference between the initial and final values is ca 3.2‰, which is somehwat smaller compared with 5‰ reported by Vogel, Lerman, and Mook (1975).

SAMPLING-SITE STUDIES OF CO_2 EVOLUTION. The apparatus used for CO_2 evolution at sampling sites is shown in figure 1. Water traps used in the laboratory were replaced with silica gel contained in two transparent plastic containers. Two metal cylinders ($500cm^3$) containing Linde 5A[1] molecular sieve replaced the liquid nitrogen traps for collecting CO_2 (Fergusson, 1963; Fairhall, Young, and Bradford, 1972). The molecular sieve was evacuated and heated to 350°C under the vacuum (overnight) to remove any moisture or CO_2 before use at the sampling site. At the sampling site, 100L of groundwater sample contained in two carboys were acidified with concentrated H_2SO_4. Pure N_2 from a gas cylinder was slowly bubbled through the water at a flow rate of $1000cm^3$/min for 30 min, then gradually increased to 2000 cm^3/min and purged at this flow rate for 2 1/2 hr. To estimate the possible loss of dissolved CO_2 during the sample filling process and shipment from the sampling site to the laboratory in Denver, sample PRB 6 was purged for 30 min at the flow rate of $1000cm^3$/min without acidification and CO_2 collected in two metal cylinders. Then, the first two cylinders were replaced with a third cylinder and it collected the remaining carbonate by acidification. The results are shown in table 3. For sample PRB 6, the CO_2 collected in the first two cylinders amounted to ca 29% of total CO_2. Therefore, it is advisable to adjust the pH of water to ca 10 by addition of fresh NaOH solution just before water collection, so that dissolved CO_2 can be converted to carbonate species to avoid the outgassing loss during transportation if precipitation at the sampling site is not feasible.

---

[1] The use of brand names in this report is for identification only and does not constitute endorsement by the US Geological Survey.

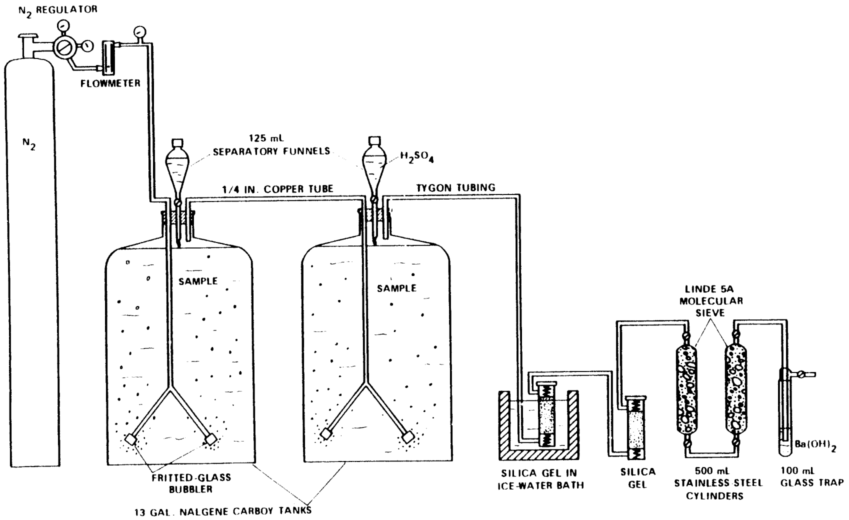

Fig 1. Carbon dioxide evolution system for extraction of dissolved carbonate species from natural water

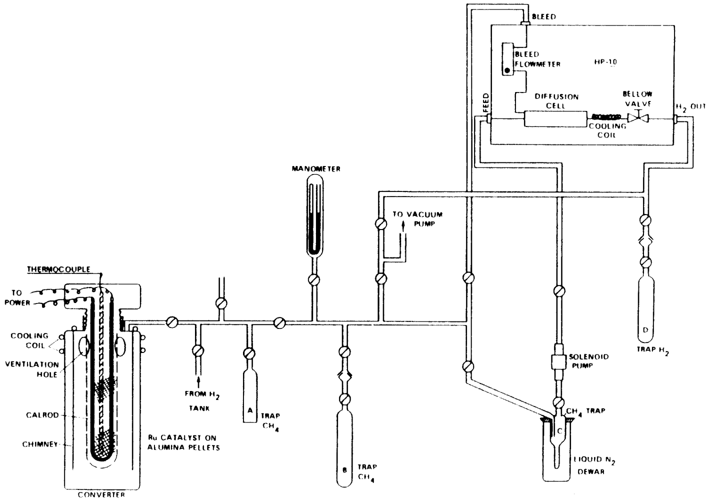

Fig 2. Carbon dioxide to methane conversion system

SAMPLING-SITE STUDIES OF CARBON-ISOTOPE FRACTIONATION. The results of carbon-isotope fractionation by GEM are shown in the last column of table 3; the first cylinder collected the lighter carbon isotope, and the last cylinder collected the heavier carbon isotope (except in the instance of the second cylinder for sample PRB 6). The second cylinder trapped lighter carbon isotope ($\delta^{13}C = -24.2$ ‰) compared with the first cylinder (-19.0‰). The possible explanation is that the flow rate of N_2 sweeping at the beginning of purging might have been too fast (not well controlled), resulting in the escape of CO_2 from the first cylinder and collection in the second. After normal flow rate was established, most of the CO_2 was collected in the first cylinder. Table 3 demonstrates that only 1% of CO_2 was collected in the second cylinder compared with 28% collected in the first cylinder.

DIRECT-PRECIPITATION METHOD (DPM)

A groundwater sample of 140L was collected in the conical-shaped precipitation tank with a 2L Mason jar screw-attached to the bottom of the tank. A top plate was provided to seal the tank from contact with the atmospheric CO_2 and a stirrer also was provided to mix the content uniformly. Barium chloride ($BaCl_2$) or strontium chloride ($SrCl_2$) were used to precipitate the carbonate as $BaCO_3$ or $SrCO_3$; the precipitate was collected in the Mason Jar. After several hours of standing, the valve directly above the jar was closed, the top was unscrewed, capped immediately, and edges sealed with tape. The jar was sent to the laboratory.

Samples for carbon-isotope fractionation study were precipitated in four batches of approximately equal volumes of carbonate by adding 1/4 of the required amount of $SrCl_2$-NH_4OH solution to the sample water each time. In the laboratory, carbonate precipitate was acidified with phosphoric acid (H_3PO_4) to generate CO_2 gas for mass-spectrometric analysis. The results are shown in table 3. There are very few differences among the four fractions in both samples as indicated by the $\delta^{13}C$ values. The decrease in heavier isotopes from the first fraction toward the fourth fraction also is evident in both instances. However, the difference is only a fraction of 1‰.

COMPARISON OF $\delta^{13}C$ VALUES BETWEEN DPM AND GEM

Results of GEM invariably are isotopically lighter than those of DPM. The difference for sample PRB 6 between the two methods is 3‰, whereas for sample PRB 11, the difference is only 1.2‰. This can be explained by examining the processes of fractionation in some detail. Strontium sulfate ($SrSO_4$) precipitates with $SrCO_3$. The increase in sulfate concentration decreases the carbonate-precipitate yield because the amount of $SrCO_3$ precipitated does not vary linearly with the amount of $SrCl_2$ added; this process precipitates the heavier carbon isotope and leaves behind the lighter carbon isotope in the solution. Hassan (1982) found that the increase in the sulfate concentration to 0.01 molar decreases the efficiency of carbonate recovery to 90% by precipitation; thus, the heavier carbon isotope by DPM compared to GEM (which collects 95% or more) is observed. In contrast, GEM generates isotopically lighter carbon at the beginning of the process and heavier isotopes at the end. Consequently, incomplete recovery of carbon results in lighter $\delta^{13}C$ values. The two processes enhance each other yielding even larger differences for the two methods if complete recovery of inorganic carbon is not attained. These processes partly account for the isotopically heavier $\delta^{13}C$ values by DPM compared to GEM in table 3.

THE SMALL BENZENE SAMPLE

In the laboratory, CO_2 is allowed to react with metallic lithium (Li) to produce lithium carbide (Li_2C_2), which is then hydrolyzed to produce acetylene (C_2H_2). The acetylene is then passed over a Mobil Durabead catalyst[1] to form benzene (C_6H_6). Benzene is placed in Teflon vials and counted on liquid-scintillation counters (Yang and Emerson, 1980). For clean carbonate precipitate, the CO_2-C_2H_2 conversion step normally results in > 95% efficiency and ca 88% efficiency in the C_6H_6 step. However, in quite a few instances, impure gas generated from the acidification of carbonate precipitate poisons the Li, resulting in low yields on subsequent steps of C_2H_2 and C_6H_6 syntheses. In other instances, small C_6H_6 samples were obtained due to low carbonate concentrations in the ground water itself. From preliminary sampling-site data, indications were that GEM invariably yielded more C_6H_6, probably because of the cavity size of the molecular sieve that trapped the CO_2 and excluded other gases. More data are required to support the finding.

For small samples, gas counting is preferred over liquid-scintillation counting. Methane gas is used as a counting gas, because the same system also can be used to assay tritium activity. In 1980 a CO_2-CH_4 conversion system was developed that was similar to the design of Buddemeier et al (1970), except that model HP-10 is used in CH_4 purification instead of the A-5 palladium diffusion cell. Other modifications also were made on the converter and CH_4-gas trap (fig 2). For a 4L CO_2 sample, the conversion can be accomplished in 3 hr with a 98% yield. The proportional counters are similar to those of previous designs at the Quaternary Research Center of the University of Washington in Seattle (Stuiver, Robinson, and Yang, 1979).

CONCLUSION

GEM for extracting carbonate species from a large volume of ground water for ^{14}C dating is little affected by the presence of high concentrations of sulfate ions, is less susceptible to contaminations from atmospheric CO_2, is less time-consuming, and results in a higher yield. Thus, GEM is a better method for ^{14}C determination than DPM. However, possible large carbon-isotope fractionation by GEM, which is ca 1.1%, can be avoided by sweeping with carrier gas at a flow rate of 2000cm^3/min for 3 to 4 hours. A separate 500ml water sample should be collected for ^{13}C/^{12}C analysis by DPM to calculate the contributions of various sources of dissolved carbonate species to the ^{14}C ages.

REFERENCES

Buddemeier, RW, Young, AY, Fairhall, AW, and Young, JA, 1970, Improved system of methane synthesis for radiocarbon dating: Rev Sci Instruments, v 41, no. 5, p 652-654.

Fairhall, AW, Young, AW, and Bradford, PA, 1972, Radiocarbon in the sea, in Rafter, TA and Grant-Taylor, T, eds, Internatl ^{14}C conf, 8th, Proc: Wellington, Royal Soc New Zealand, p C2-C16.

Fergusson, GJ, 1963, Upper tropospheric carbon-14 levels during spring 1962: Jour Geophys Research, v 68, p 3933-3941.

Gleason, JD, Friedman, I, and Hanshaw, BB, 1969, Extraction of dissolved carbonate species from natural water for carbon-isotope analysis: US Geol Survey Prof Paper 650-D, pD248-D250.

Hassan, AA, 1982, Methodologies for extraction of dissolved inorganic carbon for stable carbon-isotope studies-Evaluation and alternatives: US Geol Survey Water Resources Inv, 82-6, 51p.

Stuiver, M, Robinson, SW, and Yang, IC, 1979, Carbon-14 dating to 60,000 years BP with proportional counters, in Berger, R and Suess, HE, eds, Radiocarbon dating, Internatl ^{14}C conf, 9th, Proc: Berkeley, Univ California Press, p 202-215.

Thatcher, LL, Janzer, VJ, and Edwards KW, 1977, Carbon-14, dissolved, apparent age, liquid scintillation method, Denver Laboratory: US Geol Survey Techniques of Water Resources Inv, Bk 5, Chap A5, p 17-22.

Yang, IC and Emerson, RL, 1980, Teflon vials for low-level carbon-14 liquid scintillation counting, in Peng, Horrocks, and Alpen, EL, eds, Liquid scintillation counting: recent applications and development: New York, Academic Press, v 2, p 181-197.

Vogel, JC, Lerman, JC, and Mook, WG, 1975, Natural isotopes in surface and groundwater from Argentina: Bull Hydrol Sci, v 2C p 203-221.

[Radiocarbon, Vol 25, No. 2, 1983, P 519-527]

AN INTERNATIONAL REFERENCE MATERIAL FOR RADIOCARBON DATING*

W B MANN

National Bureau of Standards, Washington, DC, 20234

ABSTRACT. In August 1980, the National Bureau of Standards (NBS) issued, in the form of oxalic acid, a new International Reference Material of contemporary ^{14}C for use in radiocarbon dating laboratories. This reference material was to replace the 1975 oxalic-acid standard, supplies of which had been practically exhausted in 1978. The preparation of the new oxalic-acid standard was described in a preliminary report, as were, also, the results then available for the activity-concentration ratio of the new to the old standard obtained by a number of leading international laboratories.

With the recent completion of the analysis of all results submitted by the participating laboratories, NBS plans to issue these recently calibrated samples of oxalic acid as an NBS Standard Reference Material. There is, however, no significant difference in the reported value of its activity concentration, relative to that of the 1957 standard, from that given provisionally in 1980.

Subsequent to our report (Cavallo and Mann, 1980) a further measurement of relative activity concentration was reported by the Radiocarbon Laboratory of Peking University. Their value, and that also for $\delta^{13}C$, is insignificantly different from the average value of the results submitted by the eleven laboratories that participated in the international comparison organized by NBS.

Cavallo and Mann (1980) gave a preliminary value for a new radiocarbon-dating standard, NBS Research Material RM-49 (see also Stuiver, 1980). Since then the results have received scrutiny in various laboratories, some slight modifications and suggestions have been received, and one new result has been submitted. In spite of considerable correspondence there is some residual doubt about the statements of uncertainty by various laboratories. None had given a statement of systematic uncertainty; in fact some claimed zero such uncertainty. After many discussions it appeared to us that systematic uncertainties involving the threshold voltage of the counter plateau, pressure and temperature measurements, incomplete chemical-reaction yields, and mass-spectrometric measurements of ^{13}C abundance might amount to as much as 0.05 to 0.2%. We therefore included, as a matter of prudence, an estimate of 0.1% for the

---

* Contribution of the National Bureau of Standards, not subject to copyright.

systematic uncertainty in the final estimate of the overall uncertainty. After further consideration, however, the estimate of systematic error in the present paper, assessed at a level approximately equivalent to one standard deviation of the mean, has been reduced to 0.05%.

In the final analysis in the preliminary certificate, however, we treated the average value from each laboratory as an independent sampling of the same population, deriving an overall average at a 99% level of confidence for the mean value of the activity concentration of the new NBS oxalic-acid standard relative to that of the old. But from the discussion at the 11th International Radiocarbon Conference in Seattle a preference seemed to be expressed for a weighted-average value of the results to be given.

The aim of NBS in inviting participation of an international comparison of its old and new oxalic-acid standards was simply to obtain a reliable value for the ratio of the activity concentration of the new standard relative to that of the old. Three half-pound samples of oxalic acid were distributed to several laboratories -- one sample of the old oxalic-acid standard (SRM-4990) and two of the new standard. These latter comprised one sample with aliquants taken from all of 198 5-lb jars of specially prepared oxalic acid, generously provided by Pfizer Inc, and one sample taken from a single 5-lb jar randomly selected, in order to check the homogeneity of all 198 jars. The samples taken from single 5-lb jars were designated "I", and the mixed samples from all the 5-lb jars, "M" (this is described more fully in Cavallo and Mann, 1980). The measurements made by the University of Peking, Beijing, were on material from NBS Research Material RM-49 that was taken, however, from the same batch of oxalic acid as were the samples "I" and "M".

The comparison of the activity concentration of the new standard with the old standard (NBS SRM-4990) involves the measurement of activity per unit mass of each standard. The only other consideration is that in the preparation of carbon dioxide, or acetylene, from the oxalic-acid samples the yield should not be significantly different from 100%, apart from random fluctuations. In the old standard this could be assessed by measuring the isotopic abundance of ^{13}C relative to ^{12}C in the gas sample. The ^{13}C abundance had been carefully measured in the old standard and is usually expressed in terms of the quantity $\delta^{13}C$, which is a measure of the difference in the ratio $^{13}C/^{12}C$ in the standard from the ratio of $^{13}C/^{12}C$ in the deposit of Belemnitella americana in the Pee Dee formation (PDB) in South Carolina.

Participants in the international measurement of the new NBS oxalic-acid standard not only measured the ratio of activity concentrations of the two standards, but also the value of $\delta^{13}C$

for the old and new standards. The reliability of these measurements clearly depends on complete chemical yield being achieved in the conversion of the oxalic acid to carbon dioxide; as with the old oxalic-acid standard, individual values obtained for $\delta^{13}C$ in future samples can be used to estimate the yield in the conversion to the counting material, and to correct for the corresponding $\delta^{14}C$. In the new NBS standard it would appear, from the results shown in Table 1, that $\delta^{13}C$ is somewhat smaller in absolute magnitude -- about 17.6‰ -- than in SRM-4990. Such a decrease corresponds to an enhancement of the $^{13}C/^{12}C$ ratio, relative to SRM-4990, in the growing of the French beet or its subsequent fermentation.

The results shown in Table 1 are also plotted as histograms in Figures 1(A) and 1(B). In these figures the shaded results represent values obtained in Groningen for counting-gas samples (or carbon dioxide representative of the liquid-scintillation-counting solution) submitted to W G Mook for mass-spectrometric analysis. It is very clear, from casual inspection, that neither the distribution of results for the old standard nor that for the new standard is very normal. There is indeed a very strong indication of systematic error. The average values of the two distributions, old and new, are respectively -19.1‰ and -17.6‰. The difference between them is 1.5‰ and this, fortunately, is the only quantity used in determining the final activity-concentration ratio of the new-to-old NBS standards.

Several earlier measurements have been made of $\delta^{13}C$ for the old NBS standard, which is now accepted as lying in the range of -19.2 to -19.3‰. The corresponding range of values for the new NBS standard corresponding to the difference of 1.5‰, would be -17.7 to -17.8‰. Any values greater, in absolute magnitude, would represent possibly incomplete chemical conversion to carbon dioxide.

If, however, one takes differences in paired $\delta^{13}C$ values from individual laboratories the results, shown in Figure 2 are quite remarkable. (The values of $\Delta\delta^{13}C$ for laboratory 2, shown in Table 1, were not used in plotting Figure 2.) The distribution of results, although limited in number, looks reasonably normal. The mean value and its estimated standard deviation are (1.49 ± 0.05)‰. This dramatic improvement strongly suggests the existence of systematic biases in the results, shown in Figure 1, obtained by individual participants.

The weighted averages of the ratio of the activity concentrations obtained by the participants in the intercomparison are shown in Table 2. All adjustments to different values of $\delta^{13}C$ have been made using the factor

$$(1+\delta_1{}^{13}C/1000)^2/(1+\delta_2{}^{13}C/1000)^2.$$

TABLE 1. Reported values of $\delta^{13}C$

Participating Laboratory	Reported Values of $\delta^{13}C$ (^{o}/oo vs PDB)			$\Delta\delta^{13}C$ between old and new standards (^{o}/oo vs PDB)
	I	M	4990	
1. Arizona, University of, Austin Long	-17.4	-17.4	-18.7 ± 0.1	1.3
2. Bern, University of, Hans Oeschger	-17.2 ± 0.1 -17.12*	-16.4 ± 0.1 -17.78*	-17.4 ± 0.1 -20.02*	0.6 2.57*
3. California Inst of Tech, Pasadena Sam Epstein Susan Kurisu	-16.8	-16.8	-18.2	1.4
4. California, Univ of, Los Angeles Rainer Berger W F Libby	-17.91	-18.04	-19.48	1.51
5. California, Univ of, San Diego T W Linick Hans Suess	-17.7	-17.5	-19.3	1.7
6. National Physical Research Laboratory, Pretoria J C Vogel	-17.54	-17.61	-19.28	1.71
7. Peking, University of, Beijing Chen Tei-mei Yun Si-xun	-17.14**	-17.52**	-18.52 -19.02	1.44
8. Queens University, Belfast G W Pearson	-17.75 ± 0.12 -17.73 ± 0.11 -18.26*	-17.78 ± 0.14 -17.77 ± 0.11 -17.81*	-19.59 ± 0.1 -19.53*	1.83 1.50*
9. Rijksuniversiteit, Groningen W G Mook	-17.63 -17.67	-17.48 -17.65	-19.09 -19.24 -19.35	1.54 1.58
10. U S Geological Survey, Denver Irving Friedman	-17.50 ± 0.02	-17.52 ± 0.02	-18.75 ± 0.02	1.24
11. U S Geological Survey, Menlo Park S W Robinson J R O'Neill	-18.00 -18.45*	-18.11 -18.36*	-19.47 ± 0.48	1.42
12. U S Geological Survey, Reston Meyer Rubin Tyler B Coplen	-17.95	-	-19.12	1.17
13. Washington, Univ of, Seattle Minze Stuiver Pieter Grootes	-17.49 -17.84*	-17.48 -17.79*	-19.00 ± 0.04 -19.26 ± 0.01*	1.52 1.45*

*Results of measurements by Professor W G Mook on samples of counting gas or carbon dioxide, in case of liquid-scintillation counting, sent to for isotopic-abundance measurements.

**Measurements carried out using NBS Research Material, RM-49, which was distributed from same new batch of oxalic acid.

TABLE 2. Activity-concentration ratios of new-to-old NBS radiocarbon-dating standards

Laboratory	Reported values of activity-concentration ratios of new-to-old oxalic acid standards		δ^{13}C values for reported ratios ($^{o}/_{oo}$ vs PDB)			Ratios normalizes to δ^{13}C = $-19^{o}/_{oo}$ for I, M, and 4990 (weighted averages and and their estimated standard deviations)	
	I/4990	M/4990	I	4990	M	I	M
2 Bern	1.2925 ± 0.0056 1.2896 ± 0.0055	1.2941 ± 0.0057 1.2876 ± 0.0059	-17.2	-17.4	-16.4	1.2905 ±0.0039	1.2883 ±0.0041
	1.2986 ± 0.0053 1.2898 ± 0.0053	1.2955 ± 0.0052 1.2865 ± 0.0053	-17.12	-20.02	-17.78	1.2866 ±0.0037	1.2852 ±0.0037
						(1.2875 ± 0.0019)	
4 UCLA	1.2854 ± 0.0096	1.2887 ± 0.0097	-17.91	-19.48	-18.04	1.2813 ±0.0096	1.2849 ±0.0097
						(1.2831 ± 0.0069)	
5 UCSD	1.2898 ± 0.0026	1.2914 ± 0.0017	-17.7	-19.3	-17.5	1.2856 ±0.0026	1.2867 ±0.0014
						(1.2864 ± 0.0014)	
6 NPRL	1.2943 ± 0.0018	1.2912 ± 0.0015	-17.54	-19.28	-17.61	1.2897 ±0.0018	1.2868 ±0.0015
						(1.2880 ± 0.0012)	
7 Peking	1.2852 ± 0.0066	1.2975 ± 0.0065	-17.14	-18.52 -19.02	-17.52	1.2816 ±0.0064	1.2936 ±0.0064
	(Measurements made on NBS RM-49)						
						(1.2876 ± 0.0046)	
8 Queen's	1.2901 ± 0.0015 1.2894 ± 0.0015	1.2900 ± 0.0015 1.2885 ± 0.0015	-19	-19	-19	1.2897 ±0.0011	1.2892 ±0.0011
						(1.2895 ± 0.0008)	
9 Rijks-univ.	1.2972 ± 0.0054 1.2947 ± 0.0037 1.2962 ± 0.0017	1.2904 ± 0.0054 1.2954 + 0.0039 1.2966 ± 0.0018	-17.63 -17.67	-19.09 -19.24 -19.35	-17.48 -17.65	1.2921 ±0.0015	1.2917 ±0.0016
						(1.2910 ± 0.0008)	
11 USGS	1.2917 ± 0.0025	1.2882 ± 0.0025	-19	-19	-19	1.2917 ±0.0025	1.2882 ±0.0025
						(1.2900 ± 0.0018)	
13 Washington Univ.of	1.28863 ± 0.00145	1.29049 ± 0.00148	-19	-19	-19	1.28863 ±0.00145	1.29049 ±0.00148
						(1.2895 ± 0.0010)	

WEIGHTED AVERAGE = $1.2893_{49} \pm 0.0004_{1}$

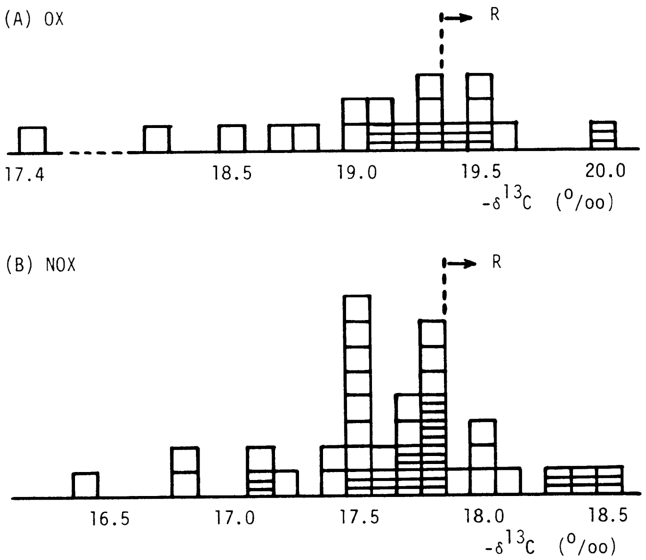

Fig 1. Histograms for values of $-\delta^{13}C$ for (A) NBS SRM 4990 (OX) and (B) for NBS RM-49 -- "I" and "M" (NOX). R in each of (A) and (B) represents values of $-\delta^{13}C$ beyond which the data may possibly indicate incomplete chemical conversion. Shaded data points represent results obtained in the laboratory of Professor W G Mook. The average value of OX is -19.1‰, and its estimated standard deviation is 0.1‰. For NOX, the corresponding values are -17.6 and 0.1‰.

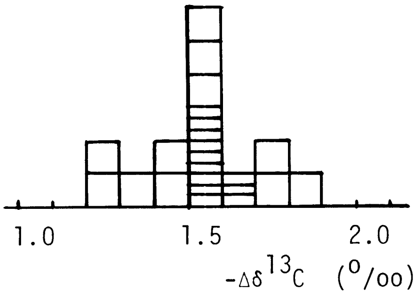

Fig 2. Histograms for values of the differences between $-\delta^{13}C$ for the old and new NBS radiocarbon-dating standards. The average value of $-\Delta\delta^{13}C$ is 1.49‰ and its estimated standard deviation is 0.05‰.

It is clear that there is no statistically significant difference between the ratios measured with samples "I" and "M". The question also arises as to the best method of treating these data; whether by taking a weighted average, or an unweighted average, the latter treating the results as a small sampling, all of equal weight, of a population. Any difference between methods of averaging might similarly give some inkling as to whether the estimate of systematic uncertainty may have been realistic or not.

The unweighted average gives ratios of the activity concentration of the new-to-old NBS standards, both normalized to δ^{13}C equal to -19.00‰, of

$$1.2881 \pm 0.0008,$$

where the stated uncertainty is the estimated standard deviation of the average value.

The weighted average of the ratio and its estimated standard deviation, also normalized to a value of δ^{13}C equal to - 19.00‰, with each laboratory's submitted value weighted by the inverse of the estimated variance of that value, is

$$1.2893 \pm 0.0004.$$

The difference between the weighted and unweighted averages is 0.10%, and the final results from each laboratory seem to represent an excellent set of data.

As, however, I still had some reservations as to the homogeneity of the results, I consulted, as has been my wont in such situations during the last two decades, my friend and colleague Dr H H Ku. Fortunately he was able to direct me to some recent work by two other colleagues, R C Paule and J Mandel (1982), that dealt with the statistical analysis of data pertaining to the measurement of the same physical quantity by different groups of experimenters, that took into account intergroup differences.

Very briefly this method calculates the weighted average, $\tilde{\underline{Y}}$, or the $\underline{\bar{Y}}_i$ quantities submitted by m different laboratories, namely $\underline{Y}1$, $\underline{Y}_2, \ldots . \underline{Y}_i \ldots .$ The best estimate of the concensus value is then given by

$$\tilde{\underline{Y}} = \frac{\sum_{i=1}^{m} \omega_i \bar{\underline{Y}}_i}{\sum_{i=1}^{m} \omega_i}, \tag{1}$$

where ω_i is the reciprocal variance of $\bar{\underline{Y}}_i$, as defined below. Paule and Mandel then consider the two components of uncertainty, namely the within-laboratory variance for each laboratory, and the between-laboratory component, given respectively by $\underline{s}^2_{\underline{w}_i}$ and $\underline{s}^2_{\underline{b}}$, to estimate ω_i as

$$\omega_i = (\underline{s}^2_{w_i} + \underline{s}^2_{\underline{b}})^{-1} . \qquad (2)$$

The values of ω_i and $\underline{s}_b$ are obtained by an iterative process, and ω_i is substituted in equation (1). ($s^2_{w_i}/n_i$ in Paule and Mandel's paper corresponds to $\underline{s}^2_{\underline{w}_i}$ above.)

Dr. Paule and Dr. Mandel applied their method to the set of data shown in the last column of Table 2, for all samples normalized to $\delta^{13}C$ equal to -19.00‰, and obtained a weighted average for the ratio of activity concentrations equal to $1.2891_3 \pm 0.005_3$ (the uncertainty being the estimated standard deviation of the weighted average) and the value of $\underline{s}_b$ of 0.0008_1. They concluded that these values indicated an extremly homogeneous set of data.

The ratio of activity concentration of the new-to-old NBS radiocarbon-dating standards is not given by the weighted average of the results shown in the last column of Table 2. This value, 1.2893 ± 0.0004, must be normalized to reflect the actual ^{14}C isotopic abundances in the two standards, and the normalization is derived from the measured difference in abundance of ^{13}C between them. The normalization used is in the form of

$$(1 + \delta_n{}^{13}C/1000)^2/(1 + \delta_o{}^{13}C/1000)^2.$$

As was seen from the data shown in Figures 1 and 2, the difference in $\delta^{13}C$ is known more precisely than the actual values of $\delta^{13}C$ for each standard. The normalization can therefore be calculated in the form

$$\frac{(1 - (19.30 - 1.49)/1000)^2}{(1-19.30/1000)^2} ,$$

which is quite insensitive to the value of $\delta^{13}C$ of the old standard, and whether it is taken as -19.0 or -19.3‰ makes no significant difference. In either case the normalization factor is 1.00304, which gives a value for the ratio of activity concentrations of new-to-old standards of $1.2932_7 \pm 0.0004_1$. Allowing for a systematic uncertainty of 0.0006 (i e , 0.05%) gives a final result of

$$1.2933 \pm 0.0010$$

The weighted average and its estimated standard deviation normalized by the factor 1.00304, are 1.2920 ± 0.0008. Within the stated estimates of uncertainty the two values are certainly not discordant.

At the 10th International Radiocarbon Dating Conference held in Bern and Heidelberg in 1979 it was agreed, for reasons to which I am not privy, that the new standard should be normalized to a value corresponding to $\delta^{13}C$ equal to -25‰, normalization of the old NBS standard having, by agreement, always been made to $\delta^{13}C$ equal to -19‰. For these two values of $\delta^{13}C$ the ratio of new-to-old NBS standards would be

$$1.2736 \pm 0.0004$$

where the uncertainty is the estimated standard deviation of the weighted average.

ACKNOWLEDGMENTS

I wish to thank all the participants in this intercomparison for their generous help, advice, and cooperation. W G Mook kindly made and sent me an analysis of the data deriving the weighted averages of the ratio of the two standards for $\delta^{13}C$ respectively -19‰ (old) and -25‰(new) which provided a most valuable check, to within 0.001%, of my own calculations made by the -19, -19‰ route described above. I especially acknowledge the active collaboration of Lucy Cavallo who helped with the organization of this venture until her retirement in August 1980, and both she and I are grateful to Lloyd Currie, Meyer Rubin, and Minze Stuiver who gave us substantial advice in the field that was relatively new to us. I also wish to thank J Mandel, R C Paule, and M P Unterweger for a helpful discussion on the assessment of uncertainty in intercomparisons between any number of equally competent laboratories, and also B M Coursey and D D Hoppes for reading this paper and for help in the details of preparing the standard and its certificate for distribution. And last, but by no means least, we at NBS and the members of the international radiocarbon-dating community wish gratefully to acknowledge the help and cooperation of G D Lauback, H F Hammer, A J Schatz, and A J Schmitz of Pfizer Inc , for not only providing the oxalic acid for this new standard but for assuring the quality and homogeneity of the final product.

REFERENCES

Cavallo, L M and Mann, W B, 1980, New National Bureau of Standards contemporary carbon-14 standards, in Stuiver, M and Kra, R S, eds, Internatl ^{14}C conf, 10th, Proc: Radiocarbon, v 22, no. 3, p 962-963.

Paule, R C and Mandel, J, 1982, Consensus values and weighting factors: NBS Jour Research, v 87, p 377-385.

Stuiver, M, 1980, Workshop on ^{14}C reporting, in Stuiver, M and Kra, R S, eds, Internatl ^{14}C conf, 10th, Proc: Radiocarbon, v 22, no. 3, p 964-966.

[Radiocarbon, Vol 25, No. 2, 1983, P 529-532]

STABLE ISOTOPE FRACTIONATION DURING BENZENE SYNTHESIS FOR RADIOCARBON DATING *

HECTOR O PANARELLO, MIGUEL C ALBERO, and
FERNANDO E ANGIOLINI

Instituto de Geocronología y Geología Isotópica (INGEIS)
Pabellón 2, Ciudad Universitaria
1428 Buenos Aires, Argentina

ABSTRACT. ^{13}C isotope analyses of different stages of benzene synthesis have been made to study partial isotope fractionation. More than 60 analyses of carbonates, charcoal, carbon dioxide, and benzene were made in a double collector mass spectrometer. In the first stage of the synthesis (conversion to carbon dioxide) little or no fractionation was observed, beyond the analytical error of the method. Later stages of the process, show a greater and systematic fractionation. The experimental techniques are described.

INTRODUCTION

Routine ^{14}C samples were isotopically analyzed for carbon isotope fractionation. The results obtained will be used to correct ^{14}C ages and to control the general behavior of the benzene synthesis line (Tamers, 1975). The $\delta^{13}C$ values obtained in the Stable Isotopes Laboratory (SIL) on the CO_2 released from the samples by H_3PO_4 (100 %) (carbonate samples) or V_2O_5 oxidation (organic samples) are used as reference to evaluate fractionation in successive stages of benzene synthesis.

TECHNICAL PROCEDURE

In order to produce CO_2 from different samples, the following procedures are carried out.

BENZENE SAMPLES. 1) 4μl of benzene are introduced in a ca 3ml quartz vial, containing 120mg of previously vacuum-baked V_2O_5, by using a microsyringe; 2) Ten quartz vials are connected by means of PVC tubes to a stainless steel manifold. While the samples are frozen with liquid nitrogen, the gases are pumped out until a vacuum of ca 10^{-4} mbar is achieved; 3) The vials are then introduced into the purification line by breaking the vial into the vacuum. The CO_2 is released, purified and the yield is estimated.

---

* Contribution no.65 of the Instituto de Geocronología y Geología Isotópica (INGEIS), supported by the Consejo Nacional de Investigaciones Científicas y Técnicas (CONICET)

CARBONATE SAMPLES. These samples are processed according to the technique of McCrea (1950) and Panarello *et al* (1980).

SOLID ORGANIC MATERIAL SAMPLES. These samples are processed according to Hoefs and Schidlowski (1967). The CO_2 obtained in this manner is then measured against a Carrara Marble reference in a Micromass 602-D mass spectrometer. The results are expressed as $\delta^{13}C$ ‰ vs PDB, defined as

$$\delta^{13}C = \left[\frac{Rs}{Rstd} - 1\right] x\ 1000\ ‰$$

Where Rs: $^{13}C/^{12}C$ in the sample
Rstd: $^{13}C/^{12}C$ in the PDB standard defined by Craig (1957).

RESULTS AND DISCUSSION

Table 1 shows the values obtained for the analyzed samples. In column 1, the $\delta^{13}C$ obtained on CO_2 by H_3PO_4 (100 %) dissolution of carbonates or V_2O_5 oxidation of organic samples are listed. In 2, the $\delta^{13}C$ of CO_2 obtained on the first stage of the benzene synthesis are shown.

The two sets of values show the lack of isotope fractionation in this first stage. The mean value of the difference between these two columns is (0.16 ± 0.49) ‰.

The "t" Student test:

$$t = \frac{\bar{d} - 0}{s/(n-1)^{1/2}} \quad \text{in the zero point}$$

Where $\bar{d}$: 0.16 mean value of the difference
s: 0.49 standard deviation
n: 23 number of samples
gives t: 1.532, inside the critical interval defined by $t_{.95,\ 22} = 2.074$ (2 tails).

Column 3 shows the $\delta^{13}C$ values of benzene. The systematic difference between these values and those in column 2, shows an isotope depletion in the CO_2 conversion to benzene.

The mean value of the difference among 23 samples is now (-1.72 ± 0.87) ‰.

The "t" Student test:

$$t = \frac{\bar{d} - 0}{s/(n-1)^{1/2}} \quad \text{in the zero point}$$

Where $\bar{d}$: -1.72 mean value of the difference
s: 0.87 standard deviation
n: 23 number of samples
gives t: -9.27 outside of the critical interval defined $t_{.95,\ 22} = 1.72$ (1 tail)

TABLE 1. $\delta^{13}C$ values in the different stages of benzene synthesis

Sample no.	Material	(1)* $\delta^{13}C \pm 0.1$ ‰	(2)** $\delta^{13}C_{CO_2} \pm 0.1$ ‰	(2) - (1) ‰	(3)† $\delta^{13}C_{Bz} \pm 0.3$ ‰	Yield %	(3) - (2) ‰
AC0352	Marine shell	1.3	1.6	0.3	-1.3	83	-2.9
AC0379	" "	0.3	-0.6	-0.9	-2.0	82	-1.4
AC0383	" "	1.4	1.3	-0.1	-0.2	82	-1.5
Ac0343	" "	0.6	1.0	0.4	-0.9	83	-1.9
AC0371	Freshwater shell	-0.3	-0.8	-0.5	-2.1	89	-1.3
AC0344	Marine shell	1.5	1.5	0.0	-0.8	86	-2.3
AC0384	" "	2.8	2.6	-0.2	1.5	82	-1.1
AC0340	Freshwater shell	0.3	0.2	-0.1	-2.0	89	-2.2
AC0307	" "	-6.2	-6.4	-0.2	-8.2	75	-1.8
AC0339	Marine shell	1.7	1.8	0.1	-1.8	78	-3.6
AC0390	" "	1.5	1.5	0.0	-1.1	76	-2.6
AC0391	" "	2.8	3.1	0.3	0.6	84	-2.5
AC0323	Sediment	-4.5	-4.8	-0.3	-5.8	81	-1.0
AC0375	Marine shell	0.0	-0.1	-0.1	-1.2	85	-1.1
AC0326	" "	1.8	2.2	0.4	-0.2	86	-2.4
AC0333	" "	0.9	1.6	0.7	-0.2	80	-1.8
AC0334	" "	1.2	1.3	0.1	-1.7	80	-3.0
AC0345	" "	-2.1	-2.1	0.0	-4.0	84	-1.9
AC0077	Vegetal charcoal	-23.0	-22.2	0.8	-23.2	83	-1.0
AC0080	" "	-23.4	-22.1	1.3	-22.9	76	-0.8
AC0217	" "	-23.0	-22.0	1.0	-22.7	81	-0.7
AC0273	" "	-9.5	-9.0	0.5	-9.3	80	-0.3
Secondary Standard							
$BaCO_3$ ‡		-26.0	-26.2	0.2	-26.7	85	-0.5
$\bar{x} \pm s$		-	-	0.16 ± 0.49	-	-	-1.72 ± 0.87

*$\delta^{13}C$: H_3PO_4 (100 %) attack or V_2O_5 oxidation in the SIL

**$\delta^{13}C_{CO_2}$: first stage, $HClO_4$ (70 %) attack or O_2 stream combustion, in ^{14}C laboratory

†$\delta^{13}C_{Bz}$: Benzene + V_2O_5 in SIL

‡ See Angiolini & Albero (1983)

Therefore, a systematic fractionation can be assumed. The benzene yield, about 80 %, may cause this fractionation; however, the error it introduces into the ^{14}C activity measurement is much lower than the statistical error of the activity. Similar errors introduced by fractionation in sample and standard cancel each other out in age calculations.

Two conclusions can be made: 1) Benzene yields around 80% do not result in major fractionation, and thus do not cause appreciable errors in activity measurements. 2) The correction for isotopic fractionation needed in the activity measurement will not change noticeably by using either the δ^{13}C from the CO_2 released from the sample in the first stage or the δ^{13}C of the CO_2 evolved from the benzene by catalytic combustion.

ACKNOWLEDGMENTS

The autors thank the Stable Isotopes Laboratory members who assisted in this research. Also thanks are due to E Linares, who supported this research.

REFERENCES

Angiolini, FE and Albero, MC, 1983, A Secondary standard for radiocarbon dating, in Stuiver, M and Kra, RS, eds, Internatl ^{14}C Conf, 11th, Proc: Radiocarbon, v 25.

Craig, H, 1957, Isotopic standards for carbon and oxygen and correction factors for mass spectrometric analysis of carbon dioxide: Geochim et Cosmochim Acta, v 12, p 133-150.

Hoefs, J and Schidlowski, M, 1967, Carbon isotope composition of carbonaceous matter from the Precambrian of the Witwatersrand system: Science, v 155, p 1096-1097.

McCrea, JM, 1950, The isotopic chemistry of carbonates and a paleotemperature scale: Jour Chem Physics, v 18, p 849-857.

Panarello, HO, García, CM, Valencio, SA, and Linares, E, 1980, Determinación de la composición isotópica del carbono en carbonatos. Su utilización en Hidrogeología y Geología: Rev Asoc Geol Argentina, v 35, no. 4, p 460-466.

Tamers, M, 1975, Chemical yield optimization of benzene synthesis for radiocarbon dating:Internatl Jour Appl Radiation Isotopes, v 26, p 676-682.

[Radiocarbon, Vol 25, No. 2, 1983,P 533-539]

RADIOCARBON DATING OF FOSSIL EGGSHELL

AUSTIN LONG*, R B HENDERSHOTT**, and P S MARTIN*

ABSTRACT. Controlled feeding experiments demonstrate that the ^{14}C content of the carbonate fraction of fossil avian eggshell should reliably reflect the ^{14}C activity of feed and contemporary atmospheric CO_2 regardless of amounts of ^{14}C depleted scratch injested. Consideration of biochemical pathways and exchange rates across lung membranes leads to the possibility that the carbonate fraction may, in some instances, be slightly ^{14}C depleted. ^{14}C dates on eggshell carbonate should require little or no correction. As with marine shell carbonate, normal soil-forming processes may alter the surficial carbon isotopes in eggshell carbonate. ^{14}C dates on the protein fraction should be even more reliable than those on the carbonate fraction, but only if special precautions or separation techniques exclude non-indigenous carbon from the sample. Original protein contents are likely to be too low for conventional ^{14}C dating techniques.

INTRODUCTION

Avian eggshells occur in the Pleistocene and Holocene fossil record, often with sufficient diagnostic morphology and/or stratigraphic association to make ^{14}C dating of eggshell critical in testing hypotheses (Williams, 1981; Haynes, in press). For all ^{14}C dated material, either explicit or implicit assessments of two basic assumptions in the dating method must be made: 1) the initial ^{14}C activity of the dated material, and 2) the sample as a closed system with respect to carbon. We assess both assumptions with regard to eggshells, and report experiments on initial ^{14}C activity of chicken eggs.

PHYSIOLOGY AND BIOCHEMISTRY OF EGGSHELLS

Eggshells contain carbon in two basic fractions: carbonate and organic matter, primarily protein. For quantitative reasons, the carbonate fraction is more attractive for conventional ^{14}C dating than the protein fraction, which is comparatively small. The protein carbon is more likely to obey the closed system assumption, and direct ion counting technology

---

*Department of Geosciences, University of Arizona, Tucson, Arizona 85721.

**Feed Tuffs Processing Company, 28100 South Highway 33, Tracy, California 95376.

will utilize this fraction most effectively. Thus, both sources of carbon are of interest in ^{14}C dating. We evaluated each fraction for its source of carbon and the factors controlling its initial ^{14}C activity.

Fossil eggshells of interest to paleontologists and paleoecologists are from Pleistocene species, especially extinct ratites, such as the moas of New Zealand, the elephant birds of Madagascar, and the dromornithids (not ratites) of Australia. We assume that the egg physiology of modern avian species are analogous to extinct species.

Taylor (1970) and Taylor and Stringer (1965) summarized the physiology of eggshell formation. Chicken eggshells consist of columns of calcite ($CaCO_3$) perpendicular to the shell's surface. Column diameters are typically 0.05 mm in diameter and separated by a thin proteinaceous film. The protein constituents are synthesized in the liver from food-product metabolites and should, therefore, carry the ^{14}C label of nutrient organic carbon. The shell $CaCO_3$ carbon derives from the dissolved inorganic carbon in the blood plasma. A likely mechanism involves the enzyme carbonic anhydrase catalyzing the reaction

$$CO_2 + H_2O \rightarrow HCO_3^- + H^+.$$

The bicarbonate ion equilibrates with carbonate ion by

$$HCO_3^- = CO_3^= + H^+.$$

Calcium ions (Ca^{++}) from the plasma and $CO_3^=$ ions are attracted to the shell protein onto locations spaced at their approximate interionic distances in calcite. The protein may then act as a template for the nucleation of eggshell calcite. Other mechanisms are possible, but all derive the carbon from inorganic carbonate ions dissolved in blood plasma.

Before ^{14}C dating of shell carbonates can be interpreted, the derivation of the plasma carbonate must be known. It could originate from respiration of organic foodstuff, in which case, like the eggshell protein, the fresh egg carbonate natural ^{14}C label would be the same as that in the chicken's organic nutrient, when corrected for istopic fractionation. But chickens habitually ingest small pebbles, often limestone or shell, which help pulverize grains in their gizzards prior to digestion. Thus, it is possible that some carbon labeled with the ^{14}C of ingested mineral carbonate makes its way to the plasma-dissolved inorganic carbon. If this happens, and the mineral carbonate contains little or no ^{14}C, as could be the case in limestone, the initial ^{14}C activity of the shell carbonate might be lower than that of the shell organic matter. An erroneously old ^{14}C age on the shell carbonate would result.

It would seem that this "limestone" effect on the shell carbonate ^{14}C age should be minimal for two reasons: 1) a large, probably major portion of the plasma-dissolved inorganic carbon must be the product of respiration of organic nutrients, and 2) CO_2 exchange between plasma and the atmosphere through the lung membranes tends to bring plasma into isotopic equilibrium with the atmosphere. Since we found sufficient uncertainty about the effects on ^{14}C dates of mineral carbonate "scratch" in avian diets, we carried out a series of experiments to maximize the probability of ^{14}C date bias, and then looked for the effect.

EXPERIMENTAL APPROACH

We measured ^{14}C activities and $^{13}C/^{12}C$ ratios on both carbonate and organic fractions on four sets of eggs from chickens that were fed controlled diets. We also measured carbon isotope contents of the feed. Two groups of chickens received feed high in limestone $CaCO_3$ (ca 22%) while two groups received feed low in limestone $CaCO_3$ (ca 11%). The eggs were collected in each case after 5 to 8 (early group) and 20 to 25 (late group) days on the special feed.

RESULTS AND DISCUSSION

Table 1 shows the carbon isotope analysis results. As expected, the mineral carbonate in the feeds contained no measurable ^{14}C. All other carbon fractions in the experiment,

TABLE 1. Carbon isotopic analyses of eggs and feed

	Sample no.	Fraction	Description		$\delta^{13}C$ PDB (‰)	^{14}C% modern (normalized to $\delta^{13}C$ = 25‰)
Eggs	1058A	organic	early group	fed high $CaCO_3$ feed	-	243 ± 14*
	1058B	carbonate			-	166 ± 2
	1059A	organic	first group		-	**
	1059B	carbonate			+ 2.6	161 ± 2
	1060A	organic	early group	fed low $CaCO_3$ feed	- 29.8	170 ± 4
	1060B	carbonate			+ 3.1	160 ± 2
	1061A	organic	late group		-	**
	1061B	carbonate			+ 2.4	168 ± 2
Feed	1062A	organic	high $CaCO_3$ content		- 19.7	165 ± 2
	1062B	carbonate			+ 2.3	< 2.5
	1063A	organic	low $CaCO_3$ content		-	163 ± 2
	1063B	carbonate			+ 2.2	< 2.5

*Sample very small, highly diluted for analysis

**Too small for ^{14}C analysis

when normalized to the same $\delta^{13}C$ value, had essentially the same ^{14}C activity of contemporary atmosphere at the time of the feeding (1969). In our experiment, "dead" mineral carbonate was absorbed by chickens and had no measurable effect on the initial ^{14}C content of eggshell carbonate or organic matter.

One curiosity is the $\delta^{13}C$ values of the eggshell carbonate all slightly positive (enriched in ^{13}C) with respect to PDB, and similar to other chicken eggshells we measured. This is closer to the value expected for isotopic equilibrium in atmospheric CO_2 than expected for food respiration products. Interestingly, the $\delta^{13}C$ values Folinsbee et al (1970) show for chicken eggshell range from $-13^{o}/oo$ to $-7^{o}/oo$. Similarly, the $\delta^{13}C$ values for Aepyornis reported in Folinsbee et al (1970), Berger et al (1975), and in this study fall in the $-14^{o}/oo$ range. These more negative values may represent varying degrees of isotopic equilibrium attainment in chicken lung membranes. Isotopic equilibrium can be tested by measuring $\delta^{13}C$ in blood bicarbonate.

A single comparison of $\delta^{13}C$ values in eggshell carbonate and chicken blood revealed the eggshell to be $9.6^{o}/oo$ more enriched in ^{13}C, too great for either equilibrium or kinetic explanations (Turner, 1982). Further such tests are needed.

POST-DEPOSITIONAL EFFECTS

Time and subaerial processes will affect both the calcite and protein fractions of fossil eggshells, similar to effects on carbonate in molluscan shells. Original protein will gradually disintegrate into smaller fragments and wash away. Rate of disappearance of protein will depend on soil conditions and thickness of shell fragments. Soil organic matter will tend to adsorb onto calcite surfaces, thus affecting the ^{14}C age of total organic matter.

Soil process may alter ^{14}C dates on eggshell calcite by surficial exchange of carbonate or deposition of $CaCO_3$. A number of studies conclude isotopic alteration of calcite. Accurate ^{14}C dating of marine shells requires removal of outer layers of calcite: ^{14}C dating of Foraminifera tests (Eriksson and Olsson, 1963), fine-grained carbonate material subjected to subaerial processes (Long, unpub ^{14}C data), and $^{13}C/^{12}C$ and $^{18}O/^{16}O$ ratio alteration studies in calcitic sediments (Gross, 1964).

APPLICATIONS TO DATING FOSSIL EGGSHELLS

We now consider the applicability of this study on chicken eggs to avians in general and large extinct birds in particular. Williams (1981) reported a ^{14}C date on modern Emu eggshell of

560 ± 70 BP (SUA-1069). He did not note whether this date is ^{13}C normalized, nor did he measure ^{14}C in diet. This could mean that larger birds may incorporate small but significant amounts of mineral carbon in their eggshells and, as suggested above, plasma-dissolved inorganic carbon may not entirely equilibrate isotopically with atmospheric CO_2. The $^{13}C/^{12}C$ ratio may prove to be an indicator of such isotopic equilibrium.

Clearly, more analyses on modern large bird eggshells are needed, but evidence so far suggests that fossil eggshell carbonate dates cannot be more than a few hundred years too old if properly pretreated to remove surficial carbonate. Ideally, carbonate dates should be compared with shell protein or amino acid ^{14}C dates on fossil eggs. The latter could be done by isolating specific organic compounds and performing ^{14}C measurements by direct ion counting accelerator techniques.

CARBON ISOTOPE ANALYSIS ON FOSSIL EGGSHELL

Recently, we analyzed several fossil eggshells for ^{14}C and ^{13}C. In two cases we were able to analyze both calcite and organic matter fractions (table 2). Note that the carbonate-organic matter pairs, A-2515, 2516 and A-3106, 3105 are within one standard deviation of agreement. Although surficial carbonate was removed from 2515 and 3106 before analysis, exchange with more recent carbon possibly affected its ages to a minor degree, thus producing a fortuitous agreement. We consider it

TABLE 2. Carbon isotope analyses on fossil eggshell

Lab no.	Bird	Fraction dated	^{14}C date*	$\delta^{13}C$ (PDB) (‰)	Loc, ref
A-2515	Ostrich	Carbonate	6270 ± 50	− 3.4	Egyptian Sahara, Haynes (in press)
A-2516	Ostrich	Organic residue from A-2515	6660 ± 320	− 19.8	Egyptian Sahara, Haynes (in press)
A-2517	Ostrich	Carbonate	4780 ± 50	− 4.4	Egyptian Sahara, Haynes (in press)
A-2518	Ostrich	Carbonate	6290 ± 150	− 4.4	Egyptian Sahara, Haynes (in press)
A-3106	Ostrich	Carbonate	8280 ± 60	− 5.6	Egyptian Sahara, Haynes (in press)
A-3105	Ostrich	Organic residue from A-3106	8680 ± 450	− 21.6	Egyptian Sahara, Haynes (in press)
A-2833	Aepyornis	Carbonate	7450 ± 150	− 12.3	Madagascar (coll by P S Martin)
A-2834	Aepyornis	Carbonate	1550 ± 90	− 14.6	Madagascar (coll by P S Martin)

*Normalized to $\delta^{13}C = -25$‰

more likely that the eggshell carbonate and organic matter had similar ^{14}C activity when the egg was laid, and the δ^{13}C signals a significant trend toward isotopic equilibrium during shell growth.

It does not seem likely that diet is an important factor in controlling the δ^{13}C of eggshell carbonate for the following reasons: 1) The experimental eggs (table 1) showed ca 32°/oo enrichment of ^{13}C in carbonate over the organic fraction. 2) One fossil ostrich egg carbonate (table 2) is ca 16°/oo enriched over its organic matter. 3) Aepyornis eggshell carbonate seems to be in the -13 to -15°/oo δ^{13}C range, which is likely to be less than 16°/oo enriched with organic matter. 4) Other chicken egg δ^{13}C values on carbonate/organic matter pairs analyzed (Long, unpub data) are +3.2, -21.2, and +2.2, -27.0.

CONCLUSIONS

1) Fossil avian eggshell carbonate ^{14}C dates should reliably represent the date of organic nutrients the bird consumed if the carbonates undergo laboratory pretreatments which are standard for other carbonate samples. 2) Although ingestion of "old" carbonate may affect the ^{14}C content of eggshell, we find no compelling evidence that it has. 3) The ^{13}C/^{12}C of eggshell carbonate is evidently not solely controlled by diet. It may be related to kinetic or equilibrium processes at the lung membrane, but our evidence cannot yet make this distinction.

ACKNOWLEDGMENTS

This manuscript benefited greatly from discussions with C V Haynes and K Brendel. B L Reid provided chemical analyses of feed. I Kuch, R Donnelly, R Ronstadt, C Ratto, J Schaller, and L Warneke helped with isotope analyses.

REFERENCES

Berger, R, Ducote, K, Robinson, K, and Walter, H, 1975, Radiocarbon date for the largest extinct bird: Nature, v 258, p 709.

Eriksson, K G and Olsson, I U, 1963, Some problems in connection with ^{14}C dating of tests of Foraminifera: Geol Inst Univ Uppsala Bull, v 42, p 1-13.

Follinsbee, R E, Fritz, P, Krouse, H R, and Robblee, A R, 1970, Carbon-13 and oxygen-18 in dinosaur, crocodile, and bird eggshells indicate environmental conditions: Science, v 168, p 1353-1356.

Gross, M G, 1964, Variations in the $^{18}O/^{16}O$ and $^{13}C/^{12}C$ ratios of diagenetically altered limestones of the Bermuda Islands: Jour Geol, v 72, p 170-194.

Haynes, C V, in press, Great sand sea and selima sand sheet, eastern Sahara: Geochronology of desertification: Science, in press.

Taylor, T G, 1970, How an eggshell is made: Sci Am, v 222, p 88-95.

Taylor, T G and Stringer, D A, 1965, Eggshell formation and skeletal metabolism, _in_ Sturkie, P D, ed, Avian physiology: Ithaca, Comstock Pub Assoc.

Turner, J V, 1982, Kinetic fractionation of carbon-13 during calcium carbonate precipitation: Geochim et Cosmochim Acta, v 46, p 1183-1191.

Williams, D L G, 1981, _Genyornis_ eggshell (Dramornithidae; Aves) from the late Pleistocene of South Australia: Alcheringa, v 5, p 133-140.

[Radiocarbon, Vol 25, No. 2, 1983, P 541-546]

A SECONDARY STANDARD FOR RADIOCARBON DATING *

FERNANDO E ANGIOLINI and MIGUEL C ALBERO

Instituto de Geocronología y Geología Isotópica (INGEIS)
Pabellón 2, Ciudad Universitaria
1428 Buenos Aires, Argentina

ABSTRACT. The preparation and calibration of a secondary standard for the INGEIS Radiocarbon Dating Laboratory are presented. This standard is barium carbonate with a specific activity almost twice that of NBS oxalic acid. It was prepared from $BaCO_3$ with high specific activity and commercial potassium carbonate by an isotopic dilution technique. The advantages of this standard are: 1) the preparation is simple and can be achieved with ordinary labware; 2) the production of CO_2 by acid attack from this carbonate shows minimum isotopic fractionation. At least, it has less fractionation than wet oxidation of oxalic acid, the problems of which are described in the literature. This standard ensures better reproducibility in activity measurements; 3) despite some problems of activity exchange with atmospheric CO_2 concerning carbonates, measurements of activity over a period of about two years have shown no significant deviation from the mean value. A tentative explanation of this phenomenon is also given. The activity ratio between $BaCO_3$ and NBS oxalic acid is given with its error, and the statistical tests used in the calibration are briefly explained. Finally,a control chart for the activity of the standard over a long period is drawn, showing non-significant deviation and supporting the usefulness of this standard.

INTRODUCTION

Because NBS oxalic acid standard for ^{14}C dating is available only in limited quantities, we saw the need for a ^{14}C-labeled substance that could be used as a secondary standard. This substance should show stability and reproducibility in activity measurements, it should be easily obtained, and its specific activity should be similar to that of modern ^{14}C activity.

Our ^{14}C laboratory has been operating since 1979 using benzene synthesis and liquid scintillation counting techniques (Tamers, 1975) and dates ca 200 archeologic and geologic samples per year.

The criteria that the standard should achieve are: 1) The activity must be similar to that of NBS oxalic acid. If specific activity is too high, it could cause contamination in the synthesis line. Low specific activity would increase the counting times. A specific activity about twice that of NBS was

---

*: Contribution no. 55 of the Instituto de Geocronología y Geología Isotópica (INGEIS), supported by Consejo Nacional de Investigaciones Científicas y Técnicas (CONICET)

chosen. 2) Easy preparation-the standard should be synthesized with ordinary labware and easily converted to benzene. It could be processed as any sample; 3) It should not show isotopic fractionation, a problem with NBS oxalic acid (Grey et al, 1969), which shows appreciable fractionation in derived CO$_2$. This is because the reaction of oxalic acid with a sulfuric solution of potassium permanganate is a redox reaction of slow kinetics. We wanted a carbonate because the reaction with acid to obtain CO$_2$ is one of quick kinetics, so that it should show no isotopic fractionation; 4) Homogeneity of the standard-synthesis of the standard should ensure that the product is homogeneous which is important for the reproducibility of its activity.

PREPARATION OF THE STANDARD

From ^{14}C labeled barium carbonate of high specific activity (ca 88000dpm/g), an isotopic dilution was performed as follows: The labeled barium carbonate was dissolved with concentrated phosphoric acid under vacuum and the CO$_2$ was absorbed in a potassium hydroxide solution. This solution was mixed with a saturated solution of commercial potassium carbonate. The dilution of the specific activity and the homogeneity was achieved by gently stirring. A warm solution of barium chloride is neutralized because the hydrolysis of Ba^{2+} gives a pH of ca 4.5 and the carbonate precipitated would redissolve at this pH; then it is mixed with the former carbonate solution. The barium carbonate is precipitated with a crystal size suitable for filtering. The precipitate is then washed and dried at ca 110°C.

We observed that potassium chloride was coprecipitated with the barium carbonate as a result of reacting with saturated solutions; this potassium chloride does not affect the usefulness of the standard. Ca 2200g of the standard were obtained from 45 mg of high specific activity barium carbonate. This quantity will be enough for about two years' work.

CALIBRATION OF THE STANDARD

MEAN VALUE OF δ^{13}C. In order to check the hypotesis that this standard should not show problems of isotopic fractionation, the δ^{13}C value was determined for seven samples with the following results (table 1):

TABLE 1. δ^{13}C values of the secondary standard

Sample no.	1	2	3	4	5	6	7
δ^{13}C(‰)	-26.4 ± .4	-26.5 ± .4	-27.1 ± .6	-26.1 ± .6	-26.5 ± .4	-26.4 ± .5	-26.4 ± .6

Mean value = -26.5% ; Standard deviation = 0.3‰

The $\delta^{13}C$ measurements were performed in the Stable Isotopes Laboratory of INGEIS using a double collector Micromass 602-D mass spectrometer. The small standard deviation shows that the criteria 3) in the introduction is fulfilled and the mean value is considered as a reference to correct the activity of the standard by isotopic fractionation.

ACTIVITY CALIBRATION. Following the technique described by Tamers (1975), 5 benzene synthesis of the standard and two of NBS oxalic acid were made. The activity of these samples, together with background, were measured in a Packard 3255 Liquid Scintillation Spectrometer. The measured activities of the NBS oxalic acid were corrected according to Faure, (1977):

$$A_{NBS}^{corr} = (A_{NBS} - A_F) . \left[1- \frac{2.(\delta^{13}C_{NBS} + 19.0)}{1000} \right] \qquad (1)$$

where A_{NBS}^{corr} = corrected activity of the NBS oxalic acid

A_{NBS} = gross activity of the NBS oxalic acid

A_F = background

$\delta^{13}C_{NBS}$ = measured value of NBS oxalic acid $\delta^{13}C$ vs PDB

Similarly the activity of the standard was corrected using the following equation:

$$A_P^{corr} = (A_P - A_F) . \left[1- \frac{2.(\delta^{13}C_P + 26.5)}{1000} \right] \qquad (2)$$

where A_P^{corr} = corrected activity of the standard

A_P = gross activity of the standard

$\delta^{13}C_P$ = measured value of $\delta^{13}C$ of the standard vs PDB

The activity measurements of the standard and the NBS oxalic acid are shown in tables 2 and 3.

TABLE 2. Activity measurements of NBS oxalic acid

NBS	A_{NBS} (cpm)	A_F (cpm)	$\delta^{13}C_{NBS}$(‰)	A_{NBS}^{corr} (cpm)	Counting time(min)
1	56.02±.20	9.65±.08	-20.3±.5	46.50±.22	1380
2	57.23±.22	10.80±.09	-18.2±.2	46.36±.24	1220

TABLE 3. Activity measurements of the secondary standard

Secondary standard	A_P (cpm)	A_F (cpm)	$\delta^{13}C_P$(‰)	A_P^{corr} (cpm)	Counting time(min
1	109.88±.27	10.06±.08	-26.4±.4	99.80±.28	1480
2	110.22±.27	10.06±.08	-26.4±.4	100.17±.28	1480
3	109.94±.33	9.64±.08	-26.4±.4	100.29±.34	1000
4	109.15±.33	9.64±.08	-26.5±.4	99.52±.34	980
5	110.96±.30	10.80±.09	-26.2±.6	100.10±.31	1200

Samples of 5ml of benzene corresponding to the standard and NBS oxalic acid were measured in different runs. Counting time was divided in periods of twenty minutes, allowing statistical treatment of the data. Using Chauvenet's criterion, we rejected data that deviated significantly from the mean. For NBS oxalic acid samples, the net corrected activities were compared by means of the statistic "t" (Student) for a confidence of 95%, with no significant difference between the two corrected activity values. We were able to obtain a mean value of:

$$A^{corr}_{NBS\ mean} = (46.47\pm.15)\text{cpm}$$

For the standard, we had to stablish whether differences in measurements were due to statistical or systematic errors. If the former, the standard would be isotopically homogeneous. This can be determined by an analysis of variance (ANOVA) of the five sets of activity values (20-minute measurement each) corresponding to the standard samples. First we had to determine that the five sets showed quality of variances by using statistic "F" (for a confidence of 95%). The results of the ANOVA showed that the differences between the mean value of each set (table 3) was due only to the statistical deviation of radioactivity (Poisson) and not to systematic errors. Thus, the homogeneity of the standard was also proven. We were then able to obtain a mean value for the standard activity:

$$A^{corr}_{P\ mean} = (99.98\pm.15)\text{cpm}$$

The activity factor between the secondary standard and the NBS oxalic acid and its error were then calculated:

$$\gamma = \frac{A^{corr}_{NBS\ mean}}{A^{corr}_{P\ mean}} = .4648 \qquad \sigma_\gamma = .0016 \tag{3}$$

STATISTICAL CONTROL OF THE STANDARD

Each time a new series of samples to be dated is measured, the net corrected activity of the standard is controlled by means of a "t" test (95% confidence), using the value of 99.98 cpm as a reference value:

$$t_{.95,\ n-1} = \frac{\bar{X} - \mu}{S/\sqrt{n}} \tag{4}$$

where $\bar{X}$ = net corrected activity of the measured standard.

S = standard deviation

n = number of cycles of measurement

μ = 99.98cpm

The result of 14 measurements are presented in table 4, and plotted vs time in figure 1. The areas of ±1σ and ±2σ levels of confidence are also drawn in figure 1.

TABLE 4. Results of measurements made with the secondary standard.

Month/ year	A_P^{corr} (cpm)	$\delta^{13}C$ (‰)	no. of 20 min counts	t(Student)
8/80	99.80±.28	-26.4±.7	74	-.64
8/80	100.17±.28	-27.1±.6	74	.68
11/80	100.29±.34	-26.4±.4	50	.91
11/80	99.52±.34	-26.1±.5	49	-1.35
2/81	100.29±.27	-26.8±.2	83	1.15
3/81	99.50±.25	-26.8±.2	50	-1.92
4/81	100.10±.31	-26.2±.6	60	.39
5/81	100.05±.29	-26.2±.6	69	.24
6/81	100.68±.35	-26.5±.2	49	2.03
6/81	99.86±.34	-26.2±.6	50	-.35
7/8/81	100.05±.48	-26.5±.3	25	.15
8/81	100.30±.35	-26.1±.3	49	.91
9/81	99.79±.34	-26.1±.3	50	-.56
11/81	99.44±.34	-26.1±.3	50	-1.59

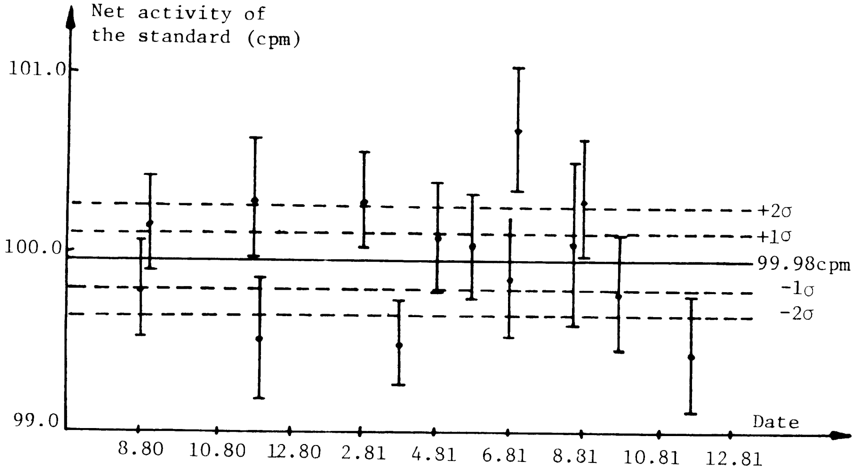

Fig 1. Net activity of the secondary standard vs time

CONCLUSIONS

The secondary standard has achieved the goals set out at the beginning of our project.

The resulting activity is about twice that of the NBS oxalic acid:

$$A_P = A_{NBS} \cdot (2.1515 \pm .0074)$$

The data show good reproducibility resulting from homogeneous dilution of the initial high specific activity; reproducibility of the whole synthesis and measurement procedures are also shown.

Isotopic fractionation of the standard is negligible, as shown in the $\delta^{13}C$ values of tables 1 and 4.

It has been noted that a ^{14}C exchange occurs between ^{14}C labeled carbonates and atmospheric CO_2 and these carbonates lose activity with time. This is a result of the following exchange reaction:

$$^{14}CO_3^{=} + CO_2 \xrightleftharpoons{H^+} CO_3^{=} + {}^{14}CO_2 \qquad (5)$$

catalized by small quantities of CO_3H_2.

Our secondary standard has not shown this behavior; its specific activity has been constant right along. A tentative explanation is that the rate of the exchange depends on the difference of activity of the carbonate and the CO_2. The exchange has been noticed in carbonates with high specific activity, which is much higher than the natural levels of CO_2. In our case, both activities, atmospheric CO_2 and the standard, are comparable, making the exchange negligible.

ACKNOWLEDGMENTS

The authors want to thank E Linares who made this project possible. We also thank HO Panarello who made the $\delta^{13}C$ measurements and JL Nogueira who performed most of the benzene synthesis.

REFERENCES

Faure, G, 1977, Principles of isotope geology: New York, John Wiley & Sons.

Grey, DC, Damon, PE, Haynes, CV, and Long A, 1969, Carbon-isotope fractionation during wet oxidation of oxalic acid: Radiocarbon, v 11, p 1-2.

Tamers, M, 1975, Chemical yield optimization of the benzene synthesis for radiocarbon dating: Internatl Jour Appl Radiation Isotopes, v 26, p 676-682.

[Radiocarbon, Vol 25, No. 2, 1983, P 547-552]

A MULTIPLE PROPORTIONAL ^{14}C COUNTER SYSTEM FOR MILLIGRAM-SIZED SAMPLES

GERT HUT, JAN KEYSER, and STEF WIJMA

Isotope Physics Laboratory, University of Groningen
The Netherlands

ABSTRACT. A system of 10 proportional ^{14}C counters has been designed. The counters have a volume of 35ml and are operated with CO_2 at a pressure of 1 bar and a voltage of 3300V. The amplified signals of the counters are fed through an analog multiplexer to the inputs of three discriminators. The Geiger signal is fed to a separate discriminator. A logic circuit selects from these discriminators the alpha, beta, muon, and purity counts which are then stored in a microcomputer (ITT 2020 with 48K RAM), where the necessary calculations are also performed. The purity of the gas sample is monitored by counting a part of the muon spectrum. The alpha and beta pulses are stored during 95% of the measuring period; the remaining 5% is used for registration of the muon and purity pulses. The overall accuracy of the system for modern carbon samples is 2% after a counting period of 6 days.

INTRODUCTION

The determination of $^{14}C/^{12}C$ ratios in very small quantities of carbon would yield results of scientific and/or practical value to such research areas as archaeology, oceanography, environmental studies, climatology, and authentication of museum objects.

Parallel to the development of the mass-spectrometric separation of ^{14}C and ^{12}C ions followed by counting of the ^{14}C with electrostatic accelerators, conventional proportional counter operation using CO_2 as a counter gas has been extended to very small counters and samples. Although the latter method is slow (counting times up to several weeks may be required for 20mg of carbon) no operator intervention is necessary and many samples may be counted simultaneously.

New installations with small counters are under construction or in the planning stage, eg, at the National Bureau of Standards (Currie, 1978), Brookhaven Laboratory (Harbottle, Sayre, and Stoenner, 1979), Harwell (Sayre et al, 1981) and the Isotope Physics Laboratory of the University of Groningen.

In existing ^{14}C counting set-ups (Tans and Mook, 1978), the electronic system of one ^{14}C counter consists of an amplifier, a set of 3 adjustable discriminators, a selection circuit and 4 counting channels, each with a 6-decade counter and display. For a system with several counters, this data acquisition system would become quite complicated. Also, the calibrating procedure of the discriminators would be time-consuming.

In our application, we developed a relatively small data acquisition system with a microcomputer for 10 small ^{14}C counters. After the 10 amplifiers for ^{14}C counter pulses, an analog multiplexer is used with 1 set of 3 adjustable discriminators. After address encoding, a ^{14}C counter pulse is selected as an alpha, beta, muon, or purity count, which, together with the ^{14}C counter address is then fed to the peripheral interface adapter (PIA) of the microcomputer where the count is stored in the memory. The dead time is ca 0.2% of the total measuring time. An internal timer selects the alpha-beta counts and the muon-purity counts at a ratio of 95:5.

COUNTERS

Two types of proportional counters were designed (pl 1). One type is made from high-purity quartz and uses a gold layer of ca 0.01μ as a cathode. The insulating end pieces are obtained by a shadow technique during vacuum deposition of the gold layer. The small amount of gold which still may be deposited on the end pieces is then removed by careful immersion in aqua regia. The wire support is similar to the one in the counters described by Tans and Mook (1978). The length and diameter of the gold layer are 120 and 19mm,

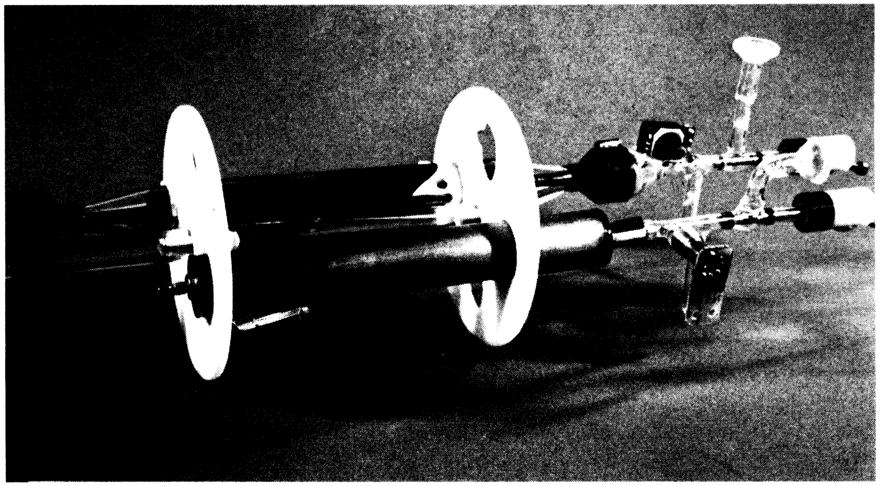

PLATE 1. The two types of proportional counters. The top one is made out of quartz and has a vacuum-deposited gold layer as a cathode. The bottom one is made out of oxygen-free copper.

respectively. The other type is made from oxygen-free copper[1]. The end pieces are manufactured from high-purity quartz. The anode wire is connected at one side to an Amphenol, hermetically sealed mini-coax receptacle, the outside of which is used as a guard ring. The length and diameter of the cathode are 135 and 20mm respectively. The pressure in both counters is measured by a monolithic pressure transducer with a range of 2 bar and an overall accuracy of 0.5%. Both types have a stainless-steel anode wire with a diameter of 50μm. Both types have a small cold finger at the gas inlet side. The counters remain in their position during sample changing.

The inlet valves were specially designed at the Isotope Physics Laboratory. A stainless-steel plunger with two viton "O"-rings can be moved in a quartz tube with an inner diameter of 4 mm. Movement is made possible by a self-centering brass disk which can rotate in a housing of "Delrin". The counters are surrounded by a cylinder of old lead, 35mm thick, surrounded by 34 Geiger-Müller counters, each 500mm long. Perpendicular to the 34 counters at one end of the cylinder are 7 Geiger-Müller counters 200mm long. The shielding is similar to the one used by Tans and Mook (1978) and also consists of 100mm of lead and a layer of 200mm boron-paraffine around the counters. At the upper part of the shielding is a layer of 200mm of iron. The system is located in the basement of a three-story building. The counters are accessible by front and rear doors made of lead, 100mm thick. These doors move on a rail along the shielding.

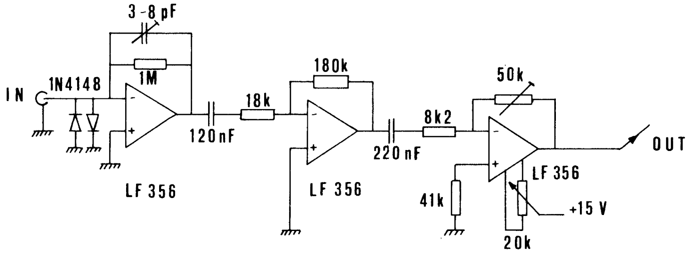

Fig 1. One of the amplifiers for the current pulses from the ^{14}C counters

---

[1] Kindly provided by R Nydal, Radiological Dating Laboratory, Trondheim

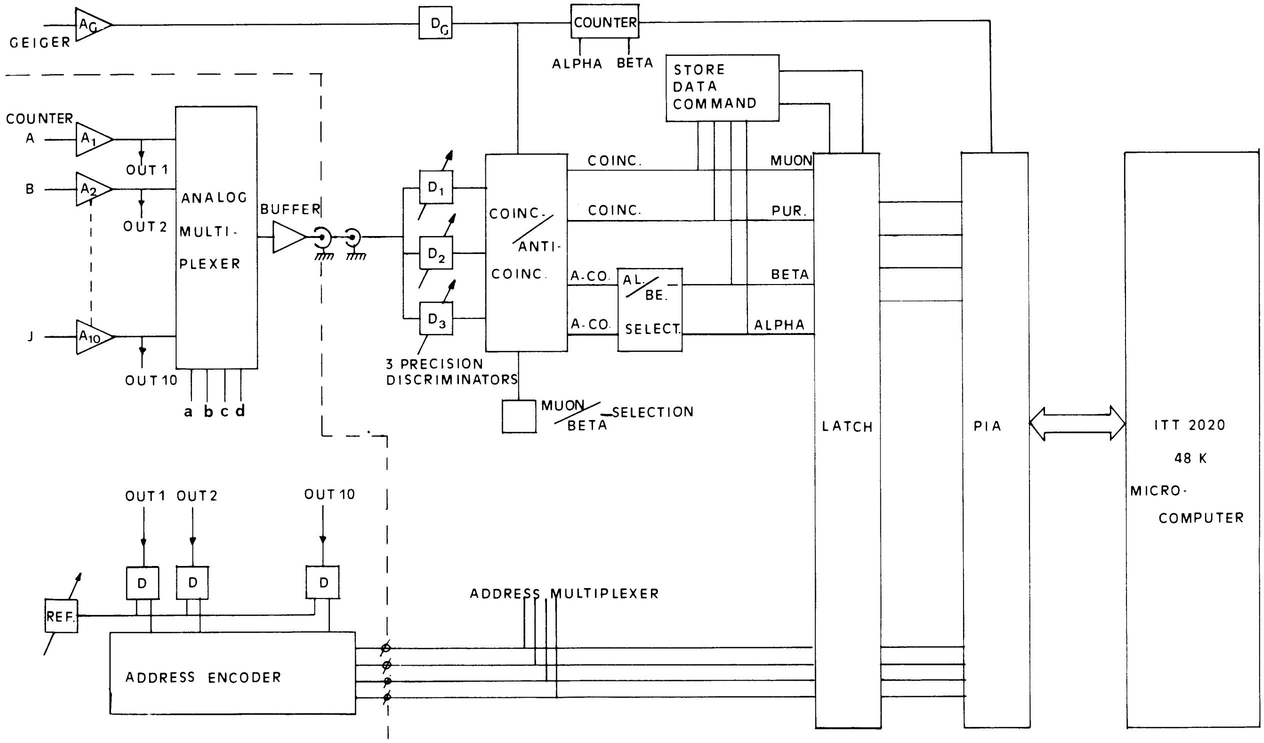

Fig 2. Data-acquisition system

DATA ACQUISITION SYSTEM WITH AMPLIFIERS AND ADJUSTABLE DISCRIMINATORS

Figure 1 shows 1 of the 10 amplifiers for the current pulses from the ^{14}C counters. It consists of a current-to-voltage converter followed by 2 inverting voltage amplifiers. The output voltage is $5.10^7.iV$, where i is the current pulse from the ^{14}C counter. The slew rate and output noise of the amplifier are 10V/µsec and 10mV RMS, respectively. Figure 2 shows the total data acquisition system. The output of each amplifier is connected to 1 of 10 rather simple discriminators and an input of the analog multiplexer. The discriminators (D) have a common reference; their outputs generate the ^{14}C counter address for the multiplexer through an encoder. The output of the multiplexer is fed through an analog buffer to 3 adjustable precision discriminators where the alpha, beta and purity energy levels are set. One of the 3 adjustable discriminators is shown in figure 3. The reference level can be adjusted with R. The hysteresis and response time are 5mV and 110nsec, respectively. The maximum temperature drift of the circuit with amplifier, multiplexer, buffer and adjustable discriminator is 25µV/°C. The Geiger pulse is fed to a separate discriminator. The muon and purity pulses are selected from the discriminators D_1 and D_2. The alpha and beta pulses are in anti-coincidence with the Geiger pulse and are separated in the alpha/beta select circuit. After a pulse appears at one of the alpha, beta, muon or purity lines, the latch will get a delayed strobe pulse and hold the signal with the ^{14}C counter address information available at the input of the PIA (CCS type 7720A) for 9ms; during this time the data are stored in the memory of the microcomputer. A separate muon/beta selection circuit controls the time ratio between the alpha-beta and muon-purity measurements, after

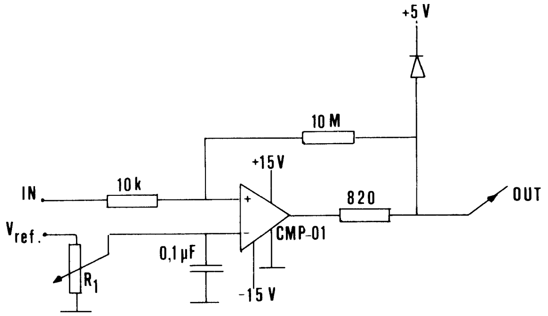

Fig 3. 1 of the 3 adjustable discriminators, D_1, D_2, and D_3. The comparator CMP-01 is from PMI

every 950s of alpha-beta counting follows 50s of muon-purity counting. The alpha, beta, and Geiger pulses are totalized in a preset counter which generates an interrupt in the data acquisition after reaching its preset value, which is then stored in the microcomputer. The circuit left of the dotted line in the diagram of figure 2 is mounted inside the shielding around the Geiger tubes and the ^{14}C counters. The remaining part of the circuit is mounted on a standard eurocard.

RESULTS

Testing both types of counters for one month yielded the following results:

	Quartz counter	Copper counter
Length	120mm	135mm
Cathode diameter	19mm	20mm
Anode diameter	50μm	50μm
Operating pressure	1 bar	1 bar
Working voltage	3300V	3300V
Muon counting rate (cpm)	14.43 ±0.12	15.44 ±0.38
Purity counting rate (cpm)	8.51 ±0.09	9.35 ±0.06
Net beta counting rate (cpm)	0.219±0.023	0.198±0.075
Background (cpm)	0.273±0.007	0.380±0.010

The alpha and beta pulses were counted separately for correction of the dead time which is ca 0.2% for an alpha-beta count rate of 0.5cpm and a Geiger count rate of 1400cpm.

ACKNOWLEDGMENTS

The authors wish to thank Henk Been, Eric Kuperus, and Bert Metz for their contribution to this project.

REFERENCES

Currie, LA, 1978, Environmental radiocarbon measurements, in Gove, HE, ed, Conf on radiocarbon dating with accelerators, 1st, Proc: Univ Rochester, p 372-390.

Harbottle, G, Sayre, EV, and Stoenner, RW, 1979, Dating of small samples by proportional counting: Science, v 206, p 683-685.

Sayre, EV, Harbottle, G, Stoenner, RW, Otlet, RL, and Evans, GV, 1981, Small gas proportional counter for the ^{14}C measurement of very small samples, in Methods of low level counting and spectrometry, Proc: Berlin, IAEA Symposium, p 391-407.

Tans, PP and Mook, WG, 1979, Design, construction and calibration of a high accuracy carbon-14 counting set up: Radiocarbon, v 21, p 22-40.

[Radiocarbon, Vol 25, No. 2, 1983, P 553-564]

MINIATURE SIGNALS AND MINIATURE COUNTERS: ACCURACY ASSURANCE VIA MICROPROCESSORS AND MULTIPARAMETER CONTROL TECHNIQUES

L A CURRIE, R W GERLACH, G A KLOUDA, F C RUEGG, AND
G B TOMPKINS
Center for Analytical Chemistry, National Bureau of Standards
Washington, DC 20234

ABSTRACT. When ^{14}C signals approach background levels, the validity of assumptions concerning Poisson counting statistics and measurement system stability becomes crucial in interpreting the resultant low-level counting observations. This has been demonstrated in our previous work on detection limits for non-Poisson error and it is critical in our current studies of carbonaceous pollutants, where the ^{14}C signal from just 5 mg C is comparable to that of the background for our miniature gas proportional counters. To assure data quality, our multi-detector system is designed for the on-line monitoring of critical parameters that reflect both the (statistical) nature of the non-Poisson errors and the underlying (physical) causes. It sends >60 bits of information/pulse to a microprocessor which automatically generates, for each counting period, two-dimensional spectra and multiparameter correlation and control charts. To evaluate the validity of long-term counting of 1-10 mg C we use robust (statistical) estimators, optimal counting interval subdivision, and time series analysis of the individual pulses. New opportunities for selective sampling and chemical fractionation which come with the small sample measurement capability have led us to give special attention also to higher control levels, involving e g, isotopic heterogeneity and representative standard materials.

INTRODUCTION

The growing popularity of small (∿10 mL) gas proportional counters for environmental studies and ^{14}C dating has led us to re-examine some of the assumptions connected with counting errors, and to consider means for monitoring data quality when a multi-counter array is operating, when signals are comparable to backgrounds, and when counting periods (and hence required system stability) of weeks to months are involved (Currie, Noakes, and Breiter, 1979; Sayre et al, 1981; Polach et al, 1982). Under the best of circumstances in low-level counting, the absolute activity (or age) of a sample can be deduced from three observations: background (B), gross signal (S+B), and gross standard (M+B) — where the symbols refer to the number of counts due to the background events, net signal, and "modern" standard, respectively. The uncertainty of the estimated normalized net signal (S/M) may then be calculated by appropriately propagated Poisson counting errors. Replication is important for monitoring major deviations from Poisson behavior, and the more conservative investigator will base uncertainty statements on observed replicate variability and Student's-t.

At extremely low levels however, when $S \lesssim B$ and the imprecision (σ) sought corresponds to a small fraction of the background rate, or when few if any real replicates are possible within the overall counting time available, some fundamental limitations must be recognized. First, <5 replicates lead to large uncertainties and large values of Student's-t; second, this statistic carries the assumption that all errors are random and normal. Non-Poisson random error may be estimated by replication, and bias may be estimated by comparison with standards or comparison among laboratories, but most such comparisons have limited statistical power. It can be shown, eg, that even with considerable segmentation (internal replication) of the overall counting period, the smallest non-Poisson random error component that can be detected is comparable to the Poisson component (Currie, 1973); and bias may remain undetected until it exceeds the standard error by about a factor of four or more (Currie, 1978). Thus, even with some replication and comparison with "knowns", a several-month extreme low-level measurement may contain significant but undetected imprecision and bias. For these reasons we have chosen to supplement conventional measures of quality control with several on-line controls which, together, greatly reduce unanticipated error and often point to physical causes when such error occurs.

LEVELS OF CONTROL. The overall measurement process for environmental ^{14}C may be viewed as a hierarchical system of basic levels each of which may contain potential errors (or erroneous assumptions) which may invalidate the final result. We refer to these levels as 1) sampling and sample assumptions, 2) sample preparation, 3) treatment of the counter gas (storage, replicate counter fillings, etc), and 4) individual measurements (counting periods). In this report we focus on level 4, ie, counting system design and on-line monitoring of the quality of each measurement. We also briefly review assumptions to be monitored at the higher control levels, especially for isotopic measurements of carbonaceous particles. Table 1 outlines the overall control strategy.

COUNTING SYSTEM AND ON-LINE CONTROLS

DATA ACQUISITION; SEGMENTED OUTPUT (Level 4). For this fundamental control level we have instituted several automatic (on-line) controls, plus specific pre- and post-counting

TABLE 1. Hierarchical control scheme: ^{14}C in atmospheric particles

Level		Factors
1	Source, Environmental Assumptions	- f_c = 0 or 1 (tree age)
	samples (regime)	- filter blank - particle size
2	sample preparation (5-10 mg-C)	- isotopic heterogeneity - organic, elemental-C
3	counters	- accuracy (SRM's)
	fillings	- repeatability - purity
	observations (vs time)	- radon - stability (pressure, composition)
4	counting segments	- precision - stability - noise, failures - efficiency, gain

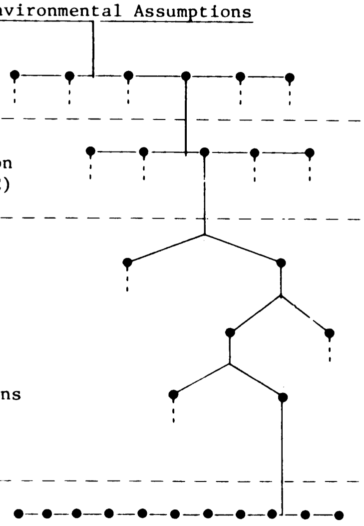

(on-line control: 7 parameters)

protocols. Examining the structure of the acquisition system (fig 1), we see that the basic mode of operation is two-parameter (pulse amplitude, rise time), anticoincidence and coincidence (meson) spectroscopy. While meson cancellation and β^- energy spectroscopy are common for low-level ^{14}C counting, rise time and meson (energy) spectroscopy are not. Although, under ideal circumstances, these added dimensions are unnecessary for ^{14}C counting, they provide important diagnostic information on noise, gas purity, and drift. Briefly, behavior which must be monitored in extended-period, small-signal ($S \lesssim B$) counting may be classified as 1) counter instability (counting gas loss or impurity introduction through leakage, diffusion, desorption; electrical breakdown), 2) system instability (power surges or failure, electronic or computer breakdown; environmental excursions — temperature, humidity, electromagnetic radiation [E-M]), and 3) background variations and radioactive impurity effects. Such difficulties are minimized by system design and pre-acquisition protocol: i e , chemical and radiochemical (^{222}Rn) impurities are removed by rigorous CO_2 purification and precounting decay ($\sim$1 month); external E-M radiation is eliminated through extensive electronic shielding; and our new laboratory incorporates rigorous environmental controls plus an "uninterruptible power supply". Prior to extended counting we monitor meson and CuKα x-ray pulse characteristics and rates, and we visually inspect guard and sample counter pulse shapes and noise levels.

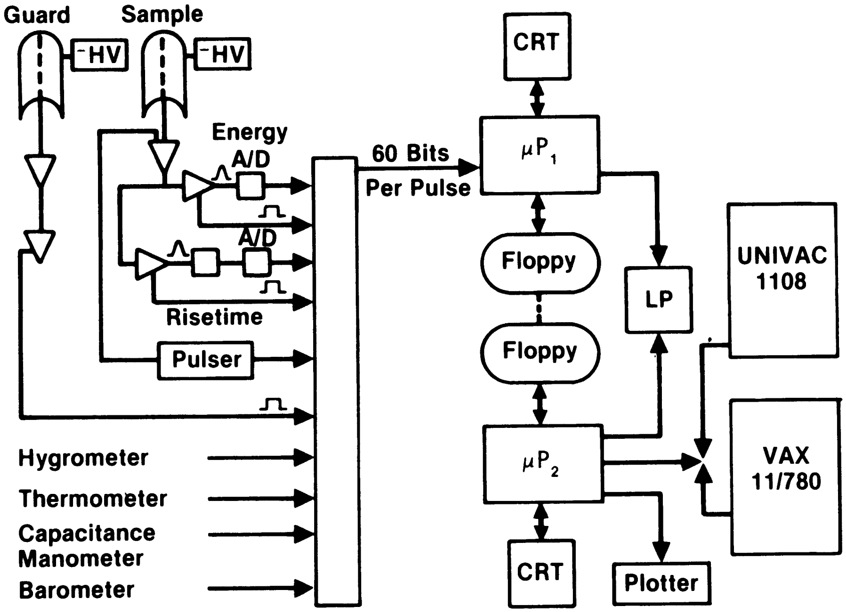

Fig 1. Structure of the microprocessor(μP)-controlled data acquisition and processing systems. LP = Line Printer

The individual data acquisition periods (6-24 hours each) are subdivided into 6-12 segments (fig 2) to gain information on actual variability of the critical parameters and to guard against isolated outliers and failures. The number of intervals selected is based on a balance between tolerable information-loss (if one interval is faulty) and the broad segmentation optimum (Currie, 1973; Currie, Noakes, and Breiter, 1979) for detecting non-Poisson error. We include automatic (microprocessor controlled) monitoring of the several parameters shown in fig 2, plus environmental variables and pulser signals. Special attention is given to "noise," as manifest by unreasonably fast rise time, lack of coincidence between energy and rise time signals ("singles"), odd spectrum shape, or unusual "peaking time" (time between peaks of energy and rise time output pulses). Evaluation of the counting data quality thus follows from visual examination of the multiple control charts, limits for critical variables (eg, meson and guard rates, noise), and bounds for three test statistics that assess variability and outliers. Since our experience indicates that occasional positive outliers do occur, especially when a counter has been freshly filled, we have elected to use a robust statistic (the median) to estimate the mean over the entire counting period (Kafadar, Rice, and Spiegelman, 1983). Isolated outliers then have little effect on the results, and we sacrifice a little

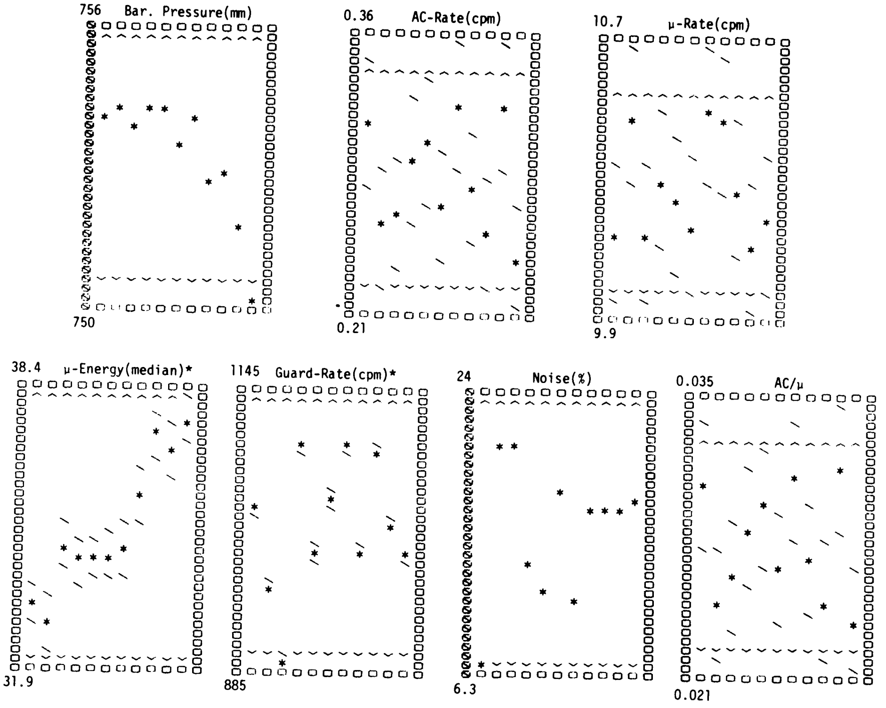

Fig 2. **Multiparameter** control chart (aerosol sample #561-562) showing parameters monitored on-line during 11-segment, 2200 min counting period. (*) indicates χ^2 significant at 5% level. (⟍) equals ± Poisson-σ; (◇) equals ±2s limits. (Imperfect run, selected to show drift and noise.)

precision (median vs arithmetic mean standard errors) to avoid the subjective trap of rejecting a datum simply because it appears to be outlying. Finally the quantity used for computation is the ratio "AC/μ", ie, the anticoincidence count rate divided by the meson (coincidence) rate, as this ratio gives automatic compensation for small changes in counter efficiency. (In fig 2, eg , the final result is AC/μ, median = 0.0266 ± 0.0011).

INDIVIDUAL PULSE DATA STREAM. As an alternative to sorting pulses into discrete two-parameter (energy, rise time) bins, we have the capability of preserving the entire time series of individual events. Thus, we may estimate activity levels from the distribution of pulse time intervals rather than counts per unit time. As with rise time analysis, this exercise would be rather uninteresting under the null hypothesis (pure Poisson process), because the information derivable from the Poisson distribution of counts is exactly equivalent to that from the exponential distribution of time intervals (Cox and Lewis, 1966). However, when real systems with imperfect counters and electronics are involved, the complete information record can provide important insights and defense against artifacts such as multiple pulses. Also, statistical problems of extreme low-level counting, when few if any counts occur in given segments, are avoided. Table 2 gives a brief record from a sequence of anticoincidence events and electronic pulser signals. One important derived quantity, the time interval since the preceding coincidence event, is given in the last column — this particular data set exhibits one surprisingly small value: 3 ms. Further investigation of the diagnostic value of the pulse time record is actively underway.

TABLE 2. Pulse data stream

Cntr		**Coinc**		**Peak**		**Guard**		**Pulser**			**Energy**		**ADP**		**Time**					**Δt**
Part A: Partial record of electronic pulser events																				
1	1	0	0	1	0	0	0	1	0	0	45	12	86	29	253	39	35	20	100	
1	1	0	0	1	0	0	0	1	0	0	90	22	173	42	257	39	35	20	100	
1	1	0	0	1	0	0	0	1	0	0	45	12	86	29	748	38	15	22	100	
1	1	0	0	1	0	0	0	1	0	0	90	22	173	42	753	38	15	22	100	
1	1	0	0	1	0	0	0	1	0	0	45	12	86	29	404	21	55	23	100	
1	1	0	0	1	0	0	0	1	0	0	90	22	174	42	409	21	55	23	100	
Part B: Partial record of anticoincidence pulses																				
1	1	0	0	0	0	0	0	0	0	0	60	15	62	22	47	13	49	22	100	15019
1	1	0	0	0	0	0	0	0	0	0	61	58	62	62	4	49	54	22	100	5913
1	1	0	0	1	0	0	0	0	0	0	11	2	50	14	865	37	56	22	100	7088
1	1	0	0	0	0	0	0	0	0	0	60	60	62	50	973	37	56	22	100	7196
1	0	0	0	0	0	1	0	0	0	0	0	0	0	0	657	46	58	22	100	543
1	0	0	0	0	0	0	0	0	0	0	6	0	7	0	914	58	58	22	100	3
1	1	0	0	1	0	0	0	0	0	0	10	2	48	11	119	1	1	23	100	11960
1	0	0	0	0	0	0	0	0	0	0	6	0	9	0	388	57	4	23	100	16
1	1	0	0	0	0	0	0	0	0	0	61	17	41	11	871	53	6	23	100	2680
1	1	0	0	0	0	0	0	0	0	0	26	6	20	6	143	17	8	23	100	14197
1	0	0	0	0	0	1	0	0	0	0	0	0	0	0	533	23	7	23	100	2410
1	1	0	0	0	0	0	0	0	0	0	16	4	14	3	992	33	11	23	100	23156
C	**D**														**ms**	**s**	**min**	**hr**	**day**	**ms**
Channel																				

Code: The 6 double columns have bits indicating for each of 2 counters: (1) a counter pulse, (2) coincidence with guard (selected out, here), (3) "peaking time" (noise monitor), (4) guard scaler (10^4 counts), (5) pulse amplitude (E), (6) rise time parameter (ADP). Quintuple column gives pulse time (nearest ms); last column: interval (ms) since preceding coincidence event.

REPLICATION, REPORTING, AND LONG-TERM CONTROL [Level 3]. Level 3 control of quality is achieved through independent counting replicates in which the counting gas is placed alternately in different counters (following repurification and volumetric mass measurement, when appropriate), and counted at different times (separated by at least one ^{222}Rn half-life) and interleaved with measurements of standards and blanks. Occasional higher-order replication occurs also, using independent sample preparation from the starting material (oxalic acid, aerosol particles, etc). Our goal is to achieve an adequate degree of control through independent measurements to expose problems with contamination, efficiency, stability, or counter calibration while minimizing the overall elapsed and handling time. This generally means at least two measurements each in two independent counters.

Table 3 presents a recent data set, selected to illustrate level 3 controls (including outlier treatment). The table is derived from the medians of the segmented counting periods (AC/μ, level 4) combined into weighted means (for each counter); and then converted to the tabulated f_M values (% of modern carbon) using mean AC/μ ratios from background and standard measurements in the respective counters. Weighted means across counters give final f_M values, which are converted to % "contemporary carbon" (f_C) for environmental samples. As shown in the table, χ^2 is used to monitor consistency between replicates (for a given detector) as well as between detectors for a given sample. Our treatment of outliers (note 3) is to report the final result both with and without the apparent outlier. Outright rejection is not done without cause. Finally, background and standard measurements are performed on a weekly basis, and both long-term means and time-bracketing observations are used to assess control and the ^{14}C content of samples (fig 3).

TABLE 3. Summary report for aerosol samples*

Sample No.	Mass Carbon (mg)	f_M(±SE),(χ^2/df,df)** Detector N	f_M(±SE),(χ^2/df,df)** Detector M	Average f_M** (±SE),(χ^2/df,df)	f_C(±SE)**
557-558	9.4	102±6(1.8,5)	107±6(1.4,5)	105±4(0.3,1)	84±3
559-560	7.9	88±7(2.1,3)	80±7(3.0,4)	84±5(0.7,1)	67±4
561-562	7.3	110±8(3.3,3)	124±8(0.7,3)	118±6(1.4,1)	94±5
563-564	7.4	104±9(0.5,2)	114±8(0.5,5)	110±6(0.6,1)	88±5
572-573	7.5	133±9(1.2,3)	130±7(1.9,7)	131±5(0.1,1)	105±4

* Illustrative data from samples recently provided by the US EPA (1981).

**f_M - "Modern carbon" (%); f_C - contemporary carbon (%), = f_M/1.25 [1980 vegetation]; (χ^2/df,df) = chi-square per degree of freedom, no. of degrees of freedom.

COMMENTS: 1) f_M is derived from at least 2 replicate measurements each in 2 independent detectors.

2) Standard error, SE, is the Poisson standard deviation of the weighted mean for f_M and f_C values. Quality control is monitored with chi-square for both internal replicates and between detectors.

3) Weighted average f_M value for sample 572-573 in detector M omits two measurements which proved to be marginal outliers. Weighted average f_M including these outliers is 136±6.

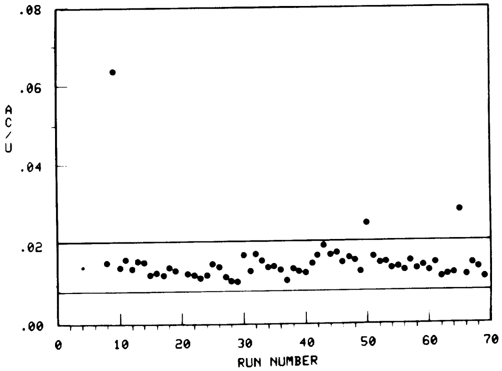

Fig 3. Background-counter M. Control chart, covering a 9 month period, for normalized background observations (18 mL quartz counter). Each observation is equivalent to 900-1200 min; and ±2s bounds are indicated. Outliers are rare and isolated; the first is unexplained, but the latter two are associated with gaseous impurities.

ARCHIVING. All original data files including segment data, and merge (summary) files, are retained on floppy disk. For each observation, all variables monitored are stored in vector format on archive files for subsequent quality control plots. For efficient, exploratory data evaluation, we have developed a Fortran routine, ANALYZER, which permits rapid data subset selection (according to sample, detector and date), error propagation and pooling, and generation of test statistics.

HIGHER (NON-COUNTING) CONTROL LEVELS

SAMPLE PREPARATION AND REFERENCE SAMPLES [Level 2]. Apart from the need for rigorous chemical purification of the CO_2 counting gas and removal of ^{222}Rn (by chromatography or decay), environmental aerosol samples bring with them some special sample preparation needs and pitfalls. These concern standards or reference materials, the (particle filter) blank, isotopic heterogeneity and recovery, and accurate separation/identification of different carbonaceous species.

Before turning to the first of these topics (standards), brief comments on accuracy requirements and on radon levels are in order. Unlike ^{14}C dating in which relative uncertainties must be <1%, aerosol studies generally require no better than ∿10% uncertainty levels, the primary limitations being sample (C) mass and separation of molecular species. As our smallest counter has a background rate of 0.058 cpm and a modern/background ratio ($M/B = \rho_M$) of 1.8 for 10 mg carbon (table 4; Currie, Noakes, and Breiter, 1979), the random (σ_f) and systematic (Δ_f) errors in the estimated fraction of modern carbon (f_M) due to counting statistics, radon contamination, and background variations are, respectively

$$\sigma_f = \phi_B \left(\frac{\sqrt{f_M \rho_M + 2}}{\rho_M}\right) \quad \text{and} \quad \Delta_f = \frac{Rn/B}{\rho_M} , \frac{\Delta B/B}{\rho_M} \qquad (1)$$

where ϕ_B is the relative Poisson standard deviation for the background count ($\phi_B = 1/\sqrt{B}$), and Rn/B and $\Delta B/B$ are the systematic errors from radon or background shifts relative to the background counts. The largest Poisson error obtains when f_M is unity (ignoring bomb contamination for the moment); σ_f will therefore be 10% when ϕ_B equals $10\%/[\sqrt{3.8}/1.8] = 9.2\%$. Thus, $B = 118$ counts which is equivalent to ca 2000 min counting time. Taking Δ_f to be 5%, eg, contamination or background instability ($\Delta B/B$) may not exceed ∿9% for this detector. Finally, for radon, we have (occasionally) seen contamination levels as high as 1-2 cpm immediately following atmospheric aerosol sample preparation. Thus, for this to be reduced adequately (to ∿0.005 cpm), ca 8 half-lives (∿30 days) must elapse before counting.

TABLE 4. Small sample detector characteristics*

Detector	Volume (mL)	Background rate (cpm)	Modern (gross) rate (cpm)	$\rho_M (=\frac{M}{B})$
P	4.8	0.058	0.16_0	1.8
N	6.1	0.067	0.17_3	1.6
M	17.7	0.15_2	0.25_2	0.7

*The modern (gross) rate (= background rate + 0.95*SRM 4990B) and the modern (net rate, M) to background (B) ratio (ρ_M) refer to samples having 10 mg carbon.

Table 5 lists reference materials used for calibration and quality control. The two oxalic acids, ANU sucrose, and the two fossil carbon samples calibrate and check the response for contemporary ^{14}C levels and the background, while the dated wood sample is used to check an intermediate age (∿ mean life). Of major importance for aerosol studies are the two urban particulate standard reference materials (SRM's) which were collected in St Louis and Washington, DC, respectively. They were designed primarily for control of interlaboratory measurements of trace elements, and have become very useful also for organic compounds and carbon isotopes. These SRM's are necessary to continually demonstrate measurement accuracy in materials resembling real samples both in analyte concentration and in overall composition.

Isotopic heterogeneity can be significant for aerosol samples because they contain compounds coming from many different (biogenic and fossil) sources. Thus, if sample conversion to GO_2 is not quantitative, the average isotopic composition in the counting gas may be very different from that in the original sample. (The situation is not analogous to isotopic fractionation of samples that are isotopically homogeneous;

TABLE 5. Quality control (reference) samples

Control sample	% Carbon	^{14}C activity (dpm/10 mg carbon)
NBS SRM 4990B Oxalic Acid	19	0.142
NBS RM 49 Oxalic Acid	19	0.184
ANU Sucrose	42	0.214
NBS SRM 1648 Urban Dust	13	ca 0.11
NBS SRM 1649 Urban Dust	16	ca 0.09
USGS Wood (7060 ± 250y BP)	44	0.057
Bituminous Coal - SRM 1632a	81	0
Spectrograde Graphite - RM 21	99.9	0

rather, large chemical fractionation effects produce different mixes of compounds which are initially isotopically heterogeneous.) More important than accurate average aerosol isotopic compositions, however, are isotope ratios for individual molecular species. This represents the area of greatest experimental difficulty, but it presents the greatest promise for understanding aerosol origins and it is well suited to work with miniature counters. An illustration was given for Denver aerosol where we found that the more volatile sample component contained considerable biogenic carbon (∿55%) whereas the elemental carbon was mostly fossil (∿14% biogenic) (Currie et al, 1982).

SAMPLING AND SOURCES — ASSUMPTIONS AND ARTIFACTS [Level 1]. A significant aerosol sampling problem is the carbon blank associated with the particle filter. When pollution is slight, the chemical and isotopic composition of the blank may cause substantial perturbations in the observed results. The nature of the blank is incompletely understood, but there is evidence that it has both human and natural origins; that it is primarily volatile; and that it may be contemporary. The blank level ranges from ∿2 μg C/cm^2 to ∿8 μg C/cm^2 for carefully prepared, pre-fired filters, with the lower value being obtained with special quartz filters. Assuming the blank to be contemporary, the correction factor is $(1-[\phi_b/f])/(1-\phi_b)$, where ϕ_b is the blank carbon mass fraction and f is the observed fraction of contemporary carbon. The largest correction to our Houston samples (Currie et al, 1982), eg , occurred with sample 8 where $\phi_b = 0.145$ and the total mass was 6.4 mg carbon. Blank-correction reduced the observed value (18% contemporary) to just 4% contemporary carbon.

A principal assumption in the application of radiocarbon to aerosol studies is the two source hypothesis. That is, we assume (within ∿10%) that all major contributing sources are either fossil or contemporary. This appeared valid at the outset, for even soil carbon which may be mobilized is unlikely to be older than ∿800 years. However, one major difficulty plus some subtle ones are now emerging with this hypothesis. The subtle difficulties relate to societal changes which lead to mixing of contemporary carbon in primarily fossil fuel, and the converse, eg , synthetic fireplace logs containing a paraffin binder, and auto-fuel containing (biogenic) ethanol ("gasohol"). The major effect relates to ^{14}C variations associated with wood-burning. The economic incentive to use wood as a fuel has made this a primary seasonal source of carbonaceous aerosols. In order to assess its impact one must estimate the average ^{14}C content of the firewood by integrating over the radiocarbon variations during the growth period. Prior to 1954 this was unimportant, but the doubling of atmospheric $^{14}C/^{12}C$ in 1964 followed by a slow decline leads to significant corrections for more recent vegetation (Currie, Klouda, and Gerlach, in Cooper and Malek, 1981).

Finally, accuracy of the overall measurement process has been assessed. Some support comes from our rather large body of measurements of atmospheric particles for which the natural bounds (fossil, contemporary) have not been exceeded, but more especially from consistency of conclusions when just one primary carbon source was believed present (vegetation: Cooper, Currie, and Klouda, 1981; diesel exhaust: Klouda, unpublished data, 1982). A recent more conclusive test took place when aerosol samples submitted "blind" gave results which agreed to within 5% based on completely independent approaches involving ^{14}C and trace element receptor modeling (personal communication, J A Cooper, 1982).

CONCLUSION

Realization of the full potential of miniature gas counters for archaeological and environmental ^{14}C applications requires strict attention to measurement quality and assumptions. Though precision needs are often modest, sample size and composition, signals close to background, and long-term counting demand a tightly-linked multi-level system of quality control. Four such levels are used in our program, ranging from aerosol sampling and separation to segmented multiparameter data acquisition. Special attention has been given to the diagnosis of errors in simplistic assumptions involving Poisson error dominance, isotopic heterogeneity, and background and blank variability.

ACKNOWLEDGMENTS

Assistance in designing the counting system came from JR DeVoe with software input from FJ Barkley. Support is gratefully acknowledged for a National Research Council - National Bureau of Standards Postdoctoral Research Associateship held by RW Gerlach. Partial support for the environmental research was provided by the Energy-Environment Program (EPA-IAG-D6-E684), US EPA.

REFERENCES

Cooper, JA, Currie, LA, and Klouda, GA, 1981, Assessment of Contemporary carbon combustion source contributions to urban air particulate levels using C-14 measurements: Environmental Sci Technol, v 15, p 1045.

Cooper, JA and Malek, D, eds, 1981, Conference on residential solid fuels, environmental impacts and solutions: Oregon Graduate Center, p 365-385.

Cox, DR and Lewis, PAW, 1966, The statistical analysis of series of events: New York, Wiley & Sons, Chap 6.

Currie, LA, 1973, The limit of precision in nuclear and analytical chemistry: Nuclear Instruments Methods, v 100, p 387-395.

__________ 1978, Bias Detection, in Kolthcff, IM and Elving, PJ, eds, Treatise on analytical chemistry: New York, John Wiley and Sons, p 151.

Currie, LA, Klouda, GA, Continetti, RE, Kaplan, IR, Wong, WW, Dzubay, TG, and Stevens, RK, 1983, On the origin of carbonaceous particles in American Cities: Results of radiocarbon "dating" and chemical characterization, in Stuiver, M and Kra, RS, eds, Internatl ^{14}C conf; Radiocarbon, v 25.

Currie, LA, Noakes, J, and Breiter, D, 1979, Measurement of small radiocarbon samples: Power of alternative methods for tracing atmospheric hydrocarbons, in Berger, R and Suess, HE, eds, Radiocarbon dating, Internatl ^{14}C conf, 9th, Proc: Berkeley/Los Angeles, Univ California Press, p 158-175.

Kafadar, K, Rice, J, and Spiegelman, C, 1983, One-sided trimming in small samples with asymmetric contamination: Commun in statistics, theory and methods, v 12, no. 4, p 477-496.

Polach, HA, Soini, E, Kojola, H, Robertson, S, and Kaihola, L, 1982, Radiocarbon dating of milligram-size samples using gas proportional counters: an evaluation of precision and of design parameters, in Australian conf on archaeometry, 1st, Proc: Sydney, Australian Museum.

Sayre, EV, Harbottle, G, Stoenner, RW, Otlet, RL, and Evans, GB, 1981, The use of the small gas proportional counters for the carbon-14 measurement of very small samples, in Internatl symposium on methods of low-level counting and spectrometry: IAEA, Vienna, in press.

[Radiocarbon, Vol 25, No. 2, 1983, P 565-575]

DEVELOPMENT AND OPERATION OF THE HARWELL SMALL COUNTER FACILITY FOR THE MEASUREMENT OF ^{14}C IN VERY SMALL SAMPLES

R L OTLET, GEORGE HUXTABLE, G V EVANS, D G HUMPHREYS
T D SHORT*, and S J CONCHIE

Nuclear Physics Division, AERE Harwell, Oxfordshire, OX11 ORA
United Kingdom

ABSTRACT. The Harwell system for measuring milligram size samples using Brookhaven miniature gas counters is fully operative. It comprises 12 counters of different sizes which operate simultaneously within a single NaI crystal (300mm diameter x 300mm long) acting as an anti-coincidence guard counter. Brief details are given of the construction and commissioning of the system, including counter assembly, shield design, electronics, data capture, data analysis, and chemical processing and filling procedures. The performance of the system and an overall view of the fields of application for which the counters have important applications are discussed.

INTRODUCTION

This paper describes the development and first few months of operation of the Harwell small sample ^{14}C measurement facility which uses Brookhaven miniature gas counters (Harbottle, Sayre, and Stoenner, 1979). The collaboration with Brookhaven National Laboratory began in the initial testing of the counters and the design and planning of the proposed facility with its multi-counter array were previously described (Sayre et al, 1981; Otlet and Evans, in press). Up to that time, work had been confined to test, background and calibration samples with no actual samples.

COUNTER ASSEMBLY AND SHIELD

Six 5mℓ 'micro-counters' and six 30mℓ 'mini-counters' which, filled to 4 atmospheres pressure of carbon dioxide, mean equivalent quantities of ca 11mg and 66mg respectively, are employed.

---

* Computing Centre, North Staffordshire Polytechnic, Blackheath Lane, Stafford, United Kingdom

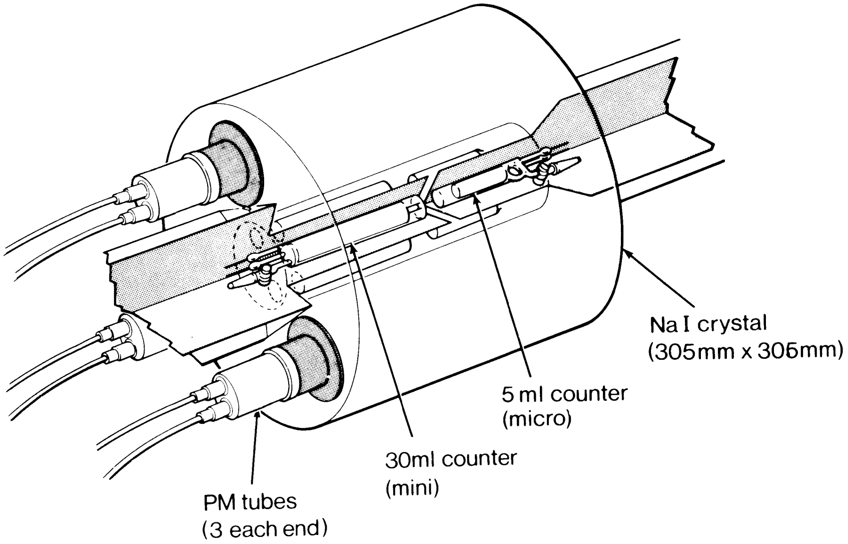

FIG 1. **NESTING OF COUNTERS IN GUARD COUNTER CAVITY**
Showing a 'micro'-counter (5 ml) back to back with a 'mini'-counter (30ml) in one of the segmented compartments

Figure 1 shows nesting of the full array of counters inside the guard counter, which is a large, 300mm diameter by 300mm long, NaI crystal with three photomultiplier tubes on opposite parallel faces (six in all), providing annular shielded volume for the counters ca 90mm internal diameter. The complete assembly, guard counter, and gas counters are further shielded within a large passive shielding castle. The shield comprises old steel, total thickness 230mm, with an inner layer of boron-loaded paraffin wax (neutron shield) arranged in the order, 204mm steel, 150mm paraffin wax plus 26mm steel as the inside layer. During commissioning we found it necessary to contain each counter in its own individual metal (copper) box. This design feature greatly assists removal for counter filling and minimizes spurious cross-talk-type interference among neighboring counters 'in operation. The individual, segment-shaped containers are illustrated in plate 1, designed to pack numerous counters (six at each end) inside the concentric cavity of the guard counter, with the EHT filter components and pre-amplifiers as close to the counter as possible, as well as to leave space for the photomultiplier tube terminations.

Table 1 lists characteristics of the counters operated within the shield and, in the case of the micro-counters, can be compared with the Brookhaven values. The background so far obtained, although very low and acceptable from an operational point of view, is not so low as the best Brookhaven result, the achievement of which will be further considered. On the other hand, the modern carbon to background ratio achieved with the larger mini-counters (∿ 8) is close to the Brookhaven value and compares favourably with large sample scintillation counting.

TABLE 1. Comparison of some miniature counter characteristics in different shields

Guard shield	Place	Counter Volume (mℓ)	Background (counts/day)	Modern carbon to background ratio
Conventional multi-gas counters	Brookhaven	5	56	3.3
Conventional multi-gas counters	Harwell	30	180*	5.3
Conventional multi-wire gas counter	Harwell	5	124	1.5
Conventional multi-wire gas counter	Harwell	30	400	2.4
254mm x 254mm NaI crystal	Brookhaven	5	21	8.9
300mm x 300mm NaI crystal	Harwell	5	30	6.2
300mm x 300mm NaI crystal	Harwell	30	130	7.5
300mm x 300mm NaI crystal	Harwell	10	80**	∿4.7
Gas multi-wire counter with inner plastic phosphor shield (10mm thick)	Harwell	5	72	2.6

*Approximate result with a 4-atmosphere filling of P10 gas

** Counter tested for Wallac, Finland - filled to 4 atmospheres CH_4

Other counters all of Brookhaven origin - filled to 4 atmospheres CO_2

The validity of the decision to use the large NaI crystal as the guard counter instead of a less expensive gas proportional or plastic phosphor type is still under investigation. The comparative tests with a multi-wire gas proportional guard counter operated in the same passive shield (table 1) support the Brookhaven results and our decision. Further tests will include a direct comparison with a plastic phosphor guard shield.

ELECTRONICS AND DATA HANDLING

Recent improvements in technology, eg, monolithic integrated circuit components and micro-processor data capture have been fully exploited, facilitating multi-counter operations and providing stability throughout the counting times. The electronics hardware is made at Harwell using standard, commercially available components. The full system,including micro-processor and computer display, acts as 14 multi-channel analysers, each of 512 channels and split-store operational capability. Additional features of the Harwell circuitry enable 1) full spectrum display of both coincident (cosmic) and anticoincidence (sample and background) pulses, 2) pulse height analysis of events recorded simultaneously in any counter (without which it would be impossible to record the coincident spectra of every counter separately), 3) variable dead time (blanking time) following guard counter (veto) pulses. The relatively high count-rate of the large NaI crystal detector and the excessively large amplitude range of pulses ca 1000:1 made this necessary. Figure 2 is a simplified schematic diagram of the electronics and data handling circuitry EHT for the 12 counters which are currently in operation is individually provided from a single unit (Le Croy 4032A) which uses plug-in EHT pods. Positive high voltage is used, applied (after filtering) directly to the anodes, the signal being taken from the cathode terminations at ground level. This particular connection arrangement means that any spurious break down pulses in the EHT filter circuit have an opposite polarity to the genuine counter pulses and is more convenient from the point of view of the physical layout in the confined space of the counter box.

Output from the preamplifiers is passed to the amplification, pulse shaping, discrimination and peak stretching (sample and hold) circuits. All are internally connected to a common logic board which includes the analogue to digital converter and logic circuitry which encodes all signals ready for acceptance and storage by the dedicated micro-processor (NASCOM). Data transfer is effected on a priority interrupt basis and in the case of multi-events (simultaneous triggering of more than one counter at a time) a hierarchical system reads

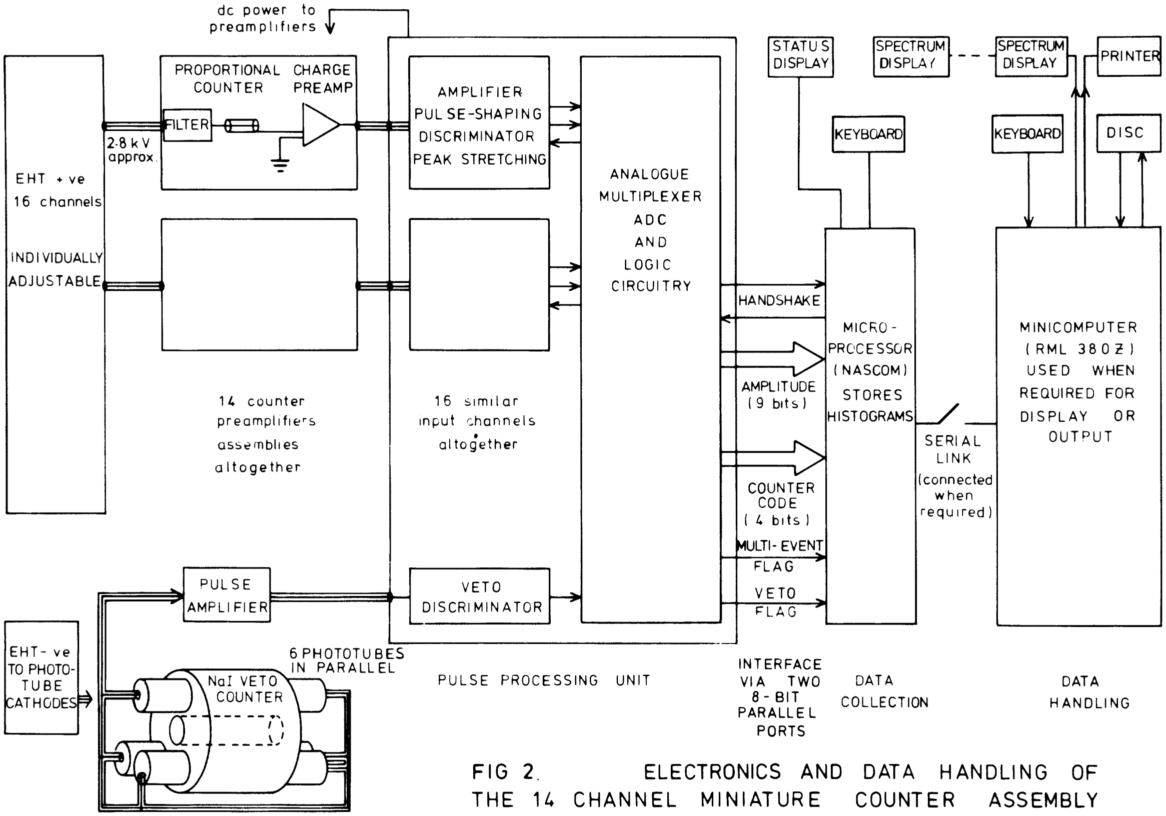

FIG 2. ELECTRONICS AND DATA HANDLING OF THE 14 CHANNEL MINIATURE COUNTER ASSEMBLY

PLATE 1. Individual counter assembly

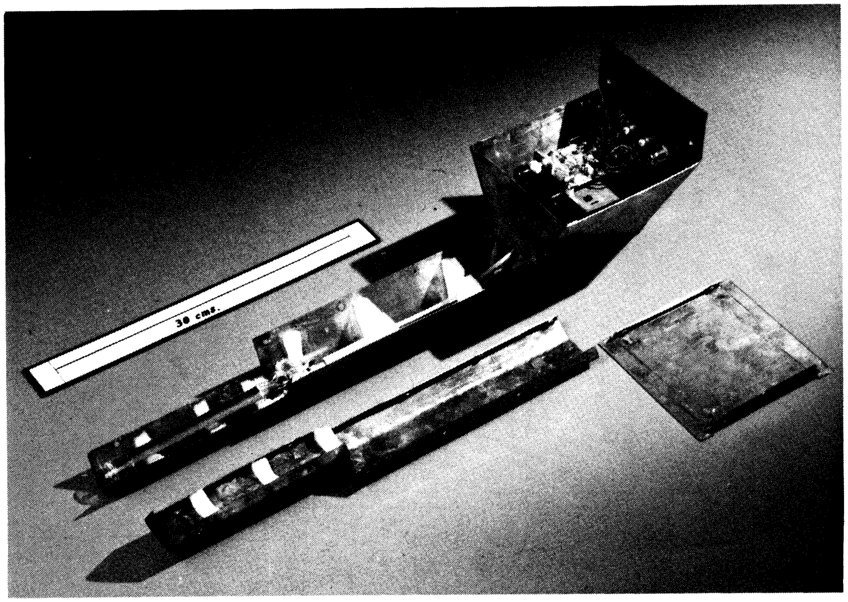

PLATE 2. Complete set-up - shield, counter assembly, electronics, and micro-computers

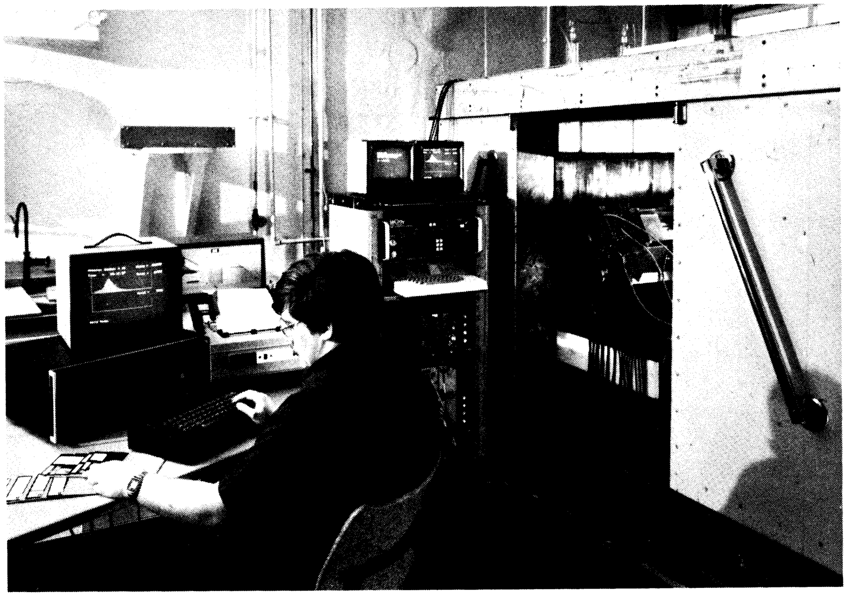

from each counter in turn whilst the peak stretching facility holds the sampled pulse waiting for its turn to transfer. Priority interrupt also ensures that data transfer from the counter electronics is not impeded by read-out of the Nascom stores by the data handling general purpose computer.

Data collection and handling is enacted by two Z80 based devices. The first is a simple, inexpensive extended memory (16K) microprocessor (NASCOM), the basic function of which is to accept pulses from the counters and to store them as histograms according to the encoded label. For each counter 256 locations are for multi- and veto-flagged events and 256 for non-flagged pulses. The NASCOM is permanently connected to the counter electronics circuitry and buffers the system breakdowns or malfunction caused by other activities of the second, more sophisticated, general purpose micro-computer (RML 380Z). This second computer, which includes full facilities for high resolution graphics provides display of the counter pulse-height spectra, analysis and long term (back-up) floppy disk storage. In these first few months of operation, display of spectra has been made frequently but the dumping to disk should only need to be carried out twice a week, each time resetting the NASCOM stores to zero. This procedure enables possible problems to be spotted rapidly enough and at no time is there any risk of losing a set of data which may have taken up to 7 days to collect. A photograph of the complete shield, electronics and data-handling set-up is given in plate 2.

INTERPRETATION OF SPECTRA

Figure 3 A-D shows a set of print-outs derived from displays of spectra obtained with the micro and mini-counters under different conditions. Each display is a composite of the coincident (cosmic) spectrum, above, with the anticoincident spectrum below. Counts per channel are plotted against channel number which, in terms of energy, is linear up to channel 255. Counts below channel 10 are cut off by the preset discriminator contained in the pulse processing unit (see fig 2). The displayed range represents ca 2 KeV to 59 KeV for both sizes of counter. All pulses above the equivalent energy of channel 255 (> 59 KeV) are dumped into channel 256 but are included in the total count calculations. A new counter filling is set up, using an external ^{241}Am or ^{238}Pu gamma-ray source to excite the Kα X-ray spectrum off the iron cathode, before the counter is put into the shield. The peak is moved to channel 31 (both sizes of counter) by adjusting the EHT and forming the primary energy calibration of the channel's scale (6.4 KeV at channel 31). The sharpness of the peak is important for assessing the quality of the filling gas (Sayre et al,

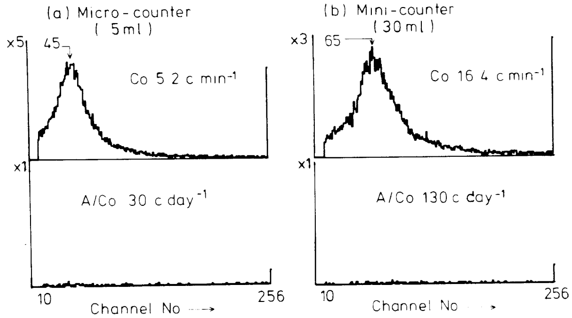

3A Background good spectra

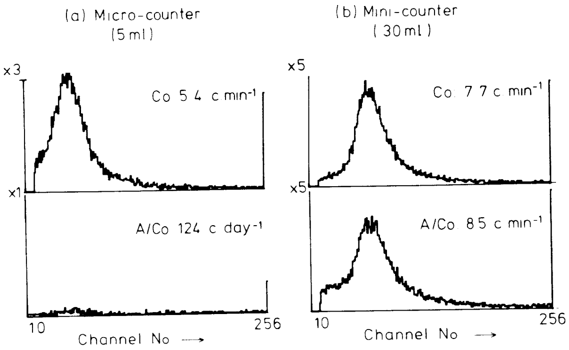

3C Background (a) Inefficient guard counter (b) Guard counter failure

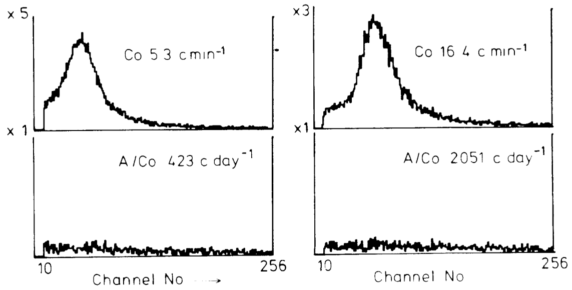

3B Twice modern ^{14}C good spectra

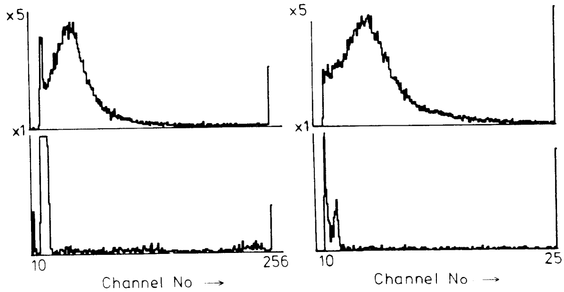

3D EHT Breakdown problems

FIG 3 EXAMPLE COINCIDENT / ANTICOINCIDENT SPECTRA FROM "MICRO" AND "MINI" GAS COUNTERS

1981). A resolution of the order of 25% should be obtained or repurification will be necessary.

The counter is then put into the shield and the position of its cosmic peak and its resolution determined. The occurrence of these peaks, shown in the upper half, coincident, spectra, in fig 3 at ca 9.5KeV and 13.6KeV for the micro- and mini-counters, respectively, are characteristic of gas counters generally (Wolfendale, 1963). They are produced from charged particles (muons) causing ionization during passage through the counter, the total energy deposited being a function of the product of the track length possible in the dimensions of the counter and of the gas density for the particular gas filling, thus it reflects the pulse produced by the passage of such a particle across the diameter of the counter and for larger counters filled to the same pressure, the equivalent energy it represents appears at higher levels. The peak is used to provide a continuous monitor of the gas quality and electronics (EHT and gain) stability throughout the long counting periods. This technique has been used for many years in our laboratory for ^{14}C gas counting, having been developed from a similar procedure we used in ^{3}H counting (Otlet, 1968) but has also been reported independently by Oona and Fan (1977). No change in either its position or resolution is expected even after 70 days of counting.

Examination of the anticoincidence (sample) spectra also provides valuable confirmation of valid counting. Figure 3A and B shows good background and ^{14}C (2 x modern) plus background spectra for both sizes of counter. The difference between these good spectra and the others, which demonstrates problems, is clearly seen. So far, sporadic EHT breakdown has been the only problem which has had to be contended with and the ability to identify it and to cure it quickly on the occasions when it has arisen has been invaluable.

GAS PURIFICATION AND COUNTER FILLING

Sample preparation basically follows the well established procedures for gas counting with CO_2 (Srdoč and Sliepčevic, 1963; Sayre et al, 1981) but using rigs suitably scaled down for the smaller size of samples being handled. Dry reagents are used throughout, the essential stages of the final purification being thermal cycling for 2 to 3 hours, first over copper at 700°C and afterwards over silver and platinum at the same temperature in the presence of a small quantity of added oxygen. The last step is the passage of the CO_2 through activated charcoal at 0°C as Bruns (ms) followed by freezing and pumping.

The filling procedure is similar to that which Brookhaven uses (Harbottle, Sayre and Stoenner, 1979). Mercury under pressure is used to compress the purified CO_2 into the counter. The mercury passes through the pre-filling measurement vessel and connecting lines right into the counter filling leg stopping only 2-3mm short of the counter sensitive volume. In this way, dead volume is absolutely minimized and no loss of sample CO_2 occurs even for samples which yield amounts very close to the minimum required to fill the counter. When the counter stopcock is closed the mercury above it helps the seal and prevents the gas making contact with the stopcock grease.

CONCLUSIONS

Operation of the 12-counter assembly began in November, 1981. Since then a simultaneous programme of sample measurements and calibration of the counters has been operated. Preliminary experience with the multi-counter set-up suggests that miniature counters have a promising future for low-level ^{14}C measurements in a variety of applications including Art, Archaeology, Hydrology and the Environment. The obvious limitation of counting time required for acceptable statistics is minimized when several counters are operated simultaneously. For many applications, the sample quantities available enable use of the larger sized counters and a corresponding reduction in counting time for a given measurements precision to be realized (table 2).

TABLE 2. Poisson precision from micro- and mini-counters

Age of sample (years)	± 1σ precision*(%)					
	Micro-counters (5mℓ)			Mini-counters (30mℓ)		
Count time (days)	30	60	90	15	30	60
Modern	1.5	1.1	0.9	1.0	0.7	0.5
1000	1.7	1.2	1.0	1.0	0.7	0.5
2000	1.8	1.3	1.0	1.1	0.8	0.5
5000	2.3	1.6	1.3	1.4	0.9	0.7
10 000	3.6	2.5	2.1	2.1	1.5	1.1
20 000	9.6	6.8	5.5	5.7	4.0	2.8
30 000	18.4	13.0	10.6	17.0	12.0	8.5

* Represents minimum errors in the full procedure, based on the statistics of the estimated sample and background counts only

Modern electronics simplify the operation of many counters simultaneously and their small size allows for containment within an efficient guard counter shield. Experience with a large NaI crystal guard counter reinforces Harbottle, Sayre, and Stoenner's (1979) conclusions that a substantial reduction in background, over and above conventional gas proportional guard systems, is obtained by its use.

ACKNOWLEDGMENTS

The continued collaborative support of the Brookhaven National Laboratory (G. Harbottle and staff) in this project is gratefully acknowledged. Also the assistance of our colleagues L L Wassell and D B Punter, in the design and construction of the counter assembly, and D Sanderson (Research Assistant, Bradford University), who has recently joined the Group, for the provision of some of the latest data, should be mentioned.

REFERENCES

Bruns, M, (ms), 1976, Gas chromatography with Radon-222, Doctoral thesis: Inst Environmental Physics, Univ Heidelberg.

Callow, WJ, Baker, MJ, and Pritchard, DH, 1963, National Physical Laboratory radiocarbon measurements I: Radiocarbon, v 5, p34.

Harbottle, G, Sayre, EV, and Stoenner, RW, 1979, Carbon-14 dating of small samples by proportional counting: Science v 206, p683-685.

Oona, H, and Fan, CY, 1977, A counter system for natural ^{14}C measurements: Nuclear Instruments and Methods, v 143, p391-397.

Otlet, RL, 1968, Low-level tritium measurements for hydrological applications, in Nucleonic Instrumentation Conf, Proc: Conf Publication No. 47, Institution of Electrical Engineers.

Otlet, RL, and Evans, GV, in press, Progress in the application of miniature gas counters to radiocarbon dating of small samples: in ^{14}C and Archaeology Symposium, 1st, Proc: Groningen, in press.

Sayre, EV, Harbottle, G, Stoenner, RW, Otlet, RL, Evans, GV, 1981, Small gas proportional counters for the carbon-14 measurement of very small samples, in Methods of Low Level Counting and Spectrometry: IAEA Vienna, p393-407.

Srdoc, D, and Sliepcevic, A, 1963, Carbon dioxide proportional counters; effects of gaseous impurities and gas purification methods: Internatl Jour Appl Radiation Isotopes, v 14, p68.

Wolfendale, AW, 1963, Cosmic Rays: London, Newnes, p46.

[Radiocarbon, Vol 25, No. 2, 1983, P 577-580]

AN EVALUATION OF SHIELDING CHARACTERISTICS APPLICABLE TO MINI-GAS PROPORTIONAL-COUNTER-BASED ^{14}C DATING SYSTEMS

LAURI KAIHOLA*, HANNU KOJOLA**, HENRY POLACH+,
ERKKI SOINI** AND ROBERT OTLET‡

ABSTRACT. A mini-gas-proportional counter prototype of 10ml capacity (at NTP) was constructed of oxygen-free Finnish copper. The counter tube will be one of 16 equivalent tubes of a small-sample gas counting system, which is equipped with passive graded shield made of lead, cadmium, and copper and a dual active anticoincidence shield, consisting of an external cosmic gas-proportional and an internal plastic scintillation guard. The aim of this study was to evaluate the parameters leading to the design of a cost-effective and compact shielding package for mini-counters.

INTRODUCTION

A joint project was initiated in February 1982 between the Australian National University, Wallac Oy, and University of Turku to design a commercially viable multiple, gas-proportional β-counting system capable of ^{14}C age resolution of small samples, ie, 10 to 100mg of elemental carbon. The heart of the device will be 16 10ml capacity gas counters capable of operation at pressures from 1 to 10atm (abs). Flexibility will be achieved by loading each detector with a separate sample (parallel mode) or by loading the same sample into several counters (serial mode). It was estimated that the precision of a mini-gas counter in determination of the age of a sample would approach that of a good liquid scintillation counter (Polach et al, 1982). A predecessor of the proposed microprocessor-controlled instrument was constructed for tritium counting (Soini and Kojola, 1977).

SHIELDING CONCEPT

The passive shield consists of 600kg of low activity lead distributed asymmetrically around the sample counter: a maximum thickness of 20cm above, 12cm underneath, and 7cm in the sidewalls of the cylindrical counting cavity (fig 1). An excentrically hollow cylindrical plastic scintillator (NE 102) is

---

* University of Turku, Department of Physical Sciences, Turku, Finland

** Wallac Oy, Research Department, Turku, Finland

\+ Radiocarbon Dating Research, Australian National University, Canberra

‡ Low Level Measurement Laboratory, AERE, Harwell, UK

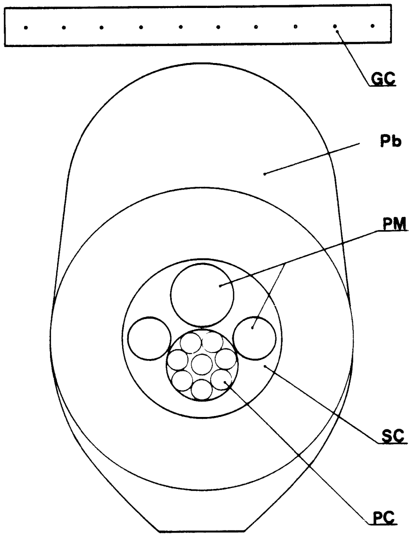

Fig 1. A cross-sectional view of the multicounter shield consisting of: gas-proportional flow counter (GC), massive asymmetric lead shield (Pb), photomultipliers (PM) facing plastic scintillator (SC) and sample gas-proportional counters (PC). The copper and cadmium layers as described in the text are not shown.

viewed with 6 photomultiplier tubes (3 on each end) and is surrounded by 3mm of copper. The inner wall of the plastic container is made of 1.5mm thick cadmium and a copper cylinder with a wall thickness of 5mm. The photomultipliers viewing the plastic scintillator are in anticoincidence with the sample counters, and the upper guard counter, which is a flat multiwire gas-proportional flow counter. The concept and reasons leading to the adoption of this shielding design will be described elsewhere.

SAMPLE COUNTER

The experimental counter (fig 2) was made of Finnish oxygen-free copper with nylon end-plugs and viton O-rings. The inner diameter of the counter tube is 13mm and its wall thickness is 1.5mm. The anode is a 10mm gold-coated tungsten wire. The voltage plateau, using pure CH_4, extends over a range of 1kV with a slope of 1%/100 V. The capacity of the counter is 10ml at STP. The tube is designed to withhold pressures of 4ATM and future design modifications will ensure that a pressure is expected to lie within 4 to 7ATM. Selection of materials was governed by the need to achieve a very low background signal within the ^{14}C β-energy region.

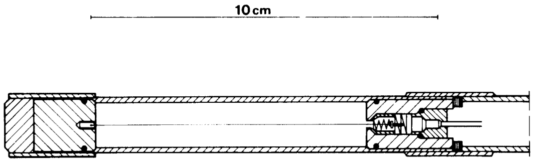

Fig 2. The prototype proportional gas counter. In this version the gas is admitted to and evacuated through the spring cavity, the gas capillary serving as the HV lead at the same time.

Good counters currently achieve a contemporary carbon-to-background count rate ratio of 8 (Harbottle, Sayre, and Stoenner, 1979). Based on this, our design goals at 7ATM are to achieve a modern count rate of ca 0.5cpm (≅720 counts per day) and background of ca 0.06cpm (≅90 counts per day).

TEST DATA

Background tests were carried out in Turku using the shielding described in figure 1 and at AERE, Harwell, using the iron/sodium iodide shielding as described by Otlet et al (1983). Results are given in table 1. A number of automatic on-line controls, as well as pre- and post-counting protocols can be instituted (Currie et al, 1983). These will deal with such parameters as counting gas purity, HV setting, detector long-term stability, detection of spurious (non-Poisson) signals, electronic system instability and environmental factors.

TABLE 1. Sample counter background

		CPM
Outside the lead shield		35
Inside the lead shield		7.8
Inside the lead shield + flat guard on top	*	5.5
Inside the lead shield + plastic scintillator	*	0.35
Inside the lead shield + plastic scintillator + flat guard on top	*	0.20
Old iron + borated paraffin + NaI(Tl) guard	**	0.06

* 50μs anticoincidence resolving time

** 114 hr count at Harwell (80 counts per day)

CONCLUSION

The performance of our sample gas-proportional counter at Harwell shows that it was possible to build an all-metal (copper) detector that meets our requirements. The increase in background, as observed when the same counter is located within our double anti-coincidence graded shield, located in Turku, is due to a number of factors. The most significant possibly are environmental gamma radiation and difference in attenuation of environmental gammas between plastic (Turku) and sodium iodide (Harwell) active coincidence guards. An experiment is planned late this year (1982) at the Harwell location, which will yield data to answer the above questions.

ACKNOWLEDGMENTS

This work was supported by a research grant from the Australian National University, Canberra, Australia, and Wallac Oy, Turku, Finland. Their support is gratefully acknowledged.

REFERENCES

Currie, LA, Gerlach RW, Klouda, GA, Ruegg, FC, and Tompkins, GB, 1983, Miniature signals and miniature counters: Accuracy assurance via microprocessors and multiparameter control techniques, in Stuiver, M and Kra, RS, eds, Internatl ^{14}C conf, 11th, Proc: Radiocarbon, v 25.

Harbottle, G, Sayre, EV, and Stoenner, RW, 1979, Carbon-14 dating of small samples by proportional counting: Science, v 206, p 683-685.

Otlet, RL, Huxtable, G, Evans, GV, Humphreys, DG, Short, TD, and Conchie, SJ, 1983, Development and applications of the Harwell small counter facility for the measurement of ^{14}C in very small samples, in Stuiver, M and Kra, RS, eds, Internatl ^{14}C conf, 11th, Proc: Radiocarbon, v 25.

Polach, H, Soini, E, Kojola, H, Robertson, S, and Kaihola, L, 1982, Radiocarbon dating of milligram-size samples using gas proportional counters: an evaluation of precision and of design parameters, in Ambrose, W and Duerden, P, eds, Archaeometry: An Australasian perspective: Canberra, ANU Press, p 343-350.

Soini, E, and Kojola, H, 1977, An automatic gas counter for quantitative microdetermination of tritium in biological material: Acta Pharmacol Toxicol, v 41, p 79.

VI. ANTHROPOGENIC ^{14}C VARIATIONS

[Radiocarbon, Vol 25, No. 2, 1983, P 583-592]

ANTHROPOGENIC ^{14}C VARIATIONS*

MONIKA SEGL, INGEBORG LEVIN, HILLA SCHOCH-FISCHER,
MARIANNE MÜNNICH, BERND KROMER, JOCHEN TSCHIERSCH
and KARL OTTO MÜNNICH

Institut für Umweltphysik
Universität Heidelberg
Federal Republic of Germany

ABSTRACT. Continuous ^{14}C data of 1 or 2 weekly samples of atmospheric CO_2 are presented, collected near two nuclear power plants (NPP-Biblis and NPP-Philippsburg) located in the rather densely populated upper Rhine valley. Tree-leaf and tree-ring samples from the area of a boiling water reactor in northern Germany (NPP-Würgassen) are also presented and discussed. Additional atmospheric $^{14}CO_2$ samples from two continental 'clean-air' stations in Germany and Austria were used as reference for the polluted areas. For January 1982, these samples yield a 'clean-air' ^{14}C concentration in central Europe of $\Delta^{14}C=255\pm5‰$[1] (7.7pCi/gC=1.45pCi/m^3 air).

In the vicinity of boiling water reactors we found a mean excess in $\Delta^{14}C$ activity of ca 53‰ (0.05pCi/m^3 air) above the local level during normal periods of reactor operation. During revision, however, the $\Delta^{14}C$ excess may reach up to 300‰ above the local background. From this, we calculate source strengths of ca 20Ci/GWa on the average, with peak values of up to 2Ci/week during specific periods. Pressurized water reactors emit ^{14}C mainly as hydrocarbons, and consequently, we found no additional $^{14}CO_2$ near the Biblis reactor.

Stations located in the Rhine valley show significant summer-winter $^{14}CO_2$ variation due to

---

*This paper is from an invited talk.

[1] Heidelberg ^{14}C measurements are systematically $\Delta^{14}C=9\pm2‰$ high compared to the NBS Oxalic Acid standard; if to be compared all Heidelberg ^{14}C data should be shifted by $\Delta^{14}C=-9‰$. A careful standard comparison and recalibration is presently under way.

intensive fossil-fuel combustion. The fossil-fuel admixture leads to a depression of the ^{14}C level and reaches $\Delta^{14}C_{depr}=120‰$ in winter; summer values, however, are only slightly lower than the 'clean-air' level.

INTRODUCTION

In populated areas the 'clean-air' ^{14}C level is modified by two opposite anthropogenic sources:

- fossil fuel CO_2 causes a depletion of the regional ^{14}C level ($^{14}C/^{12}C$ ratio) in industrial areas (Vogel and Uhlitzsch, 1975),
- the emission of ^{14}C from nuclear power and reprocessing plants leads to increased local ^{14}C concentration (Kunz, Mahoney, and Miller, 1974;1975).

The present study continues a previous one by Levin, Münnich, and Weiss (1980). Measurements have been made at the Biblis nuclear power plants (Plants A and B together=2500 MWe) and at the Vermunt and Schauinsland reference stations. A new sampling site was established close to the Philippsburg nuclear power plant (900 MWe). Tree-leaf and tree-ring samples were collected in the area of the Würgassen nuclear power plant (670 MWe). These two plants are boiling water reactors (BWR), emitting mainly $^{14}CO_2$, while pressurized water reactors (PWR) like Biblis primarily emit hydrocarbons (Schwibach, Riedel, and Bretschneider, 1979).

CLEAN-AIR BACKGROUND

'Clean-air' ^{14}C and ^{13}C isotopic measurements are being made at two stations in central Europe, at the Vermunt water power plant (Silvretta 1800m) in Austria (no fossil-fuel contamination, electric power and heating only), and at the UBA-(Federal Environment Agency) observation station on the Schauinsland mountain top (1200m, Black Forest, southern Germany), 1000m above the city of Freiburg.

Figure 1a shows the ^{14}C data for 1976-1982. After the nuclear weapon test ban in 1963, the ^{14}C level decreased exponentially ($\tau \simeq 15$yr), due to the exchange between atmosphere and ocean (see Levin, Münnich, and Weiss, 1980, Fig 1).

For the last few years, a linear regression fits to the observed data equally well:

$\Delta^{14}C = 375 - 20 * t$[2] t = years since 1/1/76 (1)

The fact that Vermunt and Schauinsland data agree well indicates that the data of both stations may be used as ^{14}C reference on the continent, not influenced locally, but rather representing the general ^{14}C level in central Europe. The summer-winter peak-to-peak variations up to $\Delta^{14}C = 40‰$ are essentially due to a generally higher pollution level of the continental air during winter: The corresponding $\delta^{13}C$ values indicate that the Schauinsland station, although only 1000m above Freiburg and the Rhine valley measures the local pollution level sufficiently low except for a remaining contribution of about 4 to 5 ppm fossil-fuel CO_2 ($\Delta^{14}C_{depr} = 15‰$, $\Delta^{14}C_{depr}$ = depression below the 'clean-air' level) in winter. The remaining long-term deviation, especially during 1978/79 when the 'clean-air' ^{14}C level was ca $\Delta^{14}C = 14‰$ above the linear fit shows no significant seasonal variation. It presumably results from post-test-ban atmospheric nuclear weapon tests in China (9/17/77, 3/15/78, 12/14/78) (Fry et al, 1981, Levin, Münnich, and Weiss, 1980).

ATMOSPHERIC SAMPLES FROM BIBLIS AND HEIDELBERG STATIONS

Both sampling locations, Biblis and Heidelberg, are situated in the Rhine valley, a region rather densely and evenly populated. Figure 2 shows their locations and the regional fossil-fuel pollutant sources in the Rhine valley, i e , primarily the cities of Mannheim, Ludwigshafen (industrial area), Worms, and Speyer.

Levin, Münnich, and Weiss (1980) found that the nuclear power plant Biblis A, a pressurized water reactor, is not a source for $^{14}CO_2$. Figure 1b shows the time variations of the $^{14}CO_2$ concentration in Biblis where the ^{14}C level is obviously only influenced by fossil-fuel CO_2. The mean depression during the winter half of the year is ca $\Delta^{14}C_{depr} = 60‰$ with peak depressions up to 100‰, while the summer values are only slightly lower than the 'clean-air'

---

[2] See footnote 1

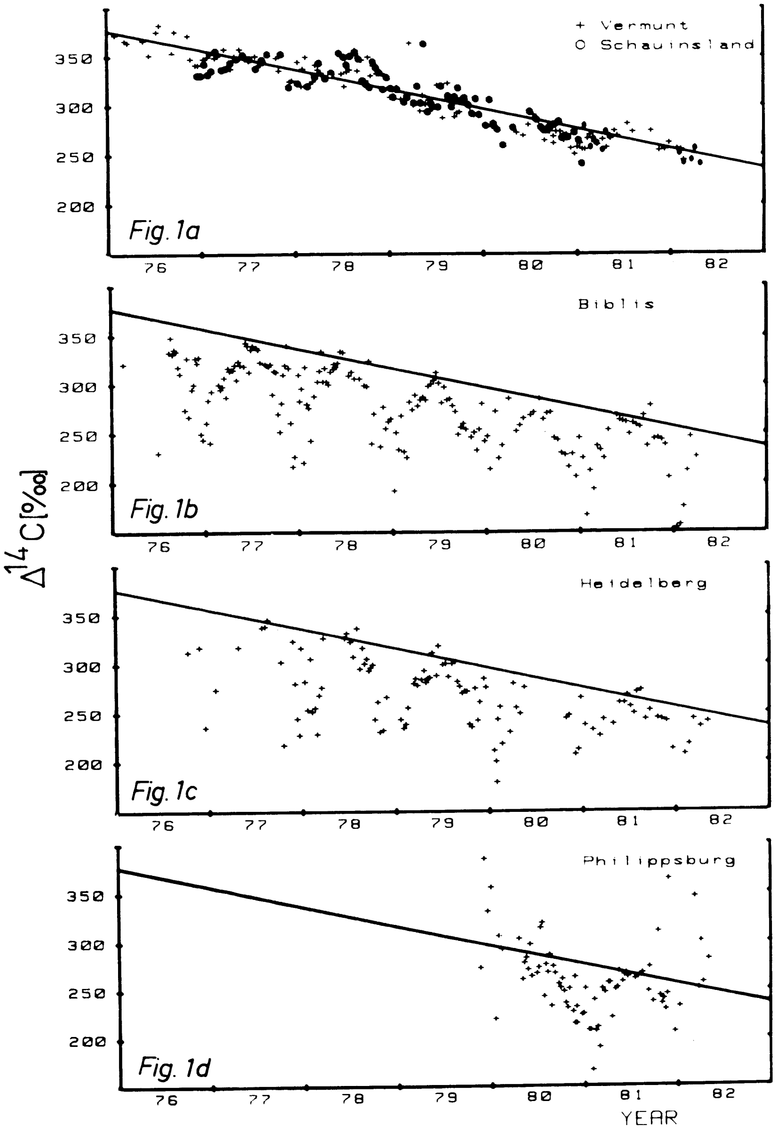

Fig 1. ^{14}C concentration of atmospheric CO_2 at Vermunt and Schauinsland reference stations, 1a. At NPP-Biblis in the Rhine valley, 1b. At the Heidelberg institute ca 15m above the ground, 1c. At sampling site ca 1.5 km northwest of the NPP-Philippsburg, 1d. (See map, Fig 2). The straight line is a least squares fit through the reference station data.

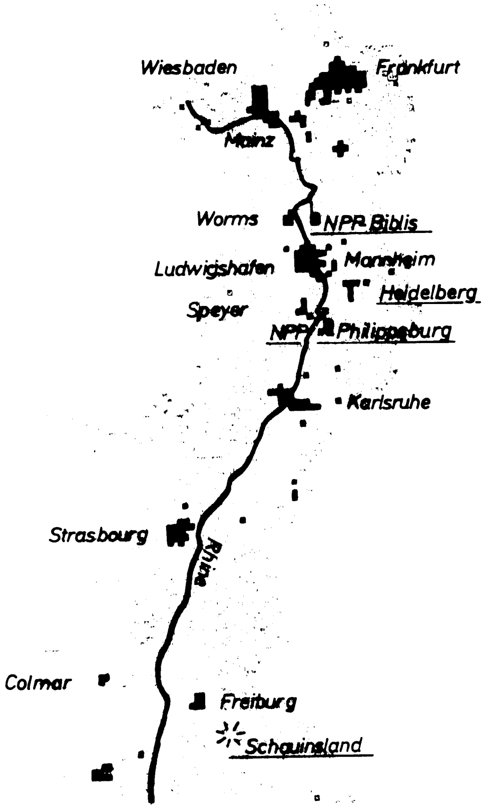

Fig 2. Sources of ^{14}C-free CO_2 from fossil-fuel combustion in the Rhine valley; shaded areas represent the homogeneously distributed smaller anthropogenic sources like villages, traffic, etc. Black areas indicate cities. Underlined names stand for sampling sites (modified from Bartholomäi and Kinzelbach, 1980).

reference level. The same winter depression is observed at the Environmental Physics Institute (Fig 1c), located on the outskirts of Heidelberg. Similar summer-winter variations were observed by Tans (1978) on the Smilde Drenthe radio tower station 100m above the ground (Netherlands). Tans interprets part of these variations as the result of pulsed stratospheric injections of natural and bomb ^{14}C. Unfortunately, there is only one year overlap with our Biblis and Heidelberg data. From the little corresponding 'clean-air' data that we have from Vermunt for 1975/76 we cannot distinguish any significant summer-winter variation. But as indicated before the slight seasonal ^{14}C variations in the period from 1977 to 1981 have no significant contribution from stratospheric ^{14}C injections.

Moreover, the summer maximum observed by Tans lies on the reference fit[3] of the mountain stations of southern Germany and Austria. The low winter values observed by Tans are in phase with those of Biblis and Heidelberg, but the amplitude is only ca 40% of the one in the Rhine valley. If the Tans minima are in fact due to fossil-fuel CO_2, the reduced amplitude might roughly represent the time fraction during which air masses originate from land, while the rest of the time, unpolluted air comes from the ocean.

ATMOSPHERIC SAMPLES FROM THE PHILIPPSBURG BOILING WATER REACTOR

The Philippsburg nuclear power plant is a BWR of about the same power production as each of the Biblis reactors. It is located at the Rhine river south of Mannheim and Ludwigshafen. Spot measurements in the reactor stacks of BWRs yielded source rates of 5-16Ci/GWa of ^{14}C emitted as $^{14}CO_2$, PWRs emit hydrocarbons at a rate of 3-11 Ci/GWa (Schwibach, Riedel, and Bretschneider, 1979).

The Philippsburg reactor stopped in May 1980, resuming operation in October 1981. It is now inoperative since May 1982. In 1980/81 we observed the same winter depression as in Biblis and Heidelberg. In spring 1980 and winter 1981/82 $^{14}CO_2$ levels were observed significantly above the reference line (see Fig. 1d). From November 1979 to May 1980 we found $\Delta^{14}C$ to be 10 to 130‰ higher than the level in the Rhine valley which is uninfluenced by the nuclear power plant. The mean value is $\Delta^{14}C=296\pm5$‰[1], that is 24‰ above the Rhine valley level and 14‰ above the 'clean-air' level. The highest ^{14}C activities (eg. $\Delta^{14}C=570$‰[1] in October 1981) occurred a short time before or a few days after operation. Perhaps the containment was flushed during these periods.

Using a Gaussian plume model with dispersion parameters of Vogt (1970), and the actual synoptic data from the Mannheim Weather Service station (Deutscher Wetterdienst, 1979-1982) we calculated dispersion factors at the sampling location for the periods when the reactor was running. Together with

---

[3] See footnote 1

the excessive Δ^{14}C levels of the two periods above, we have estimated the ^{14}C source strengths. The mean source strength for November 1979 to May 1980 was 16Ci/yr and 18Ci/yr for October 1981 to May 1982. The samples with highest ^{14}C levels indicated source strengths of up to 2Ci/week (≃100Ci/yr) during the sampling period. There are no published direct measurements of the source strength from stack samples of the Philippsburg reactor. Our results, however, fit the average source strength of boiling water reactors in western Germany quite well.

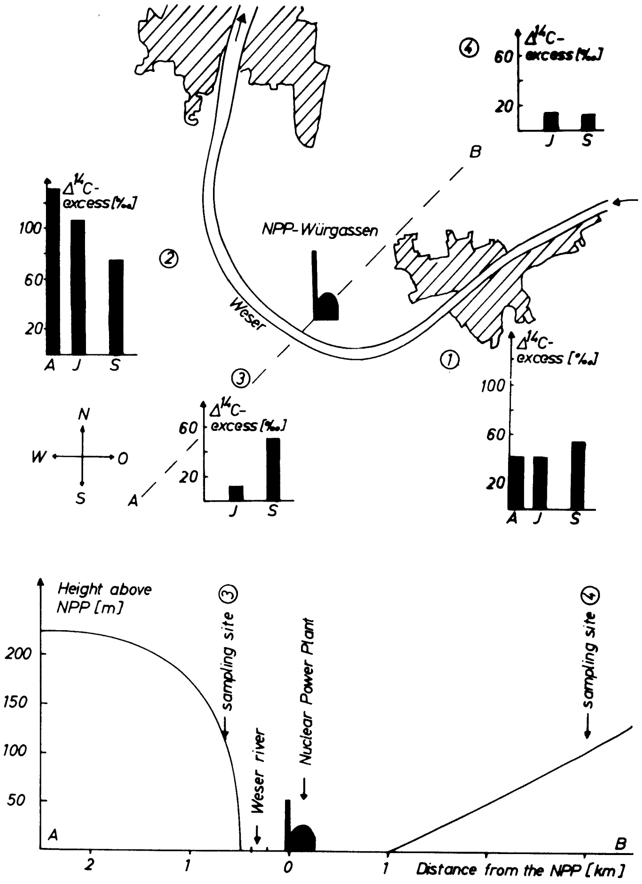

Fig 3. Top: geographic location map of the Würgassen NPP in the Weser valley. Diagrams 1-4 represent the observed Δ^{14}C excess over the 'clean-air' level in tree leaves collected at different times of 1981 at the corresponding sites (1-4). Bottom: topographic profile along line A - B (see top) illustrating hilly terrain.

PLANT SAMPLES FROM THE WÜRGASSEN NUCLEAR POWER PLANT

Würgassen is a BWR of 670MWe, in the Weser River valley of the northern part of western Germany near Kassel and Göttingen. Tree-leaf samples were collected at four sites around the reactor (Fig 3) in April, June, and September 1981; tree-ring samples were taken from trees at Sites 1 and 4. The greatest ^{14}C effects were expected at Site 1, the lowest at Site 4, because of the mean geostrophical wind direction from the west, and because ground-level wind is canalized by the valley (hills in the south and west of the river reach heights up to 250m). Atypically, there was a very stable weather pattern in April 1981, with constant winds from the east causing a strong ^{14}C increase in the leaves collected at Site 2 ($\Delta^{14}C_{excess}=130‰$, $\Delta^{14}C_{excess}$ = positive deviation from the 'clean-air' level). Leaves collected at Site 1 show only little excess, $\Delta^{14}C_{excess}=40‰$ (Fig 3). Although the situation changed

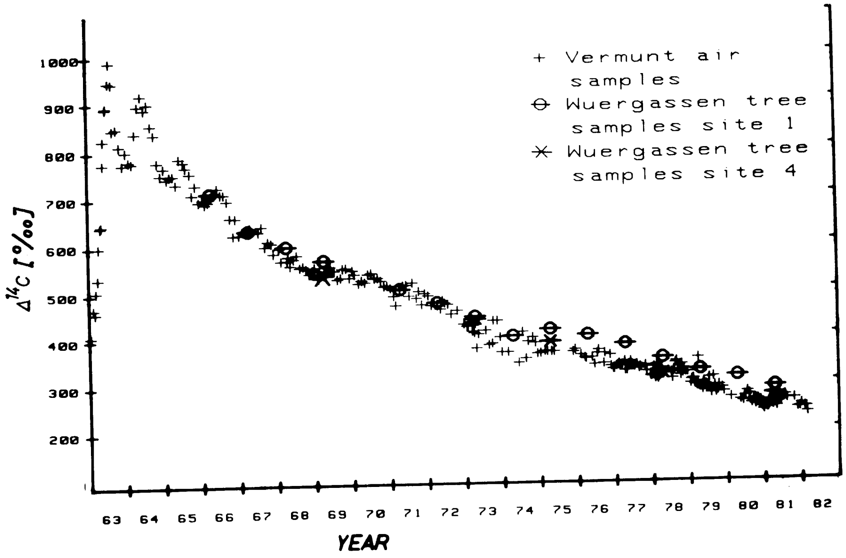

Fig 4. ^{14}C concentration of atmospheric CO_2 at Vermunt together with the tree-ring samples from trees felled near Würgassen NPP at Sites 1 and 4 (see map Fig 3).

due to 'normal' weather conditions with wind from the northwest, all tree leaves collected in the course of the vegetation period 1981 (in June and September) show only slight changes in ^{14}C content (decrease at Site 2, increase at Site 1).

Figure 4 shows the results of tree-ring measurements from Sites 1 and 4. The reactor has been operative since 1972. During this time, the tree-rings of Site 1 are generally ca 35‰ higher in $\Delta^{14}C$ than at Site 4, which shows nearly background concentrations (mean $\Delta^{14}C_{excess}$ =10‰).

Dispersion models are not as yet applicable to hilly terrain which prevents the calculation of source strengths from observed ^{14}C data. Nevertheless, our measurements do not indicate higher source strengths than expected for older type German BWRs (up to 20Ci/GWa).

COMPARISON OF INTERHEMISPHERIC MIXING DATA AS DERIVED FROM BOMB ^{14}C AND FROM ^{85}Kr

On the basis of nuclear test ^{14}C data Münnich and Vogel (1963) used a global diffusion model for deriving a relaxation time of ca 5 months for the lowest order sperical harmonic representing an interhemispheric atmospheric concentration difference. This corresponds to a hemispheric residence time of 10 months. Czeplak and Junge (1974) used a similar, but more sophisticated model and also reviewed all available data of other tracers. They concluded that ca 1 year was the most probable value for the hemispheric residence time.

Until recently, nuclear bomb ^{14}C provided the most reliable basis for estimating interhemispheric exchange. Since very accurate ^{85}Kr data are available (Weiss et al, in press) it is interesting to compare the respective results since bomb ^{14}C has its source primarily in the stratosphere while ^{85}Kr originates from fuel reprocessing at ground level. The meridional ^{85}Kr profiles show a significant concentration drop at the Intertropical Convergence, suggesting a slightly longer hemispheric residence time. However, the difference is not positively significant.

ACKNOWLEDGMENTS. This study is supported by the Federal Minister of the Interior, Bonn. We wish to thank B Becker, Hohenheim, for tree-ring identification and J Volpp for tree-ring and tree-leaf sampling in Würgassen, C Junghans for running the ^{13}C measurements, A Ebert, U Kühnel, C Picke, and M Rabbel for running the ^{14}C measurements. Special thanks are due the Departments of Radiation Protection of the Biblis and the Philippsburg nuclear power plants for their cooperation.

REFERENCES

Bartholomäi, G and Kinzelbach, W, 1980, Das Abwärmekataster Oberrheingebiet:Kernforschungszentrum Karlsruhe,KfK 2869 UF.

Czeplak, G and Junge, C, 1974, Studies of interhemispheric exchange in the troposphere by a diffusion model: Adv Geophysics, 18B,p57-72.

Deutscher Wetterdienst, 1979-1982, Europäischer Wetterbericht, Amtsblatt des DWD: Verlag Deutscher Wetterdienst.

Fry, FA, Dodd, NJ, Green, N, Major, RO, and Wilkins, Bt, 1981, Environmental radioactivity surveillance programme: Results for the UK for 1980, Natl Radiol Protection Bd, Chilton, Didcot, Oxon.

Kunz, CO, Mahoney, WE and Miller, TW, 1974, C-14 gaseous effluents from pressurized water reactors, in Health physics symposium on population exposures:Knoxville,Tennessee.

---- 1975, C-14 gaseous effluents from boiling water reactors, in Am Nuclear Soc ann mtg: New Orleans, Louisiana.

Levin, I, Münnich, KO, and Weiss, W, 1980, The effect of anthropogenic CO_2 and ^{14}C sources on the distribution of ^{14}C in the atmosphere, in Stuiver, M and Kra, RS, eds, Internatl ^{14}C conf, 10th, Proc: Radiocarbon, 22, no.2,p379-391.

Münnich, KO and Vogel, JC, 1963, Investigation of meridional transport in the troposphere by means of carbon-14 measurements, in Radioactive Dating, IAEA Vienna, Proc: STI/PUB/ 68, 189.

Schwibach, J, Riedel, H, and Bretschneider, J, 1979, Untersuchungen über die Emission von Kohlenstoff-14 Verbindungen aus grosstechnischen Anlagen: Inst Strahlenhygiene Bundesgesundheitsamt, StH-Bericht 20/79.

Tans, PP, (ms), 1978, Carbon-13 and carbon-14 in trees and the atmospheric CO_2 increase. PhD thesis, Univ Groningen.

Vogel, JC and Uhlitzsch, I, 1975, Carbon-14 as an indicator of CO_2 pollution in cities. Isotope ratios as pollutant source and behaviour: Vienna, IAEA symposium.

Vogt, KJ, 1970, Umweltkontamination und Strahlenbelastung durch radioaktive Abluft aus Kerntechnischen Anlagen: Kernforschungsanlage Jülich, Jül 637 St.

Weiss, W, Sittkus, A, Stockburger, H, Sartorius, H, and Münnich, KO, in press, Large-scale atmospheric mixing derived from meridional profiles of krypton-85: Jour Geophys Research, in press.

[Radiocarbon, Vol 25, No. 2, 1983, P 593-602]

THE USE OF ^{14}C IN NATURAL MATERIALS TO ESTABLISH THE AVERAGE GASEOUS DISPERSION PATTERNS OF RELEASES FROM NUCLEAR INSTALLATIONS

R L OTLET*, A J WALKER*, and H LONGLEY**

ABSTRACT. The Harwell Low Level measurements Laboratory has been measuring a variety of natural materials from locations close to United Kingdom nuclear installations since 1977. The measurements are made first, to establish the past effects of releases to the atmosphere of ^{14}C as observed from individual tree rings and second, to establish dispersion contours averaged over extended periods. The main study area has been in Cumbria, around the BNFL nuclear installation at Sellafield. ^{14}C, which can be measured to good precision even at values close to the normal natural levels, provides a powerful technique for the provision of practical experimental values much wanted for theoretical dispersion models.

INTRODUCTION

The many and varied applications of low-level ^{14}C measurements play an important role in a large number of research disciplines. The measurement technique has been developed to a very high standard to meet the demands of its original and major application, ^{14}C dating. For ^{14}C dates to be of value to an archaeologist, they must be made to a precision of at least ± 1% and this on levels well below those occurring naturally, i e below 6 pCi/g of carbon. With this precision, it is clear that levels only a few picocuries above natural can be easily detected and measured. We present here some new applications of particular relevance to the nuclear industry and, on a wider scale, the protection of the environment. Investigations were made by Harwell in the vicinity of the BNFL nuclear installation at Sellafield in collaboration with BNFL, the operators of the plant, and the Department of the Environment. The goal was to obtain data on gaseous dispersion patterns and the effect of releases of ^{14}C to the atmosphere.

*Low Level Measurements Laboratory, AERE, Harwell, Oxfordshire,
OX11 0RA, UK
**Environmental Section, British Nuclear Fuels Ltd, Sellafield,
Cumbria, CA20 1PF, UK

BACKGROUND AND EARLY WORK

The natural level of ^{14}C has been extensively studied in recent years (Vogel and Marais, 1971, Levin, Münnich, and Weiss, 1980; Barrette et al 1980) etc. Research began in Britain with Baxter, Ergin, and Walton (1969) and was continued by Harwell from 1971 onwards (fig 1).

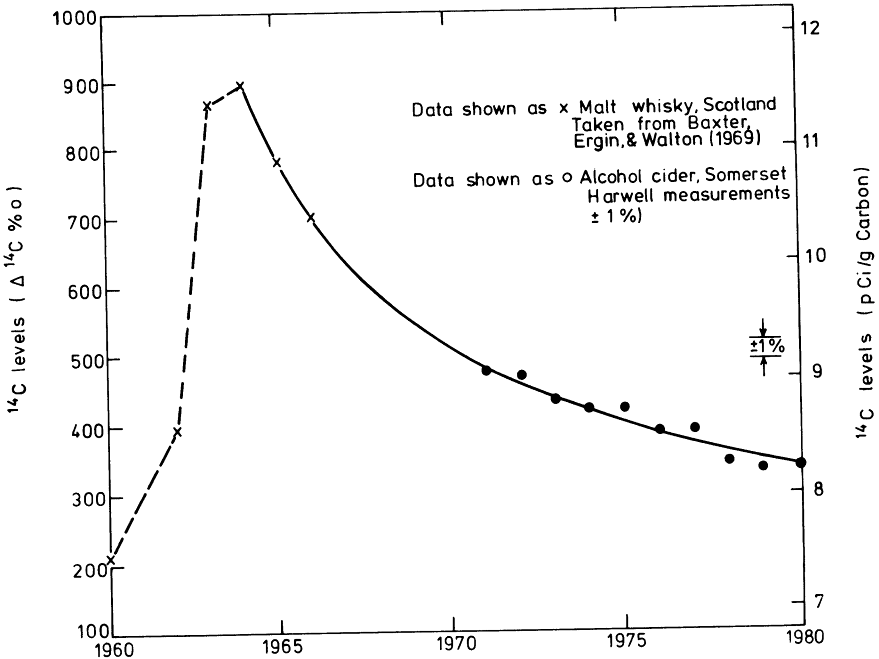

FIG 1. ^{14}C LEVELS IN ALCOHOL SINCE 1960 (UK)

The now familiar profile rises in 1963 to twice (ie ∿ 12 pCi/g carbon) the natural level which is close to the ^{14}C standard value (0.95 x NBS oxalic acid ^{14}C value of 6.16 pCi/g carbon equivalent to $\Delta^{14}C \pm 0^o/_{oo}$). The 1963 peak provides an important time-marker for a number of applications. The measurements were made on alcohol (malt whisky by Baxter, cider by Harwell) but supporting measurements were also made at Harwell on grain and sugar from various locations. In 1976, we began work on a monitoring survey of samples of milk, grain, and potatoes from local farms close to BNFL, Sellafield. Some results of these measurements averaged between 1976 and 1979 are given in table 1. They show levels above the northern hemisphere of figure 1 from locations close to the site and to a lesser extent at distances up to and beyond 10km.

TABLE 1. ^{14}C in foods

Distance from Sellafield (km)	^{14}C in foods (pCi/g^{-1} C)* Milk	Grain	Potatoes
up to 1	2.90	3.23	0.88
1 to 2	6.28	0.68	4.42
2 to 4	2.40	3.29	3.62
5 to 7	1.64	1.44	0.59
ca 30	0.25	0.22	-

* Averages calculated from available data of 1976 to 1979, after subtraction of the contribution due to global levels.

Although discernible by ^{14}C measuring techniques, these levels are insignificant in terms of radiation exposure to the public, ie < 0.2% of the dose-equivalent limit recommended for critical groups by ICRP (ICRP, 1977). Their importance in providing much needed experimental dispersion parameters was, however, realized and promoted the investigations reported here.

DEMONSTRATION OF CHRONOLOGIC RECONSTRUCTION

The first of these, the establishment of a chronology of emissions of ^{14}C from the site, began with individual tree-ring measurements on a sycamore felled in April, 1979 ca 3km NE of the site. The tree was a large sycamore, felled for road widening. A slice was taken through the trunk, from the butt end of the tree. It was not particularly circular, with major and minor diameters of ca 0.90m, respectively. The pith was almost centrally placed but the ring widths varied considerably around the whole circumference. A sector was chosen in which the rings were even and visible and ring widths increased from ca 1mm near the bark to ca 10mm at ring 30.

Annual measurements were made on the last 30 years' growth of the tree. The samples (∿ 15g dry wood from each ring) were pretreated using the standard 'AAA method' (acid-alkali-acid). Each sample was first boiled for 30 minutes in 3M $HC\ell$, backwashed to neutral, boiled for 30 minutes more in 1M NaOH and backwashed again. A final acid (3M $HC\ell$) wash removed any carbonates deposited in the sample from the tap water. The acid was washed out with distilled water. Supporting measurements were also made on cellulose but full details of these comparative results will be described elsewhere. Liquid scintillation counting techniques were employed using an optimum sample size of 6g C_6H_6. Samples were converted to C_6H_6 using the normal procedures of the laboratory and were processed in sequence starting with the bark and finishing with ring 30.

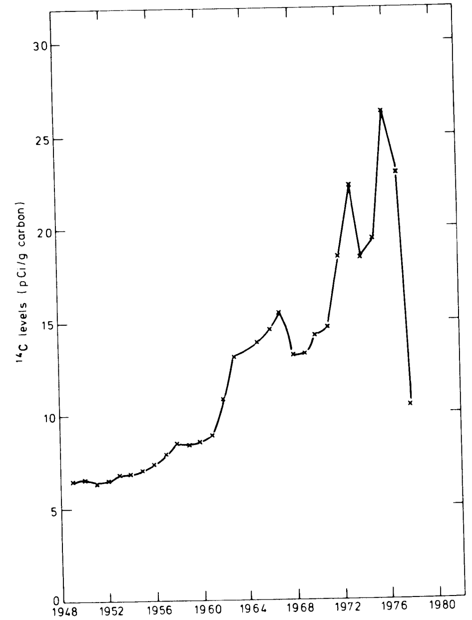

FIG 2 ^{14}C LEVELS FROM TREE RINGS OF A SYCAMORE TREE NEAR SELLAFIELD

Figure 2 presents absolute ^{14}C levels which include the contribution of the global average values. The initial rise between 1956 and 1963 is approximately coincident with the northern hemisphere average rise (fig 1) over the same period. The values from 1976 to 1978 are also broadly consistent with the values of ^{14}C in milk, potatoes and grain (table 1). The detailed structure of the profile probably relates to the nuclear fuel reprocessing programmes at BNFL, Sellafield. It is of interest to note that no significant variation can be attributed to the 1957 Windscale incident.

Following these preliminary measurements, we repeated the experiment using five trees from selected locations at increasing distances and different directions from the site. The results from annual measurements on these generally support the initial results but showed attenuation of the ^{14}C levels at greater distances.

The introduction of micro-sample (micro-counter) measurement facilities (Sayre et al, 1981) should greatly facilitate the tree ring measurement research. The two counter sizes require only 60mg and 10mg of carbon, respectively. The 60mg sample can be measured to ± 1% (counting statistics) in ca 10 days, and with simultaneous operations of a group of such counters, sample throughput need not be a problem.

The advantage of using miniature samples is that they can be obtained by boring and extracting a complete core from healthy living trees. Coring can be done without damage to the tree which facilitates the collection of suitable samples at required locations. Preliminary experiments using a 12mm core borer on a variety of tree species shows that the size of core from a healthy tree provides well-defined ring sections which are not difficult to isolate and of ample weight for the larger counter size (fig 3).

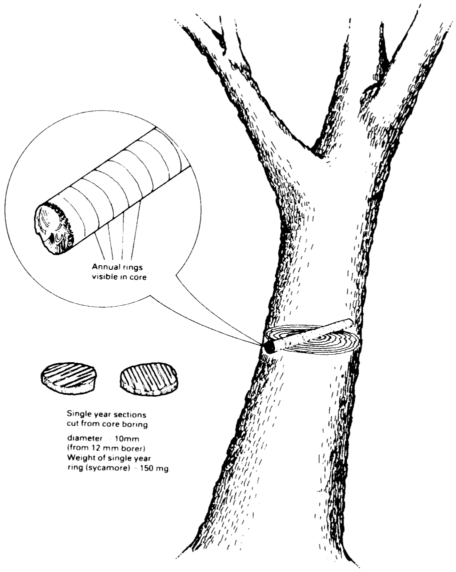

FIG 3 A CORE EXTRACTED FROM A BORING ACROSS A FULL DIAMETER AND ITS BREAK-UP INTO ANNUAL SECTIONS

These tree-ring methods can provide simultaneous chronologic and dispersion information. However, at the study site, the problem of obtaining trees even suitable for the microcounter severely limited the possibility of finding full spatial dispersion data quickly. Thus, we sought a different type of environmental material for this purpose.

DEMONSTRATION OF GASEOUS DISPERSION PATTERNS

Advice was sought from the Department of Forestry, Oxford on the most suitable material for this study. A number of criteria had to be satisfied: 1) the material should be truly representative of a single years growth; 2) it should be readily available throughout the area; 3) it should grow for a period long enough to provide an average of wind and weather patterns, and 4) it should occur naturally rather than being planted and tended for the experiment. We were advised that fruit would be better than grass, fresh shoots or leaves. The growth period of grass is short and difficult to prove even at all sampling points. New shoots are difficult to identify later in the year and are known to be produced partly from carbohydrate stored in the tree from the previous year (Kramer and Kozlowski, 1960). Leaves of a tree species found widespread in the area seemed more suitable and have been used successfully for this type of application. However, as with shoots, the first leaves of the season are made from the previous years' carbohydrate and only when photosynthesis has been active for some time can the leaves be certainly attributed to that year. Thus, we decided to use a fruit since it fits all the criteria and appeared to have no intrinsic problems.

Extensive research on the apple has shown (E Reynolds, (pers comm) that it is produced solely from photo-synthesis in the surrounding leaves. In the area under study, the hawthorn (Crataegus Monogyna) which belongs to the apple family is ubiquitous and was therefore selected.

The first samples of hawthorn berries were collected in October, 1981 at 32 sites, 31 in the study area (fig 4) and 1 in Yorkshire, 110km away, as a control.

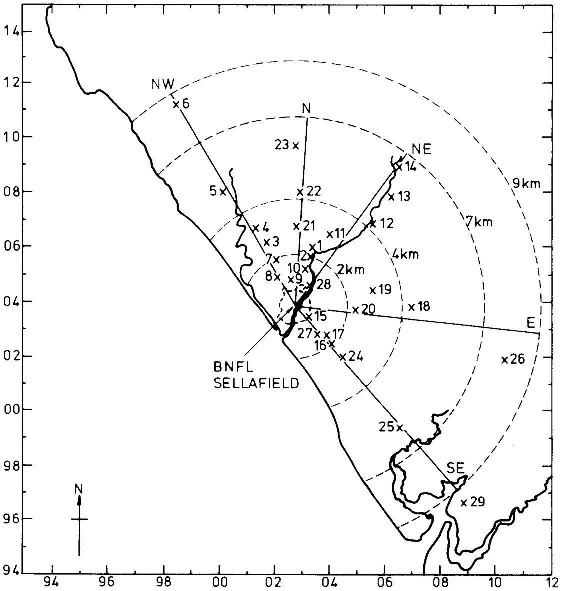

FIG 4. HAWTHORN BERRY SAMPLING SITES, OCTOBER 1981

The sites were located along 5 transects radiating inland from the site along different compass directions. The three major transects, along each of which 6 to 8 samples were collected, lay at approximately NE, NW and SE'ly directions. The two minor transects, lying N and E provided 4 more samples each. For each sample, ca 200g of ripe hawthorn berries were collected. Pretreatment consisted of removing stems and leaves, washing, boiling in acid, washing again in distilled water and drying in a hot cupboard. The process produced 40 to 50g of dry weight; 17g of this produced ∿ 12 STP 1 of CO_2 which provided 6g of benzene for liquid scintillation counting.

Figure 5 shows preliminary results of the first sampling, in which the ^{14}C levels, expressed as picocuries ^{14}C/g of carbon minus the expected global levels, are plotted as a function of distance from Sellafield. The individual transects are identified by lines hand-drawn through the relevant experimental points. These lines indicate the dilution along each of the transects, from which the two-dimensional pattern of dispersion can be derived. Thus, these measurements provide an opportunity to study the actual dispersion of ^{14}C around Sellafield, to compare the observed concentrations with those predicted from theoretical dispersion models (eg Clarke, 1979), and to consider the effects of local topography and meteorology. These further studies are now in hand.

We have observed that all the lines show a reduction of ^{14}C concentration with distance from Sellafield, but the concentration gradient varies for different directions and the spatial dispersion of ^{14}C appears to be non-uniform.

Similar dispersion patterns are observed for the N, NE and E transects. However, the lines are considerably different for the NW and SE transects which show lower concentrations of ^{14}C and very different concentration gradients. The highest concentrations are seen on the NE transect, and are ca 5 times those of the NW transect. Figure 5 shows that the NW and SE transects are approximately parallel to the coast and 1 to 2km inland; in general, the sampling points are at lower elevations than those on the N, NE and E transects. The ^{14}C concentrations on the NW transects are about half those on the SE transect. Thus, it seems that both topography and proximity to the sea appear to be influencing the dispersion pattern. Directional dispersion is affected by the average wind vectors during the growing season, but this does not account for the differences observed.

CONCLUSIONS

Both experiments provide basic data for more detailed analysis and interpretation. They indicate the importance of low-level ^{14}C measurements on natural materials in providing

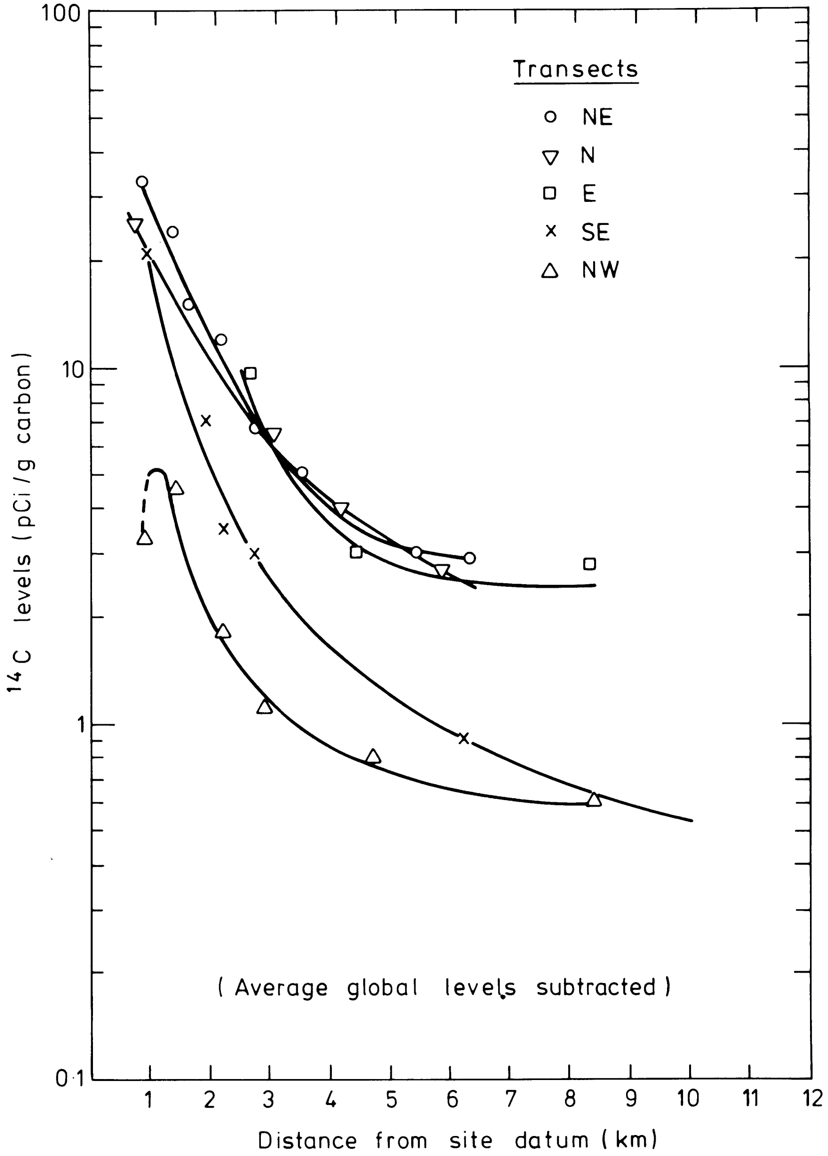

FIG 5. PRELIMINARY DISPERSION PATTERN DATA FOR 5 TRANSECTS OF THE 1981 HAWTHORN BERRY SURVEY

data that would be difficult to collect by physical instrumentation. The difficulties of setting up and tending instruments at 31 sites for several months are considerable.

Since not enough is known of the rate of carbon uptake of natural materials during growth, we plan to investigate this problem. Direct air sample measurements are also being made to determine the relation of air concentration to plant uptake. With the data on the dispersion parameters for specific sites, this relationship will correlate the ^{14}C tree-ring data to chronologic discharges from Sellafield.

Further, these ^{14}C measurements will help to assess the past and present environmental impact of ^{14}C discharges on the radiation exposure of the public, since ^{14}C levels in locally grown foods will be similar to those recorded in tree-rings and hawthorn berries. The studies will also refine our knowledge of the effects of ^{14}C emissions even though observed levels are low and represent only a small fraction of the ICRP dose limit for the public. Although much more research is needed, these initial measurements make a valuable contribution to the nuclear power industry in providing the first experimentally determined dispersion data for ^{14}C.

ACKNOWLEDGMENTS

The financial support of the Department of the Environment, British Nuclear Fuels Ltd, and the Atomic Energy Research Establishment, Harwell is gratefully acknowledged. This research is conducted by agreement with these agencies and is part of a comprehensive study of radioactive materials in the Cumbrian environment.

REFERENCES

Barrette, L, Lasalle, P, Martel, Y, and Samson, C, 1980, Variations of ^{14}C in oats grown from 1957 to 1978 in Quebec, in Stuiver, M and Kra, RS, eds, Internatl ^{14}C Conf, 10th, Proc: Radiocarbon, v22, no. 2, p 410-414.

Baxter, MS, Ergin, M, and Walton, A, 1969, Glasgow university radiocarbon measurements I: Radiocarbon, v 11, p 43-52.

Clarke, RH, 1979, A model for short and medium range dispersion of radionuclides released to the atmosphere: NRPB-R91, London HMSO, Nat Radiol Protection Bd

ICRP Pub 26, 1977, Internatl Comm on Radiol Protection, Annals of the ICRP, v 1, no. 3.

Kramer, PJ and Kozlowski, TT, 1960, Physiology of trees: New York, McGraw-Hill Book Co, p 150-159.

Levin, I, Münnich, KO, and Weiss, W, 1980, The effect of anthropogenic CO_2 and ^{14}C sources on the distribution of ^{14}C in the atmosphere, in Stuiver, M and Kra, RS, eds, Internatl ^{14}C Conf, 10th, Proc: Radiocarbon, v 22, no. 2, p 379-391.

Sayre, EV, Harbottle, G, Stoenner, RW, Otlet, RL, and Evans, GV, 1981, The use of small gas proportional counters for the carbon-14 measurement of very small samples, in Methods of low level counting and spectrometry: Vienna, IAEA, p 393-408.

Vogel, JC and Marais, M, 1971, Pretoria radiocarbon dates I: Radiocarbon, v 13, p 378-399.

[Radiocarbon, Vol 25, No. 2, 1983, P 603-614]

ON THE ORIGIN OF CARBONACEOUS PARTICLES IN AMERICAN CITIES: RESULTS OF RADIOCARBON "DATING" AND CHEMICAL CHARACTERIZATION[1]

L A Currie[2], G A Klouda[2], R E Continetti[2],
I R Kaplan[3], W W Wong[3],
T G Dzubay[4], and R K Stevens[4]

ABSTRACT. During the past three years radiocarbon assay has emerged as a primary tool in the quantitative assignment of sources of urban and rural particulate pollution. Its use in several major field studies has come about because of its excellent (fossil/biogenic) discriminating power, because of advances in ^{14}C measurements of small samples, and because of the increased significance of carbonaceous particles in the atmosphere. The problem is especially important in the cities, where increased concentrations of fine particles lead to pollution episodes characterized by poor visibility and changes in the radiation balance (absorption, scattering), and immediate and possibly long-term health effects. Efforts in source apportionment in such affected areas have been based on emissions inventories, dispersion modeling, and receptor modeling — ie, chemical and physical (and statistical) characterization of particles collected at designated receptor sites. It is in the last category that ^{14}C has become quite effective in helping to resolve particle sources. Results are presented for studies carried out in Los Angeles, Denver, and Houston which incorporated ^{14}C measurements, inorganic and organic chemical characterization, and receptor modeling. The ^{14}C data indicated wide ranging contributions of biogenic and fossil carbon sources — eg, <10% to 60% contemporary (biogenic) in Houston — depending on meteorological, biological, and anthropological activity. The combined (chemical, isotopic, statistical) data point to sources such as vehicles, wood combustion, power plants, and vegetation.

INTRODUCTION

Measurements of ^{14}C, and to a lesser extent, ^{13}C have been utilized during recent years to define the origin of carbonaceous species in the atmosphere (Currie, Klouda and

---

[1] Contribution of the National Bureau of Standards; not subject to copyright

[2] Center for Analytical Chemistry, National Bureau of Standards, Washington, DC 20234

[3] Global Geochemistry Corporation, Canoga Park, CA 91303

[4] Environmental Sciences Research Laboratory, US Environmental Protection Agency, Research Triangle Park, NC 27711

Cooper, 1980; Currie and Klouda, 1982; Polach and Ferrari, 1982). Carbonaceous particles, especially black "soot" (Rosen et al, 1980), are of special concern because of their significant effects on visibility, atmospheric heating, and health (Novakov, 1978; Wolff and Klimisch, 1982), the health effects being connected with inhalable particles and associated polycyclic aromatic hydrocarbons (Kaden and Thilly, 1978). ^{14}C measurements are becoming broadly applied to atmospheric particulate studies because ^{14}C serves as a unique tracer for biogenic carbon and because of the development of counting systems capable of measuring small samples — 5 to 10 mg-carbon (Currie and Murphy, 1977; Sayre et al, 1981). Early applications of the technique surveyed urban and rural areas to ascertain the relative significance of fossil and vegetative carbon sources (Currie et al, 1978). Subsequently, a practical application demonstrated the impact of vegetative burning — field, slash, residential wood — on the particulate burden in Portland, Oregon (Currie, Klouda and Cooper, 1980). The increased popularity of wood stoves has led to still further demand for ^{14}C measurements of wintertime ambient particles in populated areas (Cooper and Malek, 1981).

The studies reported below go beyond the simple measurement of ^{14}C to assess the fossil carbon fraction in total ambient particles. Our objective now includes the quantitative apportionment of all (major) carbonaceous sources in a given sampling region. This requires: (1) accurate measurement of ^{14}C in individual chemical and size fractions, often corresponding to submilligram quantities of carbon, (2) accurate trace element and organic analysis of atmospheric particles, and (3) accurate evaluation of multidimensional (chemical, isotopic) analytical data for individual source contributions. We are meeting the first requirement for samples containing as little as 100 μg-C by means of Accelerator Mass Spectrometry (AMS), in cooperation with the Univ of Arizona. A critical element in meeting the second is the use of urban particulate Standard Reference Materials (SRM's 1648 and 1649), for example, in connection with our recent AMS measurements, and for the assessment of analytical methods for elemental and organic carbon (Groblicki et al, 1982). Finally, the accuracy and sensitivity of source apportionment methods (chemical mass balance, factor analysis) applied to the full Houston data set were evaluated by a receptor modeling exercise, in which we used computer simulation to prepare reference sets of data having known model and random error structure. One outcome was a quantitative indication of the improvement in source resolving power which comes when observations include both ^{14}C and chemical characterization (Currie, Gerlach and Lewis, ms).

REVIEW OF URBAN STUDIES

LOS ANGELES — AN EXPLORATORY INVESTIGATION. Samples were collected during 1978–79 by I R Kaplan at a receptor site atop the City of Hope hospital (COH) in Duarte, CA in connection with the development of a comprehensive scheme of analysis by particle size and organic and inorganic composition of urban ambient aerosols (Brenner et al, 1980). The site is located in the foothills of the San Gabriel Valley where photochemical smog is often intense. It lies northeast of downtown Los Angeles (LA) and south of the vegetation of the Angeles National Forest. The normal wind pattern at COH during the day indicates a continuous flow from LA, toward the northeast. At night, wind from the north adds biogenic input from the vegetation on the San Gabriel Mountains.

Detailed organic analysis, which included extraction with a series of organic and aqueous solvents followed by chromatographic and spectroscopic measurements, was feasible because of the use of the Battelle Megavolume Sampler (Mitchell et al, ms). This device collects aerosol particles in three size ranges (<1.7 µm, 1.7-3.5 µm, and >3.5 µm), and at high flow rates (19 m^3/min) by impaction followed by electrostatic precipitation. With several days sampling, gram quantities of aerosol could be collected. Besides the separation and measurement of organic constituents (carboxylic acids, polynuclear aromatic hydrocarbons, n-alkanes, ...), anions and metals, the aerosol was analyzed directly for carbon, hydrogen, nitrogen, electron spin density, $^{13}C/^{12}C$, and $^{14}C/^{12}C$. The distribution of certain homologous series of organic compounds, the high spin densities, $\delta^{13}C$, and the finding from ^{14}C measurements that only about half the non-carbonate aerosol was fossil, all indicated that a substantial part of the aerosol was biogenic, in addition to the expected anthropogenic material (Brenner et al, 1980).

Data highlights are given in Table 1 and Figure 1. The ^{14}C results, for a sample collected from Aug 31 to Sept 5, 1979 (140 m^3-air), are of some importance because they give the only quantitative measure for the biogenic contribution. Also, they demonstrate the dependence of this contribution on particle size. It is noteworthy that we used both miniature gas counting and accelerator mass spectrometry to obtain the ^{14}C data, the latter at the University of Arizona tandem with ∿50 µg and 500 µg carbon samples. The chromatogram of aromatic compounds (Fig 1A) illustrates the separation that was achieved and provides abundance patterns which may lend insight as to combustion sources and toxicological properties (Novakov, 1978). The pattern for n-alkanes (Fig 1B) supports

TABLE 1. ESR and isotopic carbon data — Los Angeles aerosol

Particle size (μm)	Color	Spins/g	^{14}C (f_c)*	^{13}C ($\delta^{13}C_{PDB}$)
<1.7	Black	3.8×10^{19}	0.52±0.05	
1.7-3.5	Dark Gray	8.2×10^{19}	0.57±0.04	-25.9‰**
>3.5	Light Gray	7.5×10^{19}	0.85±0.03	

*Fraction contemporary carbon, assuming a correction factor of 1.30 for the increase in biospheric ^{14}C due to nuclear testing (standard error based on Poisson counting statistics)

**$\delta^{13}C_{PDB}$, which is the deviation in parts per thousand from the Pee Dee Belemnite standard, is given as an average value over all size fractions, determined from acid-washed samples

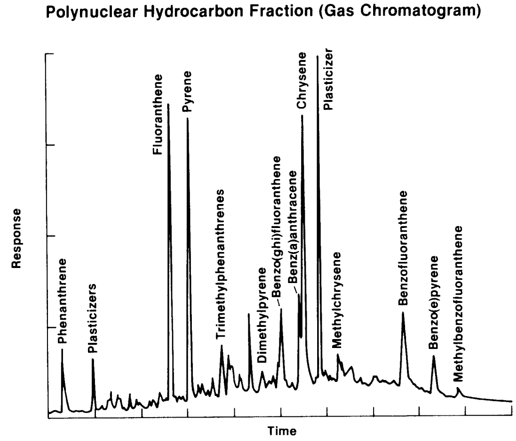

Fig 1A. Gas chromatogram of polynuclear aromatic hydrocarbons (DMSO extract). Los Angeles aerosol.

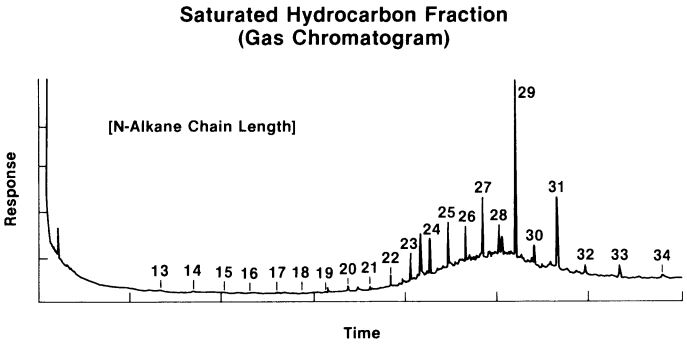

Fig 1B. Gas chromatogram of saturated hydrocarbon fraction, LA aerosol (carbon-chain lengths for n-alkanes are shown).

the ^{14}C data in that, (1) the large hump of branched cyclic hydrocarbons in the C_{22} - C_{33} region of the chromatogram indicates fossil emissions, and (2) the distinctive odd-even pattern of straight-chain hydrocarbons indicates vegetative material (plant wax derivatives). Biogenic sources were also reflected by predominantly even-carbon fatty acids, camphor, phorone, and the tri-isoprenoid structure in the trimethylpentadecanone. Complementing these studies of the COH ambient aerosol were measurements on source aerosol, coal fly ash whose chromatogram, unlike Fig 1B, showed a large hump of unresolved mixture in the $\underline{n}$-C_{13}-$\underline{n}$-C_{21} region, a small hump between $\underline{n}$-C_{22}-$\underline{n}$-C_{29}, and a distinct pattern of $\underline{n}$-alkanes with maxima at $\underline{n}$-C_{17}-$\underline{n}$-C_{20}. (See Eganhouse, Simoneit and Kaplan, 1981 for a concise discussion of molecular characterization of fossil/biogenic sources of urban organic pollution.)

DENVER — THE "BROWN CLOUD". An extensive field study of the nature and sources of the particulate pollution that envelops Denver, Colorado each winter was made recently under the technical direction of the General Motors Research (GMRL) Laboratory (Heisler et al, 1980). It took place over a period of 40 days during Nov and Dec , 1978, and involved monitoring of chemical and physical properties of aerosols, emissions inventories, source studies, and both dispersion and receptor modeling. ^{14}C was the only direct means to estimate the residential wood-burning component and for the first time, was assayed as a function of both temporal regime (weekday, weekend, level of pollution) and organic compound volatility. The latter was specially directed at identifying the sources of elemental, combustion carbon. (This component is of some concern because of its presumed influence on atmospheric temperature and health, and its catalytic properties leading to acid sulfates (Novakov, 1978; Wolff and Klimisch, 1982).)

Samples were collected at the GMRL site, 8 km northeast of downtown Denver. During the sampling period Denver experienced an air pollution alert (Dec 18-19, 1978) the proximate contaminant of which was CO. For 4 days the total suspended particulate (TSP) secondary standard (150 $\mu g/m^3$) was exceeded. On the average, during the 40 day period, carbon comprised 20% of the TSP mass and 36% of the fine (<2.5 μm) particle mass; 42% of the carbon was elemental, and most of this (∿80%) occurred in the fine particle mode.

Table 2 shows results for ^{14}C measurements ordered according to decreasing particulate air pollution. It is clear from this table and figure 2 that the relative importance of fossil sources increased significantly with increasing levels of pollution, accounting for essentially all of the carbon during

TABLE 2. Radiocarbon in Denver winter aerosol*

Sample No.	Conditions	Mass-C (mg)	Percent volatile-C	C-concentration (μg/m^3)	Contemporary** carbon (%)
9	High pollution (P)	23.9	45	78	11±3
7	-3 °C	16.4	54	49	29±7
4 [5]†	Weekday (WD)	20.7	54	46	26±5 [14±5]†
2 [3]	Weekend (WE)	12.3	55	32	35±8 [24±6]
8	-20 °C	11.1	--	17	38±5
6	Clean air (U)	9.8	70	8	39±8
1 (composite) [C]	---	17.7	55	47	37±4 [25±5]
10 (fine fraction, <2.5μm)	---	5.6	50	--	58±12
Blank -glass	---	0.67	97	--	---
Blank -quartz	---	0.37	--	--	93±8

* All samples were total suspended particulate, except No. 10

**Percent of "modern carbon," divided by 1.3 to correct for the excess bomb ^{14}C in living matter

† Percent of contemporary carbon in the non-volatile ("elemental") fraction is given in brackets. The elemental component in each case is shifted toward fossil carbon. "Organic" (volatile) carbon is necessarily more biogenic — corresponding to 55±21% for the weekday sample, for example

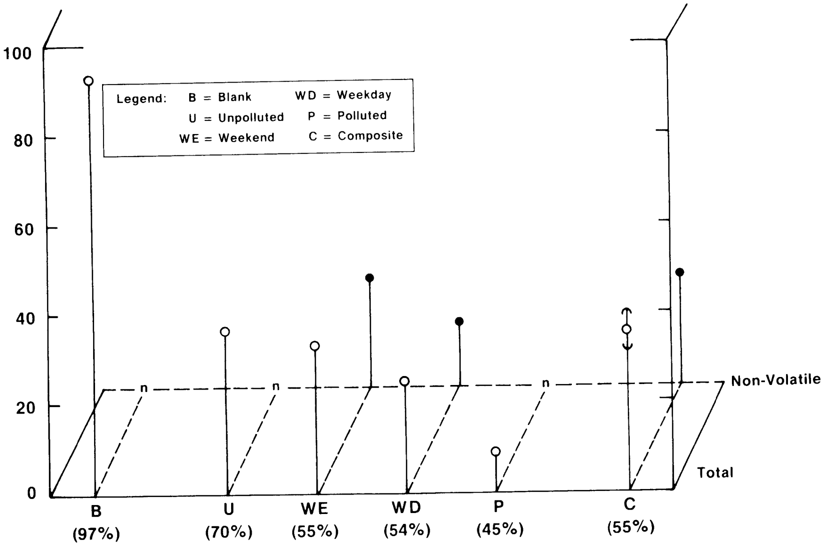

Fig 2. Contemporary carbon in the Denver aerosol vs pollution level for total and non-volatile carbon. Also shown are a filter blank (B) and composite (C) with its Poisson error. Percent of volatile carbon is shown (in parentheses) at the bottom of the figure (n=no sample).

the worst episode. The relative amount of elemental (non-volatile) carbon followed the same pattern (4th column of the table); and ^{14}C measurements of the separate chemical fractions of the particles in each case showed a significant shift of the elemental carbon fraction toward fossil carbon. In fact, during the weekday period of only moderate pollution, practically all (80–90%) of the elemental carbon was fossil in origin.

By contrast, the data indicate that weekends, especially cold periods, and "organic" (volatile) carbon have a greater proportion of biogenic carbon. Based on our ^{14}C data for a composite sample (No. 1), and appropriate source data, Wolff _et al_ (1981) concluded that the biogenic source was wood-burning, and that it contributed some 12% of the fine particle mass. (For comparison, auto exhaust was responsible for 18% of the fine particle mass; coal combustion, 20%; and crustal dust, 12%.) Carbonaceous particles, which constituted _ca_ 1/3 of the mass of all fine particles were deemed responsible for _ca_ 1/2 of the visibility reduction associated with the "brown cloud." Wood-burning, in turn, was concluded to be the major contributor to this impairment in Denver's visibility. Receptor modeling approaches including diurnal and weekend/weekday variations in such species as Pb (a motor vehicle tracer) and K/Fe (an indirect wood burning tracer) have lent semiquantitative support to the importance of motor vehicles during commuting periods and wood burning during nights and weekends (Courtney _et al_, ms). The fact that particles arising from the combustion of wood are predominantly in the fine particle fraction ($\sim$90%) is consistent with the maximum in the fine particle carbon mass reported for the evening sampling periods (Countess _et al_, 1981) and with the large fraction of contemporary carbon found in our sample No. 10 (<2.5 μm particles). The most severe carbon pollution, however, cannot be ascribed to wood-burning, because of the near absence of ^{14}C (sample No. 9) and because the wood-burning CO emission factor is too small to account for a significant portion of the observed CO (Courtney _et al_, ms).

HOUSTON. A second major urban field study was organized by the Environmental Sciences Research Laboratory of the US Environmental Protection Agency. Sampling took place during a one week period in Sept. 1980, with size fractionated atmospheric particles being collected simultaneously in 5 samplers operating on 12 hour cycles at a receptor site on the University of Houston campus. The objects of the study were to evaluate chemical species responsible for visibility reduction, and to apportion aerosol sources on the basis of the variability patterns and "chemical [and isotopic] fingerprints" observed in the ambient aerosol. To this end, measurements were made of visual range, aerosol concentration, and size distribution; particles were characterized by optical and electron microscopy and x-ray diffraction; and some 19 elements, 4 ions (H^+, NH_4^+, NO_3^-, $SO_4^=$), 3 gases (O_3, NO, NO_2), and one isotope ratio ($^{14}C/^{12}C$) were measured routinely.

Results of the visibility study indicated that fine particle carbon ("soot") was responsible for 17-24% of the daytime light extinction coefficient, with the bulk of the remainder due to sulfate (and associated cations) and water (Dzubay et al, 1982). The average fine fraction mass ($\sim$42 μg/m^3) was also dominated by sulfate and carbon; the coarse particle mass ($\sim$27 μg/m^3), by crustal components and carbon (see Fig 3).

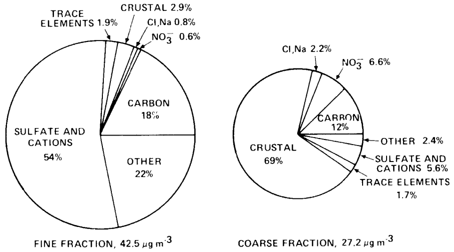

Fig 3. Eight-day average of Houston daytime fine and coarse aerosol masses apportioned by chemical species. (Sept 11 to 19, 1980).

Unlike the prior studies, the Houston study was designed from the start to collect a full set of fine particle samples for ^{14}C assay. This was useful, because apportionment of carbonaceous sources on the basis of ambient variability and elemental composition alone is very difficult. Traditionally, source deconvolution has rested heavily on trace elements, yet these comprise only a small fraction ($\lesssim$2%) of the ambient particle mass (Fig 3). Also, collinearity and variability of trace element source profiles cause serious error amplification. Quantitative investigation of these issues as well as source apportionment results for the Houston data were treated in depth at the 1982 Quail Roost II Workshop on Receptor Modeling (Stevens, 1983). Among the most important outcomes were the need to: (1) define compatible source classes and obtain receptor compatible source signatures; and (2) utilize isotopic, diffraction and microscopic data to verify the "statistical" source deconvolution results. Also, it was found that the number of resolvable source classes ranged from ca 10 to 20 with interlaboratory (modeling) differences ranging from 20% to 50%.

Figure 4 shows the ^{14}C data which provided direct information on the fine carbonaceous aerosol, plus some of the most pertinent elemental data. ^{14}C measurements, made with

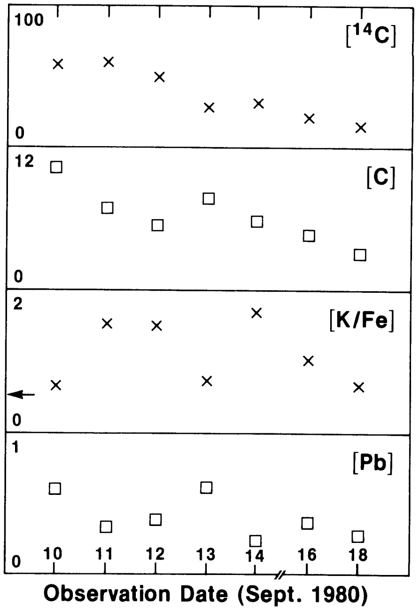

Fig 4. Receptor data for Houston fine particle aerosol. Time record is given for ^{14}C (percent contemporary), total carbon, K/Fe (vegetation marker), and Pb (auto marker). Arrow (K/Fe) indicates approximate crustal ratio. (Units for C, Pb are μg/m^3.)

miniature gas proportional counters at NBS, were obtained from 5 to 18 mg (carbon) samples collected on pre-fired type 2500 QAST Pallflex quartz filters. In both Denver and Houston contemporary carbon accounted for about ca 1/3 of the total carbon on the average, and the major portion of the carbon was volatile (>80% in Houston). However, the average (carbon) pollution levels and the ^{14}C trends with those levels were very different. The Houston carbonaceous aerosol concentration (median ∿6 μg/m^3) was about seven times smaller than that of Denver, and the biogenic fraction decreased with decreasing pollution, rather than the converse. For the Houston aerosol sampled, therefore, the ^{14}C observations stimulate the search for a significant source of contemporary carbon during the period of higher pollution. This is one of the most important outcomes of the study, because the trace element receptor modeling is insufficiently precise or direct to lead to the discovery of an unanticipated source of biogenic carbon.

The elemental data are supportive, however. Lead (Pb) is useful for indicating auto-exhaust carbon, and the ratio K/Fe is a qualitative indicator of vegetative carbon when it exceeds the crustal ratio of ca 0.5 (Core and Terraglio, 1978; Countess et al, 1981). Viewing the data (Fig 4) in four-space demonstrates an interesting feature: a discontinuity in each of the temporal trends occurs on Saturday, Sept 13. Although C (μg/m^3) increased, the fraction of contemporary carbon dropped sharply, while Pb increased and K/Fe decreased. The overall pattern is thus consistent with an injection of fossil fuel (automotive) carbon together with a decrease in vegetative carbon, possibly due to altered weekend activities and/or wind patterns. Several potential sources of the contemporary carbon aerosol have been suggested, such as long-range transport of the fine carbon aerosol, botanical emissions, agricultural burning, municipal incineration, etc.

CONCLUSION

Our survey of three cities shows that: (1) both fossil and biogenic carbon make significant contributions to the carbonaceous urban aerosol, (2) there are many variables involved in fixing the ^{14}C concentration, so an "average", TSP ^{14}C/^{12}C ratio for a given locale gives limited information, per se, and (3) miniature gas proportional counting systems can play a useful role in regional field studies for sample sizes down to 5 mg-C. Radiocarbon, being a direct and robust tracer for biogenic carbon, provides information otherwise unobtainable — because of basic uncertainties associated with both dispersion and receptor modeling. As we saw in the earlier study of radiocarbon in the Portland aerosol (Currie, Klouda and Cooper, 1980), contemporary carbon is not necessarily all natural in origin. Man's activities, especially the burning of vegetation, can make a substantial contribution to this fraction.

Further progress in understanding the distribution (sources, transport, sinks) of carbonaceous species in the atmosphere will depend on continued monitoring of the fine particle aerosol together with careful attention to modeling, standards, and selective radiocarbon (organic) chemistry. One of the most important new tools for high resolution atmospheric ^{14}C data is Accelerator Mass Spectrometry (AMS). With the capability of measuring submilligram samples, one can more readily search for ^{14}C fine structure such as we saw in Los Angeles (particle size), Denver (chemical form) and Houston (temporal variations). In view of this, we have just completed exploratory AMS measurements (in cooperation with the University of Arizona) of ^{14}C in a specific chemical fraction of SRM-1649 together with urban and rural ambient samples containing as little as ca 100 μg-carbon.

ACKNOWLEDGMENT

R W Gerlach and G Tompkins made substantial contributions to the program at NBS. AMS measurements (Univ of Arizona) were made possible through the cooperation of D Donahue, T Jull, and T Zabel. Denver samples were provided by R J Countess (now at Environmental Research at Technology, Inc) and laboratory assistance came from D P Stroup through the courtesy of G T Wolff (GM Research Labs). Work at NBS was supported through NBS funds and the Energy-Environment Program (EPA-IAG-D6-E684), US Environmental Protection Agency. The work at Global Geochemistry Corp (Los Angeles study) was sponsored by the Electric Power Research Institute, Inc. Use of product names does not imply endorsement by NBS.

REFERENCES

Brenner, S, Brewer, RL, Kaplan, IP, Wong, WW, 1980, Collection and analysis of organic and inorganic components in particulates and volatiles in the Southern California air basin. final report, submitted to the Electric Power Research Inst.

Cooper, JA and Malek, D, ed, 1981, Residential solid fuels, Oregon Graduate Center, Portland.

Core, JE and Terraglio, FP, 1978, Field and slash burning particulate characterization: the search for unique natural tracers: Air Pollution Control Assoc report.

Countess, RJ, Cadle, SH, Groblicki, PJ and Wolff, GT, 1981, Chemical analysis of size-segregated samples of Denver's ambient particulate, J Air Pollution Control Assoc, v 31, p 247.

Courtney, WS, Tesch, JW, Russworm, GM, Stevens, RK and Dzubay, TG, 1980, Characterization of the Denver aerosol between December 1978 and December 1979, Air Pollution Control Assoc, Paper 80-58.1 (Montreal meeting).

Currie, LA, Gerlach, RW, and Lewis, CW, 1982, The aerosol simulation data set, in Stevens, RK, ed, Receptor Modeling Workshop — Quail Roost II, US Environmental Protection Agency, ms.

Currie, LA, Klouda, GA and Cooper, JA, 1980, Mini-radiocarbon measurements, chemical selectivity, and the impact of man on environmental pollution and climate, in Stuiver, Minze and Kra, Renee, eds, Internatl Radiocarbon Conf, 10th, Proc: Radiocarbon, v 22, p 349-362.

Currie, LA and Klouda, GA, 1982, Counters, accelerators and chemistry in Nuclear and Chemical Dating Techniques, Currie, LA, ed, ACS Sympos Series, No. 176, p 159.

Currie, LA, Kunen, SM., Voorhees, KJ, Murphy, RB, and Koch, WF, 1978, Analysis of carbonaceous particulates and characterization of their sources by low-level radiocarbon counting and pyrolysis/gas chromatography/mass spectrometry, in Novakov, T, ed. Conf on carbonaceous particles in the atmosphere; Berkeley, Univ of California Press, p 36-48.

Currie, LA and Murphy, RB, 1977, Origin and residence times of atmospheric pollutants: application of ^{14}C, in Methods and Standards for Environmental Measurement, Kirchoff, WH, ed, NBS Spec Pub 464, NBS, Washington, DC Nov, p 439.

Dzubay, TG, Stevens RK, Lewis, CW, Hern, D, Courtney, WJ, Tesch, JW and Mason, MA, 1982, Visibility and aerosol composition in Houston, Texas: Environ Sci Tech, 16 514.

Eganhouse, RP, Simoneit, BRT and Kaplan, IR, 1981, Extracted organic matter in urban stormwater runoff: II Molecular Characterization, Environ Sci Tech, 15, 315.

Groblicki, PJ, Cadle, SH, Ang, CC, and Mulawa, PA, 1982, Interlaboratory comparison of methods for the analysis of organic and elemental carbon in atmospheric particulate matter, presented at the National Sympos on Recent Advances in Pollutant Monitoring of Ambient Air and Stationary Sources, ms.

Heisler, SL, Henry, RC, Watson, JG and Hidy, GM, 1980, The 1978 Denver winter haze study, Motor Vehicle Manufacturers Assoc, Detroit, Michigan, report.

Kaden, DA and Thilly WG, Mutagenic activity of fossil fuel combustion products, in Novakov, T, ed, Conf on carbonaceous particles in the atmosphere: Berkeley, Univ California Press, v 193.

Mitchell, RI, Henry, WM, Anderson, NC, Thompson, RJ and Burton, RM, 1977, Megavolume respirable particulate sampler (Mark II), presented at the 70th Annual Meeting of the Air Pollution Control Association, Toronto, Canada, June 20, ms.

Novakov, T, ed, 1978, Conference on carbonaceous particles in the atmosphere, Proc: LBL-9037 (Lawrence Berkeley Lab).

Polach, HA and Ferrari, LM, 1982, Tracing particulate fallout by carbon isotopes, the urban atmosphere - Sydney, a case study, CSIRO, North Hyde Australia, in press.

Rosen, H, Hansen, ADA, Dod, RL and Novakov, T, 1980, Soot in urban atmospheres: determination by an optical absorption technique, Science, v 208, p 741.

Sayre, EV, Harbottle G, Stoenner, RW, Otlet, RL and Evans, GB, 1981, The use of the small gas proportional counters for the carbon-14 measurement of very small samples: Internatl Sympos on Methods of Low-Level Counting and Spectrometry, IAEA, Vienna.

Stevens, RK and Pace, TG, 1983, Status of source apportionment methods: Quail Roost II, Jour Air Pollution Control Assoc, in press.

Wolff, GT, Countess, RJ, Groblicki, PJ, Ferman, MA, Cadle, SH and Muhlbaier, JL, 1981, Visibility-reducing species in the Denver "brown cloud", II sources and temporal patterns, Atmos Environ, v 15, p 2485.

Wolff, GT and Klimisch, RL, eds, 1982, Particulate carbon: atmospheric life cycle: New York, Plenum Press.

[Radiocarbon, Vol 25, No. 2, 1983, P 615-620]

RADIOCARBON MEASUREMENTS OF PARTICULATES IN SMOG

RAINER BERGER*, R M JOHNSON**

and J R Holmes†

ABSTRACT. In recent years in California, smog aerosols have been observed in metropolitan and rural areas. We wondered what the relative contribution is from sources such as fossil fuel combustion (eg, cars, factories) and emissions from trees and other plants. Pollution produced by fossil fuel combustion can be distinguished from biological sources using radioactive carbon. Carbon in fossil organic materials is radioactively dead whereas carbon in living plants contains ^{14}C. Smog particles were collected on clean glass or quartz fiber paper and analyzed in a small volume CO_2 proportional counter for ^{14}C content. Results are given for sampling locations at UCLA, El Monte, Riverside, and Lake Tahoe showing the relative contributions of fossil and modern carbon sources ranging from 0 to 74% and 26 to 100% respectively.

INTRODUCTION

A special aspect of the carbon cycle in nature involves the presence of carbon-containing particles in smog aerosols. Generally, the carbonaceous portion of smog consists mainly of a gaseous phase and ca 3% particulates (Grosjean and Friedlander, 1975). Even though the latter contribution is relatively small, it causes much air pollution and visibility problems affecting eg, air traffic.

Smog largely occurs in areas where the downward air motion of the Hadley cell produces, mainly in the summer, high pressure areas near 30° N or S latitude. As these high pressure cells are associated with little wind, temperature inversions often develop, placing warm over cool air near the surface of the earth. This condition causes the trapping of atmospheric pollutants below the inversion layer.

At the same time, photochemical reactions operate due to strong insolation. Nitrogen oxides formed give rise to

---

*Institute of Geophysics and Planetary Physics, Depts of Anthropology, and Geography, UCLA

**Department of Earth and Space Sciences, UCLA

†State of California Air Resources Board, Sacramento, 95812

ozone which, in turn, oxidizes hydrocarbons to such irritants as aldehydes, peroxides, or epoxides. Briefly summarized, some of the principal chemical reactions are: (Varney and McCormac, 1971)

1) $N_2 + 2O_2 \rightarrow 2NO_2$

2) $NO_2 + h\nu \rightarrow NO + O$

3) $O + O_2 + M \rightarrow O_3 + M$ (where M is a third body)

4) $NO + O_3 \rightarrow NO_2 + O_2$

5) O_3 + hydrocarbons → aldehydes, peroxides, and epoxides

This combination of meteorologic and chemical processes will produce smog with its attendant particulates.

In recent years, appreciable concentrations of smog reaching from ca 32° N to 42° N latitude, have been observed in previously unaffected rural or semi-rural areas of California. The need arose to determine if smog drifts in from large metropolitan centers or if trees and other plants contribute enough organic substances (eg, terpenes and pollen) to become an alternate source of air pollution (Sandberg, Basso, and Okin, 1978; Bufalini, 1979; Miller, Pitts, and Winer, 1979; Sandberg, Basso, and Okin, 1979; Currie et al, 1983). This question can be answered by analyzing aerosol particles for their ^{14}C content. Biospheric origin manifests itself in ^{14}C concentrations in the recent biosphere. On the other hand, fossil origin is indicated by the absence of ^{14}C, which because of its half-life of 5730 ± 30 years, has long ceased to exist in measurable quantities in fossil fuels formed millions of years ago.

SAMPLE COLLECTION

In 1978, personnel from the State of California Air Resources Board began collecting particulates, using first air samplers containing chemically isotopically clean glass filters and later quartz paper. The latter does not melt in the intense heat of the combustion process causing cracking of the Vycor-tubes in which the sample burning is accomplished. Both glass and quartz filter papers were checked for contaminating organic compounds by heating blanks. No measurable gas or activity was found.

At the outset of the sampling program, three stations were set up in southern California: at UCLA, El Monte, and Riverside. Since westerly breezes blow smog mainly toward

Riverside and beyond, it was thought that the lowest air contamination might exist at UCLA increasing in severity toward El Monte and Riverside (fig 1). In 1982, several other stations such as Lake Tahoe and more in the greater Los Angeles area were added to this ongoing program of particulate analysis.

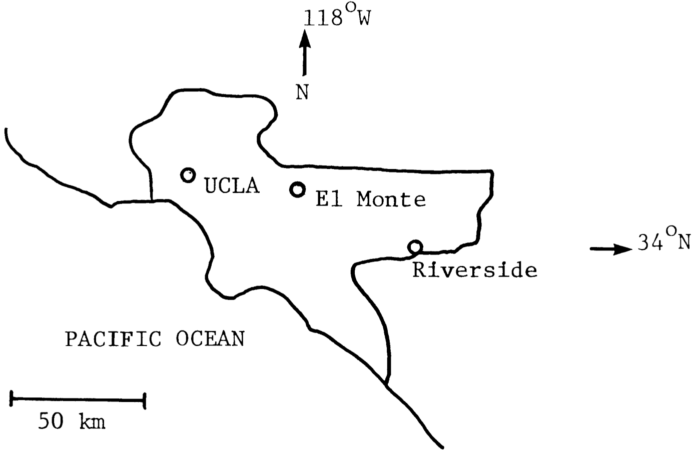

Fig 1. The area shown is the air basin of metropolitan Los Angeles. The surrounding region is mountainous or hilly except for the Pacific coastline. Winds during most of the year are from the west. During the winter Santa Ana winds occur which blow from the desert areas east of Los Angeles toward the ocean. The wind velocity precludes then any accumulation of smog over Los Angeles.

RADIOISOTOPIC ASSAY

As aerosol particles occur in relatively small quantities, a special low-level counting system had to be designed, constructed, and tested, based on previous experience with CO_2 proportional counters. Typically, aerosol phases contain only ca 100μg of organic material in 1m^3 of air. Thus, a small 200mL copper proportional counter was built which needs only 100mg of carbon for filling, obtainable often within 1-3 days on the inert particulate filters. This unit was placed inside an anti-coincidence guard assembly which is, in turn, protected from ambient environmental radiation by a 7.5 ton radioactively clean steel shield. The electronics unit consists of 3 anti-coincidence and 3 coincidence channels powered by ultrastable high voltage supplies. Three standard are used: 1) by international convention, 95% of the count rate of NBS oxalic acid (1.88cpm), 2) CO_2 derived from marble as primary source (0.87cpm), and 3) a CO_2 gas sample derived from a deck plank of the funerary boat of Sesostris III, historically dated to 1800 B C (0.63cpm). The latter standard is used to assure that the equipment performs accurately.

Depending on the filter loading which varies from ca 0.5 to 2.9g one or more filters are placed into an isotopically clean Vycor-quartz tube and burned in a stream of analytically pure oxygen. The resulting CO_2 is purified by washing in silver nitrate and chromic acid solutions. Any CO is converted to CO_2 by copper oxide at 500°. Finally, all electronegative impurities such as O_2 or NO_2 which interfere with proportional counting are removed by passage over clean elementary copper at 500°. Subsequently, these clean CO_2 samples are stored for one month in high-pressure steel cylinders to allow all radon to decay. Typically, samples are then counted for about 2000 minutes to a standard deviation of 2%.

RESULTS

Table 1 lists the data for particulates by percentage of fossil fuel and by inference of recent biospheric contributions. In addition to the ^{14}C measurements, a series of $^{13}C/^{12}C$ stable isotope measurements were made to ascertain that there was no inclusion of carbonate-dust in the particulate samples. The range of $\delta^{13}C$ determinations is from -26.30% to -29.72% with respect to the PDB standard. Since carbonate-derived CO_2 has a $\delta^{13}C$ near zero no inorganic contamination is present.

TABLE 1. Carbon Composition of Total Suspended Particles

From UCLA

UCLA no	Collection date	Weight sample(g)	Fossil fuel contribution(%)*
2210B	9/26/78	1.752	65 ± 2
2210C	9/29/78	1.657	60 ± 2

From El Monte			
2209A	8/11-15/78	0.784	66 ± 2
2209B	8/16-18/78	0.949	74 ± 2
2209C	8/21-24/78	0.759	59 ± 2
2427A,B	3/25-26 and 4/7-9/82	0.506	16 ± 2
2427C,D,E	4/12-19/82	0.877	0 ± 2
2427F	4/19-22/82	0.526	55 ± 2
From Riverside			
2211A	9/29/78	2.670	58 ± 2
2211B	10/3/78	2.708	59 ± 2
2211C	10/6/78	1.246	66 ± 2
2211E	10/13/78	2.880	55 ± 2
From Lake Tahoe			
2426A,B	2/11-14/82	0.593	53 ± 2
2426C,D	2/24-3/4/82	0.879	53 ± 2
2426E	3/4-10/82	1.146	53 ± 2
2426F	3/10-16/82	0.450	53 ± 2

*Based on $^{14}CO_2$ concentration of +35% for 1978 and +25% for 1982 in troposphere above 95% of the count rate of NBS oxalic acid (Berger, ms in preparation).

DISCUSSION

The initial data show that there is considerable variation in the composition of particulates in the Los Angeles air basin, eg, UCLA 2209B is composed of almost 75% of fossil carbon due to anthropogenic emissions. On the other hand, UCLA-2427CDE contains only recent biospheric material. Could it be that this latter sample is made up entirely of pollen from a nearby tree? If so, the choice of sampling location is very critical. Yet on the whole, except for two samples, all data show a clear preponderance of fossil over recent biospheric carbon. This is even true for a High Sierra resort such as Lake Tahoe during February-March 1982.

All these determinations compare well with appropriate measurements obtained by Currie, Klouda, and Cooper (1980) and Currie et al (1983). However, the variations in the data call for more detailed studies linking location, meteorology, and seasonal factors. Such a program of research is now being continued at UCLA.

ACKNOWLEDGMENTS

This study was supported by the State of California Air Resources Board. Our gratitude is extended to D Sullivan, D McJunkin, I Kaplan, and D Winter, whose cooperation has been invaluable. This is publication no 2347 of the Institute of Geophysics and Planetary Physics, UCLA.

REFERENCES

Bufalini, J J, 1979, Factors in summer ozone production from the San Francisco air basin: Science, v 203, p 81.

Currie, L A, Klouda, G A, Continetti, R E, Kaplan, I R, Wong, W W, Dzubay, T G, and Stevens, R K, 1983, On the origin of carbonaceous particles in American cities: results of radiocarbon "dating" and chemical characterization, in Stuiver, M and Kra, R S, eds, Internatl ^{14}C conf, 11th, Proc: Radiocarbon, v 25.

Currie, L A, Klouda, G A, and Cooper, J A, 1980, Miniradiocarbon measurements, chemical selectivity, and the impact of man on environmental pollution and climate, in Stuiver, M and Kra, R S, eds, Internatl ^{14}C conf, 10th, Proc: Radiocarbon, v 22, no 2, p 349-362.

Grosjean, D and Friedlander, S K, 1975, Gas and particle distribution factors for organics and other pollutants in the Los Angeles atmosphere: Jour Air Pollution Control Assoc, v 25, p 1038-1044.

Miller, P R, Pitts, J N, and Winer, A M, 1979, Factors in summer ozone production in the San Francisco air basin: Science, v 203, p 81-82.

Sandberg, J S, Basson, M J, and Okin, B A, 1978, Winter rain and summer ozone: a predictive relationship: Science, v 200, p 1051-1054.

________ 1979, Factors in summer ozone production in the San Francisco air basin: Science, v 203, p 82-83.

Varney, R and McCormac, B M, 1971, Atmospheric pollutants, in McCormac, B M, ed, Introduction to the scientific study of atmospheric pollution: Dordrecht, Reidel Pub Co, p 8-52.

[Radiocarbon, Vol 25, No. 2, 1983, P 621-628]

ANTHROPOGENIC CHANGES IN ORGANIC CARBON AND TRACE METAL INPUT TO LAKE WASHINGTON

WR Schell*, JR Swanson, and LA Currie

National Bureau of Standards
Washington, DC 20234

ABSTRACT. An example of how man's contaminants are introduced, deposited, and retained in sediments giving a chronological record of events has been developed for Lake Washington, Seattle. Significant amounts of both inorganic and organic compounds in the environment originate from fossil fuel sources, such as power plants and motor vehicles. Many organic compounds are introduced also from contemporary biogenic materials. Through the combined carbon isotope analysis technique (CCIA), we can distinguish between fossil and contemporary carbon sources classes (using ^{14}C), as well as sources within each class (using ^{13}C). To establish the chronology of the organic carbon pollutant input to the lake sediment, the ages of the layers were determined using ^{210}Pb dating techniques. Sediment profiles of trace metals and a fallout radionuclide plutonium were also obtained and compared with the carbon isotope profiles. The results show that the total organic carbon (TOC) concentration correspond to 93% modern carbon before 1905. This ^{14}C concentration in TOC decreased to ~60% modern in the 1930's and now is between 95 and 80% modern. The lipid fraction is ca 30% modern and the total aromatic hydrocarbon fraction reached a minimum of 5% modern in 1954. The large decrease in ^{14}C of TOC around 1930 is believed to be due to coal dust or fly ash. The trace metal concentration also increased substantially at this time. The pattern observed in the sediment thus reflects the change in the local energy consumption pattern from a predominately coal to an oil-based economy. From the plutonium profile we infer that mixing occurs for 3 or 4 years before the sediment layers are compacted.

INTRODUCTION

One of the key concerns of society is the introduction of large amount of organic compounds into the environment, as well as their sources, history, (Hites, LaFlamme and Farrington, 1977) and effects on the ecosystem. The overall impact of

---

* University of Pittsburgh, Department of Radiological Health, Graduate School of Public Health, Pittsburgh, Pennsylvania 15261

these organic pollutants often cannot be determined simply by the methods of compound identification by separation and gas chromatography/mass spectrometry as was done for trace metals. The large number of compounds identified by the sophisticated instruments often are confused with those derived from natural oil seeps, coal dust, exometabolites from photosynthesis, and organic degradation products from chemical and bacterial activity. Since many organic compounds are produced and decompose naturally, a means of distinguishing pollution from biogenic chemicals is needed.

ORGANIC-ISOTOPIC METHODS

Swanson (1980) developed a method to detect anthropogenic pollution and tested it on the chronology of organic pollutants in Lake Washington and Puget Sound. This combined carbon isotope analysis (CCIA) measures ^{12}C, ^{13}C, and ^{14}C in carbonaceous compounds found in sediment layers. The total organic carbon, total aliphatic hydrocarbons, and polycyclic aromatic hydrocarbons are separated from kilogram quantities of sediments which have been dated by ^{210}Pb methods. The separation steps include freeze drying, extraction, fractionation, column chromatography, and evaporation. A large Soxhlet extraction apparatus is used for the sediment with ultrapure (nanograde) benzene-methanol solution in which 97% of the total lipids and all hydrocarbons with boiling points higher than that of tetradecane (n-C_{14}) are extracted. Isolation of the aliphatic and aromatic hydrocarbon fractions is achieved by column chromatography using Sephadex and alumina/silica columns. Combustion and quantitative CO_2 measurements (Swanson, 1980) determine the amount of each fraction recovered.

This method is based on natural isotopic differences in organic compounds derived from various sources. Since 1952, all carbon that participates in photosynthesis also contains excessive ^{14}C,ie, greater than the cosmic-ray-produced level ($13.6 dpm \cdot g^{-1}$), produced by atomospheric thermonuclear explosions. The CCIA method makes use of these levels of ^{14}C in organic compounds to develop a chronology and a relative biogenic-to-fossil signature of carbon compounds found in sediments. Measurements of ^{12}C and ^{13}C are used also to identify sources of carbon, since isotopic fractionation occurs in photosynthesis and in decomposition processes of organic compounds (Deines, 1980). Thus, the source of a compound can often be distinguised by its $^{13}C/^{12}C$ ratio. The

CCIA method makes use of these isotopic differences together with the ^{14}C content in natural organic compounds (Swanson, 1980). Because of the small amount these organic fractions (5 to 10Mg) in a reasonable sediment sample size, special low-level counting methods must be employed to measure the ^{14}C content. These methods include the use of small quartz counters of 5 to 15m volume, rise time pulse shape analysis, and statistical methods of data interpretation for the "few count" region (Davis, Harmer, and Hoffman, 1968; Currie, 1972; Currie, Noakes, and Breites, 1979; Cooper, Currie, and Klouda, 1981). The CCIA method provides data on pollution and the impact of chronic levels of toxicants.

RESULTS AND DISCUSSION

Figure 1 shows the CCIA method, (B) ^{14}C, (C) $^{13}C/^{12}C$ isotopic ratio measurements (after Swanson, 1980). The chronology of the sedimentary layers was established using ^{210}Pb methods, correlated with known historical time markers, along with trace metal (Fig 1A) and fallout radionuclides (Fig 1D) information (Schell and Barnes, in press). The ^{14}C profile of total organic carbon (TOC with depth gives ca 100% modern carbon (based on 0.95 oxalic acid standard of NBS) at the surface layers, decreasing to 63% at 1930, then increasing to 95% modern at 1900 and earlier. To interpret these data, three sources of ^{14}C must be imposed. Prior to 1880, the Lake Washington area was a pristine forest with no significant anthropogenic fossil carbon output. The ^{14}C in the TOC of the sediments reflected the atmospheric or cosmic-ray-produced carbon in organic and inorganic detritus settling to the bottom. The value, 95% modern(equal to ~400 years)shows that a small dilution of contemporary carbon does occur, probably due to short storage time (400 years) and/or by utilization of lake water CO_2 which originates partly from dissolution of carbonate rocks. At ca 1905, a rapid dilution of contemporary ^{14}C in TOC occurred, reaching the greatest dilution of contemporary ^{14}C at ca 1930. The source of old or fossil carbon then decreased gradually to the present as indicated by the approach to 95% modern ^{14}C. The minimum in the ^{14}C content of TOC at ca 1930 corresponds to the greatest net dilution by fossil carbon. It is expected that this period corresponds to the maximum particulate carbon input from coal dust, coal burning, or fly ash. This is supported by increased lead and zinc concentrations, shown in figure 1C. Subsequently, natural gas and/or petroleum products were burned; these do not produce as many carbon particles for deposition. Increased ^{14}C in the 1960's and 1970's is not necessarily due to decreased fossil carbon input but rather to excessive environmental ^{14}C from atmospheric thermonuclear testing.

The upper layers of the sediment contain more ^{14}C than the pre-industrial levels of 90 to 95%. This excess is due to the nuclear weapons tests which produced about one-year equivalent of cosmic-ray produced ^{14}C for each megaton of nuclear test (Singer, 1962). The first thermonuclear detonation that produced excessive ^{14}C was in 1952; Fig 1D shows the input of fallout $^{239, 240}Pu$ for comparison. The increase in ^{14}C reached a maximum of ca 80 to 100% excess of modern ^{14}C in 1963 and 1964 (Nydal, Lovseth, and Gulliksen, 1979), and in 1980, the level decreased to ca 30% excess of modern at this latitude. Increased fossil carbon since 1952 may be represented by the ^{14}C measurements but the input to the biosphere is a complicated function depending on the nuclear weapons testing schedule and the response of the atmosphere. Thus, because of this source of excessive ^{14}C the upper layers of sediment should give a minimum of fossil-fuel-derived carbon unless appropriate corrections are made. This dilution could be calculated only if comparable ^{14}C measurements were available, eg on surface sediments of a nearby lake which had not experienced pollution effects.

The extractable lipid fraction (Fig 1B) illustrates the dilution of biogenic carbon (with a ^{14}C content of 90 to 95% modern) by carbon compounds from pollution. The value at the 1915 level is already contaminated by fossil carbon at 65% modern with the greatest contamination at the upper layers of 30 to 40% modern. The total aliphatic hydrocarbons and polycyclic aromatic hydrocarbons also show the contamination of biogenic carbon by fossil carbon compounds with values in the top 40 years between 9 and 30% modern (Swanson, 1980).

The $^{13}C/^{12}C$ ratio ($\delta^{13}C_{PDB}$) in TOC (Fig 1C) shows that $\delta^{13}C$ values of ca $-27^{o}/oo$ are characteristic of the total organic carbon in sediment before man's impact in 1880 (Swanson, 1980). $\delta^{13}C$ in organic carbon seems to have increased (became less negative) during the initial clearing of forests in 1880 to 1915 when large increases in sediment deposition occurred. Above 1915, the $\delta^{13}C$ appears to have decreased up to a surface value of $-29^{o}/oo$. These more depleted values in the upper region of the layers may be due to increased pollution chemical inputs or perhaps to processes of eutrophication in the water column (Deines, 1980). Extractable lipids measured in the upper layers also show a more depleted trend in $\delta^{13}C$ although the data are limited.

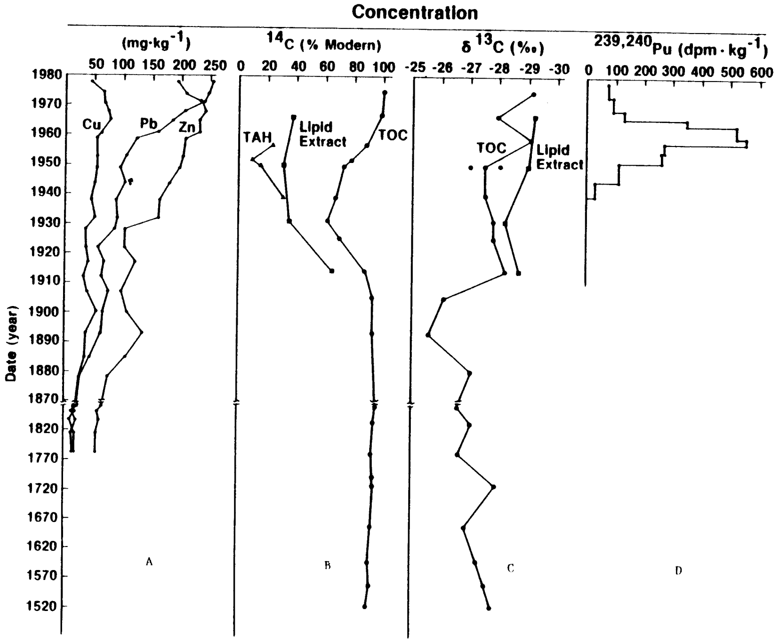

Fig 1. Concentration profiles of trace metals organic carbon and plutonium in Lake Washington as a function of year of sediment deposited at the 62m deep station. A. Concentrations of Cu, Pb, and Zn with time illustrating anthropotenic sources which contribute to the increase. B. Changes in the organic ^{14}C concentration with time using 0.95 oxalic acid of NBS as standard for 100% modern. The decrease from the natural biogenic level of 93% modern (400 year old) before 1900 to the minimum in 1930 shows the fossil fuel dilution. TOC is total organic carbon, TAH is total aromatic hydrocarbon. C. Profiles of the $^{13}C/^{12}C$ isotopic ration as a function of depth based on the PDB carbonate standard of $0\delta^{13}$. Increasing δ^{13} values from 1890 to 1915 may indicate the contribution of inorganic carbonates to the lake from land erosion. D. Concentrations of $^{239,\ 240}Pu$ with time illustrate the fallout from nuclear weapons tests which deposited in the lake. The early 1960's maxima is at the correct time but the presence of plutonium below the 1952 layer shows mixing or diffusion.

The trend toward smaller $\delta^{13}C$ with decreasing depth illustrates the fact that the isotopically lightest carbon compounds,, eg, asphalt and crankcase oil, have diluted the natural biogenic carbon isotopic compounds (Deines, 1980). $\delta^{13}C$ values in biogenic sources of carbon in plankton are all larger than in the surface sediment, eg, Lake Washington plankton - 26°/oo, (mostly C_3 plants) terrestrial plants - 12°/oo (mostly C_4 plants) (Swanson, 1980).

The concentration of the total aliphatic hydrocarbon (TAH) fraction extracted from the Lake Washington sediments was measured. The present flux (surface sediment values) of $9 \times 10^4 g \cdot m^{-2} \cdot yr^{-1}$ is ca 40 times greater than the flux in 1905, assuming no degradation (Swanson, 1980). If this flux were due only to fossil carbon, the ^{14}C content of TAH should be ca 2% modern. However, the value, 15 to 30% modern ^{14}C, shows that a significant part of the TAH comes from contemporary biogenic carbon and not from coal or oil burning.

The concentrations of the polycyclic aromatic hydrocarbon (PAH) fraction were measured. The present flux of $3 \times 10^3 g \cdot m^{-2} \cdot yr^{-1}$ is about ten times greater than the flux of PAH in 1905, assuming no degradation (Swanson, 1980). The ^{14}C content of 10% modern is about the expected level considering that all the excess PAH comes from fossil fuel (ie, coal and oil).

Fig 1D shows $^{239, 240}Pu$ measurements in sediment as a function of years of deposition. The layers dated by ^{210}Pb fix the time period and the high concentrations of $^{239, 240}Pu$ in the early 1960's confirming the chronology determined by ^{210}Pb. However, the peak concentration of $^{239, 240}Pu$ is found from 1958 to 1964, a few years before the maximum fallout peak of 1963 for the northern hemisphere. This time difference may define the "error interval" for mixing of the upper sediment layers at this station. Such a mixing interval of 3 to 4 years may be the time the tracer spends in the upper flocculent layer before final deposition as sediment particles. In addition, $^{239, 240}Pu$ is found in small but significant concentrations below the 1952 layer when significant levels of radioactive fallout from nuclear weapons tests could not have reached Lake Washington. The depth of penetration to the 1940 layer suggests that plutonium either may be mixed with sediment particles to a significantly deeper level than 3 or 4 years, or that part of the plutonium is not permanently fixed to the sediment particles but diffuse across the deposited layers in the pore water. The diffusion coefficient for plutonium would necessarily be much greater than that of lead in these sediments. Plutonium can exist in four possible oxidation states in the aquatic environment: Pu(III), Pu(IV), Pu(V), Pu(VI). To explain this diffusion in the sediments, we suggest that a portion of the initially deposited plutonium diffuses in the pore water in the form of complexes produced by organic and inorganic chemical reactions occurring during sediment diagenesis. Organic compounds also could diffuse in the pore water resulting in a less-defined maximum with date of the layers.

CONCLUSIONS

The total aliphatic plus polycyclic aromatic hydrocarbons comprise only ca 14% of the total carbonaceous compounds in sediment layers (Swanson, 1980). The major fraction, 86%,of the total organic compounds is non-extractable in benzene-methanol and is believed to be coal dust or fly ash. The input of coal dust has decreased from the late 1920's, 40% of the total organic carbon, to 5 to 20% at present (Swanson, 1980). This change, which is recorded in the sediments, must reflect the change in the local use pattern of energy consumption from a predominantly coal- to an oil-based economy. The previous atmosphere must have contained much more particulate carbon pollutants than at present.

Concentrations of trace metals (Cu, Pb, Zn) in sediments show a trend of increasing enrichment towards the sediment surface with Pb reaching the highest value of 250μg/kg at the surface; Cu and Zn concentrations decrease at the surface indicating either a decreasing recent input or, more likely, a diffusion of these metals out of the upper layers. The $^{239,240}Pu$ concentration profile shows a maximum at about the correct time but also that part of the $^{239,240}Pu$ is diffusing and/or mixing to the 1940 level. The quantitative amounts and the history of these contaminants may be found by further interpreting the sedimentary record.

ACKNOWLEDGMENTS

We would like to acknowledge the assistance of Craig Curro, University of Washington, for the analyses of plutonium in sediments, AW Fairhall, University of Washington, for support in the early laboratory analytical program for ^{14}C, and the Gas and Particulate Science Division, Center for Analytical Chemistry, National Bureau of Standards, for the financial support of WR Schell via an intergovernmental personnel act loan from the University of Washington.

REFERENCES

Currie, L A, 1972, The limit of precision in nuclear and analytical chemistry: Nuclear Instruments Methods, v 100, p 387-395.

Currie, L A, Noakes, J E, and Breiter, D N, 1979, Measurement of small radiocarbon samples: power of alternative methods for tracing atmospheric hydrocarbons, in Berger, R and Suess, H E, eds, Radiocarbon dating, International ^{14}C conf, 9th, Proc: Berkeley, Univ California Press, p 158-175.

Cooper, J A, Currie, L A and Klouda G A, 1981, Assessment of contemporary carbon combustion source contributions to urban air particulate levels using carbon-14 measurements: Environmental Sci Technol, v 15, p 1045-1050.

Davis, R, Harmer, D S, and Hoffman, K C, 1968, Search for neutrinos from the sun: Phys Rev Letters, v 20(21), p 1205-1209.

Deines, P, 1980, The isotopic composition of reduced organic carbon: Handbook of environmental isotope geochemistry, Vol A, in Fritz, P and Fontes, JC, eds, The terrestial environment: Amsterdam, New York, Elsevier, p 329-406.

Hites, R A, LaFlamme, R E, and Farrington, J W, 1977, Sedimentary polycyclic aromatic hydrocarbons: The historical record: Science, v 198, p 829-831.

Nydal, R, Loveseth, K, and Gulliksen, S, 1979, Accuracy of radiocarbon variations in nature since the test ban treaty, in Berger, R and Suess, H E, eds, Radiocarbon dating, International ^{14}C conf, 9th, Proc: Berkeley, Univ California Press, p 313-323.

Schell, W R and Barnes, R S, in press, Environmental isotope and anthropogenic tracers of recent lake sedimentation: Handbook of environmental isotope geochemistry, vol B, in Fritz, P and Fontes, J C, eds, The terrestial environment Amsterdam, New York, Elsevier in press.

Swanson, J R, (ms) 1980, Carbon isotope analysis of carbonaceous compounds in Puget Sound and Lake Washington: PhD thesis, Univ Washington.

Singer, S F, 1962, Nuclear explosions in space: Nature, v 196, p 307-314.

[Radiocarbon, Vol 25, No. 2, 1983, P 629-636]

TIME HISTORY OF HUMAN GALLSTONES: APPLICATION OF THE POST-BOMB RADIOCARBON SIGNAL

ELLEN M DRUFFEL* and HENRY Y I MOK**

ABSTRACT

Bomb-produced ^{14}C is a valuable tool for studying rates of short-term processes involving carbon cycling. This study shows that bomb ^{14}C is an excellent tracer of a biochemical process that takes place in the human body, namely the accretion of stones in the gallbladder. The methods developed for obtaining time histories of $^{14}C/^{12}C$ and $^{13}C/^{12}C$ in concentric layers from a large gallstone (30mm diameter) are reported. Formation times are assigned by matching the $^{14}C/^{12}C$ obtained from individual layers with those found for known-aged tree rings. Results show that the gallstone grew over a period of 10 years and seems to have lain dormant within the gallbladder for a period of 11 years. The average growth rate was 1.5mm/year.

INTRODUCTION

The evolution of the pathogenesis of gallstones (GS) is divided into five stages (Small, 1974): metabolic, chemical, physical, growth, and symptomatic. In the first stage, the individual is predisposed to the formation of abnormal bile which then becomes supersaturated with cholesterol. Cholesterol crystals appear in the bile and a conglomeration of numerous crystals develops into a macroscopic stone. Finally, the stones give rise to symptoms or complications, such as jaundice or biliary colic, which cause the patient to seek medical attention. In order to interrupt or reverse the natural progression of cholelithiasis (gallstones), it is important to know the temporal relationship between the various stages.

The temporal history of GS was studied by Stenhouse (1979) and is studied here in a similar manner using the level of bomb-produced ^{14}C in individual concentric layers. Material that was accreted before the testing of thermonuclear bombs (pre-1955) contained ambient levels of ^{14}C ($\Delta^{14}C$ = -25 to 0‰). One of the three donors studied by Stenhouse (1979) had GS that were this old.

---

*Department of Chemistry, Woods Hole Oceanographic Institution, Woods Hole, Massachusetts 02543
**Woodland Clinic Medical Group, Woodland, California 95695

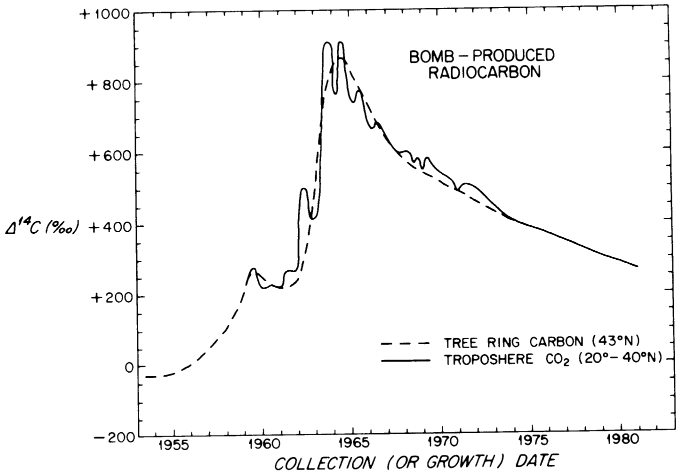

Fig 1. Post-bomb $\Delta^{14}C$ in tree rings (1950-1975)(Cain and Suess, 1976) and in atmospheric CO_2 (1960-1981)(Nydal, Löveseth, and Gulliksen, 1979; Levin, Munnich, and Weiss, 1980; Druffel, ms in preparation)

^{14}C in tree rings as determined by Cain and Suess (1976) was used to assign dates to the growth layers. The curve in figure 1 represents $\Delta^{14}C$ values of annual rings obtained from a Bear Mountain oak from rural New York State (43°N, 74°W). The tree ring curve was preferred over measurements made directly on atmospheric CO_2, because of the large annual variations in atmospheric ^{14}C concentration observed between 1963 and 1973 due to the spring leak. It is of utmost importance, however, to address the offset observed between atmosphere/tree ring and contemporary human ^{14}C levels. Broecker, Schuler, and Olson (1959) found that it took 1 and 1.8 years before the ^{14}C concentration in blood and lung tissue, respectively, reached that in the atmosphere. Likewise, Nydal, Lövseth, and Syrstad (1971) examined human blood and hair samples over a long period (1963-1970) and concluded that bomb ^{14}C enters the body 1.4 years after production in the atmosphere. As cholesterol and bile pigments are the chief constituents in GS, the ages assigned to individual GS layers will be dependent upon the residence time for these chemicals in the body.

APPROACH

The GS discussed below (No. XVIII) was obtained with the GS and common bile duct stones (CBS) from the Veterans Administration Hospital, San Diego, California (32°N). Only stones containing significant amounts of organic material (mostly cholesterol and bile pigments) were chosen. Stones were obtained only from patients who lived in the northern hemisphere and who never received radioisotopes.

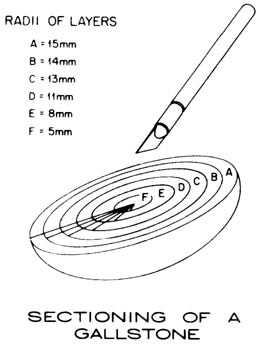

Fig 2. Schematic drawing showing the procedure for sectioning GS No. XVIII

The stone was washed in distilled water and dried at room temperature. It was cut in half using a jeweler's saw. Concentric layers were carefully sectioned with a scalpel, starting with the nucleus of the stone and working out toward the surface (fig 2). The diameter of the stone was 30.0±1mm; the thickness of each of the 6 layers, was measured with an accuracy of ± 0.4mm.

At least 0.3g of material was needed per sample to generate a sufficient amount of CO_2 to analyze for ^{14}C. Each sample was ground in a mortar and pestle in preparation for combustion. An aliquot of material was removed from some samples before combustion to determine per cent cholesterol (Fieser and Fieser, 1959). ^{14}C analyses were performed on extracted cholesterol from some samples other than the GS reported here. These measurements did not differ from those made on whole stones (Mok, Druffel, and Rampone, ms in preparation).

Combustion of each sample was performed by heating the material slowly in a flow of medical-grade oxygen ($80cm^3$/min, 8-10cm Hg). The combusted sample was passed through cupric oxide at 600°C to convert CO to CO_2, and bubbled through chromic acid to remove impurities. The sample was absorbed onto calcium oxide at 600°C, pumped free of contaminants at 400°C and then removed at 800°C. The purified CO_2 was passed through activated charcoal at 0°C to remove any residual contaminating gases.

All CO_2 samples were counted twice in a $100cm^3$ quartz and/or a $200cm^3$ copper counter at 900mm Hg and 25°C. Each sample was counted for a minimum of five days. All measurements were corrected for isotope fractionation to a

$\delta^{13}C$ of $-25.0^{o}/oo$ relative to the PDB-1 standard. The standard used was 95% of the net count rate of NBS oxalic acid standard. All results are reported in terms of $\Delta^{14}C$, according to the Lamont normalization (Broecker and Olson, 1961).

Dates were assigned to layers by matching the $\Delta^{14}C$ value of each sample to the corresponding date using the $\Delta^{14}C$ curves for tree rings, human diet, and human blood (fig 3). It is possible to obtain two sets of dates for each stone, one set from each side of the bomb ^{14}C curve. We chose the set for which the oldest date corresponded to the nucleus and the most recent date corresponded to the outermost layers. Using the dates assigned to the nucleus and the outermost layer, we determined an average growth rate (both in d(radius)/dt and d(Volume)/dt) for the GS.

RESULTS

Results for GS XVIII, obtained from an asymptomatic patient, are reviewed. Table 1 lists ^{14}C and stable isotopic measurements, as well as age assignments. All $\Delta^{14}C$ values found for this GS $<+400^{o}/oo$. According to the composite ^{14}C curve in figure 3, this reflects growth before 1963 or after 1975. As the cholecystostomy (GS operation) was performed in March 1975, we concluded that growth took place during the earlier period. For comparison, the ages of the six GS layers are determined using each of the three ^{14}C curves shown in figure 3 (table 1).

The ages range from 1953.7-1962.0, 1955.6-1963.3 and 1955.6-1964.0 for the tree ring curve, dietary curve and blood curve, respectively. Despite an offset of 1-2 years among the three curves, the growth period of the GS determined using each of these three curves is the same, ca 8 ± 1.5 years. However, as these age assignments reflect the midpoint of each layer, assumptions must be made in order to calculate the growth period for the entire GS. First, a constant growth rate (d radius/d time) is postulated throughout the period of stone formation. In reality, the GS appears to have grown significantly faster during the formation of layers B and C. Second, we assume that the GS did not experience a hiatus at any point during its growth. Thus, assuming a constant growth rate of 1.5mm/yr, the growth period of the GS is determined (from tree ring curve) to have been from 1952.6 to 1962.3, representing a growth interval of ca 10 years. This estimate does not change significantly when either the diet or blood curves are used (fig 3).

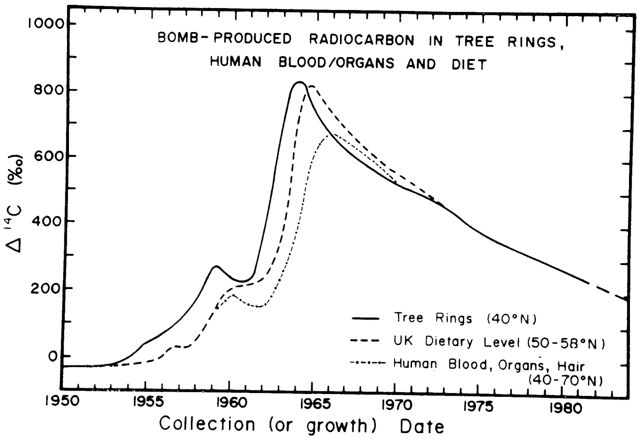

Fig 3. $\Delta^{14}C$ time histories in each of three carbon reservoirs: tree rings (Cain and Suess, 1976), computed dietary level for humans in the United Kingdom (Harkness and Walton, 1972; Stenhouse and Baxter, 1977) and composite human blood/ organs (Broecker, Schuler, and Olson, 1959; Harkness and Walton, 1972; Nydal, Lövseth, and Syrstad, 1971).

These results indicate that the GS stopped growing from ca 1963 to the time of removal from the gallbladder (March 1975), a period of 11-12 years. This is an approximation of the period of no growth, as we cannot determine if the GS grew at a significantly reduced or accelerated rate during the formation of the outermost layer. Although we cannot totally dismiss the possibility of dissolution of other layers that may have formed subsequent to 1963, clinical evidence indicates that conditions favorable to dissolution of stones are not easily achieved in the gallbladder (Wolpers, 1968).

Figure 4 shows a positive correlation between $\delta^{13}C$ (table 1) and distance of the GS layers from the center. The values range from -19.1°/oo in the nucleus to -17.4°/oo in the outermost layer. This may indicate that bile pigment , which was enriched in the inner layers, has a significantly lighter $\delta^{13}C$ signature than cholesterol. Another possibility could be higher concentrations of calcium carbonate (Bills and Lewis, 1975), a mineral enriched in ^{13}C compared to both bile and cholesterol, in the outer layers.

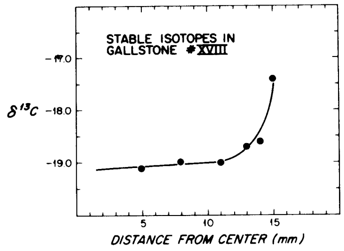

Fig 4. $\delta^{13}C$ results of GS layers as a function of distance from the center

TABLE 1. $\Delta^{14}C$, stable isotope measurements, and corresponding growth years of individual growth layers of GS XVIII

Sample	Layer	Thickness of layer (mm)	$\delta^{13}C$ (‰)	$\Delta^{14}C$ (‰)	Growth years* Tree ring	Diet	Blood/organs
LJ-4178	A (outermost)	1	-17.4	+390±10	1962.0±.2	1963.1±.4	1964.0±.4
-4179	B	1	-18.6	+128±25	1957.2±.3	1959.0±.4	1959.0±.4
-4180	C	2	-18.7	+110±25	1956.8±.4	1958.8±.7	1958.8±.7
-4181	D	3	-19.0	+100±25	1956.6±.4	1958.6±.7	1958.6±.7
-4182	E	3	-19.0	-5±25	1953.7±1.2	1955.6±1.2	1955.6±1.2
-4183	F (nucleus)	5	-19.1	+30±15	1954.7±.5	1957.0±1.5	1957.0±1.5

---

*From figure 3. Errors (in years) are determined from curves in figure 3 using $\pm 1\sigma$ counting error reported with $\Delta^{14}C$ results in previous column.

CONCLUSIONS

Chronology of cholelithiasis can now be determined using the level of bomb-produced ^{14}C in concentric layers of the stone. The growth period of the GS examined in this work spanned ca 10 years and seems to have lain dormant within the gallbladder for ca 10-12 years. The average growth rate of this stone was 1.5mm/year (or $1.6cm^3/yr$). Further studies that include ^{14}C results for GS from symptomatic patients are needed for determining the progression of GS formation from the asymptomatic to the symptomatic stage.

ACKNOWLEDGMENTS

E M Druffel made isotopic measurements at the Mount Soledad Radiocarbon Laboratory, UCSD. Our thanks go to the patients who donated their gallstones for this study, including H E Suess. The technical skills of W Rampone, M Stenhouse, M Harvey, T W Linick, and G Calta are gratefully acknowledged. Our thanks are also given to an anonymous reviewer who contributed greatly to our interpretation. This work was supported by NSF Grant Nos. EAR 78-15183 and OCE 81-11954. This is Woods Hole Oceanographic Contribution No. 5185.

REFERENCES

Bills, P M and Lewis, D, 1975, A structural study of gallstones: Gut, v 16, p 630-637.

Broecker, W S and Olson, E A, 1961, Lamont radiocarbon measurements VIII: Radiocarbon, v 3, p 176-204.

Cain, W F and Suess, H E, 1976, Carbon-14 in tree rings: Jour Geophys Research, v 81, p 3688-3694.

Druffel, E M, 1980, Radiocarbon in annual coral rings from the Atlantic and Pacific Oceans: PhD thesis, Univ California, San Diego.

Fieser and Fieser, 1959, Steroids: New York, Reinhold Pub Co.

Harkness, D D and Walton, A, 1972, Further investigations of the transfer of bomb ^{14}C to man: Nature, v 240, p 302-303.

Levin, I, Munnich, K O, and Weiss, W, 1980, The effect of anthropogenic CO_2 and ^{14}C sources on the distribution of ^{14}C in the atmosphere, in Stuiver, Minze and Kra, Renee, eds, Internatl radiocarbon conf, 10th, Proc: Radiocarbon, v 22, no 2, p 379-391.

Lonsdale, K, 1968a, Human stones: Scientific American, v 219, p 104-111.

Lonsdale, K, 1968b, Human stones: Science, v 159, p 1199-1207.

Nydal, R, Lövseth, K, and Gullicksen, S, 1979, A survey of radiocarbon variation in nature since the test ban treaty, in Berger, Rainer and Suess, H E, eds, Internatl radiocarbon conf, 9th, Proc: Radiocarbon dating, Berkeley, Univ California Press, p 313-323.

Nydal, R, Lövseth, K, and Syrstad, O, 1971, Bomb ^{14}C in the human population: Nature, v 232, p 418-421.

Small, D M, 1974, Management of gallstones, particularly the silent variety: advantages of a varied and individualized approach, in Ingelfinger, F J, Ebert, R B, Finland, M and Relman, A S, eds, Controversy in Internal Medicine, p 545-559.

Stenhouse, M J and Baxter, M S, 1977, Bomb ^{14}C as a biological tracer: Nature, v 267, p 828-832.

Stenhouse, M J, 1979, Further application of bomb ^{14}C as a biological tracer, in Berger, Rainer and Suess, H E, eds, Radiocarbon dating, Internatl radiocarbon conf, 9th, Proc: Berkeley, Univ California Press, p 342-352.

Wolpers, C, 1968, Spontaneous dissolution of gallstones, Deutsch Med Wschr, v 93, p 2525-2532.

VII. ARCHAEOLOGY

[Radiocarbon, Vol 25, No. 2, 1983, P 639-644]

THE INTEGRATION OF RADIOCARBON DATING IN ARCHAEOLOGY*

H T WATERBOLK

Biologisch-Archaeologisch Instituut
Poststraat 6, 9712 ER Groningen
The Netherlands

In the past 30 years many hundreds of archaeologic samples have been dated by radiocarbon laboratories. Yet, one cannot say that ^{14}C dating is fully integrated into archaeology. For many archaeologists, a ^{14}C date is an outside expertise, for which they are grateful, when it provides the answer to an otherwise insoluble chronologic problem and when it falls within the expected time range. But if a ^{14}C date contradicts other chronologic evidence, they often find the 'solution' inexplicable. Some archaeologists are so impressed by the new method, that they neglect the other evidence; others simply reject problematic ^{14}C dates as archaeologically unacceptable. Frequently, excavation reports are provided with an appendix listing the relevant ^{14}C dates with little or no discussion of their implication. It is rare, indeed, to see in archaeologic reports a careful weighing of the various types of chronologic evidence. Yet, this is precisely what the archaeologist is accustomed to do with the evidence from his traditional methods for building up a chronology: typology and stratigraphy. Why should he not be able to include radiocarbon dates in the same way in his considerations?

One reason, of course, is that the archaeologist does not produce the evidence himself. In most cases, he is not trained in physics and chemistry, and therefore has little feeling for the subtleties of the dating method. There is, however, another reason. In my opinion archaeologists often do not clearly realize why they want ^{14}C dates. In this paper, it is my purpose to specify the various functions ^{14}C dates can have in archaeologic reasoning. All examples are taken from old world prehistory.

First of all, ^{14}C provides us with an absolute time scale which extends not only far beyond the historic time scale, but also beyond the time scales provided by geochronology and dendrochronology. We can place archaeologic phenomena on the radiocarbon time scale and along it we can measure the duration of developments or periods. So we know that the expansion of cereal growing and cattle breeding from the Aegean coasts to those of the North Sea took 1500 years and that the period during which Bell Beakers were made in the Netherlands lasted just about 300 years.

---

* This paper is from an invited talk.

The archaeologic interest of such statements is limited, once the absolute time scale is roughly known. Far more interesting is that radiocarbon dating provides us with a tool for establishing relative chronology. Our own methods, typology and stratigraphy, both have their inherent weaknesses. Good stratigraphies are rare in any case, and hiatuses may be very difficult to discern. Typologic sequences are, by their very nature, impressionistic and speculative. It is often difficult to isolate the chronologically significant features in the observed variability. In the past years, radiocarbon has solved many problems of relative chronology. The sequence of the main archaeologic stages is now well established in many areas. Gaps in the sequences are easily identified; hypotheses as to how they should be filled up can be tested by active sampling. In the Netherlands, typochronology has, for some periods, been pushed to the limit, to the degree of detail where the statistical error of the measurements starts to interfere. As an example, I may point to the sequence of Beaker cultures in the later part of the Neolithic period (Lanting and Mook, 1977). For such well-analyzed periods, further dates are in themselves pointless; they will always be 'according to expectation'.

Even more important for archaeology is the importance of ^{14}C dating in establishing correlations between archaeologic sequences that are too far apart in the geographic sense to permit the direct application of stratigraphy and typology. For long-distance correlations, we have in principle a method of our own which is sometimes called 'comparative stratigraphy': the cross-dating of regional sequences by means of exports, imports, or imitations, and by observed parallels in stylistic or technologic developments. A spectacular example of this is Milojčič's (1949) correlation of the historic Egyptian and Mesopotamian sequences with the protohistoric and prehistoric sequences of Anatolia, Crete, Greece, the Balkans, central Europe, and northwestern Europe. For large parts of this geographic range, his correlations have turned out to be correct; that he was completely wrong in the correlation between the Aegean and the Balkans is not a fault of the method, but of its application at a time when the material available for comparison was too limited and a Near Eastern origin of any cultural innovation was still commonly presupposed.

For northern Europe and parts of central Europe, pollen analysis provided a means for long-distance correlations. It worked well for the late glacial and early postglacial periods, such as the Allerød, Upper Dryas, and Preboreal periods, but for the later postglacial periods, the major changes in vegetation were not quite synchronous and too few in number to be of practical use for archaeologic synchronizations.

In the same area, Quaternary geology should provide another means for long-distance correlations, especially for the earlier periods of prehistory. But in practice, there are great difficulties in correlating the moraines of the Alpine glaciers with those of the Scandinavian glaciers, of the loess sections in western Europe with those in central Europe, of the river terraces in the different river systems, of the cave sequences in different limestone areas. Radiocarbon has been able to correct a few errors, but unfortunately, its range of application does not extend far enough backwards in time.

For the late and postglacial periods, however, radiocarbon has been of enormous help in studying such problems as the spread of farming, megalithic burial customs, copper metallurgy, in short, any cultural process occurring on a continental scale. Comparison of local sequences gives the direction of cultural movement and suggests possible areas of origin.

As a fourth contribution of ^{14}C dating to archaeology, I consider its power for independent correlation of archaeologic sequences with environmental sequences, such as derived from geology or vegetational history. For prehistoric man in the Netherlands, the fertile but subsiding and ephemeral delta environment was very attractive. Cultural deposits are often found deeply buried under later sediments. For reconstructing and understanding the settlement history of the delta, the independent dating of environmental sequences has proved to be of vital importance (Waterbolk, 1981).

The four aspects I mentioned - absolute chronology, relative chronology, long-distance correlation of regional sequences, and correlations with environmental sequences - are, in my opinion, the major outside contributions of radiocarbon dating to archaeology. But radiocarbon can do more for archaeology.

Quite often, I have the feeling that a submitter presents a sample for the sole purpose of having an independent check on his or her identification of pottery, grave, or house type, or on its stratigraphic position. The pottery may be typologically a little deviant, the grave may be in an area where, hitherto, the same grave type has not been found, the house may be incompletely preserved, an important find may have been brought to light without professional control, stratigraphic complications may render difficult the attribution of a cultural deposit to the standard geologic sequence of the area. In all these situations, a radiocarbon date will be of great help - not for dating the find itself, but for verifying archaeologic considerations of the find, as a check on the conclusions derived from typology and stratigraphy. In these cases, dates will often turn out to be 'according to expectation', but this does not mean that the measurement has been superfluous. If there is reason for some frowning on the part of the ^{14}C laboratory, it is because the archaeologist has not stated explicitly why he needed the date. But, as I said before, he may not have realized that what he wanted was anything else than the date itself.

I can elaborate a little further on this point. In strict archaeologic reasoning, find associations, in particular so-called closed finds, form the basis for connecting typologic sequences with each other and for the abstraction of units of material culture. The underlying supposition is that associated finds were deposited together. Wether this is true or not will, in each individual case, depend not only on the circumstances of deposition but also on the quality of the stratigraphic observations and may be open to some doubt. But even accepting contemporaneous deposition, this need not mean that all associated objects were made simultaneously. In the light of new finds, doubts may arise as to the reliability of earlier find associations. The same applies to stratigraphies that should provide proof for the chronologic value of typologies. Field data may be less convincing than published reports. In fact, archaeologists are constantly turning back to the old data, to see whether they are in need of reinterpretation in the light of new evidence. It is in this process of continuous critical analysis that ^{14}C dates can be of great help and the recovery of suitable organic materials from museum stores can be most profitable. Here again, the dates themselves are of less importance than their contribution to archaeologic discussion.

We can go a step further. In planning new excavations or in typologic treatment of new find groups, ^{14}C dates can be used to analyze complicated stratigraphies and to bring an initial chronologic order in the find group. The resulting stratigraphies and typologies will have already profited from radiocarbon and need no verification afterwards. A condition for applying this procedure is, of course, that ^{14}C samples are available in sufficient numbers, so that a selection can be made which is relevant to the problem being studied.

Finally, I want to point out the great advantage of having ^{14}C dates available soon after the first campaign of an excavation that is planned for a number of years. Such dates may help in the preliminary analysis of the findings and in the detailed planning of the campaigns for future. This will be particularly true for sites with complicated stratigraphies such as tells. In the end, we will perhaps have more dates than seem necessary for a chronologic analysis of the site as a whole, but the improvement of the quality of the excavation is worth the effort.

In the examples mentioned - verification of typologic or stratigraphic identifications, critical analysis of closed finds, assistance in establishing reliable typologies and stratigraphies, and monitoring excavation projects - ^{14}C dating serves goals in archaeology that go much further than chronology. It functions as a basic method in the search for chronologic order in the material remains of the past, alongside the traditional methods of typology and stratigraphy. It can fulfil this function because of its nearly universal applicability. Of course, archaeology is more than only chronology. But a sound chronology is a necessary starting point for the definition of cultural units and for all considerations of cultural change and cultural movement.

It is, however, clear that such an integration of ^{14}C dating in archaeology can only be successful if the archaeologist is constantly aware of the subtleties of the method, in the same way as he knows the strong and weak points of typology and stratigraphy. This awareness can only be achieved by training. Some problems involved in ^{14}C dating should not be so difficult to appreciate for the archaeologist: the varying reliability of the association between the dated organic material and the diagnostic finds is just another manifestation of the problem surrounding closed finds. That dates of charred wood are always older than the moment the tree in question was cut is a problem akin to the problem which the archaeologist has when he studies hoards of bronzes or coins. The possibility that samples may be contaminated or even mixed will be easily appreciated by an archaeologist who knows by experience that in complex stratigraphies isolated Neolithic sherds keep turning up in overlying Bronze Age layers and vice versa. In 1971 I published a paper with some guidelines for the use of ^{14}C dates in archaeology (Waterbolk, 1971). In an abbreviated and slightly amended form it will appear again (Waterbolk, in press).

Only radiocarbon scientiests are qualified to teach the physical and chemical side of radiocarbon dating. By this I mean the fundamental aspects of the method, the laboratory procedures, the statistical side of the measurements, the role played by the variations in the ^{14}C content of the atmosphere, the estimation of the quantitative effect of contamination, the problems involved in the use of samples from aquatic or volcanic environments, the calibration of the ^{14}C time scale, etc. I refer once more to the Proceedings of the Groningen symposium, which, in its introductory and invited papers, contains useful material for teaching purposes.

I want to end with a call to fellow archaeologists to include courses in radiocarbon dating in their curricula, and to radiocarbon scientists to help the archaeologists in implementing such courses. There are a few places in the world where such courses exist, but they are still far too few. If radiocarbon dating is allowed to grow from an outside expertise to a basic method of archaeology, training is a vital matter. And to make this training successful, archaeologists and radiocarbon scientists must join forces.

REFERENCES

Lanting, JN and Mook, WG, 1977, The pre- and protohistory of the Netherlands in terms of radiocarbon dates: Groningen, 247 p.

Milojčić, VM, 1949, Chronologie der jüngeren Steinzeit Mittel- und Südosteuropas: Berlin, Verlag Mann, 137 p.

Waterbolk, HT, 1971, Working with radiocarbon dates: Proc. Prehistoric Soc, v 37, p 15-33.

----- 1981, Archaeology in the Netherlands: delta archeology: World Archaeology, v 13, p 240-254.

----- in press, Ten guidelines for the archaeological interpretation of radiocarbon dates, in Mook, WG and Waterbolk, HT, eds, First internatl Symp on ^{14}C and archaeology - Groningen 24-28 August 1981: Strassbourg.

[Radiocarbon, Vol 25, No. 2, 1983, P 645-646]

THE RELIABILITY OF ARCHAEOLOGIC INTERPRETATION OF ^{14}C DATES

HORST WILLKOMM

Institut für Reine und Angewandte Kernphysik der Universität Kiel
Olshausenstr 40-60, D-2300 Kiel 1, W-Germany

ABSTRACT. ^{14}C dates of a medieval settlement with archaeologically well-dated strata are compared with the true ages of the respective layers. The ^{14}C values indicate that each layer may contain older material reaching up to the beginning of settlement. Therefore, the ^{14}C measurement of only a few wood or charcoal samples may lead to age estimations several hundred years too old.

The excavations of the medieval village of Starigard at Oldenburg, Schleswig-Holstein, northwest Germany, provided a rare opportunity of comparing ^{14}C ages of wood and charcoal samples with the age of the surrounding layer determined by archaeologic methods.[1] Figure 1 shows the results. On the lower x-axis, the conventional ^{14}C age is given. The bars equal 1σ lying, in most cases, between 50 and 70 years. The upper x-axis gives the age corrected for variations of the recent activity. Instead of the calibrations of Bruns, Münnich, and Becker, (1980), this scale is simply shifted against the lower scale by a mean value of 35 years. This may be justified because the samples of Starigard usually consisted of charcoal containing a mixture of many tree rings. On the y-axis, the archaeologic age is given with a precision of ca 25 years. The accuracy is still better, eg, for the "separation layer," assigned to AD 967 or 968, when the Slavonic fortification was destroyed by fire and subsequently reconstructed as a bishop's see. Other strata can be clearly differentiated and dated by ceramic finds.

The ^{14}C values have a rather poor correlation to the real age. At the younger side, except for statistical variations, no value is younger than expected archaeologically (see the diagonal lines in figure 1). But at the left (older) side, excepting one sample, all ^{14}C ages found in the different strata end within a common short period near AD 600, possibly indicating the beginning of the settlement.

There are several well-known reasons for the difference between the (older) ^{14}C age and the real age of the layer in question (cf Waterbolk, 1971). Also, the excavation of Starigard shows that every stratum contains material from the beginning of the settlement to contemporaneous samples in spite of the difference of >3m between the lowest and uppermost layer. In this case, the obvious reasons are frequent burning and reconstruction of fortifications, digging new ditches, or leveling the ground. On other excavation sites, such "anthropogenic bioturbation" usually can be expected to produce large errors in age estimation.

---

[1] My thanks go to Ingo Gabriel, Schleswig, who collected and submitted the samples, did the dating, and made the comments.

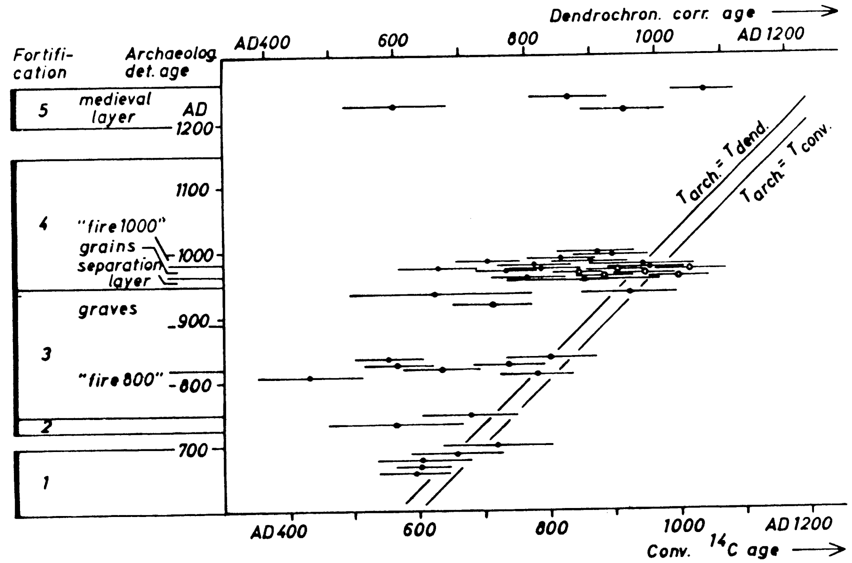

Fig 1. Comparison of ^{14}C values with archaeologically determined ages. ● = wood and charcoal; o = carbonized cereals.

For a single layer with different ^{14}C ages, it is interesting to decide on the basis of these values, whether the samples belong to a single common age or whether the real ages are spread over a larger time span. Only if there is a single common age, it is justified to calculate a mean value giving a more precise estimation of the real age. In the other case, the mean value is of no practical use.

On the basis of measured values only, it is impossible to decide between these two cases. Consequently, it is invalid to combine several ages to get a more exact mean except when there are strong archaeologic or stratigraphic reasons indicating that the samples really belong to the same age. Mere coincidence of measured ages is not enough.

ACKNOWLEDGMENT

This work was financially supported by the Deutsche Forschungsgemeinschaft within the program of the Sonderforschungsbereich 17 (Skandinavien- und Ostseeraumforschung).

REFERENCES

Bruns, M. Münnich, KO, and Becker, B, 1980, Natural radiocarbon variations from AD 200 to 800, in Stuiver, Minze and Kra, Renee, eds, Internatl radiocarbon conf, 10th, Proc: Radiocarbo v 22, no. 2, p 273-277.

Waterbolk, HT, 1971, Working with radiocarbon dates: Prehistoric Soc Proc, v 37, pt 2, p 15-33.

[Radiocarbon, Vol 25, No. 2, 1983, P 647-654]

NON-CONCORDANCE OF RADIOCARBON AND AMINO ACID RACEMIZATION DEDUCED AGE ESTIMATES ON HUMAN BONE

R E TAYLOR

Department of Anthropology
Institute of Geophysics and Planetary Physics
University of California, Riverside
Riverside, California

ABSTRACT. Radiocarbon determinations, employing both decay and direct counting, were obtained on various organic fractions of four human skeletal samples previously assigned ages ranging from 28,000 to 70,000 years on the basis of their D/L aspartic acid racemization values. In all four cases, the ^{14}C values require an order of magnitude reduction in age.

INTRODUCTION

Some of the earliest ^{14}C measurements carried out in 1948-1949 were concerned with the question of the antiquity of Homo sapiens in the Western Hemisphere (Arnold and Libby, 1950). By the mid-1960's, ^{14}C values were being used to establish the presence of human populations in the New World at a maximum of ca 12,000 to 13,000 ^{14}C years BP (Haynes, 1967). In the early 1970's, ^{14}C values on the "collagen" (typically, the acid-insoluble) fraction of human bone samples (cf Hassan and Hare, 1978; Taylor, 1980) were used to adjust the upper limit upward to ca 20,000 to 25,000 ^{14}C years (Berger et al, 1971; Berger, 1975). By the mid 1970's, amino-acid racemization (Bada and Protsch, 1973) and its application to bone samples from anatomically modern Homo sapiens from central and southern California (Bada and Helfman, 1975) provided aspartic acid derived age assignments up to as much as 70,000 years (Sunnyvale skeleton).

Based, in part, on the ^{14}C and amino acid racemization estimates of age, several archaeologists conversant with the evidence (MacNeish, 1976; 1978) suggested that human populations moved into North America more than 35,000 to 50,000 years ago. Recently, the amino acid racemization values were used as evidence to support a view that human populations arrived in the New World as early as the last interglacial (Carter, 1980). The 70,000-year age of the Sunnyvale skeleton has even been cited to support the view that modern Homo sapiens evolved in the New World (Goodman, 1981).

At the same time, several geochemists have been quite skeptical concerning the validity of such age assignments on bone (Hare, 1974; Bender, 1974; Williams and Smith, 1977; Von Endt, 1979; Kessels and Dungworth, 1980). An undercurrent of uncertainty prevails concerning the validity of some ^{14}C and amino acid racemization values assigning ages older than ca 15,000 years to New World human skeletal remains (Willey, 1978, p 269-270; Taylor and Payen, 1979; Meighan, 1983). There is clearly a need to resolve some basic questions focused on both ^{14}C and amino acid racemization deduced ages on presumed early New World human skeletal samples.

DATA AND DISCUSSION

Up to 1982, there were ten published examples in which North American Homo sapiens skeletal materials were assigned ages older than about 15,000 years BP based on direct ^{14}C, amino acid racemization, and/or uranium series determinations on bone. The oldest values are assigned by the amino acid racemization technique. These include, in order of the age indicated by D/L aspartic acid racemization values, the Sunnyvale (70,000 years), Haverty or Angeles Mesa (>50,000 years), and Del Mar (41,000-48,000 years) skeletons. This paper reports direct comparisons between ^{14}C and amino acid deduced age estimates for the two oldest skeletons as well as comparisons on samples assigned somewhat younger ages (37,000 and 28,000 years) by the amino acid racemization method. The method of preparation of the organic fractions of the bone samples used for the ^{14}C analysis in the UCR laboratory is presented in figure 1.

The Sunnyvale skeleton was excavated in 1973 from an exposed section of the Sunnyvale East Drainage Channel in the southern portion of San Francisco Bay, California (Lajoie, Peterson, and Gerow, 1980). An anthropometric examination showed the skeleton was a morphologically fully modern, nearly complete female, statistically indistinguishable in 32 standard measurements and indices from a local population of females previously dated by ^{14}C and cultural association to between ca 400 and 1600 ^{14}C years ago (Gerow, 1981). Both archaeologic and geologic contexts pointed to a late to middle Holocene age. The skeleton was found in a well-defined grave pit 2.7m deep. The pit was excavated through a layer of dispersed freshwater shell that yielded ages of 10,110±260 (I-8084) and 10,430±150 (I-6476) ^{14}C years BP. Charcoal associated with a bone artifact found ca 400m south of the burial and ca 2m deep, in sediments similar to those in the burial pit, yielded an age of 4460±95 ^{14}C years BP (I-6977). On this evidence Lajoie, Peterson and Gerow (1980) and Gerow (1981) argued that the Sunnyvale skeleton was less than 10,000 years and probably less than 4500 years.

Four ^{14}C ages have been obtained, by both decay and direct counting on three organic fractions of post-cranial bone of the Sunnyvale skeleton. Decay counting was done by a 500cc

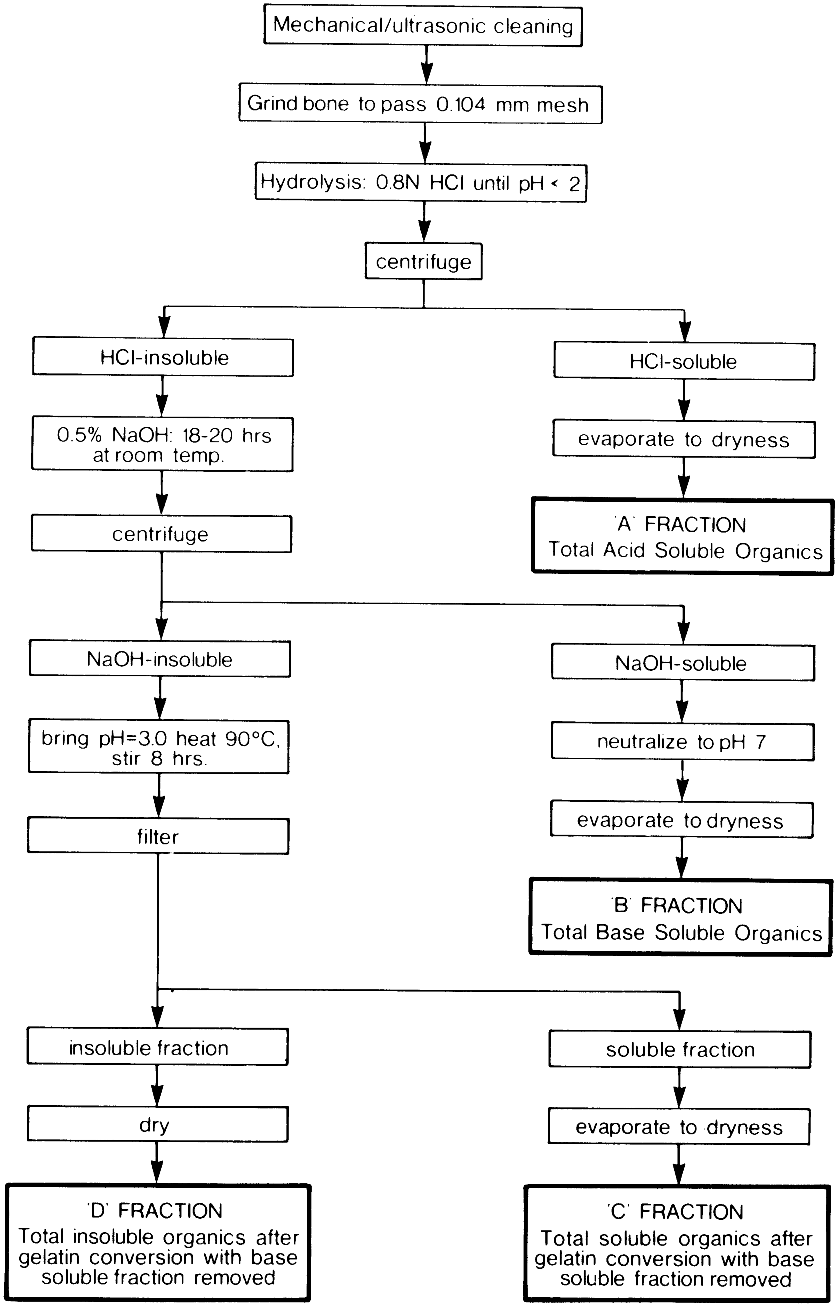

Fig 1. Preparation of organic fraction of bone for ^{14}C analysis. See also Taylor 1980, 1982.

CO_2 gas proportional counter (Taylor, 1975). Insufficient carbon yield from two of the organic fractions required the use of direct counting. The analyses were made at the NSF Regional Facility for Radioisotope Dating at the University of Arizona with sample gases prepared at the UCR laboratory; details are discussed in Chapter VIII (Donahue et al, 1983). The direct counting values are identified in table 1 by the dual laboratory number, ie, UCR-1437A/AA-50 with AA identifying a University of Arizona Accelerator determination. All four ^{14}C determinations on the Sunnyvale skeleton support a middle Holocene age assignment in the range between 3500 and 5000 ^{14}C years BP in contrast to the aspartic acid racemization deduced age.

In 1924, a group of human skeletons were found between 5.75 and 7m deep in an area ca $1m^2$ during trenching operations being carried out by the Haverty Construction Company in the Baldwin Hills area of western Los Angeles County, California (Stock, 1924). The horizontal proximity of the skeletons strongly suggest that all of the skeletons were interred at the same time. Interest in the age of the Haverty or Angeles Mesa skeletons was heightened by the 1970 ^{14}C determination on the Los Angeles (Baldwin Hills) human skeleton which was recovered in 1936 ca 0.8km north of Haverty at a depth of 4m (Lopatin, 1940; G Kennedy, pers commun). Its ^{14}C age, >23,600 years BP, was obtained on the total amino acid fraction of a portion of the skull (Berger et al, 1971; Berger, 1975). Subsequently, a D/L aspartic acid racemization value of 26,000 years was obtained using the ^{14}C-dated Laguna human skull to provide the temperature calibration (Bada and Helfman, 1975). With the same temperature calibration, an aspartic acid measurement on the Haverty skeleton resulted in an inferred age of greater than 50,000 years (Austin, 1976, p 5; Masters, pers commun). By contrast, the four ^{14}C determinations on the Haverty skeletons by three radiocarbon laboratories point to a middle Holocene age in the range between ca 5000 and 8000 ^{14}C years.

The La Jolla Shores skeleton (SDM 16755) was unearthed in 1926 during construction operations at the San Diego Museum of Man (SDM) W-2 site. As an Olivella shell bead was cemented to one of the ribs, the remains were interpreted as a burial. The sample was collected by M J Rogers and stored at the Museum of Man until selected for amino acid racemization analysis by George F Carter. The Laguna skull was used as the SDM 16755 "calibration" sample for the purpose of inferring its aspartic acid racemization age of 28,000 years BP (Bada, Schroeder, and Carter, 1974). Three ^{14}C values on La Jolla Shores bone obtained by two laboratories place its age at less than 2000 years. The D/L aspartic acid ratios of both bone and teeth from the Riverside or San

TABLE 1. North American human skeletal samples with direct ^{14}C and amino-acid racemization-deduced ages. Details of the method of preparing bone for ^{14}C analysis in the UCR laboratory is presented in figure 1.

	Locality	Age/technique*	Fraction employed for ^{14}C	Reference
1	Los Angeles (Angeles Mesa), California (Haverty)	>50,000(A)	-	Austin, 1976; P Masters pers commun
		5200±400(C) (GX-1140)	Total bone organics after pyrolysis	S Brooks, pers commun
		7900±1440(C) (UCLA-1924A)	Total acid-insoluble organics with base extraction	R Berger, pers commun
		5680±180(C) (UCR-1349A)	Total acid-soluble organics	This report
		5280±180(C) (UCR-1349D)	Total acid-insoluble organics after gelatin conversion with base-soluble fraction removed	This report
2	Los Angeles (Baldwin Hills), California	>23,600(C) (UCLA-1430)	Total amino acids (ion exchange chromatography)	Berger et al, 1971
		26,000(A)	-	Bada, Schroeder, and Carter, 1974
3	San Diego, La Jolla Shores (W-2, SDM 16755), California	28,000(A)	-	Bada, Schroeder, and Carter, 1974
		1770±790(C) (UCR-1511D)	Total acid insoluble organics after gelatin conversion with base soluble fraction removed	This report
		1850±200(C) (UCLA-2368)	Gelatin fraction	R Berger, pers commun
		1930±200(C) (UCLA-2384)	Gelatin Fraction	R Berger, pers commun
4	San Jacinto (Riverside), California	37,000(A)		Bada, et al, 1979; P Masters, pers commun
		3020±140(C) (UCR-1420A)	Total acid-soluble organics	This report
5	Sunnyvale, California	70,000(A)		Bada and Helfman, 1975
		4390±150(C) (UCR-1437A)	Total acid-soluble organics	This report
		3600±600(C)** (UCR-1437A/AA-50)	Total acid-soluble organics	This report
		4850±400(C)** (UCR-1437B/AA-52)	Total base-soluble organics	This report
		4650±400(C)** (UCR-1437D/AA-51)	Total insoluble organics after gelatin conversion with base soluble fraction removed	This report

---

*(C)=^{14}C value, (A)=aspartic acid racemization value

**Preliminary values for the ^{14}C determinations obtained by direct counting at the NSF Regional Facility for Radioisotope Dating at the University of Arizona were originally reported with respect to 5050 BC wood. The values cited here represent a large number of subsequent measurements and have been expressed in ^{14}C years BP.

Jacinto skeleton was published by Bada et al, 1979. This skeleton had been recovered in 1938 by H Garbani at the Charlotte Site near San Jacinto in Riverside County, California (H Garbani, pers commun). The k_{asp} value used to determine the aspartic acid racemization age of the La Jolla Shores (and Laguna skull) sample has been employed to calculate an aspartic acid racemization age of approximately 37,000 years for the San Jacinto skeleton (P Masters, pers commun). Its ^{14}C age is approximately 3000 years.

CONCLUSION

A significant number of amino acid racemization ages on bone have previously been validated by their concordance with ^{14}C values. An example of this is the ^{14}C and aspartic acid racemization dates on the Los Angeles (Baldwin Hills) skeleton. In other instances, however, the racemization deduced values can be significantly anomalous. Such is the case for the ages assigned to the Sunnyvale, Los Angeles (Angeles Mesa/Haverty), La Jolla Shores, and San Jacinto (Riverside) skeletons. In all four instances, the ^{14}C values require an order of magnitude reduction in age. Future studies will be required to determine what factors are involved in causing these samples to yield greatly inflated racemization-deduced ages.

ACKNOWLEDGMENTS

Research support of the UCR Radiocarbon Laboratory by NSF Grant BNS 7815069 and 8011764 (Anthropology Program), the dedicated laboratory assistance of P Ennis, A Payen, C Prior, and P J Slota, Jr, and the collaboration of D J Donahue, T H Zabel, A J T Jull, and P E Damon (University of Arizona) is gratefully acknowledged. The Regional Accelerator Facility at the University of Arizona is supported by an NSF Regional Instrumentation Facilities Grant. This is contribution number 82/12 of the Institute of Geophysics and Planetary Physics, University of California, Riverside.

REFERENCES

Arnold, J R and Libby, W F, 1950, Radiocarbon dates: Science, v 113, p 111-120.

Austin, J, 1976, A test of Birdsell's hypothesis on New World migration: Paper, Ann mtg Soc California Archaeology, April 1976.

Bada, J L and Helfman, P M, 1975, Amino acid racemization dating of fossil bones: World Archaeol, v 7, p 160-173.

Bada, J L and Protsch, R, 1973, Racemization reaction of aspartic acid and its use in dating fossil bones: Natl Acad Sci Proc, v 70, p 1131-1334.

Bada, J L, Schroeder, R, and Carter, G F, 1974, New evidence for the antiquity of man in North America deduced from aspartic acid racemization: Science, v 184, p 791-793.

Bada, J L, Masters, R M, Hoopes E, and Darling, D, 1979, The dating of fossil bones using amino acid racemization, in Berger, R and Suess, H E, eds, Radiocarbon dating: Berkeley, Univ California Press, p 740-773.

Bender, M L, 1974, Reliability of amino acid racemization dating and paloeotemperature analysis on bones: Nature, v 252, p 378-379.

Berger, R, 1975, Advances and results in radiocarbon dating: early man in America: World Archaeol, v 7, p 174-184.

Berger, R, Protsch, R, Reynolds, R, Rozaire, C, and Sackett, J R, 1971, New radiocarbon dates based on bone collagen of California paleoindians: Contr Univ of Calif Archaeol Research Fac, v 12, p 43-49.

Bischoff, J L and Rosenbauer, R J, 1981, Uranium series dating of human skeletal remains from the Del Mar and Sunnyvale sites, California: Science, v 213, p 1003-1005.

Carter, G F, 1980, Earlier than you think: a personal view of man in America: College Station, Texas A&M Univ Press.

Donahue, D J, Zabel, T H, Jull, A J T, and Damon, P E, 1983, Results of tests and measurements from the NSF Regional Accelerator Facility for radioisotope dating, in Stuiver, M and Kra, R S, eds, Internatl ^{14}C Conf, 11th, Proc: Radiocarbon, v 25.

Gerow, B A, 1981, Amino acid dating and early man in the New World: A rebuttal: Soc for California Archaeology occasional papers, v 3, p 1-11.

Goodman, J, 1981, American genesis, the American Indian and the origins of modern man: New York, Summit Books.

Hare, P E, 1974, Amino acid dating--A history and an evaluation: MASCA Newsletter, v 10, p 4-7.

Hassan, A A, and Hare, P E, 1978, Amino acid analysis in radiocarbon dating of bone collagen, in Carter, G F, ed, Archaeol chemistry II: Washington DC, Am Chemical Soc, p 109-116.

Haynes, C V, Jr, 1967, Carbon-14 dates and early man in the New World, in Martin, P S and Wright, H E, eds, Pleistocene extinctions: the search for a cause: New Haven, Yale Univ Press, p 267-286.

Kessels, H J and Dungworth, G, 1980, Necessity of reporting amino acid compositions of fossil bones where racemization analyses are used for geochronological application: Inhomogeneties of D/L amino acid in fossil bones, in Hare, P E, Hoering, T C, and King, E, eds, The biogeochemistry of amino acids: New York, John Wiley and Sons, Inc, p 477-489.

Lajoie, K R, Peterson, E, and Gerow, B A, 1980, Amino acid bone dating: A feasibility study--south San Francisco Bay region, in Hare, P E, Hoering, T C, and King, E, eds, The biogeochemistry of amino acids, New York, John Wiley and Sons, Inc, p 477-489.

Lopatin, I A, 1940, Fossil man in the vicinity of Los Angeles, California, in Pacific Sci Cong, 6th, Proc: v 4, p 177-181.

MacNeish, R S, 1976, Early man in the New World: American Scientist, v 63, p 316-327.

——————— 1978, Late Pleistocene adaptations: A new look at early peopling of the New World: Jour Anthropological Research, v 34, p 475-496.

Meighan, C W, 1983, Early man in the New World, in Masters, P M and Flemming, N C, eds, Quaternary coastlines and marine archaeology: towards a prehistory of landbridges and continental shelves: New York, Academic Press.

Protsch, R R, 1978, Catalog of fossil hominids of North America: Stuttgart, Gustav Fisher.

Smith, F H, 1976, The skeletal remains of the earliest Americans: a survey: Tennessee Anthropologist, v 1, p 116-147.

Stock, C, 1924, A recent discovery of ancient human remains in Los Angeles, California: Science, v 60, p 2-5.

Taylor, R E, 1975, UCR radiocarbon dates II: Radiocarbon, v 7, p 396-406.

——————— 1980, Radiocarbon dating of Pleistocene bone: toward criteria for the selection of samples, in Stuiver, M and Kra, R S, eds, Internatl ^{14}C conf, 10th, Proc: Radiocarbon, v 22, no 3, p 969-979.

——————— 1982, Problems in the radiocarbon dating of bone, in Currie, L A, ed, Nuclear and chemical dating techniques: interpreting the environmental record: Washington DC, Am Chemical Soc, p 453-473.

Taylor, R E and Payen, L A, 1979, The role of archaeometry in American archaeology: approaches to the evaluation of the antiquity of *Homo sapiens* in California, in Schiffer, M, ed, Advances in archaeological method and theory: New York, Academic Press.

Von Endt, D W, 1979, Techniques of amino acid dating, in Pre-Llano cultures of the American: paradoxes and possibilities, Washington DC, Anthropol Soc Washington, p 71-100.

Williams, K M and Smith G G, 1977, A critical evaluation of the application of amino acid racemization to geochronology and geothermometry: Origins of Life, v 8, p 91-144.

Willey, G R, 1978, A summary scan, in Taylor, R E and Meighan, C W, eds, Chronologies in New World archaeology: New York, Academic Press.

[Radiocarbon, Vol 25, No. 2, 1983, P 655-659]

DIRECT BONE DATING IN A SMALL CO_2 COUNTER

RAINER BERGER

Archaeology Program, Departments of
Anthropology and Geography, and Institute
of Geophysics and Planetary Physics
University of California, Los Angeles, California 90024

ABSTRACT. A small 200ml capacity CO_2 proportional counting system has been developed which uses only 100mg of carbon for complete filling. Thus, with respect to the small quantities needed, it compares favorably to dedicated accelerators at significantly lower cost. The performance of this equipment is demonstrated using a variety of samples including some human bone fragments from La Jolla which had been estimated to be 28,000 years old by aspartic acid racemization analysis.

INTRODUCTION

Direct dating of artifacts or bone is very valuable in archaeology inasmuch as association problems can be avoided. At Gypsum Cave (Harrington, 1933) atlatl shaft fragments and dung from giant sloths were found mixed together. The dung was dated to 10,455 ± 340 years (C-221, Libby, 1952) which led Harrington to believe that sloth and early man coexisted. However, direct dating of the atlatl shafts showed them to be only 2900 ± 80 years old (UCLA-1233) (Berger and Libby, 1967).

BONE DATING

Most bone samples recovered archaeologically tend to retain little native protein (collagen) on which to base a direct ^{14}C date when measured in conventionally-sized counters. Moreover, samples are often small or may be morphologically valuable so that only little can be sacrificed. Consequently, it became desirable to develop a special counting system which requires only small amounts of sample while yielding dates with acceptable standard deviations within reasonable counting time. Polach et al (1982) recently published a review of this approach.

In order to obtain the native organic fraction in bone, collagen is isolated by mild hydrochloric acid treatment followed by conversion to gelatin (Longin, 1971). This process eliminates most chemical contamination experienced in the field (Protsch, ms). However, when serious organic contamination is expected or outright asphalt impregnation is noticed, collagen is hydrolyzed completely into its component amino acids which are then dated directly (Ho, Marcus, and Berger, 1969). Generally, the selection of the most suitable isolation technique for obtaining radiochemically pure amino acids or proteinaceous matter depends largely on the geochemistry and geomorphology of the recovery site. For example, dry cave deposits may not be chemically contaminated at all, while bone from the La Brea tar pits requires exhaustive decontamination, isolation, and characterization procedures.

In order to produce a clean CO_2 gas sample suitable for counting, the collagen fraction or amino acids are burned in a stream of pure oxygen. The CO_2 so generated is absorbed in carbonate-free 4N sodium hydroxide. This solution is flushed with oxygen gas to remove most radon dissolved in the solution. Then the original CO_2 is liberated by adding analytically pure hydrochloric acid. Subsequently, this CO_2 gas is cleaned in wash towers containing consecutively dilute silver nitrate and concentrated chromic acid. The next step involves passing the counting gas repeatedly over elementary copper at 500°C to remove such electro-negative impurities as oxygen or nitrogen oxides which interfere with CO_2 proportional counting. Finally, the counting gas is stored for about two weeks to permit complete radon decay.

The counter itself has a volume of 200ml equivalent to ca 8mM of CO_2 or 100mg of carbon all of which is used in the actual counting chamber. It is constructed of pure copper, epoxy-sealed, and fitted with a 1 mil anode wire at 3400V. The counter and separate anticoincidence system is located in a steel shield, 20cm thick, at the base of a five-story steel-reinforced concrete building. After preamplification the counter pulses are sorted into 3 anticoincidence and 3 coincidence channels for ultimate data reduction. With present shielding the dating range is ca 30,000 years but can be extended with additional modifications or made more accurate. Typically, a modern sample is counted for 2000 min to a standard deviation of 2%, a 3800-yr-old sample to 3% in 5000 min and a 18,000-yr-sample to 10% in one week. Thus this 200ml unit can produce about one date list/year when used for general archaeological/geological purposes.

TABLE 1. 200ml counter dates of bone samples

UCLA No.	Provenience	Counting time(min)	Age*(yr)
2380	Burial LAn717	2000	1125 ± 300
2384	La Jolla Shores W-2, #16755	4000	1930 ± 200
2347	Rancho La Brea	1000	Modern
2315A	Lake Taguatagua	5900	15,250 ± 910

*Age based on half-life 5568 ± 30; not calibrated or corrected

UCLA-2380 shows the kind of date to be expected from a relatively recent sample counted over a conventional period of 2000 min equivalent to 33.3 hours or ca 1 1/2 days. Such exploratory dates with an error on the order of ±300 years still permit archaeologic judgments, in many cases, on the chronologic period of a sample.

UCLA-2384 was analyzed to compare directly ^{14}C and aspartic acid racemization dates of the same human skeleton. The sample was composed of a few long bone fragments from site W-2, La Jolla Shores, California, where in 1926, Malcolm Rogers recovered a human skeleton without a cranium (SDM-16755). In 1973, bone fragments from this skeleton were dated by aspartic acid racemization and estimated to be 28,000 years old, using $K_{asp} = 1.08 \times 10^{-5}\ yr^{-1}$. This date was used besides four others as new evidence for the antiquity of man in North America (Bada, Schroeder, and Carter 1974). The oldest racemization date in this suite of specimen was 48,000 years for SDM-16704, also called "The Del Mar Skeleton" which Spencer Rogers (1963) described earlier. Recently, Bischoff and Rosenbauer (1981) determined an age of 11,300 (+1300 -1200) years for the same skeleton (SDM-16704) by uranium series dating. If, indeed, the 48,000-year-old skeleton were actually 11,300 years old, then the 28,000-year-old specimen might also be more recent and datable by ^{14}C in the 200ml counter at UCLA.

For a direct bone ^{14}C date, ca 50g of bone were treated to isolate the gelatine fraction. After processing, the age was 1850 ± 200 yr. As a double check, a second set of bone fragments was treated similarly and dated at 1930 ± 200 yr. This compares with an age of 1770 ± 790 yr determined independently at the Riverside ^{14}C laboratory (UCR-1511D) and discussed in this volume by Taylor (1983). Consequently, SDM-16755 is actually $<$ 2000 yr old. The discrepancy between ^{14}C and racemization dates may be caused by the need for a revised racemization rate based on a better localized environmental estimate for the Del Mar site. The ^{14}C age for SDM-16755 raises the question of whether the Del Mar skeleton (SDM-16704) also is really much more recent, in line with the uranium series date. However, it should be noted that elsewhere, good correspondence has been found between ^{14}C and racemization dates (Bada et al, 1974).

Another bone sample, UCLA-2347, from the tar pits of Rancho La Brea was dated to determine whether deer occupied the Rancho La Brean landscape of the Late Pleistocene. The amino acids native to bone were isolated according to the chromatographic procedure by Ho, Marcus and Berger (1969).

A 1000 minute count showed overnight that the deer bones were < 300 yr old and did not belong to the prehistoric fauna of the site.

Finally, to illustrate Late Pleistocene dating capability, a small bone sample from Lake Taguatagua, Chile was dated to assess the age of a large deposit of animal bones found in a former marsh environment near the perimeter of a lagoon. After collagen isolation and purification with dilute sodium hydroxide, the sample was assayed and calculated to be 15,210 ± 910 yr old (UCLA-2315A). Counting time for this sample was 5900 minutes or ca 4 days.

Ultimately, we hope that accelerator-based dates combining short measuring times and even smaller samples sizes with small standard deviations will become available. In the meantime, appropriately designed small gas counters can perform effectively many duties bridging the gap between liter-sized gas counters and accelerators.

ACKNOWLEDGMENTS

The design and construction of this counting equipment was funded by the State of California. Bone samples were provided by C W Meighan (UCLA), Antonia Tejada-Flores (Page Museum, Los Angeles), and Ruth Tyson (San Diego Museum of Man). D McJunkin assisted in the measurement of samples. This is publication 2345, Institute of Geophysics and Planetary Physics, UCLA.

REFERENCES

Bada, J L, Schroeder, R A, and Carter, G, 1974, New evidence for the antiquity of man in North America deduced from aspartic acid racemization: Science, v 184, p 791-793.

Bada, J L, Schroeder, R A, Protsch, R, and Berger, R, 1974, Concordance of collagen-based radiocarbon and aspartic acid racemization ages: Proc US Natl Acad Sci, v 71, p 914-917.

Berger, R and Libby, W F, 1967, UCLA radiocarbon dates VI: Radiocarbon, v 9, p 477-504.

Bischoff, J L and Rosenbauer, R J, 1981, Uranium series dating of human skeletal remains from the Del Mar and Sunnyvale sites, California: Science, v 213, p 1003-1005.

Harrington, M R, 1933, Gypsum Cave, Nevada: Southwest Mus Papers, no. 8.

Ho, T Y, Marcus, L F and Berger, R, 1969, Radiocarbon dating of petroleum-impregnated bone from tar pits at Rancho La Brea, California: Science, v 164, p 1051-1052.

Libby, W F, 1952, Radiocarbon Dating: Chicago, Univ Chicago Press.

Longin, R, 1971, New method of collagen extraction for radiocarbon dating: Nature, v 230, p 241-242.

Polach, H, Soini, E, Kajola, H, Robertson, S, and Kaihola, L, 1982, Radiocarbon dating of milligram-size samples using gas proportional counters: An evaluation of precision and of design parameters: Wallac Rept.

Protsch, R (ms), 1973, The dating of Upper Pleistocene subsaharan fossil hominids and their place in human evolution with morphological and archaeological implications: PhD dissert, UCLA.

Rogers, S, 1963, The physical characteristics of the aboriginal La Jollan population of Southern California: San Diego Mus Papers, No. 4.

Taylor, R E, 1983, Non-concordance of radiocarbon and amino acid racemization-deduced age estimates on human bone, in Stuiver, M and Kra, R S, eds, Internatl ^{14}C conf, 11th, Proc: Radiocarbon, v 25.

[Radiocarbon, Vol 25, No. 2, 1983, P 661-666]

RADIOCARBON DATABASE: A PILOT PROJECT

STEINAR GULLIKSEN

Radiological Dating Laboratory, The Norwegian
Institute of Technology, Trondheim, Norway

ABSTRACT. Computer storage and surveys of large sets of data should be an attractive technique for users of ^{14}C dates. Our pilot project demonstrates the effectiveness of a text retrieval system, NOVA STATUS. A small database comprising ca 100 dates, selected from results of the Trondheim ^{14}C laboratory, is generated. Data entry to the computer is made by feeding typewritten forms through a document reader capable of optical character recognition. A text retrieval system allows data input to be in a flexible format. Program systems for text retrieval are in common use and easily implemented for a ^{14}C database.

INTRODUCTION

The value of information is, of course, dependent on its accessibility to users. This basic principle is obviously valid for the information contained in the rapidly increasing multitude of ^{14}C dates. Global accumulation rate of dates is probably > 20,000 a year. For scientists using ^{14}C dates, keeping "up-to-date" can be quite laborious.

A gallup poll of the majority of Norwegian scientists using ^{14}C dates revealed that more than 90% would like to see the establishment of a ^{14}C database, for efficient and thorough information retrieval. At Ninth International Radiocarbon Conference a recommendation was made to set up a format for reporting dates compatible with computer-assisted information retrieval (Berger and Suess, 1979). Otlet and Walker (1981) discussed the possible development of their system for filing and reporting dates into a database suitable for information retrieval. Polach (1980) tackles the problems of retrieving ^{14}C data through a bibliographic approach. Expensive searching through eight relevant databases yields unsatisfactory recovery due to the multidisciplinary nature of radiocarbon literature; consequently, a specialized bibliography is necessary for efficient retrieval.

DATABASE DESIGN

A pilot project was initiated to evaluate database design for storage and retrieval of ^{14}C dates. Information contained in a database may vary from pure text to sets of numerical or numerically-coded data. Typical for the data associated with a ^{14}C date is the combination of these types of data. The text that describes the environmental background of a sample, the general aspects of the research project of which the sample is a part, and the specific chronologic goal of the measurement, could all be coded by using selected descriptive categories. An information retrieval system that provides for a search in free text will permit the entry of such data with restrictions only on space and relevant terminology and abbreviations.

Users of dates produced by the Trondheim ^{14}C laboratory were asked to suggest parameters that should be available for searching the database. Such a variety of terms appeared that we decided to consider a system able to search in free text, ie, specific dates could be recovered by searching for any term or combination of terms that appears in the description of the date. The output from this type of database would be less cryptic.

We consulted the Norwegian Computing Center for the Humanities, at The University of Bergen. Their system, NOVA STATUS, is a redesigned and extended version of the STATUS I system developed at AERE Harwell, England. We considered this system suitable for our project.

DATA INPUT FORMAT

All information associated with a ^{14}C date is contained in a document assigned to this date. Descriptive parts of the document will be in free text, but a relatively large part of the information is formalized, ie, given in standardized format, eg, numerically arranged. To obtain high retrieval efficiency for such mixture of free text and formalized data, we must structure the documents. This is done by reserving fields in the document for formalized information with assigned prefixes.

We try to conform to the extent of information given in RADIOCARBON date lists, assuming that the optimum compromise between precision and space requirements is represented by the date list layout.

Data entry can be made in several modes; the choice will mainly depend on the availability of computer peripherals. University mainframe computers are preferred for housing the database, with access through a local terminal, which is also convenient for updating the file. The documents may be prepared gradually along sample routing through the dating process, appearing as an extract from computerized laboratory household routines. Printouts of date reports, date lists, laboratory status reports, etc (Otlet and Walker, 1981) can be

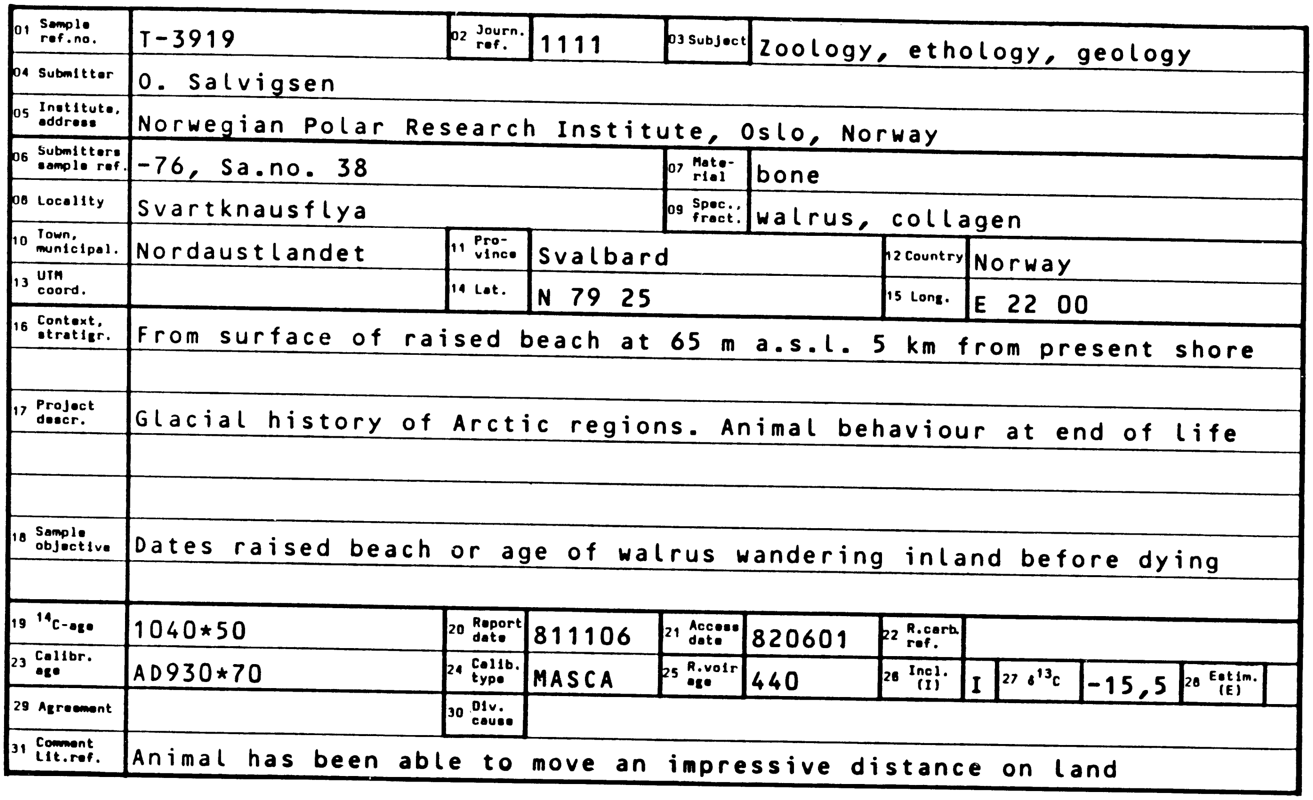

01 Sample ref.no.	T-3919	02 Journ. ref.	1111	03 Subject	Zoology, ethology, geology						
04 Submitter	O. Salvigsen										
05 Institute, address	Norwegian Polar Research Institute, Oslo, Norway										
06 Submitters sample ref.	-76, Sa.no. 38	07 Mate-rial	bone								
08 Locality	Svartknausflya	09 Spec., fract.	walrus, collagen								
10 Town, municipal.	Nordaustlandet	11 Pro-vince	Svalbard	12 Country	Norway						
13 UTM coord.		14 Lat.	N 79 25	15 Long.	E 22 00						
16 Context, stratigr.	From surface of raised beach at 65 m a.s.l. 5 km from present shore										
17 Project descr.	Glacial history of Arctic regions. Animal behaviour at end of life										
18 Sample objective	Dates raised beach or age of walrus wandering inland before dying										
19 ^{14}C-age	1040*50	20 Report date	811106	21 Access date	820601	22 R.carb. ref.					
23 Calibr. age	AD930*70	24 Calib. type	MASCA	25 R.voir age	440	26 Incl. (I)	I	27 δ^{13}C	-15,5	28 Estim. (E)	
29 Agreement		30 Div. cause									
31 Comment Lit.ref.	Animal has been able to move an impressive distance on land										

Fig 1. Sample form for optical document reading - all the information is for one ^{14}C date.

incorporated into the system. A microcomputer employed as a terminal should be useful for this purpose.

For the pilot project, dates previously produced by the Trondheim laboratory were selected. Optical document reading is preferred for the data entry. The information is typewritten, using the IBM OCR-B font designed for optical character recognition, on forms with guidelines for document structure printed in a non-reproducible color. Documents can be prepared off-terminal by personnel without computer experience and at convenient periods. Figure 1 shows a completed form.

THE SEARCH

Entering a search session, the system requests identification. Several security levels can be defined for different sections, allowing retrieval only for password-holders at the appropriate priority level. The search is activated by queries listing search words, phrases, or combinations defined by Boolean operators. As the free text information is based on descriptions supplied by submitters, terminology varies, and the search must include several synonyms to ensure complete recovery of relevant information. For this purpose, it is useful

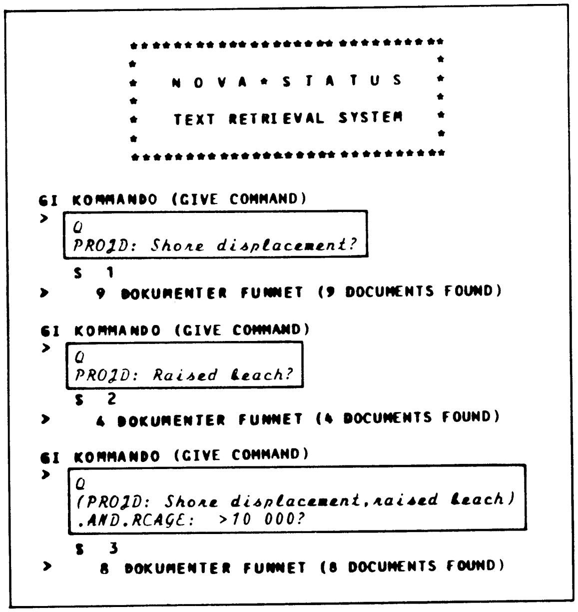

```
*******************************
*                             *
*   N O V A * S T A T U S     *
*                             *
*   TEXT RETRIEVAL SYSTEM     *
*                             *
*******************************

GI KOMMANDO (GIVE COMMAND)
>  Q
   PROJD: Shore displacement?
   S  1
>    9 DOKUMENTER FUNNET (9 DOCUMENTS FOUND)

GI KOMMANDO (GIVE COMMAND)
>  Q
   PROJD: Raised beach?
   S  2
>    4 DOKUMENTER FUNNET (4 DOCUMENTS FOUND)

GI KOMMANDO (GIVE COMMAND)
>  Q
   (PROJD: Shore displacement,raised beach)
   .AND.RCAGE:  >10 000?
   S  3
>    8 DOKUMENTER FUNNET (8 DOCUMENTS FOUND)
```

Fig 2. Search for documents containing expressions "shore displacement" or "raised beach" with ^{14}C age > 10,000 yr.

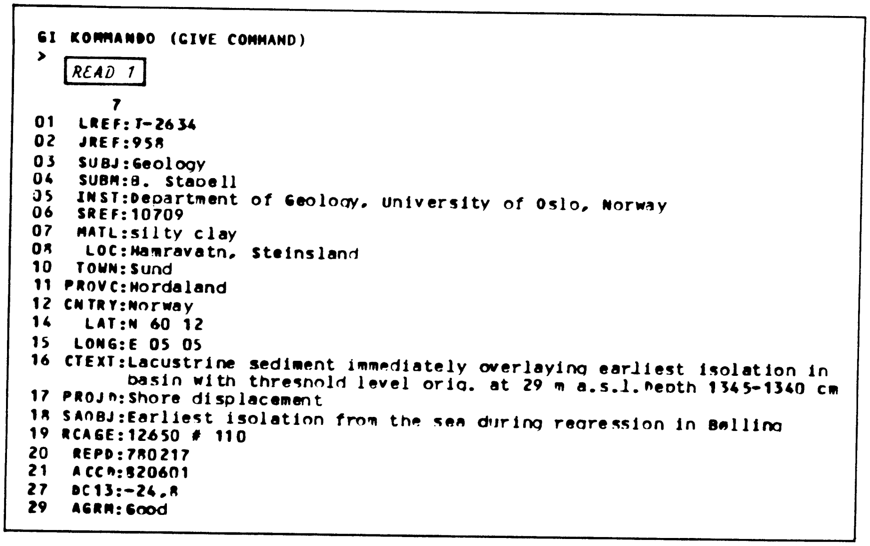

```
GI KOMMANDO (GIVE COMMAND)
> READ 1
      7
01  LREF:T-2634
02  JREF:958
03  SUBJ:Geology
04  SUBM:B. Stapell
05  INST:Department of Geology, University of Oslo, Norway
06  SREF:10709
07  MATL:silty clay
08   LOC:Hamravatn, Steinsland
10  TOWN:Sund
11 PROVC:Hordaland
12 CNTRY:Norway
14   LAT:N 60 12
15  LONG:E 05 05
16 CTEXT:Lacustrine sediment immediately overlaying earliest isolation in
         basin with threshold level orig. at 29 m a.s.l.Depth 1345-1340 cm
17 PROJD:Shore displacement
18 SADBJ:Earliest isolation from the sea during regression in Bølling
19 RCAGE:12650 # 110
20  REPD:780217
21  ACCD:820601
27  DC13:-24.8
29  AGRM:Good
```

Fig 3. Document retrieved in search shown in figure 2.

to define macros, which are groups of synonyms that can be used to retrieve documents in which at least one of the words appear.

Structuring of documents implies that either the whole document or parts of it may be searched. Searching in a field is executed by addressing a prefix assigned to the field. This function is vital, especially when retrieval is based on specific values of numerical data. Relation operators are applied when values within a range are searched. Only numerical data in a standard format can be compared by using relation operators.

The output of a search session may be a complete formatted printout of all documents retrieved, or a short-form presentation defined by users to consist of any desired combination of document fields. Figure 2 shows how the pilot database responds to a search for the expression "shore displacement" or "raised beach" in the project description field.

The query about documents containing either of these expressions and a ^{14}C age $>$ 10,000 resulted in a recovery of eight documents (fig 3).

PROSPECTIVES

Many university computers are linked together by international datanets. If local databases are generated with standardized information formats, simultaneous searches in several databases should be possible. Although conversion programs may enable conversation between different database program systems, they should preferably be of the same type with respect to handling capacity of mixed free text and formalized information. The standardization of an information format and eventually a database system should probably be evaluated by the European Study Group on Physical, Chemical and Mathematical Techniques Applied to Archaeology (PACT).

A new general-purpose information retrieval system has been developed jointly by several Norwegian institutions. It is based on experiences with NOVA STATUS and will be portable, ie, adaptable to any computer equipped with a FORTRAN 77 compiler. The SIFT (Search In Free Text) information retrieval system will be made available free of charge (in English). The Council of Europe will implement the system for retrieving judicial information.

CONCLUSIONS

Retrieval of selected data by searching a database for radiocarbon dates should be of great value to scientists utilizing such data. Standardization of information format is desirable for searches through multinational datanets. Database systems capable of searching in free text are well suited for radiocarbon data.

ACKNOWLEDGMENTS

The pilot database was generated and searched by Sigbjørn Århus at the Norwegian Computing Center for the Humanities. The work was financially supported by the Norwegian Research Council for Science and the Humanities (NAVF).

REFERENCES

Berger, R and Suess, HE, eds, 1979, Radiocarbon dating, Internatl radiocarbon conf, 9th, Proc: Berkeley, Univ California Press, p xii.

Otlet, RL and Walker, AJ, in press, The computer writing of radiocarbon reports and further developments in the storage and retrieval of archaeological data, in Mook, WG and Waterbolk, HT, eds, Internatl symp on ^{14}C and archaeology, 1st, Proc: Strasbourg, PACT, in press.

Polach, D, 1980, The first 20 years of radiocarbon dating, An annotated bibliography, 1948-68; a pilot study, in Stuiver, M and Kra, R, eds, Internatl radiocarbon conf, 10th, Proc: Radiocarbon, v 22, no. 3, p 997-1004.

[Radiocarbon, Vol 25, No. 2, 1983, P 667-668]

DATABASE MANAGEMENT SYSTEMS, RADIOCARBON AND ARCHAEOLOGY

JC MOFFETT and RE WEBB*

Institute of Archaeology, 31-34 Gordon Square,
London WC1H OPY, England

An annotated card index of ^{14}C dates directly relating to Old World cultural material of Palaeolithic and Mesolithic age (>50,000 - ~7000 BP) and New World material older than 7000 BP was compiled in 1972 to include all previously published dates. It is updated annually and currently correct to the end of 1981. The need for such an index to reduce duplication of research time spent in primary data acquisition has long been implicity recognized. Indeed, many such data files may already exist. We wish to discover the nature, scope, and intercompatibility of other lists both to improve our own system and to allow for an exchange of information without unnecessary duplication. Our sources include SCIENCE and NATURE but RADIOCARBON is the major source of information. The general scientific and archaeologic literature has not been systematically searched. Where possible, other published lists have been consulted and additional dates incorporated in our list.

The data file has now been transferred for ease to retrieval to a Z80A microcomputer at the Institute of Archaeology, London. Part of the cost of data input was met by the Department of Archaeology, Cambridge University. The Z80A has a 20 Mbyte hard disk and a single 8-inch double-density double-sided 1 Mbyte floppy disk drive, and uses a CP/M 2.2 operating system but can also read non-CP/M formatted disks, eg, DEC disks. A database has been set up using the MDBS package (MDBS, 1980), which is based on the CODASYL model (Gagle, Koehler, and Whinston, 1981). Retrieval is permitted of all or part of the data file selected by one or any combination of the following keywords: site; layer; culture; sample type; age range. Other options are possible. Detailed information about the structure of the database and its manipulation are given in Moffett and Webb (1983).

Radiometric age determinations are particularly suited to analysis by database management systems since the necessary

---

*Department of Extra-Mural Studies, 26 Russell Square, London WC1B 5DQ, England information can be broken down easily into a number of fields or keywords and selectively retrieved to answer different research problems. Data are input into three files which are updated annually. The main file comprises the individual dates which are broken down into the following fields: site name; site layer; cultural attribution; quality of association; sample type; sample quality; age; error factor; $\delta^{13}C$; laboratory identifier; laboratory number; publication reference. Two separate library files are maintained giving all available site bibliographic information and standard laboratory pretreatment and counting details. The database is primarily intended as a research tool giving keyword access to the full publication of age estimates. Therefore, for a small charge, any interested researcher may request hard copy printout of part or all of the data file for any given range of keywords. For example, it is possible to list all dates for west European Magdalenian sites, or for the South African Later Stone Age, or all dates obtained on bone collagen or mollusk shells. It is hoped that floppy disks of the full database will soon be made available to institutions with compatible host equipment.

REFERENCES

Gagle, M, Koehler, GJ, and Whinston, A, 1981, Database management systems: powerful newcomers to microcomputers: Byte, v 6, no. 11, p 97-122.

Micro Data Base Systems (MDBS), 1980, MDBS data management system documentation: Lafayette, Indiana, Micro Data Base Systems Inc.

Moffett, JC and Webb, RE, 1983, Database management of radiocarbon dates, in Aspinall, A and Warren, SE, eds, Internatl symposium on archaeometry and archaeological prospection, 22nd, Proc: Bradford, England, Univ Bradford Press, 67-72.

[Radiocarbon, Vol 25, No. 2, 1983, P 669-674]

POSSIBILITIES IN THE DATING OF WRITING MATERIALS AND TEXTILES

RICHARD BURLEIGH and A D BAYNES-COPE

Research Laboratory, The British Museum, London WC1B 3DG, England

This paper discusses the characteristics of the commoner classes of writing materials and textiles deriving from ancient and more recent historical sources and the problems they present for ^{14}C dating. The materials under consideration are, firstly, paper in various forms, parchment, and vellum (ancient papyrus, which poses different kinds of dating problems, is not considered) and secondly, fabrics such as linen, cotton, and woolen textiles, to which, from the dating point of view, similar technical considerations apply. Our main concern is with problems associated with the dating of paper.

The purpose of applying ^{14}C dating to paper (and parchment or vellum) will be to authenticate an archival document ("document" is used here to mean anything written, drawn, or painted on these materials, and "archival" to mean material bearing a date or datable by art-historical methods). Thus, much may depend on the result of any such ^{14}C measurement and an understanding of possible sources of error in the interpretation of the date obtained is of great importance.

Until recently, the relatively large amount of sample needed (ca 10g) has precluded the application of conventional ^{14}C measurement (by standard gas-proportional and liquid scintillation counting methods) to the dating of documents, as it has never been permissible to remove a sufficient quantity of material for worthwhile analysis. The same difficulty has sometimes arisen with ancient textiles, eg, two tunics from Tarkhan, Egypt (Burleigh, Matthews, and Ambers, 1982; Hall, 1982), with which individual garments have been too important to allow even partial destruction for dating (although without a precise date their archaeologic value may have been correspondingly diminished). With the advent of (in R L Otlet's terminology) "micro-" and "mini-" methods of ^{14}C measurement by means of accelerators (Hedges, 1981; Stuiver, 1978) and small counters (Harbottle, Sayre, and Stoenner, 1979; Otlet and Evans, 1982; Sayre et al, 1981), for which a few milligrams or less of sample are needed, the former constraint of minimum sample size has been removed. As a result, among many other important applications, the dating and authentication of a great diversity of hitherto imprecisely dated archaeologic finds and museum objects has become possible. In many, perhaps most, such instances, positive results will be obtained that will have real benefit to scholarship, but in some others the answers may be equivocal or even wrong. This risk applies particularly to the dating of paper documents and it is with the consequences of the inevitable application of the new methods to these (and not the technical aspects of the methods themselves) that this paper is chiefly concerned. The procedures suggested for the preparation of paper for dating (see Appendix) are appropriate also to textiles, although dates for textiles will not necessarily share the same sources of possible error. To explain the sources of systematic error to which ^{14}C dates for paper will be subject (apart, that is, from the random errors inherent in all ^{14}C measurements, and errors of the ^{14}C time scale itself), it is necessary to give a summary of the technological history of paper manufacture.

Until the early 1840s, paper was made from shredded and pulped cellulose rags (cotton and linen). These were indiscriminately collected and may have been of any age, perhaps commonly up to 100 years old, but the use of mummy wrappings from Ancient Egypt for paper manufacture in the mid-19th century has also been recorded (Hunter, 1957). This is an extreme example, but it serves to illustrate the nature of the problem. After ca 1840 the use of rags for paper manufacture was superseded by the introduction first of mechanical and later of chemical wood pulp, although a limited amount of higher quality rag paper is still made today for specialized uses. Wood pulp averages the age of the (de-barked) trees from which it is manufactured and again probably incorporates material representing up to 100 years or more of growth. Esparto (grass) papers, although in principle "annual," may also incorporate wood fibers. The practice of re-pulping paper, although known from China as early as ca AD 1380, was not in use in Europe before 1800. Thus, it is evident that any apparent age obtained for paper will antedate its manufacture and use, sometimes by a large margin (also, paper may have been stored for a considerable period before use). From this it is clear that the only valid ^{14}C date for a paper document will be one that is significantly older than its purported historical date. Even so, this will not always be sufficient proof of the authenticity of that document which must ultimately rest upon independent evidence such as handwriting (Harrison, 1958), although it may indicate that it is contemporaneous, or at the very least not inconsistent with, the age expected on historical grounds. By contrast, parchment and vellum were made from the skins of young animals (sheep or goat and calf, respectively), generally used soon after manufacture, and therefore, can be expected to have much smaller, usually negligible, apparent ages. Nevertheless, long after first use, parchment and vellum were often cleaned to remove the original ink and re-used, such documents being known as palimpsests. Similarly, although the basic textiles of antiquity - linen, wool, and silk - were probably manufactured from the products of a single season's growth more or less immediately after harvesting, re-use, in particular of wool for the manufacture of felt, is to be considered. A date for a textile provides essentially a *terminus post quem* as the period of time over which it was in use may remain indeterminate, while it is the date of the making of a document, the single event of the use of the paper, that is principally of interest, which may differ widely from the apparent ^{14}C age of the paper.

Finally, as a result of natural ^{14}C variations over the last few hundred years, a single measured ^{14}C age may correspond ambiguously to more than one alternative calendar date (Stuiver, 1982).

In view of these problems and the abundant historical documentation of almost all aspects of paper manufacture and technology, it is essential that a detailed technical examination of any document should be carried out before it is subjected to ^{14}C dating. If ^{14}C dating is to be used for this purpose at all it should be applied with a reluctance amounting to last resort. From an essentially non-destrictive preliminary examination of a paper document, such highly diagnostic features as the kind of fibers of which it is composed and their mode of preparation, the presence of specific chemical substances (eg, aluminum sulphate in modern papers), the nature of the size used, the use of "wove" or "laid" paper, the spacing of laid lines, the ink, and above all, watermarks, can all be determined (the last by beta-radiography, a mandatory procedure). A combination of the information obtained in this way may provide very precise historical dating as well as an indication of provenance, although it should be noted that, strictly, it is the application of the ink alone that dates the document. It would be difficult to obtain an adequate sample of the ink itself for ^{14}C dating and to add to this difficulty, ink may sometimes contain dead carbon. In contrast, therefore, to the precise information that will most probably be obtained from detailed technical examination of a document, it is unlikely that its age can be resolved satisfactorily by the application of ^{14}C dating, the results of which are more likely to provide confirmation of known trade practices in the manufacture and use of paper than an exact date (disregarding the additional problem of the ambiguities in the recent ^{14}C time scale). An example of the kind of "corroborative" application that might, however, be worth attempting is the dating of printed documents bearing, say, 16th or 17th century dates (and often of great value today if genuine), but on paper with unrecorded watermarks believed to be much later, perhaps 18th century date, implying later discovery and re-use of the original printing blocks (Baynes-Cope, 1981; Burleigh, 1981). The parchment of the Vinland Map, on the other hand, would probably not be datable as it is almost certainly a palimpsest made using ink that analysis has shown to be of 20th century origin (Baynes-Cope, 1974; McCrone and McCrone, 1974).

In summary and in conclusion, the only unequivocal application of radiocarbon dating to documents appears to be for invalidation purposes, where a document purporting to be much earlier was actually made from material incorporating artificial ^{14}C derived from thermonuclear weapon tests, in which the characteristic bomb-carbon signal can be observed. The dating of textiles by the new micro- and mini-methods of ^{14}C measurement appears much less problematic and, within the limits of resolution of the radiocarbon time scale, reliable results for these materials should be obtainable.

APPENDIX. Chemical pretreatment of paper and textiles before radiocarbon dating

The purpose of the pretreatment of paper and textiles is to isolate the original cellulose or protein, removing altogether other substances that may have been added during manufacture and which may contain carbon. For paper, these may include glue (or rosin), size, starch, casein, chalk, oils, gums and resins, and coloring such as Prussian blue, ultramarine, or indigo. Of these, generally only dyes were added to textiles (procedures for pretreatment of textiles have already been proposed by Elmore et al, 1981, and by Harbottle, Stoenner, and Sayre, 1981, with particular reference to the Turin Shroud). Preliminary standard tests should be made for evidence of heavy sizing (cold water does not wet paper), the presence of starch (addition of 0.1% iodine solution gives blue color), resins (drop of alcohol/chloroform produces ring), and for blue papers, Prussian blue (slowly turned brown by a drop of 10% NaOH), ultramarine (fades quickly with addition of 10% HCl), indigo (unchanged by solutions of acid or alkali). A generalized procedure that will remove all of these added substances from paper (and textiles) without destroying cellulose or protein fibers, simultaneously removing extraneous organic and other contaminants, and give a clean sample containing up to approximately 40% by weight of carbon ready for conversion to elemental carbon or CO_2 for ^{14}C measurement, is as follows: soak in cold, de-ionized water for 1 hour (use preliminary protease digestion if paper proves unwettable); boil for 1 hour in water; boil in 5% NaOH to disintegrate material into separate fibers, centrifuge, rinse with hot water; add 5% HCI (break up wad of fibers), warm, centrifuge, rinse to neutrality and dry ready for radiochemical conversion and final analysis. Additions or modifications to this procedure that may be needed are solvent extraction of persistent dyes, bleaching of persistent brown coloration with sodium chlorite/formaldehyde, and the substitution of dilute (5%) ammonia solution for NaOH, for the pretreatment of woolen textiles; silk that has disintegrated badly with age would be much more difficult to pretreat successfully and any such samples would need to be separately considered.

REFERENCES

Baynes-Cope, AD, 1974, The scientific examination of the Vinland Map at the Research Laboratory of the British Museum, in The strange case of the Vinland Map (Symposium Royal Geog Soc, London, Feb 4, 1974, paper 7): Geog Jour, v 140, pt 2, p 208-211.

__________ 1981, The investigation of a group of globes: Imago Mundi, v 33, p 9-19.

Burleigh, Richard, 1981, Note on radiocarbon (dating) of the Ambassadors' Globe: Imago Mundi, v 33, p 20.

Burleigh, Richard, Matthews, Keith, and Ambers, Janet, 1982, British Museum natural radiocarbon measurements XIV: Radiocarbon, v 24, p 229-261.

Elmore, D, Gove, HE, Beukens, RP, Litherland, AE, Purser, KH, and Rubin, M, 1981, A method for dating the Shroud of Turin, in Sox, HD, 1981, The image on the Shroud - is the Turin Shroud a forgery?: London, Unwin, p 163-169.

Hall, RM, 1982, Garments in the Petrie Museum of Egyptian Archaeology: Jour Textile Hist and Conserv, v 13, pt 1, p 27-45.

Harbottle, G, Sayre, EV, and Stoenner, PW, 1979, Carbon-14 dating of small samples by proportional counting: Science, v 206, p 683-685.

Harbottle, G, Stoenner, RW, and Sayre, EV, 1981, Procedure for the treatment of historical linen fabrics before carbon-14 dating, in Sox, HD, 1981, The image on the shroud - is the Turin Shroud a forgery?: London, Unwin, p 170.

Harrison, WR, 1958, Suspect documents, their scientific examination: London, Sweet & Maxwell, 583 p.

Hedges, REM, 1981, Radiocarbon dating with an accelerator-review and preview: Archaeometry, v 23, p 3-18.

Hunter, D, 1957, Papermaking, the history and technique of an ancient craft (2nd ed): London, Cresset Press, 611 p.

McCrone, WC and McCrone, LB, 1974, The Vinland Map ink, in The strange case of the Vinland Map (Symposium Royal Geog Soc, London, Feb 4, 1974, paper 8): Geog Jour, v 140, pt 2, p 212-214.

Otlet, RL and Evans, GV, in press, Progress in the application of miniature gas counters to radiocarbon dating of small samples in Mook, WG and Waterbolk, HT, eds, Internatl symposium on C-14 and archaeol, 1st, Proc: Groningen, PACT Jour, in press.

Sayre, EV, Harbottle, G, Stoenner, RW, Otlet, RL, and Evans, GV, 1981, Small gas proportional counters for the carbon-14 measurement of very small samples, in Methods of low-level counting and spectrometry: Vienna, IAEA, p 393-407.

Stuiver, Minze, 1978, Carbon-14 dating - a comparison of beta and ion counting: Science, v 202, p 881-883.

________ 1982, a high-precision calibration of the AD radiocarbon time scale: Radiocarbon, v 24, p 1-26.

VIII. TECHNICAL ASPECTS OF ACCELERATOR MASS SPECTROMETRY

[Radiocarbon, Vol 25, No. 2, 1983, P 677-691]

ACCELERATOR MASS SPECTROMETRY: FROM NUCLEAR PHYSICS TO DATING*

WALTER KUTSCHERA
Argonne National Laboratory, Argonne, Illinois 60439

INTRODUCTION

One of my former teachers in nuclear physics, H Morinaga, once pointed out to me that essentially all the fundamental discoveries in nuclear physics were done without the use of accelerators. At first, this statement seemed extremely exaggerated, but now I think there is much truth in it. Once we build an instrument to investigate a specific problem we have already realized the existence of the problem and do not need the instrument to discover it. It is almost inevitable that the most interesting discoveries with a new technique will be made in fields for which the technique was not invented. Accelerators, built for nuclear physics, produced a great amount of data on nuclear structure and forces but the most fundamental discoveries were made in elementary particle physics. In any case, for almost 40 years the sole purpose of accelerators was to deliver beams of ever increasing energy and versatility to perform experiments _after_ the accelerator. The analytic properties of accelerators were almost completely ignored even after the very early use of the Lawrence cyclotron at Berkeley as a mass spectrometer to discover ^{3}He in nature (Alvarez and Cornog, 1939 a; b). The enormous analytic power of accelerators is now fully recognized, but the joy of the revival is mixed with some disappointment that the great prospects for studying ^{14}C problems (Muller, 1977; Bennet _et al_, 1977; Nelson, Korteling, and Stott, 1977) have not yet been fulfilled. Fortunately, some of the papers of this conference show that a big step forward has been taken. But in view of what I said before it is not surprising that most of the studies were actually done with other radioisotopes.

Part of the reason for this situation is that Accelerator Mass Spectrometry (AMS) is independent of half-life and decay characteristics which allows for the selection of almost any radioisotope. Since the precision of conventional ^{14}C measurements cannot easily be achieved with such a highly

---

*Work supported by the U S Department of Energy under Contract W-31-109-Eng-38. This paper is from an invited talk.

complex instrument as an entire accelerator system, it is no wonder that interest first focused on other radioisotopes. Figure 1 gives an overview of the ca 140 radioisotopes with half-lives greater than one year. For shorter half-lives, decay counting will almost always be more practicable. It is interesting to note that ^{14}C is the only convenient radioisotope in a half-life range of almost two decades (5×10^2 to 5×10^4 yr). A similar outstanding position is occupied by ^{40}K. Only a very small fraction of the radioisotopes shown in the figure has been touched by AMS. A fairly complete account of ongoing and future AMS projects can be found in Henning et al (1981a). It seems quite possible that the whole range of radioisotopes (fig 1) will eventually be accessible to AMS. This will largely be determined by the energy of heavy ion beams available at the future generation of accelerators.

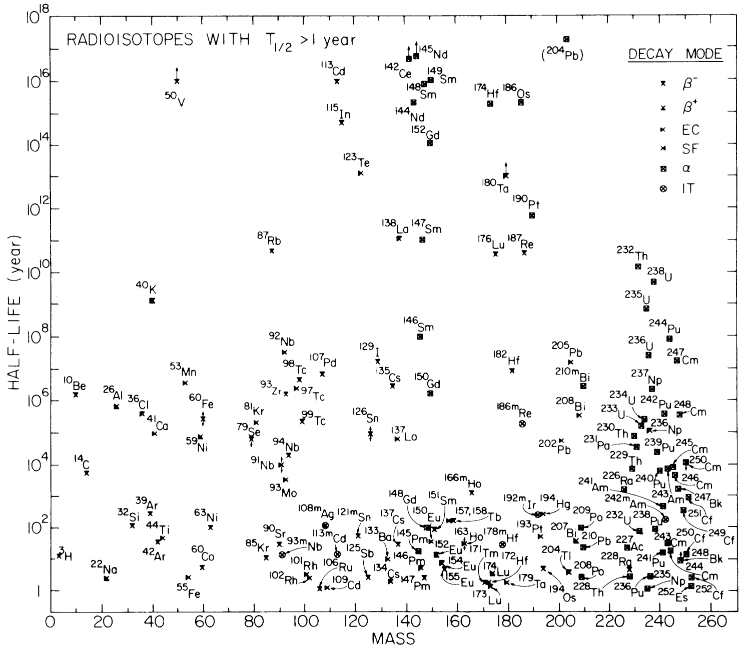

Fig 1. Overview of long-lived radioisotopes. Data are taken from Lederer and Shirley (1978) except ^{32}Si (Kutschera et al, 1980; Elmore et al, 1980) and ^{202}Pb (Nagai, Nitoh, and Honda, 1981). Arrows on data points indicate that the half-life is only approximately known in the respective direction. Isotopes in brackets are of uncertain assignment.

SOME TECHNICAL ASPECTS OF AMS

Figure 2 shows the key for high-energy mass spectrometry, namely, the energy-loss separation of isobaric ions in matter. Since for every radioisotope below Bi there is a stable isobar in nature (except for mass 5 and 8), the main problem in AMS is to separate these usually interfering ions from the radioisotope ions. For an efficient separation, ion energies above the maximum in the energy loss curves are required. In this region, most of the electrons (> 70%) are removed from the ions and the Z^2/v^2 dependence of the energy loss (Bethe, 1930) results in a good separation of isobars especially for the lighter ions. Qualitatively, heavy ions passing swiftly through matter lose all the electrons for which orbital velocity is smaller than ion velocity (Bohr, 1940). Since the velocity of the innermost electrons increases proportionally to the atomic number Z, very high energies are required to strip off these electrons for the heavier ions. The dramatic increase in energy required to match the velocity of the last electron (hydrogen-like atom) is shown in figure 3. At these high energies, a relatively large fraction (> 10%) of the ions are fully stripped and a

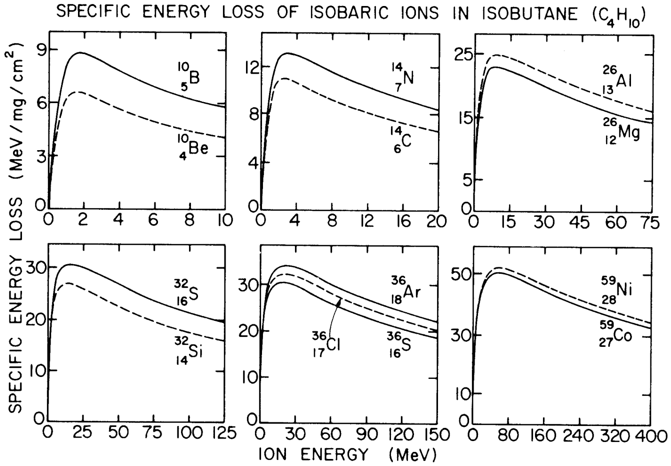

Fig 2. Energy loss in a typical counter gas of a heavy ion detector. The compilation of Ziegler (1980) was used to calculate the solid and dashed curves for stable and radioactive isotopes, respectively. N, Mg, and Ar do not form negative elemental ions (Mg and N, however, form negative hydride ions) and are, therefore, greatly suppressed in AMS with tandem accelerators.

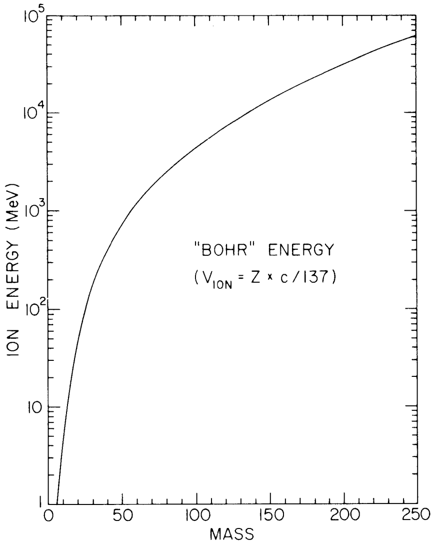

Fig 3. Ion energy required to strip off all but the last electron. According to Bohr (1940), all electrons with an orbital velocity smaller than the ion velocity are lost. At the "Bohr" energy, ca 10-20% of the ions are fully stripped.

separation of the radioisotope from the interfering stable isobar by magnetic or electrostatic devices is possible if the radioisotope has the higher Z (eg, ^{26}Al, ^{36}Cl, and ^{59}Ni in fig 2). The feasibility of this technique has been demonstrated for the isobar pairs ^{26}Al - ^{26}Mg (Raisbeck and Yiou, 1979), ^{41}Ca - ^{41}K (Raisbeck and Yiou, 1980), ^{59}Ni - ^{59}Co (Henning et al, 1981), and ^{36}Cl - ^{36}S (Gustavsson et al, 1981). Figure 4 gives an example of the ^{59}Ni - ^{59}Co separation when the tandem energy of 93.5 MeV was boosted to 328 MeV with the new superconducting linac at Argonne and the fully-stripped ions were separated magnetically. Table 1 gives the fraction of fully-stripped ions at energies presently available at Argonne. It is evident that much higher energies (cf fig 3) are required for an efficient stripping of Ni and Co . These will be available within a few years at Argonne and other new-generation heavy ion facilities. A drawback of these more complex accelerator systems is that they often require a beam feedback signal for a stable operation (eg, to synchronize the pulsing system of a dc beam from a tandem with the rf of a linac post-accelerator). Thus, the "zero-beam" radioisotope acceleration mode is not possible. The background beam of an ion-optically identical particle (^{59}Co in our example) must be

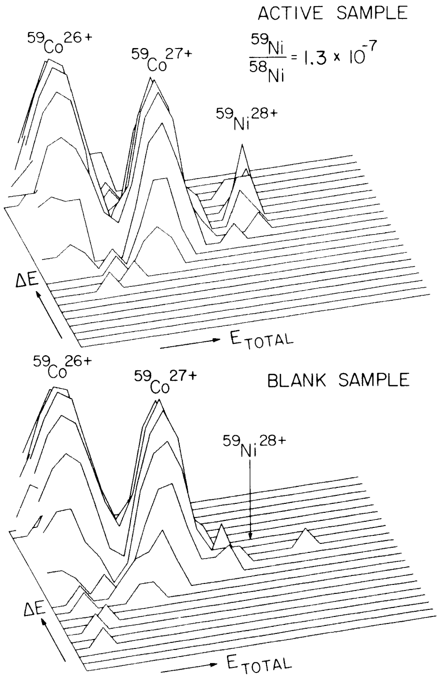

Fig 4. E_{total} vs ΔE spectra measured in a Si ΔE-E telescope detector system. Ions of 328 MeV were stripped in a 100μg/cm^2 carbon foil and separated with a magnet set to accept mass-59, charge-28+ ions of full energy. The ^{59}Co background beam was 10^7 times stronger than the ^{59}Ni component before the charge state separation.

raised to the level required for the generation of the feedback signal. Although such an operation can guarantee long-term stability of the system, it has severe effects on the radioisotope detection sensitivity. The development of sophisticated beam pick-up devices operating at extremely low current levels are required if the sensitivity of free-running accelerators is to be matched.

SEARCH FOR THE UNKNOWN

One of the most exciting applications of AMS is the search for hitherto unobserved particle species (eg, quarks, anomalously heavy isotopes). Since particles with properties very different from normal matter are generally sought, the background can be very low and, consequently, the sensitivity very high. The main problem in these studies is that we are

TABLE 1. Some highly stripped heavy ion beams from the Argonne tandem-superconducting linac system

Ion	Energy (MeV)	Charge state	Fraction* (%)	"Bohr" energy** (MeV)
$^{17}_{8}O$	130	7^+	16	25
		8^+	84	
$^{35}_{17}Cl$	165	16^+	39.5	251
		17^+	11.5	
$^{40}_{20}Ca$	170	19^+	6.3	397
		20^+	0.4	
	260	19^+	33.7	
		20^+	8.7	
$^{59}_{27}Co$	328	26^+	0.97	1067
		27^+	0.023	
$^{58}_{28}Ni$	314	27^+	0.45	1128
		28^+	0.014	

*Measured after stripping in a 100μg/cm^2 carbon foil except ^{17}O where a 150μg/cm^2 gold foil was used.
**See figure 3

searching in the dark and must take great care to reliably scan a certain parameter space. Figure 5 summarizes searches for anomalously heavy isotopes (Klein, Middleton, and Stephens, 1981). Not included in this figure is the search for anomalous hydrogen in extremely enriched D_2O with a low-energy time-of-flight spectrometer (Smith _et al_, 1981). Due to the large enrichment factor (~ 10^{11}), extremely low limits on the concentration of heavy hydrogen in normal hydrogen (~ 10^{-30}) were reported.

The experimental limits for the concentration of the different species measured so far are all considerably lower than the theoretical predictions. These are based on considerations of the early universe, where, under extreme conditions of the big bang, a certain fraction of anomalous particles may have formed and survived until today. Although none of the searches have yet yielded positive result, they will be continued as long as we are curious.

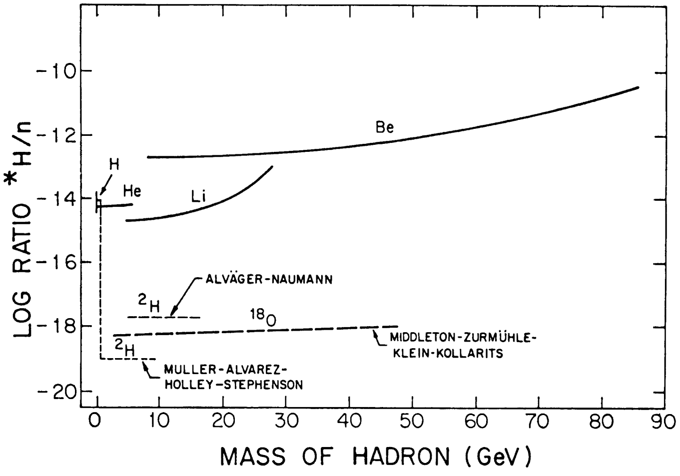

Fig 5. Summary of searches for anomalously heavy isotopes of various elements (Klein *et al*, 1981). He, Li, Be, and ^{18}O measurements were done with a tandem (Middleton *et al*, 1979; Klein *et al*, 1981), one ^{2}H search with a mass separator (Alväger and Naumann, 1967), and the other H and ^{2}H searches with a cyclotron (Muller *et al*, 1977).

ON THE USE OF COSMOGENIC RADIOISOTOPES

As mentioned above, the half-life of a radioisotope is not a limiting factor for the AMS technique. What counts most is the beam current from the sample. Since most of the AMS experiments use tandem accelerators, the efficiency of negative ion formation largely determines the lower detection limit. For many elements, negative ion beams of ca 1μA (~ 6 x 10^{12} ions/sec) can be produced. If we assume a 10% transmission from the ion source to the detection system (including charge state selection) and one count per hour as the lower limit to detect a radioisotope ion in a background-free condition, then we reach a radioisotope abundance limit of ca 10^{-15}. In practice, this limit may well turn out to be several orders of magnitude higher. Low negative ion yield, low transmission, and high background level can be reducing factors. It is interesting to note that, by far, the most used radioisotope in AMS, ^{10}Be, falls into the latter category.

Figure 6 gives an overview of the abundance of cosmogenic radioisotopes in various samples (Nishiizumi and Arnold, 1981). In general, the abundance is larger for extra-terrestrial material since the radioisotope is not diluted by

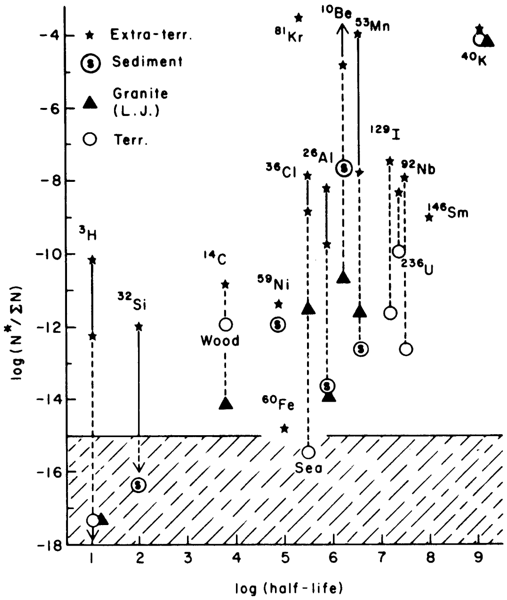

Fig 6. Ratio of cosmogenic radioisotopes, N*, to the sum of the respective stable isotopes, ΣN, as a function of the half-life in years in various natural materials (Nishiizumi and Arnold, 1981). The hatched area shows the detection limit of AMS for the most favorable conditions. Enrichment processes prior to the AMS measurement could lower the limit further.

the large reservoir of stable isotopes on earth. ^{10}Be has an exceptionally high abundance even in terrestrial material because of the low abundance of stable Be in nature (Suess and Urey, 1956). The high abundance makes it relatively easy to measure ^{10}Be/^{9}Be ratios with AMS despite the difficulties mentioned above. In addition, the specific energy loss separation of ^{10}Be from the interfering ^{10}B background is large (cf fig 2). Figure 7 summarizes AMS measurements with ^{10}Be. It shows that ^{10}Be has been measured in many different reservoirs covering a large range of concentrations. This great use is due to some outstanding properties of ^{10}Be : 1) high production rate in the atmosphere by spallation of nitrogen and oxygen (Lal and Peters, 1967), 2) short residence time in the atmosphere of about one year which makes it useful to study secular variations in the production rate with possible implications on cosmic ray variations (Raisbeck and Yiou, 1981; Wahlen et al, 1982), 3) long half-life (1.6×10^6 yr) which allows us to study slow geophysical processes such as the growth rate of manganese nodules (Turekian et al, 1979) and the mixture of deep-sea sediments into lava (Brown et al, 1982).

As demonstrated in the pioneering work at Orsay (Raisbeck et al, 1978b; a) and in many measurements of this group thereafter, ^{10}Be can well be measured with a cyclotron. Although, at present, all other work in AMS is done with tandems, the cyclotron or any other accelerator starting with positive ions may well turn out to be an important alternative whenever elements are involved which do not easily form negative ions (or not at all as do the noble gases except He).

With respect to dating applications of ^{10}Be and other radioisotopes now available through AMS (eg, ^{26}Al, ^{32}Si, ^{36}Cl), it will be most important to measure ratios of different radioisotopes such as ^{10}Be/^{26}Al or ^{10}Be/^{36}Cl (Raisbeck and Yiou, 1981). In contrast to ^{14}C, there exists

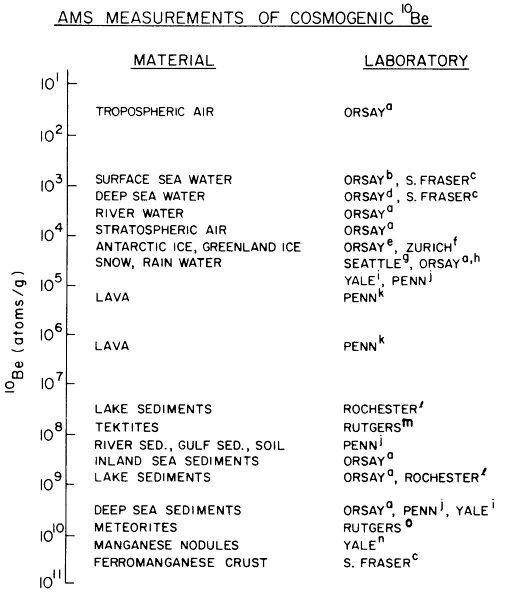

Fig 7. Summary of ^{10}Be measurements in various materials. The ordering is done according to the ^{10}Be concentration measured in the respective materials. [a]Raisbeck et al (1981), [b]Raisbeck et al (1979a), [c]Nelson et al (1983), [d]Raisbeck et al (1980), [e]Raisbeck et al (1978a), [f]Beer et al (1983), [g]Farwell et al (1983), [h]Raisbeck et al (1979b), [i]Thomas (1982), [j]Brown et al (1981), [k]Brown et al (1982), [l]Wahlen et al (1982), [m]Pal et al (1982), [n]Turekian et al (1979), [o]Kruse et al (1983).

no well-equilibrated "time-zero" abundance of any of these radioisotopes with respect to its stable isotope(s). The reliability of a date based on the time variation of the ratio of two or more radioisotopes will critically depend on the understanding of the respective chemical and physical fractionation effects.

THE MEASUREMENT OF HALF-LIVES WITH AMS

Perhaps one of the most important contributions AMS can make to dating is the measurement of uncertain or believed-to-be-certain half-lives. I became interested in this subject when I learned at the first conference on AMS at Rochester that the half-lives of some interesting long-lived radioisotopes produced by cosmic rays are still uncertain (Arnold, 1978).

Long half-lives can be determined uniquely from the relation $dN/dt = -\lambda N$, when both the decay rate, dN/dt, and the number of radioisotope atoms, N, is measured. The latter quantity is traditionally measured with low-energy mass spectrometry if sufficient material is available. Much lower radioisotope concentrations can be measured with AMS; thus, the method can be extended to more difficult cases such as ^{32}Si, the half-life of which was assumed to be ca 300 yr. AMS measurements at Argonne (Kutschera et al, 1980) and Rochester (Elmore et al, 1980) on different samples yielded half-lives of 101 ± 18 yr and 108 ± 18 yr, respectively. Figure 8 shows the history of ^{32}Si half-life measurements. First, we note an intriguing trend toward shorter half-life values with time. All the measurements marked with a cross relied on estimates of the respective production cross-sections, since the ^{32}Si concentration was not measured explicitly. Based on more recent cross-section systematics, arguments can be found (Kutschera et al, 1980) to bring these values down to the accelerator results. A serious disagreement exists with the results of two geophysical half-life measurements, where the depth profile of natural ^{32}Si activity was measured in ice-cores from Greenland (Clausen, 1973) and in a varved sediment core from the Gulf of California (Demaster, 1980). Assuming that the AMS results are correct, we are encouraged to measure the decay rate as a function of time for a half-life determination. A measurement over a period of a year or longer with a high-precision differential counting technique (Harbottle, Koehler, and Withnell, 1973) is currently underway at Brookhaven (Alburger, 1982 pers commun). It will hopefully give a decisive answer.

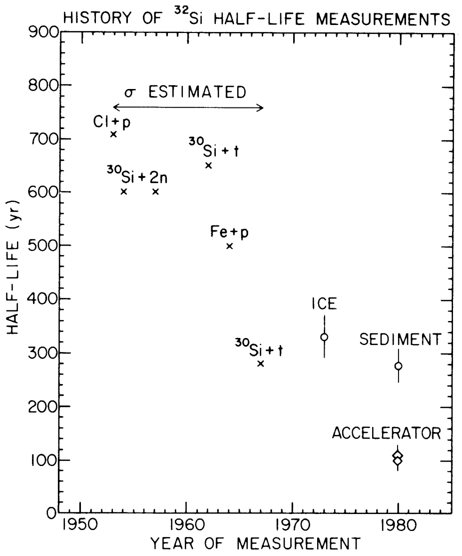

Fig 8. Summary of the attempts to measure a ^{32}Si half-life in the last 30 years (see text for references to the various measurements).

CONCLUSION

The encouraging results on high-precision measurements of $^{14}C/^{12}C$ or $^{14}C/^{13}C$ ratios described in various contributions to this issue justify optimism for this field. Details of the current status of the various facilities can be found in the respective contributions. Ironically, perhaps the strongest reaction to the original excitement about ^{14}C measurements with AMS was the development of miniature gas counters capable of measuring milligram quantities of carbon. The concurrent development of microprocessors allowing the automatic measurement of arrays of counters probably had a strong impact on this field as well.

It is interesting to speculate about a possible correlation between ^{14}C variations and ancient cultural events. Although it seems purely accidental, I should like to mention an amazing coincidence pointed out to me during a recent visit to Jerusalem (Paul, 1982, pers commun)

$T_{1/2}(^{14}C) = 5730 \pm 40$ yr
Genesis (Bible) = 5743 yr B P

ACKNOWLEDGMENTS

I should like to thank HR Andrews, I Brissaud, D Donahue, D Elmore, M Furukawa, J Heinemeier, T Kruse, P Kubik, R Middleton, G Possnert, KH Purser, F Schmidt, J Thomas, G Wallace, and N White for supplying valuable information on ongoing AMS experiments, and CN Davids for critical comments on the paper.

REFERENCES

Alväger, T and Naumann, RA, 1967, Search for stable heavy massive particles of positive integral charge: Physics Letters, v 24B, p 647-648.

Alvarez, LW and Cornog, R, 1939a, ^{3}He in helium: Physical Rev, v 56, p 379; 1939b, Helium and hydrogen of mass 3: Physics Rev, v 56, p 613.

Arnold, JR, 1978, The importance of direct detection of other radioisotopes, in Gove, HT, ed, Conf on ^{14}C dating with accelerators, 1st, Proc: Rochester, New York, p 345-352.

Beer, J Andrée, M Oeschger, H, Stauffer, B, Balzer, R, Bonani, G, Stoller, Ch, Suter, M, Wölfli, W, and Finkel, RC, 1983, Temporal ^{10}Be variations in ice, in Stuiver, M and Kra, RS, eds, Internatl ^{14}C conf, 11th, Proc: Radiocarbon, v 25.

Bennet, CL, Beukens, RP, Clover, MR, Gove, HE, Liebert, RB, Litherland, AE, Purser, KH, Sondheim, WE, 1977, Radiocarbon dating using electrostatic accelerators: Negative ions provide the key: Science, v 198, p 508-510.

Bethe, H, 1930, Zur Theorie des Durchgangs Schneller Korpuskularstrahlen durch Materie: Annals Physics, v 5, p 325-400.

Bohr, N, 1940, Scattering and stopping of fission fragments: Physics Rev, v 58, p 654-655.

Brown, L, Klein, J, Middleton, R, Sacks, IS, and Tera, F, in press, Beryllium-10 in island - arc volcanos and implications about subduction: Nature, in press.

Brown, L, Sacks, SI, Tera, F, Klein, J and Middleton, R, 1981, Beryllium-10 in continental sediments: Earth Planetary Sci Letters, v 55, p 370-376.

Clausen, HB, 1973, Dating of polar ice by ^{32}Si: Jour Glaciology, v 12, p 411-416.

Demaster, DJ, 1980, The half-life of ^{32}Si determined from a varved Gulf of California sediment core: Earth Planetary Sci Letters, v 48, p 209-217.

Elmore, D, Anantaraman, N, Fulbright, HW, Gove, HE, Hans, HS, Nishiizumi, K, Murrel, MT, and Honda, M, 1980, Half-life of ^{32}Si from tandem-accelerator mass spectrometry: Phys Rev Letters, v 45, p 589-592.

Farwell, GW, Grootes, PM, Leach, DD, Schmidt,FH, and Stuiver, M, 1983, Current ^{14}C measurements with the University of Washington FN tandem accelerator, in Stuiver, M and Kra, RS, eds, Internatl ^{14}C conf, 11th, Proc: Radiocarbon, v 25.

Gustavsson, S, Korschinek, G, Kubik, PW, Morinaga, H, Nolte, E, and Pravikoff, MS, 1981, Nachweis mikroskopischer Mengen von ^{36}Cl: Ann rept tandem lab, Tech Univ Munich, p 104-105.

Harbottle, G, Koehler, C, and Withnell, R, 1973, A differential counter for the determination of small differences in decay rates: Rev Sci Instruments, v 44, p 55-59.

Henning, W, Kutschera, W, Smither, RK, and Yntema, JL, eds, 1981a, Symposium on accelerator mass spectrometry, Proc: Argonne, Illinois, Argonne Natl Lab Rept ANL/PHY-81-1.

Henning, W, Kutschera, W, Myslek-Laurikainen, B, Pardo, RC, Smither, RK, and Yntema, JL, 1981b, Accelerator mass spectrometry of ^{59}Ni and Fe isotopes at the Argonne superconducting linac, in Henning et al, eds, Symposium on accelerator mass spectrometry, Proc: Argonne, Illinois, Argonne Natl Lab Rept ANL/PHY-81-81, p 320-329.

Klein, J, Middleton, R, and Stephens, WE, 1981, Search for anomalously heavy isotopes, in Henning et al, eds, Symposium on accelerator mass spectrometry, Proc: Argonne, Illinois, Argonne Natl Lab Rept ANL/PHY-81-1, p 136-153.

Kutschera, W, Henning, W, Paul, M, Smither, RK, Stephenson, EJ, Yntema, JL, Alburger, DE, Cumming, JB, and Harbottle, G, 1980, Measurement of the ^{32}Si half-life via accelerator mass spectrometry: Phys Rev Letters, v 45, p 592-596.

Lal, D and Peters, B, 1967, Cosmic-ray produced radioactivity on the earth, in S Flügge, ed, Encyclopedia of Physics: Berlin-Heidelberg-New York, Springer, v XLVI/2, p 551-612.

Lederer, CM and Shirley, VS, eds, 1978, Table of isotopes: New York, John Wiley & Sons.

Middleton, R, Zurmühle, RW, Klein, J, and Kollarits, RV, 1979, Search for an anomalously heavy isotope of oxygen: Phys Rev Letters, v 43, p 429-431.

Muller, RA, 1977, Radioisotope dating with a cyclotron: Science, v 196, p 489-494.

Muller, RA, Alvarez, LW, Holley, WR, and Stephenson, EJ, 1977, Quarks with unit charge: A search for anomalous hydrogen: Science, v 196, p 521-523.

Nagai, H, Nitoh, O, and Honda, M, 1981, Half-life of ^{202}Pb: Radiochim Acta, v 29, p 169-172.

Nelson, DE, Korteling, RG, and Stott, WR, 1977, Carbon-14: Direct detection at natural concentrations: Science, v 198, p 507-508.

Nelson, DE, Korteling, RG, Southon, JR, Vogel, JS, Nowikow, I, Ku, TL, Kusakabe, M, and Reyss, JL, 1983, Tandem accelerator measurements of ^{10}Be deposition rates, in Stuiver, M and Kra, RS, eds, Internatl ^{14}C conf, 11th, Proc: Radiocarbon, v 25.

Nishiizumi, K and Arnold, JR, 1981, Measurement of cosmogenic nuclides in extraterrestrial material, in Henning et al, eds, Symposium on accelerator mass spectrometry, Proc: Argonne, Illinois, Argonne Natl Lab Rept ANL/PHY-81-1, p 262-276.

Pal, DK, Tuniz, C, Moniot, RK, Kruse, TH, and Herzog, GF, in press, ^{10}Be in Australasian tektites: Evidence for a sedimentary precursor: Science, in press.

Raisbeck, GM, Yiou, F, Fruneau, M, Lieuvin, M, and Loiseaux, JM, 1978a, Measurement of ^{10}Be in 1,000- and 5,000-year-old Antarctic ice: Nature, v 275, p 731-732.

Raisbeck, GM, Yiou, F, Fruneau, M, and Loiseaux, JM, 1978b, Beryllium-10 mass spectrometry with a cyclotron: Science, v 202, p 215-217.

Raisbeck, GM, Yiou, F, Fruneau, M, Loiseaux, JM, and Lieuvin, M, 1979a, ^{10}Be concentration and residence time in the ocean surface layer: Earth Planetary Sci Letters, v 43, p 237-240.

Raisbeck, GM, Yiou, F, Fruneau, M, Loiseaux, JM, Lieuvin, M, and Ravel, JC, 1979b, Deposition rate and seasonal variations in precipitation of cosmogenic ^{10}Be: Nature, v 282, p 279-280.

Raisbeck, GM and Yiou, F, 1979, ^{26}Al measurement with a cyclotron: Jour Physique, v 40, p L-241-L-243.

_________1980, Progress report on the possible use of ^{41}Ca for radioactive dating: preprint, Lab Rene Bernas, Orsay: Rev Archeometrie, in press.

_________1981, Accelerator mass spectrometry with the Grenoble and Orsay cyclotrons: in Henning, et al, eds, Symposium on accelerator mass spectrometry, Proc: Argonne, Illinois, Argonne Natl Lab Rept ANL/PHY-81-1, p 23-33.

Raisbeck, GM, Yiou, F, Fruneaux, M, Loiseaux, JM, Lieuvin, M, Ravel, JC, Reyss, JM, and Guichard, F, 1980, ^{10}Be concentration and residence time in the deep ocean: Earth Planetary Sci Letters, v 51, p 275-278.

Raisbeck, GM, Yiou, F, Lieuvin, M, Ravel, JC, Fruneau, M, and Loiseaux, JM, 1981, ^{10}Be in the environment: Some recent results and their implications, in Henning et al, eds, Symposium on accelerator mass spectrometry, Proc: Argonne, Illinois, Argonne Natl Lab Rept ANL/PHY-81-1, p 228-243.

Smith, PF, Bennet, JRJ, Homer, GJ, Lewin, JD, Walford, HE, and Smith, WA, 1981, A search for anomalous hydrogen in enriched D_2O, using a time-of-flight spectrometer, in Henning et al, eds, Symposium on accelerator mass spectrometry, Proc: Argonne, Illinois, Argonne Natl Lab Rept ANL/PHY-81-1, p 170-192.

Suess, HE and Urey, HC, 1956, Abundances of the elements: Rev Modern Physics, v 28, p 53-74.

Thomas, JH, (ms), 1982, Ultra-sensitive mass spectroscopy using a tandem van de Graaff accelerator to detect ^{10}Be and ^{26}Al: PhD thesis, Yale Univ, New Haven.

Turekian, KK, Cochran, JK, Krishnaswami, S, Lanford, WA, Parker, PD, and Bauer, KA, 1979, The measurement of ^{10}Be in manganese nodules using a tandem van de Graaf accelerator: Geophysics Research Letters, v 6, p 417-420.

Wahlen, M, Kothari, B, Elmore, D, Tubbs, L, Newman, D, Ma, XC, and Gove, HE, (ms), 1982, ^{10}Be in lake sediments.

Ziegler, JF, 1980, Handbook of stopping cross-sections for energetic ions in all elements, vol 5: New York, Pergamon Press.

[Radiocarbon, Vol 25, No. 2, 1983, P 693-700]

TANDEM ACCELERATOR MEASUREMENTS OF ^{10}BE DEPOSITION RATES

DE NELSON, RG KORTELING, JR SOUTHON*, JS VOGEL* AND I NOWIKOW*

Archaeology and Chemistry Departments, Simon Fraser
University, Burnaby, British Columbia, Canada

and

TL KU, MASASHI KUSAKABE AND JL REYSS**

Department of Geological Sciences, University of Southern
California, Los Angeles

ABSTRACT. A Tandem Van de Graaff accelerator has been modified for use in the direct measurement of natural abundances of ^{10}Be and ^{14}C. A description of the system is given and some ^{10}Be results on oceanographic samples are discussed.

INTRODUCTION

We present a short review of our work with the McMaster University Tandem accelerator for the study of the radioisotopes ^{10}Be and ^{14}C. We have made over 100 ^{10}Be measurements on oceanographic samples. We find ^{10}Be is an ideal isotope for testing developing systems while providing useful geophysical information. We have not yet begun natural ^{14}C measurements, as our initial system did not have sufficient sensitivity. This deficiency is now rectified, and we should soon be starting ^{14}C dating.

TECHNICAL METHODS

The general features of our system are similiar to those of most other laboratories. Negative ions are accelerated and then magnetically and electrostatically selected before detection with Faraday cups and solid-state particle detectors. Our system differs from others in that we inject, accelerate, and detect both the stable and rare isotopes simultaneously instead of sequentially. We make no attempt to determine the absolute efficiency of the system, but measure

---

* Also: Department of Physics, McMaster University, Hamilton, Ontario, Canada

** Permanent address: Centre des Faibles Radioactivités, 91190 Gif-sur-Yvette, France

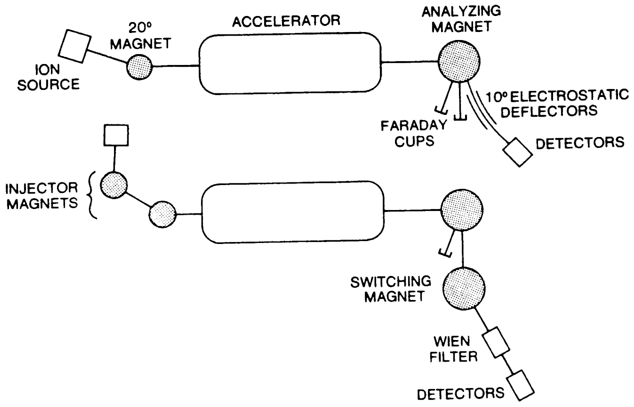

Fig 1A. (Top) The first-generation accelerator system used in making the measurements reported here. Fig 1B. (Bottom) The second-generation system which is now being completed, and which will be used in future studies.

all samples relative to a standard measured alternately with the unknowns. We operate the system as an analogue of a conventional isotope-ratio mass spectrometer.

Figure 1A shows our first-generation system. The ions from a reflected-beam Cs sputter source are injected by the 20° inflection magnet. This is not ideal, as only the rare isotope can be injected on-axis, resulting in very different optical properties for the rare and major beams. This problem was compounded by the optics of the inclined-field tubes that were used in the accelerator until recently. These tubes further accentuated the differences between the beams. After acceleration, the ions were analyzed with the normal accelerator analyzing-magnet which has an enlarged vacuum chamber to accommodate the different beams. The rare isotope was further selected by a 10° electrostatic deflection 80cm from the analyzing magnet exit point. Detection was done by commercial E-ΔE detectors for the rare isotope and Faraday cups for the major beams.

This system has been quite adequate for natural ^{10}Be measurements. Under typical operating conditions, for BeO samples of 0.1 to 1mg, we obtained ~0.5μA of BeO$^-$ current and 30 to 40nA of analyzed $^{9}\text{Be}^{4+}$ current. Detection sensitivity was ca $^{10}\text{Be}/^{9}\text{Be} = 5 \times 10^{-13}$, limited primarily by nuclear reactions in the Al guard foil preceding the detectors and sometimes by the ^{10}Be count-rate, as not all natural samples yield the same output from the source. The measurement accuracy with respect to our ^{10}Be standard ranged from 2 to 10%, and was very dependent on the condition of the accelerator.

This system did not provide sufficient sensitivity for ^{14}C measurements. ^{13}C ions from the stable-isotope beam were scattered into the rare-isotope beam by residual gas molecules in the magnet chamber. This background intensity was about equal to the intensity of ^{14}C from modern carbon, and so precluded useful measurement. Further magnetic filtering is required to eliminate these contaminant ions.

We are now completing second-generation modifications to every part of the system (fig 1B). A new injection system (Lobb et al, 1981) is nearing completion. This should simultaneously inject all isotopes of interest into the accelerator in a uniform fashion. The accelerator itself has been extensively upgraded in the past two months. The beam tubes and charging system were replaced with better designs. A new rare-isotope detection line including further magnetic and electrostatic filtering (the laboratory switching magnet and a Wien filter) is now complete. Preliminary tests show that there is now sufficient sensitivity for ^{14}C measurement. These modifications should allow us to determine ^{14}C and ^{10}Be concentrations with much better accuracy and sensitivity. Southon et al (1982) give detailed description of our system and measurement methods.

^{10}BE RESULTS

Most of our ^{10}be measurements were made on deep-sea manganese nodules as part of the manganese nodule program (MANOP) sponsored by the US National Science Foundation. We studied several of these in considerable detail and found that accelerator ^{10}Be determinations provide a powerful new tool for studying these sea-floor concretions. Much information on the long-term growth history of nodules was learned. The growth rates of mms/Myr determined from the ^{10}Be concentrations compared very well with those by uranium-series isotopes measured on the same nodules.

We also studied ^{10}Be concentrations in two manganese crusts which are similar to nodules but fixed to the ocean floor and not subject to possible roll-over. They can provide a several-million-year record of ^{10}Be deposition near the sample. If the logarithms of the ^{10}Be concentrations are a linear function of the sampling depth in the crust, it is reasonable to suggest that both the average ^{10}Be deposition and the crust accretion rate have been constant, where the average is taken over the time-interval represented by the thickness of the successive sample layers analyzed.

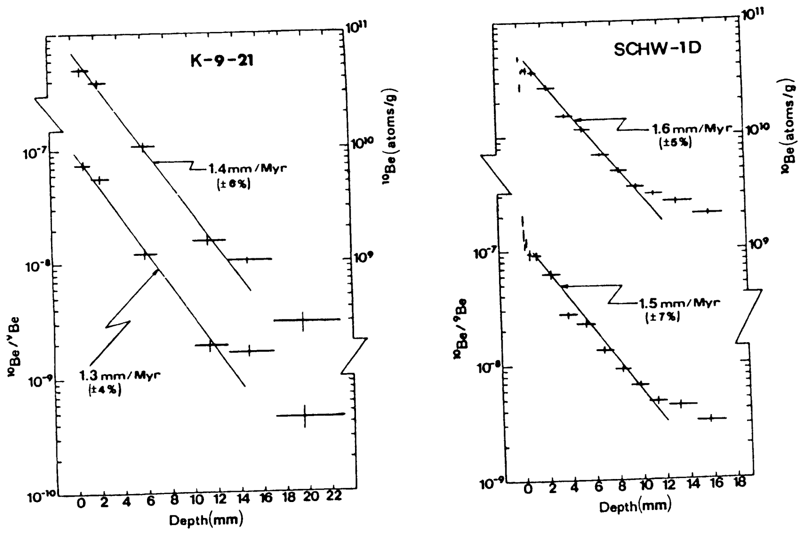

Fig 2. Plots of the ^{10}Be concentrations (on a residue-free basis) and ^{10}Be/^{9}Be ratios in two Mn crusts. Least squares fits for the linear segments of the plots give estimates for the accretion rates. The horizontal lines on each point give the depth intervals analyzed, and the positions of the vertical lines (measurement uncertainty) are placed at the effective measurement depths.

Figure 2 shows both the ^{10}Be concentrations (upper plots) and the ^{10}Be/^{9}Be ratios in a crust from the equatorial Atlantic (K-9-21 at 7°58'N, 21°02'W) and one from the North Pacific (SCHW-1D at 30°N, 140°W). The ^{9}Be measurements that were required to obtain the ^{10}Be/^{9}Be ratios were made by atomic absorption spectroscopy. Except near the very surface of sample SCHW-1D, the sampling intervals on these crusts represent depositions averaged over time spans of the order of a million years.

For both crusts, the plots are log-linear for the first ~10mm of sample. This indicates that the ^{10}Be production and deposition rate and the crustal growth rate have remained quite constant (the data suggest to within ~±6-7%) for the past 7-9 Myr. Prior to that time, the crusts from both oceans show a very similar deviation, which could be due either to a higher ^{10}Be deposition rate in both oceans prior to 7-9 Myr ago or to a global change in the oceans which would similarly change the growth rates of these two crusts. The growth rate change is deemed unlikely, though, because no discernible major changes in the Fe/Mn ratio or in the concentrations of ^{9}Be and alumino-silicates occur across the 7-9 Myr boundary in these crusts (Ku et al, 1982). Ciesielski et al (1982) suggested that the formation of the West Antarctic ice shelf at ca 7-9 Myr ago caused a permanent change in the global abyssal circulation; perhaps these crusts recorded that event.

The detailed study of the Pacific crust shows that ^{10}Be concentration changes markedly in the outermost millimeter. There was not sufficient sampling resolution to detect such a change in the Atlantic crust, but we saw this feature in all the manganese nodules we studied. We cannot determine from these data whether this indicates a gradual decrease in the ^{10}Be production rate from 0.5 Myr ago to the present, or whether it is due to the nature of the chemical processes by which the Be is incorporated into the manganese deposits. Kusakabe and Ku (ms in preparation) have developed a model which explains but does not prove the latter possibility.

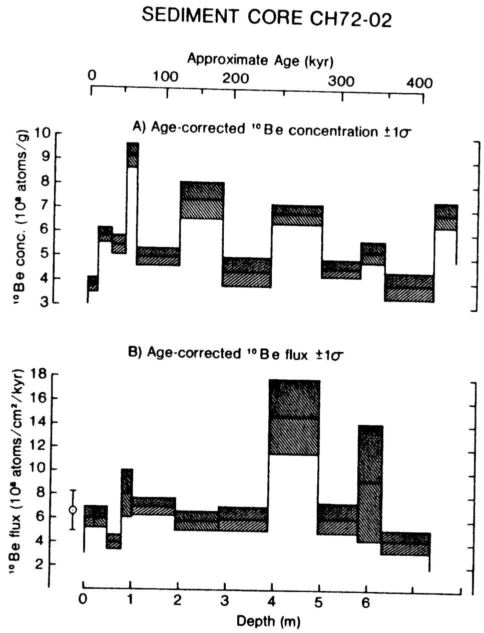

Fig 3. Plots of the age-corrected ^{10}Be concentrations in, and the calculated ^{10}Be fluxes into, a deep-sea sediment core. Each step in the histogram represents the average value for oxygen-isotope states I-XII, reading from left to right. An approximate age-scale is given at the top.

On the million-year time-scale, then, ^{10}Be can provide a good chronometer for oceanographic studies. For shorter periods, we have information from a preliminary analysis of ^{10}Be concentrations in a sediment core (CH72-02 from 40°36'N, 21°42'W; 3485m) from the Atlantic, representing ~500 kyr of depositional history (fig 3) as determined by ^{230}Th and oxygen-isotope measurements. The core was divided into sections corresponding closely to the oxygen-isotope stages. The upper histogram of figure 3 gives the age-corrected average ^{10}Be concentrations as a function of down-core depth. For this core, age estimates as a function of depth were determined from the ^{230}Th data, from a comparison of the oxygen-isotope record of this core with the isotope record of Morley and Hays (1981) and from the first appearance of the micro-organism, E Huxleyi. Linear-regressions of the age-depth data gave high correlation coefficients ($r \simeq 0.996$). At first glance, this suggests that the sedimentation rate for the core is constant, and that the ^{10}Be concentration histogram also gives the variation with time of the ^{10}Be deposition rate at this location. We see, eg, a variation between isotope stages 1 and 2 that is very similar to that found by Raisbeck et al (1981) in an Antarctic ice core, and it is tempting to conclude that this indicates a global change in ^{10}Be production.

We believe this interpretation is incorrect. A plot of the non-carbonate fraction (or the "clay" fraction) of our core vs depth gives a histogram identical in shape to the ^{10}Be concentration histogram, indicating that the ^{10}Be concentration variations primarily reflect the changes in biogenic carbonate production and not ^{10}Be production. (The effect of carbonate dissolution should be minor, as this core is well above the lysocline depth. The constancy of the core sedimentation rate is more apparent than real.

The time-dependent fluxes of ^{10}Be into the core are given in the lower histogram of figure 3. We have used the isotope-stage boundary ages of Morley and Hays (1981) to determine the average sedimentation rate for each stage. We then calculated the ^{10}Be fluxes with these average rates, the age-corrected ^{10}Be concentrations, and the in situ sediment densities. The uncertainties include an estimate of the uncertainty in transposing the Morley and Hays' ages to this particular core, the uncertainty in the ^{10}Be measurement, and the uncertainty in the core-density estimates.

Any examination of this histogram for evidence of change in ^{10}Be (and thus, ^{14}C) production rates must be done with the caution that the values plotted here depend strongly on the ages of the stage boundaries. Perhaps it is preferable to base the flux calculations on the ^{230}Th ages measured for this core, but these determinations have analytical uncertainties (especially for the older samples) that are quite large. The age values we have chosen from the literature (Morley and Hays, 1981) are derived from a variety of methods and are perhaps the best current estimates, but an assessment of the absolute accuracy of these ages has not been made.

The point plotted to the left of this histogram gives the ^{10}Be production-rate predicted by Reyss, Yokoyama and Guichard (1981) from spallation cross-sections and cosmic-ray intensities. There is very good agreement between this predicted value and the observed flux into the core.

If the age estimates are correct, the histogram gives no evidence that the ^{10}Be flux averaged over each isotope stage (hence, climatic cycle) has changed more than ca 25 to 30% over the past 1/2 Myr, with the possible exception of stages 3 and 8. Further, whether we use the isotope-record ages or the ^{230}Th ages, there is no evidence of differences between the average ^{10}Be fluxes for stages 1 and 2.

We are also attempting to examine ^{10}Be production on a shorter time scale, with detailed ^{14}C and ^{10}Be measurements on a 20,000 year-old lake core from Tennessee. The topography indicates that the catchment area of the pond has not changed a great deal during that time. Only preliminary determinations on two segments of the core have been made; one for a modern sample and one for a sample of age ~14,000 ^{14}C years. The results indicate that, 1) the ^{10}Be concentration in the modern sample is 3 times higher than that in the 14,000-year-old sample, 2) the ^{10}Be flux into the core is about a factor of 4 lower in modern times than at 14,000 years ago, and 3) the ^{10}Be/^{9}Be ratio in the modern sample is approximately a factor of two lower than the ratio in the 14,000-year-old sample.

These data are apparently inconsistent and do not provide any reliable general information on ^{10}Be production and distribution of these times. In order to extract such information from this core, we will at least have to derive very accurate estimates for the sedimentation rates, so that the ^{10}Be fluxes can be accurately determined. At present, the only method by which this can be done is ^{14}C dating, and a calibration scale for that technique exists only for the past 8000 years.

CONCLUSION

These studies have examined the production and distribution of the radioisotope ^{10}Be, both to evaluate its potential as a dating tool, and to gain information on the production rate variation. We have found that measurements of ^{10}Be concentrations do not always provide unambiguous information on ^{10}Be production rates. To translate ^{10}Be concentrations in a sample to ^{10}Be flux for short time scales compared to the mean-life of ^{10}Be, we require accurate, independent dating techniques.

ACKNOWLEDGMENTS

We thank the staff of the McMaster University Accelerator Laboratory for their continuing support of our program, Tom Brown for permission to discuss his preliminary lake-core data, and Gord Richards, John Sheppard, and Nadine Bohna for technical assistance. Funding is provided by the NSF Manganese Nodule Program, by NSERC of Canada, and by Simon Fraser and McMaster Universities.

REFERENCES

Ciesielski, PF, Ledbetter, MT, and Ellwood, BB, 1982, The development of Antarctic glaciation and the Neogene paleo-environment of the Maurice Ewing Bank: Marine Geol, v 46, p 1-51.

Ku, TL, Kusakabe, M, Nelson, DE, Southon, J, Korteling, RG, Vogel, J, and Nowikow, I, 1982, Constancy of oceanic deposition of ^{10}Be as recorded in Mn crusts: Nature v 299, p 240-242.

Lobb, DE, Southon, JR, Nelson, DE, Wiesehahn, W, and Korteling, RG, 1980, An ion injection system for use in tandem accelerator radioisotope dating devices: Nuclear Instruments Methods, v 179 p 171-180.

Morley, JJ and Hays, JD, 1981, Towards a high-resolution, global, deep-sea chronology for the last 750,000 years: Earth Planetary Sci Letters, v 53, p 279-295.

Raisbeck, GM, Yiou, F, Fruneau, M, Loiseaux, JM, Lieuvin, M, Ravel, JC, and Lorius, C, 1981, Cosmogenic ^{10}Be concentrations in Antarctic ice during the past 30,000 years: Nature, v 292, p 825-826.

Reyss, J-L, Yokoyama, Y, and Guichard, F, 1981, Production cross-sections of ^{26}Al, ^{22}Na, ^{7}Be from argon and of ^{10}Be, ^{7}Be from nitrogen: implications for production rates of ^{26}Al and ^{10}Be in the atmosphere: Earth Planetary Sci Letters, v 53, p 203-210.

Southon, JR, Vogel, JS, Nowikow, I, Nelson, DE, and Korteling, RG, 1983, The measurement of ^{10}Be concentrations with a Tandem accelerator: Nuclear Instruments Methods, in press.

[Radiocarbon, Vol 25, No. 2, 1983, P 701-710]

RECENT ^{14}C MEASUREMENTS WITH THE CHALK RIVER TANDEM ACCELERATOR

R M BROWN, H R ANDREWS, G C BALL, NEIL BURN,
W G DAVIES, YOSHIO IMAHORI, J C D MILTON,
AND WAYNE WORKMAN

Chalk River Nuclear Laboratories, Chalk River,
Ontario KOJ 1JO, Canada

ABSTRACT. The Chalk River Tandem Accelerator Mass Spectrometry System has reached a state of reliable measurement of ^{14}C using 2 to 5mg elemental carbon prepared by Mg reduction of CO_2. For two comparisons of a near-modern unknown with the NBS oxalic acid standard we obtain a total error of ~±4.5%, consisting of a random system error of about ± 3.5% combined with the statistical counting error. Measurements have been made on 70 samples in 30 days of running time during the past year. Samples included deep rock carbonates, cosmogenic ^{14}C in meteorites, charcoal from earthquake fault zones, collagen of bone artifacts and fossil beetle- fragments.

INTRODUCTION

At the last Radiocarbon Conference in 1979 we detailed the evolution of a Tandem Van de Graaff ^{14}C dating system at Chalk River (Andrews and others, 1980). At an International Atomic Energy symposium in West Berlin in 1981 we described further development of the system and gave an appraisal of its capabilities, limitations, and prospects for improvement (Brown and others, 1981). During the past year our facilities and techniques have remained essentially unchanged. We have gained operating experience and measured a variety of sample types to demonstrate the validity and value of the technique. This paper recounts our experience and presents some illustrative results. Papers dealing with the significance of the results for specific studies will be published separately in collaboration with the submitters of the samples.

The Chalk River ^{14}C system is based on a MP Tandem Van de Graaff accelerator operating at 8 MV terminal voltage. C^{4+} ions of 40 MeV energy emerge from the accelerator, pass through two analyzing magnets and a Wien

AECL-7992

cross-field velocity filter and are measured by a Faraday cup in the case of ^{12}C or an E/ΔE counter telescope in the case of ^{14}C. Ions of the desired isotope are switched automatically through the system by adjusting the magnetic elements. ^{14}C is counted for five 45-second periods followed by a 50-second integration of the ^{12}C current. Normally, the ^{13}C current is not monitored. The $^{14}C/^{12}C$ ratio obtained for a sample is normalized to that of carbon prepared from the NBS oxalic acid standard measured before and after each one or two samples.

OPERATING EXPERIENCE

ION SOURCE PERFORMANCE. Our standard sample material for the ion source has been 2 to 5mg of elemental carbon mixed with four times its weight of reduced Fe powder. The mixture is pressed into a ring within the bore of a cylindrical aluminum sample holder through which a 6mm diameter Cs^+ sputtering beam passes. An attempt to achieve a higher C^- emission by using a more concentrated Cs^+ beam of 1.3mm diameter was unsuccessful. No measurable increases in beam currents were observed and the beam was found to sputter through the carbon of the oxalic acid standards which were counted repeatedly throughout a run. In addition, Al was sputtered onto the rest of the source material, as a portion of the intense Cs^+ beam struck the inside of the source mount. We have tried industrial graphite, iron carbide, and graphite pyrolyzed onto a hot Ta wire from acetylene with no significant improvement in source emission. Thus, we find our original C + Fe sources to be the most satisfactory. Their output stabilizes sufficiently for measurement to start in 30 minutes, they last a long time without sputtering through, and they give as high a C^- current as industrial graphite mounted in the same geometry. The carbon preparation technique, reduction of CO_2 by Mg in a disposable stainless steel tube at 900°C, continues to be satisfactory.

We have been able to increase our beam current 2 to 3 fold without degrading our reproducibility by using a larger beam-defining aperture at the entrance to the Tandem accelerator. We now obtain $^{12}C^{4+}$ beam currents of 1 to 3 μA corresponding to ^{14}C counting rates of 100 to 300 per minute for modern carbon and 0.5 to 1.5 per minute for a background sample.

BACKGROUND. Our experience with background during the past year is shown in figure 1. Our original practice had been to carry over a background sample of carbon prepared from limestone from one loading of the ion source to another within a run. The May and September runs show that the count on such a background sample tends to rise with each successive loading, perhaps because of exposure of the caesiated surface of the carbon to atmospheric CO_2 during load change. In the fourth load of the September run, a new background sample gave a much lower value than the sample carried through the four loadings. In subsequent runs, new background samples have been used for each load. The hatched band marked "Limestone Background" is the average level obtained for all fresh background carbon samples measured during the past year. Since all the limestone carbon samples were prepared from aliquots of a single preparation of carbon by our standard procedure, the fluctuations in the measured background level must result from contamination introduced during the preparation or loading of the sample holders. Within a given load we have found the background count to remain constant.

Figure 1 also shows the results of measurements on industrial graphite and an empty Al sample holder in the standard geometry. These are significantly lower than all but one of the limestone measurements. We consider this to be the inherent background level in our machine at the present time, equivalent to a sample with an age of ~56,000 years. Attempts to reduce the background by installation of a cold trap close to the ion source and by flushing the ion source chamber with dead CO_2 just prior to pump-down have not been successful.

REPRODUCTIBILITY. Statistical analysis of multiple measurements of unknown samples with respect to the standard during the past year indicate a random system error of ~5% for a single measurement, in addition to counting statistics. For our usual practice of two measurements per sample this results in an error of ~±3.5%. When this error is combined quadratically with the counting statistical error (±3%) associated with our usual counting times, the result is a total error of ~±350 years for a modern sample.

COMPARATIVE MEASUREMENTS. We have tested our system with a series of samples prepared from a weak $^{14}CO_2$ spike diluted quantitatively with ^{14}C-free CO_2. Figure 2

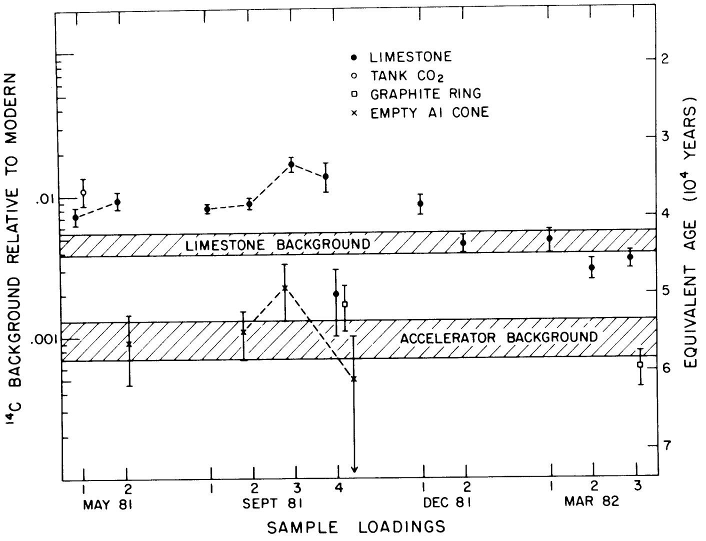

Figure 1. ^{14}C background in the Chalk River MP Tandem Accelerator, 1981-82

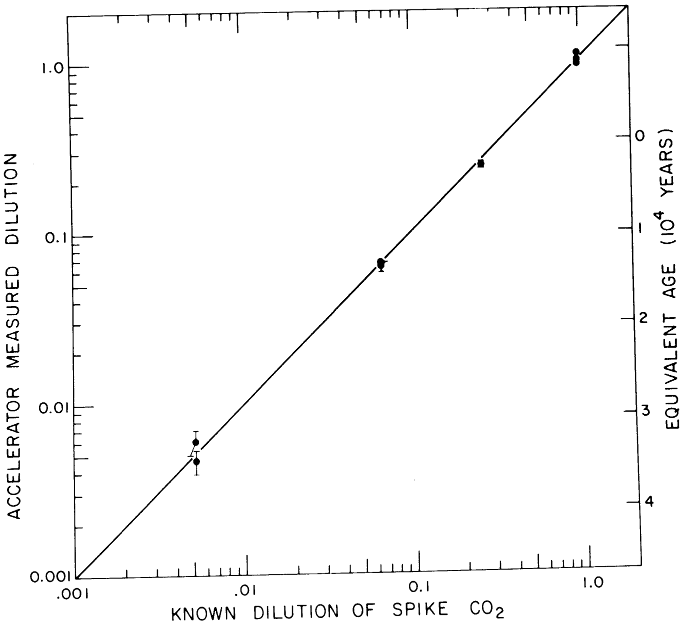

Figure 2. Accelerator measurements of quantitatively diluted spike $^{14}CO_2$

shows the linear correspondence we obtain between measured and known concentrations over a 250-fold dilution. Reasonable replication was obtained on multiple samples measured at different times over the span of more than a year. The greatest dilution corresponds to 1.2% modern or an age of ca 35,000 years.

In each group of samples we have measured, some have been measured radiometrically at a previous time. Comparative results are presented in Table 1. The errors quoted for the accelerator measurements are estimated overall measurement errors (1σ) as discussed above. Errors quoted for radiometric measurements are assumed to be simple counting statistical errors as is the usual practice.

These comparisons encompass the complete determinations involving independent sample selection and preparation in different laboratories not necessarily using exactly the same purification procedures. The accelerator samples were small discrete portions of material rather than representative fractions of the large portions used for the radiometric measurements at an earlier time. In view of the opportunities for occurrence of differences in material actually measured, the correlation of results is encouragingly good. Of the two instances where the difference in results exceeds twice the quadratically combined standard deviations of the measurements, one (the Indian campsite charcoal) is probably attributable to different sample materials and the other (the mammoth bone) to the difficulty of obtaining reproducibly-dateable material from bone. Unfortunately the radiometric value for Farmington CO_2 (from which carbon was prepared for the accelerator measurement after 20 years storage) is of low accuracy due to the small sample size. Obviously it is desirable to obtain direct intercomparisons using homogeneous CO_2 samples that have been measured radiometrically with high accuracy.

DATING RESULTS

Rather than making a Herculean effort to achieve the 1% or better accuracy attained by radiometric measurement and expected for the dedicated machines, we have accepted the 4 to 5% accuracy consistently obtainable with our system and proceeded to measure a number of samples for which this is perfectly acceptable. This is the case for most samples more than a few thousand years old.

TABLE 1. COMPARATIVE RADIOMETRIC AND ACCELERATOR MEASUREMENTS

	RADIOCARBON AGE (Years bp)#		
Sample	Radiometric	Accelerator	Difference
Charcoal-Indian campsite	1870 ± 175 "From same site"(S-501) *	270 ± 360 0 ± 320	4.σ
Bone collagen-human	2610 ± 65 (S-1285) *	2470 ± 340	0.4σ
Bone collagen-mammoth	15500 ± 130 (GSC-3053) **	17900 ± 500 17860 ± 440	4.7σ
Charcoal-Wasatch Fault	"With modern nails"	220 ± 340	0.7σ
Charcoal-Wasatch Fault	130 ± 95 †	390 ± 330	0.7σ
Charcoal-Wasatch Fault	1350 ± 70†	1560 ± 340	0.6σ
Charcoal-Wasatch Fault	4580 ± ? †	4030 ± 280	<1.5σ
CO$_2$ from Farmington meteorite. Same CO$_2$ for both measurements.	(dpm/kg meteorite)		
	47 ± 10 ‡	48.2 ± 3.2	0.1σ
CO$_2$ from Bruderheim meteorite. Independent portions of meteorite.	(dpm/kg meteorite)		
	57 ± 3 ‡	49.8 ± 1.8	2.0σ

\# ^{14}C half-life = 5568 years

* University of Saskatchewan, Saskatoon, Saskatchewan, Canada

** Geological Survey of Canada, Ottawa, Ontario, Canada

† Dicarb Radioisotopes Co , Gainesville, Florida 32601, U S A

‡ de Felice and others (1963); Fireman (1978)

During the past year we have had four runs in which we have measured 70 samples in 30 days of running time. Detailed date lists will be published elsewhere. Here we present our dates in graphical form to demonstrate the reproducibility attained in routine analysis and the range of sample types and ages that have been measured.

METEORITE SAMPLES. Measurement of the ^{14}C content of meteorites is an excellent application of the accelerator technique since only very small samples are available. Our samples have been a few mL CO_2 extracted by E L Fireman of the Smithsonian Astrophysical Observatory from North American and Antarctic meteorites. Many of these have been counted in small volume proportional counters in past years. We have obtained about 5-fold higher precision and extended the terrestrial age limit to 50,000 years from the 25,000 years limit of radiometric measurements on the small amounts of sample available. Figure 3 shows our experience with reproducibility on multiple measurements of these samples. The error bars are counting statistics only; in many cases, the spread in the repeat data exceed these estimates reflecting the presence of the ~5% system fluctuation discussed previously. In two cases (137,167) one measurement is far out and obviously should be discarded. Usually, such results can be associated with some operational aberration during the measurement. Fireman and others (1982) and Andrews and others (1982) have reported aspects of these meteorite measurements.

ARCHAEOLOGIC SAMPLES. The Archaeological Survey of Canada provided 17 bone samples which have been analyzed, some several times. Most of these were animal bones from the Yukon which showed evidence of use as tools by man when fresh. Dating was done on collagen recovered from these bones by mild HCl and NaOH extractions. Two samples had been measured radiometrically and are reported in Table 1. Significant new dates were obtained for the other samples which were too small for radiometric measurement.

Figure 4 shows the reproducibility and age range of these samples. The brackets embrace different carbon samples prepared from the same bone measured in accelerator runs separated by several months. Samples 3 and 4 were from a common preparation of carbon, as were 15 and 16, but the other pairs were processed independently from common bone samples.

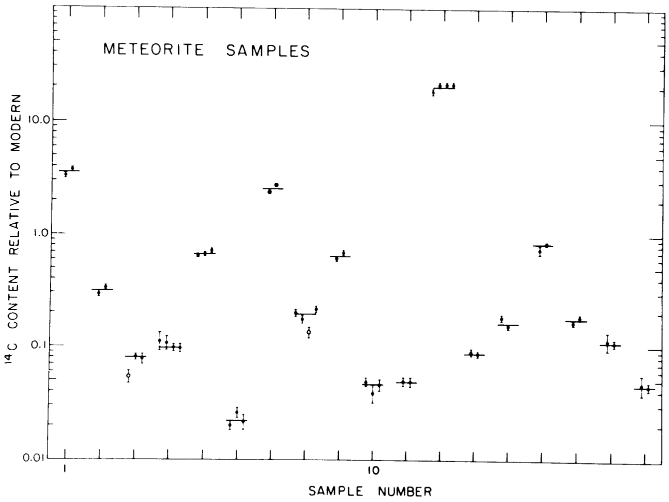

Figure 3. ^{14}C content of meteorite samples. Error bars are counting statistics only. Open points not included in mean values shown by horizontal bars.

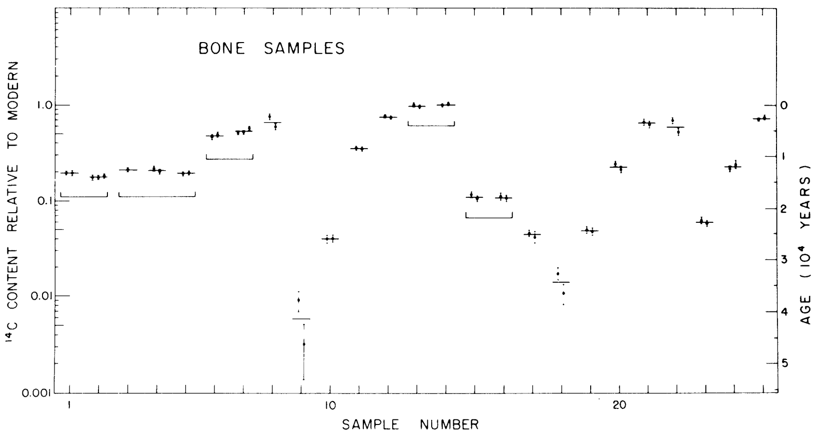

Figure 4. ^{14}C content of bone samples. Error bars are counting statistics only. Horizontal bars are the mean values of the multiple measurements on each sample. Brackets embrace different samples prepared from the same bone and measured several months apart.

Two of the bone samples we analyzed early in our program gave impossibly young ages. We have related these discrepancies to sample processing. These samples, and one done intentionally at a later time, were extracted with hot 6-molar HCl resulting in loss of most of the protein. The small acid-insoluble organic residue remaining had an age of a few thousand years. It is estimated that such a contaminant would reduce the age of a sample prepared by our usual procedure from a true age of 15,000 to 13,000 years. Since the amount and age of such contaminants are probably variable from sample to sample, they should be removed, perhaps by solubilizing the collagen in hot water and discarding insoluble material as described by Longin (1971). We have not used such treatment as yet.

EARTHQUAKE DATING. A set of charcoal samples provided by Allen Tucker, San Jose State University, have been measured for earthquake dating purposes. The samples comprise small flecks of charcoal recovered from soil at the site of the earthquake-produced Wasatch fault near Salt Lake City, Utah. The dates of such charcoal found on the two sides of faulted strata give a maximum age for the time of faulting. Hand-picking of the small samples required for accelerator measurement is the only practical means of ensuring freedom from contamination by more recent organic material such as rootlets. These samples were combusted to CO_2 and reduced to carbon in our standard procedure to ensure that sample and standard were in the same form.

PALEO-ENTOMOLOGIC SAMPLES. Information on the paleo climate at a site can be obtained from the identity and age of insect remains found. In the past, dating of the insects had to rely on stratigraphy or ^{14}C measurements on co-existing organic matter. We have directly dated insect remains provided by Allan Morgan, University of Waterloo, finding ages of 28,000 and 32,000 years for beetle parts from two related strata in the Yukon, and ca 8000 years for fossil beetles from more southerly sites.

CONCLUSION

These measurements have shown that we can obtain much valuable information at the present level of precision of accelerator ^{14}C dating. We are now shut down for the installation of a superconducting cyclotron as a post-accelerator for the MP Tandem. The Tandem will be in operation again by 1984 and we shall then continue measurements of ^{14}C and other isotopes of radiochronologic interest.

REFERENCES

Andrews, H R, Ball, G C, Brown, R M, Davies, W G, Imahori, Y, Milton, J C D, 1980, Progress in radiocarbon dating with the Chalk River MP tandem, in Stuiver, M and Kra, R S, eds, Internatl ^{14}C conf, 10th, Proc: Radiocarbon,v22,no.3,p822-828.

Andrews, H R, Ball G C, Brown, R M, Burn N, Imahori, Y, Milton J C D, Workman, W and Fireman, E L, 1982, ^{14}C content of Antarctic meteorites measured with the Chalk River MP Tandem accelerator, in Internatl conf on geochronol, cosmochronol and isotope geol, 5th, Proc: Japan, June 27 - July 2.

Brown, R M, Andrews, H R, Ball, G C, Burn, N, Davies, W G, Imahori, Y, Milton, J C D, 1981, Radiocarbon measurements with the Chalk River MP tandem accelerator, in Methods of low level counting and spectrometry, Proc: IAEA symposium, West Berlin, April 6-10, IAEA, Vienna.

de Felice, J, Fazio, G G, Fireman, E L, 1963, Cosmic ray exposure age of the Farmington meteorite from radioactive isotopes: Science, v142, p673-674.

Fireman, E L, 1978, ^{14}C in lunar soil and meteorites, Lunar and planetary sci conf, 11th, Proc: p1647-1654.

Fireman, E L, Andrews, H R, Ball, G C, Brown, R M, Burn, N, Imahori, Y, Milton, J C D, 1982, ^{14}C terrestrial ages of Antarctic meteorites measured with counters and a Van de Graaff accelerator, in Lunar and planetary sci conf, 13th: Houston, Texas, March 15-19.

Longin, R, 1971, New method of collagen extraction for radiocarbon dating: Nature, v230, p241-242.

[Radiocarbon, Vol 25, No. 2, 1983, P 711-718]

CURRENT ^{14}C MEASUREMENTS WITH THE UNIVERSITY OF WASHINGTON FN TANDEM ACCELERATOR

G W FARWELL, P M GROOTES, D D LEACH, F H SCHMIDT
AND MINZE STUIVER

Nuclear Physics Laboratory and Quaternary Isotope Laboratory
University of Washington, Seattle, Washington 98195

ABSTRACT. Our accelerator mass spectrometry (AMS) system shows a one-to-one relationship between sample ^{14}C concentrations determined by AMS - and by β-counting. Measurements of unknown samples against a standard indicate that ^{14}C concentration measurements to better than 2% can be made. For a 30-second data collection interval in a typical run of 100 intervals, the variability of the beam injected into the accelerator is ca 2%, that of the machine transmission is ca 4%, and counting statistics give 4.7% standard deviation for a sample of 80% of modern carbon.

INTRODUCTION

The University of Washington accelerator mass spectrometry (AMS) system, which uses an FN tandem Van de Graaff accelerator, has been described in Farwell et al (1980) and Farwell, Schmidt, and Grootes (1981). Technological advances in this system during the past year, including enhancement and stabilization of the overall ion transmission, are reported in Farwell et al (1983).

To minimize the influence of isotopic fractionation in ion source and accelerator, measurements are made by switching back and forth between the sample to be measured and a standard sample. For each sample, the number of $^{14}C^{+4}$ ions detected in a 30-second counting period is compared with the accompanying $^{12}C^{-}$ beam current collected simultaneously in a side Faraday cup located downstream from the inflection magnet, or with the corresponding $^{13}C^{+4}$ beam collected in a Faraday cup at the ^{14}C detector location, with the AMS system reset for this ion. Using a set of β-counted carbon samples, we tested the capability of our system to produce correct ^{14}C concentration ratios between pairs of samples. We also measured three β-counted samples of which the ^{14}C activity was unknown to the AMS experimenters. We report here the results of the ratio tests and the unknown sample measurements and discuss the stability and the apparent isotope fractionation of our AMS system. All measurements were made with a final ion energy of 35.0 MeV ($^{14}C^{+4}$); the corresponding terminal voltage for the tandem accelerator is 7.00 MV.

MATERIAL

The samples of known activity were prepared from tree rings formed in 1939, 1964, and 1968 by a Sitka spruce (*Picea sitchensis*) that grew near Quillayute, Washington (48°N, 24.6°W). Wood from a single ring was split off and chopped to match stick size. It was extracted at 60°C with a 3% NaOH solution, washed until neutral with distilled water, extracted with 2% HCl solution at 60°C, and again washed until neutral. The pretreated wood was divided into a sample for β-counting of its ^{14}C activity and a portion for AMS measurement. The AMS portion was charred in a nitrogen flow at 900°C; the resulting charcoal was powdered, mixed with coal tar pitch (sample: pitch equals 5:1 by weight), and made into graphitic pellets as described elsewhere (Grootes et al, 1980; 1981; Farwell et al, 1983).

The 1939 sample represents the normal pre-bomb, fossil-fuel-diluted ^{14}C activity which, in 1939, was 98% of modern carbon (.95x the activity of the NBS oxalic acid standard CO_2). In 1982, this has decreased to 97.5% or $\Delta^{14}C=-2.5\%$. The 1964 and 1968 samples were β-counted and gave

1964: QL-1567 $\Delta^{14}C = +86.8 \pm 1.0\%$ $\delta^{13}C$: -26.53‰
1968: QL-1568 $\Delta^{14}C = +58.9 \pm 0.5\%$ $\delta^{13}C$: -25.35‰

LINEARITY

The ^{14}C concentration ratio of different sample pairs is plotted in figure 1 against that determined by β-counting. Typical AMS count rates observed when running graphite standards correspond to a background of 0.3 to 0.5pM (% modern, Stuiver and Polach, 1977). In this comparison, the β-counted values have not been corrected for isotope fractionation ($\delta^{13}C$) and the effect of an estimated accelerator background of 0.5pM is included. The AMS data were obtained by simultaneous detection of the $^{14}C^{+4}$ beam through the whole system and the $^{12}C^{-}$ beam in the side Faraday cup, with the inflection magnet current controlled by a regulator that senses the position of the $^{12}C^{-}$ beam. The measured points scatter around the 45° line. Deviations are generally only a few percent; some of them can be attributed to minor differences in goemetry between sample and reference and can be avoided in future runs. A weighted least squares fit of a straight line gives a slope of .980±0.012 and a y intercept of .024±0.012 for all 17 points. We conclude from this set of comparisons that, when the ^{14}C concentration of a sample differs from that of the standard by less than a factor of two in either direction, the AMS measurement using this method ($^{12}C^{-}$ normalization) are accurate to better than 5%.

BLIND MEASUREMENTS

The AMS runs were made to obtain blind measurements on three samples of finely-ground cellulose supplied by the Quaternary Isotope Laboratory. In the first run, transmission

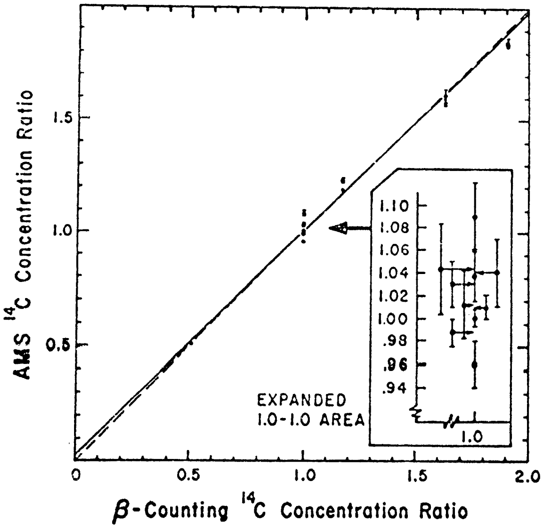

Fig 1. ^{14}C concentration ratio of two samples determined by accelerator mass spectrometry (AMS) as a function of the same ratio obtained by β-counting; insert shows the AMS results when both samples were of the same material.

through the accelerator was about a factor 2 below normal and could not be improved by tuning. After the run, it was found that a paper clip had partly shorted a compensating magnet of the gridded lens at the entrance to the accelerator (see Farwell et al, 1983). The results of this run are, therefore, considered unreliable.

The measurements were repeated several days later with good transmission. Although the samples had already been exposed to the cesium beam for several hours at $^{12}C^-$ currents of ca 6μA and conditions, therefore, were less than ideal, we measured each of the three samples at least twice during this run. Both methods of normalization (against $^{12}C^-$ and $^{13}C^{+4}$), with the inflection magnet controlled by NMR (nuclear magnetic resonance) feedback, were used to convert the observed ^{14}C counting rate to a $^{14}C/^{12}C$ concentration ratio (table 1). (To facilitate comparison, each AMS measurement is expressed as the ratio of the ^{14}C concentration to that of 1939 wood, using where appropriate, the known 1964/1939 ^{14}C concentration ratio.)

Table 1. Results of the blind measurements of three ^{14}C samples

Sample	Observed AMS ^{14}C Concentration Ratio (Sample/'39 Reference) $^{12}C^-$ NMR**	$^{13}C^{+4}$ NMR	AMS-Counted Sample Activity (pM)*	β-Counted Sample Activity (pM)	Difference (pM)
A	0.713±0.014	0.806±0.019			
	0.827±0.015	0.837±0.023			
Average	0.770±0.057	0.822±0.016†	79.5±1.5	79.24±0.18	0.3±1.5
B	0.811±0.013	0.828±0.013			
	0.810±0.014	0.865±0.018			
Average	0.811±0.001	0.847±0.019†	81.9±1.8	79.24±0.18	2.7±1.8
I	1.495±0.029	1.067±0.032			
	0.833±0.017	1.057±0.023			
	1.020±0.021	1.088±0.025			
Average	1.116±0.177	1.071±0.009†	104.0±1.0	95.05±0.18	8.9±1.0

* pM = % modern, ie, the absolute activity of AD 1950 (Stuiver and Polach, 1977)

** NMR= Inflection magnet field controlled by nuclear magnetic resonance feedback

† Data selected in blind test for comparison with β-counted activity

To compare the observed AMS ^{14}C concentration ratios (table 1) with the resulting of β-counting, it must be realized that β-counted results are normalized to 1950 AD standard activity (.95x NBS oxalic acid standard CO_2 corrected for decay since 1950) and to $\delta^{13}C = 25.0‰$ and are corrected for the background counting rate. The observed AMS ratios of table 1 are corrected for neither $\delta^{13}C$ nor background and are referenced to the 1939 Sitka spruce wood sample. They were converted to "AMS-counted sample activity" (table 1) as follows: 1) Typical AMS count rates observed when running graphite standards correspond to a background of 0.3 to 0.5%; a background of 0.5pM is, therefore, subtracted from both sample and standard. 2) The 1939 wood ^{14}C activity of 98% has decayed to 97.5% in 1982, and a correction is made for this. In addition, we assume that no serious fractionation occurred in the manufacturing of the graphitic sample pellets from wood cellulose.

Since the internal consistency of the results based upon the $^{13}C^{+4}$ normalization was clearly superior to that of the results based upon $^{12}C^{-}$, the $^{13}C^{+4}$-based averages were selected for correction and comparison, in our blind test, with the β-counted activities. The agreement for Samples A and B, which turned out to be splits from the same sample, is good. The Sample I results deviate outside statistics; however, this did not surprise the AMS experimenters unduly since there had been clear warning signals: strong disagreement between $^{12}C^{-}$ and $^{13}C^{+4}$ results for each measurement, serious inconsistency in the $^{12}C^{-}$ results, and sharp trends in the data as they came in during a given measurement.

We conclude that measurements accurate to ca 2% can be made using the $^{13}C^{+4}$ normalization method, provided that the AMS system is in favorable condition as indicated by good particle transmission and stability, and that new samples of well-defined, identical geometry are used that give consistent results in repeated measurements.

While our measurements are not intended to give absolute isotopic abundance ratios, it is possible to calculate these whenever the $^{13}C^{+4}$ beam is measured for normalization. Table 2 shows the results for the measurements of the three unknown samples. On the average, the AMS system showed a discrimination against $^{14}C^{+4}$ as compared with $^{13}C^{+4}$ of ca -10%. In earlier series, we observed ca -13% and 0% (Farwell, Schmidt, and Grootes, 1981). Obviously, the variability in the directly calculated ratios is considerably larger than in those obtained from sample comparisons, and relative measurements are indispensable for good precision.

AMS SYSTEM CONTRIBUTIONS TO THE STANDARD DEVIATION

It is of interest to assess the relative importance of several identifiable factors that contribute to the standard

Table 2. $^{14}C/^{12}C$ abundance ratios calculated from a direct comparison of the $^{14}C^{+4}$ and $^{13}C^{+4}$ beams of a single sample

	$^{14}C/^{12}C$ abundance ratio (x 10^{-12})		
Sample	AMS	β-counting	Error (%)
1964	2.18		
	2.02		
	2.30		
	1.65		
Average	2.04±0.14	2.19	-6.8±6.4
1939	1.02		
	0.89		
	0.97		
Average	0.96±0.04	1.14	-16.0±3.3
A	1.01		
	0.77		
Average	0.89±0.12	0.93	-4.1±13.2
B	0.84		
	0.75		
Average	0.79±0.04	0.93	-14.3±4.7
I	1.20		
	1.15		
	0.95		
Average	1.10±0.08	1.11	-1.1±6.7
Average for all samples			-8.5±2.9

deviation of the ^{14}C concentration ratio for a pair of samples. In the $^{12}C^-$ normalization method (data of fig 1), the principal factors are: 1) Variations in ion source output and inflection magnet and Einzel lens transmission, with resulting variations in ion input to the accelerator. These affect both the $^{14}C^{+4}$ and the $^{12}C^-$ beams and, thus, largely cancel out in the concentration ratio. 2) Variations in the collection efficiency of the $^{12}C^-$ beam in the side cup and in the transmission of the $^{14}C^{+4}$ beam through the system. These are independent and will show up in the $^{12}C^-$ and the $^{14}C^{+4}$ count rates and in the concentration ratio. 3) Poisson counting statistics governing the count rate of the $^{14}C^{+4}$ ions. (The $^{12}C^-$ count rate is actually a current measurement.)

During a comparison of two samples by the $^{12}C^-$ method, an automatic sample changer alternates the two samples (1 and 2) after every 30 seconds of data collection. The data for a full cycle (30 seconds on each sample) consist of four count rates: $^{14}C^{+4}$ for 1 and 2, obtained from the DE,E detector with appropriate gating and coincidence requirements, and $^{12}C^-$ for 1 and 2, obtained as a count rate through a current integrator on the side cup. These counts rates are displayed for a typical data run in figure 2. The calculated ^{14}C concentration ratio (1 vs 2) is also plotted for the same succession of intervals. As can be expected for such short data collection periods, the individual data points show considerable scatter.

Examination of the $^{12}C^-$ count rate records yields information about the variations in ion source output and accelerator input. We observe that both $^{12}C^-$ beams increased gradually during the first half of the run by ca 10 to 15% and then remained constant; scatter of the individual data points around the trend line is generally small, except for 4 points on Sample 1 and 1 on Sample 2. (Such outliers are often correlated with an identifiable accelerator event or other cause.) If a simple average is calculated for all data points, the standard deviation for a single point is 12% (Sample 1) or 9% (Sample 2); these reduce to 3.6% and 4.4%, respectively, when the five outliers (fig 2, $>2\sigma$) are rejected. If the increasing trend of the beam is taken out in first approximation by a straight line least squares fit, the standard deviations reduce to 1.9% (1) and 3.4% (2). Thus, the variability, from cycle to cycle, of the beam entering the accelerator is of the order of 2% for a 30-second data collection interval. (In other runs with somewhat more constant $^{12}C^-$ beam strength, the standard deviations ranged between 0.5% and 2%.) In the present case, the $^{12}C^-$ currents for 1 and 2, averaged over all collection intervals, have standard deviations of 0.2% and 0.35%, respectively.

A similar analysis of the $^{14}C^{+4}$ count rates (rejection of outliers, least squares fits) yields standard deviations of 6.1% (Sample 1) and 10.5% (Sample 2) for a second interval. These figures include contributions from accelerator input (see above), Poisson counting statistics (4.7% for 1 and 4.9% for 2), and variations in the transmission of $^{14}C^{+4}$ ions through the accelerator and downstream beam-handling system. From this, we infer that the variability of the $^{14}C^{+4}$ transmission is 3.2% for Sample 1 and 8.7% for Sample 2; this is of the same order as the counting statistics.

Comparison of the $^{14}C^{+4}$ with the $^{12}C^-$ graph of each sample and of these with the ^{14}C concentration ratio plot shows the strong advantage of making relative measurements. The gradually increasing trend in beam output and the deviating single readings are present in both $^{14}C^{+4}$ and $^{12}C^-$ and are, therefore, eliminated from the concentration ratio. The standard deviation for a single reading of the concentration ratio is 7.9%, based on the actual scatter (0.81% for the average). The standard deviation expected solely from counting statistics of both $^{14}C^{+4}$ beams is 6.8%. Therefore, the contribution from other sources, including the machine transmission of $^{14}C^{+4}$, is ca 4.1% (0.42% for the average). This agrees with the lower number estimated from the $^{14}C^{+4}$ graphs.

Finally, we note that the graphs offer an important means of detecting anomalies that could result in a poor management and, thus, provide criteria for discarding data that, in other respects, seem entirely valid.

In the above-described run, the carbon samples (activity, 80% modern carbon) gave $^{12}C^-$ beams of 11 to 12μA and $^{14}C^{+4}$ count rates of 850 to 900cpm. The run of 100 cycles took 2½

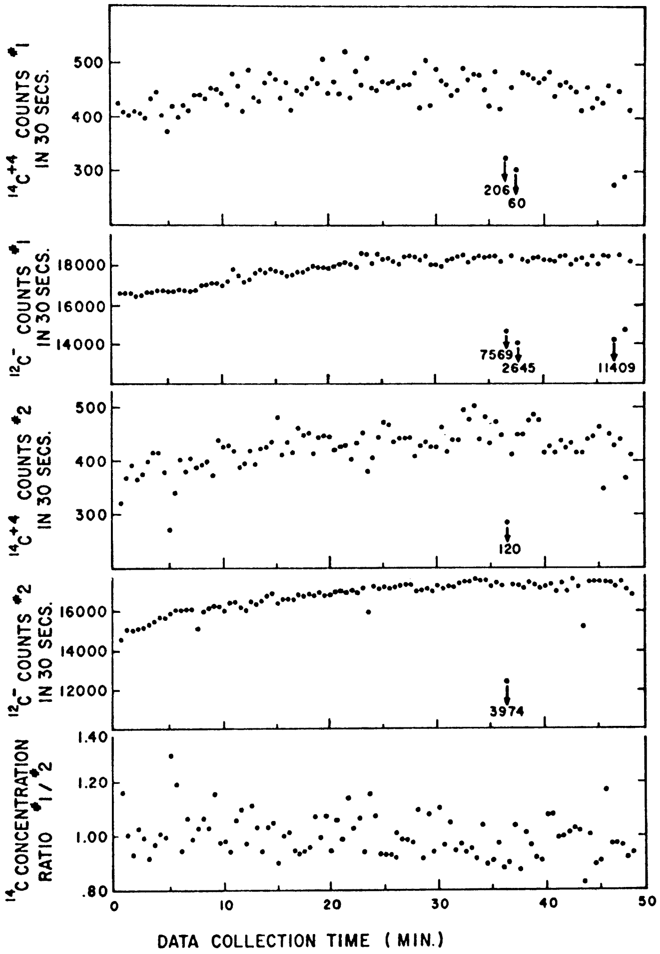

Fig 2.Data collected during a typical measurement with the inflection magnet current controlled by feedback from the position of the $^{12}C^{-}$ beam. One full cycle consists of 30 seconds of data collection on Samples 1 and 2 each, during which the $^{14}C^{+4}$ count rate is recorded by a DE,E detector system and the $^{12}C^{-}$ beam is obtained as a count rate through a current integrator on the side Faraday cup. For each cycle, a ^{14}C concentration ratio is obtained as the quotient of the ^{14}C count rates normalized to the same $^{12}C^{-}$ beam strength.

hours and gave a concentration ratio with a standard deviation of .81%; the dominant factor in this standard deviation was counting statistics rather than the stability of the AMS system. In two long and several short runs with these samples, a total of >100,000 counts was obtained from each without deterioration of the beam and with concentration ratios that repeated within their statistical uncertainty.

ACKNOWLEDGMENTS

This work has received support from the National Science Foundation (Grant EAR-8115994, Environmental Geosciences Program), the M J Murdock Charitable Trust, and the U S Department of Energy.

REFERENCES

Farwell, GW, Grootes, PM, Leach, DD, and Schmidt, FH, 1983, Technological advances in the University of Washington accelerator mass spectrometry system, in Stuiver, M and Kra, RS, eds, Internatl ^{14}C Conf, 11th, Proc: Radiocarbon, v 25.

Farwell, GW, Schaad, TP, Schmidt, FH, Tsang, M-YB, Grootes, PM, and Stuiver, M, 1980, Radiometric dating with the University of Washington tandem Van de Graaff accelerator, in Stuiver, M and Kra, RS, eds, Internatl ^{14}C Conf, 10th, Proc: Radiocarbon, v 22, no. 3, p 838-849.

Farwell, GW, Schmidt, FH, and Grootes, PM, 1981, Accelerator mass spectrometry at the University of Washington, in Kutschera, W, ed, Symposium on accelerator mass spectrometry, Proc: Argonne Natl Lab pub ANL/PHY-81-1, p 100-119.

Grootes, PM, Stuiver, M, Farwell, GW, Schaad, TP, and Schmidt, FH, 1980, Enrichment of ^{14}C and sample preparation for beta and ion counting, in Stuiver, M and Kra, RS, eds, Internatl ^{14}C Conf, 10th, Proc: Radiocarbon, v 22, no. 2, p 487-500.

Grootes, PM, Stuiver, M, Farwell, GW, and Schmidt, FH, 1981, Sample preparation for accelerator mass spectrometry at the University of Washington, in Kutschera, W, ed, Symposium on accelerator mass spectrometry, Proc: Argonne Natl Lab pub ANL/PHY-81-1, p 405-412.

Stuiver, M and Polach, HA, 1977, Discussion: Reporting of ^{14}C data, Radiocarbon, v 19, p 355-363.

[Radiocarbon, Vol 25, No. 2, 1983, P 719-728]

RESULTS OF TESTS AND MEASUREMENTS FROM THE NSF REGIONAL ACCELERATOR FACILITY FOR RADIOISOTOPE DATING

D J DONAHUE, T H ZABEL, A J T JULL, P E DAMON

University of Arizona
Tucson, Arizona 85721

and K H PURSER

General Ionex Corporation
Newburyport, Massachusetts 01950

ABSTRACT. Tests of performance of the tandem accelerator mass spectrometer at the NSF Regional Facility at the University of Arizona are discussed. Results of measurements on some tree rings and on some archaeologic samples are presented.

SYSTEM PROPERTIES

The accelerator and associated instrumentation were delivered to our laboratory by General Ionex Corporation, Newburyport, Massachusetts, on September 15, 1981. The installation was completed by November, and ^{14}C was first detected on February 2, 1982. In this paper, we present some results of tests and measurements made with the accelerator. The ion source is a cesium sputter type in which the cesium beam is incident upon a flat target at an angle of ca 35° to the normal to the target face. With graphite targets we have been able to produce currents of ^{12}C, analyzed through the injection magnet, of nearly 20 micro-amperes. The accelerator has been operated at a voltage of 2.2MV. For the ^{14}C measurements, a terminal voltage of 1.8MV was used. The system is operated using an argon gas stripper. We do not, as yet, have a vacuum pump in the terminal. Figure 1 shows, for a terminal voltage of 1.8MV, the transmission of the system,

$$T = \frac{\text{particle current of } ^{12}C^{q} \text{ at high-energy end}}{^{12}C^{-} \text{ at low-energy end}} ,$$

as a function of gas pressure as measured by a Penning ionization gauge located at the high-energy end of the accelerating tube. For $^{12}C^{+++}$ ions, the maximum transmission occurs when this pressure is 5×10^{-6} Torr, which is about a factor of ten higher than the pressure with no stripper gas. Figure 2 shows the transmission as a function of terminal voltage, when the stripper is set at its optimum value for the 3^{+}

charge state. The transmission for $^{12}C^{+++}$ is 20%. An extrapolation of the 3^+ curve indicates that at a terminal voltage of about 2.4MV, this transmission would reach a maximum of ca 25%. In figure 3, the transmission for 3^+ ions is plotted as a function of ion velocity at the terminal. The velocities of ^{12}C, ^{13}C, and ^{14}C are indicated for a terminal voltage of 1.8MV, and, as can be seen, ^{14}C ions are produced 20% less efficiently than are ^{12}C ions.

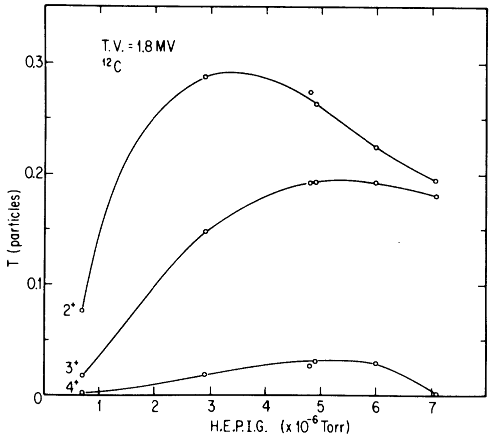

Fig 1. Particle transmission, T, through the accelerator of various charge states as a function of stripper-gas pressure, measured at the high-energy end of the accelerator tube

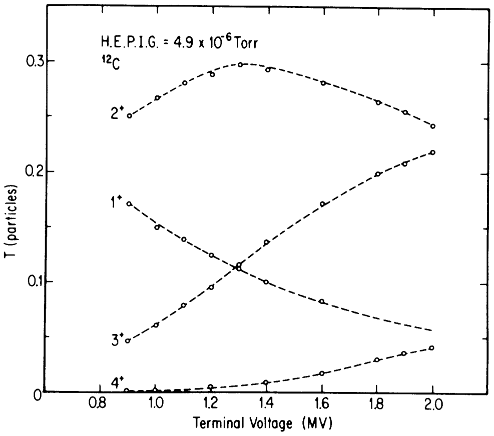

Fig 2. Particle transmission, T, vs terminal voltage

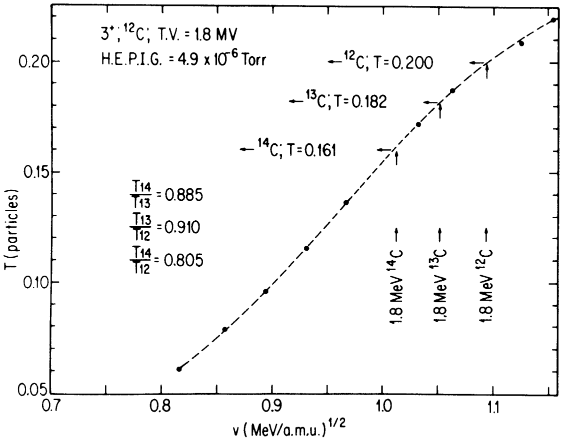

Fig 3. Particle transmission of $^{12}C^{+++}$ ions vs velocity of ^{12}C ions. Velocities of ^{14}C, ^{13}C, and ^{12}C ions with kinetic energies of 1.8MeV are indicated.

Ions of ^{14}C are detected in a silicon surface-barrier detector. Nitrogen ions are eliminated in one of two ways. The silicon detector can be operated in conjunction with a gas-ionization detector from which $\Delta E/\Delta x$ pulses are obtained for use in discriminating against nitrogen pulses. At times we use an alternative method for rejecting pulses from nitrogen. A thick absorber, 250 $\mu g/cm^2$, placed in front of the silicon detector is used to reduce the energy of the nitrogen ions by enough so that they can be rejected by energy discrimination in the silicon detector.

From the currents obtained from the ion source and from the accelerator transmission shown in figures 2 and 3, we calculate that for a current of 2.5 μamp $^{12}C^-$ (a realistic value from archaeologic samples) a ^{14}C count rate of 3 c/sec should be obtained for a modern sample. We do, in fact, observe such count rates.

TESTS WITH GRAPHITE

For most of the early tests, targets of spectroscopic graphite were used. The graphite was pumped free of nitrogen and irradiated in a nuclear reactor to produce a ^{14}C content of 1.57 ± 0.05 times the content of modern (1950) wood. We used these samples to measure the reproducibility of $^{14}C/^{13}C$ ratios in a series of targets. The methods used are best described by referring to the schematic diagram in figure 4.

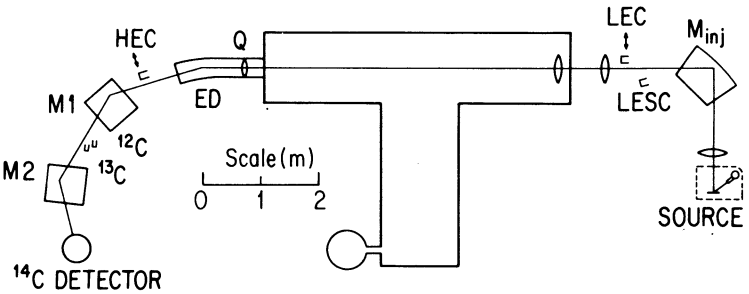

Fig 4. Schematic diagram of system. Abbreviations in the figure are: M_{inj}, injection magnet; LEC, low-energy Faraday cup (this cup can be moved in and out of the beam); LESC, low-energy side cup; Q, electrostatic quadrupole focus; ED, electrostatic deflector; M1 and M2, high-energy magnets; ^{13}C and ^{12}C, high-energy Faraday cups

The procedures used were as follows: 1) with a suitable target, enriched by a factor 2 to 10 in ^{14}C, set ion source controls, lenses, and other electrostatic and magnetic elements to optimize ^{14}C rate in detector; 2) move standard sample into appropriate position in ion source; 3) measure ^{14}C rate in detector. Counting time is from 2 to 6 minutes; 4) manually adjust injection magnet to pass M = 13. With a current integrator, measure ^{13}C current in high-energy side cup. Counting time is 10 to 30 seconds; 5) move unknown sample into position in the ion source; 6) repeat steps 3) and 4); 7) calculate the ratio

$$R = \frac{(^{14}C/^{13}C)_u}{(^{14}C/^{13}C)_s} .$$

Results of $^{14}C/^{13}C$ ratios made with a pair of graphite targets are shown in figure 5. Each point represents a cycle with the injection magnet, and gaps occur where the targets were interchanged. The measurement time for ^{14}C was 200 seconds and for ^{13}C, 10 seconds; targets were cycled about every 10 minutes. Two points should be noted. First, for target

#6, results were very stable. The standard deviation of the mean value of all the points is 0.5%, and is essentially equal to the precision from counting statistics. Second, the ratio for the upper target exhibits a trend with time. The problem is probably with the target itself. Quantitative results obtained with graphite targets appear to be very sensitive to properties of the target. We have observed that as the cesium beam produces cratering on the surface of the graphite target, $^{14}C/^{13}C$ ratios have changed by as much as a factor of two. In fact, the ratio begins to change before any obvious surface defects appear. From the results for target #6, we conclude that, in this set of data, systematic errors introduced by system fluctuations, by cycling of the injection magnet, and by moving the target in and out of position, were less than statistical errors, which were 0.5%.

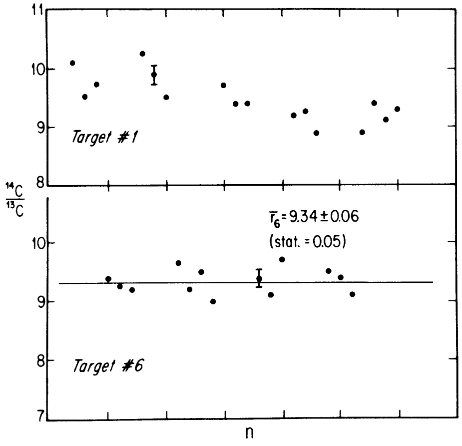

Fig 5. A plot of measurements of the ratio $^{14}C/^{13}C$ from irradiated graphite targets. Each point represents a cycle of the injection magnet and each gap in the points indicates a change on the target. The flags indicate the size of statistical error on individual points.

TESTS WITH Al_4C_3

We have tried many ways in which to prepare accelerator targets from cellulose and/or CO_2. Charcoal is easy to prepare from wood or cellulose and alternatively, CO_2 can be reduced to carbon by reduction with hot magnesium. Carbon in either of these forms is either mixed with a binder or heated to form a carbide. The product is packed into a sample holder. We have tried mixtures such as Ag-C, Pb-C Cu-C and KBr-C, and compounds such as Fe_3C, Mn_3C and Al_4C_3 and have had mixed and inconsistent results. At the present time, Al_4C_3 appears to be most satisfactory of the compounds. We consistently produce targets that yield from one to three micro-amps of $^{12}C^-$, resulting in 2 to 4 counts/sec from 1890 wood samples. The Al_4C_3 targets are easy to make and appear to stand up well under bombardment. Although cratering does occur in Al_4C_3 targets after a few hours of use, isotopic effects similar to those from graphite targets have not been observed in the 3% measurements made with these targets. Figure 6 illustrates that results of $^{14}C/^{13}C$ in two "real" targets can be made to 3%, and we expect that simply counting longer will improve that precision.

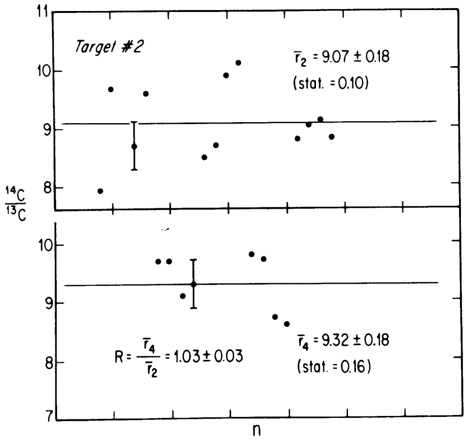

Fig 6. Plots similar to those in figure 5, but for Al_4C_3 targets.

BACKGROUND

Measurements of background are made by optimizing the parameters of the instrument with a target containing ^{14}C, and then measuring ^{14}C rates produced from a carbon target that contains no ^{14}C. Targets made from old (age > 58,000 yr) graphite, from bottled CO_2, and from limestone have been used. Results seem to depend on a variety of parameters which are not simple to define quantitatively. In figure 7, the ^{14}C rate from various targets is plotted against the total output of carbon ions from the ion source, as measured by the $^{12}C^-$ current in the low-energy cup. For these data, the gas-ionization chamber was used in conjunction with the silicon detector to ensure that the residual counts have the $\Delta E/\Delta x$ values of carbon. The figure includes data obtained with graphite and with Al_4C_3 targets made from old CO_2 and from limestone.

The value of the ^{14}C rate extrapolated to $i(^{12}C) = 0$, 1 or 2 counts per 1000 seconds, is approximately the rate observed with a pure aluminum target. Current of $^{12}C^-$ in the low-energy cup observed from pure aluminum is generally a few nanoamperes. Most Al_4C_3 targets of interest produce currents of < 4 micro-amperes, so that, for the present, a background is used as indicated by the horizontal lines in the curve; i e , we assume a ^{14}C background rate $= 0.02 \pm 0.01$ counts/sec. We expect that, eventually, this rate will be decreased. In terms of sample age, if a sample were 41,000 years old, its signal would be about equal to the background.

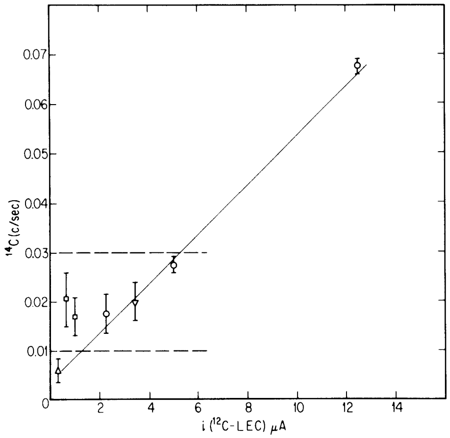

Fig 7. Background count rates plotted vs total carbon current from the ion source. Circles were obtained with graphite targets, and the others, with Al_4C_3 targets.

ARCHAEOLOGIC MEASUREMENTS

Measurements were made with Al_4C_3 targets prepared from tree rings provided by C W Ferguson, from corn obtained from Bat Cave by Austin Long, and from several CO_2 samples prepared by R E Taylor, from bones of a skeleton known as "Sunnyvale girl". The results of these measurements are listed in Table 1. Column 3 lists measured values of the ratio

$$R = \frac{(^{14}C/^{13}C)_{sample}}{(^{14}C/^{13}C)_{standard}} .$$

The measured ratio of $^{14}C/^{13}C$ in 5050 BC tree rings and in AD 1890 tree rings is shown as $R = 0.50 \pm 0.03$. The expected value for this ratio ($R = 0.48$) was obtained from the calibration curves of Klein <u>et al</u> (1982). The age of the Bat-cave corn as shown agrees well with a recent measurement by Long (pers. commun; 1982) on charcoal taken from that cave.

TABLE 1. Results of measurements

Sample	Standard	Ratio (measured)	Radiocarbon Age ^{14}C years B P ($T_{\frac{1}{2}}$ = 5568 yr)
Tree ring, 5050 BC	Tree ring, AD 1890	0.50 ± 0.03	
	(ratio from calibration (1))	0.48	
Bat-cave corn	Tree ring, AD 1890	0.84 ± 0.10	1460 ± 800
Sunnyvale, 1437A	Tree ring, 5050 BC	1.36 ± 0.10	3600 ± 600
Sunnyvale, 1437B	Tree ring, 5050 BC	1.16 ± 0.05	4850 ± 400
Sunnyvale, 1437D	Tree ring, 5050 BC	1.19 ± 0.05	4650 ± 400

Results of measurements on CO_2 from three different fractions of bone from the "Sunnyvale girl" are presented. According to Taylor (pers. commun; and (1983)), sample 1437A is from total acid-soluble organics, sample 1437B is from total base-soluble organics, and sample 1437D is from total insoluble organics, after gelatin conversion. Figure 8 shows results of $^{14}C/^{13}C$ measurements in which targets prepared from 5040-5050 BC tree rings and from sample 1437D (CO_2 from total insoluble organics) were alternated in the ion source. It is clear that the $^{14}C/^{13}C$ ratios of the two targets are comparable.

Measurements were made in collaboration with L A Currie and G A Klouda of the National Bureau of Standards on several atmospheric and standard samples. These measurements were made with our original target chamber and will be repeated. One result of interest is that a $^{14}C/^{13}C$ ratio was measured with a statistical precision of 10% with an Al_4C_3 target fabricated from oxalic acid which contained slightly $< 100\ \mu g$ of carbon.

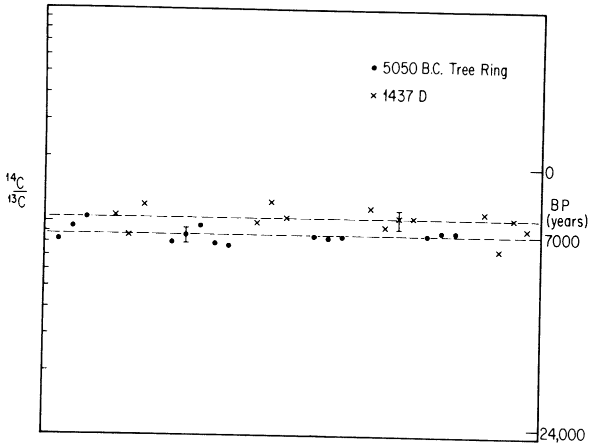

Fig 8. Successive measurements of $^{14}C/^{13}C$ ratios in Al_4C_3 targets made from 5050 BC tree rings (●) and from CO_2 from Sunnyvale bones (x). The dotted lines are averages of the two sets of points. The flags indicate the size of the statistical error for individual measurements. The right hand ordinate shows the time scale.

SUMMARY

We have presented results of initial tests of the General Ionex Corporation tandem accelerator facility which has been installed at the University of Arizona as part of a National Science Foundation Regional Facility for Radioisotope Dating. Some important results are: 1) at a terminal voltage of 1.8MV, the transmission of $^{12}C^-$ through the accelerator to $^{12}C^{+++}$ is 20%, sufficient to perform precise measurements of $^{14}C/^{13}C$ ratios; 2) to a precision of 0.5%, $^{14}C/^{13}C$ ratio measurements can be made in which the errors are predominately statistical. These measurements were made with irradiated graphite targets, and include all of the magnet cycling and target changing that are necessary to make relative age measurements; 3) experience with a large number of mixtures and compounds indicate that Al_4C_3 is a reasonable material from which to fabricate accelerator targets. Results were obtained from one such target which was fabricated from 100 μg of carbon; 4) with Al_4C_3 targets fabricated with CO_2 obtained from geophysical and archaeological samples, measurements of the ratio:

$$R = \frac{(^{14}C/^{13}C)_{\text{sample}}}{(^{14}C/^{13}C)_{\text{standard}}}$$

have been made with standard deviations of 3%. Again, these standard deviations were limited primarily by statistical uncertainties. It is our expectation that further experiments with more total counts collected will lower these uncertainties; 5) background measurements indicate that, at present, the real signal from a 40,000-year-old sample is equal to the background from a dead carbon sample. The "machine" background, obtained by looking for a signal from a blank aluminum target, is ca 60,000 years; 6) preliminary results of measurements on tree rings and on some archaeologic samples are presented.

REFERENCES

Klein, J, Lerman, J C, Damon, P E and Ralph, E K, 1982, Calibration of radiocarbon dates: tables based on the consensus data of the Workshop on Calibrating the Radiocarbon Time Scale: Radiocarbon, v 24, p 103-150.

Taylor, R E, 1983, Non-concordance of radiocarbon and amino acid racemization-deduced age estimates on human bone, in Stuiver, Minze and Kra, Renee, eds, Internatl radiocarbon Conf, 11th, Proc: Radiocarbon, v 25.

[Radiocarbon, Vol 25, No. 2, 1983, P 729-737]

THE OXFORD RADIOCARBON ACCELERATOR FACILITY

RICHARD GILLESPIE, R E M HEDGES, AND N R WHITE

Research Laboratory for Archaeology and the
History of Art, Oxford University
6 Keble Road, Oxford OX1, 3QJ, England

The Oxford ^{14}C accelerator has operated with beam for some 400 hours. This report describes the progress made towards achieving dates from milligram samples with the required accuracy of better than 2%. In summary, it shows how ^{14}C is relatively easily detected, but that the overall beam optical system is, at present, rather sensitive to effects which prevent reliable maintenance of the necessary isotope ratio stability. These effects can probably be eliminated by careful attention to details of the design rather than by major modifications.

GENERAL DESCRIPTION OF BEAM TRANSPORT SYSTEM. Figure 1 shows a general plan of the beam transport system. ^{12}C and ^{13}C are both measured after acceleration of pulses of beam (pulse length 0.1msec to 10msec for ^{12}C, 1msec to 100msec for ^{13}C, mark space ratio of 2%), and collection in Faraday cups in the focal plane of the analyzer magnet, which is set to bend the $^{13}C^{3+}$ beam 90°. ^{14}C is measured by counting each ion as it is identified from two energy loss (dE/dX) measurements and a total energy measurement from a gas counter fitted with a half-micron polypropylene window. As ^{14}C is only 0.1 to 1% of the ion beam leaving the analyzer magnet at 90°, excess ions, which depress the count rate of the detector, are removed with a Wien (velocity) filter. The velocity resolution (half-width) of the filter is variable, to a maximum of 2%. The mass resolution of the analyzer magnet is 0.05%.

The accelerator is a '3MV' Tandetron, capable of operating up to 2.4MV. The maximum voltage for reliable operation appears to be ca 2.1MV at present, but this should improve. Ideally, the terminal voltage would be chosen to optimize production of C^{3+}, and possibly to ensure that isotopic fractionation in the stripping process is at its most reproducible. The terminal voltage stability is controlled solely by a GVM feedback loop, and at 2MV, is within ± 300V, with drifts of up to 1000V over several hours. Negative ion beams are stripped by carbon foils, or, more usually, by O_2 gas leaked into the stripper canal. Optimum stripping is not realized, since all leaked gas is pumped through the accelerating tubes. However, the overall beam transmission is quite satisfactory.

Selected masses are injected with a 90°, 450mm radius double focusing magnet with a mass resolution (FWHM) of 1%. $^{12}C^-$, $^{13}C^-$ ions are injected by electrostatically accelerating the beams through the magnet, using gap lenses at the magnet

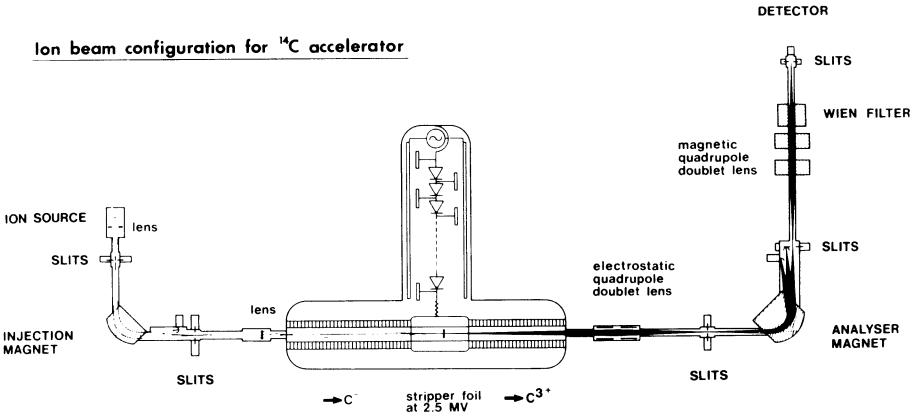

Fig 1. Beam transport system for ^{14}C accelerator (to scale)

waists. The electrostatic field is pulsed according to the schedule described above. All beam steering elements in the complete system are energy-dependent, rather than momentum-dependent. C^- beams are produced from graphite, using one or other of two Cs sputter sources, which are described below.

ION SOURCES AND SAMPLE TARGETS. Both ion sources were described previously (Hedges, Wand, and White, 1980; White, in press). The reflected source is more complex in operation and performance. It can accept 20 samples of graphite deposited on Ta wires. The 5mm length of graphite is scanned repetitively past the Cs^+ sputtering beam. Figure 2 shows the essentials of the arrangement.

In the alternative source (IS3; see figure 2) a single sample is accommodated. The operation of the source is more straightforward, but is limited by unsatisfactory fabrication procedures for the annular spherical ionizer. The source works best when the sample of graphite is crushed from the original Ta wire on which it was deposited and pressed into a hole of 1mm diameter in the center of an expendable Al holder. We have also operated (for a short time) the reflected beam source on graphite samples similarly crushed and pressed into holes of 1.2mm diameter. The resulting currents are 1/2 to 2/3 the current produced from wires; the sample is probably consumed more efficiently. In principle, it should be possible to design the IS3 source to take multiple samples. We believe that this source offers the best long-term arrangement for ^{14}C dating, but will continue to work both in parallel. Both sources have similar characteristics in performance, which also extends to finer details of isotopic ratio stability, and background ^{14}C

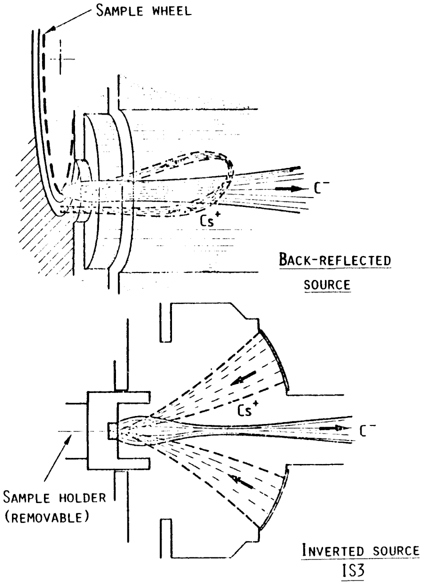

Fig 2. Schematics of beam arrangements in the back reflected and inverted sputter sources, showing sample mounting

contamination. Typical beam currents are in the 1 to 10μA region, using samples of ca 2mg of deposited graphite. When given full attention, both sources are capable of producing up to 5 times this beam current however.

BEAM TRANSPORT. The current injected as mass 14 (mainly $^{13}CH^-$) is in the region of 1nA or less. Up to 5μA ($12C^-$) at least, there is no change in overall transmission with current, although there is a significant increase in radiation at 2MV. The beam waist sizes, measured at slits, and the optical field strengths for optimum transmission, agree well with the original beam optics calculations.

The particle transmission through the accelerator at 2MV is ca 60 to 65%. This could be improved to perhaps 70 to 75% with a terminal gas stripper pump. Foil stripping at this voltage is significantly less efficient, due to greater scattering. In all cases, transmission should improve at higher voltage. The yield of C^{3+} is ca 30 to 35%, on a particle basis, from gas stripping. It is unlikely that equilibrium stripping can be obtained in our system at present, and the expected value is 42%. Transmission around the analyzer magnet and, for the 90° (ie, ^{14}C) beam, to the detector, is 95 ± 5%. For the smallest aperture (1.5mm diameter) before the detector, this is reduced to 80 to 85%, probably as a result of terminal voltage fluctuations (see below).

The stability of the terminal voltage can be monitored by measuring the position of the $^{12}C^{3+}$ beam inside the 97° Faraday cup. This can be measured to within 0.1mm, corresponding to a value of ± 25V on the terminal. There is an additional ripple at 50Hz and 300Hz with a maximum amplitude of 400V on the terminal, and it is necessary to synchronize the phase of the short $^{12}C^-$ beam pulse with the phase of the mains supply in order to eliminate a major source of noise in the measurement. Reduction of this ripple on the terminal can only be achieved with a fast-response feedback loop using an error signal derived from the Tandetron power supply. However, the ripple, while somewhat reducing transmission under conditions of highest resolution, should not lead to long-term instabilities. Monitoring of the beam position shows that the terminal is subject to random drifts typically in the range of 200V over 10 minutes, although periods of much higher stability can occur. The maximum excursion is probably ca 400V, although long-term drifts, probably due to thermal changes in the GVM and its circuitry, can lead to drifts of up to 1KV. These changes are important in the context of the stability of the $^{14}C/^{12}C$ ratio measurements.

DETECTION OF ^{14}C. With the beam transport system properly aligned, >95% of the particles reaching the detector, even with a large final aperture of 4mm, are ^{14}C ions, using a sample of oxalic acid standard (see fig 3). With the Wien filter turned off, the dominant ion is $^{13}C^{3+}$, with the same magnetic rigidity as the detected ^{14}C, and therefore, less energy. Some oxygen is also observed. There can be a small background spectrum from particles originating in the accelerating tubes during conditioning behavior, ie, irrespective of beam. Nitrogen is only observed when the injector magnet is tuned to inject mass 15 (NH^-), when the flux is maximized for a rigidity corresponding to the breakup of NH. There is no difference in observed background between foil stripping and gas stripping. (O_2 is used in preference to Ar simply because it is pumped better by our ion pumps.)

DETECTION OF ^{14}C FROM 'DEAD' SAMPLES. Although we have not done much work on the reduction of ^{14}C backgrounds, preliminary results give a ^{14}C signal equivalent to ca 60,000 years BP. This signal is undoubtedly due to ^{14}C nuclei originating from the ion source, and very probably from the region of sputtering itself. If the Cs^+ beam is interrupted before striking the target, no ^{14}C atoms are detected (age >80,000 years). Bare Ta and Pt wires have given ages between these two values. Since some C^- is detected (generally <1nA and falling with time), the ^{14}C ratio corresponds to fairly 'old' carbon. Interestingly, the oil from the turbo-pump has an equivalent age of 11,000 years. Much more work is needed to locate the sources of contamination, but it is gratifying that there is no significant cross-contamination between samples.

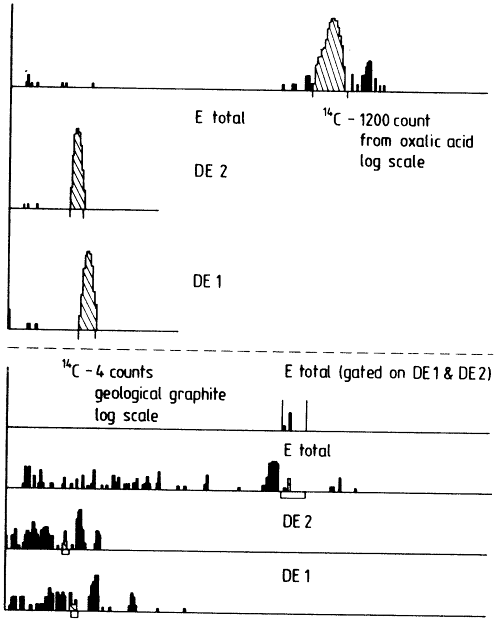

Fig 3. Energy spectra from the ^{14}C detector

MEASUREMENT OF THE ISOTOPE RATIO $^{14}/12$. This ratio is measured by comparison with that from a standard, and fractionation in the system which is linear with mass, ie, dependent on dynamic effects rather than, eg, beam alignment, is corrected for by reference to the change in $^{13}/12$ ratio. Thus, absolute measurements are not required, but the system must have a high degree of stability for accurate (<2%) measurements. Stability was measured under conditions similar to those for actual dating, but is not yet adequate for dating.

Stability of electronic measurements. By feeding stable currents into the gated integrators (which measure the pulsed beams entering the precision Faraday cups), and using a radioactive source before the detector, the dating experiment can be mimicked. The overall stability between runs is better than 1% provided the temperature of the gated integrators themselves is kept within 5°F.

Stability during a run with a single sample. Both ratios must be considered, and can be measured separately. As a rule, the $^{13}/12$ ratio is reproducible for a period of up to ca 3 hours, to within 1%. Occasionally, drifts in the value of 1 to 2% over 30 minutes are observed, and sometimes step changes of

2 to 3% take place. Such variations, which we suspect reflect varying source conditions, occur in ca 20% of runs of ca 30 minutes.

The stability of the $^{14}/12$ ratio is more difficult to measure, because of the time required to accumulate adequate statistics. We used Fermi graphite enriched to ca 4 times modern and observed quite severe drifts of the $^{14}/12$ ratio with time, nearly always falling away from the initial (set-up) value. We ascribe these to terminal voltage drifts which show a similar time-dependent behavior, and have the appropriate magnitude. We should eliminate this problem by stablizing the voltage on a signal from the pulsed ^{12}C beam position at the analyzer magnet. Table 1 lists other possible effects from the pulsed ^{14}C transmission, although there is no reason to expect other beam transport components to drift by the required amount. It is, of course, vital that the transmission of beam from the analyzer to detector can be kept constant to better than 1%, since these changes cannot be compensated.

^{14}C transmission will also probably be affected by the same causes of variation in the $^{13}/12$ ratio (apart from the linear, dynamical effects), which will have to be eliminated by study of the $^{13}/12$ ratio, since measurements to this accuracy on the $^{13}/12$ ratio take much more time.

Stability for runs with a single sample which is removed and replaced. Movement of the sample causes major changes in the 13/12 ratio, typically of ± 5%, sometimes of up to 15%. Very often the $^{14}/12$ ratio is correlated, but is not proportional to the mass difference. To some extent the same $^{13}/12$ ratio can be produced by exact repositioning of the sample, but movement of the order of 0.3mm, along beam axis, or 0.5mm, transversely, is sufficient to change the ratio significantly. We have evidence that these changes arise from only slight displacements in the three isotopic beams (see below).

Stability for runs between two samples of identical composition. The stability of these conditions is dominated by the problems mentioned above. One interesting and important feature that has emerged is that the injection conditions that maximize the transmission can be reproducibly different for different samples. In particular, a field shift of 0.5G in 2000 may be necessary to maximize the same isotopic beam from different samples on the target wheel. This corresponds to a shift of source position (transverse to the beam) of 0.25mm. Since the sputtering Cs^+ beam has a focused diameter of ca 1mm, with the target of similar size, such apparent shifts are not difficult to understand.

Stability conditions for dating. Accurate dating requires adequate stability under condition 4, above (to better than 1%) on account of dynamical fractionation effects, eg, occurring

TABLE 1. Change in HEMS system to produce 2%(5%) transmission change

Instrument	Beam	Aperture(mm)	Change in value
Terminal V	^{12}C,^{13}C pulsed		1.8 (2)kV @ 2MV
	^{14}C detector	1.5	120 (180)V
		2.3	450V
		4	550V
Analyzer magnet	^{12}C,^{13}C		18G = 0.18%
	^{14}C	1.5	0.3G = 3×10^{-5}
		4	1.5G = 1.5×10^{-4}
Wein filter	^{14}C only	1.5	0.2 (0.4)%
		4	1 (1.5)%
Magnetic quadrupole doublet lens	^{14}C only	1.5	0.5 (0.8)%
		4	1 (1.5)%
Electrostatic quadrupole doublet lens	all isotopes		5 (6)%
Stripper	(Attenuation)		~8% pressure change in gas
	C^{3+} fraction		25 (60)kV
Injector magnet	all isotopes		0.4 (0.6)G = 2×10^{-4}
Pulser voltage	^{13}C,^{12}C only		0.5(0.8)% = 1×10^{-4} for DE/E total
Injector lens			1.4 (2.3)%
Ion source lens			0.9 (2)%
Injector steerers (4)			17, 6, 17, 4%

in chemical preparation, and possibly in the mass spectrometer, and a demonstration that the measurement of ^{14}/12 is indeed linear with the ^{14}/12 ratio. Since the ^{14}C background can be shown to be sufficiently small, ie, below 1% of the sample requiring accurate dating, and the detector counts all particles, we do not expect difficulties in establishing linearity. However, the uncontrolled variations in ^{13}/12 and ^{14}/12 ratios prevent a demonstration of this at present.

THE EFFECT OF BEAM ALIGNMENT ON ISOTOPIC DISCRIMINATION. Table 2 shows the measured change in various functions of the system which bring about isotopic discrimination. The injection system is particularly sensitive, and angular or displacement changes of the order of that found in changing from one sample to the next are sufficient to bring about discrimination of the

TABLE 2. Change in HEMS system to produce 2%(5%) change in $^{13}/12$

Instrument	% change	Degree of $\frac{\text{fractionation change}}{\text{transmission change}}$
Ion source lens	1.1 (3) %	0.8
Injector lens	1 (2.5) %	1.4
Electrostatic quadrupole doublet	14%	0.3
Injector magnet	0.5,0.65 G (1G) ie 2.2×10^{-4}	0.8
Pulser voltages	0.5 (0.8) %	1.0
Injector steerers		
horizontal 1	10%	1.4
vertical 1	10%	0.6
horizontal 2	20%	0.8
vertical 2	6%	0.7
Analyzer magnet	$15G = 1.5 \times 10^{-4}$	

magnitude observed. (It is most unlikely that run to run reproducibility is affected by lack of stability in the electronic control of the beam transport fields.)

Reference to the curve showing the observed change in $^{13}/12$ as a function only of the injector magnetic field (fig 4A), suggests that if the two transmission curves for $^{12}C^-$ and $^{13}C^-$ are not exactly superimposable, ie, if the isotopic beams are not exactly co-linear, a change in the field for optimum transmission ~0.5G, will produce isotopic discrimination of the magnitude seen. This is shown in Figure 4B, where a shift of 0.5G would give a 2% change in isotope ratio for a displacement equivalent to 0.25G in the two stable isotope beams. Two effects therefore multiply each other: slight changes in beam source position and direction from sample to sample, and lack of colinearity in the injected isotope beams.

OUTLOOK. We have not collected enough evidence, nor made sufficient changes to the beam transport system to make predictions of performance with confidence. However, before the requisite accuracy can be achieved or any dynamical correction to the isotopic discrimination becomes appropriate, the following must be accomplished: 1) stabilization of the terminal voltage to within ± 150V at all times; 2) corrections to the injection system, either magnetically or with steerers synchronized with the pulsed isotopic beam, to reduce the isotope ratio sensitivity to misalignment; 3) understanding and reduction of the change of apparent source position for change of sample.

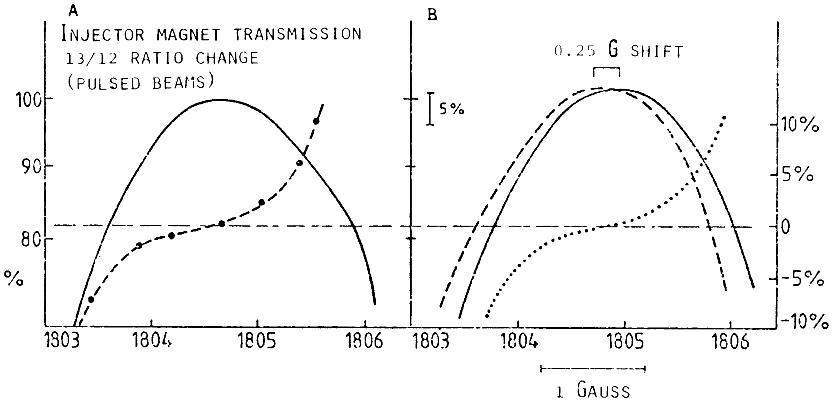

Fig 4A. Transmission of ^{13}C ion beam through the accelerator as a function of injector magnetic field. The dashed curve is the measured change in ^{13}C/^{12}C ratio as a result of changing the injector field.

Fig 4B. The continuous curve is a repeat of the transmission curve in 4A. The cashed curve is a similar curve, shifted by 0.25G, such that, if it represented the transmission of ^{12}C ion beam, the resulting isotopic discrimination would be given by the dotted curve.

REFERENCES

Hedges, REM, Wand, JO, and White, NR, 1980, The production of C$^-$ beams for radiocarbon dating with accelerators: Nuclear Instruments and Methods, v 173, p 409-421.

White, NR, in press, The inverted spherical ionizer sputter ion source (IS3): Nuclear Instruments and Methods, in press.

[Radiocarbon, Vol 25, No. 2, 1983, P 739-744]

RADIOCARBON DATING WITH THE UTRECHT TANDEM ACCELERATOR

K VAN DER BORG, JA HOOGENBOOM, RA JELMERSMA, ABRAHAM VERMEER
Fysisch Laboratorium Rijksuniversiteit Utrecht
PO Box 80.000, 3508 TA Utrecht, The Netherlands

and

GERT HUT

Laboratorium voor Isotopen Fysica,
Rijksuniversiteit, Groningen, The Netherlands

INTRODUCTION

In 1979 when accelerator mass spectrometry was started in the Netherlands, Gove (1978) and Litherland (1980) demonstrated that a tandem accelerator is eminently suited for this work. Isotope ratios below 10^{-15} could be determined and applications were stimulated on numerous fields of research. ^{14}C dating in particular would become an important application because smaller samples could be employed and more complex dating problems could be attacked. However, the 5% accuracy reached at that time had to be improved towards the 0.5% obtained with the conventional method of counting decays. Purser and Hanley (1978) pointed out that this high accuracy could be reached in facilities especially dedicated to dating. Rapid switching between measurements on different isotopes turned out to be crucial (Suter et al, 1981). We decided to proceed in two phases. In the first phase, the existing EN-tandem facility would be used as before and modified for the detection of ^{14}C ions. From measurements with ^{14}C ions from different samples, information would be obtained about the limitations of the existing facility. In the second phase, this information would be used to develop a facility in which accurate measurements of isotope ratios can be performed for elements throughout the periodic system. Conventional ^{14}C dating will be extended in collaboration with the Isotope Physics Laboratory in Groningen. Also, applications with other elements will be studied. The improved facility is scheduled for operation in the spring of 1983.

EXPERIMENTAL ARRANGEMENT AND METHOD

In analogy with laboratories where accelerator mass spectrometry was born, accelerator technology for stable heavy-ion beams of high intensity and heavy-ion detection techniques had to be developed. A sputter ion source of the Aarhus type (Tykeson et al, 1975) was constructed because the existing duoplasmatron showed a serious memory effect. Carbon samples with known $^{14}C/^{12}C$ ratios were prepared for this source from either charcoal of CO_2. Charcoal conventionally dated in

Groningen with an accuracy of 0.5% was used in the form of manganese carbide. Stable $^{12}C^-$ currents between 2 and 4 μA were obtained with these samples for periods of several hours. In a new set-up, similar to that of Beukens and Lee (1981), carbon samples were obtained by rf-cracking of acetylene, prepared from CO$_2$. Carbon samples with different $^{14}C/^{12}C$ ratios were obtained with 1% accuracy by using acetylene obtained by mixing amounts of this gas with known $^{14}C/^{12}C$ ratios. During a period of an hour $^{12}C^-$ currents up to 7 μA were obtained from these samples. A gas-filled heavy-ion detector of the Rochester design (Gove, 1978) was constructed. It combines a resistive wire counter for position read-out and an ionization chamber for measurement of energy loss and total energy of the ions. A 13° electrostatic analyser with $E/\Delta E = 200$ was constructed to reduce the background of ions in the detector. Spirally-inclined field acceleration tubes were installed in the high-energy part of the tandem in order to reduce the heavy load of the terminal and, hence, to obtain a more stable beam transmission. A generating voltmeter stabilization circuit was developed to stabilize the terminal voltage within 0.1% during acceleration of ^{14}C ions when the slit stabilization system cannot be used.

The measurements were made with the EN-tandem facility (fig 1). Negative ions with an energy of 25 keV emerging from the sputter source were mass-analyzed with the 20° inflection magnet with $m/\Delta m \simeq 20$ and were focused with Einzel lenses in

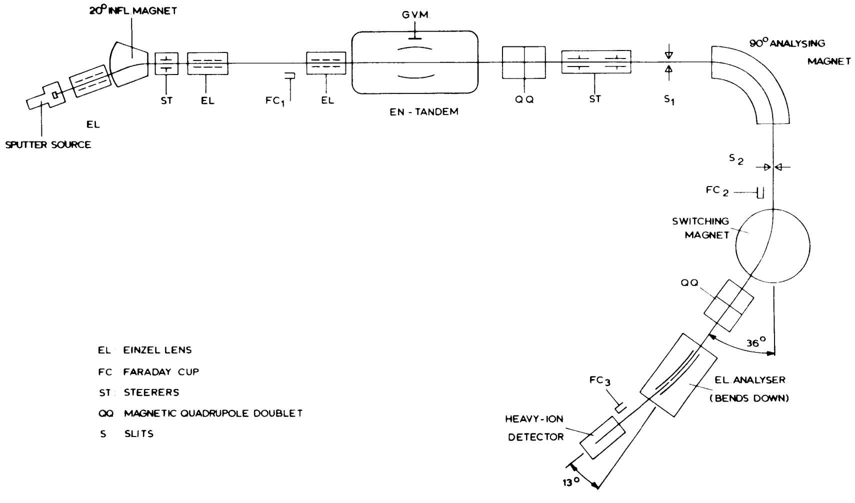

Fig 1. Schematic experimental arrangement of the present Utrecht EN-tandem facility

the stripper of the tandem accelerator. The terminal voltage was set at 4.35 MV to obtain optimal stripping efficiency for 4+ ions. The ions emerging from the accelerator were focused with a magnetic quadrupole doublet in the object slits of the 90° analysing magnet with exit slits set at $p/\Delta p \simeq 500$. The switching magnet bent the beam over 36° into the beam line used, where another magnetic quadrupole doublet focused the beam through the electrostatic analyser. ^{14}C ions were detected in the heavy-ion detector and ^{12}C and ^{13}C currents measured in a Faraday cup which can be placed pneumatically just in front of the detector. Signals of the detector with information on position, energy loss, and total energy of the detected ions were digitized by 11-bit ADC's, connected with a CAMAC interface to a PDP 11/34 computer for on-line data handling. Figure 2 shows the two-dimensional display of the data on a graphics terminal, used for event selection.

In order to determine $^{14}C/^{12}C$ ratios, the accelerator and beam transport elements were tuned for optimal transmission of a ^{12}C beam. Then tuning was done for a ^{13}C beam. The best transmission was 50%, taking stripping efficiency into account. Settings for the ^{14}C beam were obtained by scaling the magnetic elements. Further optimization of all these magnetic elements was extremely important. Hence, reproducible settings are required for the periodic measurement of ^{14}C ions alternated with ^{12}C and ^{13}C currents. However, the reproducibility proved insufficient. In particular, accelerator tuning for the intense ^{12}C beam differed from that for the weak ^{13}C and ^{14}C beams. Moreover, the interchange from slit stabilization to generating

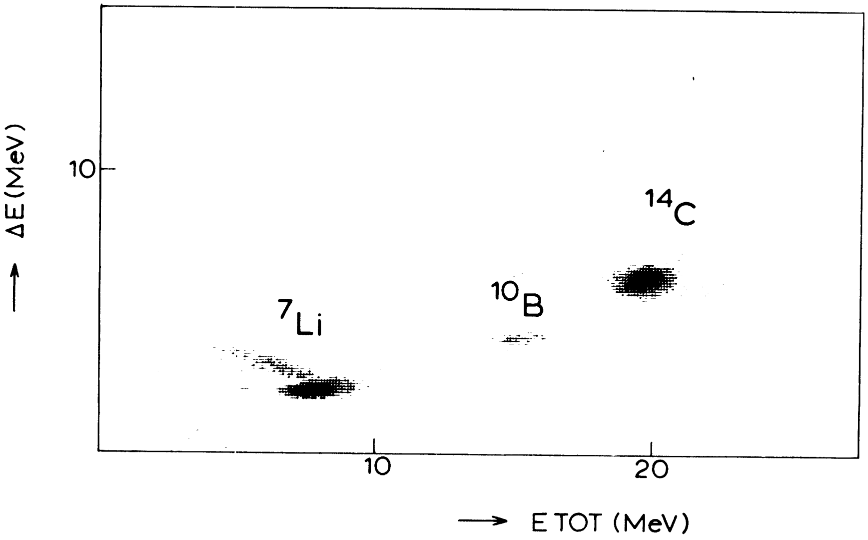

Fig 2. Two dimensional display of energy loss ΔE vs total energy E_{tot}

voltmeter (GVM) stabilization also caused a drop in transmission. Since it was impractical to measure sequentially ^{14}C ions and both the ^{12}C and ^{13}C currents, we only alternated with the ^{13}C current, which did not reproduce well within 10%. This could be due either to changes in the performance of the sputter source or to instabilities in the beam transmission. Thus, measurement of ^{14}C ions was made in short periods of 5 to 10 minutes, when ca 1000 ^{14}C ions were counted. Measuring 1 sample consisted of ca 5 short measurements. Samples were changed by inserting a new sample in the sputter source. Taking into account the lower stripping efficiency of ca 3% for the ^{14}C ions with respect to the ^{13}C ions at the terminal voltage used, the ^{14}C/^{13}C ratios obtained for the different samples were converted into percentages of modern carbon (pmC). The statistical errors of ca 3% for the short measurements were small with respect to the large systematic errors.

RESULTS

Table 1 shows the results for a series of short measurements obtained with a carbon sample prepared with the rf-cracking method with a ^{14}C/^{12}C ratio of 154.4 pmC. The values show large systematic errors and the average value of 67 ± 10 pmC is considerably lower than the expected value. Similar results were obtained for measurements made under the same experimental conditions with rf-cracked samples of different ^{14}C/^{12}C ratios. Figure 3 shows the results of these accelerator measurements compared to values obtained with 1% accuracy in the conventional decay-counting method. The same observation was made as in table 1: large systematic errors occur and average values obtained with the accelerator method are too small by about a factor of two. Similar results were obtained in other experimental runs with different samples. Mostly, the ^{14}C yield was too small, but the difference with expected values was not constant. Nevertheless, the data show a linear dependence on the ^{14}C/^{12}C ratio present in the sample, indicating that relative dating can be done with present accuracy as low as 20%.

TABLE 1. Results obtained for a ^{14}C measurement with a carbon sample containing 154.4 pmC *

Running time (sec)	^{14}C counts	^{13}C current (nA) (nA)	^{14}C/^{12}C** (pmC)
146	501	27	79
595	3155	45	73
297	1794	58	65
296	1654	60	58
297	1783	65	57

* pmC means percentage of modern carbon; 100 pmC corresponds to $^{14}C/^{12}C = 1.18 \times 10^{-12}$

** Corrected for 3% lower stripping efficiency of ^{14}C ions with respect to ^{13}C ions

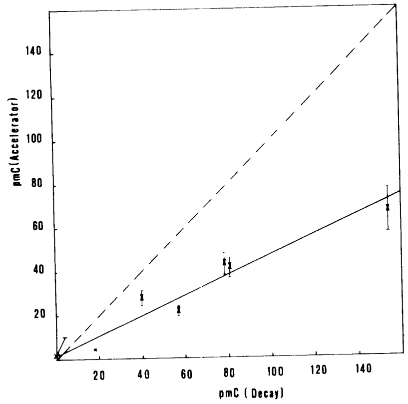

Fig 3. Comparison of results from the accelerator method and the conventional method of counting decays. The slope of the full line drawn through the data is too small with respect to the dashed line representing the expected values.

CONCLUSION

Our results show that the combination of electrostatic analyser and heavy-ion detector provides good identification of ^{14}C ions. Sample preparation is satisfactory, especially the new facility for the rf-cracking method which can create carbon samples from very little material. $^{14}C/^{12}C$ ratios determined for different samples show a linear dependence on the ratios determined in Groningen, indicating that relative dating measurements are possible with low accuracy. Absolute values of the obtained ratios are too small and show large systematic errors. These shortcomings can be ascribed to the poor beam transmission through the accelerator. The best transmission of 50% indicates that a considerable fraction of the beam is lost. Since the loss occurs in an undefined way, small changes in the performance of the accelerator or in the settings of the beam transport elements cause larger changes in beam transmission. Hence, it is difficult to obtain reproducible settings for optimal beam transmission of the different isotopes. Also, it is a drawback that the present ion source is not provided with a sample wheel. Interchange of samples involves the shutdown of the ion source, introducing a change in performance for different samples.

We have decided to improve the beam transmission in order to realize the future determination of isotope ratios within 1% accuracy. Beam transport calculations with the computer code OPTRYK (Greenway, 1978 pers commun) were made to develop a new injection system with optimal beam transmission. This injection system involves: 1) a 90° magnet with $m/\Delta m \simeq 300$, 2) pre-acceleration to 120 keV, 3) an electrostatic quadrupole triplet lens, 4) spirally-inclined field tubes in the low-energy part of the tandem. A gridded lens in the entrance of the first tube facilitates optimal focusing in the stripper.

Rapid switching between measurements on different isotopes will achieve reproducible and accurate measurement of the different isotopes. Rapid switching will be obtained by electrostatically biasing the vacuum chamber of the injection magnet, so that at a fixed magnetic field, ions of different mass can be injected in short periods by adjusting the energy of the ions. The stable isotopes will be injected in short periods of ca 100 μs to prevent instabilities in accelerator performance due to the intense ^{12}C beam. The experimental arrangement with pulsed beams will become similar to the EN-tandem facility in Zürich (Suter et al, 1981). Different isotopes with the same energy emerging from the accelerator pass through the electrostatic analyser and are separated with a 90° analyzing magnet. With computer control, the ^{14}C ions are counted in the heavy-ion detector and ^{12}C and ^{13}C currents are measured in separate Faraday cups located in the focal plane of the magnet. Another improvement is expected from a new sputter ion source similar to the Argonne design (Yntema and Billquist, 1982). Early tests showed that $^{12}C^-$-currents up to 80μA could be obtained from a spot of 1mm diameter on a graphite sample. At the moment, the sample wheel can contain eight samples.

REFERENCES

Beukens, RP, Lee, HW, The production of small carbon samples by re-dissociation of acetylene, Symp on accelerator mass spectrometry, Proc: Illinois, Argonne Natl Lab, p 416-425.

Gove, HE, ed, 1978, Conf on radiocarbon dating with accelerators, 1st, Proc: New York, Univ Rochester.

Litherland, AE, 1980, Ultrasensitive mass spectrometry with accelerators: Ann Rev Nuclear Particle Sci, v 30, p 437-473.

Purser, KH, Hanley, PR, A carbon-14 dating system, Conf on radiocarbon dating with accelerators, 1st, Proc: New York, Univ Rochester, p 165-186.

Suter, M, Balzer, R, Bonani, G, Stoller, CH, Wölfli, W, Beer, J, Oeschger, H, Stauffer, B, 1981, Improvements in the application of a tandem Van de Graaff accelerator for ultrasensitive mass spectrometry, in Symp on accelerator mass spectrometry, Proc: Illinois, Argonne Natl Lab, p 87-99

Tykeson, P, Anderson, HH, Heinemeier, J, 1975, Further investigations of ANIS: IEEE Trans Nucl Sci 1, v NS23, p 1104-1108

Yntema, JL and Billquist, PJ, 1982, High intensity inverted sputter source; Nuclear Instruments Methods, v 199, p 637-638.

[Radiocarbon, Vol 25, No. 2, 1983, P 745-753]

RADIOISOTOPE DATING WITH THE ETHZ-EN-TANDEM ACCELERATOR

WILLY WOELFLI, GEORGES BONANI, MARTIN SUTER, RICHARD BALZER,
MARZIO NESSI, and CHRISTIAN STOLLER
Laboratorium für Kernphysik, Eidgenössische Technische
Hochschule, CH-8093 Zürich, Switzerland
and
JUERG BEER, HANS OESCHGER, and MICHEL ANDRÉE
Physikalisches Institut, Universität Bern,
CH-3012 BERN, Switzerland

INTRODUCTION

During the last three years the ETH-EN-tandem accelerator facility has been adapted for the quantitative determination of the rare isotopes ^{14}C and ^{10}Be in mg samples. The goal of this project is to routinely achieve a 1% accuracy when measuring $^{14}C/^{12}C$ ratios with a minimum expenditure of human resources and beam time. The concept is similar to that proposed by Purser and Henley (1978). The early evolution of this dating facility was described previously (Suter et al , 1981a,b). This paper is a brief report on the current status of the system and its development.

INSTRUMENTATION

The schematic layout of our dating facility is shown in figure 1, consisting of a Cs sputter ion source producing the negative ion beam attached to the 90° inflection magnet at the low energy side of the machine. The accelerated beam is then separated and analyzed by a combination of a 15° electrostatic deflector, a 90° analyzing magnet and a gas ΔE-E counter (the current of the abundant isotopes is measured directly in Faraday cups). The use of electrostatic elements only, for focusing and steering of the beam from the inflection magnet to the analyzing magnet ensures that for equal beam injection conditions all paths of the various isotopes are virtually the same up to the magnetic spectrometer. In this way, systematic errors in the determination of the isotopic ratios due to changes of the transmission through the accelerator and the beam transport system can be reduced considerably.

Unfortunately, existing tandem van de Graaff accelerators are not capable of sustaining the intense currents of the abundant stable isotopes. An overall current reduction is undesirable since it affects also the rare isotope. Thus we developed a fast switching system in which the stable isotopes are only injected in short pulses (160-200μs long). Provided

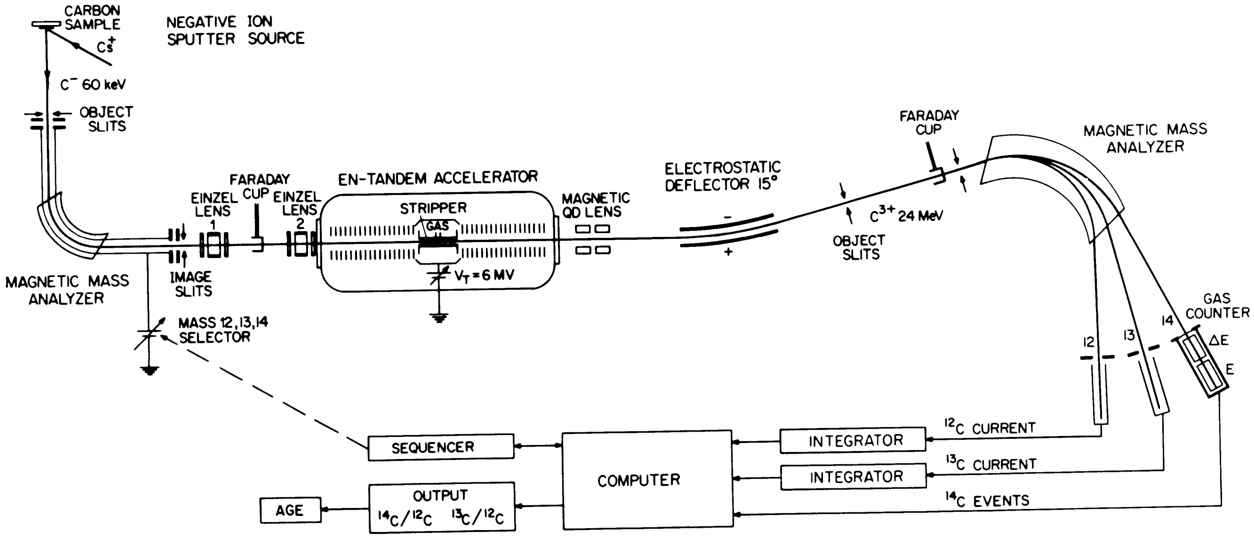

Fig 1. Layout of the accelerator based dating facility

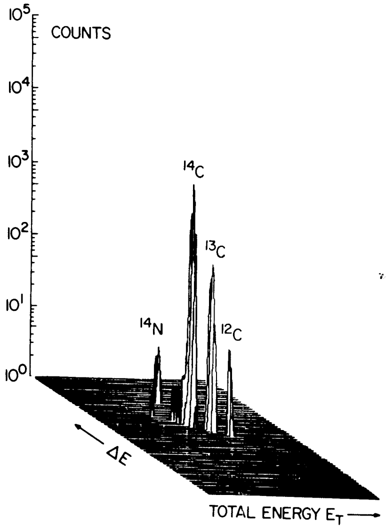

Fig 2. Two-parameter logarithmic plot of a particle spectrum from a graphitic wood sample (∿135%M) observed with the ΔE-E heavy ion gas detector. The electrostatic and magnetic analyzing system was set for particles having an energy of 18MeV, charge state 3^+ and mass 14.

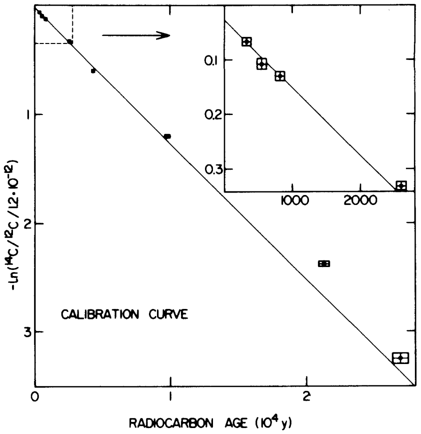

Fig 3. Calibration curve. The $^{14}C/^{12}C$ ratios are given in units of modern carbon ($1.2\cdot10^{-12}$). The carbon age of the samples was determined by beta counting. The solid line is a fit to the data using $t_{1/2}=5568$ yr. For the samples shown in the insertion, the β counting accuracy is better than ±75 yr. For the older samples, it lies between ±80 and ±590 yr. The measuring time for each sample was only 500 sec.

the duty cycle is low (2×10^{-3} in our case), loading effects on the machine are minor. The injection of 10 to 20 pulses/s allows quasicontinuous monitoring of all isotopes of interest. A more detailed description has been given by Suter et al (1983). To check the performance, the stability, the sensitivity, and the reproducibility of the whole arrangement, extensive tests with C and BeO standards were made.

RESULTS

^{14}C RESULTS. We measured $^{13}C/^{12}C$ and $^{14}C/^{12}C$ isotopic ratios using beams from calibrated graphitic C samples, ie, carbon converted into graphite under high temperature and pressure (1300 °C, 10 kb) (Polach, pers commun). Graphite was used because it yields the highest and most stable negative C currents in our ion source. Samples of charcoal and amorphous carbon obtained by various processes give lower and less stable currents, and also tend to burn out faster. From graphite we obtain up to 40μA negative ^{12}C current, which is injected into the tandem. Up to 30% of the injected particles emerge from the accelerator in the 3+ state with an energy of 18MeV (with an accelerating voltage of 4.5MV). This charge state and energy are selected by the electrostatic deflector (independently of particle mass) and finally mass-analyzed by the magnetic spectrometer.

Figure 2 shows a typical particle spectrum measured with a ΔE-E gas counter telescope using a 135% M ^{14}C standard. Only four well-separated peaks are observed, which can be attributed to ^{14}C, ^{13}C, ^{12}C, and ^{14}N ions of equal magnetic rigidity. The unwanted ions (^{13}C, ^{12}C, ^{14}N) stem from fragments of molecular beams (like $^{13}CH^-$, $^{12}CH_2^-$, ^{14}NH) or from $^{12}C^-$ and $^{13}C^-$ tails under the ^{14}C which, through multiple scattering, find their way through the electrostatic deflector and the magnet to the counter. The ^{13}C and ^{12}C peaks vary significantly from sample to sample since they are related to the hydrocarbon content of the material used.

The sensitivity of the method is limited in two ways - by ^{13}C background (the tail of the ^{13}C peak in fig 2 can reach into the region of the ^{14}C peak), or by ^{14}C contamination of the sample, be it by cross talk in the source or during sample preparation. The present sensitivity limit of 10^{-15} to 2×10^{-16} is mainly determined by sample contamination with ^{14}C.

Figure 3 shows a measurement of $^{14}C/^{12}C$ ratios for a set of calibrated graphitic samples (Polach, pers commun). The measured ratio is plotted vs the age determined by conventional β counting. The data were fitted to an exponential with only the height as a free parameter. The slope is given by the known ^{14}C half life (Libby). The weighted mean deviation of the data points from the fit is 1%.

In order to prove that this excellent agreement is not fortuitous, we made several runs to determine the long-term stability of the apparatus and the reproducibility of the results. Figure 4 shows results obtained by measuring $^{14}C/^{12}C$ and $^{13}C/^{12}C$ ratios in consecutive 50 s long cycles for one hour. We also determined the transmission of ^{12}C through the machine (ie, the ratio between ^{12}C current at the low energy side of the machine and ^{12}C current after the magnetic analyzer divided by the charge state to compare the number of particles). During a 50 s cycle we obtain ^{14}C counting statistics of ca 3%. The internal and external errors of the $^{14}C/^{12}C$ mean value were consistent with each other ($\sigma_{int} = 1/\sqrt{N_{tot}} = 0.28\%$, $\sigma_{ext} = 0.31\%$). This shows that systematic variations are smaller than 2‰, confirmed by the measurement of the $^{13}C/^{12}C$ ratio which, although measured only during a fraction

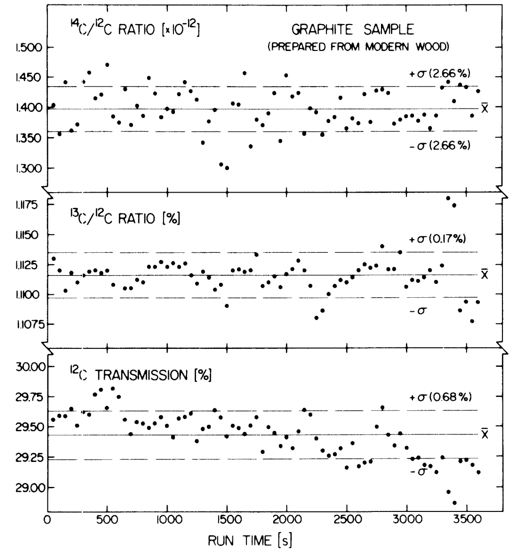

Fig 4. Carbon isotopic ratios and ^{12}C transmission for individual runs each lasting 50 sec. The mean value for the whole series is $\bar{X}$ = 1.397±0.004 (0.31%) for ^{14}C/^{12}C and $\bar{X}$ = 1.1116±0.0002 (0.02%) for ^{13}C/^{12}C. σ is the standard deviation of each single measurement.

of the time (0.1 s out of 50 s), is much better determined than ^{14}C/^{12}C. The standard deviation of a single ^{13}C/^{12}C data point in figure 4 is σ = 0.17% and the standard deviation of the mean is σ = 0.02%, although the transmission through the machine fell from 29.6% to 29.1%. This shows the inherent insensitivity of the arrangement to small drifts.

If we compare ^{13}C/^{12}C ratios when changing between samples of equal composition we sometimes find larger variations. If different samples made of the same material are measured consecutively, we find variations of the ^{13}C/^{12}C ratios of up to 1%. Preliminary data indicate that for amorphous carbon the variation is presently ca 2%. The lower reproducibility as compared to the stability is due to the fact that small changes in the sample position in the source slightly change the beam parameters. For amorphous material, reproducibility is worse because the samples burn out more quickly and also show large current variations during the measurement. In order to enhance reproducibility and thereby accuracy, the accelerator voltage regulation system must be improved. A reduction in sensitivity to changes in beam quality is expected by replacing the magnetic high-energy quadrupole lens with an electrostatic one.

^{10}Be RESULTS. The cosmogenic radioisotope, ^{10}Be($t_{1/2} = 1.6 \cdot 10^6$ yr), has been mainly used, so far, to study variations in the interaction of cosmic radiation with the atmosphere (Raisbeck et al, 1981). ^{10}Be is washed out by precipitation in a very short time of the order of 1 to 2 years and deposited on the earth. It is found in sediments, in polar ice caps, and even in organic material. The concentration of ^{10}Be in ice, eg, is very low. Raisbeck et al (1981) found a ^{10}Be concentration of $(4-12) \cdot 10^4$ atoms per gram water in ice-core samples from Antarctica. Our own measurements (Beer et al, 1983) indicate that it is about an order of magnitude smaller in ice-core samples from Dye 3 (Greenland). Usually, a well-known amount of ^{9}Be carrier (1 to 2 mg/lt water) is added and both isotopes are extracted chemically in the form of BeO. Samples with a ^{10}Be/^{9}Be concentration of the order of 10^{-12}–10^{-13} can be used for analysis without further processing, because the most intense negative ion beam obtained from a sputter ion source is formed by this molecule. However, the intensity of the molecular BeO$^-$ currents observed so far, is considerably lower than that for $^{12}C^-$. Whereas negative currents of the order of up to 40μA can be obtained for $^{12}C^-$, a maximum of only ca 1μA ^{9}BeO$^-$ has been obtained.

The acceleration of molecular ions with tandem accelerators imposes some additional problems as compared to atomic ions. The molecular ions accelerated in the first section usually desintegrate if stripped to positive charge states of 3^+ or more in the foil or gas stripper placed at the terminal of the accelerator. Consequently, the energies of the ^{9}Be and ^{10}Be fragments accelerated in the second section are not equal. Since the energy of a molecular fragment of mass m_1 and charge state q is given by $E = e(U_1\ m_1/m_2 + U_T(q+m_1/m_2))$ where m_2 is the mass and eU_1 the energy of the injected molecule and U_T the acceleration voltage, it follows that this energy difference is ca 0.7% for $q=3^+$ and U_T=5.5MV. Thus, all electrostatic focusing and bending elements placed at the high energy side of the accelerator must be modulated with a correction voltage when switching from ^{10}Be to ^{9}Be to avoid different focusing and bending of the two isotopes.

Transmission measurements made with BeO and ^{12}C-beams confirmed earlier observations (Middleton, Klein and Tang, 1981) that the transmission of a molecular beam is significantly poorer (about a factor of 4) than for elemental ions. The lower velocity of the heavier molecules in the first section of the accelerator and the Coulomb explosion of the molecules when passing through the stripper are responsible for this effect.

All analyzed BeO samples have been contaminated with Boron on the ppm level. Boron oxide forms negative ions with abut twice the efficiency of BeO (Middleton, Klein and Tang, 1981). The ^{10}B beam cannot be separated from the ^{10}Be beam by the magnetic spectrometer. Because the high ^{10}B intensity would overload the detector, the beam must be stopped in a suitable absorber before it reaches the ΔE-E counter.

Following a suggestion of Middleton, Klein and Tang (1981), we are using a gas (Ar) absorber cell into which an ionization chamber is incorporated. ^{10}B can then be used as a pilot beam for optimal tuning of the accelerator, beam transport, and isotope switching system. On the other hand, although this beam is only of the order of a few pA, it produces a disturbing background in the entrance foil of the gas cell which limits the detection sensitivity for ^{10}Be. The background results from a nuclear reaction of ^{10}B with hydrogen ($^{1}H(^{10}B,^{7}Be)^{4}He$) always present in ppm concentrations in metal foils. This reaction is exothermic ($Q = 1.146$MeV) and both reaction products are able to enter the ΔE-E counter telescope. ^{7}Be is very disturbing since it extends into the ^{10}Be region (Klein, Middleton, and Tang, 1981) limiting the $^{10}Be/^{9}Be$ concentration sensitivity to ca 10^{-14}. Obviously, this limit can be improved considerably if some way is found to reduce the Boron contamination in the BeO samples or (and) the hydrogen content of the entrance foil of the gas absorber.

At present the accuracy of measurements of Be samples with ^{10}Be concentration is determined mostly by statistics, because of the relatively low BeO^{-} currents. Systematic errors are larger than for carbon (∿2 to 3%) because of the poorer beam quality. For a $^{9}BeO^{-}$ current of 1μA and a ^{10}Be concentration of 10^{-14} only 20 counts per hour are recorded with the particle detector. Thus, the development of ion source with a negative ion efficiency comparable to that for carbon is very desirable.

The first results of measurements on ice samples from Dye 3 (Greenland) are discussed by Beer et al (1983).

CONCLUSION

We have shown that it is possible to convert a tandem Van de Graaff accelerator to a highly sensitive and accurate tool for rare isotope mass spectrometry. Using the concept of Purser and Henley (1978) we have obtained an accuracy of 1% for $^{14}C/^{12}C$ ratios using graphitic C samples. An improvement to 0.3% seems possible without major modifications. The ^{14}C concentration sensitivity is presently 10^{-15} to $2x10^{-16}$, depending on the composition and preparation of the sample.

Limitation is mainly by sample contamination with ^{14}C except for samples with a high hydrocarbon content. Molecular ^{13}C fragments from the parasitic $^{13}CH^-$ beam are the limiting factors here.

With ^{10}Be we have achieved sensitivities of 10^{-13} to 10^{-14}, depending on the amount of ^{10}B contamination in the sample. In this case systematic errors were between 2 and 3%. Present limitations in our apparatus are determined, on the one hand by the long-term variations in the sputter ion source, and on the other hand by the present long-term stability of the accelerator. The performance of the source can be improved by better sample preparation techniques and by changes in the source geometry. Higher accelerator stability requires a new stabilization system and the installation of an electrostatic quadrupole lens at the high energy end of the machine to reduce its sensitivity to small instabilities. Further improvements might be achieved by using computer-aided procedures to tune the accelerator and beam transport system so that the beam path for all isotopes is equal. We also intend to measure heavier isotopes (eg ^{36}Cl), for which major modifications will be needed.

ACKNOWLEDGMENTS

We would like to express our sincere appreciation to Henri Polach,Radiocarbon Dating Research Laboratory, ANU, Canberra, Australia, for providing the ^{14}C standards. Part of this work was supported by the Swiss National Science Foundation.

REFERENCES

Beer, J, Oeschger, H, Stauffer, B, Balzer, R, Bonani, G, Stoller, Ch, Suter, M, and Wölfli, W, 1983, Comparison of ^{10}B and ^{14}C variations, in Stuiver, Minze and Kra, Renée, eds, Internatl radiocarbon Conf, 11th, Proc: Radiocarbon, v 25.

Klein, M, Middleton, R, and Tang, H, 1982, Modifications of an FN tandem for quantitative ^{10}Be measurements, Nucl Instr Meth, v 193, p 601-616.

Middleton, R, Klein, J, Tang, W, 1981, Instrumentation of an FN tandem for the detection of ^{10}Be, ANL/PHY-81-1, p 57-86.

Purser, KH, and Henley, PR, 1978, in Gove, HE, ed, First Conf on Radiocarbon Dating with Accelerators, Proc Univ Rochester, p 165-186.

Raisbeck, GM, Yion, F, Lieuvin, M, Ravel, JC, Fruneau, M, Loiseaux, JM, 1981, ^{10}Be in the environment: Some recent results and their applications, ANL/PHY-81-1, p 228-243.

Suter, M, Balzer, R, Bonani, G, Stoller, Ch, Wölfli, W, Beer, J, Oeschger, H, and Stauffer, B, 1981a, Radioisotope Dating using an EN-tandem accelerator, IEEE transaction on Nucl Sci, NS-28, p 1475-1477.

Suter, M, Balzer, R, Bonani, G, Stoller, Ch, Wölfli, W, Beer, J, Oeschger, H, and Stauffer, B, 1981b, Improvements in the application of a tandem Van-de-Graaff accelerator for ultra-sensitive mass spectrometry, ANL/PHY-81-1, p 87-95.

Suter, M, Balzer, R, Bonani, G, Nessi, M, Stoller, Ch, Wölfli, W, Andrée, M, Beer, J, Oeschger, H, 1983, Precision measurements of rare radioisotopes with a tandem Van-de-Graaff accelerator, IEEE Transaction on Nucl Sci, NS-30, in press.

[Radiocarbon, Vol 25, No. 2, 1983, P 755-760]

TECHNOLOGICAL ADVANCES IN THE UNIVERSITY OF WASHINGTON ACCELERATOR MASS SPECTROMETRY SYSTEM

G W FARWELL, P M GROOTES, D D LEACH, AND F H SCHMIDT
Nuclear Physics Laboratory
University of Washington, Seattle, Washington 98195

ABSTRACT. During the past year we have continued to work toward greater stability and flexibility in nearly all elements of our accelerator mass spectrometry (AMS) system, which is based upon an FN tandem Van de Graaff accelerator, and have carried out measurements of $^{14}C/^{12}C$ and $^{10}Be/^{9}Be$ isotopic abundance ratios in natural samples. The principal recent developments and improvements in the accelerator system and in our sample preparation techniques for carbon and beryllium are discussed, and the results of a study of ^{10}Be cross-contamination of beryllium samples in the sputter ion source are presented.

INTRODUCTION

As all scientists engaged in accelerator mass spectrometry (AMS) are aware, the apparently simple task of adapting an accelerator constructed primarily for use in nuclear physics experiments to the measurement of minute isotopic fractions becomes formidable when accuracy in the 1% range (counting statistics permitting) is desired. During the year following the 1981 Symposium on Accelerator Mass Spectrometry held at the Argonne National Laboratory, where we reported our results up to that time (Farwell, Schmidt, and Grootes, 1981; Grootes et al, 1981), we have made substantial progress toward the desired 1% capability. Particular effort has been given to enhancement and stabilization of the overall ion transmission of the accelerator, to improvements in the cesium sputter ion source, to the measurement of cross-contamination among beryllium samples in the ion souce and the reduction of the ^{10}Be background of our system, to the construction of an automatic low-energy beam control system that enables concurrent measurement of $^{12}C^{-}$ and $^{14}C^{+4}$ beams from alternating samples, and to the study of other normalization arrangements. We have also given much attention to the preparation of beryllium and carbon ion source samples from natural materials, including the graphitization of carbon into pellets that give high (>10μA $^{12}C^{-}$) and very stable ion yields. These developments are discussed in more detail below; the results of recent measurements of isotopic abundance ratios are reported in a companion paper (Farwell et al, 1983).

ION SOURCE AND LOW-ENERGY BEAM TRANSPORT

A number of changes were incorporated into the cesium sputter ion source, including a better ion-forming electrode, steering electrodes for the negative ion beams, and improved electrode and sample alignment. These measures made it possible virtually to "dial-set" the source parameters in advance to produce any desired output of $^{12}C^-$ ions ranging from 0.5μA to 15μA, and resulted in increased ion output and stability for beryllium beams as well.

A substantial improvement in the ion optics of the low-energy beam system resulted from installation of a more highly stabilized power supply on the 12.5cm Einzel lens downstream from the inflection magnet. The mass resolution of the negative ion injection system was thereby increased from $M/\Delta M \simeq 30$ to $M/\Delta M \simeq 90$.

To facilitate rapid shifts of the AMS system from one isotope to another, we installed a two-level nuclear magnetic resonance controller on the inflection magnet; this was particularly useful in the beryllium studies and in the carbon studies in which normalization against ^{13}C is used.

Finally, an automatic low-energy beam control system was installed which enables concurrent measurement of $^{12}C^-$ and $^{14}C^{+4}$ beams; this provides a means of comparing the $^{14}C/^{12}C$ ratios of two alternating samples, a standard and an unknown (Farwell et al, 1983; Schmidt and Fauska, 1982).

ACCELERATOR TRANSMISSION: THE GRIDDED LENS

During much of the past year our studies were seriously affected by a deterioration in the overall ion transmission of the tandem Van de Graaff accelerator. However, it appears that the primary transmission problem has been solved, and recent operation has been much more satisfactory for the AMS studies. The transmission problem was associated largely with a gridded lens placed at the entrance to the accelerator tube. When this grid was first installed in May 1980, transmission of the carbon beams was increased nearly threefold. Other benefits were also derived from the grid -- most notably, a marked reduction in the criticality of low-energy tuning parameters. (This lack of criticality is very important when operating with a beam for which a current cannot be measured, as for ^{14}C or ^{10}Be.)

These benefits were seriously offset, however, by several grid-related phenomena: a lateral displacement of the high-energy beam, a reduced ability for the tandem accelerator to hold full voltage (9 MV), and increased X-radiation. These problems have been largely resolved by the installation of a suppressor magnet for electrons generated at the grid by the negative ion beam, together with three upstream compensating magnets to correct for beam displacement and deflection by the suppressor. With more favorable conditions resulting from these improvements it has been possible to achieve ^{14}C counting rates of ca 1500 per minute for 1950 carbon samples that give $^{12}C^-$ (low-energy) beams of ca 15μA.

The tandem accelerator is usually operated with a terminal voltage of 7.00 MV; the final ion energies are then 35.0 MeV ($^{14}C^- \rightarrow {}^{14}C^{+4}$) and 23.7 MeV ($^{10}Be^{16}O^- \rightarrow {}^{10}Be^{+3}$).

SAMPLE PREPARATION: CARBON

The production of small pellets (8 to 10mg) of graphite from wood samples or cracked carbon was described earlier (Grootes et al, 1980; Grootes et al, 1981). We have devised completely new equipment to make the process more reproducible and reliable. Carbonized and pulverized wood is mixed with ∿20% heavy hydrocarbon binder ("pitch") in a molybdenum mold. A set of six molds is gradually heated to 1000°C in a nitrogen atmosphere while pressure is applied to the carbon mixture to form it into a wafer of appropriate shape for insertion into the sputter ion source. The wafers are subsequently removed from the molds and heated under vacuum to 2500°C in a graphite holder inside a heavily heat-shielded graphite furnace. This produces graphitic wafers that are truncated cones, 0.090cm high x 0.236cm base diameter, with a cone angle of 20°. They are of uniform size, weigh ca 4mg, give beams of $^{12}C^-$ ions equal to or greater than high-grade commercial graphite, and reach 80% to 90% of peak output within 2 minutes after first being moved into position and subjected to the Cs sputtering ion beam.

This technique produces good graphitized carbon samples directly from wood. A more general sample preparation procedure, however, must be able to use CO_2 which can be prepared in a pure form from any carbonaceous material. Conversion of CO_2 into carbon is under study at the

Quaternary Isotope Laboratory. Reduction of CO_2 to CO over hot zinc followed by decomposition of the CO in a DC glow discharge (cracking) produces high quality carbon suitable for graphitization. The process is, however, time-consuming and the effect of gas pressure and discharge current on the cracking process needs further study.

An alternative and much faster route to elemental carbon uses reduction of CO_2 with magnesium at 900°C. Reductions between 80% and 100% can be reached without significant isotope fractionation in 5 to 10 minutes. Substantial chemical purification is required to eliminate the Mg and MgO and parts of the vicor tube used for the reduction. In addition, the carbon must be powdered and baked at 1000°C before it can be used for pellet production. Unfortunately, impurities remain in the mixture and cause serious deterioration of the pellet during the graphitization process.

SAMPLE PREPARATION: BERYLLIUM

We have found that a mixture of BeO powder and ultra-pure, finely ground silver (BeO:Ag ratio 1:6 to 1:8 by weight) gives good ion beams (BeO^-) when compressed into the central well of a Ta or an Al sputter ion source sample button. We have achieved analyzed $^9Be^{+3}$ beams of up to 80nA and routinely work with 20 to 50nA. A sample well size of 1.52mm diameter x 0.76mm depth has been as effective as a larger well size and requires only 2 to 3mg of BeO. Such samples reach full ion yield within an hour or so and have been run stably and effectively for as long as 12 hours.

The small sample size is especially beneficial in working with ^{10}Be extracted from snow, ice, and water samples when minimum expenditure of material is desired. Techniques for quantitative recovery of ^{10}Be from large volumes of water using ^9Be carrier (a few mg) and ion exchange filters and columns are currently being studied.

CROSS-CONTAMINATION STUDIES

In measuring minute isotopic abundance ratios (10^{-10} to 10^{-15}), it is tempting to use a sample rich in the rare isotope (eg, ^{10}Be or ^{14}C) while optimizing the accelerator parameters for transmission and detection of the rare isotope. We have explored the degree to which this procedure may result in contamination of unknown samples low in the rare isotope (Farwell, Grootes, and Schmidt, 1981). The results bear also upon the likelihood of mutual cross-contamination among unknown samples.

Cross-contamination was observed in the following instances: 1) ^{9}Be ions were observed from Ag and C (graphite) samples exposed to operation of the sputter ion source with a natural Be metal sample. 2) Strong contamination of the same samples with ^{10}B was also seen following brief (<10 min) operation with a B metal sample used for detector calibration. (^{10}B is the principal contaminant in analyzed ^{10}Be beams.) 3) The apparent ^{10}Be/^{9}Be ratios of low-level ($\sim 10^{-12}$ or less) BeO/Ag samples were grossly altered during operation with a Be metal sample enriched in ^{10}Be. We present here the results of this third study, which has clear implications for the measurement of low-level samples of both carbon and beryllium.

Table 1 gives the measured ^{10}Be/^{9}Be ratios for three beryllium samples made in our standard fashion (BeO powder/finely powdered Ag) both before and after exposure to extended operation of the sputter source with a Be metal sample enriched in ^{10}Be. The samples were mounted on a circle 10cm in diameter, in a 20-place rotating holder; their relative positions can be seen from the indicated position numbers (#20 is next to #1 in the sequence). While the ^{10}Be enhancement factors show an apparent correlation with distance from the contaminating source, the final ^{10}Be/^{9}Be ratios do not, and their values all lie between 10^{-5} and 10^{-4} of that of the contaminating sample.

We conclude that even a few minutes of operation with a high-ratio (high isotopic fraction) sample can contaminate exposed low-ratio samples at the level of 10^{-5} to 10^{-4} of the higher ratio.

TABLE 1. Cross-contamination with ^{10}Be. Beryllium samples were mounted on a 20-position circular holder and mutually exposed, in a cesium sputter ion source, for periods of 10 minutes or more of operation for each sample.

	Ratio ^{10}Be/^{9}Be			
Sample & position	Before exposure	After exposure	^{10}Be enhancement	^{10}Be/^{9}Be ratio relative to that for Be#20 (after exposure)
Be metal #20 (^{10}Be-enriched)	$5.4 \times 10^{-7} \pm 0.1$	(Same)	(None)	1.00 (Reference)
BeO/Ag #3	$0.8 \times 10^{-12} \pm 0.2$	$20 \times 10^{-12} \pm 1$	25	$3.7 \times 10^{-5} \pm 0.2$
BeO/Ag #7	$4.0 \times 10^{-12} \pm 0.8$	$35 \times 10^{-12} \pm 2$	8.8	$6.5 \times 10^{-5} \pm 0.4$
BeO/Ag #12	$6.0 \times 10^{-12} \pm 0.9$	$35 \times 10^{-12} \pm 2$	5.8	$6.5 \times 10^{-5} \pm 0.4$

By cleaning the sputter source components and taking other measures, we reduced our ^{10}Be background; it now corresponds typically to a $^{10}Be/^{9}Be$ ratio of $\sim 10^{-13}$ with BeO/Ag "blank" samples that have undergone the chemical extraction process used for preparing our natural samples. For high-purity, unprocessed BeO/Ag samples, which give a better indication of the possible level of ion source and accelerator contamination, the ^{10}Be background is less than 10^{-13}. For ^{14}C, the background from presumably ^{14}C-free graphite ranged from 1/200 to 1/400 of contemporary carbon until recently. Studies now indicate that the principal source of contamination is the pitch used for sample preparation. With ^{14}C-free pitch, our ^{14}C background corresponds to 55 to 58 thousand years.

ACKNOWLEDGMENTS

It is a pleasure to acknowledge the encouragement and support of Minze Stuiver. The work was materially assisted during the past year by a grant from the MJ Murdock Charitable Trust, and was also supported in part by the US Department of Energy and the National Science Foundation.

REFERENCES

Farwell, GW, Grootes, PM, and Schmidt, FH, 1981, Accelerator mass spectrometry: cross-contamination in a sputter ion source: Am Phys Soc Bull, v 26, p 1159.

Farwell, GW, Grootes, PM, Leach, DD, Schmidt, FH, and Stuiver, M, 1983, ^{10}Be and ^{14}C measurements with the University of Washington FN tandem accelerator, in Stuiver, M and Kra, RS, eds, Internatl ^{14}C Conf, 11th, Proc: Radiocarbon, v 25.

Farwell, GW, Schmidt, FH, and Grootes, PM, 1981, Accelerator mass spectrometry at the University of Washington, in Kutschera, W, ed, Symposium on accelerator mass spectrometry, Proc: Argonne Natl Lab pub ANL/PHY-81-1, p 100-119.

Grootes, PM, Stuiver, M, Farwell, GW, Schaad, TP, and Schmidt, FH, 1980, Enrichment of ^{14}C and sample preparation for beta and ion counting, in Stuiver, M and Kra, RS, eds, Internatl ^{14}C Conf, 10th, Proc: Radiocarbon, v 22, no. 2, p 487-499.

Grootes, PM, Stuiver, M, Farwell, GW, and Schmidt, FH, 1981, Sample preparation for accelerator mass spectrometry at the University of Washington, in Kutschera, W, ed, Symposium on accelerator mass spectrometry, Proc: Argonne Natl Lab pub ANL/PHY-81-1, p 405-415.

Schmidt, FH and Fauska, H, 1982, Auto-control of injected beams in accelerator mass spectrometry (AMS): Am Phys Soc Bull, v 27, p 526.

[Radiocarbon, Vol 25, No. 2, 1983, P 761-769]

PRODUCTION OF C^- DIRECTLY FROM CO_2 USING THE ANIS SPUTTER SOURCE

JAN HEINEMEIER and HANS HENRIK ANDERSEN

Institute of Physics, University of Aarhus
DK-8000 Aarhus C, Denmark

ABSTRACT. Micro-ampere beams of C^- have been produced with the Aarhus negative-ion source, operated on CO_2 gas. The efficiency of the source and memory effects have been measured, using ^{13}C-enriched CO_2, in order to evaluate the applicability of the source to ^{14}C dating by accelerator mass spectroscopy.

INTRODUCTION

Although primarily intended for solids, the Aarhus negative-ion source (ANIS) may be operated on gas feeds as its negative-ion production is based on a Penning-type discharge (Andersen and Tykesson, 1975; Tykesson, Andersen, and Heinemeier, 1976). We describe here an investigation of the production of C^- from gaseous samples, intended to evaluate the applicability of the source to ^{14}C dating by tandem-accelerator mass spectrometry. For a recent review of this technique, see Hedges (1981).

While most conventional ^{14}C dating is done by radioactivity counting on CO_2 samples, all successful accelerator dating up till now has relied on C^- production from solid graphite or carbonaceous samples used as sputter targets in various designs of the Middleton type of ion source. The preparation of CO_2 samples is a thoroughly understood process, while the further conversion into solid samples is associated with varying isotope fractionation, as discussed in detail by Hedges (1981). Several contributions to this conference report that fractionation in the sputtering and ion-extraction process is sensitive to the shape and position of the solid sample in the ion source, thus introducing severe irreproducibility in the measured isotopic ratios. Handling of solid microsamples, sufficiently small to fully exploit the high efficiency of the accelerator method, is difficult and introduces a risk of contamination with modern carbon. Thus, the use of solid samples for radioactivity counting ('the carbon black method') was abandoned during the early history of ^{14}C dating because of problems with contamination. Although the advantages thus are obvious, very few attempts to use gaseous samples for the accelerator method have been made. Middleton (1978) finds low C^- output from his source when jetting CO_2 onto a titanium sputter cone and also finds that the exit aperture of a duoplasmatron gets blocked by carbon deposits when operated on CO_2. Shea et al (1980) conclude that the Dawton-type carbon-ion source with gas charge exchange is unsuitable for dating due to memory effects. Thus, we investigated the performance of the ANIS source in terms of (i) C^- beam intensity, (ii) ionization efficiency, (iii) memory effects, and (iv) background of C^- beam originating from residual gas and the source, itself, rather than from the gas feed. All measurements described in the following were made on our ion-source test bench.

EXPERIMENTAL PROCEDURE

The ANIS source is shown schematically in figure 1. A Penning discharge is maintained on a mixture of CO_2 gas and cesium vapour in the stainless-steel discharge chamber, which is heated to ca 500°C by the two filaments, which also provide the electrons for the discharge. Positive ions from the plasma impinge on the sputter cathode at an energy corresponding to the sputtering voltage of ca -1.5keV. The cesium-enhanced negative sputtered ions are accelerated across the plasma sheath at the spherically concave cathode surface and thus directed

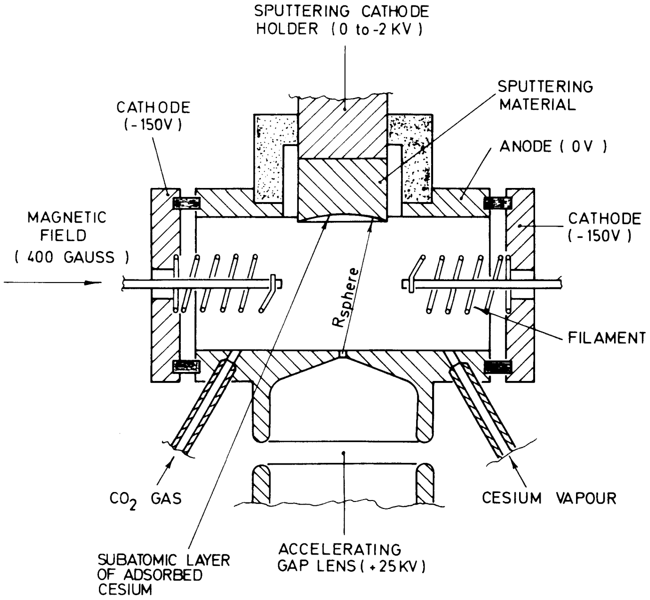

Fig 1. Schematic drawing of the ANIS source

towards the outlet aperture. Apart from beams corresponding to the cathode material, micro-ampere beams of C^- and O^- are produced from carbon and oxygen implanted in the cathode by bombardment with positive plasma ions such as C^+, CO^+, CO_2^+, and O^+. Thus, with the high sputter currents (10mA) typical of this operation, rapid sputtering of the cathode will bring the implanted ions near the surface, where they are sputtered off, with only a short delay. Adsorption of CO and CO_2 may also contribute to the process.

A simple way of evaluating the carbon memory effects down to a level of ∿0.5% consists of recording the $^{13}C^-/^{12}C^-$ beam-intensity ratio while alternating between gas feeding of natural CO_2 and ^{13}C-enriched CO_2. The gas-flow rate to the source is measured by monitoring the pressure difference ΔP across a known molecular-flow resistance with an electronic membrane differential manometer. The pressure signal is also used for feed-back regulation of the flow rate through two remote-control needle valves, one for each gas supply. Changing gas sample simply involves switching the control signal from one valve to the other. When both valves are closed, ΔP decreases exponentially with a time constant of 30 sec, which also governs the partial pressure in the gas feed of the previous gas sample after sample changes. Thus, the gas-control system not only allows an accurate determination of the ionization efficiency but also ensures a rapid change of isotopic composition of the sample gas without changing the total CO_2 flow rate or any other ion-source parameter. For memory measurements, this method is more reliable than, eg, closing off the gas supply and watching the decrease in C^- intensity, which may be affected by a change in ionization efficiency, with changing operating conditions. Likewise, the processes responsible for the liberation of the carbon deposited in various parts of the source may depend on the CO_2 supply.

After sample change from enriched to natural CO_2, the beam intensity I_{13} at mass 13 relative to the mass-12 intensity I_{12} reflects the fraction of the total C^- output which remains as a 'memory' of the previous sample. Taking into consideration mass-13 background and enrichment ε (normally 90%), we define the memory fraction

$$F = \frac{I_{13}-(I_{13}/I_{12})_0 \cdot I_{12}}{I_{12}+I_{13}} \frac{1}{\varepsilon}, \qquad (1)$$

where $(I_{13}/I_{12})_0$ is the ratio of the mass-13 to -12 beams for a natural CO_2 sample. It is usually ca 2%, due to the natural 1.1% abundance of ^{13}C as well as a component of $^{12}CH^-$. Ideally, F should vary from 100% before to zero after sample change.

In order to ensure reliable results, unaffected by a possible background of $^{12}C^-$, the ionization efficiency was normally determined from the $^{13}C^-$ intensity and the measured flow rate of 90% enriched $^{13}CO_2$. The ionization efficiency is defined as the number of C^- ions per second in the source output divided by the number of carbon atoms per second in the gas flowing to the source. Beam intensities were measured in a suppressed Faraday cup after magnetic analysis at 20keV. No correction was made for transmission losses, eg, in the two gridded lenses between the source and the magnet.

RESULTS

In this study we have used sputter cathodes made of copper since this material proved superior to other sputter materials such as magnesium, titanium, yttrium, gold, and tantalum. Typical C^- currents observed for a copper cathode were 2 to 4μA and up to 7μA on a few occasions. These values were found for CO_2 flow rates of ca 5×10^{-4} torrℓs^{-1} (0.03cm^3/min), where the ionization efficiency defined above attained 0.15%. A typical mass spectrum (fig 2) shows that the C^- production is accompanied by strong beams of O^-, C_2^-, and Cu^-. The high intensity of C_2^- cannot be exploited for dating purposes since injection of $^{14}C^{12}C^-$ into a tandem at a mass setting of 26

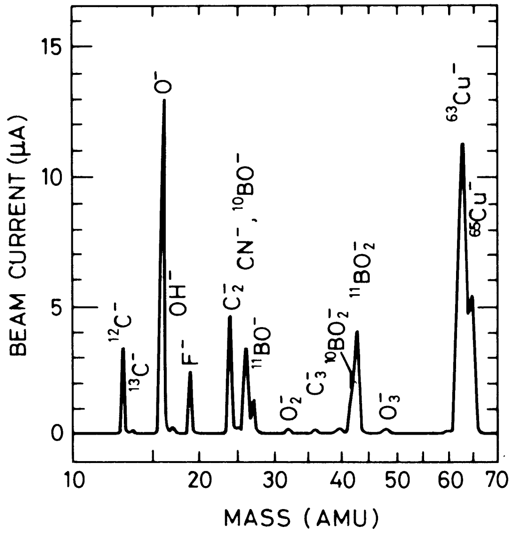

Fig 2. Output of the negative ion beams from the source using natural CO_2 gas and a copper sputter cathode. The ions are magnetically analyzed at 20keV energy.

would not allow ^{14}C to be separated from ^{14}N, abundantly accelerated as $^{12}C^{14}N^-$ at the same mass setting. The ratio of the mass-13 to -12 beams varies from 1.5 to 2.5%, depending on source parameters, and can be kept fairly constant at ca 2% if these parameters are not changed.

Sputter cathodes of yttrium and magnesium were tried because their work functions are lower than that of copper (3.1, 3.7, and 4.5eV, respectively) and therefore might be expected to increase the negative-ion production in the carbon sputtering process. However, very low yields, 0.2μA C^-, were found for yttrium, probably because of the imperfect shape of the sputter cathode, which was made of foils. The magnesium tests were stopped because of extremely unstable source operation, probably due to evaporation of the cathode material when heated by the positive-ion bombardment from the plasma. Up to 10μA C^- was recorded for a tantalum cathode (work function 4.2eV), but the output was not well correlated to the gas-flow rate, which may be consequential to the severe memory effects for tantalum, discussed below. A cathode of gold was tested despite its high work function of 5.3eV because low memory effects might be expected if chemical processes and/or gas adsorption on the cathode surface were responsible for these effects. However, the C^- output was only 0.25μA and the efficiency as low as 0.009%; memory effects are quite similar to those of copper.

A few attempts were made to feed the source on CH_4 gas in connection with cathodes of copper and tantalum. The increases in C^- beams were only minor, whereas the mass-13 to -12 ratio increased to ca 30%, due to $^{12}CH^-$. Only with a hot cathode made of thermally insulated tantalum foil did the ratio drop to 2%. In all cases, the correlation between gas-flow rate and C^- was poor; no further attempts were made.

The decay of the memory fraction measured as described above was recorded as a function of the time elapsed after switching from enriched to natural sample. This was done for several different values of 'exposure' time, T, in which the source had been operated on the enriched sample. Cathodes of copper, gold, and tantalum were used. The memory decay could not be described as a simple exponential or even as a sum of two exponentials. Rather, the decay curve follows a power law $F \propto t^{-x}$ at first and then approaches a single exponential, as shown in figure 3. The power dependence indicates a continuous distribution of time constants as known from, eg, activation analysis and thermoluminescence. The components of long time constants contribute more heavily, the longer the exposure time. Thus, as illustrated in figure 4, the value of the exponent, x, in the power decay decreases with increasing

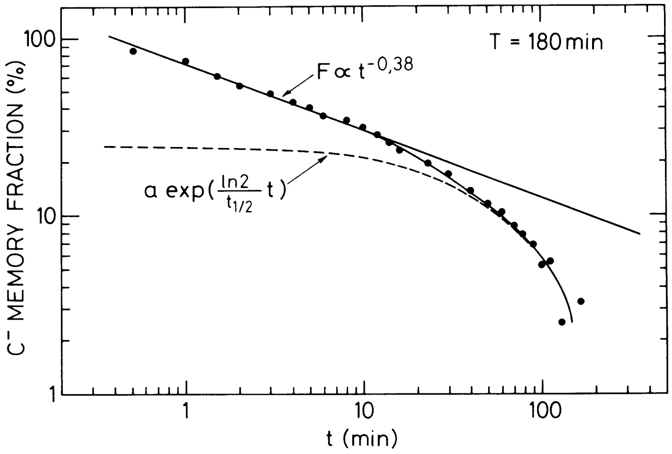

Fig 3. Double logarithmic plot of the memory fraction F (Eq (1)) as a function of time after change from 90% enriched $^{13}CO_2$ to natural CO_2. A power-law dependence has been fitted to the first part of the curve and an exponential ($t_{\frac{1}{2}}$ = 48 min) to the last part. A copper cathode was used, and the exposure time was 180 min.

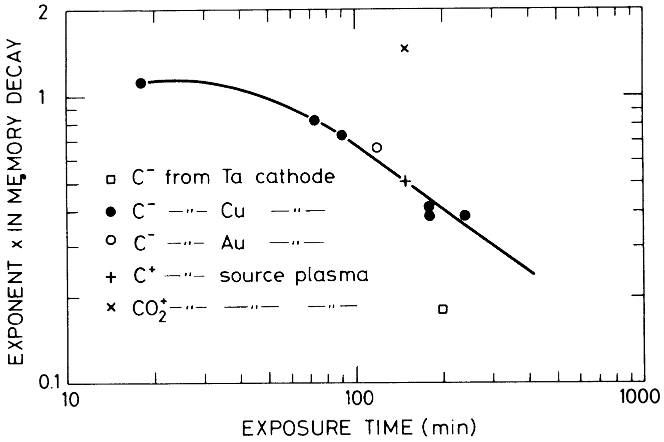

Fig 4. The exponent x in the power-law decay, $F \propto t^{-x}$, plotted as a function of exposure time for different sputter materials. Also shown are values for positive beams, extracted from the source at reversed potential (see text).

exposure time, indicating that memory effects grow with exposure time. The memory effects must be governed by a competition between, on the one hand, processes depositing carbon in the source such as C^- sputtered from the cathode being implanted around the source outlet, positive ions from the plasma being implanted in the end-plate cathodes, and adsorption of C and CO diffusing to the discharge-chamber walls, and, on the other hand, processes liberating carbon chemically or by sputtering or desorption. High deposition rates in certain parts of the source do not necessarily lead to severe memory effects since liberation rates may be correspondingly high. This seems to be the case for the copper sputter cathode, itself. Thus, changing the exposed cathode to an unexposed one (which can be done in ca 5 minutes) simultaneously with sample change did not alter the memory effects as compared to the normal procedure when the same cathode is used throughout. Probably the long-lived memory components come from the more 'remote' parts of the source, where deposition and liberation rates are low. It should be added that the copper cathode was originally chosen because it sputters readily so that carbon-implanted layers are rapidly removed from the cathode, and a layer of copper builds up on the inside of the anode cylinder, continuously 'burying' the carbon deposits, thereby reducing memory effects.

If the source is allowed to 'clean up' for 5 to 10 hours by running on cesium vapour alone, then F attains 100% within the measuring uncertainty of 2% when 90% enriched CO_2 is introduced. This is an indication that essentially all the C^- beam originates from the gas feed rather than from the vacuum system or the source, itself. Under the same conditions, the C^- beam increases by a factor of 500-1000 both absolute and relative to the Cu^- beam when CO_2 is introduced, supporting the above conclusion.

Results are summed up in figure 5, which shows the delay in reaching 2% memory level as a function of exposure time. Note the high value for the tantalum cathode, probably due to the porous nature of commercial tantalum. For copper and gold, the delay is of the order of the exposure time. Rapid changing between a sample to be ^{14}C dated and a known standard would not be practical with the ANIS source in its present design unless their compositions are matched to some extent.

Included in figure 5 are delay values for beams of C^+, CO^+, and CO_2^+, extracted from the source at a reversed potential of +20kV in intensities of 3, 12, and 0.5μA, respectively. The delay time for CO_2^+ is remarkably low, a factor of ten lower than for C^+ and C^- at similar exposure times, and only

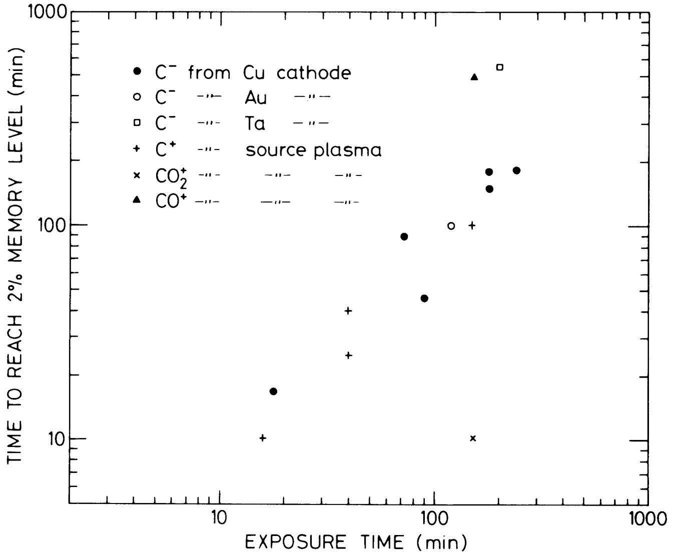

Fig 5. Time taken to reach 2% memory level after sample change, plotted as a function of exposure time.

a factor of three higher than the pumping time. This is a confirmation that adsorption of CO_2 in the gas-supply system or in the source, itself, is not responsible for the observed C^- memory effects. The observation also suggests that memory-free C^- beams could be produced by break-up and charge exchange in a metal vapour of CO_2^+ beams, extracted from a positive source. This idea was tested on a 12μA CO_2^+ beam extracted at 20kV from an RF source with 2% efficiency. The memory effects were essentially determined by the pumping time. By collision in sodium vapour, the $^{12}CO_2^+$ beam was converted into 5.5keV $^{12}C^-$ with an efficiency of 4.4%. According to the charge-exchange data (Heinemeier and Hvelplund, 1978), the expected fraction of negative carbon ions at this final energy is 35%, provided the vapour-target thickness is sufficient to break up all the molecules and bring the carbon ions into charge-state equilibrium. The low yield observed appears to be due to the difficulty of breaking up the CO_2^+ molecule as well as beam scattering reducing the transmission. The test should be repeated at higher beam energy, where both effects would be less severe.

CONCLUSION

The intensity and efficiency of C^- ions produced in the ANIS source from CO_2 gas is well below the values, 40μA C^- beam at ∿10% efficiency, routinely achieved by sources operating on solid-carbon samples (Hedges, 1981). Background beams of C^- from the ANIS source itself seem to be similar to the ∿1% values found by Hedges, Wand, and White (1980). Memory effects in the ANIS source are clearly more severe than for the Middleton type, although we are not aware of detailed studies for these sources. Berthier et al (1981) have used a carbon sputter cathode to produce a C^- beam from an ANIS source and find that ^{14}C memory drops to less than 1% after change to a copper cathode. Improved memory properties could possibly be achieved by reducing the surface area of the discharge chamber and by briefly running an intense discharge of an inert gas between successive CO_2 samples. We plan to try such measures along with further investigations of the alternative solution of C^- production by charge exchange. A comparison of the ANIS source with other gaseous sources indicates that it is superior in performance parameters relevant to the production of C^- beams for dating purposes.

ACKNOWLEDGMENTS

We gratefully acknowledge the skillful assistance of E Jans and many useful discussions with H Loft Nielson.

REFERENCES

Andersen, HH and Tykesson, P, 1975, A PIG source for negative ions: IEEE Trans Nuclear Sci, v NS-22, p 1632.

Berthier B, Bianchi, L, Delibrias, G, and Koechlin, V, 1981, Plan for mass accelerator spectrometry at Gif-sur-Yvette and Sacaly, in Symp on accelerator mass spectrometry, Proc: Argonne, Illinois, Argonne Natl Lab, p 120-129.

Hedges, REM, Wand, JO, and White, NR, 1980, The production of C^- beams for radiocarbon dating with accelerators: Nuclear Instruments and Methods, v 173, p 409-421.

Hedges, REM, 1981, Radiocarbon dating with an accelerator: review and preview: Archaeometry, v 23, p 3-18.

Heinemeier, J and Hvelplund, P, 1978, Production of 10-80keV negative heavy ions by charge exchange in Na vapour: Nuclear Instruments and Methods, v 148, p 425-429.

Middleton, R, 1978, Some remarks on negative ion sources and ^{14}C dating, in Gove, HE, ed, Conf on radiocarbon dating with accelerators, 1st, Proc: Rochester, New York, Univ Rochester, p 196-209.

Shea, JH, Conlon, TW, Asher, J, and Read, PM, 1980, Direct detection of ^{14}C at the Harwell tandem, in Stuiver, Minze, and Kra, Renee, eds, Internatl radiocarbon conf, 10th, Proc: Radiocarbon, v 22, no 3, p 830-837.

Tykesson, P, Andersen, HH, and Heinemeier, J, 1976, Further investigations of ANIS (the Aarhus negative-ion source): IEEE Trans Nuclear Sci, v NS-23, p 1104.

[Radiocarbon, Vol 25, No. 2, 1983, P 771-774]

SAMPLE CHEMISTRY FOR THE OXFORD HIGH ENERGY MASS SPECTROMETER

RICHARD GILLESPIE and ROBERT E M HEDGES

Research Laboratory for Archaeology and the History of Art
Oxford University, 6 Keble Road, Oxford OX1 3QJ, England

ABSTRACT. Chemical pretreatment procedures for the decontamination, extraction, and isolation of organic materials for ^{14}C dating using the Oxford accelerator system are described. Specific details are given for the isolation and chromatographic purification of amino acids from bone and tooth collagen, of lipids from sediments, and of cellulose and glucose from wood, paper, and textiles. A description is also given of the apparatus used for the routine preparation of 1 to 5mg graphite samples on tantalum wire, for use in the accelerator ion source.

The high energy mass spectrometer (HEMS) approach to ^{14}C dating allows the use of very small samples in the low milligram range. Sample pretreatment and decontamination procedures can be both more vigorous and more selective than those used by conventional dating laboratories. Specific chemical compounds can be isolated from archaeologic or geologic samples; such compounds may be characteristic of particular source materials and, hence, provide more detailed information than is generally possible using bulk organic samples. The Oxford Radiocarbon Unit has concentrated on three sample types that represent the kind of material we expect to work on initially: bone, lake sediment, and wood.

AMINO ACIDS FROM BONE. The usual practice of dating the acid insoluble residue ("collagen") fraction from bone is fraught with complications regarding reproducibility and contamination. It is possible to isolate the collagen amino acids and to purify these using ion exchange chromatography. This has been attempted (see, eg, Taylor and Slota, 1979), but not established as a routine procedure. The small samples required for HEMS dating allow high purity amino acids to be separated from bone using conveniently-sized apparatus.

The amino acid content of bone is first estimated using the standard Kjeldahl nitrogen analysis, or, more usefully, from GC to HPLC analyses that can separate enantiomers (see, eg, Hoopes, Peltzer, and Bada, 1978). Bones are cleaned by scraping or grinding off surface debris and sonication in distilled water and/or 0.1M HCl for a few minutes. After crushing to <25 mesh, the inorganic matrix is dissolved in 1M HCl, using sonication and several changes of acid to speed release of CO_2. The acid insoluble residue is treated with alkali to remove humic acids and hydrolyzed in 6M HCl for 8 to 12 hours at 105° in sealed tubes. Finally, the liberated amino acid mixture is desalted on Biorad AG50X8 cation exchange resin, using 2 to 3M NH_3 solution for elution.

Wand (ms) developed a method for the isolation of the specific amino acid hydroxyproline from bone hydrolysates. This involves deamination of all amino acids except proline and hydroxyproline with nitrous acid, followed by preparative high pressure liquid chromatography (HPLC) using pH2.5 phosphate buffer on Partisil 10SCX cation exchanger. Modification of this procedure by the addition of a desalting step before HPLC improves the separation of proline from hydroxyproline, and allows UV detection at 200nm to monitor the chromatography. The final amino acid products from these procedures may be assayed for purity using gas chromatography (GC) and HPLC. Such methods are also applicable to tooth, antler, and ivory collagen, and with slight modification, to shell conchiolin amino acids.

LIPIDS FROM SEDIMENTS. Lake sediments are normally dated using the total organic matter, which may not give the actual time of sedimentation because of the mixed origin of the various organic components. Insoluble compounds such as lipids may offer more attractive dating samples, because they can often be related to specific plant sources (aquatic or terrestrial) and should give a more precise date for deposition of the sediments.

A general scheme, based on work by Cranwell (1973), Brooks et al (1976) and Birks (1980), is being developed to isolate n-alkanes and n-carboxylic acids from sediments for dating. Samples are demineralized with 6N HCl/40%HF at room temperature for 2 to 3 days, filtered, and dried under vacuum at 40°. Macrofossils are removed at this stage for separate identification and dating. The dried sediment is then extracted with benzene, using sonication and several changes of solvent. This solvent extract is reduced in volume and chromatographed on a silica column, using hexane to elute hydrocarbons and more polar solvents for elution of fatty acids. Analysis of lipid fractions is carried out by GC on packed OV-1 columns, and selected chain length alkanes or acids can be isolated by preparative GC for dating.

Further fractions that may be significant for dating can be isolated from the solvent-extracted sediments. For example, humic acids can be extracted with alkali and reprecipitated for analysis; amino acids can be obtained by hydrolysis in 6M HCl and subsequent purification as for bone amino acids.

CELLULOSE AND GLUCOSE FROM WOOD. The standard method for preparation of cellulose from wood can be used for the small samples required in HEMS dating. These usually involve solvent extraction of resins, alkali, and acid extraction of other soluble components, followed by oxidation of lignin with

$NaClO_3/HCl$. It is possible to extend this treatment to complete hydrolysis of the cellulose to glucose, which can be purified by preparative HPLC for dating. This would also allow critical analysis of the final product by GC or HPLC to assess purity. Such a scheme can also be applied to cellulose-based textiles and paper samples.

GRAPHITE TARGET PREPARATION. Initial experiments (Hedges, Wand, and White, 1980) confirm that graphite is the material of choice for ion source targets. Wand (ms) developed a procedure for preparing graphite on tantalum wire supports, which has now been modified for routine production of 1 to 5mg of graphite from 5 to 10mg of sample carbon. The synthesis apparatus is shown diagramatically in figure 1.

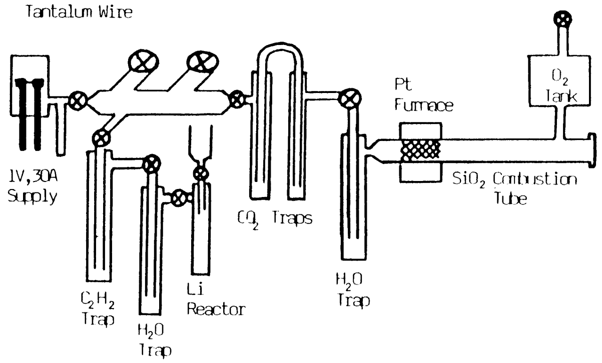

Fig 1. Graphite preparation system

Combustion takes place in a silica tube under 1 atm oxygen, with final oxidation over a supported platinum catalyst at 450°C. CO_2 is dried by passage through a dry ice/methanol trap and collected in liquid N_2 cooled traps. Lithium carbide is prepared by reacting this CO_2 with molten Li metal at 600-700°C for 5 minutes; the CO_2 may either be added to the hot Li or (for small samples) the CO_2 can be frozen into the Li reactor and heated with the lithium. After cooling the Li_2C_2, water is added to produce acetylene, which is dried by passage through a dry ice/methanol trap and collected in a liquid N_2 cooled trap. This acetylene is then expanded in a dry ice/methanol trap and frozen into the cracking vessel with liquid N_2. Routine yields are better than 90%.

The cracking reaction takes place at an acetylene pressure of 10 to 50mbar. A tantalum wire, 0.5mm diameter x 5mm long, is heated resistively between stainless steel electrodes, with a current of 25 to 30amps at 1 volt, to a temperature of ca

2000°C, measured with an optical pyrometer. Ca 10 minutes is sufficient for this reaction, yields being ca 40 to 50% based on the acetylene.

Because of the gas to solid reaction, changing composition in the gas phase may introduce isotopic fractionation in the graphite product. Even with 100% yeild, it is likely that spatially different isotope ratios will be present. The yields obtained could not be increased by changing acetylene pressure, wire temperature, or time of reaction. Wand (ms) measured stable isotope ratios on graphite prepared by this procedure, and concluded that the bulk sample could have fractionated ^{14}C by ca 2%. Such variation can probably be corrected by the use of standard linear factors during the analysis on the HEMS system.

The graphite, as prepared on tantalum wires, is compact, robust, and easily stored. Wires may be mounted directly into a reflected beam ion source (Hedges et al, 1980), or the graphite can be removed from the wire and pressed into a hole of 1mm diameter for the inverted spherical ionizer sputter source (White, in press). Both techniques have been in use at Oxford and routinely produce adequate C^- ion beams.

REFERENCES

Birks, HH, 1980, Plant macrofossils in lake sediments: Archiv Hydrobiol Beih, v 15, p 1-60.

Brooks, PW, Eglinton, G, Gaskell, SJ, McHugh, DJ, Manwell, JR, and Philip, RP, 1976, Lipids of recent sediments Part I. Straight chain hydrocarbons and carboxylic acids of some temperate lacustrine and sub-tropical lagoonal/tidal flat sediments: Chem Geol v 18, p 21-38.

Cranwell, PA, 1973, Chain length distribution of n-alkanes from lake sediments in relation to post-glacial environmental change: Freshwater Biol, v 5, p 259-265.

Hedges, REM, Wand, JO, and White, NR, 1980, The production of C^- beams for radiocarbon dating with accelerators: Nuclear Instruments and Methods, v 173, p 409-421.

Hoopes, EA, Peltzer, ET, and Bada, JL, 1978, Determination of amino acid enantiomeric ratios by gas chromatography of the N-trifluoroacetyl-L-prolylpeptide methyl esters: Jour Chromatographic Sci, v 16, p 556-560.

Taylor, RE and Slota, PS, 1979, Fraction studies on marine shell and bone samples for radiocarbon dating, in Berger, R and Suess, HE, eds, Radiocarbon dating, Internatl ^{14}C conf, 9th, Proc: Berkeley, Univ California Press, p 442-432.

Wand, JO (ms) 1981, Microsample preparation for radiocarbon dating: Unpub DPhil thesis, Univ Oxford.

White, NR, in press, The inverted spherical ionizer sputter ion source (IS3): Nuclear Instruments and Methods, in press.

[Radiocarbon, Vol 25, No. 2, 1983, P 775-784]

SURVEY OF SIMPLE CARBON COMPOUNDS FOR USE IN A NEGATIVE ION SPUTTER SOURCE

JS VOGEL*, IG NOWIKOW*, JR SOUTHON* AND DE NELSON

Department of Archaeology, Simon Fraser University
Burnaby, British Columbia, V5A 1S6, Canada

ABSTRACT. We present a survey of carbon beam yields from 20 simple carbon compounds using a caesium sputter source and the McMaster University tandem accelerator. The carbon yield was measured as a 35MeV $^{12}C^{4+}$ beam. We found that the beam intensities could be related to a grouping of the carbides according to the chemical bonding of the compounds. The usefulness of the compounds for accelerator ^{14}C dating was further related to their preparation chemistries. Strontium carbide was the equal of graphite in negative carbon ion beam production and aluminum carbide was found to be a good candidate for further tests because of its good sputter yield and preparation chemistry. Charcoal was also tested with varying amounts of silver added as a heat conduction aid.

INTRODUCTION

The use of tandem electrostatic accelerators as sensitive mass spectrometers in studying radioisotopes has become well-established in recent years (Gove, 1978; Kutschera, 1981). This technique makes possible the ^{14}C dating of small samples which were heretofore difficult or impossible to date using decay counting techniques. The accelerator method requires only a few milligrams or less of carbon but the best chemical form of the carbon for use in these systems is still under investigation. A survey of simple carbon compounds with a range of properties and preparation chemistries was made to find suitable sample preparation methods.

The criteria that the sample preparation procedure must meet for accelerator dating are generally the same as those required for decay counting. In both methods, it is very difficult to determine accurately the absolute measurement efficiencies, and for the accelerator systems, the efficiency for one isotope relative to the other. The simplest solution is to measure all unknowns with respect to standards in a system with constant relative isotopic efficiencies. This

---

* Also: Department of Physics, McMaster University, Hamilton, Ontario, Canada

requires a sample preparation technique in which all samples are treated and presented for measurement identically. The preparation chemistry must be quantitative at all stages to preclude isotopic fractionation which may vary from sample to sample. The final product must be a homomgeneous substance that remains well-mixed isotopically throughout the measurement.

For routine use, the preparation must have a reasonable through-put and be capable of handling small samples without contamination. For accelerator dating, the resultant substance should produce a long-lived intense C^- beam with a short stabilization time in the ion source lest accelerator time be wasted.

Perhaps the simplest substance to fit these needs is CO_2, which is easily prepared in a quantitative homogeneous manner. However, attempts to use CO_2 directly for accelerator dating have not been successful because of source memory effects (Shea et al, 1980; Heinemeier and Andersen, 1983).

Most laboratories use Cs sputter ion sources that require the sample to be in solid form. Various solids can be derived from CO_2. The gas can be reduced and then cracked to graphite in a slow glow discharge process which is almost quantitative but the deposit of which is thin and quickly sputtered away (Grootes et al, 1980; 1981). Alternatively, acetylene can be produced from CO_2, as is done in benzene synthesis (Tamers, 1975). Graphite can be produced from acetylene by radiofrequency dissociation (Beukens and Lee, 1981) or thermal pyrolysis (Hedges, Wand, and White, 1980). However, these methods have low yields (~60%) and produce isotopically inhomogeneous samples (Elmore, 1981; Hedges, Wand, and White, 1980). The carbonates and carbides chosen for this study can also be made from one or the other of these two gases. Charcoal is included and graphite is the standard against which all are judged.

CARBIDES. Carbides can be classified into five groups based on their macroscopic properties (Hough, 1964) and their chemical bonding (Samsonov, 1965): 1) ionic or salt-like, 2) covalent or diamond-like, 3) metallic, 4) volatile, 5) graphites (fig 1). Both the ionic and metallic groups have subgroups. Gaseous volatile "carbides", and explosive ionic-metallic carbides were not considered, as they are incompatible with the sputter source. Graphites (Hennig, 1959) were also not investigated, as they are interstitial variations on graphite and would offer no benefits over true graphite in the preparation or sputtering phases. Sixteen metal carbides (plus graphite) were chosen for study to represent the remaining major types. All of the refractory transition metal

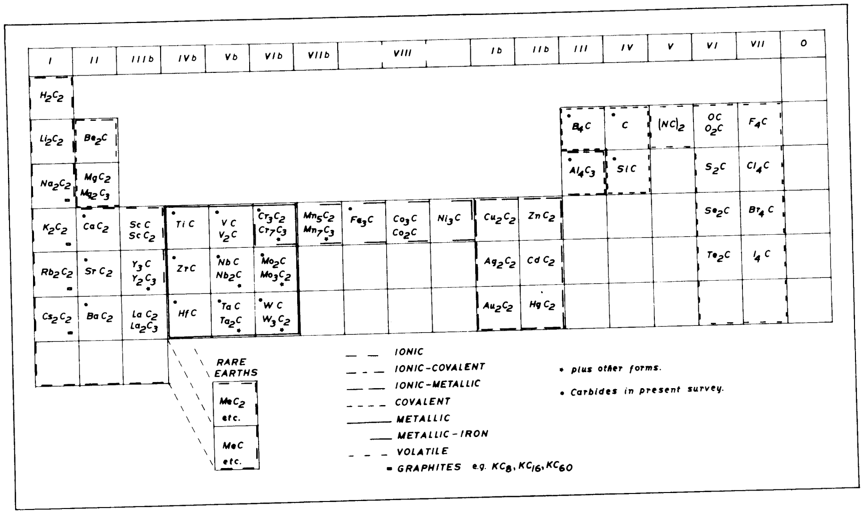

Fig 1. Periodic table of the binary carbides grouped according to the chemical bonding of the compound. Elements not included are those for which the existence of a binary carbide has not been demonstrated.

carbides were examined for any regularities in sputtering yield from within a complete group.

Frad (1968) wrote an extensive review of metal carbide properties and preparation. One general method of preparation is carburization, in which a metal or metal oxide is heated in the presence of fine carbon powder, acetylene black, or a hydrocarbon. This approach lends itself to miniaturization and can make use of the acetylene produced in benzene preparation. Vapor phase deposition (Campbell et al, 1949; Powell, 1966) is a well-documented technique in which a mixed vapor of hydrocarbon and the metal halide react, forming the metal carbide on a hot filament (tungsten or tantalum). The process is similar to thermal pyrolysis of hydrocarbons to graphite. However, unless deposition is much more efficiennt or less fractionating than pyrolysis, the latter would be preferred. The acetylides (the ionic and ionic-metallic carbides) can be produced by precipitation from a liquid ammonia solution of the metal by bubbling acetylene through it. The precipitate is primarily the metal hydro-acetylide ($MeHC_2$ or $Me(HC_2)_2$) with some ammonia and excess acetylene co-ordinated with metal ions. Gentle heating from the -30^{o} liquid ammonia temperature will drive off the ammonia and convert the hydro-acetylide to a carbide of 98 to 99% purity (Corbellini and Turner, 1960). This method is easily used for small quantities, is stoichiometric, and yields a well-mixed carbide. Some carbon will be lost as acetylene in the last heating phase, however. Other techniques of less general carbide production exist, eg, the direct production from lithium and carbon dioxide or the reduction of the carbonates of calcium, barium, and strontium to their respective carbides and oxides by heating with magnesium metal.

METHODS AND RESULTS

The caesium sputter source was of the Middleton type (Middleton and Adams, 1974) used in the reflected mode. Our meaurements were made at the FN Tandem Van de Graaff accelerator at McMaster University where the carbon yields were measured as 35MeV $^{12}C^{4+}$ at the image Faraday cup of the analyzing magnet. Using the analyzed high-energy beam eliminates any background ions introduced by the low resolution inflection magnet.

All compounds were commercial >99% pure chemicals[1]. Samples were prepared using the pure compound and using the compound mixed 1:1 with 100 mesh silver powder. Hedges, Wand, and White (1980) found that high sample temperatures impair sputtering of negative ions by evaporating caesium from the surface, whereas the addition of silver powder aids sputtering by increasing the thermal conductivity of the sample. The 1:1 ratio of silver to compound was used throughout for consistency, but much larger amounts of silver (up to 20 or more to 1) are more effective (Grootes et al, 1981). Compounds that might react with water vapor in the air were capped with a layer of silver which was scraped away before loading into the source.

Each measurement followed a sequence: 1) checking the current from the graphite standard, 2) an initial current from the sample, 3) current readings 10 and 20 minutes later, and 4) checking the current from graphite. Most samples showed increasing currents in the first few minutes as the surface became caesiated, and most had stabilized before the 20-minute reading was taken. If the current was still increasing at that time, the sample was run for another 10 minutes and the continued increase noted. The source was operated at 25 kV extraction voltage producing 5 μAmps of mass 12 negative ions from graphite.

Table 1 shows the 35MeV $^{12}C^{4+}$ current obtained as a fraction of that of graphite after 20 minutes for each compound, plain and with silver added, averaged for 2 or 3 runs on separately prepared samples. Uncertainties of up to 25% were expected due to variations in sample packing, sample holder heat conduction, and ion source behavior.

---

[1] Alfa Products, Danvers Massachusetts

TABLE 1. 35MeV $^{12}C^{4+}$ yields from sputtered carbon compounds measured relative to that of graphite

Compound	Relative yield	Relative yield with Ag added*	Compound	Relative yield	Relative yield with Ag added*
CARBIDES					
Ionic			Covalent		
CaC_2	0.19	0.48	B_4C	0.08	0.20
SrC_2	1.06	0.80	graphite	1.00	1.10
BaC_2	0.38	0.60	SiC	0.12	0.27
Ionic covalent					
Al_4C_3	0.18	0.36	CARBONATES		
Metallic			Na_2CO_3	0.01	
TiC	0.18	0.26	K_2CO_3	0.01	
ZrC	0.15	0.10	$CaCO_3$	0.01	
HfC	0.15	0.14			
VC	0.26	0.31	CHARCOAL**		
NbC	0.23	0.20	No Ag	0.09	
TaC	0.10	0.14	1:1 Ag	0.13	
Cr_3C_2	0.27	0.32	1:2 Ag	0.11	
Mo_2C	0.00	0.02	1:5 Ag	0.20	
WC	0.21	0.15	1:10 Ag	0.23	
Metallic-iron					
Fe_3C	0.03	0.03			

* silver was added in 1 to 1 ratio by weight

** ratio of added silver is by weight

TABLE 2. Carbide group average yields of $^{12}C^{4+}$ measured relative to yield of graphite

Group	Relative yield	Relative yield with Ag added
Ionic (3)*	0.54	0.63
Ionic-covalent (1)	0.18	0.36
Covalent (2)	0.10	0.24
Metallic (9)	0.17	0.18
Metallic-iron (1)	0.03	0.03

* number in parentheses is number of compounds in that group used in this study

DISCUSSION

CARBIDE SPUTTERING. Table 2 summarizes the relative sputtering yields of each carbide group. Ionic bonded compounds are more easily sputtered, with covalent and metallic compounds less so. The salt-like acetylides give over 50% the carbon current of graphite, with improvement upon addition of silver. In these compounds, the carbon clearly exists within the molecule as a negative ion attached to the positive metal ion. On several tests, pure strontium carbide was the equal (within uncertainties) of graphite. It is not clear why strontium was better than calcium or barium. Strontium carbide is produced by some laboratories as an intermediate step in acetylene and benzene production using the carbonate-magnesium process mentioned above. A sample of strontium carbide, strontium oxide, and magnesium oxide was prepared in the proportions of such a reaction. This sample, with or without silver, proved to be a poor negative carbon ion source. The strontium oxide inhibited the carbon sputtering, making an otherwise attractive production method unusable. The liquid ammonia method of preparation may still allow use of the alkali-earth carbides; however, the oxide inhibition means that the sample would have to be protected from water vapor in the air. The expensive group III and rare earth metals were not considered viable for routine use. The alkali carbides are less attractive in that, except for lithium, they tend to form compounds other than the simple carbide (Samsonov, 1965).

Magnesium, beryllium, and aluminum form carbides in which some covalent bonding of the metal ions is important. Magnesium carbide was not available, but can be made through carburization of the metal by acetylene. The difficulty in handling the powdered magnesium may preclude its use. Beryllium carbide exists as a single carbon anion attached to a covalently bound Be cation, has a high thermal conductivity and might be an excellent source of carbon ions. Health dangers of beryllium and its compounds, as well as the need to keep a low beryllium background in our source for Be dating purposes, preclude the use of this compound. Aluminum carbide is a reasonably good carbon ion source and improves greatly when heat conducting metal is added. The stronger covalent contribution to the bonding in aluminum carbide reduces its yield but also makes it much more stable against decomposition (to methane). If it were produced by carburization, a large over-supply of aluminum powder would result in a well-mixed, heat-conductive sample.

Covalent carbides, excluding graphite, are not as efficient as ionic compounds. The addition of silver to boron and silicon carbides increases their yields substantially, indicating that heat conduction is a limiting factor. (These carbides have heat conductivities 5 and 10 times smaller than graphite (Hough, 1964)).

The transition metal (refractory) carbides are commercially important and have well-studied properties (Samsonov and Vinitskii, 1980). They are all interstitial in character wherein a lattice of metal atoms accepts carbon atoms into certain positions, resulting in the formation of MeC_f where f has 1.0 as its upper limit. Except for vanadium and chromium, the sputter yields from the metal carbides are mediocre. Their heat conductivities are generally low (0.01 - 0.07cal/cm - sec^{o}C) and the addition of 1:1 silver produced little improvement. One run made on samples scrupulously similar in preparation indicated that the C- yield was related to the heat of atomization for these carbides. Vasil'yev (1980) shows a similar dependence in the sputtering yield of positive metal ions from these compounds. Vapor deposition is the standard way to make small quantities of the refractories and little appears to be gained from making these carbides instead of pyrolized graphite.

The iron metallic carbides differ from the transition metallic carbides principally in having less simple crystal lattices with vacancies for carbon. These metals do not form mono-carbides and the increased bonds may contribute to the low sputter yields, although chromium carbide, which is in a transition position between the two metallic groups, is a good sputterer. Several authors report widely differing carbon beams from cast iron and carbon-iron mixtures (Ball et al, 1981; Leavitt, Donahue, and Long, 1981: Grootes et al, 1981; Middleton, 1978). However, it is not clear in these cases how much, if any, of the carbon is in the form of iron carbide.

CARBONATES. The carbonates of sodium, potassium, and calcium were tested as representatives of the alkali and alkali-earth carbonates. These compounds are of interest because they are easily made by precipitation from CO_2. Unfortunately, the carbon sputter yields were only 1% of graphite, too low to be useful.

CHARCOAL. Charcoal as a carbon ion source is simply prepared: the sample is cleaned and then charred in an oven. However, not all samples and standards can be prepared in this way, and problems in comparisons are introduced. Table 1 indicates that at least 5:1 or 10:1 silver must be added to charcoal to get a respectable sputter yield. The grains in even hard-packed charcoal give poor thermal conduction. Grootes et al (1981) report almost 50% the beam from graphite by using 8:1 and 16:1 mixes of silver and charcoal.

CONCLUSION

From our survey of the sputtering yields of carbon from the various types of simple carbon compounds, we found that ionic and ionic-covalent carbides produce carbon beams that are a large fraction of those from graphite. Two carbides, SrC_2 and Al_4C_3, merit further investigation in order to make production techniques for small samples routinely quantitative. Aluminum carbide, in particular, offers a good beam, reasonable stability in handling, and an obvious production technique making use of acetylene from an already established sample preparation system. We have further seen that the negative ion sputtering yield from carbides depends primarily on bonding and thermal conduction effects.

ACKNOWLEDGMENTS

We thank the staff of the McMaster University Accelerator Laboratory for their continuing support of our program. Funding is provided by NSERC of Canada and by Simon Fraser and McMaster Universities.

REFERENCES

Ball, GC, Andrews, HR, Brown, RM, Burn, N, Davies, WG, Imahori, Y, and Milton, JCD, 1981, Radiocarbon dating with the Chalk River tandem accelerator, in Kutschera, Walter ed, Symposium on accelerator mass spectrometry, Proc: Argonne, Illinois, Argonne Natl Lab, p 34-42.

Beukens, RP and Lee, HW, 1981, The production of small carbon samples by RF dissociation of acetylene; in Kutschera, Walter ed, Symposium on accelerator mass spectrometry, Proc: Argonne, Illinois, Argonne Natl Lab, p 416-425.

Campbell, IE, Powell, CF, Nowicki, DH, and Gonser, BW, 1949, The vapor phase deposition of refractory materials: Jour Electrochem Soc, v 96, p 318-333.

Corbellini, M and Turner L, 1960, The alkaline and alkaline-earth acetylides and carbides (in Italian): Chemica Industria, v 42, p 251-254.

Elmore, D, 1981, Reproducibility of isotope ratio measurements, in Kutschera, Walter ed, Symposium on accelerator mass spectrometry, Proc: Argonne, Illinois, Argonne Natl lab, p 346-358.

Frad, WA, 1968, Metal carbides, in Emeleus, HJ and Sharp AG, eds, Advances in Inorganic Chemistry and Radiochemistry: New York, Academic Press, v 11, p 153-247.

Gove, HE, ed, 1978, Conference on radiocarbon dating with accelerators, 1st, Proc: Rochester, New York, Univ Rochester.

Grootes, PM, Stuiver, M. Farwell, GW Schaad, TP, and Schmidt, FH, 1980, Enrichment of ^{14}C and sample preparation for beta and ion counting; in Stuiver, Minze and Kra, Renee, eds, Internatl radiocarbon conf, 10th Proc: Radiocarbon, v 22, no. 2, p 487-500.

Grootes, PM, Stuiver, M, Farwell, GW, and Schmidt, FH, 1981, Sample preparation for accelerator mass spectrometry at the University of Washington, in Kutschera, Walter ed, Symposium on accelerator mass spectrometry, Proc: Argonne, Illinois, Argonne, Natl Lab, p 405-415.

Hedges, REM, Wand, JO, and White, NR, 1980, The production of C^- beams for radiocarbon dating with accelerators: Nuclear Instruments Methods, v 173, p 409-421.

Heinemeier, J and Andersen, HH, 1983, Production of C^- directly from CO_2 using the Anis sputter source, in Stuiver, Minze and Kra, Renee, eds, Internatl radiocarbon conf, 11th, Proc: Radiocarbon, v 25.

Hennig, GR, 1959, Interstitial compounds of graphite, in Cotton, FA, ed, Progress in Inorganic Chemistry: New York, Interscience, v 1, p 125-205.

Hough, CR, 1964, Carbides, in Mark, HF, ed, Encyclopedia of chemical technology: New York, Interscience, v 4, p 70-75.

Kutschera, Walter ed, 1981, Symposium on accelerator mass spectrometry, Proc: Argonne, Illinois, Argonne Natl Lab.

Leavitt, SW, Donahue, DJ, and Long, A, 1981, Production of charcoal for accelerator targets, (abs), in Kutschera, Walter, Symposium on accelerator mass spectrometry, Proc: Argonne, Illinois, Argonne Natl Lab, p 404.

Middleton, R, 1978, Some remarks on negative ion sources and ^{14}C dating, in Gove, HE, ed, Conference on radiocarbon dating with accelerators, 1st, Proc: Rochester, New York, Univ Rochester, p 196-219.

Middleton, R and Adams CT, 1974, A close to universal negative ion source: Nuclear Instruments Methods, v 118, p 329-336.

Powell, CF, 1966, Chemically deposited nonmetals, in Powell, CF, Oxley, JH, and Blocher, JM, Jr, eds, Vapor deposition: New York, John Wiley & Sons, p 343-420.

Samsonov, GV, 1965, On the problem of classification of carbides: Soviet Powder Metallurgy Metal Ceramics, v 25, no. 1, p 75-81.

Samsonov, GV and Vinitskii, IM, 1980, Handbook of refractory compounds: New York, IFI/Plenum Data.

Shea, JH, Conlon, TW, Asher,J, and Read, PM, 1980, Direct detection of ^{14}C at the Harwell tandem, in Stuiver, Minze and Kra, Renee, eds, Internatl radiocarbon conf, 10th Proc: Radiocarbon, v 22, no. 3, p 830-837.

Tamers, MA, 1975, Chemical yield optimization of the benzene synthesis for radiocarbon dating: Internatl Jour Appl Radiation Isotopes, v 26, p 676-682.

Vasil'yev, MA, 1980, Secondary ion emission of the borides and carbides of transition metals: Physics of Metals and Metallurgy, v 47, p 95-100.

[Radiocarbon, Vol 25, No. 2, 1983, P 785-792]

DETECTION OF THE ^{36}Cl RADIOISOTOPE AT THE REHOVOT 14UD PELLETRON ACCELERATOR

MICHAEL PAUL, ODED MEIRAV

Racah Institute of Physics, Hebrew University
Jerusalem, Israel

WALTER HENNING, WALTER KUTSCHERA

Argonne National Laboratory, Argonne, Illinois 60439
and Racah Institute of Physics

ROBERT KAIM, MARK B GOLDBERG,
JEAN GERBER*, WILLIAM HERING**

Nuclear Physics Department, Weizmann Institute of Science,
Rehovot, Israel

AARON KAUFMAN, and MORDECKAI MAGARITZ

Isotope Research Department, Weizmann Institute of Science

ABSTRACT. A program of accelerator mass spectrometry has been started at the Rehovot 14UD Pelletron Accelerator Laboratory. Part of the initial emphasis has been directed to the detection of the ^{36}Cl radioisotope. We report here on the present status of our work and describe our experimental system. Preliminary results are presented, showing that ^{36}Cl/Cl concentrations ranging down to $1\text{x}10^{-14}$ could be measured with our system.

INTRODUCTION

A program of experiments in accelerator mass spectrometry was started at the Rehovot 14UD Pelletron Accelerator Laboratory. The high-voltage terminal available at the 14UD Pelletron and its good stability properties are important features which are favorable for detection of heavy radioisotopes. Part of the initial emphasis in our program was therefore directed to the detection of the ^{36}Cl radioisotope. Tandem-accelerator mass spectrometry has indeed been demonstrated to provide a unique method for measuring extremely low ^{36}Cl concentrations (Elmore et al, 1979). The method has also been successfully applied to problems in hydrology and geology (Bentley and Davis, 1981). We report here on the present status of our work and describe the experimental system used in our measurements. Preliminary results on ^{36}Cl detection are presented.

---

*Visiting Scientist from CRN, Strasbourg, France

**Visiting Scientist from Universitat Munchen, D-8046 Garching, West Germany

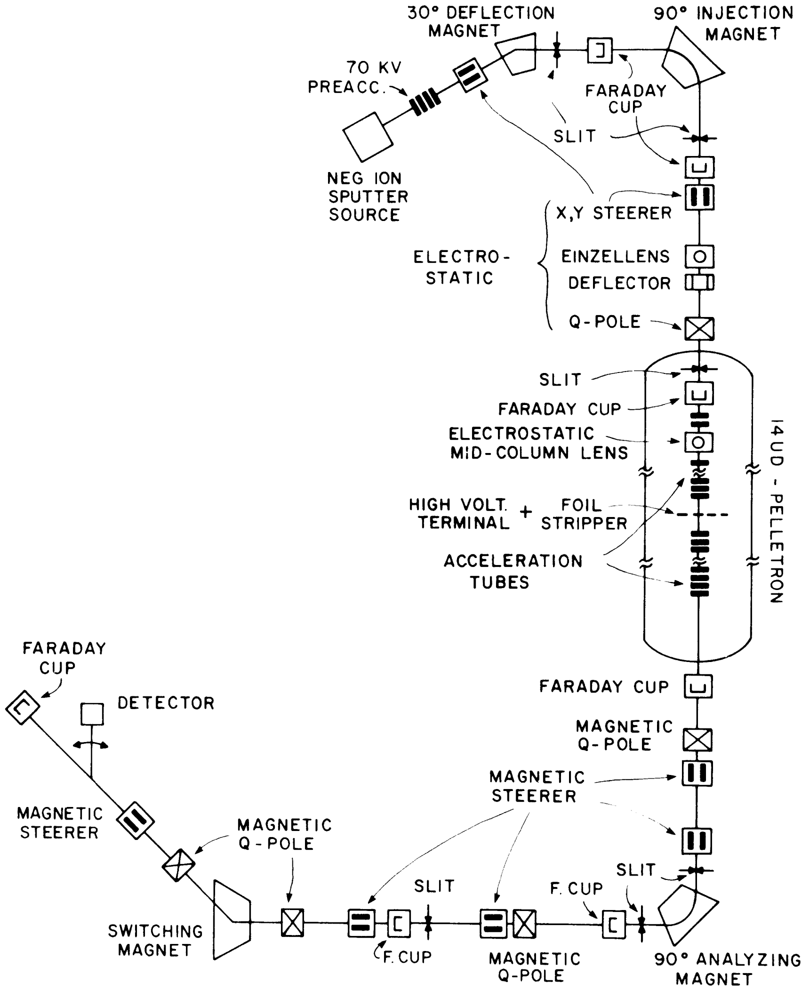

Fig 1. Schematic diagram of the accelerator set-up. The 30° magnetic deflection after the ion source, and the switching magnetic deflection, lie in a horizontal plane; the deflection of the 90° injection and analyzing magnets are in vertical planes. All other ion-optical elements of the LE(HE) sections are electrostatic (magnetic). The Faraday cup at the end of the beam line is used for the ^{37}Cl beam current measurements; the detector (fig 2) can be rotated into the beam for the ^{36}Cl counting.

EXPERIMENTAL METHOD

ACCELERATOR SYSTEM. A schematic diagram of the Rehovot 14UD Pelletron Tandem Accelerator Facility is shown in figure 1. The ion source used in our experiments was a General Ionex Hiconex 834 sputter source operated with the Cs$^+$ beam in the reflected mode. Twelve positions for sputter samples are available. The injection of the negative ion beam is achieved by two magnets with 30° and 90° deflection angles. All other ion-optical elements of the low-energy (LE) transport system (fig 1) are electrostatic. A thin C foil was used to strip the negative ions at the terminal. The vacuum in the acceleration tubes is normally in the region of 10^{-8} Torr. The high-energy (HE) ion-optical system, entirely magnetic, transports the beam after a 90° momentum analysis from the accelerator tower to the target room. A terminal voltage stabilization system (Ben-Zvi et al, 1981), based on a Generating Voltmeter, was built in our laboratory to stabilize the terminal voltage during the radioisotope measurement, when the slit system cannot be used. The GVM system stabilizes the terminal voltage within ±3kV at any value in the working range. All other elements of the accelerator used in our measurements were existing equipment routinely operating at the laboratory.

SAMPLE PREPARATION. Samples enriched in ^{36}Cl for testing and calibration purposes and several samples of natural origin were used in the ion source. The ^{36}Cl-enriched samples were produced by neutron irradiation of NaCl at the Soreq Nuclear Center and the Argonne CP5 Reactor. The integrated neutron flux was monitored by measuring the 15-hour activity of ^{24}Na simultaneously produced in the irradiation. The ^{36}Cl/Cl concentration can then be estimated from the known ^{35}Cl(n,γ) ^{36}Cl cross section. Great care was taken in a chemical procedure to reduce the level of sulphur impurity in the material, the ^{36}S stable isobar being a major source of background in the identification of ^{36}Cl (see below). The NaCl samples were first dissolved in triple distilled water. $Ba(NO_3)_2$ and $Cu(NO_3)_2$ were used to precipitate respectively SO_4^{--} and S^{--} ions. After filtration, AgCl was precipitated by $AgNO_3$ and further purified by multiple dissolution in concentrated NH_4OH and reprecipitation by HNO_3. The final AgCl precipitate was dried in darkness and pressed directly into a 4mm diameter hole in the sputter sample holder. The use of holders made of 99.99% Al was shown to reduce the ^{36}S level even further.

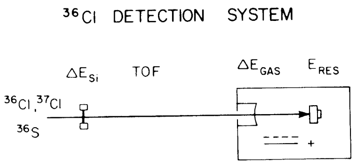

Fig 2. Schematic diagram of the detection system used for ^{36}Cl detection. Differential energy-loss signals ΔE_{Si} and ΔE_{GAS} are produced respectively by a Si detector and a gas-ionization chamber filled with isobutane at 30 Torr. The residual energy E_{RES} of the ions is measured in the last Si detector. The time-of-flight TOF of ions between the two Si detectors, ca 40cm apart, was measured.

TUNING PROCEDURE. The complete ion-optical system of the accelerator from the ion source to the final Faraday cup was set up with the ^{37}Cl stable isotope beam at a terminal voltage of 10.22 MV. The 10^+ charge state was selected to obtain sufficiently high energy for the identification system. Charge currents measured in the final Faraday cup ranged from 40 to 80 nA. After tuning, the terminal voltage was raised to 10.50 MV corresponding to a $^{36}Cl^{10+}$ beam of equal magnetic rigidity, and the source magnets (30° deflection and 90° injection) were adjusted for M=36. The detector was rotated into the beam and fine tuning of the terminal voltage was then achieved by maximizing the counting rate of the residual ^{36}S beam in the detector. This counting rate, typically of 100 to 500 sec^{-1}, was monitored during the ^{36}Cl counting time to check the stability of the system.

DETECTION SYSTEM. The detection system is designed to count the ^{36}Cl accelerated ions, while discriminating efficiently against residual ^{36}S ions and other parasitic beams degenerate in magnetic rigidity with ^{36}Cl and thus transported identically to the detector. The system, illustrated in figure 2, is a telescope composed of a Si surface-barrier detector, 13μm thick, a gas-ionization chamber (Fowler and Jared, 1975), and a $300mm^2$ Si detector. The ΔE_{Si} signal (fig 3) provided by the first detector measures the differential stopping power of the ions and gives excellent discrimination between Cl and S ions. Lighter ions from parasitic beams (not shown in the figure) are easily separated. The gas chamber, filled with isobutane at 30 Torr, was used both to provide an independent energy-loss signal ΔE_{GAS} and to act as a very homogeneous passive

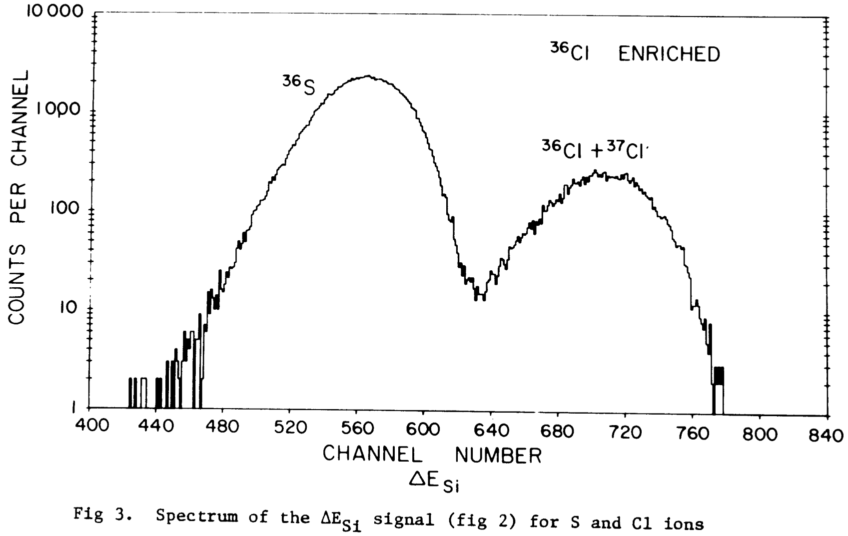

Fig 3. Spectrum of the ΔE_{Si} signal (fig 2) for S and Cl ions

energy absorber. The spectrum shown in figure 4, obtained by adding the ΔE_{Si} signal and the residual energy E_{RES} of the last Si detector, reflects the different energy losses experienced by ^{36}Cl and ^{36}S ions in the gas: indeed, it should be noted that these ions have equal energies before entering the detection system and the separation observed in figure 4 results only from the difference in the energies absorbed in the gas. The ^{37}Cl ions, identified in figure 4, result from a tail of ^{37}Cl^{-}ions injected by the source magnets and which, by means of charge-exchange processes in the residual gas along the accelerating tube, are accelerated to a magnetic rigidity equal to that of ^{36}Cl. They are separated from ^{36}Cl by their

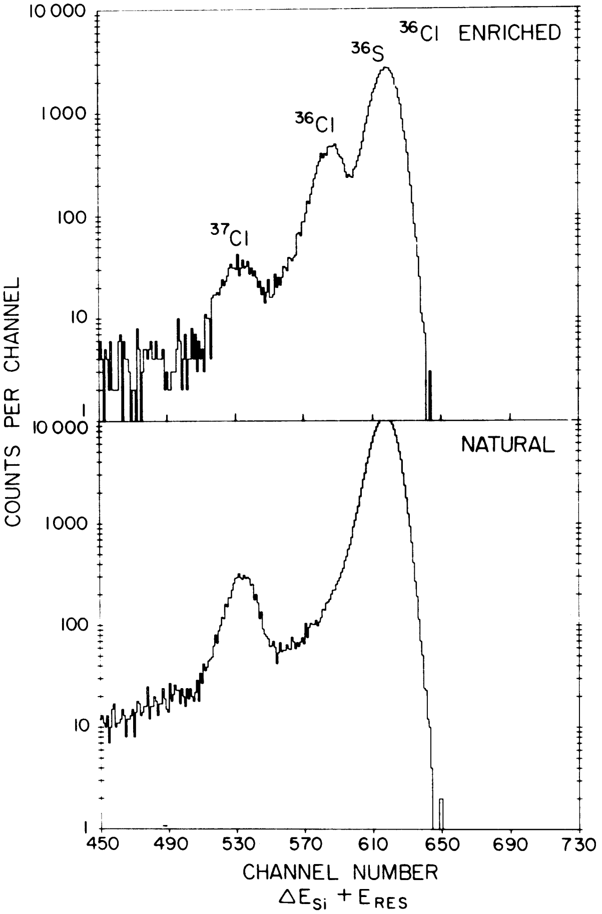

Fig 4. Spectra of the summed energies $\Delta E_{Si} + E_{RES}$, deposited in the first and last Si detectors (fig 2) for a ^{36}Cl-enriched sample and a sample of natural origin. The summation was done through software on-line treatment of the ΔE_{Si} and E_{RES} information by a PDP-11 data acquisition computer.

difference in energy, enhanced in the spectrum of figure 4 by a slightly different energy loss in the gas. A time-of-flight signal TOF was extracted from the first and last Si detectors to obtain an independent mass identification, but this gave only marginal additional information in the present measurements. Figure 5 shows a final spectrum of identified ^{36}Cl ions obtained by filtering the events through software gates on the ΔE_{Si}, ΔE_{GAS} and TOF signals.

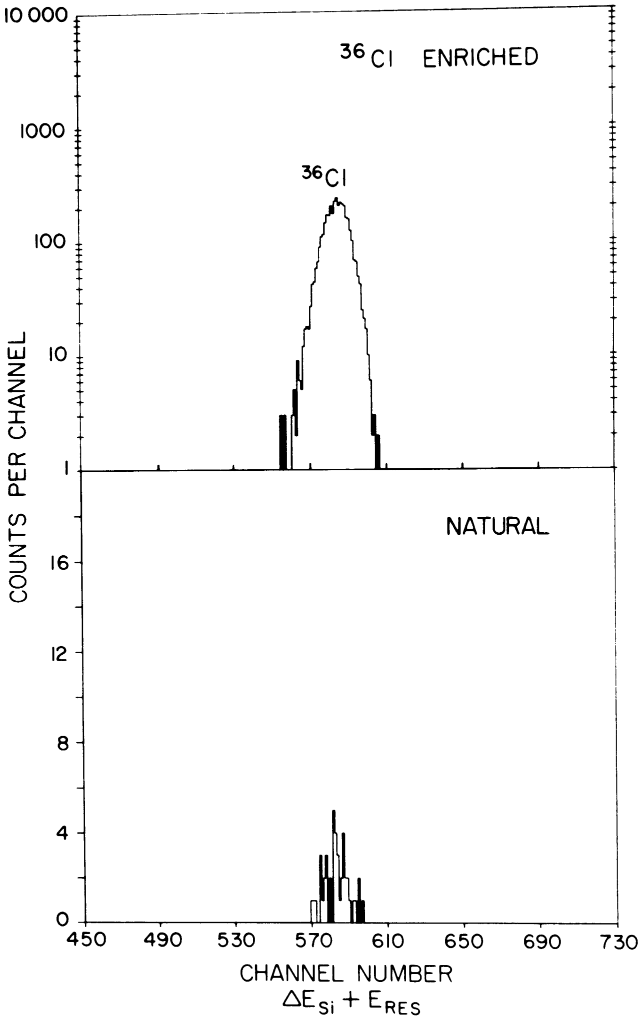

Fig 5. Spectra of summed energies $\Delta E_{Si} + E_{RES}$ for events filtered through software gates on the ΔE_{Si}, ΔE_{GAS} and TOF signals corresponding to ^{36}Cl for a ^{36}Cl-enriched sample and a sample of natural origin

PRESENT STATUS

The overall stability of the accelerator and the beam transport elements during the radioisotope counting was found to be adequate. Also, it should be emphasized that the switching between ^{37}Cl and ^{36}Cl beams could be accomplished quickly and reliably by changing only the fields of the source magnets and the charging conditions of the accelerator. Figures 4 and 5 show spectra obtained using a ^{36}Cl-enriched sample and a sample of natural origin. The low intensity of the parasitic beams such as ^{37}Cl (see fig 4) and lighter ions is attributed to the high vacuum in the accelerator tubes and to a good mass resolution of the injection magnets. Losses resulting from angular straggling of ions in the ΔE_{Si} and gas detectors were measured at ca 10%. Table 1 show our results for enriched and natural samples. The values indicate that measurements of concentrations of the order of $1x10^{-14}$ could be attained with the present system. We have not, up to now, assessed the importance of systematic errors in the measurements such as isotopic fractionation effects due to stripping efficiency, machine ion-optics, or detection efficiency. Consequently, all ^{36}Cl/Cl concentrations given in Table 1 have been measured relative to the G9 enriched sample. The level of the background and possible cross-contamination effects between source samples have yet to be established for our system.

TABLE 1. Preliminary results of ^{36}Cl/Cl concentration measurements

Sample	Counting time (sec)	$^{37}Cl^{10+}$ stable isotope charge current (nA)	^{36}Cl counts	$(^{36}Cl/Cl)^{*}_{meas}$	$(^{36}Cl/Cl)_{expected}$
G9 (Reactor enriched)	260	52	12100	$1.45x10^{-9*}$	$(1.45\pm0.10)x10^{-9}$
E11 (Reactor enriched)	600	36	124	$(1.0\pm0.4)x10^{-11}$	$(1.49\pm0.13)x10^{-11}$
S2 (Natural)	1530	80	80	$(5\pm2)x10^{-13}$	-
Z2 (Natural)	3600	41	21	$(1\pm0.5)x10^{-13}$	-
BRC2 (Natural)	3000	22	10	$(8\pm3)x10^{-14}$	-

*Normalized relatively to a value $1.45x10^{-9}$ for the G9 enriched sample. The values are not corrected for fractionation effects. The errors given include statistical and other random errors, estimated from reproducibility of the values obtained in the small number of available measurements.

CONCLUSION

The present results on the sensitivity of our system for ^{36}Cl detection are encouraging and may allow for concentration measurements of cosmogenic ^{36}Cl in nature. Interesting problems related to geology and hydrology are under study and could be attacked with the present system.

ACKNOWLEDGMENTS

This research was supported in part by a grant from the United States-Isreal Binational Foundation (BSF), Jerusalem, Israel. The assistance of Israel Felner in various chemical problems is gratefully acknowledged.

REFERENCES

Bentley, HW and Davis, SN, 1981, Application of AMS to hydrology, in Henning et al, eds, Symposium on accelerator mass spectrometry, Proc: Argonne Illinois, Argonne Nat Lab, p 193-227.

Ben-Zvi, I, Birk, M, Dafni, E, Hollos, G, Kaim, R and Sokolowski, GS, 1981, Rehovot 14 UD Pelletron - Status Report, in Internatl Conf on electrostatic accelerator technology, 3rd, Proc: IEEE 81CH1639-4, p 59.

Elmore, D, Fulton, BR, Clover, MR, Marsden, JR, Gove, HE, Naylor, H, Purser, KH, Kilius, LR, Beukens, RP, and Litherland, AE, 1979, Analysis of ^{36}Cl in environmental water samples using an electrostatic accelerator: Nature, v 277, p 22-25.

Fowler, MM and Jared, RC, 1975, A gas ionization counter for particle identification: Nuclear Instruments Methods, v 124, p 341-347.

[Radiocarbon, Vol 25, No. 2, 1983, P 793-795]

BUSINESS MEETING

INTERNATIONAL AGREEMENTS AND THE USE OF THE NEW OXALIC ACID STANDARD

MINZE STUIVER

Quaternary Research Center and Department of Geological Sciences
Seattle, Washington 98195

The international radiocarbon community met on June 25, 1982. Two reports were presented, and several measures related to radiocarbon dating discussed and adopted.

P E Damon reported on the activities of the International Calibration Committee. The efforts of the committee were directed towards the development of the calibration tables comprising the data generated by several laboratories in the 20 years following the pioneering work of de Vries. These tables were published by Klein et al (1982). The International Calibration Committee was discharged with thanks for their useful work and a smaller committee with W G Mook as chairman was reconstituted for the 1982-1985 interval. One of the tasks of the committee is to evaluate, prior to the 1985 International Radiocarbon Conference, the available high-precision data and combine these data in a "second generation" calibration curve. Sentiment was expressed at the meeting that particular attention should be given to the dendrochronologic aspects, and to the format of reporting of the calibration data.

W B Mann of the National Bureau of Standards reported the results of the international cooperative effort of calibrating the new oxalic acid standard (NOX) relative to the old oxalic standard (OX). The report, given in Chapter V, yields a weighted average of the weighted individual results:

$$NOX/OX = 1.2933 \pm 0.0004.$$

The reported $\delta^{13}C_{PDB}$ values average −17.8‰ for NOX and −19.3‰ for OX (Mann, 1983). The following normalizations apply (Stuiver and Robinson, 1974):

$$NOX(-25) = NOX\ (-17.8)\ 0.975^2\ /(1+\delta^{13}C_{nox}/1000)^2 \qquad (1)$$

and

$$OX(-19) = OX\ (-19.3)\ 0.981^2\ /(1+\delta^{13}C_{ox}/1000)^2 \qquad (2)$$

where $\delta^{13}C$ values are measured relative to PDB.

The ^{14}C activity of the international standard for radiocarbon dating is equal to 95% of the OX(−19) activity, or 0.95 OX(−19). This same activity has to equal X NOX (−25), where X is the factor to be calculated from the calibration movements.

Thus:

$$0.95\ OX(-19) = X\ NOX\ (-25),\ \text{or}$$

$$X = 0.95\ OX(-19)\ /NOX(-25) \qquad (3)$$

Substitution of (1) and (2) in (3) results in

$$X=0.95\ \frac{0.981^2(1+\delta^{13}C_{nox}/1000)^2\ OX\ (-19.3)}{0.975^2(1+\delta^{13}C_{ox}/1000)^2 NOX\ (-17.8)} \qquad (4)$$

The X value does not change materially with the absolute value of $\delta^{13}C_{ox}$ and $\delta^{13}C_{nox}$, as long as the 1.5‰ δ difference between both standards is constant. This difference in isotope ratio has been measured with excellent reproducibility (Mann, 1983).

Substitution of the measured values in (4) yields

$$X = 0.7459$$

Thus, 0.7459 times the new oxalic acid activity (when normalized on $\delta^{13}C_{PDB}$ = - 25 ‰) equals 0.95 times the old oxalic acid activity (normalized on a $\delta^{13}C_{PDB}$ = - 19‰).

The X value reported here is 0.0002 units larger than the previously reported (Stuiver, 1980) value. The 1980 report also discusses "X" values for NOX activities normalized on a $\delta^{13}C$ value of either - 17, or -19‰. These "X" values also should be increased by 0.0002 units.

The following decisions were made by majority vote:

1) The uncertainty in the ^{14}C date or $\Delta^{14}C$ value should be reported as one standard deviation, with a clear definition of the factors that are included in such a standard error.

2) The use of the Libby 5568-year half-life for reporting ^{14}C ages by all laboratories was re-affirmed. A special invitation was made to the Chinese laboratories to use the Libby half-life.

3) The weighted averages of the weighted individual results of the international NOX calibration should be used for the calculation of the X factor. The NOX standard is to be normalized on a $\delta^{13}C_{PDB}$ = -25‰. The latter measure reaffirms the adoption of the -25‰ value of NOX at the Tenth International Radiocarbon Conference (Stuiver, 1980). These decisions lead to X = 0.7459.

4) A three-year rotational schedule (with the possibility of re-appointment) applies to the term of appointment of

members of the International Calibration Committee.

5) A request was made to Reidar Nydal to host the 12th International Radiocarbon Conference in Trondheim, Norway, in the summer of 1985.

REFERENCES

Klein, Jeffrey, Lerman, J C, Damon, P E, and Ralph, E K, 1982, Calibration of radiocarbon dates: tables based on the consensus data of the Workshop on Calibrating the Radiocarbon Time Scale: Radiocarbon, v 24, p 103-150.

Mann, W B, An international reference material for radiocarbon dating, in Stuiver, M and Kra, R S, eds, Internatl ^{14}C conf, 11th, Proc: Radiocarbon, v 25.

Stuiver, Minze, 1980, Workshop on ^{14}C data reporting, in Stuiver, M and Kra, R S, eds, Internatl ^{14}C conf, 10th, Proc: Radiocarbon, v 22, no. 3, p 964-966.

Stuiver, Minze and Robinson, S W, 1974, University of Washington Geosecs North Atlantic carbon - 14 results: Earth Planetary Letters, v 23, p 87-90.

NOTICE TO READERS AND CONTRIBUTORS

Since its inception, the basic purpose of Radiocarbon has been the publication of compilations of ^{14}C dates produced by various laboratories. These lists are extremely useful for the dissemination of basic ^{14}C information.

In recent years, Radiocarbon has also been publishing technical and interpretative articles on all aspects of ^{14}C, especially in the Proceedings issues. The editors and readers agree that this expansion is broadening the scope of the Journal.

Another section is added to our regular issues, "Notes and Comments". Authors are invited to extend discussions or raise pertinent questions to the results of scientific investigations that have appeared on our pages. The section will include short, technical notes to relay information concerning innovative sample preparation procedures. Laboratories may also seek assistance in technical aspects of radiocarbon dating. Book reviews will also be included for special editions.

Manuscripts of radiocarbon papers should follow the recommendations in *Suggestions to Authors.** All copy (including the bibliography) must be typewritten in *double space*. Our deadline schedule is:

For	*Date*
Vol 26, No. 1, 1984	Sept 1, 1983
Vol 26, No. 2, 1984	Jan 1, 1984
Vol 26, No. 3, 1984	May 1, 1984

General or technical articles should follow the recommendations above and the editorial style of the *American Journal of Science* or the Proceedings of the Eleventh International Radiocarbon Conference. Date lists should follow the format shown in the most recent issue of RADIOCARBON. More detailed instructions are available upon request. Separate mailings have been discontinued.

Half life of ^{14}C. In accordance with the decision of the Fifth Radiocarbon Dating Conference, Cambridge, 1962, all dates published in this volume (as in previous volumes) are based on the Libby value, 5570 ± 30 yr, for the half life. This decision was reaffirmed at the 11th International Radiocarbon Conference in Seattle, Washington, 1982. Because of various uncertainties, when ^{14}C measurements are expressed as dates in years BP the accuracy of the dates is limited, and refinements that take some but not all uncertainties into account may be misleading. The mean of three recent determinations of the half life, 5730 ± 40 yr, (Nature, v 195, no. 4845, p 984, 1962), is regarded as the best value presently available. Published dates in years BP, can be converted to this basis by multiplying them by 1.03.

AD/BC Dates. In accordance with the decision of the Ninth International Radiocarbon Conference, Los Angeles and San Diego, 1976, the designation of AD/BC, obtained by subtracting AD 1950 from conventional BP determinations is discontinued in Radiocarbon. Authors or submitters may include calendar estimates as a comment, and report these estimates as AD/BC, citing the specific calibration curve used to obtain the estimate.

Meaning of $\delta^{14}C$. In Volume 3, 1961, we endorsed the notation Δ (Lamont VIII, 1961) for geochemical measurements of ^{14}C activity, corrected for isotopic fractionation in samples and in the NBS oxalic-acid standard. The value of $\delta^{14}C$ that entered the calculation of Δ was defined by reference to Lamont VI, 1959, and was corrected for age. This fact has been lost sight of, by editors as well as by authors, and recent papers have used $\delta^{14}C$ as the observed deviation from the standard. At the New Zealand Radiocarbon Dating Conference it was recommended to use $\delta^{14}C$ only for age-corrected samples. Without an age correction, the value should then be reported as percent of modern relative to 0.95 NBS oxalic acid (Proceedings 8th Conference on Radiocarbon Dating, Wellington, New Zealand, 1972). The Ninth International Radiocarbon Conference, Los Angeles and San Diego, 1976, recommended that the reference standard, 0.95 times NBS oxalic acid activity, be normalized to $\delta^{13}C = -19‰$.

In several fields, however, age corrections are not possible. $\delta^{14}C$ and Δ, uncorrected for age, have been used extensively in oceanography, and are an integral part of models and theories. For the present, therefore, we continue the editorial policy of using Δ notations for samples not corrected for age.

* Suggestions to Authors of the Reports of the United States Geological Survey, 6th ed, 1978, Supt of Documents, U S Govt Printing Office, Washington, DC 20402.

SPECIAL VOLUME

1983

PHILIP M. ORVILLE MEMORIAL VOLUME

in honor of our late Editor

STUDIES IN METAMORPHISM AND METASOMATISM

(24 articles — approx 500 pages)

Hugh Greenwood, editor

Special pre-publication prices to 1983 subscribers to the Journal—

Individuals	$25.00 prepaid
Institutions	35.00 prepaid
Post publication	50.00 prepaid

Send your order today to

American Journal of Science
Kline Geology Laboratory, Yale University
P.O. Box 6666
New Haven, CT 06511